



LIFE17 ENV/ES/000260

01/01/2019-31/12/2023

Deliverable Action D2. Participation and organization of networking and
information platforms related to the project objectives

NEWSLETTERS, ARTICLES IN SPECIALISED JOURNALS AND SCIENTIFIC ARTICLES

October 2023

Disclaimer

Co-funded by the European Union. Views and opinions expressed are however those of the author(s) only and do not necessarily reflect those of the European Union or CINEA. Neither the European Union nor the granting authority can be held responsible for them.

1. INTRODUCCION	3
2. INTRODUCCIÓN	3
3. Newsletters	4
4. Articles in specialised journals	8
4.1. RETEMA article	8
4.2. RETEMA article	9
4.3. RETEMA article	10
5. Scientific articles	11
6. Presentations and communications to congresses related to the Life Surfing project	13
6.1. Presentations:.....	13
6.2. Submission of abstracts to congresses:.....	14
6.3. Participation of LIFE SURFING partners in Networking sessions	16
ANNEX I. Full articles.....	18
ANNEX II. Abstracts.....	134
ANNEX III. Posters.....	148

1. INTRODUCCION

This deliverable collects that information within action D2. Participation and organization of networking and information platforms related to the project objectives such as newsletters, articles in specialized magazines and scientific articles produced for the effective dissemination of the project objectives.

In this case, the target audience is related to the technical, consulting field, scientists specializing in decontamination techniques.

It incorporates all distributed communications focused on the objectives, those of the main event of the project, the 14th International Forum on HCH and Pesticides, as well as scientific articles sent to the main international journals.

The main objectives of action D2 are to disseminate the knowledge generated by the project to the scientific community and to other stakeholders, to promote participation and fluid communication between all interested parties in the open days, and to raise awareness of the interested parties regarding the importance and priority of the LIFE SURFING project.

2. INTRODUCCIÓN

Este entregable recopila esa información en el marco de la acción D2. Participación y organización de plataformas de networking e información relacionada con los objetivos del proyecto, como boletines, artículos en revistas especializadas y artículos científicos producidos para la difusión efectiva de los objetivos del proyecto.

En este caso, el público objetivo está vinculado al ámbito técnico y de consultoría, así como a científicos especializados en técnicas de descontaminación. Incluye todas las comunicaciones distribuidas centradas en los objetivos, tanto las del evento principal del proyecto, el 14º Foro Internacional sobre HCH y Pesticidas, como los artículos científicos enviados a las principales revistas internacionales.

Los objetivos principales de la acción D2 son difundir el conocimiento generado por el proyecto a la comunidad científica y a otros interesados, promover la participación y la comunicación fluida entre todas las partes interesadas en las jornadas de puertas abiertas y concienciar a las partes interesadas sobre la importancia y prioridad del proyecto LIFE SURFING.

Mailing 8th February 2023

De: lfesurfing@sarga.es
Enviado el: miércoles, 8 de febrero de 2023 10:47
Para: lfesurfing@sarga.es
Asunto: 14th International Forum HCH&Pesticides-General information
Datos adjuntos: Block_XP_La14MarvN1.ppt

Dear Participants/Speakers,

Thank you for your registration in the "14th International HCH & Pesticides Forum" that will be held from February 21 to 24, 2023. We are pleased to inform you that you can consult the detailed [Programme](https://www.hchforum.com/programme) and download it at the following link: <https://www.hchforum.com/programme>.

All sessions will be held also via Zoom, with simultaneous interpretation in Spanish and English. We remind you that in the case of sessions with limited capacity, you can follow the session online.

On February 15, the [abstract book](#) will also be available/downloadable on the forum website, where you can consult the thematic blocks and a summary of each talk.

Speakers/Block instructions:

- Consult the session in which you participate in the program. Send an email to lfesurfing@sarga.es with the following information:
 - Complete name of speaker and session/block where you will speak.
 - Modality of the presentation: face-to-face/online.
 - Power Point of your presentation (4-8-10MB). Deadline: February 15 (After this date, organization is not responsible about its presentation).
- You can use the attached model (BlockX_NP_La14MarvN1.ppt), but in any case it is mandatory to use the indicated file name and the fields of the first side (topics, surname, name, position, company/institution, logo, article title, author/s). Please adjust your presentation to the time per session indicated in the programme.
- In the case of **online speakers**, they must be registered on the zoom platform (free) and indicate it in the presentation (Block_XP_La14MarvN1_online.ppt). They must have a cable connection and make the presentation with a microphone. The organization will provide you a link to perform tests and you must be connected since the beginning of the session.

We kindly ask speakers to have in mind the following:

Presentations should have a clear introduction and clear conclusion.
 Talks must not exceed the time indicated in the Programme per presentation.
 Speakers must speak slowly and clearly, as everything will be translated English / Spanish.
 Be aware to be registered and please make sure that all of you are registered in the 14th Forum and that you have checked that you are the **main speaker** and if not come in message that your colleagues (attendees) will help the presenters. *Miss also check if you are online or present in iZenpage. In the program you can see that those participants that have registered that they are participating online are marked with "online"*

Chair's instructions:
 In the coming days, we will provide instructions of their session speakers, so they can communicate with you on the session and discuss further details and give you some good advice on your presentation.

Please, do not hesitate to contact us for any clarification and you can find more updated information on the website www.hchforum.com.

Thank you for your cooperation.



LifeSurfing/ Secretaría del 14º foro Internacional de HCH y Pesticidas
 LifeSurfing/ 14th International HCH and Pesticides Secretariat

Proyectos Europeos/European Projects
Sociedad Aragonesa de Gestión Agroambiental, S.L.U.

Avenida de Barrios nº5 Edificio A-3ª planta 50038 Zaragoza
 Teléfono: 976 070 045 Fax: 976 070 041

Sus datos personales se utilizan para formar parte de ficheros de responsabilidad de SARGA, único destinatario de la información aportada voluntariamente por Ud.
 Esta información se utilizará para la gestión de contactos y correos electrónicos, así como la realización de consultas y comunicaciones vía telemática. Los derechos de acceso, rectificación, consulta, cancelación y oposición podrán ser ejercidos mediante escrito dirigido a lfesurfing@sarga.es y se dirigen exclusivamente a su DESTINATARIO, pudiendo contener información confidencial o privilegiada. En su caso, el destinatario indicado, queda notificado de que la utilización, divulgación o frustación de esta información o comunicación, su contenido y sus archivos adjuntos, se encuentra prohibida por la LEGISLACIÓN VIGENTE. Si ha recibido esta comunicación POR ERROR, le rogamos que nos lo comunique inmediatamente por email a través del número de teléfono 976070045 y proceda a su destrucción inmediata.

Mailing 7th March 2023

De: lfesurfing@sarga.es
Enviado el: martes, 7 de marzo de 2023 11:46
Para: lfesurfing@sarga.es
Asunto: 14th International HCH & Pesticides Forum-Information

Dear Speakers/Chairs of the 14th International on HCH and Pesticides Forum,

First of all, thank you for your collaboration in this event, your participation was essential for its development and success.

We inform you, as accepted during registration, (<https://www.hchforum.com/privacy-policy/>) we will publish photos, videos and presentations (pdf format) for their dissemination in the forum website and social media.

Please, if you did not submit your presentation (online speakers) during the forum, **send it as soon as possible to lfesurfing@sarga.es**.

We also need the full paper to prepare the paper book (some of them are still missing). Please, send it to 14forumhch.papers@gmail.com (<https://www.hchforum.com/guidance/>) Deadline 02/31/2023.

Best regards,



LifeSurfing/ Secretaría del 14º foro Internacional de HCH y Pesticidas
 LifeSurfing/ 14th International HCH and Pesticides Secretariat

Proyectos Europeos/European Projects
Sociedad Aragonesa de Gestión Agroambiental, S.L.U.

Avenida de Barrios nº5 Edificio A-3ª planta 50038 Zaragoza
 Teléfono: 976 070 045 Fax: 976 070 041

Sus datos personales se utilizan para formar parte de ficheros de responsabilidad de SARGA, único destinatario de la información aportada voluntariamente por Ud.
 Esta información se utilizará para la gestión de contactos y correos electrónicos, así como la realización de consultas y comunicaciones vía telemática. Los derechos de acceso, rectificación, consulta, cancelación y oposición podrán ser ejercidos mediante escrito dirigido a lfesurfing@sarga.es y se dirigen exclusivamente a su DESTINATARIO, pudiendo contener información confidencial o privilegiada. Si no es Ud. el destinatario indicado, queda notificado de que la utilización, divulgación o frustación de esta información o comunicación, su contenido y sus archivos adjuntos, se encuentra prohibida por la LEGISLACIÓN VIGENTE. Si ha recibido esta comunicación POR ERROR, le rogamos que nos lo comunique inmediatamente por email a través del número de teléfono 976070045 y proceda a su destrucción inmediata.

Mailing 7th March 2023

De: lifesurfing@sarga.es
Enviado el: martes, 7 de marzo de 2023 14:09
Para: lifesurfing@sarga.es
Asunto: 14th International HCH & Pesticides Forum-Information & Survey

Dear attendees of the 14th International Forum on HCH and Pesticides,

Thank you for having participated in the event and we hope it has been of interest to you. In order to improve, we would like to know your opinion through the following link:

<https://forms.gle/xyuYQPvWoiPeNv9> (Spanish)

<https://forms.gle/aKXdAcvmADk1hBL> (English)

In case you need a certificate of assistance, please send an email to lifesurfing@sarga.es

We inform you that, in the next few days, we will publish photos, videos and presentations (pdf format) for dissemination on the forum website and social networks.

Thank you for your cooperation.
Best regards,



LifeSurfing/ Secretaría del 14º Foro Internacional de HCH y Pesticidas
LifeSurfing/ 14th Forum International HCH and Pesticides Secretariat

Proyectos Europeos/European Projects
Sociedad Aragonesa de Gestión Agroambiental, S.L.U.

Avenida de Raulillas nº5 Edificio A 3ª planta 50018 Zaragoza
Teléfono 976 070 000 Fax: 976 070 001

Sus datos personales se obtienen para formar parte de ficheros de responsabilidad de SARGA único destinatario de la información aportada voluntariamente por Vd.
Estos ficheros se utilizan para la gestión de contactos y correos electrónicos, así como la resolución de consultas y comunicaciones vía telemática. Los derechos de acceso, rectificación, consulta, cancelación y oposición podrán ser ejercidos mediante escrito dirigido a info@sarga.es
Este mensaje o comunicación, su contenido y sus archivos adjuntos, se envían desde el sistema de correo electrónico de lifesurfing@sarga.es y se dirigen exclusivamente a su DESTINATARIO, pudiendo contener información confidencial o privilegiada. Si no es Vd. el destinatario indicado, queda notificado de que la utilización, divulgación y/o copia sin autorización de este mensaje o comunicación, su contenido y sus archivos adjuntos, se encuentra prohibida por la LEGISLACIÓN VIGENTE. Si ha recibido esta comunicación POR ERROR, le rogamos que nos lo comunique inmediatamente por esta misma vía o a través del número de teléfono 976070000 y proceda a su destrucción inmediata.

Mailing 15th June 2023

De: lifesurfing@sarga.es
Enviado el: jueves, 15 de junio de 2023 10:08
Para: lifesurfing@sarga.es
Asunto: 14th HCH & Pesticides Forum: Presentations and videos

Dear attendees of the 14th HCH and Pesticides Forum,

We are pleased to inform you that all the presentations and videos of the 14th HCH & Pesticides Forum (organized by blocks) are available at:

- Website of the 14th HCH Forum and pesticides: <https://www.hchforum.com/>

- YouTube channel: <https://www.youtube.com/@14thhchpesticidesforum>
(Spanish and English translation)

- The Forum Book (available soon)

In order to improve -if you had not been able to fill it out previously- we would like to know your opinion through the following link:

<http://forms.gle/xyuYQPvWoiPeNv9> (Spanish)

<http://forms.gle/19oDTpG5uPbLYZ9> (English)

Best regards,



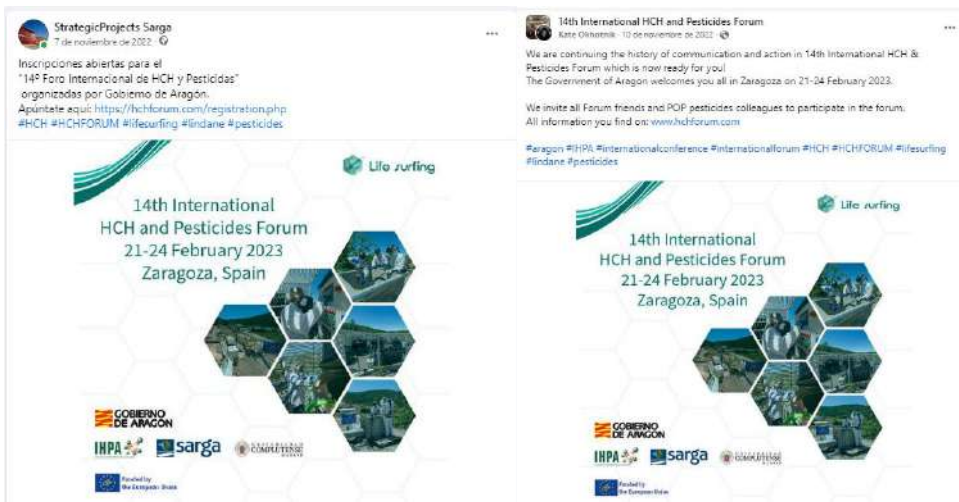
LifeSurfing/ Secretaría del 14º Foro Internacional de HCH y Pesticidas
LifeSurfing/ 14th Forum International HCH and Pesticides Secretariat

Proyectos Europeos/European Projects
Sociedad Aragonesa de Gestión Agroambiental, S.L.U.

SARGA, Avenida de Raulillas nº5 Edificio A 3ª planta 50018 Zaragoza
Teléfono 976 070 000 Fax: 976 070 001

Sus datos personales se obtienen para formar parte de ficheros de responsabilidad de SARGA único destinatario de la información aportada voluntariamente por Vd.
Estos ficheros se utilizan para la gestión de contactos y correos electrónicos, así como la resolución de consultas y comunicaciones vía telemática. Los derechos de acceso, rectificación, consulta, cancelación y oposición podrán ser ejercidos mediante escrito dirigido a info@sarga.es
Este mensaje o comunicación, su contenido y sus archivos adjuntos, se envían desde el sistema de correo electrónico de lifesurfing@sarga.es y se dirigen exclusivamente a su DESTINATARIO, pudiendo contener información confidencial o privilegiada. Si no es Vd. el destinatario indicado, queda notificado de que la utilización, divulgación y/o copia sin autorización de este mensaje o comunicación, su contenido y sus archivos adjuntos, se encuentra prohibida por la LEGISLACIÓN VIGENTE. Si ha recibido esta comunicación POR ERROR, le rogamos que nos lo comunique inmediatamente por esta misma vía o a través del número de teléfono 976070000 y proceda a su destrucción inmediata.

Social Networks



4. Articles in specialised journals

4.1. RETEMA article

The technical magazine about the environmental industry publishes the article "9 technical visits organized within the agenda of events of the EU Water Innovation Conference 2019"

- **LIFE SURFING: visita a los sitios afectados por los residuos de producción de lindano.** El Gobierno de Aragón ofrece esta visita a Sardas, Bailín para ver los trabajos que se están desarrollando en ellos, y al Centro de Referencia de Contaminantes Orgánicos Persistentes: laboratorio de control y monitorización para la Vigilancia y Plan de Control del Río Gállego.

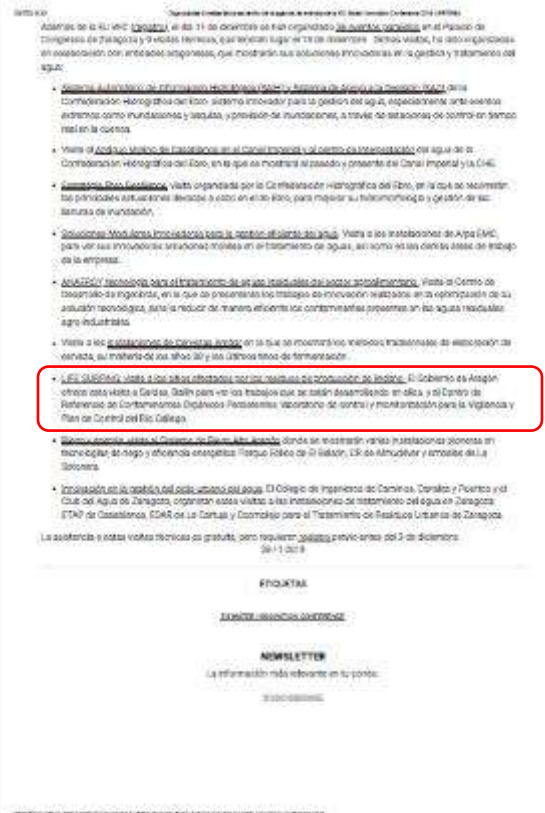



Organizadas 9 visitas técnicas dentro de la agenda de eventos de la EU Water Innovation Conference 2019

Comienza la cuenta atrás para la 7ª edición de la EU Water Innovation Conference.

Organizadas 9 visitas técnicas dentro de la agenda de eventos de la EU Water Innovation Conference 2019

Comienza la cuenta atrás para la 7ª edición de la EU Water Innovation Conference que tendrá lugar el 12 de diciembre en el Palacio de Congresos de Zaragoza. En esta ocasión, el evento y la feria son de carácter más amplio que en la edición de este evento, que reunió a todos agentes del sector del agua interesados en las nuevas tecnologías que impulsan la innovación, nuevas tecnologías y gobernanza.



Además de la EU Water Innovation Conference, el 12 de diciembre de este año se celebrará en el Palacio de Congresos de Zaragoza y 9 visitas técnicas, que se celebrarán los días 11 y 12 de diciembre. Dichas visitas, hechas conjuntamente en colaboración con entidades empresariales, que mostrarán sus soluciones innovadoras en la gestión y tratamiento del agua:

- **Visita al Laboratorio de Referencia de Contaminantes Orgánicos Persistentes (COP) del Gobierno de Aragón** para ver los trabajos que se están desarrollando en ellos, y al Centro de Referencia de Contaminantes Orgánicos Persistentes: laboratorio de control y monitorización para la Vigilancia y Plan de Control del Río Gállego.
- **Visita al Centro de Referencia de Contaminantes Orgánicos Persistentes (COP) del Gobierno de Aragón** para ver los trabajos que se están desarrollando en ellos, y al Centro de Referencia de Contaminantes Orgánicos Persistentes: laboratorio de control y monitorización para la Vigilancia y Plan de Control del Río Gállego.
- **Visita al Centro de Referencia de Contaminantes Orgánicos Persistentes (COP) del Gobierno de Aragón** para ver los trabajos que se están desarrollando en ellos, y al Centro de Referencia de Contaminantes Orgánicos Persistentes: laboratorio de control y monitorización para la Vigilancia y Plan de Control del Río Gállego.
- **Visita al Centro de Referencia de Contaminantes Orgánicos Persistentes (COP) del Gobierno de Aragón** para ver los trabajos que se están desarrollando en ellos, y al Centro de Referencia de Contaminantes Orgánicos Persistentes: laboratorio de control y monitorización para la Vigilancia y Plan de Control del Río Gállego.
- **Visita al Centro de Referencia de Contaminantes Orgánicos Persistentes (COP) del Gobierno de Aragón** para ver los trabajos que se están desarrollando en ellos, y al Centro de Referencia de Contaminantes Orgánicos Persistentes: laboratorio de control y monitorización para la Vigilancia y Plan de Control del Río Gállego.
- **Visita al Centro de Referencia de Contaminantes Orgánicos Persistentes (COP) del Gobierno de Aragón** para ver los trabajos que se están desarrollando en ellos, y al Centro de Referencia de Contaminantes Orgánicos Persistentes: laboratorio de control y monitorización para la Vigilancia y Plan de Control del Río Gállego.
- **Visita al Centro de Referencia de Contaminantes Orgánicos Persistentes (COP) del Gobierno de Aragón** para ver los trabajos que se están desarrollando en ellos, y al Centro de Referencia de Contaminantes Orgánicos Persistentes: laboratorio de control y monitorización para la Vigilancia y Plan de Control del Río Gállego.
- **Visita al Centro de Referencia de Contaminantes Orgánicos Persistentes (COP) del Gobierno de Aragón** para ver los trabajos que se están desarrollando en ellos, y al Centro de Referencia de Contaminantes Orgánicos Persistentes: laboratorio de control y monitorización para la Vigilancia y Plan de Control del Río Gállego.
- **Visita al Centro de Referencia de Contaminantes Orgánicos Persistentes (COP) del Gobierno de Aragón** para ver los trabajos que se están desarrollando en ellos, y al Centro de Referencia de Contaminantes Orgánicos Persistentes: laboratorio de control y monitorización para la Vigilancia y Plan de Control del Río Gállego.

La asistencia a estas visitas técnicas es gratuita, pero requieren registro previo antes del 3 de diciembre. 2019-12-03

ENCUENTROS

EXPOSICIÓN INNOVACIÓN CONFERENCE

NEWSLETTER

La información más relevante en tu correo.

2019-12-03

4.2. RETEMA article

The technical magazine about the environmental industry publishes the article "The Government of Aragon will work on a new European project for the decontamination of lindane"

Aragón trabaja en cuatro proyectos europeos en relación a la descontaminación del lindano

El "Pilot Project to Evaluate and Address the Presence of Lindane and Hexachlorocyclohexane (HCH) in the European Union" es el cuarto proyecto concedido por la Unión Europea a Aragón en relación al lindano. Entre todos suman 6.8 millones de euros. El ya finalizado con resultados prometedores Life Discovered (2014-2017) que perseguía la eliminación de residuos de la fabricación de lindano disueltos en el agua presentes en grietas y dotado de 1,4 millones de euros cofinanciados al 60% por la UE. Y los que todavía están en ejecución el Life Surfing (2019-2022) que investiga la extracción y eliminación de residuos densos no bombeables presentes en grietas ayudados por surfactantes (jabones industriales), que cuenta con un presupuesto de 2 millones de euros financiados al 57% por la UE y el Intereg Lindanet (2020-2023) que supone la creación de una red de regiones afectadas por los residuos de la fabricación de lindano para intercambiar experiencias de gestión y diseñar y ejecutar nuevas medidas cada uno en su emplazamiento, dotado con 1,4 millones de euros cofinanciados al 85 % por la UE.

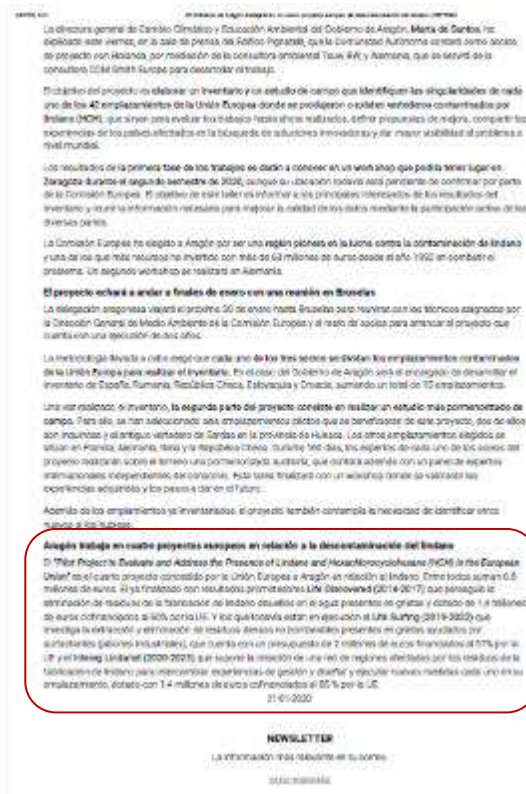



El Gobierno de Aragón trabajará en un nuevo proyecto europeo de descontaminación del lindano

El objetivo del proyecto, dotado con dos millones de euros, es elaborar un inventario y un estudio de campo que permitan conocer la contaminación de cada uno de los 42 emplazamientos de la UE donde se produjeron o fabricaron los residuos de lindano.

LIDERES
EN LA FABRICACIÓN DE EQUIPOS PARA LA CONTAMINACIÓN DE HCH, H.P.

La Comisión Europea ha concedido a la empresa javiera NARCA, del gobierno de Aragón, el proyecto "Pilot Project to Evaluate and Address the Presence of Lindane and Hexachlorocyclohexane (HCH) in the European Union" que contará con una financiación de 2 millones de euros del programa LIFE.



Aragón trabaja en cuatro proyectos europeos en relación a la descontaminación del lindano

El "Pilot Project to Evaluate and Address the Presence of Lindane and Hexachlorocyclohexane (HCH) in the European Union" es el cuarto proyecto concedido por la Unión Europea a Aragón en relación al lindano. Entre todos suman 6.8 millones de euros. El ya finalizado con resultados prometedores Life Discovered (2014-2017) que perseguía la eliminación de residuos de la fabricación de lindano disueltos en el agua presentes en grietas y dotado de 1,4 millones de euros cofinanciados al 60% por la UE. Y los que todavía están en ejecución el Life Surfing (2019-2022) que investiga la extracción y eliminación de residuos densos no bombeables presentes en grietas ayudados por surfactantes (jabones industriales), que cuenta con un presupuesto de 2 millones de euros financiados al 57% por la UE y el Intereg Lindanet (2020-2023) que supone la creación de una red de regiones afectadas por los residuos de la fabricación de lindano para intercambiar experiencias de gestión y diseñar y ejecutar nuevas medidas cada uno en su emplazamiento, dotado con 1,4 millones de euros cofinanciados al 85 % por la UE.

21/01/2020

NEWSLETTER
LA INFORMACIÓN PARA SABER MÁS DE LAS COSAS
QUE IMPORTA

4.3. RETEMA article

The technical magazine about the environmental industry publishes the article "Zaragoza hosts the XIV International Forum on Lindane (HCH) and Pesticides".

El posicionamiento de Aragón como líder en la gestión de la contaminación de los residuos del lindano en Europa y el compromiso adquirido por la región para progresar hacia la solución de la problemática han llevado a la Dirección General de Cambio Climático y Educación Ambiental del Gobierno de Aragón a ser la anfitriona del XIV Foro Internacional de Lindano (HCH) y Pesticidas. En el marco del proyecto europeo LIFE SURFING, el evento se ha inaugurado este martes, 21 de febrero de 2023, en la sede de la Caja Rural de Aragón (Zaragoza).





5. Scientific articles

Several articles have been published scientific journals of excellence. The list of articles and the link to the publication are included in the following lines. The full articles are collected in Annex I:

1. Article “Partitioning of chlorinated organic compounds from dense nonaqueous phase liquids and contaminated soils from lindane production wastes to the aqueous phase”.
David Lorenzo, Raul García-Cervilla, Arturo Romero, Aurora Santos. Chemosphere 239 (2020) 124798. **OPEN ACCESS**
<https://doi.org/10.1016/j.chemosphere.2019.124798>
2. Article “Surfactant-Enhanced Solubilization of Chlorinated Organic Compounds Contained in DNPLE from Lindane Waste: Effect of Surfactant Type and pH”.
García-Cervilla, R., A. Romero, A. Santos and D. Lorenzo. International Journal of Environmental Research and Public Health 17(12): 1-14. (2020). **OPEN ACCESS**.
<https://doi.org/10.3390/ijerph17124494>
3. Article “Compatibility of nonionic and anionic surfactants with persulfate activated by alkali in the abatement of chlorinated organic compounds in aqueous phase”.
García-Cervilla, R., A. Santos, A. Romero and D. Lorenzo. Science of The Total Environment 751: 141782 (2021). **OPEN ACCESS**
<https://doi.org/10.1016/j.scitotenv.2020.141782>
4. Article “Abatement of chlorobenzenes in aqueous phase by persulfate activated by alkali enhanced by surfactant addition”
R. García-Cervilla, A. Santos, A. Romero, D. Lorenzo. Journal of Environmental Management 306 (2022) 114475. **OPEN ACCESS**
<https://doi.org/10.1016/j.jenvman.2022.114475>.
5. Article “Simultaneous addition of surfactant and oxidant to remediate a polluted soil with chlorinated organic compounds: Slurry and column experiments”.
Raul Garcia-Cervilla, Aurora Santos, Arturo Romero, David Lorenzo. Journal of Environmental Chemical Engineering 10 (2022) 107625. **OPEN ACCESS**
<https://doi.org/10.1016/j.jece.2022.107625>
6. Article “Non-Ionic surfactant recovery in surfactant enhancement aquifer remediation effluent with chlorobenzenes by semivolatile chlorinated organic compounds volatilization”.
P. Sáez, A. Santos, R. García-Cervilla, A. Romero, D. Lorenzo. International Journal of Environmental Research and Public Health (2022) 19, 7547 **OPEN ACCESS**
<https://doi.org/10.3390/ijerph19127547>

7. Article “Regeneration of granulated spent activated carbon with 1,2,4-trichlorobenzene using thermally activated persulfate”.
Sánchez-Yepes, A. Santos, J. M. rosas, J. Rodríguez-Mirasol, T. Cordero, D. Lorenzo. Industrial & Engineering Chemistry Research (2022), 61, 9611-9620. **OPEN ACCESS**. <https://doi.org/10.1021/acs.iecr.2c00440>
8. Article “Treatment of a Complex Emulsion of a Surfactant with Chlorinated Organic Compounds from Lindane Wastes under Alkaline Conditions by Air Stripping”.
Patricia Sáez, Aurora Santos, Raúl García-Cervilla, Arturo Romero, David Lorenzo, Industrial and Engineering Chemistry Research, **OPEN ACCESS** 2022
<https://pubs.acs.org/doi/10.1021/acs.iecr.2c03722>
9. Article “European cooperation to tackle the legacies of hexachlorocyclohexane (HCH) and lindane”
John Vijgen, Boudewijn Fokke, Guido van de Coterlet, Katja Amstaetter, Javier Sancho, Carlo Bensaïah, Roland Weber. Emerging Contaminants, Volume 8, January 2022, 97112. **OPEN ACCESS**
<https://doi.org/10.1016/j.emcon.2022.01.003>
10. Article “Sustainable reuse of toxic spent granular activated carbon by heterogeneous fenton reaction intensified by temperature changes”
Sánchez-Yepes, Andrés; Santos, Aurora; Rosas, Juana M.; Rodríguez-Mirasol, José; Cordero, Tomás; Lorenzo, David. Chemosphere, Volume 341, November 2023, 140047. **OPEN ACCESS**. <https://doi.org/10.1016/j.chemosphere.2023.140047>

On the other hand, 130 scientific articles were presented at the 14th International on HCH and Pesticides Forum. They have been published in <https://www.hchforum.com/presentations/> and in the Forum Book (Deliverable D27D3). Nine (9) of these articles were specific of the LIFE SURFING project (all articles from sessions 1 and 2 of the Forum). All Forum articles will be incorporated in the Forum Book, which will be published in the website www.hchforum.com.

6. Presentations and communications to congresses related to the Life Surfing project

6.1. Presentations:

Complutense University of Madrid (UCM) has carried out presentations of the LIFE SURFING Project in several events, listed here:

1. Workshop CARESOIL 2019

Faculty of Pharmacy (UCM). October 25, 2019.

Title of the workshop: "Joining Efforts in the Characterization and Recovery of Contaminated Sites: a Necessary Multidisciplinary Approach" Organized by CARESOIL R&D Program (Coordinator: INPROQUIMA), Call for R&D Programs in Technologies 2018. Community of Madrid. In collaboration with the LIFE SURFING Project. Plenary Lecture: "Use of Surfactants and Oxidants in the Remediation of Sites with DNAPL. LIFE SURFING Project" by Eduardo Calleja Jiménez. Directorate General of Climate Change and Environmental Education. Government of Aragon.

<https://www.ucm.es/caresoil/eventos>

2. European Night of Researchers

Venue: University of Chemistry of the Complutense University of Madrid, October 27, 2019. Organized by the Madrid Region and the UCM. PÓSTER: "LIFE SURFING SURFactant enhanced chemical oxidation for remediating DNAPL".

3. XIX SCIENCE WEEK November 4-17, 2019

Organized by Madrid+d Foundation. Community of Madrid Title: Remedying Pollution Beneath Our Feet Activities: Conference and Laboratory Tour for Attendees Collaborators: CARESOIL and LIFE SURFING Location: Faculty of Chemistry, INPROQUIMA Laboratories, UCM, November 5, 2019.

<https://quimicas.ucm.es/semana-de-la-ciencia-2019>

4. LIFE Platform Meeting on Chemicals

Organized by the European Union (LIFE PROJECTS) 27 & 28 November 2019:

Seminar on Indicators to measure Improvement in Chemicals Management Vilnius, Lithuania Two posters were presented at the LIFE PROJECT: "LIFE SURFING: SURFactant enhanced chemical oxidation for remediating DNAPL." Participants: Jesús Fernández (Aragon Government) and Aurora Santos (INPROQUIMA, UCM).

<https://ec.europa.eu/easme/en/life-platform-meeting-chemicals-indicator-workshop>

5. EU Water Innovation Conference 2019

Organized by the European Union. Zaragoza, Dec 2019 Parallel Meetings: December 11, 2019, 10:00-13:00 - LIFE SURFING: Remediation of Lindane Manufacturing Wastes. Conference: Fundamentals and Techniques. Aurora Santos (INPROQUIMA, UCM).

https://ec.europa.eu/clima/events/eu-water-innovation-conference-2019_en

<https://www.eip-water.eu/side-meetings-eip-water-conference-2019>

6. Workshop CARESOIL 2022

In December 2022, the INPROQUIMA group, coordinator of the R&D Program CARESOIL in the Community of Madrid (which involves companies - stakeholders and environmental engineering firms -, environmental authorities, researchers, etc.) organized a session on the topic of "Significance of Characterization in the Remediation of Soils and Groundwater." Jesús Fernández Cascán (Government of Aragon) delivered the lecture "LIFE SURFING Project: SURfactant enhanced Chemical Oxidation for the remediatING DNAPL," which is available on YouTube at

<https://www.youtube.com/watch?v=eZZwDDRjCU>.

7. Scuola di Alta Formazione sulla Bonifica di Siti Contaminati. Labelab 20,

Ravenna, Italy, May 17-19, 2023. UCM delivered a conference on the LIFE SURFING Project by invitation in May 2023 in Ravenna, Italy. Title of the presentation: "LIFE SURFING: SURfactant enhanced chemical oxidation for remediatING DNAPL".

<https://www.fareiconticonambiente.it/corso-alta-formazione/corso-di-alta-formazione-sulla-bonifica-di-siti-contaminati/>

8. European Researchers' Night 2023

LIFE SURFING Project: A Washer to Remove Pesticides from Soils and Groundwater. Organized by the Community of Madrid-UCM, September 29, 2023. Primarily aimed at secondary school and high school students, it includes a brief talk about the LIFE SURFING project and a workshop where surfactants are applied to remove DNAPL in soils.

<https://www.madrimasd.org/lanochedelosinvestigadores/actividad/ucm-proyecto-life-surfing-una-lavadora-para-eliminar-pesticidas-de-suelos-y-aguas>

6.2. Submission of abstracts to congresses:

The UCM has sent the following communications (abstracts) of LIFE SURFING works for poster and oral presentations in soil remediation congresses:

1. "Solubilization of Dense Non Aqueous Phase Liquids produced as Lindane Wastes using Non-Ionic Surfactants" Raul García, Arturo Romero, David Lorenzo and Aurora

Santos. **Poster Presentation** in Sustainable Use and Management of Soil, Sediment and Water Resources, 5th International Conference|20–24 May 2019|Antwerp, Belgium. Aquaconsoil 2019.

2. “Post-Treatment of Aqueous Solution containing Surfactant and Chlorinated Organic Compounds from Lindane wastes” Aurora Santos, Raul García, Carmen M. Dominguez, David Lorenzo and Arturo Romero. **Poster Presentation** in Sustainable Use and Management of Soil, Sediment and Water Resources, 5th International Conference | 20–24 May 2019| Antwerp. Aquaconsoil 2019.
3. “Research on Surfactant-Supported In-Situ Oxidation for the Remediation of DNAPL-Groundwater contaminations”. Benjamin Herzog, Norbert Klaas, Jürgen Braun, David Lorenzo, Aurora Santos López. **Oral presentation** AquaConSoil 2021. June 2021 (ONLINE) (Topic 5: Sustainable remediation technologies in context of the EGD and energy transition. Session 5a6: In Situ Source Zone Remediation, surfactant & ISCO focus, Session 2.)
<https://www.google.com/search?client=firefox-b-d&q=aquaconsoil+2021>
4. “Regeneration of granulated activated carbon saturated in 1,2,4-trichlorobenzene by thermal activation of persulfate” A. Sanchez-Yepes, D. Lorenzo, A. Romero, A. Santos. **Oral Presentation** 7th International Conference on Industrial and Hazardous Waste Management “CRETE 2021” 27th - 30th July 2021, Crete -Greece.
<http://hwm-conferences.tuc.gr/program-new/>
5. “Stability of Anionic and Non-Ionic Surfactants with Alkali-Activated Persulfate and Selective Oxidation of COCs in Emulsion.” D. Lorenzo, R. García Cervilla, A. Romero, A. Santos. **Poster Presentation**. XIV Spanish Congress on Water Treatment. META 2022. June 1st-3rd, 2022. Seville- Spain
https://www.uco.es/meta2022/?page_id=66
6. “IN SITU Chemical Oxidation Enhanced by Surfactants (S-SCO): LIFE SURFING PROJECT” Aurora Santos, Jesús Fernández, Elena Cano, David Lorenzo, Salvador Cotillas, Carlos Herranz. **Poster Presentation** XXXIX Biennial Meeting of Chemistry. Zaragoza, June 23, 2023
<https://bqz2023.com/index.php/es/>
7. “Volatilization of chlorinated organic compounds from lindane wastes in non-ionic surfactant emulsion at alkaline conditions”. P. Sáez, R. García-Cervilla, A. Sánchez-Yepes, D. Lorenzo, A. Romero, A. Santos. **Poster Presentation** XXXVIII Reunion Bienal RSEQ 2022. 27th-30th June 2022 Granada-Spain.
<https://bienal2022.com/index.php/es/>

8. “Regeneration of granulated spent activated carbon with 1,2,4-trichlorobenzene by persulfate activated heat”, A. Santos, A. Sánchez-Yepes, P. Sáez, R. García-Cervilla, J.M. Rosas, J. Rodríguez-Mirasol, T. Cordero, A. Romero, D. Lorenzo, **Oral Presentation**. XXXVIII Reunion Bienal RSEQ 2022. 27th-30th June 2022 Granada-Spain.
<https://bienal2022.com/index.php/es/>
9. “DNAPL Extraction and Oxidation enhanced by Surfactant addition: LIFE SURFING PROJECT” Aurora Santos, Jesús Fernández Cascán, David Lorenzo, Elena Cano, Patricia Saez, Carlos Herranz. **Oral Presentation**. Aquaconsoil 2023, Praga 11-15 September. TOPIC 3: Sustainable remediation, emerging contaminants and prevention towards zero pollution. Session 3c5.
<https://www.aquaconsoil.com/aquaconsoil-2023/scientific-programme/abstract-booklet/>

The abstracts and the posters are included in Annex II.

6.3. Participation of LIFE SURFING partners in Networking sessions

The IHPA has participated in the following Networking sessions related to HCH remediation with other projects and groups:

1. “Is Jaworzno alone with its HCH-problem? What is the situation in other EU Countries on HCH-problems? What can we learn from that?”, Keynote Closing Speech, AMIIGA EU Interreg, Final Conference, 24-25 October 2019, Jaworzno, Poland.
2. Possibilities of Replication & Transfer of the SURFING technique to other sites in the EU and on the globe, EU Water Innovation Conference, 2019, Side Event: LIFE SURFING.
“Remediation of Lindane manufacturing waste”, 11 December 2019, Zaragoza, Spain.
3. “Call on EU Citizens to find Lindane Production sites and HCH-waste”, International Webinar HCH in EU - EU Pilot project to evaluate and address the presence of lindane and HCH in the EU, 26 November and 1. December 2020.
4. Introduction to Action Plans inclusive Brainstorming, 3rd Interregional Thematic Workshop, EU Lindanet Interreg Project, 26 November 2020. Katowice, Śląskie, Poland (Polska)
5. “Overview of contaminated sites in other parts of Europe, Lindane contamination in Europe”, Online debate, Ecologists in Action, 30. November 2020.
6. Lindane & HCH in EU Member States Problems & Solutions Keynote speech online presentation, Session Ecological Bombs – how to neutralize them? Post-industrial

pollutions' necessary remediation (part I), Green League (Strefa Zieleni), GreenDays on the Drawa River (August 28, 2021).

7. HCH and Lindane an urgent European and global problem that needs to be addressed, Webinar, Session 3 | LIFEPOPWAT, development of "Wetland+" technology, a new treatment tool for the removal of HCH and its transformation compounds, WETPOL 2021, 9th Int Symposium on Wetland Pollutant Dynamics and Control, 16 September 2021.
8. Final Workshop HCH in EU Project Lessons learnt from and the future of HCH/Lindane in the EU, Hosted by Isabel García Muñoz Member of the European Parliament, 16-17 November 2021, Hotel Thon, EU, Brussels with following presentations.
9. Closing words on the way forward. Case Hengelo the Netherlands. Strategy to manage HCH contaminated sites EU-wide. HCH Pollution, EU Problem and Solutions, Lindanet Webinar, 16 March 2022.
10. Strategy to manage HCH contaminated sites EU-wide, HCH in EU, Launch of the International Network on Soil Pollution Channelling collective action towards Zero Pollution (INSOP), FAO, 22 April 2022, Virtual format (Zoom).

ANNEX I. Full articles



Partitioning of chlorinated organic compounds from dense non-aqueous phase liquids and contaminated soils from lindane production wastes to the aqueous phase

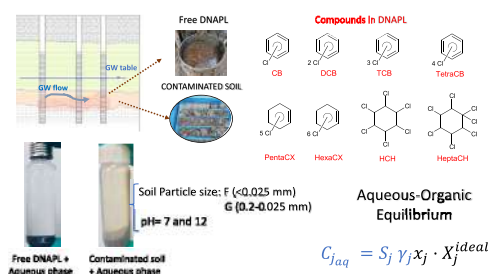
David Lorenzo, Raul García-Cervilla, Arturo Romero, Aurora Santos*

Chemical and Materials Engineering Department. University Complutense of Madrid, Spain

HIGHLIGHTS

- Partitioning behavior in water of 28 COCs in DNAPL has been studied.
- The DNAPL is a liquid waste for lindane production found in Sabinanigo Landfills.
- Concentration of COC in aqueous phase depends linearly on its mole fraction in the DNAPL.
- Similar partitioning in water was found for DNAPL as free phase or trapped into soil.
- Alkaline pH promotes dehydrochlorination to COCs with lower toxicity.

GRAPHICAL ABSTRACT



ARTICLE INFO

Article history:

Received 7 May 2019
 Received in revised form
 27 August 2019
 Accepted 5 September 2019
 Available online 7 September 2019

Handling Editor: Keith Maruya

Keywords:

Lindane wastes
 DNAPL
 Soil
 Chlorinated organic compounds
 Partitioning in water
 pH effect

ABSTRACT

Hexachlorocyclohexane (HCH) and mainly the γ -HCH isomer, namely lindane, were extensively produced and used as pesticides. Huge amounts of wastes, solids and liquids, were disposed of in the surroundings of the production sites. The liquid residuum was a complex mixture of chlorinated organic compounds, COCs, from chlorobenzene to heptachlorocyclohexane. This Dense Non-Aqueous Phase Liquid, DNAPL, migrated by density through the subsurface to greater depths, being trapped or adsorbed into the soil in this movement posing a significant risk to the groundwater. Knowledge of the partitioning in water of COCs in DNAPL is a key issue to determine its fate in the environment. However, there are no data in literature for the partitioning and/or solubility of many of the COCs in this DNAPL, such as pentachlorocyclohexene, hexachlorocyclohexene and heptachlorocyclohexane despite them constitute about 13–30% of the mole fraction of the DNAPLs. In this work, the partitioning to water of COCs in free and those adsorbed onto soil has been studied. In addition, measured and predicted aqueous concentrations of each COC in the DNAPL mixture have been compared. To do this, the solubility of a compound that is a solid crystal when pure at $P = 298 \text{ K}$ and $P = 1 \text{ atm}$ has been evaluated considering the approach of sub-cooled liquid state of solid organochlorines. Samples were obtained at Sabinanigo landfills and soils used had several grain sizes. Transformation in alkaline media of COCs had a positive environmental impact.

© 2019 Elsevier Ltd. All rights reserved.

1. Introduction

Soil and groundwater pollution caused by pesticides are a major

* Corresponding author.

E-mail address: aursan@quim.ucm.es (A. Santos).

problem in many countries all over the world (Ren et al., 2018). Their high persistency in the environment results in a high risk to human and environmental health (Weber et al., 2011; Li and Jennings, 2017). They can be transported to the atmosphere by volatilization, and may enter surface water bodies or can be leached from the superficial soil by run-off and enter to groundwater (Pirsaheb et al., 2017; Kumar and Mukherji, 2018). Among the pesticides, the Organochlorine Pesticides are a relevant group as they were widely used for agricultural pest control and for medical purposes (Cuozzo et al., 2018; Madaj et al., 2018). Many of these substances are listed by the Stockholm convention, which regulates or bans several of them (Karlagnanis et al., 2001; Lallas, 2001).

One of the most extensively used and produced organochlorine pesticides after the Second War World was lindane (Vijgen, 2006; Vijgen et al., 2011), the γ isomer of 1,2,3,4,5,6-hexachlorocyclohexane (HCH). HCHs were considered as persistent organic pollutants (POPs) and they have been banned by the Stockholm Convention since 2009 (Vijgen et al., 2011; Madaj et al., 2018). In Europe, lindane was produced in many countries mainly from the 1950s to the 1970s or 1990s as recently reported by the Directorate General for Internal Policies (EU) (Vega et al., 2016). Lindane was manufactured from photochlorination of benzene with UV light yielding a mixture of five main isomers. The only isomer with insecticide properties was the γ -HCH. Lindane was extracted and purified from the HCH mixture of isomers using fractional crystallization. In this process about 6–10 tons of other waste isomers are also obtained per ton of lindane (Vijgen, 2006; Vega et al., 2016) and the isomers α , β and γ -HCH (lindane) are included in the Stockholm Convention on Persistent Organic Pollutants (POPs) (Dorsey, 2005).

The huge amounts of wastes produced in the lindane manufacturing process have often been dumped without environmental concerns near production sites. As a result, soil and groundwater were highly contaminated (Vijgen, 2006; Fuscoletti et al., 2015; Pinto et al., 2016; Vega et al., 2016; Pawlowicz, 2017; Pirsaheb et al., 2017). Among the wastes from lindane production, a dense non-aqueous phase liquid (DNAPL) composed of HCH isomers, benzene and chlorobenzenes has been found in the subsurface of Sabiñanigo (Spain) landfills (Fernández et al., 2013), and its presence is due to the direct dumping of liquid residues from 1975 to 1992 by the company INQUINOSA. Moreover, polychlorinated dibenzo-p-dioxin/dibenzofuran (PCDD/Fs) were identified in these dense non-aqueous phase liquids (DNAPLs), as well as in landfill leachates, soil and sediments from Sabiñanigo landfills (Gómez-Lavín et al., 2018).

These liquid residues were generated from failed chlorination reactions and distillation tails in lindane production processes. Given that the average density of the DNAPL is about 1.5 g/cm^3 (Fernández et al., 2013) this phase was transported by density forces and it was found at different depths at the Sardas and Bailin landfills (Fernández et al., 2013; Casado et al., 2015). Solubilization of the DNAPL in the groundwater has caused significant pollution of the groundwater, with the associated risk for the nearby river and reservoir (Navarro et al., 2000; Fernández et al., 2013).

The detection of this dense organic chlorinated phase at the Sabiñanigo landfills was an important finding, not frequently described in other hot-sites polluted with lindane wastes. However, since a similar lindane manufacturing process was used everywhere, the presence of this DNAPL should be also expected in other sites close to lindane production points and should be more deeply investigated. The transport of this DNAPL to significant depths below ground level, due to its high density, is probably the cause of the lack of information about its occurrence in the subsurface of these hot-sites. Additionally, during the transport of this liquid organic phase through the subsurface, a significant adsorption or

trapping in the soil could occur and therefore the presence of this liquid, adsorbed or trapped in the organic phase of the soil pores, would justify the high levels of HCHs found in the groundwater at these hot-sites (Vijgen, 2006; Fernández et al., 2013; Fuscoletti et al., 2015; Vega et al., 2016).

Due to the low solubility of the Chlorinated Organic Compounds (COCs) that compose this organic phase, its presence supposes a significant risk to groundwater and nearby surface waters. Transport of COCs to the groundwater in contact with this organic phase (found as liquid pools or adsorbed/trapped in the soil) will depend on the solubility and partitioning behaviour of these COCs among the corresponding phases it comes into contact with (Xiao et al., 2004). Therefore, accurate and reliable solubility values and/or partitioning coefficients are a key factor for controlling their environmental distribution and consequences (Chiou et al., 2005; Nizzetto et al., 2011) and, are therefore, required for both the design of an effective remediation strategy and the evaluation of the risk of these COCs for human health and ecosystems.

However, there is little information about the solubility of COCs in an aqueous phase in contact with a DNAPL liquid mixture. Most of the studies on the solubility of COCs in the aqueous phase have been obtained from pure compounds (Xiao et al., 2004; Chiou et al., 2005; Nizzetto et al., 2011). However, the aqueous solubility of the COC as a pure species (often as a crystal phase) does not give a proper description of its behavior as a component of a liquid organic phase (Banerjee, 1984; Broholm and Feenstra, 1995; Jain and Yalkowsky, 2001; Yalkowsky and Wu, 2010).

Similarly, the solubility and partitioning of COCs between the soil and the aqueous phase has usually been studied by obtaining the equilibrium isotherms between the soil and this phase after the soil has been spiked with pure compounds (Duan et al., 2008; Macedo et al., 2015; Silvani et al., 2019). This procedure hardly describes the reality where a mix of COCs is historically sorbed or trapped in the soil.

One of the goals of this work is to evaluate the equilibrium of the aqueous phase in contact with seven liquid organic phases extracted from the Sardas and Bailin landfills (Sabiñanigo, Spain). Characterization and composition of six of these seven DNAPL samples was carried out elsewhere, finding that they were composed by 28 COCs (Santos et al., 2018a). Many of these compounds were not commercial and no information about their solubilities—even as pure compounds—was available in the literature. Also, the equilibrium of COCs between the aqueous phase and the soil obtained from a well drilled ad hoc in the Sardas landfill has been investigated here. While a DNAPL liquid phase was near this well, the results obtained in Milli-Q water will be compared with the composition of the groundwater extracted.

Moreover, one of the remediation strategies proposed for COCs abatement in soil and/or groundwater of the Sabiñanigo landfills is In Situ Chemical Oxidation, ISCO, using persulfate activated by alkali as an oxidant. Therefore, the effect of alkali addition on the change in composition of COCs in both soil and aqueous phases is a matter that requires investigation while dehydrochlorination reactions are produced due to the alkaline pH. To our knowledge, the solubility of COCs in an aqueous phase from liquid organic phases and contaminated soil caused by the lindane production waste has not been previously studied.

2. Materials and methods

2.1. Materials

2.1.1. DNAPLs samples

Seven DNAPL liquid samples have been used in this work. All of them have been obtained from the Sabiñanigo Landfills and kindly

provided by the company Emgrisa and the Aragon Government. One DNAPL sample was taken in a well located in the Bailin Landfill (well P55, named O1), and the other six were obtained in wells located at the Sardas landfill (wells S39G, S39I, S39F, PS15, PS23 and PD14D, called O2 to O7, respectively). The location of these wells on the site can be found in [Figures SI-1 and SI-2](#) of the Supplementary Material. Identification of COCs in samples O1 to O6 and their composition was described elsewhere ([Santos et al., 2018a](#)). Sample O7 was extracted from a new borehole drilled in April 2018 and has not been previously reported.

The seven DNAPLs used are summarized in [Tables SI-1](#) of the Supplementary Material. The well's identity, depth of the well and a photo DNAPL PS14D is included (similar to the other DNAPLs appearance). The DNAPL free phase is a black-brown liquid, with a strong smell. DNAPL samples were dissolved in 99% acetone (Sigma-Aldrich) at concentrations ranging from 20 to 25 g kg⁻¹. Then each solution was stored in a 20 mL glass vial closed with a PTFE cap. Vials had no free head space to prevent the evaporation of the most volatile compounds. COCs dissolved in acetone were analyzed by GC/MSD and GC/FID/ECD as indicated below.

2.1.2. Soil samples

The soil samples were obtained from a borehole drilled in April 2018 identified as PS14D in [Figure SI-3](#) (courtesy of the company Emgrisa, that drilled the borehole). As can be seen an anthropic fill was found from 0 to 4.8 m, a homogeneous silt layer from 4.40 to 12.50 m, a gravel-sand layer from 12.50 to 15.50 m and altered marl was identified under this gravel-sand layer. The DNAPL liquid phase obtained at this well PS14D, called O7 here, was located in the contact between the altered marls and the gravel-sand layer (then about 16.5 m below ground level).

The gravel-sand layer was permeable and the groundwater flow was in this layer. Soil samples from drilling core boxes, kindly provided by the company Emgrisa, were taken half-way down the gravel-sand layer (13.5–14.5 m) in order to avoid the presence of the free DNAPL phase. After drying at room temperature for 48 h the soil was sieved and the fraction with a particle diameter higher than 2 mm was rejected. Moreover, while the gravel-sand layer also contained some clay, the fraction with a diameter lower than 2 mm was sieved again to separate the fraction with particles less than 0.25 mm in diameter (called F fraction) from the soil particles that were larger than 0.25 mm (called G fraction).

One month after the borehole was drilled and the DNAPL phase was partially extracted groundwater samples were taken in well PS14D at 14.5 m b.g.l (therefore in the gravel-sand layer).

2.2. Solubility experiments

Solubility of COCS in DNAPL: A weighted mass of about 1 g of each DNAPL sample was in contact with 18.5 g of water in a cap sealed GC 20 mL vial without head space. The vial was sonicated for 15 min and kept at room temperature (23 °C ± 2 °C) for 48 h without agitation during this period to avoid microdroplets of the DNAPL in the aqueous phase. It was experimentally confirmed that equilibrium between organic and aqueous phase was obtained at times lower than 24 h while stable concentration of COCs in the aqueous phase were obtained at both 24 and 48 h. Then, 10 mL of the supernatant aqueous phase was taken with a syringe, filtered with a 0.1 µm nylon filter. It was confirmed that with this procedure the adsorption of COCs in the filter was negligible. Then, the filtered aqueous phase was extracted with hexane and immediately analyzed by GC/MS and GC/FID/ECD. The procedure was carried out in triplicate and differences were lower than 10%. In few cases (about 20% of the determinations) differences higher than 10% were obtained. These values were discarded and the vials were prepared

again.

Besides, it was experimentally confirmed that the equilibrium between the organic and the aqueous phase was obtained at times lower than 24 h after sonication while stable concentration of COCs in the aqueous phase were obtained at both 24 and 48 h.

Solubility of COCs from soil to the Aqueous Phase.

The experiments were carried out in batch mode by using 40 mL PTFE centrifuge tube with PTFE screw caps. In each centrifuge tube, 10 g of each fraction, F and G, of the polluted soil were treated with 30 mL of aqueous solution ($V_L/W_S = 3 \text{ mL g}^{-1}$). Head-Space was minimized by this procedure. The aqueous phase added was Milli-Q water (pH = 6.5) or Milli-Q water with 10 g/L of NaOH (pH > 12). Then, the tubes were stirred at room conditions (23 °C) with a Labolan rotary agitator (ref 51752) for 48 h. After this time, the aqueous and soil phases were separated by centrifugation. COCs in both aqueous and solid phases were extracted and analyzed by GC/MS and GC/FID/ECD. All experiments were performed in triplicate. Experimental error was less than 10%. It was experimentally confirmed that soil-water equilibrium was reached at 24 h of rotary agitation.

2.3. Analytical methods

2.3.1. Extraction of COCS from soil samples

In the case of soil samples, the 10 g of each soil fraction G (diameter from 2 to 0.25 mm) or F (diameter <0.25 mm) was mixed with anhydrous sodium sulfate and milled in a ceramic mortar. Subsequently, 25 ml of hexane/acetone mixture was added and the mixture was introduced in a microwave extraction device (Milestone Ethos One) following EPA method 3546. The temperature extraction program begins with an initial ramp of 15 min from room temperature to 110 °C, followed by a sustained temperature of 110 °C for 15 min, under a maximum power of 1000 W. Once the extraction program ends, approximately 15 ml of organic extraction phase were recovered from the supernatant, filtered with a 0.45 µm filter. The supernatant was analyzed by GC/MS and GC/FID/ECD. The extraction and analyses were carried out in triplicate.

2.3.2. Extraction of COCs from aqueous samples

A volume of 8 mL of aqueous phase was added to 2 mL of hexane in a GC 10 mL vial and sonicated for 10 min. The supernatant organic phase was taken and analyzed by GC/MS and GC/FID/ECD.

2.3.3. COCS analysis

The GC method used for COC identification and quantification in DNAPL organic phases has been described elsewhere ([Santos et al., 2018a](#)) and are summarized below:

GC/MSD analysis: COCs were identified by gas chromatography (Agilent 6890 N) coupled to a Mass Selective Detector (Agilent MSD 5975B), which operates under a vacuum. A HP-5MS column (30 m × 0.25 mm ID × 0.25 µm) was used for the COC analysis. A flow rate of 1.7 mL min⁻¹ of helium was used as carrier gas and 1 µL of liquid samples was injected. The GC injection port temperature was set to 250 °C and a programed temperature gradient was used for the GC oven, starting at 80 °C, increasing the temperature at a rate of 18 °C min⁻¹ up to 180 °C, and then keeping it constant for 15 min.

GC/ECD-FID analysis: The quantification of COCs was carried out using an Agilent 6890 gas chromatograph with both flame ionization detector (FID) and electron capture detector (ECD). An HP-5MS column (30 m × 0.25 mm ID × 0.25 µm) was also used and the Carrier gas was Helium (flow rate of 1.7 mL min⁻¹). The same temperature of the injector and GC oven as that indicated for GC/MS was used in this case. The output flow of the capillary column was split (1:1) using FID and ECD simultaneously. More details of

the procedure can be found elsewhere (Santos et al., 2018a).

3. Results

3.1. Solubility of DNAPL liquid samples in the aqueous phase

As described elsewhere (Santos et al., 2018a) the COCs identified in DNAPL liquid samples could explain about 95% of the mass of each DNAPL sample analyzed. The difference up to 100% could be attributed to the water content, to the presence of minor peaks from e.g. PCDD/Fs (Gómez-Lavín et al., 2018) or traces of tetrachlorocyclohexene isomers or to an error in the chromatographic response assigned to Pentaclorocyclohexenes (PentaCX) and Heptachlorocyclohexanes (HeptaCH) due to the same GC/FID response factor obtained for HCHs being assigned to these non-commercial compounds. Samples O1 to O7 were analyzed and mass percentages for COCs were determined. COC distribution (in weight) obtained in the analysis of samples O1 to O6 were very similar to that found elsewhere, with differences lower than 5%. Weight percentages for O1 to O7 samples are summarized in Tables SI–2 of the Supplementary Material. Values shown for O1 to O6 correspond to those obtained elsewhere (Santos et al., 2018a). Sample O7 (well PS14D), which has not been previously analyzed, has high trichlorobenzenes (TCBs) and tetrachlorobenzenes (TetraCBs) percentages, similar to those found in PS15 and PS23. This can be explained as PS14D, PS15 and PS23 were obtained in the same alluvial aquifer (Figure SI-1) and some alkaline dehydrochlorination of HCHs and HeptaCHs could take place producing TCBs and TetraCBs, respectively (Santos et al., 2018a, 2018b). From the weight percentages of each COC (%COC_{iw}) shown in Tables SI–2, the mole fraction of compound *j* in each DNAPL sample has been calculated as:

$$x_j = \frac{\frac{\%COC_{iw}}{M_j}}{\sum \frac{\%COC_{iw}}{M_j}} \quad (1)$$

Being *M_j* the molecular weight of the *j* compound. The values of *x_j* obtained are summarized in Table 1 for the seven DNAPL samples studied.

The liquid waste dumped in Sabiñanigo has been characterized elsewhere (Santos et al., 2018a) containing all the compounds summarized in Fig. 1, from chlorobenzene to heptachlorocyclohexane (HeptaCH), in agreement with reported in the literature for other wastes of the lindane production process (Wise et al., 1948; Bala et al., 2012; Fernández et al., 2013).

After the aqueous phase was equilibrated with each DNAPL sample, the concentration of each COC in this phase was determined. The results are shown in Tables SI–3 of the Supplementary Material. Due to the low mole fraction of 1,3,5 TCB; θ-PentaCX, β-PentaCX, HexaCX-b, HexaCX-c, HexaCX-d, β-HCH in all DNAPL liquid samples, the concentration of these compounds in the aqueous phase was very low and was reported as n. d. in this Tables SI–3. Moreover, the COCs measured in the groundwater extracted at well PS14D (14.5 m b.g.l) have also been included in Tables SI–3. The groundwater (GW) sample has a conductivity of 6039 μS/cm, a chloride content of 1382 mg L⁻¹ and bicarbonates of about 820 mg L⁻¹. In spite of the high conductivity of the GW, its COC composition is quite similar to that found in the Milli-Q water equilibrated with the O7 DNAPL sample, as can be seen in Tables SI–3, confirming the saturation of this groundwater with the closer DNAPL in well PS14D (O7).

The study of the equilibrium liquid-liquid (LLE) between the liquid organic phase (DNAPL) and the aqueous phase at room conditions has been accomplished using the approach of Banerjee

(1984) and Broholm et al. (Broholm and Feenstra, 1995). However, as these authors indicate, when a component in a mixture is solid (pure) and the mixture is a liquid, the difference in phase should be corrected to predict its solubility in the aqueous phase. To do this, the approach of sub-cooled liquid state of solid compounds has been applied (Jain and Yalkowsky, 2001; Yalkowsky and Wu, 2010; Schwarzenbach and Gschwend, 2016). In this way, when the equilibrium is reached, the aqueous concentration of each compound *j* present in the liquid organic phase can be predicted by the following expression:

$$C_j^{aq} = S_j \gamma_j^{DNAPL} x_j \frac{f_j^{liq}}{f_j^c} \quad (2)$$

being *C_j^{aq}* and *x_j* the concentration of the compound *j* in the aqueous phase in mg L⁻¹ (provided in Tables SI–3) and the molar fraction of the compound *j* in the DNAPL when equilibrium is reached, respectively. *S_j* is the pure-phase aqueous solubility in mg L⁻¹ of the *j* compound and *γ_j^{DNAPL}* the activity coefficient of the *j* compound in the organic phase. This *γ_j^{DNAPL}* can be assumed to be close to unity (Broholm and Feenstra, 1995). Moreover, for *x_j* in Eq. (2) the values shown in Table 1 can be used due to the ratio for mass of DNAPL to water volume used (as explained in the experimental section) is high enough to assume that the solubilized COCs in the aqueous phase yield a minor change in DNAPL composition.

The fugacity ratio of the pure compound at the right-side of Eq. (2) has been called *X_j^{ideal}*, shown in Eq. (3). It was defined in literature as the crystal/liquid solubility or fugacity ratio of a pure compound which is solid at T = 298 K and P = 1 atm (Jain and Yalkowsky, 2001; Yalkowsky and Wu, 2010):

$$X_j^{ideal} = \frac{f_j^c}{f_j^{liq}} \quad (3)$$

X_j^{ideal} is the unity when the compound *j* is liquid at 298 K and 1 atm (Smith et al., 2005). The value of the fugacity ratio can be estimated using the entropy of fusion at the melting point and the melting temperature at P = 1 atm (Yalkowsky and Wu, 2010).

$$\log_{10}(X_j^{ideal}) = \left(-\frac{\Delta S_m}{2.303 \cdot R} \cdot \frac{T_m - T}{T} \right) \quad (4)$$

Values of *ΔS_m* and *T_m* have been obtained from literature (Jain and Yalkowsky, 2001; Frenkel et al., 2005; Yalkowsky et al., 2016) being shown in Table 2. As can be seen in Table 2 this information is lacking for compounds as PentaCX, HexaCX, HeptaCH isomers. The value of *X_j^{ideal}* has been predicted by Eq. (4), and it is shown in Table 2.

Using the experimental values of *x_j* in Table 1 and *C_j^{aq}* in Tables SI–3, the product *S_jγ_j(X_j^{ideal})⁻¹* has been calculated for samples O1 to O6 by using Eq. (2). Results are shown in Table 2. Values of *S_jγ_j(X_j^{ideal})⁻¹* have also been calculated using the concentration of COCs in the GW extracted in PS14D and considering this GW in equilibrium with the organic sample O7. As can be seen in Table 2, similar values of *S_jγ_j(X_j^{ideal})⁻¹* for GW to those obtained with O7 in equilibrium with distilled water are acquired.

Besides, as can be seen in Table 2, close values of *S_jγ_j(X_j^{ideal})⁻¹* for each *j* compound have been obtained for samples O1 to O7 and for GW. Therefore, an average value of *S_jγ_j(X_j^{ideal})⁻¹* has been calculated for each specie *j*, as shown in Table 2.

If the activity coefficient is assumed to be the unity (*γ_j* = 1) the solubility *S_j* can be predicted by Eq. (5) and values obtained are shown in Table 2.

Table 1
COC Mole fraction (x_j) in each DNAPL liquid samples analyzed. Sum of COCs explain 95–97% of the DNAPL mass.

Sample			O1	O2	O3	O4	O5	O6	O7	
j Acronym	Name	CAS	M _j	BAILIN	SAR S39G	SAR S39I	SAR S39F	SAR PS15	SAR PS23	SAR PS14D
CB	chlorobenzene	108-90-7	112	0.215	0.253	0.231	0.249	0.198	0.223	0.187
1,3 DCB	1,3-dichlorobenzene	541-73-1	146	0.003	0.006	0.007	0.005	0.007	0.007	0.009
1,4 DCB	1,4-dichlorobenzene	106-46-7	146	0.033	0.055	0.077	0.056	0.083	0.071	0.080
1,2 DCB	1,2-dichlorobenzene	95-50-1	146	0.027	0.047	0.068	0.048	0.062	0.061	0.063
1,3,5 TCB	1,3,5-trichlorobenzene	108-70-3	180	0.000	0.000	0.001	0.000	0.002	0.003	0.002
1,2,4 TCB	1,2,4-trichlorobenzene	120-82-1	180	0.071	0.067	0.097	0.068	0.175	0.189	0.155
1,2,3 TCB	1,2,3-trichlorobenzene	87-61-6	180	0.006	0.009	0.013	0.009	0.031	0.026	0.024
TetraCB (1,2,4,5 + 1,2,3,5)	1,2,4,5–1,2,3,5 tetrachlorobenzene	95-94-3/634-90-2	214	0.015	0.012	0.013	0.013	0.059	0.055	0.053
TetraCB (1,2,3,4)	1,2,3,4 tetrachlorobenzene	634-66-2	214	0.026	0.004	0.014	0.004	0.077	0.083	0.074
γ-PentaCX	γ-pentachlorocyclohexene	342631-17-8	252	0.036	0.018	0.021	0.019	0.010	0.014	0.017
PentaCB	1,2,3,4,5 pentachlorobenzene	608-93-5	248	0.002	0.010	0.004	0.005	0.009	0.004	0.005
δ-PentaCX	δ-Pentachlorocyclohexene	643-15-2	252	0.031	0.015	0.015	0.015	0.012	0.020	0.016
θ-PentaCX	θ-Pentachlorocyclohexene	319-94-8	252	0.009	0.006	0.004	0.006	0.002	0.002	0.001
HexaCX-a	Hexachlorocyclohexene	1890-41-1	289	0.010	0.012	0.006	0.011	0.006	0.006	0.005
β-PentaCX	β-Pentachlorocyclohexene	319-94-8	252	0.007	0.005	0.004	0.005	0.002	0.002	0.002
η-Penta CX	η-Pentachlorocyclohexene	54083-24-8	252	0.039	0.020	0.009	0.018	0.006	0.004	0.001
HexaCX-b	Hexachlorocyclohexene	1890-41-1	286	0.011	0.004	0.002	0.003	0.001	0.002	0.002
HexaCX-c	Hexachlorocyclohexene	1890-41-1	286	0.006	0.007	0.005	0.006	0.004	0.003	0.005
α-HCH	α-hexachlorocyclohexane	319-84-6	291	0.035	0.038	0.031	0.036	0.026	0.024	0.029
HexaCX-d	Hexachlorocyclohexene	1890-41-1	286	0.016	0.002	0.001	0.003	0.001	0.000	0.000
β-HCH	β-hexachlorocyclohexane	319-85-7	291	0.000	0.000	0.000	0.000	0.000	0.001	0.000
γ-HCH	γ-hexachlorocyclohexane	58-89-9	291	0.112	0.114	0.104	0.113	0.078	0.080	0.095
HeptaCH-1	Heptachlorocyclohexane	707-55-1	322	0.108	0.102	0.097	0.110	0.052	0.039	0.072
δ-HCH	δ-hexachlorocyclohexane	319-86-8	291	0.085	0.100	0.090	0.098	0.042	0.041	0.051
ε-HCH	ε-hexachlorocyclohexane	6108-10-7	291	0.012	0.014	0.013	0.014	0.008	0.008	0.012
HeptaCH-2	Heptachlorocyclohexane	707-55-1	322	0.064	0.061	0.051	0.067	0.033	0.024	0.028
HeptaCH-3	Heptachlorocyclohexane	707-55-1	322	0.020	0.021	0.019	0.022	0.010	0.009	0.014

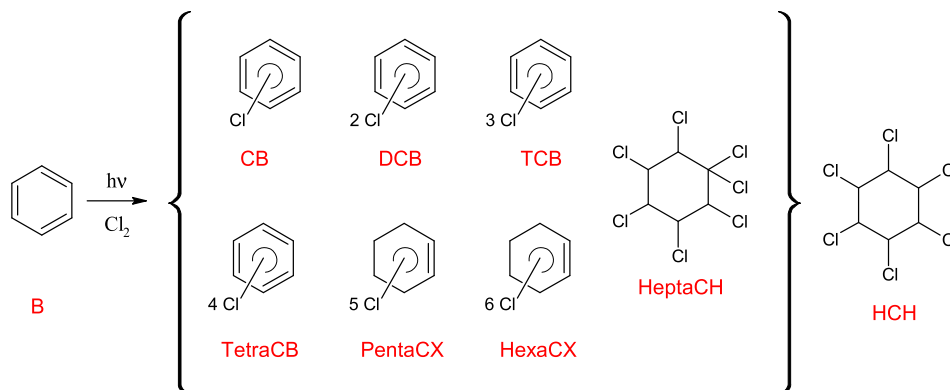


Fig. 1. Identified Chlorinated Organic Compounds in the chlorination of benzene to HCH.

$$S_j \text{ pred} = \frac{S_j \gamma_j (X_j^{\text{ideal}})^{-1}}{(X_j^{\text{ideal}})^{-1}} \quad (5)$$

The S_j values predicted with Eq. (5) have been compared with S_j values found literature (also shown in Table 2). As can be seen, a reasonable agreement has been obtained for most of the compounds which literature data is available. On the other hand, as can be seen in Table 2, there is no bibliographic data for solubility of compounds such as PentaCx, HexaCX, HeptaCH isomers. The Advanced Chemistry Development (ACD/Labs) Software V11.02 (© 1994–2019 ACD/Labs) coupled with SciFinder (educational license) was used to estimate the solubility of the latter compounds whose experimental values are not available in literature. As can be seen in Table 2, the software provides the same value for all the stereoisomers of PentaCX, HexaCX and HeptaCH. To check the reliability of the values estimated by the software, the estimated values of

solubility and the experimental values of those compounds that are found in literature are compared in Table 2. The software provides different solubility values for positional isomers of DCB, TCB and TetraCB, and the same value for the stereoisomers of HCH. In addition, the estimated values and the experimental determinations are often different. In spite of this disparity, the solubility values estimated by the software gives an adequate order of magnitude of the solubility values of the chlorinated compounds.

3.2. Solubility of COC in aqueous phase from contaminated soil

The soil obtained from 13.5 to 14.5 m b.g.l. at PS14D (Figure SI-3) was dried and sieved as explained in the experimental section. The fraction lower than 0.25 mm (F) was 31.2% of the soil with size lower than 2 mm. Therefore, the G fraction, with particle sizes between 2 and 0.25 mm, was 68.8% of the soil lower than 2 mm. During the drying and sieving procedure, the most volatile chlorinated compounds were lost. The composition in COCs of each

Table 2
Product $S_j \gamma_j (X_j^{ideal})^{-1}$ for each j compound, T_m , ΔS_{mv} , X_j^{ideal} and literature and predicted solubilities of pure compounds at $T = 298\text{ K}$ and $P = 1\text{ atm}$.

	$S_j \gamma_j (X_j^{ideal})^{-1}$ (mg L^{-1})									Appearance	T_m (+) °C	ΔS_{mv} (+) J/mol/K	$\frac{1}{X_j^{ideal}}$ Eq	S_{jpred} Eq(5) mg L^{-1}	S_j Literature ^a estimated mg L^{-1} <	Literature S_j
	O1	O2	O3	O4	O5	O6	O7	GW	Average							
CB	390.1	424.6	426.3	446.4	436.0	486.5	404	404.0	428.4	L			1	428.4	472-502/86	(Banerjee, 1984; Chiou et al., 2005; Tsai and Chen, 2007)
1,3 DCB	120.0	155.0	114.1	193.3	159.8	142.6	95.0	79.8	140.0	L			1	140	125-143/160	(Banerjee, 1984; Chiou et al., 2005; Tsai and Chen, 2007)
1,4 DCB	98.9	120.0	113.2	117.9	141.3	114.4	108.5	86.7	116.3	S	52.99	55.78	1.88	61.94	65-81.3/180	(Banerjee, 1984; Chiou et al., 2005; Tsai and Chen, 2007)
1,2 DCB	88.9	132.3	116.6	129.7	144.1	123.7	111.6	82.3	121.0	L			1	121	137-156/180	(Banerjee, 1984; Chiou et al., 2005; Tsai and Chen, 2007)
1,3,5 TCB	n.q.	n.q.	n.q.	n.q.	n.q.	n.q.	n.q.	n.q.	n.q.	S	63.5	55.82	2.38	8.97	6/3.4	(Banerjee, 1984; Yakata et al., 2006; Tsai and Chen, 2007)
1,2,4 TCB	39.5	35.7	29.4	35.2	40.1	29.3	27.8	27.7	33.9	L			1	33.9	31-49/3.6	(Banerjee, 1984; Chiou et al., 2005; Tsai and Chen, 2007)
1,2,3 TCB	34.2	42.4	32.4	40.7	45.9	31.9	29.4	21.8	36.7	S	52.5	56.78	1.88	19.54	16.3-18/3.8	(Banerjee, 1984; Chiou et al., 2005; Tsai and Chen, 2007)
TetraCB (1,2,4,5 + 1,2,3,5)	16.5	13.9	9.0	11.3	11.9	9.1	8.7	12.0	11.5	S	50.67	57.37	1.81	6.34	0.3-0.56 and 3.4/0.82 and 0.80	(Banerjee, 1984; Chiou et al., 2005; Tsai and Chen, 2007)
TetraCB (1,2,3,4)	15.4	14.0	13.6	13.0	12.5	7.8	7.5	7.3	12.0	S	46.65	53.06	1.59	7.53	3.4-5.92/0.84	(Banerjee, 1984; Chiou et al., 2005; Tsai and Chen, 2007)
γ -PentaCX	78.0	121.6	126.8	130.2	64.1	101.3	54.2	37.0	96.6	S					- ^a 7.6	
PentaCB	8.0	10.0	6.0	9.0	4.4	9.0	7.6	12.1	7.7	S	84.12	56.79	3.88	1.99	0.32-0.4/0.20	(Chiou et al., 2005; Yakata et al., 2006)
δ -PentaCX	92.7	98.2	90.2	94.1	62.4	75.3	79.6	33.7	84.7	S					-7.6	
θ -PentaCX	n.q.	n.q.	n.q.	n.q.	n.q.	n.q.	n.q.	21.6	n.q.	S					-7.6	
HexaCX-a	12.5	15.7	9.4	12.8	5.4	10.9	12.0	27.8	11.2	S					-2.4	
β -PentaCX	n.q.	n.q.	n.q.	n.q.	n.q.	n.q.	n.q.	n.q.	n.q.	S					-7.6	
η -PentaCX	38.8	42.1	36.3	47.9	38.3	40.5	60.9		43.6	S					-7.6	
HexaCX-b	n.q.	n.q.	n.q.	n.q.	n.q.	n.q.	n.q.	24.0	n.q.	S					-2.4	
HexaCX-c	n.q.	n.q.	n.q.	n.q.	n.q.	n.q.	n.q.	n.q.	n.q.	S					-2.4	
α -HCH	34.2	35.3	34.5	38.4	40.1	35.3	36.9	35.3	36.4	S	157.42	62.45	28.14	1.29	1.2-2/7.9	(Shiu et al., 1990; Health and Services, 1993; Xiao et al., 2004; Ke et al., 2007)
HexaCX-d	n.q.	n.q.	n.q.	n.q.	n.q.	n.q.	n.q.	n.q.	n.q.	S					-2.4	
β -HCH	n.q.	n.q.	n.q.	n.q.	n.q.	n.q.	n.q.	n.q.	n.q.	S	309.0			n.q.	0.15-0.7/7.9	(Shiu et al., 1990; Xiao et al., 2004; Ke et al., 2007)
γ -HCH	43.0	45.1	45.9	48.1	52.4	54.3	45.4	39.3	47.7	S	114.85	43.18	4.79	9.98	2.1-15.3/7.9	(Shiu et al., 1990; Health and Services, 1993; Xiao et al., 2004)
HeptaCH-1	19.4	21.2	14.6	17.8	8.1	16.9	8.9	14.7	15.3	S					-2.8	
δ -HCH	96.2	70.9	84.2	72.7	90.0	97.4	85.6	82.7	85.3	S	136.97	51.81	10.39	8.21	8.6-31/7.9	(Weil et al., 1974; Shiu et al., 1990; Health and Services, 1993; Ke et al., 2007)
ϵ -HCH	77.0	52.9	71.3	68.7	69.4	68.2	69.8	40.3	68.2	S	218.5				-7.9	
HeptaCH-2	10.9	14.2	9.1	11.1	7.9	11.3	10.9	9.3	10.8	S					-2.8	
HeptaCH-3	24.8	29.2	27.0	26.4	18.6	25.1	19.0	25.8	24.3	S					-2.8	

(-) Appearance at 25 °C of pure COC: L = liquid S = Solid crystal.

(+) (Jain and Yalkowsky, 2001; Frenkel et al., 2005; Yalkowsky et al., 2016).

n.q.: non-quantifiable.

^a Estimated solubility values using the Advanced Chemistry Development (ACD/Labs) Software V11.02 (© 1994-2019 ACD/Labs).

fraction F and G after drying and sieving is summarized in Table 3. As can be seen in Table 3 the most volatile COCs in the soil such as CB, DCBs are found in low concentration, due to their loss by vaporization during drying and sieving. Besides, at neutral pH, the content in TCBs is also low. In spite of the loss of the volatile compounds, the COCs content in the F soil fraction is quite high (34.57 mmol/kg that correspond to 9946 mg/kg of total COCs) and higher than the concentration found in the G fraction (11.53 mmol/kg that correspond to 3193 mg/kg of total COCs). The differences in the COC content of both soil fractions can be explained by the lower particle size of the F fraction. It is widely documented in literature that soil is comprised of various particle size fractions and most often, the contaminants are concentrated in the fraction corresponding to finer silts and clays. The higher adsorption of contaminants in the fine fraction is explained by the increased surface area, cationic exchange potential, and the innate shape of these particles. (Anderson et al., 1999).

Due to the high content of both carbonates in soil (>40% in weight in dry soil) and bicarbonates in the groundwater (820 mg L⁻¹) of the landfills (Fernández et al., 2013) and the nature of the pollutants, the persulfate activated by alkali seems to be the most reliable treatment for the groundwater of the site (Santos et al., 2018b). This can be achieved by injecting an alkali (NaOH aqueous solution) into the subsurface to reach a pH value about 10–12. Then, alkali and oxidant will be simultaneously injected. When the alkali is injected, a dehydrochlorination reaction can take place. It has been previously described that HCHs and PentaCXs are transformed into TCBs and HexaCXs and HeptaCHs are transformed to TetraCBs (Santos et al., 2018a, 2018b) as shown in Fig. 2.

However, the occurrence and distribution of TCBs and TetraCBs during these transformations in the soil phase has not been reported previously. After the alkaline treatment of F and G soil fractions –as described in the experimental section- COCs concentration in soil was analyzed and values obtained are shown in Table 3. For the scope of an easier analysis of the effect of alkali addition on the transformation of COCs in soil the concentration of

COCs is shown as mmol kg soil⁻¹. As can be seen in Table 3, 48 h after the soil has been kept at alkaline conditions (pH > 12) the PentaCX, HexaCX, HCHs and HeptaCHs have almost disappeared. On the contrary, the concentrations of TCBs and TetraCBs in the soil have significantly increased after the alkaline treatment, as predicted by reactions in Fig. 2.

An example of the GC chromatograms of the COCs extracted from the F soil before and after the addition of alkali is shown in Figure SI-4 a and SI-5 (ECD and FID detectors, respectively). This change can be explained by the dehydrochlorination reaction proposed elsewhere (Santos et al., 2018a) and summarized in Fig. 2. As these reactions do not involve a change of moles, the sum of mmol of COC per kg of soil is expected to remain constant before and after the alkaline treatment. This complies with the experimental values of total COCs as mmol kg_{soil}⁻¹ obtained and summarized in Table 3, for both F and G fractions.

For each soil fraction, the mole fraction of a compound of the *j* compound in the sum of COCs before and after addition of the alkali has been calculated by Eq (1) and the values obtained are shown in Figure SI-6 (pH 7) and SI-7 (pH 12).

The moles of HCHs and PentaCX that have disappeared from the soil after alkali addition are called Δ HCHs + PentaCX (mmol kg soil⁻¹). The moles of TCBs generated when pH changes from neutral to alkaline conditions is called Δ TCBs (mmol kg soil⁻¹).

The moles of HeptaCHs and HexaCXs that have disappeared from the soil after alkali addition are called Δ HexaCX + HeptaCHs (mmol kg soil⁻¹). The moles of TetraCBs generated when pH changes from neutral to alkaline conditions is called Δ TetraCBs (mmol kg soil⁻¹). From data in Table 3, the redistribution of COCs in soil due to the pH change is summarized in Fig. 3 and Tables SI–4. As can be seen, the balance of moles between the disappearing Δ HCHs + PentaCX and appearing Δ TCBs and between the disappearing Δ HexaCX + HeptaCHs and generated Δ TetraCBs matches quite well. The ΔTCBs produced are distributed among isomers 1,3,5; 1,2,4 and 1,2,3 and the ΔTetraCBs generated are distributed between TetraCBs a (1,2,4,5 + 1,2,3,5) and TetraCBs b

Table 3
Composition of COCs in soil (mmol j kg_{soil}⁻¹), fractions F (size < 0.25 mm) and G (size between 2 and 0.25 mm), at neutral and alkaline conditions.

Compound (mmol/kg soil)	M _j	F soil fraction pH 7	F soil fraction pH > 12	G soil fraction pH 7	G soil fraction pH > 12
CB	112	0.001	0.00	0.004	0.00
1,3 DCB	146	0.007	0.02	0.002	0.02
1,4 DCB	146	0.024	0.05	0.013	0.01
1,2 DCB	146	0.030	0.12	0.032	0.05
1,3,5 TCB	180	0.016	0.50	0.008	0.16
1,2,4 TCB	180	0.414	19.72	0.156	5.87
1,2,3 TCB	180	0.112	3.22	0.051	0.89
TetraCB (1,2,4,5 + 1,2,3,5)	214	0.673	3.40	0.383	1.46
TetraCB (1,2,3,4)	214	1.335	6.16	0.682	2.70
γ-PentaCX	252	0.777		0.463	
PentaCB	248	0.127	0.18	0.068	0.08
δ-PentaCX	252	0.822		0.447	
θ-PentaCX	252	0.065		0.028	
HexaCX-a	289	0.228		0.116	
β-PentaCX	252	0.126		0.065	
η-Penta CX	252	0.059		0.027	
HexaCX-b	286	0.100		0.036	
HexaCX-c	286	0.339		0.151	
α-HCH	291	2.672		0.851	
HexaCX-d	286	0.000		0.002	
β-HCH	291	0.057		0.013	
γ-HCH	291	14.930		3.288	
HeptaCH-1	322	3.747		1.291	
δ-HCH	291	4.328		1.303	
ε-HCH	291	1.168		0.444	
HeptaCH-2	322	1.640		0.583	
HeptaCH-3	322	0.771		0.291	
Total mmol/kg		33.568	33.38	11.158	11.25

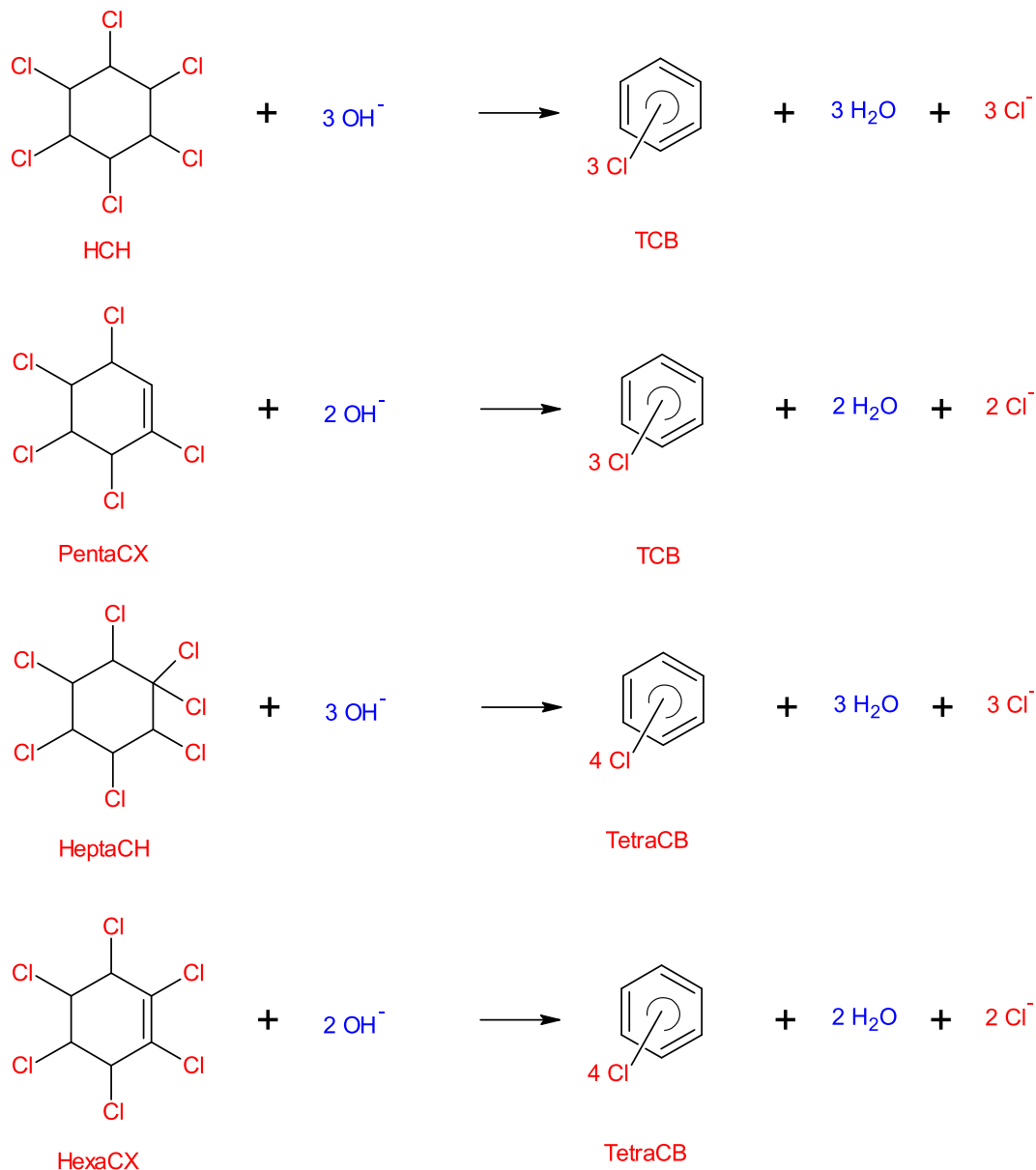


Fig. 2. Dehydrochlorination reactions at alkaline pH.

(1,2,3,4). The percentage of the Δ TCBs and Δ TetraCBs going to each isomer is also summarized in Fig. 3. As can be seen, the most favored isomer is 1,2,4 TCB (about 85% in both F and G fractions), followed by 1,2,3 TCB (13%) and finally 1,3,5 TCB (2%). The transformation to TetraCBs is favored towards 1,2,3,4 TCB (about 65%) while the sum of isomers 1,2,3,5 and 1,2,4,5 explains the 35% of the TetraCBs generated by dehydrochlorination reactions in alkaline conditions.

It should be noted that dehydrochlorination reactions take place in the soil in up to 48 h after the pH is changed from neutral to alkaline conditions (pH about 12) and that the COCs generated are much less toxic than the parent compounds (Willett et al., 1998; Tsai and Chen, 2007; Tsaboula et al., 2016). As an example, the available data on persistence of 1,2,4-trichlorobenzene, obtained from dehydrochlorination of HCHs, indicates a half-life in water of a few days and a significant biodegradation potential (van Wijk et al., 2006). Therefore, despite other treatments could be applied for soil and groundwater remediation (ISCO, S-ISCO, ISCR, etc.) the change

from neutral to alkaline pH alone could be considered a positive accomplishment from an environmental point of view.

The concentration of COCs in the aqueous phase in equilibrium with F and G fractions at neutral or alkaline pH is shown in Tables SI-4.

With data in Table 3 and Tables SI-4, the linear partition coefficient in soil-water has been calculated, defined by Eq (6), and used in some works in the literature (Djohan et al., 2005)

$$K_D = \frac{C_{js} \left(\frac{\text{mg}}{\text{kg soil}} \right)}{C_{jaq} \left(\frac{\text{mg}}{\text{L}} \right)} \quad (6)$$

Being C_{js} and C_{jaq} the concentration of j compound in soil and aqueous phase, respectively. Calculated values of K_D are also summarized in Tables SI-4. The differences in K_D between F and G soil fractions indicates that a constant linear partition coefficient soil-water cannot be used for both soil fractions.

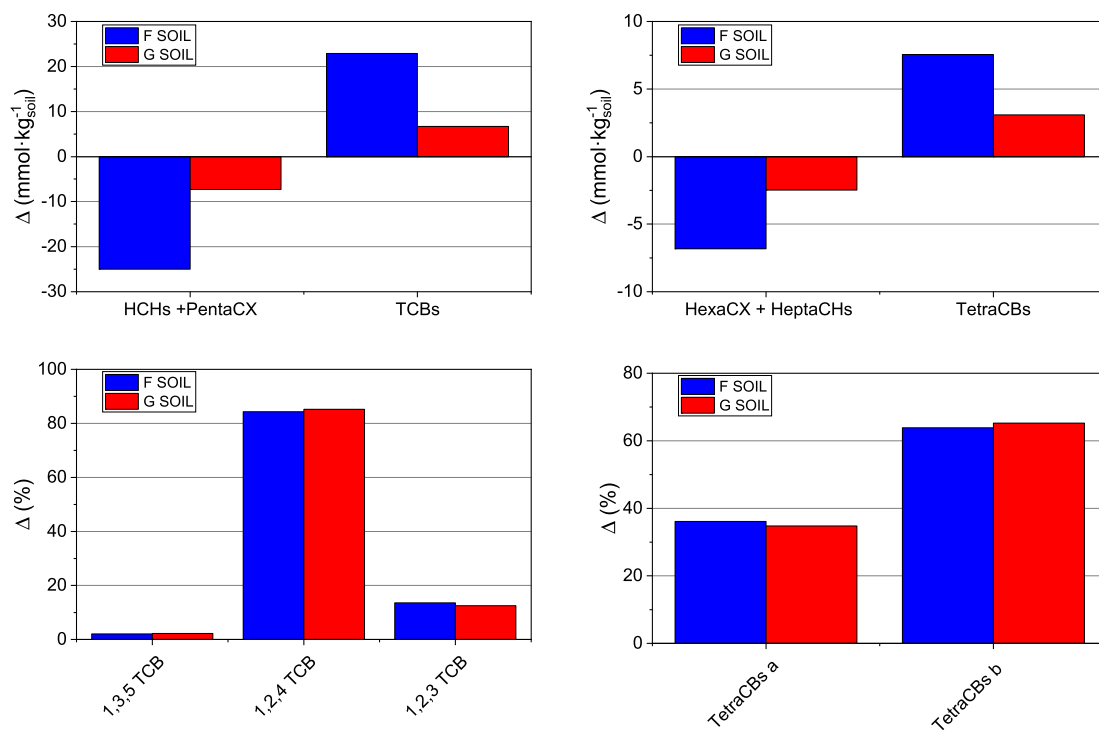


Fig. 3. Transformation of COCs in soil (fraction F and G) by dehydrochlorination reactions from neutral to alkaline pH (TetraCBs a: 1,2,4,5 + 1,2,3,5 isomers, TetraCBs b: 1,2,3,4 isomer).

To predict the solubility of each COC in the mixture of COCs in the soil, this mix has been considered as a DNAPL phase and Eq (2) has been used to calculate the $S_j\gamma_j(X_j^{ideal})^{-1}$ product of each compound for each soil fraction and pH, using the corresponding mole fraction of j , x_j , shown in Table 3 (pH = 7 and pH > 12) and the corresponding concentration of j in the aqueous phase given in

Tables SI–4.

Results are shown in Table 4. For the scope of comparison, the values of average $S_j\gamma_j(X_j^{ideal})^{-1}$ in Table 2, calculated for each compound when the aqueous phase was in equilibrium with the organic liquid phase, are also summarized in Table 4. As can be seen the values obtained for $S_j\gamma_j(X_j^{ideal})^{-1}$ after the equilibrium between

Table 4

Product $S_j\gamma_j(X_j^{ideal})^{-1}$ (mg L⁻¹) for the compounds present in soil, fractions F and G, at neutral and alkaline pH.

Compound	F soil fraction pH 7	G soil fraction pH 7	F soil fraction pH > 12	G soil fraction pH > 12	Average exptal from DNAPL liquid, Table 2
CB	nd	nd	nd	nd	428.4
1,3 DCB	nd	nd	nd	nd	140.0
1,4 DCB	nd	nd	nd	nd	116.3
1,2 DCB	nd	nd	nd	nd	121.0
1,3,5 TCB	nd	nd	9.42	7.04	n.q.
1,2,4 TCB	33.78	29.05	11.82	11.59	33.9
1,2,3 TCB	41.66	28.69	13.21	13.78	36.7
TetraCB (1,2,4,5 + 1,2,3,5)	14.38	8.15	2.75	2.70	11.5
TetraCB (1,2,3,4)	15.28	10.88	2.66	2.54	12.0
γ-PentaCX	58.98	29.54			96.6
PentaCB	8.14	4.93	1.51	1.34	7.7
δ-PentaCX	152.87	86.55			84.7
θ-PentaCX	155.98	95.22			n.q.
HexaCX-a	31.08	21.72			11.2
β-PentaCX	137.16	67.95			n.q.
η-Penta CX	120.50	68.53			43.6
HexaCX-b	39.94	32.52			
HexaCX-c	62.28	41.99			
α-HCH	39.65	38.21			36.4
HexaCX-d	nd	nd			
β-HCH	0.00	0.00			
γ-HCH	15.94	20.83			47.7
HeptaCH-1	25.60	21.57			15.3
δ-HCH	124.35	112.58			85.3
ε-HCH	77.12	60.83			68.2
HeptaCH-2	28.87	22.98			10.8
HeptaCH-3	59.17	49.07			24.3

the soil and the aqueous phase is reached at neutral pH are quite similar to those obtained at the equilibrium of a DNAPL liquid organic phase with an aqueous phase at neutral pH (Table 2). This could be explained if the COC mixture in the soil behaves as a DNAPL phase. Therefore, the solubility in the soil-water equilibrium could be predicted by Eq (5) using the same $S_j \gamma_j (X_j^{ideal})^{-1}$ values shown in Table 2.

Furthermore, in strong enough alkaline conditions (pH about 12), the $S_j \gamma_j (X_j^{ideal})^{-1}$ of the COCs is lower than the value obtained at neutral pH (Table 4). This means that lower concentration of the COC is expected in the aqueous phase, for the same mole fractions of COCs in soil. In fact, as it can be deduced from Table 3, the sum of COCs in the aqueous phase in alkaline conditions is about 1/3 of the sum of COCs at neutral pH, in addition to the lower toxicity of the compounds present in alkaline conditions.

4. Conclusions

The fate of Dense Non-Aqueous Phase Liquids, DNAPLs, in the environment strongly depends on their solubility in water. The partitioning behavior in water of pollutants in DNAPL phases present at Sabiñanigo landfills, Spain, has been studied here for the first time. This DNAPL was a liquid waste obtained in the lindane production in a factory nearby. About 28 Chlorinated Organic Compounds, COCs, from chlorobenzene to heptachlorocyclohexane were identified. Among these 20 are solid crystals as pure-phases.

The approach of Banerjee (1984) and Broholm et al. (Broholm and Feenstra, 1995) considering the sub-cooled liquid state of solid compounds (Jain and Yalkowsky, 2001; Yalkowsky and Wu, 2010) has been successfully applied to predict the solubility of the organochlorines in aqueous phase. However, for compounds as pentachlorocyclohexene, hexachlorocyclohexene and heptachlorocyclohexane isomers, which constitute 20–45% in weight of the DNAPL organic phase, neither the solubility nor other data as the entropy of fusion at the melting point and the melting temperature at $P = 1 \text{ atm}$ are available in literature. Therefore, their solubility as pure compounds has not been calculated but the product $S_j \gamma_j (X_j^{ideal})^{-1}$ has been obtained. This value would allow to predict the concentration in the aqueous phase from the composition of the organic phase, when both phases are in equilibrium.

The solubility values obtained at neutral pH were similar for both DNAPL as free liquid phase or for DNAPL trapped into the soil. Moreover, it was found in this work that alkaline condition promotes dehydrochlorination of PentaCX, HexaCX, HCHs and Hep-taCHs in soil to pollutants with lower toxicity in less than 48 h. Moreover, a decrease of the solubility of the dehydrochlorination products in alkaline conditions was found.

Acknowledgements

This work was supported by Regional Government of Madrid, project CARESOIL (S2018/EMT-4317), from the Spanish Ministry of Economy, Industry and Competitiveness, projects CTM2016-77151-C2-1-R and for the European Union Life Program (LIFE17 ENV/ES/000260). The authors thank the Department of Agriculture, Live-stock and Environment, Government of Aragon, Spain, as well as EMGRISA for their support during this work.

Appendix A. Supplementary data

Supplementary data to this article can be found online at <https://doi.org/10.1016/j.chemosphere.2019.124798>.

References

- Anderson, R., Rasor, E., Van Ryn, F., 1999. Particle size separation via soil washing to obtain volume reduction. *J. Hazard Mater.* 66, 89–98.
- Bala, K., Geueke, B., Miska, M.E., Rentsch, D., Poiger, T., Dadhwal, M., Lal, R., Holliger, C., Kohler, H.-P.E., 2012. Enzymatic conversion of ϵ -hexachlorocyclohexane and a heptachlorocyclohexane isomer, two neglected components of technical hexachlorocyclohexane. *Environ. Sci. Technol.* 46, 4051–4058.
- Banerjee, S., 1984. Solubility OF organic mixtures IN water. *Environ. Sci. Technol.* 18, 587–591.
- Broholm, K., Feenstra, S., 1995. Laboratory measurements OF the aqueous solubility OF mixtures OF chlorinated solvents. *Environ. Toxicol. Chem.* 14, 9–15.
- Casado, I., Mahjoub, H., Lovera, R., Fernandez, J., Casas, A., 2015. Use of electrical tomography methods to determinate the extension and main migration routes of uncontrolled landfill leachates in fractured areas. *Sci. Total Environ.* 506, 546–553.
- Chiou, C.T., Schmedding, D.W., Manes, M., 2005. Improved prediction of octanol-water partition coefficients from liquid-solute water solubilities and molar volumes. *Environ. Sci. Technol.* 39, 8840–8846.
- Cuozzo, S.A., Sineli, P.E., Costa, J.D., Tortella, G., 2018. *Streptomyces* sp is a powerful biotechnological tool for the biodegradation of HCH isomers: biochemical and molecular basis. *Crit. Rev. Biotechnol.* 38, 719–728.
- Djohan, D., Yu, Q., Connell, D.W., 2005. Partition isotherms of chlorobenzenes in a sediment-water system, pp. 157–173. Dec 161.
- Dorsey, A., 2005. Toxicological Profile for Alpha-, Beta-, Gamma, and Delta-hexachlorocyclohexane. Agency for Toxic Substances and Disease Registry.
- Duan, L., Zhang, N., Wang, Y., Zhang, C.D., Zhu, L.Y., Chen, W., 2008. Release of hexachlorocyclohexanes from historically and freshly contaminated soils in China: implications for fate and regulation. *Environ. Pollut.* 156, 753–759.
- Fernández, J., Arjol, M., Cachó, C., 2013. POP-contaminated sites from HCH production in Sabiñanigo, Spain. *Environ. Sci. Pollut. Control Ser.* 20, 1937–1950.
- Frenkel, M., Chirico, R.D., Diky, V., Yan, X., Dong, Q., Muzny, C., 2005. ThermoData Engine (TDE): software implementation of the dynamic data evaluation concept. *J. Chem. Inf. Model.* 45, 816–838.
- Fuscoletti, V., Achene, L., Gismondì, F., Lamarra, D., Lucentini, L., Spina, S., Veschetti, E., Turrio-Baldassarri, L., 2015. Presence of epsilon HCH together with four other HCH isomers in drinking water, groundwater and soil in a former lindane production site. *Bull. Environ. Contam. Toxicol.* 95, 108–115.
- Gómez-Lavín, S., San Román, M.F., Ortiz, I., Fernández, J., de Miguel, P., Urtiaga, A., 2018. Dioxins and furans legacy of lindane manufacture in Sabiñanigo (Spain). The Bailín landfill site case study. *Sci. Total Environ.* 624, 955–962.
- Jain, N., Yalkowsky, S.H., 2001. Estimation of the aqueous solubility I: application to organic nonelectrolytes. *J. Pharm. Sci.* 90, 234–252.
- Karlaganis, G., Marioni, R., Sieber, I., Weber, A., 2001. The elaboration of the 'Stockholm Convention' on persistent organic pollutants (POPs): a negotiation process fraught with obstacles and opportunities. *Environ. Sci. Pollut. Control Ser.* 8, 216–221.
- Ke, R., Wang, Z., Huang, S., Khan, S.U., 2007. Accurate quantification of freely dissolved organochlorine pesticides in water in the presence of dissolved organic matter using triolein-embedded cellulose acetate membrane. *Anal. Bioanal. Chem.* 387, 2871–2879.
- Kumar, R., Mukherji, S., 2018. Threat posed by persistent organochlorine pesticides and their mobility in the environment. *Curr. Org. Chem.* 22, 954–972.
- Lallas, P.L., 2001. The Stockholm Convention on persistent organic pollutants. *Am. J. Int. Law* 95, 692–708.
- Li, Z.J., Jennings, A., 2017. Worldwide regulations of standard values of pesticides for human health risk control: a review. *Int. J. Environ. Res. Public Health* 14.
- Macedo, L.D., Maneo, F.P., Mondelli, G., 2015. Batch test methodology applied at a site contaminated with hexachlorocyclohexane. *Environ. Geotechnics* 2, 371–381.
- Madaj, R., Sobiecka, E., Kalinowska, H., 2018. Lindane, kepone and pentachlorobenzene: chloropesticides banned by Stockholm convention. *Int. J. Environ. Sci. Technol.* 15, 471–480.
- Navarro, J.S., López, C., García, A.P., 2000. Characterization of groundwater flow in the Bailín hazardous waste-disposal site (Huesca, Spain). *Environ. Geol.* 40, 216–222.
- Nizzetto, L., Gioia, R., Galea, C.L., Dachs, J., Jones, K.C., 2011. Novel system for controlled investigation of environmental partitioning of hydrophobic compounds in water. *Environ. Sci. Technol.* 45, 7834–7840.
- Pawłowicz, E.T., 2017. Organic pollution OF water and human health. *Health Probl. Civiliz.* 11, 32–39.
- Pinto, M.I., Burrows, H.D., Sontag, G., Vale, C., Noronha, J.P., 2016. Priority pesticides in sediments of European coastal lagoons: a review. *Mar. Pollut. Bull.* 112, 6–16.
- Pirsaheb, M., Hossini, H., Asadi, F., Janjani, H., 2017. A systematic review on organochlorine and organophosphorus pesticides content in water resources. *Toxin Rev.* 36, 210–221.
- Ren, X.Y., Zeng, G.M., Tang, L., Wang, J.J., Wan, J., Liu, Y.N., Yu, J.F., Yi, H., Ye, S.J., Deng, R., 2018. Sorption, transport and biodegradation - an insight into bioavailability of persistent organic pollutants in soil. *Sci. Total Environ.* 610, 1154–1163.
- Santos, A., Fernandez, J., Guadaño, J., Lorenzo, D., Romero, A., 2018a. Chlorinated organic compounds in liquid wastes (DNAPL) from lindane production dumped in landfills in Sabiñanigo (Spain). *Environ. Pollut.* 242, 1616–1624.

- Santos, A., Fernandez, J., Rodriguez, S., Dominguez, C.M., Lominchar, M.A., Lorenzo, D., Romero, A., 2018b. Abatement of chlorinated compounds in groundwater contaminated by HCH wastes using ISCO with alkali activated persulfate. *Sci. Total Environ.* 615, 1070–1077.
- Schwarzenbach, R.P., Gschwend, P.M., 2016. *Environmental Organic Chemistry*. John Wiley & Sons.
- US Department of Health and Human Services, 1993. Hazardous Substances Data Bank (HSDB, Online Database). J National Toxicology Information Program. National Library of Medicine. Bethesda, MD.
- Shiu, W.Y., Ma, K.C., Mackay, D., Seiber, J.N., Wauchope, R.D., 1990. Solubilities OF pesticide chemicals IN water .2. Data compilation. *Rev. Environ. Contam. Toxicol.* 116, 15–187.
- Silvani, L., Cornelissena, G., Halea, S.E., 2019. Sorption of alpha-, beta-, gamma- and delta-hexachlorocyclohexane isomers to three widely different biochars: sorption mechanisms and application. *Chemosphere* 219, 1044–1051.
- Smith, J.M., Van Ness, H.C., Abbott, M., 2005. *Introduction to Chemical Engineering Thermodynamics*. McGraw-Hill Education.
- Tsaboula, A., Papadakis, E.-N., Vryzas, Z., Kotopoulou, A., Kintzikoglou, K., Papadopoulou-Mourkidou, E., 2016. Environmental and human risk hierarchy of pesticides: a prioritization method, based on monitoring, hazard assessment and environmental fate. *Environ. Int.* 91, 78–93.
- Tsai, K.-P., Chen, C.-Y., 2007. An algal toxicity database of organic toxicants derived by a closed-system technique. *Environ. Toxicol. Chem.* 26, 1931–1939.
- van Wijk, D., Cohet, E., Gard, A., Caspers, N., van Ginkel, C., Thompson, R., de Rooij, C., Garny, V., Lecloux, A., 2006. 1,2,4-Trichlorobenzene marine risk assessment with special emphasis on the Osparcom region North Sea. *Chemosphere* 62, 1294–1310.
- Vega, M., Romano, D., Utila, E., 2016. Lindane (Persistent Organic Pollutant) in the EU. European Parliament, Brussels [Visited: 06/06/2019]. Study for the PETI Committee (PE 571.398). Available in: [http://www.europarl.europa.eu/RegData/etudes/STUD/2016/571398/IPOL_STU\(2016\)571398_EN.pdf](http://www.europarl.europa.eu/RegData/etudes/STUD/2016/571398/IPOL_STU(2016)571398_EN.pdf). European Parliament. B-1047 Brussels.
- Vijgen, J., 2006. The legacy of lindane HCH isomer production. Main report. IHPA 383, 384. January.
- Vijgen, J., Abhilash, P., Li, Y.F., Lal, R., Forter, M., Torres, J., Singh, N., Yunus, M., Tian, C., Schäffer, A., 2011. Hexachlorocyclohexane (HCH) as new Stockholm Convention POPs—a global perspective on the management of Lindane and its waste isomers. *Environ. Sci. Pollut. Control Ser.* 18, 152–162.
- Weber, R., Watson, A., Forter, M., Oliaei, F., 2011. Persistent organic pollutants and landfills - a review of past experiences and future challenges. *Waste Manag. Res.* 29, 107–121.
- Weil, L., Dure, G., Quentin, K., 1974. Wasserlöslichkeit von insektiziden chlorierten Kohlenwasserstoffen und polychlorierten Biphenylen im Hinblick auf eine Gewässerbelastung mit diesen Stoffen. *Wasser- Abwasser- Forsch.* 6, 169–175.
- Willett, K.L., Ulrich, E.M., Hites, R.A., 1998. Differential toxicity and environmental fates of hexachlorocyclohexane isomers. *Environ. Sci. Technol.* 32, 2197–2207.
- Wise, W.S., Abbott, A.H.A., Robinson, F.A., 1948. Abstracts of papers published in other journals. *Agric. Analyst* 73, 108–109.
- Xiao, H., Li, N.Q., Wania, F., 2004. Compilation, evaluation, and selection of physical-chemical property data for alpha-, beta-, and gamma-hexachlorocyclohexane. *J. Chem. Eng. Data* 49, 173–185.
- Yakata, N., Sudo, Y., Tadokoro, H., 2006. Influence of dispersants on bio-concentration factors of seven organic compounds with different lipophilicities and structures. *Chemosphere* 64, 1885–1891.
- Yalkowsky, S.H., Wu, M., 2010. Estimation of the ideal solubility (crystal–liquid fugacity ratio) of organic compounds. *J. Pharm. Sci.* 99, 1100–1106.
- Yalkowsky, S.H., He, Y., Jain, P., 2016. *Handbook of Aqueous Solubility Data*. CRC press.



Article

Surfactant-Enhanced Solubilization of Chlorinated Organic Compounds Contained in DNAPL from Lindane Waste: Effect of Surfactant Type and pH

Raúl García-Cervilla , Arturo Romero, Aurora Santos and David Lorenzo *

Chemical and Materials Engineering Department, University Complutense of Madrid, 28040 Madrid, Spain; raugar05@ucm.es (R.G.-C.); aromeros@quim.ucm.es (A.R.); aursan@quim.ucm.es (A.S.)

* Correspondence: dlorenzo@quim.ucm.es

Received: 20 May 2020; Accepted: 19 June 2020; Published: 23 June 2020



Abstract: Application of surfactants in the remediation of polluted sites with dense nonaqueous phase liquid (DNAPL) still requires knowledge of partitioning between surfactants and pollutants in the organic and aqueous phases and the time necessary to reach this balance. Two real DNAPLs, generated as wastes in the lindane production and taken from the polluted sites from Sabinigo (Spain), were used for investigating the solubilization of 28 chlorinated organic compounds (COCs) applying aqueous surfactant solutions of three nonionic surfactants (E-Mulse[®] 3 (E3), Tween[®]80 (T80), and a mixture of Tween[®]80-Span[®]80 (TS80)) and an anionic surfactant (sodium dodecyl sulfate (SDS)). The initial concentrations of surfactants were tested within the range of 3–17 g·L⁻¹. The pH was also modified from 7 to >12. The uptake of nonionic surfactants into the organic phase was higher than the anionic surfactants. Solubilization of COCs with the nonionic surfactants showed similar molar solubilization ratios (MSR = 4.33 mmol_{COCs}·g⁻¹_{surf}), higher than SDS (MSR = 0.70 mmol_{COCs}·g⁻¹_{SDS}). Furthermore, under strong alkaline conditions, the MSR value of the nonionic surfactants was unchanged, and the MSR of SDS value increased (MSR = 1.32 mmol_{COCs}·g⁻¹_{SDS}). The nonionic surfactants did not produce preferential solubilization of COCs; meanwhile, SDS preferentially dissolved the more polar compounds in DNAPL. The time required to reach phase equilibrium was between 24 and 48 h, and this contact time should be assured to optimize the effect of the surfactant injected on COC solubilization.

Keywords: DNAPL; surfactants; partition; lindane wastes; chlorinated organic compounds

1. Introduction

Contamination of soil and groundwater by organic compounds from industrial activities has become a major environmental problem [1]. This contamination is often due to the accidental release or intentional dumping of hydrophobic organic liquid phases into the environment, resulting in a separate liquid phase, referred to as nonaqueous phase liquids (or NAPLs), that persists in the subsurface [2]. Nonaqueous Phase Liquids are hydrophobic organic phases that show properties and behavior other than dissolving contaminant plumes. NAPLs whose density is lower than that of water are light NAPLs (LNAPLs) [3,4], and NAPLs with a higher density than water are called dense nonaqueous phase liquids (DNAPL).

DNAPLs include common industrial solvents (trichloroethylene, perchloroethylene, carbon tetrachloride, dichloromethane) or other hazardous substances such as creosote and coal tar. Other chlorinated organic pollutants forming DNAPLs include pesticides and chlorinated compounds used for their synthesis [5–7]. Most of these DNAPLs are persistent in the environment due to their hydrophobic nature and low biodegradability, characterized by high toxicity and bioaccumulation and,

in some cases, carcinogenesis [8]. DNAPLs can migrate by density through the subsurface to greater depths, and a significant mass of DNAPL can be trapped in the soil pores [9,10] or soil fractures [5,11].

The remediation of sites polluted by DNAPLs poses essential technical and economic challenges. Conventional treatment technologies such as pump and treat have potentially high life cycle costs [12,13], and a feasible solution to improve the solubilization and mobilization of these DNAPLs is the Soil Flushing treatment where an aqueous solution containing the surfactant (with other possible amendments) is injected into the subsurface and then extracted and treated on-site [14–22].

Surfactants are amphiphilic compounds, and the hydrophilic group is an ionic (cationic, anionic) or highly polar group (nonionic) [23]. When a surfactant is added to the aqueous phase, surface tension decreases as surfactant concentration increases until the critical micelle concentration (CMC) is reached. At this point, tension remains constant as more and more surfactant is added to the solution [24]. However, although surface tension remains constant, the concentration of solubilized chlorinated organic compounds (COCs) increases when the concentration of surfactants in the solution increases [25].

Therefore, the equilibrium of the compounds presented in the DNAPL between the aqueous and the organic phase must be known for a reliable design of the Soil Flushing remediation treatment. This equilibrium is modeled using the mass solubilization ratio (WSR) or molar solubilization ratio (MSR). WSR is the ratio of the mass of solubilized organic compounds per unit of surfactant mass in micellar solution. MSR is defined as the moles of solubilized organic compounds per mole of surfactant in micellar solution [26,27]. Sharmin et al. calculated the MSR for perchloroethylene with Triton X-100 as a surfactant obtaining a value of $2.1 \text{ mol}_j \cdot \text{mol}^{-1}_{surf}$ [28]. Kibbey et al. reported values of MSR in the range of $3.99\text{--}17.82 \text{ mol}_j \cdot \text{mol}^{-1}_{surf}$ depending on the volume ratio of organic and aqueous phases using tetrachloroethylene and Tergitol NP15 as surfactants [29]. Zimmerman et al. reported apparent MSR values for different compounds (trichloroethylene, tetrachloroethylene, chlorobenzene, 1,2-dichlorobenzene) and by using different nonionic surfactants in the range of 0.5 to $4 \text{ mol}_j \cdot \text{mol}^{-1}_{surf}$ [30]. Kang et al. also provided values of MSR for Tween 80, 40, and 20 using trichloroethylene and tetrachloroethylene as organic compounds. They found values around $8.3 \text{ mol}_j \cdot \text{mol}^{-1}_{surf}$ for the Tween 40/trichloroethylene system and around $5 \text{ mol}_j \cdot \text{mol}^{-1}_{surf}$ for Tween 80/tetrachloroethylene [31].

The extent of micellar solubilization depends on many factors (surfactant structure, aggregation number, micelle geometry, hydrophilic/lipophilic balance (HLB), ionic strength, temperature, and the size and chemistry of the solute) [32]. The HLB value is one of the most investigated parameters, but this number cannot confirm the required concentration of the emulsifying agent or the stability of the emulsions [23]. Moreover, there is a lack of studies carried out using real mixtures of organic compounds [33].

Additionally, due to the amphiphilic nature of the surfactant molecule, when a surfactant solution is in contact with an organic phase (such as the DNAPL), the partition of the surfactant between aqueous and organic phases has to be considered to determine the remaining amount of surfactant in solution [30,31]. The partition of surfactant between phases can reduce their active concentrations in an aqueous phase for the solubilization and mobilization of pollutants [31,34], affecting the effectiveness of the remediation treatment. The partition of the surfactant between both phases has been scarcely studied in literature [31,32,35]. Moreover, in these studies, the organic phase, as a DNAPL model, was composed of a single compound (chlorobenzene, 1,2-dichlorobenzene, 1,1,2-trichloroethane [36], perchloroethylene [28], tetrachloroethylene [29,30,36], dichloromethane, chloroform [30]). Only Yang et al. [37] studied binary mixtures of trichloroethylene and perchloroethylene. From literature results, it seems that nonionic surfactants present a higher affinity for the organic phases than anionic surfactants [31].

Correlations between the partition of a surfactant in both phases and the properties of that surfactant have been investigated in the literature. Catanoiu et al. [38] used three commercial nonionic surfactants (polyoxyethylene alkyl ethers, alkyl dimethyl phosphine oxides, and alkyl glycosides) with

different water-in-alkane systems. They found that the affinity of the surfactant for the organic phase increases by increasing the surfactant alkyl chain length. Cowell et al. [36] studied the partitioning of ethoxylated nonionic surfactants in pure organic compounds (chlorobenzene, 1,2-dichlorobenzene, tetrachloroethylene, 1,1,2-trichloroethane), reporting that the concentration of the surfactant in the organic phase decreases when the polarity of this organic phase increases. This conclusion was also supported by the results of Kang et al., who studied the partitioning of different nonionic surfactants using pure compounds as an organic phase [31]. As commented before, the partitioning of surfactants between organic and aqueous phases using real DNAPL mixtures is not available in literature.

The pH effect on the partitioning equilibria has been scarcely studied, although it is proved that alkaline conditions can produce dehydrochlorination reactions of pesticides as lindane [39,40] or alkaline hydrolysis of organophosphorus pesticides, such as parathion and methyl parathion [33], generating less toxic products. Muff et al. [33] studied the solubilization of a NAPL compounded of two organophosphorus pesticides (50% w:w) in a polluted soil under strong alkaline conditions using several surfactants.

In this research, the partitioning equilibrium of surfactants and organic compounds between the organic and the aqueous phases has been studied using two different DNAPL samples. These DNAPLs were extracted from Sardas (S) and Bailin (B) landfills, caused by the dumping of liquid wastes from lindane production [7] containing up to 28 different chlorinated organic compounds [6]. The residues of the lindane produced by the company INQUINOSA were first disposed in the Sardas landfill, and later, in the Bailin landfill (Sabiñanigo, Spain), both unlined. The liquid waste dumped (DNAPL) had migrated by density forces through the subsoil in both landfills (Sardas and Bailin), with the corresponding conceptual models available in the literature [7,41]. The detection of this liquid waste was found at very variable depths, from 40 m deep under the ground level to the surface [7]. The groundwater in both landfills is connected to the Gallego river, and the solubilization of DNAPL in groundwater is a significant risk for the nearby river and reservoir [7,41].

To the best of our knowledge, the works available in literature studying these partitioning equilibria use pure organic compounds [30,31,36] or binary mixtures [42] at neutral pH.

In addition, the effect of alkaline pH on partition equilibria (scarcely studied in literature) is analyzed since strong alkaline conditions can be used in a real treatment to promote the dehydrochlorination reactions of the most toxic COCs in DNAPLs.

Biodegradable nonionic and ionic surfactants have been selected, while good biodegradability is required for the application of a surfactant in aquifer remediation. Tween 80 and Span 80 or their mixtures have been proved to be readily biodegradable [43,44] and will be studied in this research. A commercial surfactant, E-Mulse[®] 3, used in the remediation of sites with DNAPLs at full scale [22] has also been tested. Finally, sodium dodecyl sulfate (SDS), a widely used surfactant in soil remediation studies [45], has been selected as an anionic surfactant.

2. Materials and Methods

2.1. Chemicals

Three nonionic surfactants and an ionic surfactant were used. The nonionic surfactants tested were E-Mulse[®] 3 (E3), Tween[®]80 (T80), and a mixture of Tween[®]80 at 35% and Span[®]80 at 65% (TS80). This mixture was tested in a previous laboratory study carried out by the Aragon Government using a DNAPL from the Sardas landfill (Sabiñanigo, Spain) [46]. Moreover, the three nonionic surfactants were biodegradable and non-toxic.

The anionic surfactant selected was sodium dodecyl sulfate (SDS), which is also typically used in soil washing. The identification of surfactants and their main chemical properties are shown in the Supplementary Material, Table S1. As can be seen, a nonionic surfactant presents a lower micellar concentration (CMC) than SDS.

Two different DNAPL samples obtained from the Sabiñánigo landfills and provided by the company EMGRISA and the Aragon Government were used. One DNAPL sample was obtained from the Sardas landfill (S) and the other sample from the Bailin landfill (B). The composition (molar fraction) of DNAPLs used in this research is summarized in Table S2 of the Supplementary Information. In this table, the average molecular weight MW_{DNAPL} for both DNAPLs is also included (232 $\text{mg}\cdot\text{mmol}^{-1}$ and 191 $\text{mg}\cdot\text{mmol}^{-1}$ for DNAPL: B and S, respectively). As can be seen, both DNAPLs contain up to 28 chlorinated organic compounds (COCs): chlorobenzene (CB) and different isomers of dichlorobenzene (DCBs), trichlorobenzenes (TCBs), tetrachlorobenzene (TetraCBs), pentachlorocyclohexene (PentaCXs), hexachlorocyclohexanes (HCHs), and heptachlorocyclohexanes (HeptaCHs). Compound distribution is quite similar to that mentioned in previous research [6]. These COCs represent more than 95% of the DNAPL mass.

2.2. Solubility Experiments

Solubility experiments were conducted in sealed GC 20 mL glass vials without headspace, closed with PTFE caps. A mass of 0.4 g of each organic phase, DNAPL: B, and DNAPL: S, was added to 19.6 g of the aqueous phase containing the surfactant (surfactant concentration ranging from 0 to 17 g L^{-1}). These experiments were carried out on both neutral and alkaline pH ($\text{pH} > 12$). An alkaline pH was achieved by adding NaOH up to 7 g L^{-1} in the aqueous phase containing the surfactant. Table S3 provides a summary of the conditions of the experiments carried out. Six identical vials, which were sacrificed at different times of agitation, were prepared for each test.

The biphasic mixture (organic and aqueous) was agitated using a magnetic stirrer under room conditions for 5 h at room-controlled temperature ($T = 22 \pm 2$ °C). Then, the agitation was stopped and different vials were sacrificed at 0.5, 1, 3, 24, 48, and 75 h to analyze the aqueous emulsion. The experiments were carried in triplicate. The differences were lower than 10%.

2.3. Analytical Methods

The qualitative identification of dissolved COCs in the aqueous phase was carried out using a gas chromatograph (GC) (Agilent 6890 N, Sante Clara, CA, USA) along with a mass selective detector (Agilent MSD 5975B, Sante Clara, CA, USA). The quantification of COCs in the emulsion was carried out using a GC (Agilent 6890, Sante Clara, CA, USA) with both a flame ionization detector (FID) (Sante Clara, CA, USA) and an electron capture detector (ECD) (Sante Clara, CA, USA), simultaneously. The GC methods are described elsewhere [6]. The aqueous phase samples containing surfactants were previously diluted 1:10 with methanol to analyze the COCs.

The total organic carbon (TOC) of the supernatant (aqueous phase with the surfactant and solubilized COCs) was measured once the equilibrium was reached between phases (COC concentration in emulsion did not change over time). A Shimadzu TOC-V (Kyoto, Japan) analyzer was used. The concentration of nonionic surfactant under equilibrium conditions was determined from the TOC value and sum of COCs in the emulsion.

Ionic surfactant (SDS) concentration in aqueous phases was quantified by measuring sulfate anions in an aqueous solution using IC (Metrohm 761 Compact IC, Herisau, Switzerland). The column used as a stationary phase was Metrosep A SUPP5 5-250 (250 mm long, 4 mm wide) (Gallen, Switzerland), and the mobile phase used was an aqueous solution of Na_2CO_3 (3.2 $\text{mmol}\cdot\text{L}^{-1}$) and NaHCO_3 (1 $\text{mmol}\cdot\text{L}^{-1}$).

To ensure that pH conditions were maintained throughout the entire experiment, the pH was also analyzed in the samples using a 914 pH/Conductometer (Metrohm, Herisau, Switzerland).

3. Results and Discussions

3.1. Partitioning of a Surfactant under Equilibrium Conditions

When equilibrium was reached, the concentration of surfactant absorbed in the organic phase ($C_{surf,ORG}^{eq}$) and the aqueous phase ($C_{surf,AQ}^{eq}$) were calculated from the surfactant mass balance as

shown in the Supplementary Information. The mass of organic phase not dissolved at equilibrium conditions ($w_{org})_{EQ}$ was obtained from the DNAPL mass balance, as shown in equation (S1) to (S3) in the Supplementary Information. It was found that equilibrium conditions for the concentration of COCs in solution were obtained in under 24 h, remaining almost constant in the range of the 24–75 h time interval studied here.

The partition of surfactant between organic and aqueous phases for both DNAPLs (B and S) under equilibrium conditions is plotted at pH = 7 in Figure 1a,b and at pH > 12 in Figure 1c,d. (Data obtained after 48 h are used).

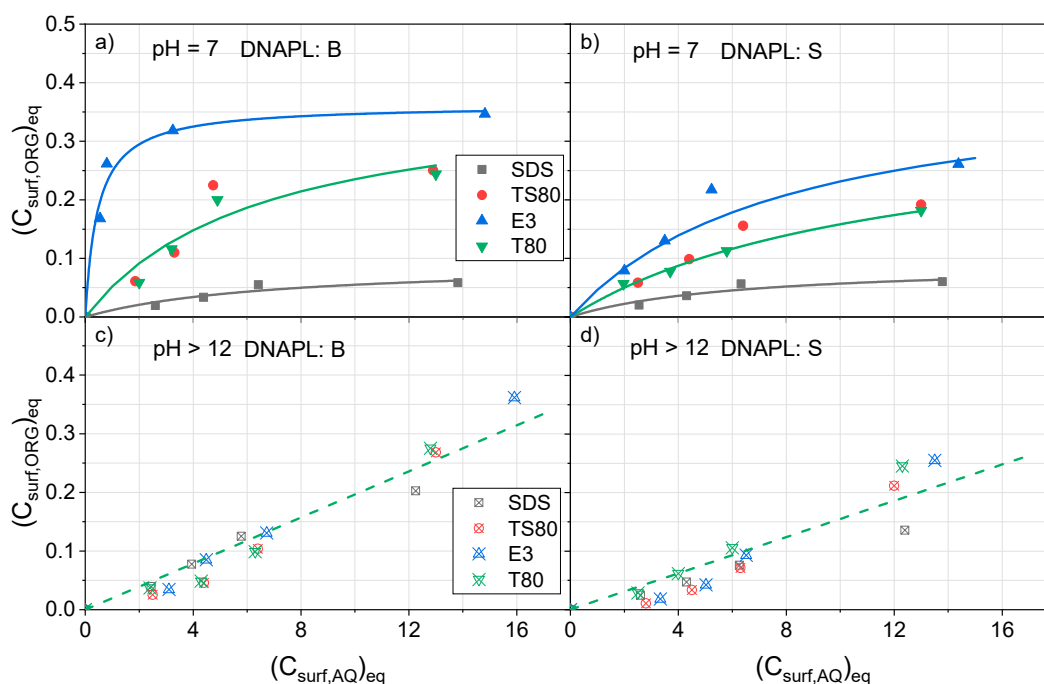


Figure 1. Partitioning of surfactants in organic-aqueous phases at (a) pH = 7, dense nonaqueous phase liquid (DNAPL): Bailin (B), (b) pH = 7 DNAPL: Sardas (S) (c) pH > 12 DNAPL: B (d) pH > 12 DNAPL: S ($C_{surf,ORG}eq$ in $g_{surf}g_{ORG}^{-1}$ and $C_{surf,AQ}eq$, in $g_{surf}L^{-1}$). Experimental values as symbols and predicted values by Equation (1) or Equation (2) with parameters in Table 1 as lines.

Table 1. Parameters estimated by fitting experimental data in Figure 1a,b to the Langmuir isotherm in Equation (1) and experimental data in Figure 1c,d to the linear partitioning model in Equation (2). The statistical significance of parameters is summarized in Table S4.

Surf.	pH = 7 DNAPL: B			pH = 7 DNAPL: S		
	$C_{s,ORG}$ $g_{surf}g_{ORG}^{-1}$	K_S $L \cdot g_{surf}^{-1}$	K_L $g_{surf,ORG} \cdot L \cdot g_{surf}^{-1} \cdot g_{ORG}^{-1}$	$C_{s,ORG}$ $g_{surf}g_{ORG}^{-1}$	K_S $L \cdot g_{surf}^{-1}$	K_L $g_{surf,ORG} \cdot L \cdot g_{surf}^{-1} \cdot g_{ORG}^{-1}$
SDS	0.093	0.143	0.013	0.093	0.159	0.015
T80 and TS80	0.387	0.155	0.059	0.354	0.097	0.034
E3	0.362	2.179	0.789	0.415	0.126	0.052
All	pH > 12			pH > 12		
	$C_{s,ORG}$ $g_{surf}g_{ORG}^{-1}$	K_S $L \cdot g_{surf}^{-1}$	K_L $g_{surf,ORG} \cdot L \cdot g_{surf}^{-1} \cdot g_{ORG}^{-1}$	$C_{s,ORG}$ $g_{surf}g_{ORG}^{-1}$	K_S $L \cdot g_{surf}^{-1}$	K_L $g_{surf,ORG} \cdot L \cdot g_{surf}^{-1} \cdot g_{ORG}^{-1}$
			0.020			0.016

As can be seen in Figure 1a, the concentration of E3 in organic phase B at neutral pH reaches an asymptotic value, about $0.35 g_{surf}g_{ORG}^{-1}$, when surfactant concentration in the aqueous phase is higher than $4 g \cdot L^{-1}$. Lower partition ratios between the organic and aqueous phases were obtained using T80, TS80, and SDS. The partition ratios of T80 and TS80 were similar. Meanwhile, the lowest

values were found with SDS. Moreover, asymptotic values are not achieved with T80, TS80, and SDS for concentrations lower than $15 \text{ g}\cdot\text{L}^{-1}$. Differences in the partition behavior of the surfactant tested at neutral pH indicate a higher affinity of E3 for organic phase B.

By comparing the results in Figure 1a,b, it can be deduced that surfactants have a lower affinity for DNAPL: S than for DNAPL: B. The highest discrepancies are found for the nonionic surfactant. This fact can be explained by differences in the composition of each organic phase B and S. It has been described in literature that the lower the polarity of the organic compounds, the higher the absorption of the nonionic surfactant in the organic phase [36]. As can be seen in Table S2, molar fractions of PentaCX, HexaCX, HCH, and HeptaCH isomers are higher in DNAPL: B than in DNAPL: S. On the contrary, molar fractions of DCB, TCB, and TetraCB isomers are higher in DNAPL: B. Therefore, the polarity of DNAPL: B is expected to be higher and, consequently, the affinity of the nonionic surfactant lower [36].

Results obtained at $\text{pH} > 12$ are shown in Figure 1c,d for DNAPL: B and S, respectively. As can be seen, the partition behavior of the four surfactants is similar for each DNAPL, and the differences found can be due to experimental error. Moreover, almost linear relationships are found between surfactant concentration in the organic and aqueous phases, and asymptotic values are not noticed in the concentration range studied. Surfactant concentration in the organic phase is slightly lower in DNAPL: S than in DNAPL: B. It can be generally noted that the affinity of the nonionic surfactants for the organic phase is more inferior in alkaline conditions than at neutral pH, at least when the surfactant concentration in the aqueous phase is lower than $15 \text{ g}\cdot\text{L}^{-1}$. On the contrary, the higher the pH, the higher the affinity of SDS for the organic phase. These effects can be explained, taking into account that the presence of electrolytes in the aqueous phase can modify the partition of the surfactant [34]. Moreover, alkaline conditions can alter both the polarity of the DNAPL surface and the surfactant micelles, thus affecting the surfactant partition.

To model the partition of surfactant between organic and aqueous phases, some authors [30,31,37] have used Langmuir isotherms, as shown in Equation (1).

$$(C_{surf,ORG})_{eq} = [C_{s,ORG} \cdot K_s \cdot (C_{surf,AQ})_{eq}] / (1 + K_s \cdot (C_{surf,AQ})_{eq}), \quad (1)$$

where $C_{s,ORG}$ is the saturation concentration of surfactant in the organic phase, in $\text{g}_{surf} \cdot \text{g}^{-1}_{ORG}$, and K_s the constant affinity of the surfactant for the organic phase, in $\text{L} \cdot \text{g}^{-1}_{surf}$.

The experimental values shown in Figure 1a,b were fitted to Equation (1) by using non-linear regression, and the corresponding parameters calculated are shown in Table 1. Taking into account that similar behavior was obtained with surfactants T80 and TS80 (Figure 1a,b) and the differences can be explained by uncertainty in the experimental data, the results obtained with both surfactants were joined together. The statistical significance of parameters is summarized in Table S4. On the other hand, in Figure 1c,d, the partition of the surfactants between the organic and the aqueous phase presents a linear trend at $\text{pH} > 12$ and the concentrations applied. In this case, the expression in Equation (2) was proposed:

$$(C_{surf,ORG})_{eq} = K_L \cdot (C_{surf,AQ})_{eq}. \quad (2)$$

K_L is the linear partitioning parameter [31] in $\text{g}_{surf,ORG} \cdot \text{L} \cdot \text{g}^{-1}_{surf} \cdot \text{g}^{-1}_{ORG}$. Equation (1) can be simplified using Equation (2) for small values of K_L . The latter parameter is the product of $C_{s,ORG}$ by K_s in Equation (2).

The experimental data obtained in alkaline conditions was fitted to Equation (2) using linear regression and a K_L parameter was estimated. Since the four surfactants had a similar partitioning behavior under alkaline conditions, the experimental data was fitted together. A unique value of K_L was obtained for each DNAPL, which is also shown in Table 1. As can be seen in Table 1, slightly lower values of K_L were obtained with DNAPL: S, indicating that a lower affinity of this organic phase S for the surfactant is also found at an alkaline pH.

The corresponding values of K_L at $\text{pH} = 7$ are also shown in Table 1. As can be seen, higher K_L values for nonionic surfactants are obtained at a neutral pH, for both DANPLs B and S. On the contrary,

higher K_L values are obtained using the anionic surfactant SDS under alkaline conditions. In all cases, it is confirmed that pH has a strong influence on the affinity of the surfactant for the organic phases.

3.2. Solubilization of COCs

The solubilization experiments carried out are summarized in Table S3. In Figures S1–S5 of the Supplementary Material, some photos of the emulsions before agitation (up), after stirring (centrum), and 75 h after the agitation stopped are shown. As can be seen, the emulsions had a light brown appearance after agitation, being darker in the experiments with DNAPL: S. The brown color settled overtime after the agitation stopped, due to the presence of some clay interbedded in both DNAPL: B and S (more evident in DNAPL: S). As the total amount of COCs quantified represents more than 95% of the mass in both DNAPLs, the percentage of clay is lower than 5% in all cases.

As explained in the experimental part, for each experiment in Table S3, a vial was sacrificed at different settling times, and the amount of COCs in the aqueous phase was measured. The profiles of COCs in solution with the settling time is shown in Figure 2. As can be seen, although the clay gradually precipitated during the settling of the COC, the concentration in the aqueous phase remained constant 24 h after the agitation had stopped and the equilibrium was achieved.

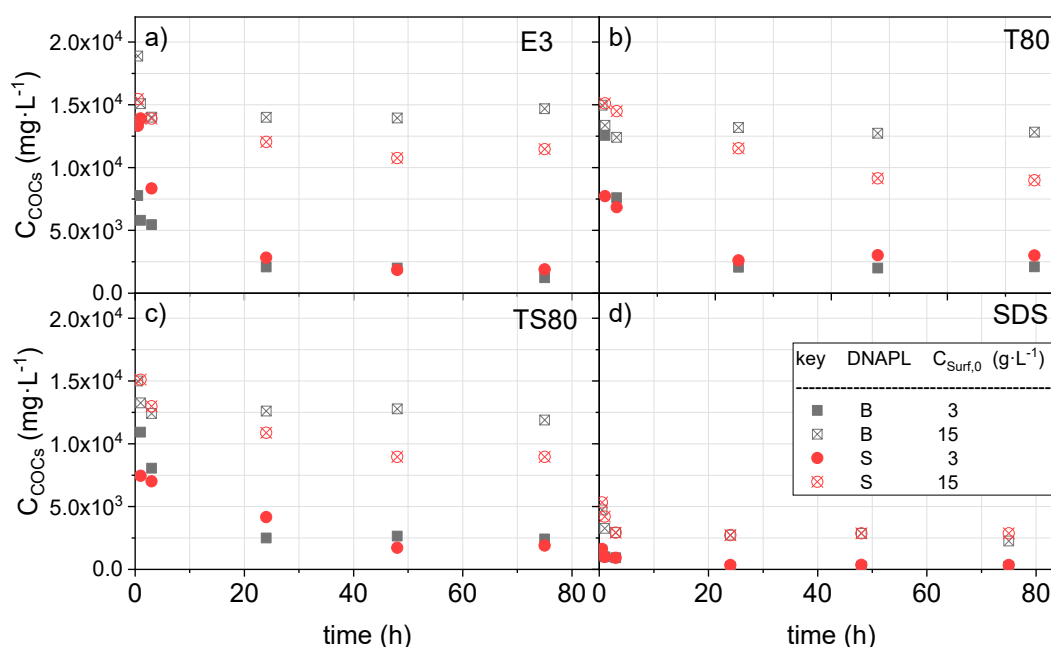


Figure 2. Evolution of chlorinated organic compounds (COCs) concentration in aqueous phase with (a) E3 at 3 and 15 $\text{g}\cdot\text{L}^{-1}$; (b) T80 at 3 and 15 $\text{g}\cdot\text{L}^{-1}$; (c) TS80 at 3 and 15 $\text{g}\cdot\text{L}^{-1}$; (d) sodium dodecyl sulfate (SDS) at 3 and 15 $\text{g}\cdot\text{L}^{-1}$ and $\text{pH} = 7$.

3.2.1. Distribution of Solubilized COCs

As the DNAPL samples used in this research are a complex mixture of COCs, a study has been conducted to see if the surfactants selectively dissolve some compounds in the mixture. The molar distribution of COCs in the DNAPL sample is summarized in Table S2. The percentage of each solubilized COC in the aqueous phase is calculated as follows:

$$y(\% \text{mole}) = 100 \cdot [(C_{j,AQ}/MW_j) / (\sum C_{j,AQ}/MW_j)]_{eq}, \quad (3)$$

where $C_{j,AQ}$ is the concentration of j in the aqueous phase, $\text{mg}\cdot\text{L}^{-1}$ and MW_j are the molecular weight of j . In $\text{mg}\cdot\text{mmol}^{-1}$, COC isomers have been lumped together, so j refers to CB, the sum of DCBs, TCBS, TetraCBs, PCB, PentaCXs, HexaCXs, HCHs, and HeptaCHs isomers.

The molar percentages of solubilized COCs (calculated by Equation (3)) under equilibrium conditions at two different initial surfactant concentrations ($3 \text{ g}\cdot\text{L}^{-1}$ and $15 \text{ g}\cdot\text{L}^{-1}$) at neutral pH are shown in Figures 3 and 4, for DNAPL: B and S, respectively. As can be seen, the higher the surfactant concentration, the higher the sum of solubilized COCs.

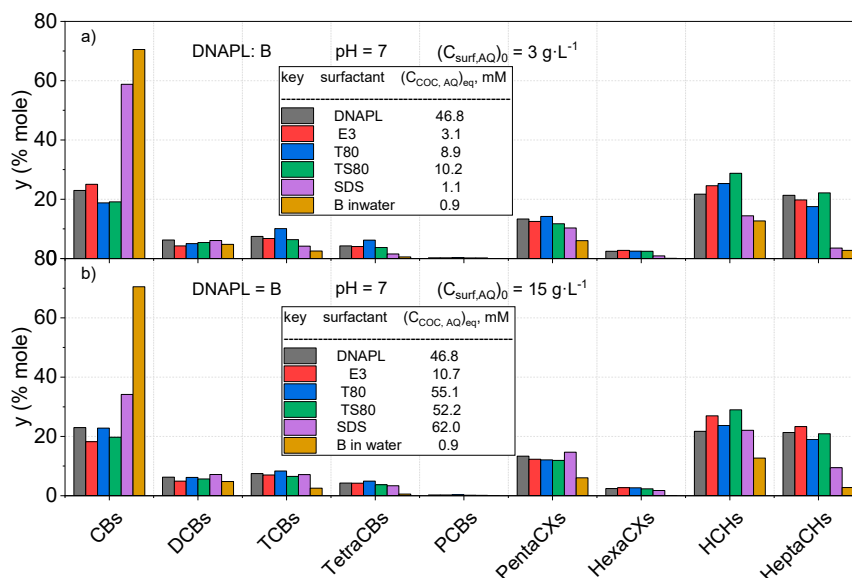


Figure 3. Molar distribution (%) of COCs in the initial DNAPL: B as a sum of isomers and COC distribution in the aqueous phase using an initial surfactant concentration of (a) $(C_{surf,AQ})_0 = 3 \text{ g}\cdot\text{L}^{-1}$ (b) $(C_{surf,AQ})_0 = 15 \text{ g}\cdot\text{L}^{-1}$ at pH = 7. The distribution of solubilized COCs in the aqueous phase saturated in DNAPL (without surfactant) is given as B in water.

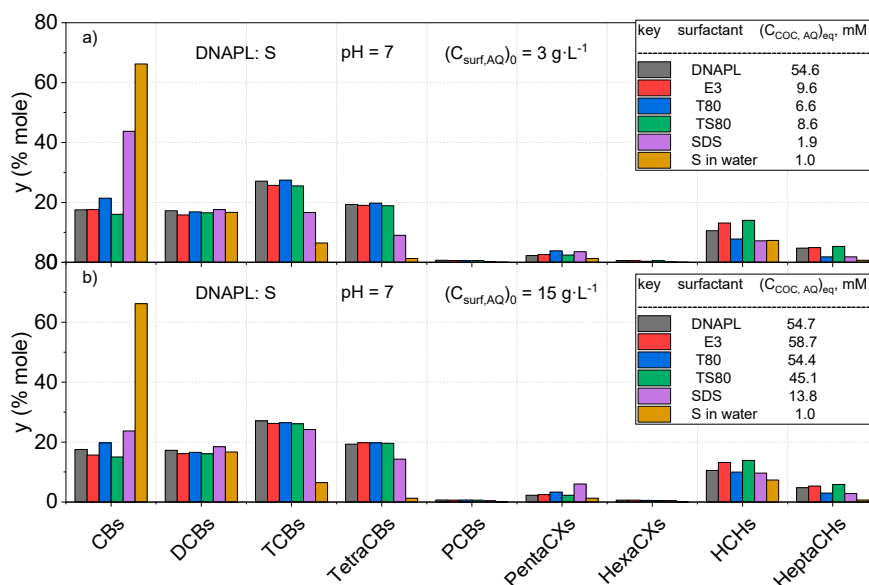


Figure 4. Molar distribution (%) of COCs in the initial DNAPL: S as the sum of isomers and COC distribution in the aqueous phase using an initial surfactant concentration of (a) $(C_{surf,AQ})_0 = 3 \text{ g}\cdot\text{L}^{-1}$ (b) $(C_{surf,AQ})_0 = 15 \text{ g}\cdot\text{L}^{-1}$ at pH = 7. The distribution of solubilized COCs in water is also provided as DNAPL saturated in water.

Moreover, the distribution of COCs in the aqueous phase without surfactant and DNAPL are also included. As can be seen, the distribution of COCs solubilized by nonionic surfactants is quite similar to the initial distribution of COCs in the organic phase (the latter is shown in Table S2),

for both DNAPL: B (Figure 3) and S (Figure 4). Differences are lower than 15%, regardless of the initial surfactant concentration in the aqueous phase. This fact can be explained assuming that the organic phase is trapped in the micellar cores and the aqueous phase is emulsified. Therefore, for the nonionic surfactants tested, the complex mixture forming the DNAPL can be joined together as a single compound.

On the contrary, the solubilization of COCs without surfactant presents a different distribution, following the partitioning of these compounds in the aqueous phase reported elsewhere [6,39]. The distribution of COCs in the aqueous phase without surfactants is quite different from their distribution in the organic phase, where chlorobenzene is the most abundant dissolved COC.

On the other hand, COC distribution obtained with SDS at a low surfactant concentration is more similar to that found in the aqueous phase without surfactant, as can be seen in Figures 3 and 4. However, the higher the SDS concentration, the more similar the distribution of dissolved COCs to that found in the organic phase, although some selectivity is still noticed.

The total COCs concentrations in the aqueous phase from the solubility experiments are shown in the legends of Figures 3 and 4.

The effect of the addition of alkali on solubilized COC distribution in the presence of surfactants under equilibrium conditions was analyzed. COC distribution in the aqueous phase obtained at initial surfactant concentrations of 3 and 15 g·L⁻¹ is summarized in Figures S6 and S7 for DNAPL: B and S, respectively. For comparison purposes, COC distribution at neutral pH and the total moles of dissolved COCs at neutral and alkaline pHs are also shown in these figures. The concentration of COCs in the aqueous phase is also summarized in the captions of the figures mentioned above.

As can be seen in Figures S6 and S7, for a given surfactant concentration, the total moles of dissolved COCs are similar at both pHs, but their distribution changes. PentaCX, HexaCX, HCH, and HeptaCH isomers are not detected in the aqueous emulsions under alkaline conditions while TCBs and TetraCB molar percentages have remarkably increased under these conditions. It has been reported elsewhere [39] that under alkali conditions, HCH and PentaCX isomers in the aqueous phase produce TCB and HeptaCHs compounds and HexaCXs are transformed into TetraCBs. Dehydrochlorination reactions and selectivity concerning TCB and TetraCB isomers obtained are shown in Figures S8 and S9, following that reported by Lorenzo et al. [39]. Therefore, the alkaline conditions produced the transformation of some compounds in a solubilized fraction of DNAPL inside the micelles generated by the surfactant due to alkaline conditions; however, similar molar total concentration of COCs in solution is obtained at neutral and alkaline pHs. Moreover, the TCBs and TetraCBs produced under alkaline conditions are less toxic than the precursors' organic compounds (HCHs and HeptaCHs, respectively) [47–50].

3.2.2. Partition Equilibria of Solubilized COCs

From the results shown in Table S5, it is clear that the concentration of solubilized COCs depends on the concentration of the surfactant added. In addition, it has been found that for a nonionic surfactant, the complex mixture of compounds in DNAPL can be joined together as a single solubilized compound.

The partition of COCs and equilibrium conditions can be modeled employing the MSR (or WSR) parameters defined in Equation (4).

$$\begin{aligned} MSR &= (C_{COCs,AQ})_{eq} / (C_{surf,AQ} / MW_{surf})_{eq} \\ WSR &= (\sum C_{j,AQ})_{eq} / (C_{surf,AQ})_{eq} \end{aligned} \quad (4)$$

where MW_{surf} is the molecular weight of the surfactant summarized in Table S1 (but for E3 that is unknown). The sum of COCs dissolved has been called $C_{COCs,AQ}$, in mmol·L⁻¹ defined as

$$(C_{COCs,AQ})_{eq} = \sum (C_{j,AQ} / MW_j) \quad (5)$$

In Figure 5, the concentration of solubilized COCs calculated by (5), in $\text{mmol}\cdot\text{L}^{-1}$, vs. the concentration of surfactant in the aqueous phase under equilibrium conditions, calculated by Equation (S2) in the Supplementary Information), in g L^{-1} , has been plotted for both pHs and DNAPLs studied. As can be seen in Figure 5a,c and Figure 5b,d, similar plots are obtained for nonionic surfactants at both pHs. It is in concordance with the assumption that the DNAPL is mobilized as an organic phase in the micellar core and the reaction of dehydrochlorination by NaOH takes place in this aqueous phase. Moreover, similar results are obtained regardless of the DNAPL used. The pH only affects the solubilization capacity of SDS. The higher the pH, the higher the COC concentration solubilized with SDS. The explanation for this is that SDS selectively solubilized the COCs as explained in the previous section.

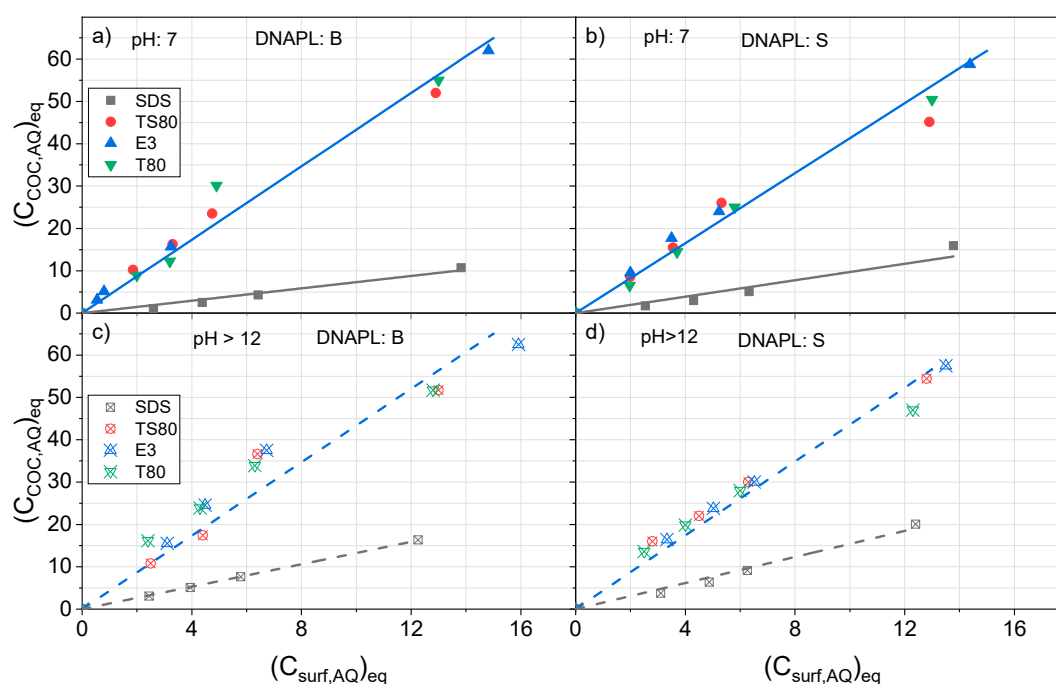


Figure 5. Aqueous phase solubility of COCs in $\text{mmol}_{\text{COCs}}\cdot\text{L}^{-1}$ versus the concentration of surfactant in the aqueous phase in $\text{g}_{\text{surf}}\cdot\text{L}^{-1}$ after reaching equilibrium at pH = 7 using (a) B, (b) S, and at pH > 12 using (c) B and (d) S.

Moreover, the higher the surfactant concentration in solution, the higher the solubilized COC concentration, meaning that an almost linear trend is found between both variables in the concentration range studied. On the other hand, lower solubilization is achieved with SDS in comparison with that obtained with nonionic surfactants, following that reported by Zhou et al. in previous research [51].

The slope of the plots in Figure 5 can be related to the MSR or MWR values obtained in Equation (4), which are summarized in Table 2. Nonionic surfactant data at both pHs and for both DNAPLs were joined together. The statistical significance of linear regression parameters obtained is summarized in Table S6.

The SMR values obtained were in line with those reported by Pei et al. for the solubilization of DCBs using different surfactants [52].

In the linear regressions, the intercept corresponds to the solubilized DNAPL in the absence of the surfactant: $0.9 \text{ mmol}\cdot\text{L}^{-1}$ and $1.0 \text{ mmol}\cdot\text{L}^{-1}$ for B and S, respectively, following previous results [39].

Table 2. Molar solubilization ratios (MSR) and mass solubilization ratio (WSR) values calculated from the slopes in Figure 5 for nonionic surfactants and SDS *.

Nonionic Surfactants pH = 7 and >12, DNAPL: B and S			
	WSR $\text{mg}_{\text{COCs}} \cdot \text{g}^{-1}_{\text{surf}}$	MSR $\text{MW}_S \text{mmol}_{\text{COCs}} \cdot \text{g}^{-1}_{\text{surf}}$	MSR $\text{mmol}_{\text{COCs}} \cdot \text{mmol}^{-1}_{\text{surf}}$
T80			5.66
TS80	1005	4.33	3.11
E3			-
Anionic surfactant: SDS surfactant			
	WSR $\text{mg}_{\text{COCs}} \cdot \text{g}^{-1}_{\text{surf}}$	MSR $\text{MW}_S \text{mmol}_{\text{COCs}} \cdot \text{g}^{-1}_{\text{surf}}$	MSR $\text{mmol}_{\text{COCs}} \cdot \text{mmol}^{-1}_{\text{surf}}$
pH = 7 DNAPL: B	162	0.7	0.43
pH = 7 DNAPL: S	186	0.97	0.68
pH > 12 DNAPL: B	307	1.32	0.8
pH > 12 DNAPL: S	295	1.54	0.94

* The statistical significance of linear regression parameters obtained is summarized in Table S6.

4. Conclusions

The surfactants studied here (three nonionic surfactants (E3, TS80, and T80) and one anionic surfactant (SDS)) significantly improved the solubilization of a complex mixture of chlorinated organic compounds contained in real DNAPL present in two landfills polluted with liquid organic wastes from lindane production. This improvement was remarkably greater for all nonionic surfactants tested, finding similar values of molar solubilization ratios (MSR) regardless of the pH used. Moreover, a significant partition of the surfactants was found between the organic and the aqueous phases. The nonionic surfactant presented a higher affinity for the organic phase at neutral pH. For each DNAPL, the composition of COCs in the micellar core was similar to the initial composition of the organic phase for the three nonionic surfactants tested. In contrast, the anionic surfactant selectively solubilized the most polar compounds in DNAPL. Moreover, under strong alkaline conditions, dehydrochlorination of some COCs trapped in the micelles was noticed obtaining an emulsion with less toxic COC. These findings are relevant in the design of the surfactant-enhanced remediation process of the site.

Supplementary Materials: The following are available online at <http://www.mdpi.com/1660-4601/17/12/4494/s1>, Table S1: Surfactant tested in DNAPL solubilization and main properties. Table S2: Mole fraction of COCs from B and S DNAPLs samples used. Table S3: Experimental conditions of the solubility tests carried out. wORGO = 400 mg, $V_{aq} = 0.02 \text{ L}$, pH = 7 and >12 ($7 \text{ g L}^{-1} \text{ NaOH}$); DNAPL: B and S. Table S4: Parameters and statically significance obtain to fit Equations (4) and (5) to the data in Figure 1 at pH = 7 and pH > 12 for both DNAPLs, B and S. Table S5: Concentrations of surfactants and COCs in aqueous phase at neutral and alkaline pH and equilibrium state. Table S6: Parameters and statically significance obtain to fit Equation (9) to the data in Figure 4 at pH = 7 and pH > 12 for both DNAPLs, B and S. Figure S1: Left: organic phase S; right: organic phase B adding E3 at several concentrations (initial surfactant concentration from the left to the right: 3, 5, 7.5, and 15 g L^{-1}) and pH = 7. Top: Appearance before agitation. Center: Appearance after agitation (5 h). Bottom: Appearance after 75 h of settling. Figure S2: Left: organic phase S; right: organic phase B adding T80 at several concentrations (initial surfactant concentration from the left to the right: 3, 5, 7.5, and 15 g L^{-1}) and pH = 7. Top: Appearance before agitation. Center: Appearance after agitation (5 h). Bottom: Appearance after 75 h of settling. Figure S3: Left: organic phase S; right: organic phase B adding TS80 at several concentrations (initial surfactant concentration from the left to the right: 3, 5, 7.5, and 15 g L^{-1}) and pH = 7. Top: Appearance before agitation. Center: Appearance after agitation (5 h). Bottom: Appearance after 75 h of settling. Figure S4: Left: organic phase S; right: organic phase B adding SDS at several concentrations (initial surfactant concentration from the left to the right: 3, 5, 7.5, and 15 g L^{-1}) and pH = 7. Top: Appearance before agitation. Center: Appearance after agitation (5 h). Bottom: Appearance after 75 h of settling. Figure S5: Appearance of emulsion at 75 h of settling after alkali addition: from the top to the bottom: E3, T80, TS80, and SDS. Left: Results with DNAPL from S, right: Results with B. Initial surfactant concentration from the left to the right: 3, 5, 7.5, and 15 g L^{-1} . Figure S6: Molar distribution (%) of COCs in the initial DNAPL: B as sum of isomers and COCs distribution in aqueous phase using a surfactant initial concentration of (a) $C_{\text{surf,AQ0}} = 3 \text{ g L}^{-1}$ (b) $C_{\text{surf,AQ0}} = 15 \text{ g L}^{-1}$ at pH > 12. Figure S7: Molar distribution (%) of COCs in the initial DNAPL: S as sum of isomers and COCs distribution in aqueous phase using a surfactant initial

concentration of (a) $C_{surf,AQ0} = 3 \text{ g}\cdot\text{L}^{-1}$ (b) $C_{surf,AQ0} = 15 \text{ g}\cdot\text{L}^{-1}$ at $\text{pH} > 12$. Figure S8: Reaction of HCH and PentaCX isomers in DNPLS to TCBS under alkali conditions adapted from (Lorenzo et al., 2020). Figure S9. Reaction of HeptaCH and HexaCX isomers in DNPLS to TetraCBs under alkali conditions. Adapted from (Lorenzo et al., 2020).

Author Contributions: Conceptualization, A.R., A.S., and D.L.; data curation, R.G.-C. and D.L.; funding acquisition, A.R. and A.S.; investigation, R.G.-C. and D.L.; methodology, R.G.-C. and A.S.; supervision, A.S. and D.L.; writing—original draft, R.G.-C.; writing—review & editing, A.S. and D.L. All authors have read and agreed to the published version of the manuscript.

Funding: This research was supported by the EU LIFE Program (LIFE17 ENV/ES/000260), the Regional Government of Madrid, through the CARESOIL project (S2018/EMT-4317), and the Spanish Ministry of Economy, Industry and Competitiveness, through project CTM2016-77151-C2-1-R. Raúl García-Cervilla acknowledges the Spanish FPI grant (ref. BES-2017-081782).

Acknowledgments: The authors thank the Department of Agriculture, Livestock and the Environment, Government of Aragon, Spain, as well as EMGRISA, for kindly supplying the samples.

Conflicts of Interest: The authors declare no conflict of interest.

References

1. van Liedekerke, M.; Prokop, G.; Rabl-Berger, S.; Kibblewhite, M.; Louwagie, G. *Progress in the Management of Contaminated Sites in Europe*; Reference Report; Joint Research Centre of The European Union: Ispra, Italy, 2014.
2. Siegrist, R.L.; Crimi, M.; Simpkin, T.J. *Situ Chemical Oxidation for Groundwater Remediation*; Springer: New York, NY, USA, 2011. [[CrossRef](#)]
3. Sulaymon, A.H.; Gzar, H.A. Experimental investigation and numerical modeling of light nonaqueous phase liquid dissolution and transport in a saturated zone of the soil. *J. Hazard. Mater.* **2011**, *186*, 1601–1614. [[CrossRef](#)] [[PubMed](#)]
4. Soga, K.; Page, J.W.; Illangasekare, T.H. A review of NAPL source zone remediation efficiency and the mass flux approach. *J. Hazard. Mater.* **2004**, *110*, 13–27. [[CrossRef](#)] [[PubMed](#)]
5. Parker, B.L.; Bairos, K.; Maldaner, C.H.; Chapman, S.W.; Turner, C.M.; Burns, L.S.; Plett, J.; Carter, R.; Cherry, J.A. Metolachlor dense non-aqueous phase liquid source conditions and plume attenuation in a dolostone water supply aquifer. In *Groundwater in Fractured Bedrock Environments: Managing Catchment and Subsurface Resources*; Ofterdinger, U., Macdonald, A.M., Comte, J.C., Young, M.E., Eds.; Geological Society of London: London, UK, 2019; Volume 479, pp. 207–236.
6. Santos, A.; Fernandez, J.; Guadano, J.; Lorenzo, D.; Romero, A. Chlorinated organic compounds in liquid wastes (DNAPL) from lindane production dumped in landfills in Sabinanigo (Spain). *Environ. Poll.* **2018**, *242*, 1616–1624. [[CrossRef](#)] [[PubMed](#)]
7. Fernández, J.; Arjol, M.; Cacho, C. POP-contaminated sites from HCH production in Sabinanigo, Spain. *Environ. Sci. Pollut. Res.* **2013**, *20*, 1937–1950. [[CrossRef](#)] [[PubMed](#)]
8. Council, N.R. *Alternatives for Managing the Nation's Complex Contaminated Groundwater Sites*; National Academies Press: Washington, DC, USA, 2013.
9. Agaoglu, B.; Coptly, N.K.; Scheytt, T.; Hinkelmann, R. Interphase mass transfer between fluids in subsurface formations: A review. *Adv. Water Resour.* **2015**, *79*, 162–194. [[CrossRef](#)]
10. Brusseau, M.L. *The Impact of DNAPL Source-Zone Architecture on Contaminant Mass Flux and Plume Evolution in Heterogeneous Porous Media*; ARIZONA UNIV TUCSON: Tucson, AZ, USA, 2013.
11. Schaefer, C.E.; White, E.B.; Lavorgna, G.M.; Annable, M.D. Dense Nonaqueous-Phase Liquid Architecture in Fractured Bedrock: Implications for Treatment and Plume Longevity. *Environ. Sci. Technol.* **2016**, *50*, 207–213. [[CrossRef](#)]
12. Kavanaugh, M.C.; Suresh, P.; Rao, C. *The DNAPL Remediation Challenge: Is there a Case for Source Depletion*; Environmental Protection Agency: Washington, DC, USA, 2003.
13. McGuire, T.M.; McDade, J.M.; Newell, C.J. Performance of DNAPL source depletion technologies at 59 chlorinated solvent—Impacted sites. *Groundw. Monit. Remediat.* **2006**, *26*, 73–84. [[CrossRef](#)]
14. Atteia, O.; Estrada, E.D.; Bertin, H. Soil flushing: A review of the origin of efficiency variability. *Rev. Environ. Sci. Bio. Technol.* **2013**, *12*, 379–389. [[CrossRef](#)]

15. Strbak, L. *Situ Flushing with Surfactants and Cosolvents*; National Network of Environmental Studies Fellowship Report for US Environmental Protection Agency; Office of Solid Waste and Emergency Response Technology Innovation Office: Washington, DC, USA, 2000.
16. Svab, M.; Kubala, M.; Muellerova, M.; Raschman, R. Soil flushing by surfactant solution: Pilot-scale demonstration of complete technology. *J. Hazard. Mater.* **2009**, *163*, 410–417. [[CrossRef](#)]
17. Pennell, K.D.; Capiro, N.L.; Walker, D.I. Surfactant and cosolvent flushing. In *Chlorinated Solvent Source Zone Remediation*; Kueper, B.H., Stroo, H.F., Vogel, C.M., Ward, C.H., Eds.; Springer: New York, NY, USA, 2014; Volume 7, pp. 353–394.
18. Maire, J.; Joubert, A.; Kaifas, D.; Invernizzi, T.; Marduel, J.; Colombano, S.; Cazaux, D.; Marion, C.; Klein, P.Y.; Dumestre, A.; et al. Assessment of flushing methods for the removal of heavy chlorinated compounds DNAPL in an alluvial aquifer. *Sci. Total Environ.* **2018**, *612*, 1149–1158. [[CrossRef](#)]
19. Londergan, J.; Yeh, L. *Surfactant-Enhanced Aquifer Remediation (SEAR) Implementation Manual*; INTERA INC.: Austin, TX, USA, 2003.
20. Acosta, E.J.; Quraishi, S. Surfactant Technologies for Remediation of Oil Spills. In *Oil Spill Remediation: Colloid Chemistry-Based Principles and Solutions*; Somasundaran, P., Patra, P., Farinato, R.S., Papadopoulos, K., Eds.; Wiley & Sons: Hoboken, NJ, USA, 2014; pp. 317–358.
21. Mulligan, C.; Yong, R.; Gibbs, B. Surfactant-enhanced remediation of contaminated soil: A review. *Eng. Geol.* **2001**, *60*, 371–380. [[CrossRef](#)]
22. Beshia, A.T.; Bekele, D.N.; Naidu, R.; Chadalavada, S. Recent advances in surfactant-enhanced In-Situ Chemical Oxidation for the remediation of non-aqueous phase liquid contaminated soils and aquifers. *Environ. Technol. Innov.* **2018**, *9*, 303–322. [[CrossRef](#)]
23. Rosen, M.J.; Kunjappu, J.T. *Surfactants and Interfacial Phenomena*; John Wiley & Sons: Hoboken, NJ, USA, 2012.
24. Mukerjee, P.; Mysels, K.J. *Critical Micelle Concentrations of Aqueous Surfactant Systems*; National Standard Reference Data system: Washington, DC, USA, 1971.
25. Mao, X.; Jiang, R.; Xiao, W.; Yu, J. Use of surfactants for the remediation of contaminated soils: A review. *J. Hazard. Mater.* **2015**, *285*, 419–435. [[CrossRef](#)]
26. Swe, M.M.; Yu, L.Y.E.; Hung, K.C.; Chen, B.H. Solubilization of selected polycyclic aromatic compounds by nonionic surfactants. *J. Surfactants Deterg.* **2006**, *9*, 237–244. [[CrossRef](#)]
27. Bouzid, I.; Maire, J.; Brunol, E.; Caradec, S.; Fatin-Rouge, N. Compatibility of surfactants with activated-persulfate for the selective oxidation of PAH in groundwater remediation. *J. Environ. Chem. Eng.* **2017**, *5*, 6098–6106. [[CrossRef](#)]
28. Sharmin, R.; Ioannidis, M.A.; Legge, R.L. Effect of nonionic surfactant partitioning on the dissolution kinetics of residual perchloroethylene in a model porous medium. *J. Contam. Hydrol.* **2006**, *82*, 145–164. [[CrossRef](#)] [[PubMed](#)]
29. Kibbey, T.C.G.; Chen, L.C. Phase volume effects in the sub- and super-CMC partitioning of nonionic surfactant mixtures between water and immiscible organic liquids. *Colloid Surf. A* **2008**, *326*, 73–82. [[CrossRef](#)]
30. Zimmerman, J.B.; Kibbey, T.C.G.; Cowell, M.A.; Hayes, K.F. Partitioning of ethoxylated nonionic surfactants into nonaqueous-phase organic liquids: Influence on solubilization behavior. *Environ. Sci. Technol.* **1999**, *33*, 169–176. [[CrossRef](#)]
31. Kang, S.; Lim, H.S.; Gao, Y.; Kang, J.; Jeong, H.Y. Evaluation of ethoxylated nonionic surfactants for solubilization of chlorinated organic phases: Effects of partitioning loss and macroemulsion formation. *J. Contam. Hydrol.* **2019**, *223*, 103475. [[CrossRef](#)]
32. Paria, S. Surfactant-enhanced remediation of organic contaminated soil and water. *Adv. Colloid Interface Sci.* **2008**, *138*, 24–58. [[CrossRef](#)]
33. Muff, J.; MacKinnon, L.; Durant, N.D.; Bennedsen, L.F.; Ruge, K.; Bondgaard, M.; Pennell, K.D. Solubility and reactivity of surfactant-enhanced alkaline hydrolysis of organophosphorus pesticide DNAPL. *Environ. Sci. Pollut. Res.* **2020**, *27*, 3428–3439. [[CrossRef](#)] [[PubMed](#)]
34. West, C.C.; Harwell, J.H. Surfactants and subsurface remediation. *Environ. Sci. Technol.* **1992**, *26*, 2324–2330. [[CrossRef](#)]
35. Babaei, M.; Coptoy, N.K. Numerical modelling of the impact of surfactant partitioning on surfactant-enhanced aquifer remediation. *J. Contam. Hydrol.* **2019**, *221*, 69–81. [[CrossRef](#)] [[PubMed](#)]

36. Cowell, M.A.; Kibbey, T.C.G.; Zimmerman, J.B.; Hayes, K.F. Partitioning of ethoxylated nonionic surfactants in water/NAPL systems: Effects of surfactant and NAPL properties. *Environ. Sci. Technol.* **2000**, *34*, 1583–1588. [[CrossRef](#)]
37. Yang, J.-S.; Yang, J.-W. Partitioning effects of nonionic surfactants on the solubilization of single or binary chlorinated solvents: Batch and column experiments. *J. Ind. Eng. Chem.* **2018**, *58*, 140–147. [[CrossRef](#)]
38. Catanoiu, G.; Carey, E.; Patil, S.R.; Engelskirchen, S.; Stubenrauch, C. Partition coefficients of nonionic surfactants in water/n-alkane systems. *J. Colloid Interface Sci.* **2011**, *355*, 150–156. [[CrossRef](#)]
39. Lorenzo, D.; García-Cervilla, R.; Romero, A.; Santos, A. Partitioning of chlorinated organic compounds from dense non-aqueous phase liquids and contaminated soils from lindane production wastes to the aqueous phase. *Chemosphere* **2020**, *239*, 124798. [[CrossRef](#)]
40. Casado, I.; Mahjoub, H.; Lovera, R.; Fernandez, J.; Casas, A. Use of electrical tomography methods to determinate the extension and main migration routes of uncontrolled landfill leachates in fractured areas. *Sci. Total Environ.* **2015**, *506*, 546–553. [[CrossRef](#)]
41. Navarro, J.S.; López, C.; García, A.P. Characterization of groundwater flow in the Bailin hazardous waste-disposal site (Huesca, Spain). *Environ. Geol.* **2000**, *40*, 216–222. [[CrossRef](#)]
42. Rhue, R.D.; Rao, P.S.C.; Annable, M.D. Single-phase microemulsification of a complex light-nonaqueous-phase-liquid: Laboratory evaluation of several mixtures of surfactant alcohol solutions. *J. Environ. Qual.* **1999**, *28*, 1135–1144. [[CrossRef](#)]
43. Cheng, M.; Zeng, G.; Huang, D.; Yang, C.; Lai, C.; Zhang, C.; Liu, Y. Advantages and challenges of Tween 80 surfactant-enhanced technologies for the remediation of soils contaminated with hydrophobic organic compounds. *Chem. Eng. J.* **2017**, *314*, 98–113. [[CrossRef](#)]
44. Franzetti, A.; Di Gennaro, P.; Bevilacqua, A.; Papacchini, M.; Bestetti, G. Environmental features of two commercial surfactants widely used in soil remediation. *Chemosphere* **2006**, *62*, 1474–1480. [[CrossRef](#)] [[PubMed](#)]
45. Muherei, M.A.; Junin, R.; Bin Merdhah, A.B. Adsorption of sodium dodecyl sulfate, Triton X100 and their mixtures to shale and sandstone: A comparative study. *J. Pet. Sci. Eng.* **2009**, *67*, 149–154. [[CrossRef](#)]
46. Corcho, D.; Fernández, J.; Laperou, L.; Guadaño, J. Laboratory evaluation of mixed surfactants solutions to mobilise hexachlorocyclohexane (DNAPL) from sardas landfill (Aragón, Spain). In Proceedings of the 13th HCH & Pesticides Forum, Zaragoza, Spain, 3–6 November 2015.
47. Tsaboula, A.; Papadakis, E.-N.; Vryzas, Z.; Kotopoulou, A.; Kintzikoglou, K.; Papadopoulou-Mourkidou, E. Environmental and human risk hierarchy of pesticides: A prioritization method, based on monitoring, hazard assessment and environmental fate. *Environ. Int.* **2016**, *91*, 78–93. [[CrossRef](#)]
48. Willett, K.L.; Ulrich, E.M.; Hites, R.A. Differential toxicity and environmental fates of hexachlorocyclohexane isomers. *Environ. Sci. Technol.* **1998**, *32*, 2197–2207. [[CrossRef](#)]
49. Tsai, K.-P.; Chen, C.-Y. An algal toxicity database of organic toxicants derived by a closed-system technique. *Environ. Toxicol. Chem.* **2007**, *26*, 1931–1939. [[CrossRef](#)]
50. van Wijk, D.; Cohet, E.; Gard, A.; Caspers, N.; van Ginkel, C.; Thompson, R.; de Rooij, C.; Garny, V.; Lecloux, A. 1,2,4-Trichlorobenzene marine risk assessment with special emphasis on the Osparcom region North Sea. *Chemosphere* **2006**, *62*, 1294–1310. [[CrossRef](#)]
51. Zhou, M.F.; Rhue, R.D. Screening commercial surfactants suitable for remediating DNAPL source zones by solubilization. *Environ. Sci. Technol.* **2000**, *34*, 1985–1990. [[CrossRef](#)]
52. Pei, G.P.; Zhu, Y.E.; Cai, X.T.; Shi, W.Y.; Li, H. Surfactant flushing remediation of o-dichlorobenzene and p-dichlorobenzene contaminated soil. *Chemosphere* **2017**, *185*, 1112–1121. [[CrossRef](#)]





Compatibility of nonionic and anionic surfactants with persulfate activated by alkali in the abatement of chlorinated organic compounds in aqueous phase

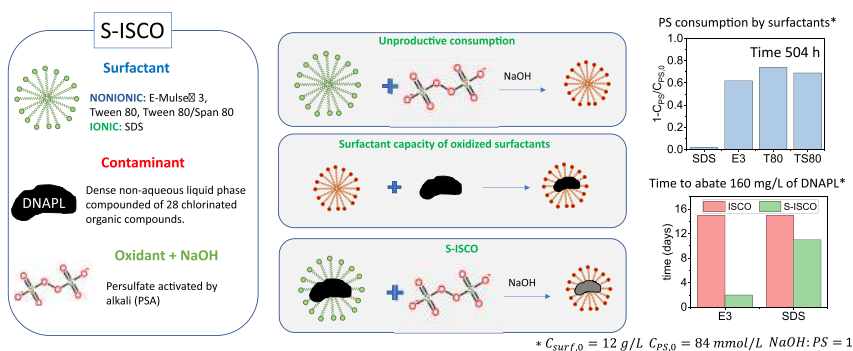
Raul García-Cervilla, Aurora Santos, Arturo Romero, David Lorenzo*

Chemical Engineering and Materials Department, University Complutense of Madrid, Spain

HIGHLIGHTS

- The oxidation of surfactant reduces the pollutant solubilization.
- Nonionic surfactants have higher MSR but are more easily oxidized by PSA.
- S-ISCO with nonionic surfactants reduces removal time of DNAPL with PSA.
- The S-ISCO treatment was more efficient with Emulse-3 than SDS.

GRAPHICAL ABSTRACT



ARTICLE INFO

Article history:

Received 10 June 2020
Received in revised form 16 August 2020
Accepted 17 August 2020
Available online 19 August 2020

Editor: Jay Gan

Keywords:

DNAPL
Nonionic and anionic surfactants
Persulfate activated by alkali
Lindane wastes S-ISCO

ABSTRACT

Surfactant Enhanced In-Situ Chemical Oxidation (S-ISCO) is an emerging technology in the remediation of sites with residual Dense Non-Aqueous Phase Liquids (DNAPLs), a ubiquitous problem in the environment and a challenge to solve. In this work, three nonionic surfactants: E-Mulse3® (E3), Tween80 (T80), and a mixture of Tween80-Span80 (TS80), and an anionic surfactant: sodium dodecyl sulfate (SDS), combined with persulfate activated by alkali (PSA) as oxidant have been investigated to remove the DNAPL generated as liquid waste in lindane production, which is composed of 28 chlorinated organic compounds (COCs).

Because the compatibility between surfactants and oxidants is a key aspect in the S-ISCO effectiveness the unproductive consumption of PS by surfactants was investigated in batch (up to 864 h) varying the initial concentration of PS (84–42 mmol·L⁻¹) and surfactants (0–12 g·L⁻¹) and the NaOH:PS molar ratio (1 and 2). The solubilization capacity of a partially oxidized surfactant was analyzed by estimating its Equivalent Surfactant Capacity, ESC, (as mmol_{COCs dissolved} g_{surf}⁻¹) and comparing it to the expected value for an unoxidized surfactant, ESC₀. Finally, the abatement of DNAPL with simultaneous addition of surfactant and PSA was studied.

At the conditions used, a negligible unproductive consumption of PS was found by SDS; meanwhile, PS consumption at 360 h ranged between 70 and 80% using the nonionic surfactants. The highest ratios of ESC/ESC₀ were found with SDS and E3 and these surfactants were chosen for the S-ISCO treatment. When oxidant and surfactant were simultaneously applied for DNAPL abatement the COC conversion was more than three times higher with E3 (0.6 at 360 h) than SDS. Moreover, it was obtained that the time needed for the removal of a mass of DNAPL by PSA in the absence of surfactants was notably higher than the time required when a suitable mass of surfactant was added.

© 2020 Elsevier B.V. All rights reserved.

* Corresponding author.

E-mail addresses: raugar05@ucm.es (R. García-Cervilla), aurasan@quim.ucm.es (A. Santos), aromeros@quim.ucm.es (A. Romero), dlorenzo@ucm.es (D. Lorenzo).

1. Introduction

Petroleum hydrocarbons, pesticides, or chlorinated solvents are hydrophobic organic compounds (HOCs) that have been released in the environment. Do the low solubility in the aqueous phase of these compounds they form non-aqueous phase liquids (NAPLs) that pollute the soil and groundwater for decades (Interstate Technology Regulatory Council, 2000; Soga et al., 2004; Katsoyiannis and Samara, 2005; National Research Council, 2013; Waclawek et al., 2016). Moreover, many of these NAPLs are formed by complex mixtures rather than single compounds (Mobile et al., 2016; Tomlinson et al., 2017). This constitutes a ubiquitous problem in the environment and it is a challenge to solve, especially in the case of Dense NAPL while this phase percolated through the saturated zone.

To shorten the required time for the remediation of sites polluted with NAPLs, surfactants and cosolvents have been recently proposed and applied (Mulligan et al., 2001; Dugan et al., 2010; Mao et al., 2015; Trellu et al., 2016; Besha et al., 2018; Dominguez et al., 2019b; Santos et al., 2019). Surfactants reduce the interfacial tension between the organic phase (NAPL) and the aqueous phase (Paria, 2008; Dugan et al., 2010) due to their amphiphilic properties (Rosen and Kunjappu, 2012) and increase the solubility of HOCs in the aqueous phase. Moreover, a partition of the surfactant between the aqueous and organic phase occurs, decreasing the viscosity of the organic phase and facilitating its extraction (Paria, 2008; Kang et al., 2019).

The SEAR (Surfactant Enhancement Aquifer Remediation) treatment consists of injecting an aqueous solution of surfactant-cosolvent into the areas contaminated by HOCs, and subsequently extracting the injected fluid and treating it *on-site* (Londergan and Yeh, 2003; Dugan et al., 2010; Mao et al., 2015; Dahal et al., 2016; Besha et al., 2018). This technology has already been implemented, but it presents some concerns. The dispersion of contamination by the injection of the surfactant must be avoided, and *on-site* treatment of the extracted fluid is required since the contamination has only changed from the soil phase to the aqueous phase.

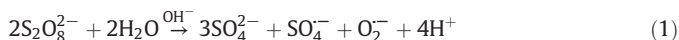
Surfactant Enhanced In-Situ Chemical Oxidation (S-ISCO) consists of the simultaneous injection of a surfactant solution and oxidants to increase the solubility of HOCs in the aqueous phase, where the oxidation takes place, and thus reduce the time required for the removal of the contaminant mass in the aquifer (Lanoue et al., 2011; Besha et al., 2018). S-ISCO treatment minimizes the inconvenience of the SEAR technology since a lower concentration of surfactant is used: the problem of contaminant dispersion is minimized, and the injected oxidant produces the destruction of the HOCs *in-situ*. Although this technology is emerging, studies in the literature on its application are scarce (Dugan et al., 2009; Dugan et al., 2010; Hoag and Collins, 2011; Wang et al., 2013; Lominchar et al., 2018a).

Hydrogen peroxide and persulfate have often been applied to remove the contaminants in the subsoil (Siegrist et al., 2011). Both oxidants can produce radicals under certain conditions. H_2O_2 catalyzed by iron salts (Fenton Reagent) generates hydroxyl radicals ($\cdot OH$) and persulfate (PS), activated by Fe(II), heat, or alkali, can produce sulfate ($SO_4^{\cdot -}$) and/or hydroxyl radicals, which both have high oxidation capacity (Bacocchi, 2013; Devi et al., 2016).

However, the Fenton process frequently exhibits significant limitations for *in-situ* applications due to the high unproductive consumption of this oxidant by the soil. Moreover, the optimal pH for the Fenton process is 2.8–3, and it not feasible to maintain these conditions in the subsoil. The optimal acidic conditions are quite difficult to obtain in the subsoil due to the high content of carbonates in the groundwater usually (Siegrist et al., 2011).

These disadvantages explain the increase in the use of activated PS as the oxidant in ISCO treatments in recent years. PS is highly stable in the subsoil, which means that it can be transported for long distances, is easy to handle and produces benign end-products (Sra et al., 2014; Ike et al., 2018). Among the activation methods of PS, the use of bases

(mainly NaOH) is gaining attention in recent years (Furman et al., 2010; Lominchar et al., 2018b). In the alkaline activation of PS, multiple reactive species are produced (Liang and Lei, 2015), according to Eqs. (1) and (2), making the process highly versatile against a wide variety of pollutants. Moreover, it does not require either heat or acidic conditions (such as activation by metals), which are both challenging to achieve in the subsoil.



In works elsewhere, it was found that in the presence of alkali some Chlorinated Organic Compounds (COCs) suffered dehydrochlorination reactions generating species of lower toxicity, which adds an advantage in the use of alkali as an activator (Santos et al., 2018b; García-Cervilla et al., 2020b; Lorenzo et al., 2020).

The success of the application of S-ISCO technology depends on the selection of the most suitable oxidizer-surfactant/pollutant system. The oxidant must be effective in abating the contaminants, and the surfactant must increase the solubility of these contaminants and be relatively stable with the oxidant. The oxidants can attack the surfactant and the pollutants because both are organic compounds. Therefore, the surfactant stability can be a crucial aspect in the design of an S-ISCO process. Another important aspect to consider is the possible loss of surfactant into the soil by adsorption, which depends on both the nature of the surfactant and the type of soil (Lee et al., 2000; Yang et al., 2006).

However, only a few works are available in the literature studying the oxidation of pollutants in the presence of surfactants, and few of them use PS as an oxidant. Moreover, most of these works are carried out in two steps. In the first step, the pollutant is solubilized by a surfactant in the aqueous emulsion. Usually, an artificially spiked soil with a single pollutant or a DNAPL of a pure pollutant is in contact with the aqueous surfactant emulsion. In the next step, the aqueous emulsion with the surfactant and the pollutant extracted is treated *on-site* using PS. Some works used PS activated by UV radiation (Long et al., 2013; Bai et al., 2019) with toluene and phenanthrene as pollutants and SDS or Tween 80 as surfactants. Another work studied the abatement of phenanthrene in the emulsion of three surfactants (SDS, lauryl betaine, and Neodil 25-7) by temperature (Bouزيد et al., 2017). Zheng et al. (2016) and Tsai et al. (2009) studied the removal of tetrachloroethylene (in spiked sand) using Tween 80 as a surfactant and PS activated by Fe (II), respectively (Tsai et al., 2009; Zheng et al., 2016). Long et al. (2014) studied the selective abatement of toluene in an emulsion with SDS and iron as a PS activator (Long et al., 2014). In these last works, iron was used to maintain the pH acidic (Tsai et al., 2009) or was presumably adjusted to the acidic range while this variable was not controlled with the reaction progress (Long et al., 2014; Zheng et al., 2016). Even though methods cited above are effective in an *on-site* treatment of the pollutant-surfactant emulsion, they cannot be applied in the subsoil and are not, therefore, the most suitable for an *in-situ* S-ISCO treatment.

In this work, the simultaneous addition of biodegradable surfactants (nonionic and anionic) and PS activated by alkali (PSA) to remove a real DNAPL consisting of 28 COCs (Santos et al., 2018a) originated as a liquid waste in the lindane production process is studied. Stability of the surfactant with the oxidant and the surfactant capacity remaining after surfactant oxidation are firstly studied to choose the most suitable surfactants for the S-ISCO treatment. Influence of the initial surfactant concentration, initial concentration of PS and NaOH:PS molar ratio on the unproductive consumption of oxidant by the surfactant and the solubilization capacity of oxidized surfactants are analyzed. For the selected surfactants the time required for the abatement of a mass of DNAPL by PSA with and without simultaneous addition of surfactants

is determined, in order to assess the advantages of S-ISCO vs. ISCO process.

2. Materials and methods

2.1. Chemicals and DNAPL

In this work, four surfactants were tested: Sodium dodecyl sulfate (SDS), an anionic surfactant applied in soil washing treatments and three nonionic surfactants: *E*-Mulse®3 (E3), Tween®80 (T80), and a mixture of 35%w of Tween®80 and 65%w:w of Span®80 (TS80). The first three are commercial surfactants, and the last one is a mixture of two commercial surfactants, which was successfully tested in a previous study (Corcho et al., 2015) using a Dense Non-Aqueous Phase Liquid (DNAPL) similar to the one employed in this work. In Table SM-1, the properties of these surfactants are summarized.

Persulfate (PS) was provided by Sigma-Aldrich and the activator (sodium hydroxide), by Riedel-de Haën. PS quantification was carried out using a titration method with potassium iodide (KI, Fisher Chemical), sodium hydrogen carbonate (NaHCO₃, Panreac), sodium thiosulfate pentahydrate (Na₂S₂O₃·5H₂O, Sigma-Aldrich) and acetic acid (C₂H₄O₂, Sigma-Aldrich) as reactants. The aqueous solutions were prepared using Milli-Q water. Moreover, sodium bisulfite (NaHSO₃, Sigma-Aldrich) was used to quench PS in the reaction samples taken.

The DNAPL sample used was obtained at Bailin landfill (Sabiñanigo, Spain). This sample was characterized in a previous work finding that it was composed of 28 Chlorinated Organic Compounds COCs (Santos et al., 2018a). In Table SM-2, the composition of the DNAPL sample (CAS and acronym) is provided. Moreover, as the oxidation of surfactant and COCs was carried out in strong alkaline conditions, dehydrochlorination reactions of pentachlorocyclohexene (PentaCXs) and hexachlorocyclohexane (HCHs) isomers to trichlorobenzene isomers (TCBs), and hexachlorocyclohexane (HexaCXs) and heptachlorocyclohexane isomers (HeptaCHs) to tetrachlorobenzenes (TetraCBs) are expected in the aqueous phase (Lorenzo et al., 2020). For a mass of DNAPL completely solubilized in the aqueous phase, the molar fraction of each COC in alkaline conditions (pH > 12) is also shown in Table SM-2.

The quantification of COCs was accomplished using commercial compounds (analytical quality, Sigma-Aldrich) to prepare calibration curves: Chlorobenzene (CB), 1,2-dichlorobenzene (1,2-DCB), 1,3-dichlorobenzene (1,3-DCB), 1,4-dichlorobenzene (1,4-DCB), 1,2,3-trichlorobenzene (1,2,3-TCB), 1,2,3,4-tetrachlorobenzene (1,2,3,4-TetraCB), 1,2,3,5-tetrachlorobenzene (1,2,3,5-TetraCB), and 1,2,3,4-tetrachlorobenzene (1,2,3,4-TetraCB), HCHs (α , β , γ , δ and ϵ -HCH). The calibration samples were prepared, dissolving the COCs in methanol. Bicyclohexyl (C₁₂H₂₂, Sigma-Aldrich) and tetrachloroethane (C₂H₂Cl₄, Sigma-Aldrich) were used as internal standards (ISTD) for quantification in flame ionization detector (FID) and electron capture detector (ECD), respectively.

2.2. Experimental runs and procedures

Four sets of runs were carried out. In the first set, the influence of NaOH and NaCl concentration on the Critical Micellar Concentration (CMC) of the surfactants was determined. In set 2, the unproductive consumption of persulfate of each one of the tested surfactants was studied. Operating conditions similar to those used in a S-ISCO treatment were applied (Beshu et al., 2018). In set 3, the surfactant capacity remaining after oxidation treatment was studied. In set 4, the removal of COCs from the surfactant emulsion was evaluated. The procedure is described below.

2.2.1. Set 1: effect of NaOH and NaCl concentration on CMC

The effect of salinity (NaCl concentration) and pH (NaOH) on the CMC value was studied for the four surfactants (SDS, E3, T80, and TS80). Aqueous solutions of 12 g·L⁻¹ of the surfactant and NaOH or

NaCl concentration within the range 0–500 mmol·L⁻¹ were prepared in closed glass vials of 20 mL. After magnetic agitation for 2 h and 24 h of rest at room conditions, the CMC of the surfactant solution was measured by the procedure described elsewhere (Dominguez et al., 2019b).

2.2.2. Set 2: unproductive consumption of oxidant by surfactants

In set 2, the consumption of PS due to the oxidation reaction of the surfactant was studied to determine the unproductive consumption of oxidant. In this set of experiments, 22 runs were carried out in the absence of DNAPL. The variables considered were the initial concentration of surfactant (within the range 3–12 g·L⁻¹), the initial PS concentration (42–84 mmol·L⁻¹) and the NaOH:PS molar ratio (1:1 and 2:1). The experimental conditions are summarized in Table SM-3. In runs C1–C5, C6–C11, C12–C16, and C17–C22, SDS, E3, T80, and TS80 were used as surfactants, respectively. Moreover, four experiments were accomplished without surfactants as blank experiments.

This set of runs was carried out in well-mixed batch reactors, consisting of a 40 mL PTFE tube with PTFE screw caps. A volume of 35 mL of the aqueous solution with the corresponding concentrations of NaOH, PS, and surfactant was placed in the PTFE tube (time zero). The tubes were stirred using a Labolan rotary agitator (ref 51752) under controlled room conditions (22 °C ± 1) up to 860 h. At different reaction times, a tube was sacrificed, and the remaining PS, pH, Surface Tension, and total organic carbon (TOC) were quantified. Furthermore, at 360 h of reaction, a sample of the oxidized solution was analyzed by GC–MS to identify the byproducts of surfactant oxidation. The experiments were carried out in triplicate finding a standard deviation of <10%. In the following section, an average of the measured values is used. All experimental conditions are shown in Table SM-3.

2.2.3. Set 3: study of solubilization capacity of the partially oxidized surfactant

The solubilization capacity that remains in the partially oxidized surfactant solution was checked by the dissolution of an amount of DNAPL. This amount was compared with the amount of DNAPL solubilized at time zero (before the partial oxidation of surfactant).

After 168 and 360 h of reaction time in runs C1, C5, C6, C10, C11, C15, C16, C20 in Table SM-3 samples of 20 mL were taken and quenched, adding 1.5 g of Na₂S₂O₃·5H₂O. Then a mass of DNAPL was added. The mixtures were magnetically agitated for 6 h to ensure that the equilibrium between the organic and aqueous phase was achieved. After that, the emulsions settled for 24 h. The aqueous phase was analyzed by GC-FID/ECD to quantify the solubilized COCs. The experimental conditions of this set of runs are shown in Table SM-4.

2.2.4. Set 4: oxidation of COCs in emulsion

In these runs, the surfactant and the pollutant were in contact with the oxidant (PS) at the activator (NaOH) from time zero. The surfactants used were SDS and E3. Firstly, the emulsion with solubilized COCs was prepared by adding 1.85 mmol of DNAPL to 500 mL of an aqueous solution of 12 g·L⁻¹ of SDS or 3 g·L⁻¹ of E3 in alkaline conditions (84 mmol L⁻¹ of NaOH). These solutions were stirred at 400 rpm for 6 h and settled for 24 h. Then, samples of 30 mL of each supernatant were taken, placed in PTFE tubes with PTFE screw caps and PS was added (time zero) to each tube to reach a concentration of 84 mmol L⁻¹. The experimental conditions are shown in Table SM-5. The PTFE tubes were agitated at 80 rpm in the rotatory agitator previously described. At different reaction times, a tube with SDS (run S1) or E3 (run S2) was sacrificed, and the remaining PS, COCs, TOC, and pH were measured.

2.3. Analysis

The CMC was determined with a Krüss tensiometer (Hamburg, Germany) by measuring the surface tension (ST) of a concentration series of samples of surfactant (0.001–3 g·L⁻¹) in pure water and constant concentration of NaOH and NaCl in each experiment. The CMC

resulted from the intersection between the regression line of surfactant concentration vs. ST data (in the region where both variables are linearly dependent) and the straight line which passes through the plateau obtained above the CMC (in the region where the ST is independent of the concentration of surfactant).

The total organic carbon (TOC) concentration of the aqueous emulsion was measured with a Shimadzu TOC-V CSH analyzer (Kyoto, Japan) using an infrared detector.

The concentration of PS in aqueous solution was determined by iodometric titration using a potentiometric titration analyzer (Metrohm, Tiamo 2.3, Gallen, Switzerland). The pH was measured using a Basic 20-CRISON pH electrode (Barcelona, Spain).

COCs were identified in the aqueous phases by using a gas chromatograph (GC) coupled with a mass selective detector (Agilent MSD 5975B, Santa Clara, CA, USA). The quantification of COCs was carried out using a GC (Agilent 6890, Santa Clara, CA, USA) with a flame ionization detector (FID, Santa Clara, CA, USA) and electron capture detector (ECD, Santa Clara, CA, USA), simultaneously. The chromatographic method was described elsewhere (Santos et al., 2018a). The samples were taken at different reaction times. Due to the presence of a surfactant in the aqueous solution, the following procedure was performed for COC analysis. When SDS was used, a mass of salt (NaCl) was added to a volume of the emulsion until it broke. After that, hexane was added, and the mixture was vigorously shaken for 2 min. The hexane phase with the COCs extracted was injected in the GC.

When using the nonionic surfactants, it was not possible to break the emulsion with the addition of salt. In this case, 0.1 mL of the emulsion was added to 0.9 mL of methanol and injected in the GC.

Carboxylic acids were measured by ionic chromatography (Metrohm 761 Compact IC, Gallen, Switzerland) with anionic chemical suppression and a stationary-phase conductivity detector was a column from Metrosep (A SUPP5 5-250, which dimensions are 25 cm in length and 4 mm in diameter) and the mobile phase was a solution of NaHCO_3 (1 mM) and Na_2CO_3 (3.2 mM) in water at $0.7 \text{ mL} \cdot \text{min}^{-1}$. The Results injection system (injection volume = 250 μL) was coupled with an on-line filtering system (0.45 μm).

3. Results

3.1. Effect of NaOH and NaCl concentration on the CMC of surfactants

The concentration of NaOH (activator of PS) in the medium could modify the capacity of the surfactant to generate micelles (Rosen and Kunjappu, 2012). Moreover, the groundwater in the polluted site is likely to present high concentrations of salt (conductivity of the groundwater in the landfill is higher than 3000 $\mu\text{S}/\text{cm}$ (Santos et al., 2018b)) and these salts could also affect the surfactant properties. For this reason, NaCl was selected to study the effect of the ion concentration on the surfactant properties. The CMC values of surfactants selected were measured at different concentrations of NaOH and NaCl, as indicated in Sections 2.2.1 and 2.3. The results obtained are plotted in Fig. SM-1.

As can be seen in Fig. SM-1, both NaOH and NaCl concentration greatly affect the CMC of SDS (ionic surfactant). In contrast, the CMCs of the nonionic surfactants do not change in the range of NaOH or NaCl concentration tested. The observed effect of ions on the CMC of the anionic surfactant SDS coincides with that reported by Rosen (Rosen and Kunjappu, 2012). Moreover, for a given molar concentration of salt in the media, no differences were found with NaOH or NaCl.

As is plotted in Fig. SM-1a, the higher the concentration of NaOH or NaCl, the lower the CMC of SDS. The drop in the CMC value with SDS at high concentrations of salts can be attributed to the decrease in the electrostatic repulsions among the ionic head groups of the anionic surfactant, located at the micelle outside, in the presence of the additional electrolyte (Rosen and Kunjappu, 2012). Moreover, it should be expected that the lower the CMC value of SDS in the presence of an electrolyte, the higher the solubilization of DNAPL. An increase in the

molar solubility ratio (MSR) of COCs when the NaOH was added to the SDS solution was reported elsewhere ($MSR_{without \text{ NaOH}} = 0.7 \text{ mmol}_{\text{COCs}} \cdot g_{\text{surf}}^{-1}$ and $MSR_{with \text{ NaOH}} = 1.32 \text{ mmol}_{\text{COCs}} \cdot g_{\text{surf}}^{-1}$) (García-Cervilla et al., 2020a). Moreover, in that work it was also found that the solubility of DNAPL with the three nonionic surfactants studied here was not affected by the addition of alkali, in accordance with the constant CMC shown in Fig. SM-1b. For the nonionic surfactant here used an almost constant value $MSR = 4.33 \text{ mmol}_{\text{COCs}} \cdot g_{\text{surf}}^{-1}$ was obtained. Therefore, it can be concluded that the CMC of the nonionic surfactants tested is not affected by the NaCl or NaOH addition in the whole range of concentration studied here. On the other hand, the electrolyte concentration in the medium has a remarkable influence on CMC of the anionic surfactant SDS, but this effect does change with the type of electrolyte used (NaOH or NaCl). The remediation treatment selected requires the addition of alkali to activate PS, but the addition of chloride is not needed. Although chloride is naturally present in the groundwater of the polluted site at a concentration in the range 11–28 $\text{mmol} \cdot \text{L}^{-1}$ (Santos et al., 2018b; Santos et al., 2019) this concentration did not modify the results obtained in the abatement of COCs by PS activated by alkali (Santos et al., 2018b).

3.2. Unproductive consumption of persulfate by the surfactants

In this section, a study of the main variables that can affect the rate of persulfate consumption in the presence of surfactants and absence of DNAPL is accomplished.

Firstly, some blank runs were carried out to evaluate the consumption of PS activated by alkali in the absence of surfactants, experiments (B1 to B4 in Table SM-3). After 864 h of reaction time, the consumption of persulfate was lower than 0.05 under the more powerful oxidant conditions tested ($C_{\text{PS},0} = 84 \text{ mmol} \cdot \text{L}^{-1}$, $C_{\text{NaOH},0} = 186 \text{ mmol} \cdot \text{L}^{-1}$). For this reason, it was assumed that the consumption of PS in the absence of surfactants was negligible in the range of variables and time used here, in accordance with previous reports (Lominchar et al., 2018b; García-Cervilla et al., 2020b).

3.2.1. Effect of the initial surfactant concentration

The effect of the initial concentration of surfactant (3, 6 and 12 $\text{g} \cdot \text{L}^{-1}$) on PS decomposition was studied at $C_{\text{PS},0} = 84 \text{ mmol} \cdot \text{L}^{-1}$, the molar ratio of NaOH:PS = 1 and room temperature. The experimental conditions of the runs were summarized in Table SM-3. The remaining PS concentration at different reaction times and different initial concentrations of surfactants was measured, and results obtained are plotted in Fig. 1.

Fig. 1a shows the experimental values of the remaining PS when SDS was used. As can be seen, the fraction of the remaining persulfate was close to 0.9 in the different initial concentrations of SDS tested. Therefore, it can be considered that the anionic surfactant is stable against PS and did not produce a significant unproductive consumption of the oxidant.

The remaining concentration of PS when nonionic surfactants were used is shown in Fig. 1b, c, and d for E3, T80, and TS80, respectively. In contrast to the results obtained when employing SDS, the presence of nonionic surfactants enhanced the consumption of PS, in accordance with that previously reported in the literature (Wang et al., 2017; Lominchar et al., 2018a; Wang et al., 2020). Wang et al. (Wang et al., 2020) studied the consumption of PS by anionic and nonionic surfactants using thermally activated PS. They found higher consumption of PS by nonionic surfactant than by anionic surfactant. The higher stability of SDS against PS was already reported by Wang et al. (2020), using thermal activated PS. These authors reported the existence of repulsion forces between the anionic radicals (SO_4^- in that work) and the sulfonate anions located at the exterior of the SDS micelle (Wang et al., 2020). Using PSA, the repulsions are the consequence of the anionic radical O_2^- , according to Eq. (1) and the activator (OH^-). Moreover, Wang et al. (2020) considered that the hydroxyl radical can attack the C—H

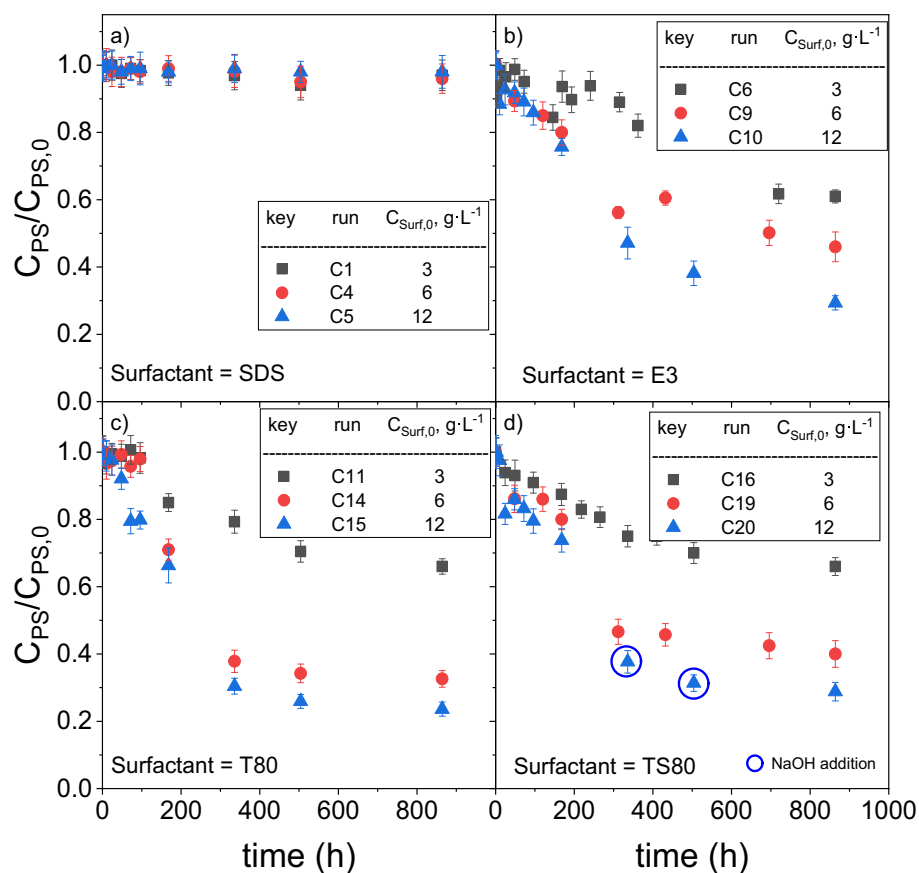


Fig. 1. Remaining PS vs. reaction time at different initial surfactant concentrations (3, 6 and $12 g \cdot L^{-1}$) at $C_{PS,0} = 84 mmol \cdot L^{-1}$ and NaOH:PS = $1 mmol \cdot mmol^{-1}$. Runs in Table SM-3 (a) SDS, (b) E3, (c) T80, and (d) TS80. In run C20, NaOH was added twice (marked with circles) to keep pH over 12.

bond of the linear alkyl chain of SDS molecules in solution (by hydrogen abstraction). The alkyl radical formed can react with $(S_2O_8)^{2-}$ to cause persulfate decomposition and generate more radicals (in this work, hydroxyl and superoxide radicals). However, as these authors explain, the linear alkyl radical is relatively stable against PS and retards the PS decomposition. The fact that the linear alkyl chain of SDS is more refractory to oxidation than the polyethoxylated chains of nonionic surfactants (E3, T80 y TS80) has also been reported by Brand et al. (1998) and Pagano et al. (2008).

As can be seen in Fig. 1b to d, if nonionic surfactants are used, the higher the initial concentration of surfactant, the lower the remaining PS concentration. This behavior was also found by other authors (Wang et al., 2020) in the consumption of thermally activated PS using Brij 35, whose chemical structure is similar to some of the surfactants used here.

For the three nonionic surfactants used, the persulfate conversion was about 0.3 at $t = 900$ h when the initial surfactant concentration was $3 g \cdot L^{-1}$ ($C_{PS,0} = 84 mmol \cdot L^{-1}$ and NaOH:PS = $1 mmol \cdot mmol^{-1}$). However, the consumption of PS was about 0.7 for E3 and TS80 and 0.8 for T80 when the initial concentration of surfactant was $12 g \cdot L^{-1}$. Therefore, the increase in surfactant concentration has a remarkable effect on PS consumption. Moreover, the unproductive consumption of PS by E3 or TS80 is slightly lower than that by T80 in the same conditions.

Runs in Table SM-3 were carried out at a pH close to 13. However, in run C20 (using $12 g \cdot L^{-1}$ of TS80) the pH dropped to 10 at reaction times of 168 h and 336 h. At each of these times, NaOH was added to raise the pH to 13. This drop of pH could indicate that the oxidation of TS80 produces byproducts with stronger acidity since this decrease was only detected using this surfactant and PS consumption obtained was similar with TS80, E3 and T80.

The mineralization of the surfactants was studied from results in runs C1 and C5 for SDS; C6 and C10 for E3; C11 and C15 using T80 and C16 and C20 for TS80. The remaining TOC was measured at 864 h of reaction time. The corresponding initial TOC was calculated with the fraction of C in the surfactant mass ($FR_{TOC, surf}$) in Table S1. Regardless of the type of surfactant and PS conversion, experimental data provided in Fig. SM-2, negligible surfactant mineralization was achieved at all of the initial surfactant concentrations tested (3 and $12 g \cdot L^{-1}$). This finding has also been reported in the literature (Pagano et al., 2008; Mendez-Diaz et al., 2010).

3.2.2. Effect of the initial concentration of PS

The effect of the initial concentration of PS was studied for the four surfactants selected at a concentration of $3 g \cdot L^{-1}$ and using two initial concentrations of PS (84 and $42 mmol \cdot L^{-1}$). The results of the fractional remaining PS vs. reaction time are plotted in Fig. 2.

As can be seen in Fig. 2a, the consumption of PS by SDS was negligible at the two PS concentrations used, and their effect on PS conversion cannot be discerned. On the contrary, when nonionic surfactants were used a decrease in oxidant conversion was always observed when the initial concentration of PS decreases. For instance, at 864 h the degradation of PS were 0.2 and 0.4 when the initial PS concentration was $42 mmol \cdot L^{-1}$, or $84 mmol \cdot L^{-1}$, respectively. This fact agrees with the reported by Wang et al. (2020), considering that the reactions between surfactants and PS involved a radical-chain mechanism. The surfactant molecules react with the radicals, and these react with the PS anion to produce more radicals, increasing the PS consumption. In this way, the higher the initial concentration of PS used, the faster the initiation and propagation reactions are. This effect is more noticeable when nonionic surfactants are used due to the higher reactivity of the

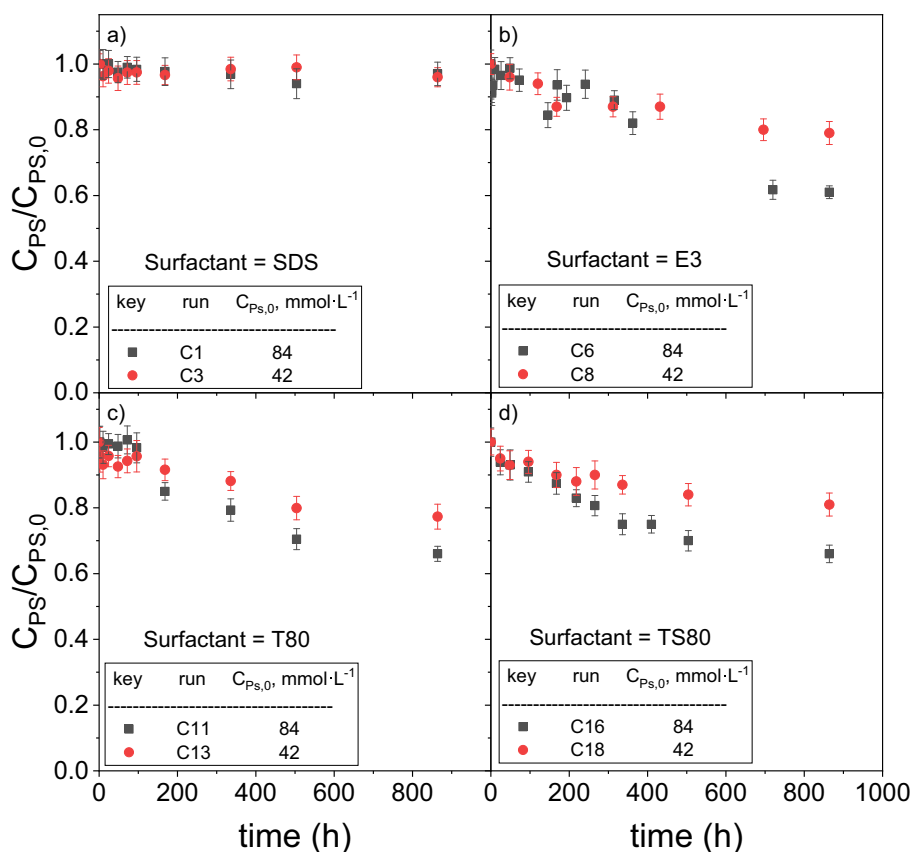


Fig. 2. Fractional remaining PS at different initial concentrations of PS (42 and $84 \text{ mmol} \cdot \text{L}^{-1}$) for the surfactants (a) SDS, (b) E3, (c) T80 and (d) TS80. Runs in Table SM-3, $C_{\text{surf},0} = 3 \text{ g} \cdot \text{L}^{-1}$ NaOH:PS = $1 \text{ mmol} \cdot \text{mmol}^{-1}$.

radicals formed compared with the alkyl radicals produced with SDS (Wang et al., 2020).

The highest mineralization conversion (5% at 864 h) was obtained using TS80 and $84 \text{ mmol} \cdot \text{L}^{-1}$ of PS (run C18), in accordance with the data plotted in Fig. SM-2.

3.2.3. Effect of NaOH:PS molar ratio

When an alkali is used to activate PS, the molar ratio between the activator (NaOH) and the oxidant (PS) could influence the production of radicals. In Fig. 3, the fractional remaining PS vs. reaction time obtained with NaOH:PS molar ratios 1 and 2 are shown. In these runs, PS and surfactant concentrations were $84 \text{ mmol} \cdot \text{L}^{-1}$ and $3 \text{ g} \cdot \text{L}^{-1}$, respectively. As can be seen, small differences were found in PS conversion with both molar ratios tested. The pH change with time noticed in runs plotted in Fig. 3 was also monitored, and the pH profiles are shown in Fig. SM-3 of the Supplementary material. It was found that the pH was quite constant for 864 h, being slightly lower when the NaOH:PS ratio had a value of 1 (pH was higher than 12 in all cases). An almost negligible influence of this activator:oxidant ratio was found on the PS or pollutant conversion if pH was high enough (>12) in accordance with that reported in the literature (Santos et al., 2018b; Dominguez et al., 2019a; Dominguez et al., 2020; García-Cervilla et al., 2020b).

3.3. Effect of the oxidant on surfactant solubilization capacity

It is expected that the reaction between the oxidant and the surfactant modify the surfactant properties, among them, the solubilization capacity of the latter. The runs in Table SM-4 (set 3) were carried out to study the loss of solubilization capacity of the partially oxidized surfactant. This information and the unproductive consumption of PS obtained from runs in set 1 are used in the selection of the more appropriate surfactants in an S-ISCO application.

As indicated in Section 2.2.3, the aqueous surfactant solutions were in contact with the oxidant under the experimental conditions in Table SM-3. After 360 h of reaction time, the reaction was quenched with sodium bisulfite, and an amount of DNAPL was added to the partially oxidized surfactant solution. After the agitation and settling of the resulting mixture for 24 h, the concentration of dissolved COCs was measured.

The molar solubilization ratios (MSR) of each surfactant for the DNAPL used here were experimentally found elsewhere (García-Cervilla et al., 2020a). The MSR in conditions of equilibrium is calculated using Eq. (3).

$$MSR = \frac{(\sum C_{jAQ})_{eq}}{(C_{\text{surf}AQ})_{eq}} \quad (3)$$

where C_{jAQ} is the concentration of COC j in the aqueous phase ($\text{mmol}_{\text{COC}} \cdot \text{L}^{-1}$) and $C_{\text{surf}AQ}$ the surfactant concentration in the aqueous phase ($\text{g}_{\text{surf}} \cdot \text{L}^{-1}$) after equilibrium was reached. The MSR values obtained elsewhere under strong alkaline conditions (García-Cervilla et al., 2020a) were $1.32 \text{ mmol}_{\text{COCs}} \cdot \text{g}_{\text{surf}}^{-1}$ with SDS and $4.33 \text{ mmol}_{\text{COCs}} \cdot \text{g}_{\text{surf}}^{-1}$ with the nonionic surfactants (E3, T80, and TS80) and DNAPL employed here.

The surfactant initially added has been partially oxidized after a period of contact with the oxidant. An equivalent surfactant concentration (ESC in $\text{g}_{\text{surf}} \cdot \text{L}^{-1}$) is defined as the concentration of virgin surfactant that would yield the solubilization the COCs found in runs in Table SM-4, carried out with partially oxidized surfactants. The value of ESC can be estimated according to Eq. (4), using the corresponding MSR for each surfactant and the sum of solubilized COCs obtained in runs in Table SM-4, after the addition of an amount of DNAPL to the partially oxidized surfactant solution.

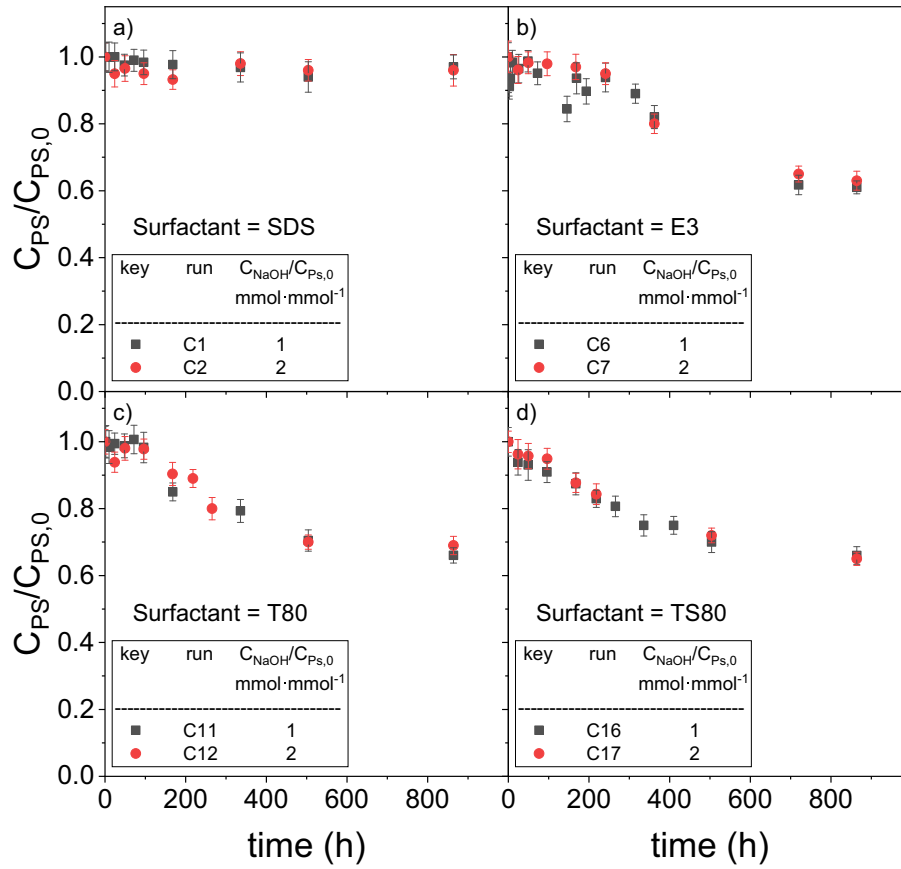


Fig. 3. Fractional remaining PS vs. reaction time at initial molar ratios NaOH:PS 1 and 2. (a) SDS, (b) E3, (c) T80, and (d) TS80. Runs in Table SM-3 $C_{Surf,0} = 3 \text{ g} \cdot \text{L}^{-1}$ and $C_{Ps,0} = 84 \text{ mmol} \cdot \text{L}^{-1}$.

$$ESC = \frac{\sum COC_j \left(\text{mmol} \cdot \text{L}^{-1} \right)}{MSR \left(\text{mmol}_{COC} \cdot \text{g}_{surf}^{-1} \right)} \quad (4)$$

The ESC value obtained by Eq. (4) is compared with the ESC value expected if the initial surfactant added were not oxidized, called ESC_0 . The value of ESC_0 is lower than $C_{surf,0}$ while the partitioning of the surfactant between aqueous and organic phases should be considered. The relation between ESC_0 and $C_{surf,0}$ is obtained by Eq. (5).

$$C_{surf,0} \cdot V_{aq} = ESC_0 \cdot V_{aq} + (C_{surf,org})_{eq} \cdot w_{DNAPL} \quad (5)$$

where V_{aq} is the volume of the aqueous phase and w_{DNAPL} the mass of DNAPL added to this volume (experiments summarized in Table SM-4).

The distribution of the surfactant among organic (DNAPL) and aqueous phases was well predicted by a linear partitioning equilibrium as shown in Eq. (6).

$$(C_{surf,org})_{eq} = K_L \cdot ESC_0 \quad (6)$$

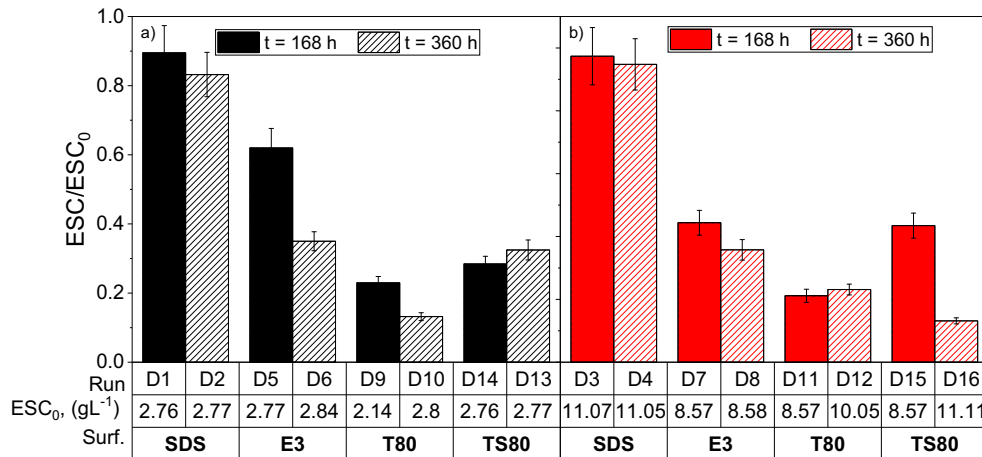


Fig. 4. Loss of surfactant solubilization capacity as ESC/ESC_0 after the surfactant solution and PS/NaOH were in contact for 168 and 360 h (a) $C_{surf,0} = 3 \text{ g} \cdot \text{L}^{-1}$, (b) $C_{surf,0} = 12 \text{ g} \cdot \text{L}^{-1}$. Experimental runs in Table SM-4.

A value of the linear partitioning coefficient $K_L = 0.02 \text{ g}_{\text{surf,ORG}} \cdot \text{L} \cdot \text{g}_{\text{surf}}^{-1} \cdot \text{g}_{\text{ORG}}^{-1}$ was found elsewhere (García-Cervilla et al., 2020a) for all the surfactants and DNAPL used in this work at $\text{pH} > 12$ and using the DNAPL from Bailin landfill.

From Eqs. (5) and (6) the value of ESC_0 can be obtained as:

$$\text{ESC}_0 = \frac{C_{\text{surf},0} \cdot V_{\text{aq}}}{V_{\text{aq}} + K_L \cdot W_{\text{DNAPL}}} \quad (7)$$

and the remaining solubilization capacity of the surfactant after its partial oxidation can be calculated by the ratio of ESC/ESC_0 . This remaining ESC/ESC_0 value is a crucial point in the S-ISCO treatment.

The ratios ESC/ESC_0 obtained at 168 and 360 h of contact between the surfactant and the oxidant are shown in Fig. 4. As can be seen, for a given surfactant, the higher the reaction time with the oxidant, the higher the loss of surfactant capacity. Moreover, the ESC/ESC_0 ratio depends on both the initial concentration of the surfactant and the surfactant studied. Some surfactants (T80 and TS80) show a quick loss of ESC in the early stages. This fact can be explained by the preferential chemical attacks of PS on the polyethoxylated functional groups (Wang et al., 2020). This oxidation can produce clouding/oiling in the solutions (Mukherjee et al., 2011) and a decrease in the ESC value. The remaining surfactant capacity could be attributed to the surfactant properties of the oxidation byproducts (Pagano et al., 2008).

The highest values of ESC/ESC_0 (close to unity) are obtained with SDS (anionic surfactant) in accordance with the lowest consumption of PS noticed using this surfactant (Fig. 1). The loss of solubilization capacity was higher with the nonionic surfactants; among these, the lowest decrease was obtained with E3.

The DNAPL used was composed of a total of 28 COCs, as detailed in Section 2.1, that can be gathered in compounds with the same number of chlorine atoms in the molecule. The COCs dissolved in the aqueous phase in runs in Table SM-4 were analyzed to figure out if the oxidized surfactant showed preference in solubilizing some type of COCs. Molar fraction (as a percentage) of COCs in solution when the surfactant was partially oxidized (at 168 and 360 h) is shown in Fig. SM-4 in the Supplementary material. The corresponding distribution of COCs in the original DNAPL phase in alkaline conditions (Lorenzo et al., 2020) was summarized in Table SM-2 and is also shown in Fig. SM-4. It can be seen that the distribution of COCs in the DNAPL (at alkaline conditions) is similar to that obtained for the solubilized COCs in the partially oxidized surfactant aqueous emulsion, independently of oxidation time. Differences are lower than 15%. This fact can be explained assuming that the organic phase is similarly trapped in the micelles formed by virgin molecules of partially oxidized surfactant.

3.4. Oxidation of COCs in aqueous surfactant emulsion by PS activated with alkali

Surfactants and oxidants are simultaneously injected in an S-ISCO treatment with the scope of enhancing the solubilization of hydrophobic organic pollutants. Consequently, a decrease in the time required for the removal of the NAPL mass from the site is expected. However, this time is not proportional to the increase in pollutant solubilization. The competition of surfactants and contaminants for the oxidant, and the protective effect of the surfactant against the oxidation of pollutants trapped in the micelles should also be considered.

The experiments in Table SM-5 were carried out, adding the oxidant (PS) and the activator (NaOH) to the aqueous emulsion containing the pollutant (DNAPL solubilized) and the surfactant, according to the procedure in Section 2.2.4. SDS and E3 were selected as the anionic and nonionic surfactants, respectively, for this study. As mentioned above, SDS presented lower MSR than nonionic surfactants but a negligible consumption of PS. On the other hand, E3 was the nonionic surfactant that yielded less PS consumption and a higher ESC/ESC_0 ratio.

Taking into account the MSR values ($\text{MSR}_{\text{SDS}} = 1.32 \text{ mmol COCs g}_{\text{SDS}}^{-1}$ and $\text{MSR}_{\text{E3}} = 4.33 \text{ mmol COCs g}_{\text{E3}}^{-1}$) the solubilization of the DNAPL added (3.7 mmol in 1 L of aqueous surfactant solution) was complete with the initial concentration used for SDS ($12 \text{ g} \cdot \text{L}^{-1}$) and E3 ($3 \text{ g} \cdot \text{L}^{-1}$). In both runs in Table SM-5, PS concentration and NaOH/PS molar ratio were $84 \text{ mmol} \cdot \text{L}^{-1}$ and 1, respectively.

At time zero (when PS was added), the concentration of COCs dissolved was $3.70 \text{ mmol}_{\text{COCs}} \cdot \text{L}^{-1}$. At different reaction times, a vial with SDS (run S1) or E3 (run S2) was sacrificed, and the remaining PS, COCs, TOC, and pH were measured. In this set of runs, the total reaction volume was diluted in MeOH (1:10 in volume) and analyzed. In this way, the total amount of COCs in the reaction media was quantified, regardless of the phases present in the vial. The PS and COCs profiles showing time are plotted in Fig. 5.

In Fig. 5a, the remaining fractional PS vs. time in runs S1 and S2 in Table SM-5 (simultaneous oxidation of COCs and surfactants from time zero) is plotted with crossed symbols. For the scope of comparison, the results obtained at the same oxidant, activator and surfactant concentrations but without dissolved COCs (runs C5 and C6 in Table SM-3) are also shown (plotted with solid symbols). It can be observed that similar PS consumption was obtained despite the presence or not of COCs in solution.

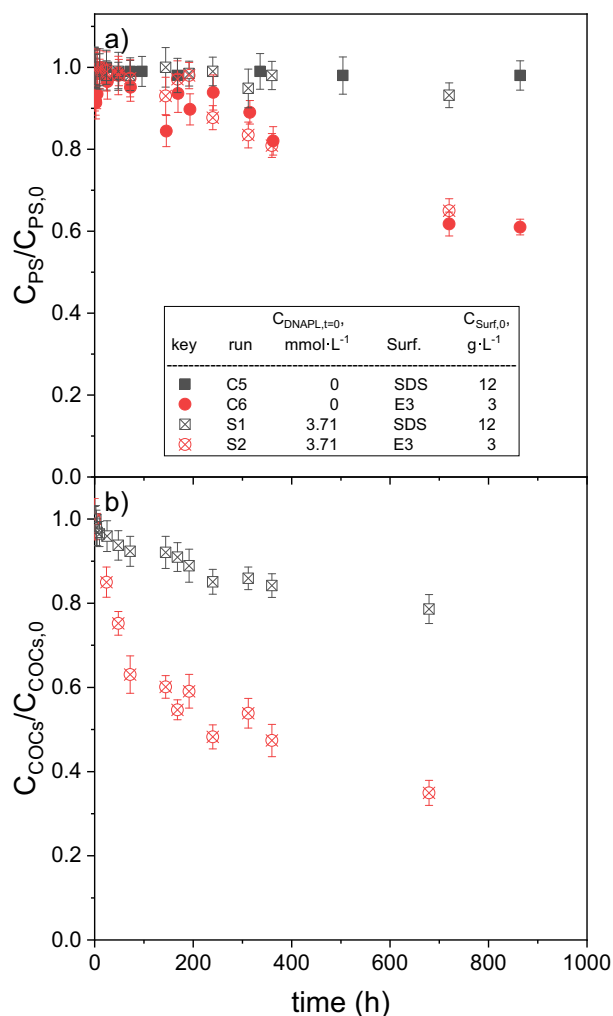


Fig. 5. Fractional remaining of a) PS and b) COC vs. time using SDS ($12 \text{ g} \cdot \text{L}^{-1}$) and E3 ($3 \text{ g} \cdot \text{L}^{-1}$) and $C_{\text{ps},0} = 84 \text{ mmol} \cdot \text{L}^{-1}$, NaOH:PS molar ratio = 1. Solid symbols correspond to runs without COCs in solution (Runs C5, C6, Table SM-3) and data with initial solubilized DNAPL ($3.709 \text{ mmol COCs L}_{\text{aq}}^{-1}$, runs S1 and S2 in Table SM-5) are plotted with crossed symbols.

The remaining fractional COCs with the reaction time in runs S1 and S2 (Table SM-5) are plotted in Fig. 5b. As can be seen, the conversion of COCs with time was much higher with E3 than with SDS, despite the higher unproductive PS consumption in the first case. At 679 h, the conversion of COCs dissolved in E3 (run S2) and SDS (run S1) was 0.65 and 0.21, respectively. As can be seen, the conversion of COCs with time was much higher with E3 than with SDS, despite the higher unproductive PS consumption in the first case. At 679 h, the conversion of COCs dissolved in E3 (run S2) and SDS (run S1) was 0.65 and 0.21, respectively. The inhibition of the potential oxidation of PS caused by SDS can be explained by the electrostatic repulsion forces between the oxidant ($S_2O_8^{2-}$) and activator (OH^-) and the hydrophilic anionic groups of SDS. These repulsions result in lower unproductive consumption of PS and lower degradation of COCs when SDS is the surfactant used. The Coulomb forces hinder the accessibility of oxidant and activator to the inside of SDS micelle. Consequently, the production of radicals in the micelle inside decreases, resulting in lower oxidation of COC, and the organic compounds in the inside of the micelles staying isolated from the attack of the radicals (Trellu et al., 2017).

The role of hydroxyl radical in oxidation of chlorinated organics, including HCHs has been recently discussed by Wacławek et al. (2019).

On the contrary, these repulsion forces and inhibition effects are lower with nonionic surfactants. Moreover, some polar compounds, such as chlorobenzenes, can diffuse to the outside of the micelle, favoring contact between pollutants and oxidants (Rosen and Kunjappu, 2012). Therefore, despite the higher PS consumption obtained with E3, a higher conversion of COCs is obtained with this surfactant.

Moreover, the conversion of COCs with time in S-ISCO (runs S1 and S2, Table SM-5) can be compared with those calculated if the oxidation of the same mass of DNAPL took place in the absence of surfactant (ISCO). For this comparison, it is considered that an amount of 0.07 mmol of DNAPL is added to the aqueous volume ($V_{aq} = 0.02 L$) with an initial oxidant concentration $C_{PS,0} = 84 mmol \cdot L^{-1}$ and a NaOH:PS molar ratio = 1. To estimate the time required to remove this DNAPL amount in the absence of surfactant, the following assumptions have been made:

- 1) The mass transfer resistance between the organic (DNAPL) and the aqueous phase has been neglected. Therefore, the concentration of COCs in the aqueous solution corresponds to the partitioning equilibrium with the organic phase.
- 2) 1,2,4 TCB is the most abundant compound in DNAPL in alkaline conditions –Table SM-2– and this compound also has the highest solubility in these conditions ($0.17 mmol \cdot L^{-1}$) among all TCBs and TetraCBs isomers. Therefore, the concentration of COCs in solution in the absence of surfactant is set to this value ($C_{COCs}^0 \approx 0.17 mmol \cdot L^{-1} \forall time$).
- 3) The kinetics of the oxidation of chlorobenzenes in aqueous phase with PS and NaOH was obtained elsewhere (Santos et al., 2018b). The kinetic model is summarized in Eq. (8).

$$r_{j,aq} = k_{j,aq} \frac{C_{j,aq}}{M_j} C_{PS} C_{NaOH}^0 \left(mmol \cdot j \cdot L^{-1} \cdot h^{-1} \right) \quad (8)$$

where $k_{j,aq}$ is the kinetic constant of the oxidation of compound j in the aqueous phase ($j = CB, DCB, TCB, TetraCB$). A similar value of the kinetic constant $k_{j,aq}$ for all chlorobenzenes ($k_{j,aq} = 3.9 \cdot 10^{-3} L \cdot mmol^{-1} \cdot day^{-1}$) was obtained elsewhere (Santos et al., 2018b).

Based on the above assumptions, the removal rate of the moles of COCs in DNAPL added can be seen in Eq. (9).

$$-\frac{dn_{COCs}}{dt} = r_{j,aq} V_{aq} = k_1 C_{NaOH}^0 \cdot C_{PS} \cdot C_{COC}^{eq} \cdot V_{aq} \quad (9)$$

where k_1 is the kinetic constant ($0.0039 L \cdot mmol^{-1} \cdot day^{-1}$), C_{PS} the PS concentration in $mmol \cdot L^{-1}$, V_{aq} the volume of the aqueous phase and C_{COC}^{eq} the concentration of COCs in the aqueous phase. Under hypothesis

Table 1

Comparison of time required in the removal of 0.07 mmol of DNAPL in 0.020 L of the aqueous phase with surfactant (S-ISCO, Fig. 5) and without surfactant (ISCO), Eq. (11) surfactant $C_{PS,0} = 84 mmol \cdot L^{-1}$, NaOH:PS molar ratio = 1.

X_{COCs}	ISCO, time (days) (Eq. (11))	Surfactant	S-ISCO, time (days) (Fig. 5)
0.2	>15 (>360 h)	SDS	11 (264 h)
	>15 (>360 h)	E3	2 (48 h)
0.65	>51 (<1224 h)	SDS	No data
	>51 (<1224 h)	E3	28 (672 h)

2, the latter is assumed to be a constant value with time ($C_{COC}^{eq} = 0.17 mmol \cdot L^{-1}$). Integrating Eq. (9) and taking into account the conversion of COC defined in Eq. (10), the relationship between time and COC conversion in the absence of surfactants is obtained by Eq. (11).

$$X_{COCs} = 1 - \frac{n_{DNAPL}}{n_{DNAPL,0}} \quad (10)$$

$$t = n_{COCs,0} \cdot \frac{X_{COCs}}{(k_1 \cdot C_{PS} \cdot C_{TCB}^{eq} \cdot V_{aq})} \quad (11)$$

The reaction times needed to reach COC conversion values of 0.2 and 0.65 without a surfactant at $C_{PS,0} = 84 mmol \cdot L^{-1}$ and NaOH:PS molar ratio = 1, have been estimated with Eq. (11), and values are shown in Table 1. The reaction time values experimentally found to reach this conversion with SDS and E3, in the same oxidant conditions and mass of DNAPL added, are also summarized in Table 1 (values taken from Fig. 5). As can be seen, the time required to reach a certain COC conversion is remarkably lower with nonionic surfactant addition (E3) than without surfactant addition. The time needed without a surfactant, underestimated due to the equilibrium between phases, has been assumed. Moreover, the solubility of 1,2,4 TCB has been used as the concentration of dissolved COCs.

Neither non-chlorinated nor aromatic compounds were detected by GC-MS or GC-ECD-FID as oxidation byproducts of COCS in DNAPL, with or without surfactants.

4. Conclusions

The results obtained in the present work indicate that the selection of suitable surfactants for the application of an S-ISCO treatment is a complex task. It should take into account issues such as the compatibility of surfactants and oxidants, the solubilization capacity of virgin and partially oxidized surfactants, and the oxidation rate of COCs in the aqueous surfactant emulsion.

It was observed that the anionic surfactant studied (SDS) did not produce an appreciable consumption of PS in the conditions tested. However, this surfactant showed a lower molar solubility ratio (MSR) and a lower rate of COC oxidation in the emulsion. The low unproductive oxidant consumption and the low oxidation rate of COCs in the SDS micelles can be explained by the electrostatic repulsions between the reagents producing radicals (oxidant and activator) and the hydrophilic groups of SDS. The decrease in radical generation inside the micelles explains the lower oxidation rate of COCs in the micelles.

In contrast, higher PS conversions were found using the three nonionic surfactants studied (E3, T80 and TS80), where E3 showed slightly lower unproductive oxidant consumption. Of note is the increase of nonionic surfactant concentration, which increases the unproductive consumption of the oxidant.

Despite the higher unproductive PS consumption found with the nonionic surfactants, the conversion of DNAPL in the surfactant emulsion was higher, due to the absence of the electrostatic repulsions mentioned above. Moreover, some polar compounds, such as chlorobenzenes present in DNAPL, can diffuse to the outside of the micelle, favoring contact between pollutants and oxidants. Therefore, for the DNAPL and surfactants studied here, the higher the

surfactant stability in relation to the oxidant, the higher the protective effect of surfactants against oxidant attack on the pollutants trapped in the core of the micelles.

The choice of optimal surfactant dosages should balance the higher solubilization of COCs, and the increase in unproductive consumption of the oxidant found when the surfactant concentration increased. Still, results obtained in this paper encourage further research on the simultaneous application of surfactants and oxidants in DNAPL removal in the environment.

CRedit authorship contribution statement

Raul García-Cervilla: Methodology, Investigation, Writing - original draft. **Aurora Santos:** Funding acquisition, Resources, Conceptualization, Supervision. **Arturo Romero:** Funding acquisition, Resources. **David Lorenzo:** Conceptualization, Methodology, Supervision, Writing - original draft.

Declaration of competing interest

The authors declare that they have no known competing financial interests or personal relationships that could have appeared to influence the work reported in this paper.

Acknowledgments

This work was supported by the EU LIFE Program (LIFE17 ENV/ES/000260), the Regional Government of Madrid, through the CARESOIL project (S2018/EMT-4317), and the Spanish Ministry of Economy, Industry, and Competitiveness, through project CTM2016-77151-C2-1-R. Raúl García-Cervilla acknowledges the Spanish FPI grant (ref. BES-2017-081782). The authors thank the Department of Agriculture, Livestock and the Environment, Government of Aragon, Spain, as well as EMGRISA, for kindly supplying the DNAPL samples.

Appendix A. Supplementary data

Supplementary data to this article can be found online at <https://doi.org/10.1016/j.scitotenv.2020.141782>.

References

- Bacocchi, R., 2013. Principles, developments and design criteria of in situ chemical oxidation. *Water Air Soil Pollut.* 224. <https://doi.org/10.1007/s11270-013-1717-8>.
- Bai, X., Wang, Y., Zheng, X., Zhu, K., Long, A., Wu, X., et al., 2019. Remediation of phenanthrene contaminated soil by coupling soil washing with Tween 80, oxidation using the UV/S2082- process and recycling of the surfactant. *Chem. Eng. J.* 369, 1014–1023. <https://doi.org/10.1016/j.cej.2019.03.116>.
- Besha, A.T., Bekele, D.N., Naidu, R., Chadalavada, S., 2018. Recent advances in surfactant-enhanced in-situ chemical oxidation for the remediation of non-aqueous phase liquid contaminated soils and aquifers. *Environ. Technol. Innov.* 9, 303–322. <https://doi.org/10.1016/j.eti.2017.08.004>.
- Bouzid, I., Maire, J., Brunol, E., Caradec, S., Fatin-Rouge, N., 2017. Compatibility of surfactants with activated-persulfate for the selective oxidation of PAH in groundwater remediation. *Journal of Environmental Chemical Engineering* 5, 6098–6106. <https://doi.org/10.1016/j.jece.2017.11.038>.
- Brand, N., Mailhot, G., Bolte, M., 1998. Degradation photoinduced by Fe(III): method of alkylphenol ethoxylates removal in water. *Environ. Sci. Technol.* 32, 2715–2720. <https://doi.org/10.1021/es980034v>.
- Corcho, D., Fernández, J., Laperou, L., G., 2015. Laboratory evaluation of mixed surfactants solutions to mobilise hexachlorocyclohexane (DNAPL) from sardas landfill (Aragón, Spain). 13th HCH & Pesticides Forum 2015, Zaragoza, Spain.
- Dahal, G., Holcomb, J., Succi, D., 2016. Surfactant-oxidant co-application for soil and groundwater remediation. *Remediation-the Journal of Environmental Cleanup Costs Technologies & Techniques* 26, 101–108. <https://doi.org/10.1002/rem.21461>.
- Devi, P., Das, U., Dalai, A.K., 2016. In-situ chemical oxidation: principle and applications of peroxide and persulfate treatments in wastewater systems. *Sci. Total Environ.* 571, 643–657. <https://doi.org/10.1016/j.scitotenv.2016.07.032>.
- Dominguez, C.M., Rodriguez, V., Montero, E., Romero, A., Santos, A., 2019a. Methanol-enhanced degradation of carbon tetrachloride by alkaline activation of persulfate: kinetic model. *Sci. Total Environ.* 666, 631–640.
- Dominguez, C.M., Romero, A., Santos, A., 2019b. Selective removal of chlorinated organic compounds from lindane wastes by combination of nonionic surfactant soil flushing and Fenton oxidation. *Chem. Eng. J.* 376. <https://doi.org/10.1016/j.cej.2018.09.170>.
- Dominguez, C.M., Rodriguez, V., Montero, E., Romero, A., Santos, A., 2020. Abatement of dichloromethane using persulfate activated by alkali: a kinetic study. *Sep. Purif. Technol.* 241, 116679.
- Dugan, P.J., Siegrist, R.L., Crimi, M.L. 2009. Method and Compositions for Treatment of Subsurface Contaminants. United State Patent US7553105-B1.
- Dugan, P.J., Siegrist, R.L., Crimi, M.L., 2010. Coupling surfactants/cosolvents with oxidants for enhanced DNAPL removal: a review. *Remediation* 20, 27–49. <https://doi.org/10.1002/rem.20249>.
- Furman, O.S., Teel, A.L., Watts, R.J., 2010. Mechanism of base activation of persulfate. *Environ. Sci. Technol.* 44, 6423–6428. <https://doi.org/10.1021/es1013714>.
- García-Cervilla, R., Romero, A., Santos, A., Lorenzo, D., 2020a. Surfactant-enhanced solubilization of chlorinated organic compounds contained in DNAPL from lindane waste: effect of surfactant type and pH. *Int. J. Environ. Res. Public Health* 17, 4494. <https://doi.org/10.3390/ijerph17124494>.
- García-Cervilla, R., Santos, A., Romero, A., Lorenzo, D., 2020b. Remediation of soil contaminated by lindane wastes using alkaline activated persulfate: kinetic model. *Chem. Eng. J.* 393. <https://doi.org/10.1016/j.cej.2020.124646>.
- Hoag, G.E., Collins, J., 2011. Soil remediation method and composition. United State patent US7976241.
- Ike, I.A., Linden, K.G., Orbell, J.D., Duke, M., 2018. Critical review of the science and sustainability of persulfate advanced oxidation processes. *Chem. Eng. J.* 338, 651–669. <https://doi.org/10.1016/j.cej.2018.01.034>.
- Interstate Technology Regulatory Council, 2000. *Dense Non-Aqueous Phase Liquids (DNAPLs): Review of Emerging Characterization and Remediation Technologies*.
- Kang, S., Lim, H.S., Gao, Y., Kang, J., Jeong, H.Y., 2019. Evaluation of ethoxylated nonionic surfactants for solubilization of chlorinated organic phases: effects of partitioning loss and macroemulsion formation. *J. Contam. Hydrol.* 223. <https://doi.org/10.1016/j.jconhyd.2019.03.007>.
- Katsoyiannis, A., Samara, C., 2005. Persistent organic pollutants (POPs) in the conventional activated sludge treatment process: fate and mass balance. *Environ. Res.* 97, 245–257. <https://doi.org/10.1016/j.envres.2004.09.001>.
- Lanoue, M., Kessell, L., Athayde, G., 2011. *Surfactant-Enhanced In Situ Chemical Oxidation (S-ISCO®). Águas Subterráneas*.
- Lee, J.F., Liao, P.M., Kuo, C.C., Yang, H.T., Chiou, C.T., 2000. Influence of a nonionic surfactant (Triton X-100) on contaminant distribution between water and several soil solids. *J. Colloid Interface Sci.* 229, 445–452. <https://doi.org/10.1006/jcis.2000.7039>.
- Liang, C.J., Lei, J.H., 2015. Identification of active radical species in alkaline persulfate oxidation. *Water Environ. Res.* 87, 656–659. <https://doi.org/10.2175/106143015x14338845154986>.
- Lominchar, M.A., Lorenzo, D., Romero, A., Santos, A., 2018a. Remediation of soil contaminated by PAHs and TPH using alkaline activated persulfate enhanced by surfactant addition at flow conditions. *J. Chem. Technol. Biotechnol.* 93, 1270–1278. <https://doi.org/10.1002/jctb.5485>.
- Lominchar, M.A., Santos, A., de Miguel, E., Romero, A., 2018b. Remediation of aged diesel contaminated soil by alkaline activated persulfate. *Sci. Total Environ.* 622, 41–48. <https://doi.org/10.1016/j.scitotenv.2017.11.263>.
- Londergan, J., Yeh, L., 2003. *Surfactant-Enhanced Aquifer Remediation (SEAR) Implementation Manual*. No. NFESC, Technical Report: TR-2219-ENV, INTERA INC AUSTIN TX.
- Long, A., Zhang, H., Lei, Y., 2013. Surfactant flushing remediation of toluene contaminated soil: optimization with response surface methodology and surfactant recovery by selective oxidation with sulfate radicals. *Sep. Purif. Technol.* 118, 612–619. <https://doi.org/10.1016/j.seppur.2013.08.001>.
- Long, A., Lei, Y., Zhang, H., 2014. Degradation of toluene by a selective ferrous ion activated persulfate oxidation process. *Ind. Eng. Chem. Res.* 53, 1033–1039. <https://doi.org/10.1021/ie402633n>.
- Lorenzo, D., García-Cervilla, R., Romero, A., Santos, A., 2020. Partitioning of chlorinated organic compounds from dense non-aqueous phase liquids and contaminated soils from lindane production wastes to the aqueous phase. *Chemosphere* 239. <https://doi.org/10.1016/j.chemosphere.2019.124798>.
- Mao, X., Jiang, R., Xiao, W., Yu, J., 2015. Use of surfactants for the remediation of contaminated soils: a review. *J. Hazard. Mater.* 285, 419–435.
- Mendez-Diaz, J., Sanchez-Polo, M., Rivera-Utrilla, J., Canonica, S., von Gunten, U., 2010. Advanced oxidation of the surfactant SDBS by means of hydroxyl and sulphate radicals. *Chem. Eng. J.* 163, 300–306. <https://doi.org/10.1016/j.cej.2010.08.002>.
- Mobile, M., Widdowson, M., Stewart, L., Nyman, J., Deeb, R., Kavanaugh, M., et al., 2016. In-situ determination of field-scale NAPL mass transfer coefficients: performance, simulation and analysis. *J. Contam. Hydrol.* 187, 31–46. <https://doi.org/10.1016/j.jconhyd.2016.01.010>.
- Mukherjee, P., Padhan, S.K., Dash, S., Patel, S., Mishra, B.K., 2011. Clouding behaviour in surfactant systems. *Adv. Colloid Interf. Sci.* 162, 59–79. <https://doi.org/10.1016/j.cis.2010.12.005>.
- Mulligan, C.N., Yong, R.N., Gibbs, B.F., 2001. Surfactant-enhanced remediation of contaminated soil: a review. *Eng. Geol.* 60, 371–380. [https://doi.org/10.1016/s0013-7952\(00\)00117-4](https://doi.org/10.1016/s0013-7952(00)00117-4).
- National Research Council, 2013. *Alternatives for Managing the Nation's Complex Contaminated Groundwater Sites*. The National Academies, Washington, DC.
- Pagano, M., Lopez, A., Volpe, A., Mascolo, G., Ciannarella, R., 2008. Oxidation of nonionic surfactants by Fenton and H2O2/UV processes. *Environ. Technol.* 29, 423–433. <https://doi.org/10.1080/09593330801983862>.
- Paria, S., 2008. Surfactant-enhanced remediation of organic contaminated soil and water. *Apr.* 138, 24–58. <https://doi.org/10.1016/j.cis.2007.11.001>.
- Rosen, M.J., Kunjappu, J.T., 2012. *Surfactants and Interfacial Phenomena*. John Wiley & Sons.

- Santos, A., Fernandez, J., Guadano, J., Lorenzo, D., Romero, A., 2018a. Chlorinated organic compounds in liquid wastes (DNAPL) from lindane production dumped in landfills in Sabinanigo (Spain). *Environ. Pollut.* 242, 1616–1624. <https://doi.org/10.1016/j.envpol.2018.07.117>.
- Santos, A., Fernandez, J., Rodriguez, S., Dominguez, C.M., Lominchar, M.A., Lorenzo, D., et al., 2018b. Abatement of chlorinated compounds in groundwater contaminated by HCH wastes using ISCO with alkali activated persulfate. *Sci. Total Environ.* 615, 1070–1077. <https://doi.org/10.1016/j.scitotenv.2017.09.224>.
- Santos, A., Dominguez, C.M., Lorenzo, D., Garcia-Cervilla, R., Lominchar, M.A., Fernandez, J., et al., 2019. Soil flushing pilot test in a landfill polluted with liquid organic wastes from lindane production. *Heliyon* 5. <https://doi.org/10.1016/j.heliyon.2019.e02875>.
- Siegrist, R.L., Crimi, M., Simpkin, T.J., 2011. *In Situ Chemical Oxidation for Groundwater Remediation*. Springer-Verlag New York, New York.
- Soga, K., Page, J.W., Illangasekare, T.H., 2004. A review of NAPL source zone remediation efficiency and the mass flux approach. *J. Hazard. Mater.* 110, 13–27. <https://doi.org/10.1016/j.jhazmat.2004.02.034>.
- Sra, K.S., Thomson, N.R., Barker, J.F., 2014. Stability of activated persulfate in the presence of aquifer solids. *Soil Sediment Contam.* 23, 820–837. <https://doi.org/10.1080/15320383.2013.722142>.
- Tomlinson, D.W., Rivett, M.O., Wealthall, G.P., Sweeney, R.E.H., 2017. Understanding complex LNAPL sites: illustrated handbook of LNAPL transport and fate in the subsurface. *J. Environ. Manag.* 204, 748–756. <https://doi.org/10.1016/j.jenvman.2017.08.015>.
- Trellu, C., Mousset, E., Pechaud, Y., Huguenot, D., van Hullebusch, E.D., Esposito, G., et al., 2016. Removal of hydrophobic organic pollutants from soil washing/flushing solutions: a critical review. *J. Hazard. Mater.* 306, 149–174. <https://doi.org/10.1016/j.jhazmat.2015.12.008>.
- Trellu, C., Oturan, N., Pechaud, Y., van Hullebusch, E.D., Esposito, G., Oturan, M.A., 2017. Anodic oxidation of surfactants and organic compounds entrapped in micelles - selective degradation mechanisms and soil washing solution reuse. *Water Res.* 118, 1–11. <https://doi.org/10.1016/j.watres.2017.04.013>.
- Tsai, T., Kao, C., Hong, A., 2009. Treatment of tetrachloroethylene-contaminated groundwater by surfactant-enhanced persulfate/BOF slag oxidation—a laboratory feasibility study. *J. Hazard. Mater.* 171, 571–576.
- Waclawek, S., Antoš, V., Hrabák, P., Černík, M., 2016. Remediation of hexachlorocyclohexanes by cobalt-mediated activation of peroxymonosulfate. *Desalin. Water Treat.* 57, 26274–26279. <https://doi.org/10.1080/19443994.2015.1119757>.
- Waclawek, S., Silvestri, D., Hrabák, P., Padil, V.V.T., Torres-Mendieta, R., Waclawek, M., et al., 2019. Chemical oxidation and reduction of hexachlorocyclohexanes: a review. *Water Res.* 162, 302–319. <https://doi.org/10.1016/j.watres.2019.06.072>.
- Wang, W.H., Hoag, G.E., Collins, J.B., Naidu, R., 2013. Evaluation of Surfactant-enhanced In Situ Chemical Oxidation (S-ISCO) in contaminated soil. *Water Air Soil Pollut.* 224, 1713. <https://doi.org/10.1007/s11270-013-1713-z> <https://ARTN>.
- Wang, L., Peng, L., Xie, L., Deng, P., Deng, D., 2017. Compatibility of surfactants. And thermally activated persulfate for enhanced subsurface remediation. *Environ. Sci. Technol.* 51, 7055–7064. <https://doi.org/10.1021/acs.est.6b05477>.
- Wang, L., Wu, H., Deng, D., 2020. Role of surfactants in accelerating or retarding persulfate decomposition. *Chem. Eng. J.* 384. <https://doi.org/10.1016/j.cej.2019.123303>.
- Yang, K., Zhu, L., Xing, B., 2006. Enhanced soil washing of phenanthrene by mixed solutions of TX100 and SDBS. *Environ. Sci. Technol.* 40, 4274–4280. <https://doi.org/10.1021/es060122c>.
- Zheng, F., Gao, B., Sun, Y., Shi, X., Xu, H., Wu, J., et al., 2016. Removal of tetrachloroethylene from homogeneous and heterogeneous porous media: combined effects of surfactant solubilization and oxidant degradation. *Chem. Eng. J.* 283, 595–603.



Abatement of chlorobenzenes in aqueous phase by persulfate activated by alkali enhanced by surfactant addition

Raul Garcia-Cervilla, Aurora Santos, Arturo Romero, David Lorenzo*

Chemical and Materials Engineering Department, Complutense University of Madrid, Spain

ARTICLE INFO

Keywords:

Surfactant
Chlorinated organic compounds (COCs)
DNAPL
S-ISCO
Persulfate activated by alkali

ABSTRACT

Sites polluted by dense non-aqueous phases (DNAPLs) constitute an environmental concern. In situ chemical oxidation (ISCO) application is limited since oxidation often occurs in the aqueous phase and contaminants are usually hydrophobic. In this work, ISCO enhanced by the surfactant addition (S-ISCO) was studied for a complex liquid mixture of chlorinated organic compounds (COCs) using persulfate (PS) activated by alkali (PSA) as oxidant and Emulse-3® as a commercial non-ionic surfactant. The reaction between E3 and PSA was investigated in the absence and presence of solubilized COCs in the following concentration ranges: COCs 1.2–50 mM, PS 84–336 mM, NaOH:PS molar ratio of 2, and surfactant concentration 1–10 g·L⁻¹.

In the experiments carried out in the absence of COCs, the unproductive consumption of PS was studied. The higher the surfactant concentration, the lower the ratio PS consumed to the initial surfactant concentration due to more complex micelle structures hindering the oxidation of surfactant molecules. This hindering effect was also noticed in the oxidation of solubilized COCs. The reduction of chlorobenzenes by PSA was negligible at surfactant concentrations above 2.5 g·L⁻¹, independently of the COCs concentration solubilized. Instead, a surfactant concentration of about 1 and PS concentration of 168 mM yielded a significant decrease in the time required to abate a mass of DNAPL, compared with an ISCO process, with a bearable increase in the unproductive consumption of PS.

1. Introduction

Sites polluted by organic compounds are an environmental issue, contaminating soil and groundwater (van Liedekerke et al., 2014). In many cases, this contamination originated from spills of organic compounds from storage tanks (fuels, solvents) or from dumping in unsafe conditions (Interstate Technology Regulatory Council, 2000; Mobile et al., 2016; Soga et al., 2004; Tomlinson et al., 2017). On the other hand, the low water solubility of organic compounds present in spills and/or releases can originate their presence in the subsurface, as non-aqueous phase liquids (NAPLs) (Brusseau, 2013; CLU-IN, 1991; Tomlinson et al., 2017).

In situ chemical oxidation (ISCO) is one of the technologies that have been successfully applied in the remediation of groundwater contamination with organic compounds (Bacocchi et al., 2014; Siegrist et al., 2011). In the ISCO treatment, the oxidants are injected into the subsurface, reacting with the contaminants dissolved in the aqueous phase (Albergaria and Nouws, 2016). Therefore, the solubility of the organic compounds and the contact between the aqueous and organic phases are

critical factors for the ISCO process to be time- and cost-effective. However, this contact is often hindered because the organic phase is a residue trapped tightly in subsurface pores or fractures (Schaefer et al., 2009, 2016). Groundwater in contact with this phase generates a contamination plume that will persist until the removal of the organic phase, the contamination enduring for decades (Stroo et al., 2012).

A recently evaluated technology is the simultaneous injection of oxidants and surfactants into the subsurface (S-ISCO) (Besha et al., 2018; Lanoue et al., 2011). The surfactant increases the solubility of the organic compound in the aqueous phase and improves its oxidation rate. Thereby, S-ISCO decreases the time required to remove the residual organic phase trapped in the soil (Dahal et al., 2016). However, surfactants are organic molecules, which may compete with the contaminant for the oxidant (Bouzd et al., 2017; Wang et al., 2017). The unproductive consumption of oxidants by the surfactant also generates a loss of surfactant that decreases the solubility of the organic compound in the aqueous phase (García-Cervilla et al., 2021).

The higher the surfactant concentration, the more complex the micelle aggregation structures are expected (Acharya et al., 1997; Lin

* Corresponding author.

E-mail address: dlorenzo@quim.ucm.es (D. Lorenzo).

<https://doi.org/10.1016/j.jenvman.2022.114475>

Received 13 September 2021; Received in revised form 22 December 2021; Accepted 6 January 2022

Available online 13 January 2022

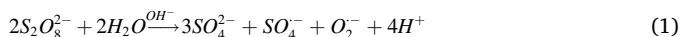
0301-4797/© 2022 The Authors. Published by Elsevier Ltd. This is an open access article under the CC BY license (<http://creativecommons.org/licenses/by/4.0/>).

et al., 2011; Rosen and Kunjappu, 2012). These structures could affect the reactivity of surfactants and solubilized contaminants against the oxidant. Besides, the selective oxidation of solubilized organic compounds in the micelle structure will also depend on the relative reactivity of both compounds (contaminant and surfactant) to the oxidant.

The oxidizing system and the characteristics of the organic compounds and surfactants will influence the efficiency of the process. In the still-limited studies in the literature on S-ISCO tests, oxidants such as persulfate (PS) and hydrogen peroxide or permanganate have been analysed in the removal of polyaromatic hydrocarbons (PAHs) (Bai et al., 2019; Bouzid et al., 2017; Li et al., 2019; Petitgirard et al., 2009; Qiu et al., 2019; Wang et al., 2017), total petroleum hydrocarbons (TPHs) (Lominchar et al., 2018; Wang et al., 2013) or organic phases formed by single compounds: toluene, (Long et al., 2014), tetrachloroethylene (Zheng et al., 2016), trichloroethylene (Li, 2004; Tsai et al., 2009). Most of these works generally focus on contaminant removal, paying less attention to unproductive oxidant consumption and loss of surfactant capacity.

The effect of surfactant and oxidant concentration on the selective COCs oxidation, unproductive consumption of oxidants and loss of surfactant capacity has not been previously studied in literature. However, the proper design of S-ISCO for a field application strongly depends on the interaction between surfactants, contaminants, and oxidants in the reaction media. Surfactant and organic pollutants in the aqueous phase compete for the oxidant, causing unproductive consumption of the oxidant and the loss of the surfactant capacity.

In this work, PS was selected as an oxidant since it is stable in the soil, allowing the transport of the injected fluid. PS can be activated by iron, heat or alkali. However, there is a lack of studies with alkali-activated persulfate (PSA) as an oxidizing system when surfactants are used. The alkali used as an activator (NaOH) generates a pull of radicals (Eq. (1) and (2)), being hydroxyl, OH^\bullet and superoxide, O_2^- , the prominent radicals at $pH > 12$ (Furman et al., 2010). Hydroxyl radicals produced in PSA are non-selective and strong oxidants (Gligorovski et al., 2015). Superoxide radicals play a non-negligible role in abating chlorinated pollutants (Checa-Fernandez et al., 2021; Dominguez et al., 2019).



PSA can be applied in soils with a neutral or alkaline pH. On the contrary, the addition of iron as an activator would require, in these cases, the addition of chelating agents (Pardo et al., 2015b; Rodrigo and Dos Santos, 2021). Chelating agents are organic compounds that can also compete with the pollutant for the oxidant (Pardo et al., 2015a) decreasing the efficiency of the process. On the other hand, other PS activations such as light (Bai et al., 2019) or temperature (Wang et al., 2017) cannot be applied in the subsoil.

The selected surfactant, Emulse 3 (E3), is a non-ionic and biodegradable commercial surfactant with a lower CMC and higher molar solubility ratio than anionic surfactants, such as SDS (García-Cervilla et al., 2020a). In addition, it was found that SDS blocks the oxidation of the dissolved COCs. Electrostatic repulsions among the sulfate groups of the surfactant and hydroxide and PS anions hinder the transport of PS and OH^- into the micelle and, consequently, the formation of radicals that attack the contaminants (García-Cervilla et al., 2021).

This work analyses the influence of the oxidant, surfactant, and contaminant concentration on removing an organic phase formed by different chlorinated organic compounds (COCs) through the simultaneous addition of PSA and surfactant. In this case, chlorobenzenes (chlorobenzene, dichlorobenzene, trichlorobenzene, tetrachlorobenzene) have been used as the Dense NAPL phase (DNAPL). This organic phase composition has been chosen to include compounds that frequently appear in spills or leaks (Wang and Jones, 1994) (Boutonnet et al., 2004; Djohan et al., 2005; Lecloux, 2003; Santos et al., 2018a; van

Wijk et al., 2006; Van Wijk et al., 2004). Moreover, these compounds have different solubility in the aqueous phase (Lorenzo et al., 2020).

The results obtained by S-ISCO are analysed and compared with those obtained in the absence of surfactant (ISCO). For this purpose, an instantaneous equilibrium between the aqueous and organic phases was assumed in the ISCO treatment. This hypothesis overestimates the effectiveness of the ISCO treatment since this equilibrium is not reached quickly under subsurface conditions.

2. Material and methods

2.1. Chemicals

The DNAPL used was formulated from commercial compounds. The COCs selected were purchased from Sigma-Aldrich with analytical quality: Chlorobenzene (CB), 1,2-dichlorobenzene (1,2-DCB), 1,2,3-trichlorobenzene (1,3,5-TCB), 1,2,4-trichlorobenzene (1,2,4-TCB), 1,2,3,4-tetrachlorobenzene (1,2,3,4-TeCB), 1,2,3,5-tetrachlorobenzene (1,2,3,5-TeCB). The purity of all commercial COCs used was higher than 99.9%.

The DNAPL was prepared by mixing the selected COCs in a 20-mL glass vial with a PTFE screw cap. The molar (x_j) and mass (w_j) fractions of each j COC in DNAPL were summarized in Table 1. Five vials were performed in total.

Bicyclohexyl (C12H22, Sigma-Aldrich) and tetrachloroethane (C2H2Cl4, Sigma-Aldrich) were used as internal standards (ISTD) in GC/FID/ECD analysis.

The surfactant selected was E-Mulse 3® (E3), supplied by EthicalChem®. This biodegradable polyethoxylated surfactant was successfully applied in the laboratory and full-scale remediation runs with S-ISCO (EthicalChem, 2016n; García-Cervilla et al., 2020a). This surfactant is formulated with limonene as a co-solvent (15–25%).

Sodium Persulfate (PS, Sigma-Aldrich) was used as an oxidant and sodium hydroxide (NaOH, Fisher Scientific) was the activator selected; this system being successfully (PSA) applied in previous studies for chlorobenzenes (García-Cervilla et al., 2020b; Santos et al., 2018b). Potassium iodide (KI, Fisher Chemical), sodium hydrogen carbonate (NaHCO3, Panreac), sodium thiosulfate pentahydrate (Na2S2O3·5H2O, Sigma-Aldrich), and acetic acid (C2H4O2, Sigma-Aldrich) were used for PS quantification. All aqueous solutions were carried out with Milli-Q water.

2.2. COCs solubility with surfactant

The solubilisation of the DNAPL mixture of chlorobenzenes with E3 at basic pH was carried out in 20-mL glass vials with PTFE screw caps. Five aqueous solutions were prepared with different concentrations of E3 (0, 2.5, 5, 10 and 15 $g \cdot L^{-1}$). The alkaline conditions were achieved by adding NaOH (168 mM). An 18-mL volume of this alkaline aqueous solution was added to the corresponded vials. Then, a mass of DNAPL, was added to each vial. Vials were shaken, with a magnetic stirrer, for 5 h. Once the aqueous phase was homogenized, the agitation was stopped for 24 h, which was enough to reach the equilibrium between the aqueous and DNAPL phases (García-Cervilla et al., 2020a). Experiments

Table 1

Molar fraction x_j , and mass fractions, w_j , (as a percentage) of chlorobenzenes in formulated DNAPL. The average molar weight was $165.5 \text{ g} \cdot \text{mol}^{-1}$.

COCs	$x_j \cdot 100$	$w_j \cdot 100$	MW
CB	27.25	18.5	112.5
1,2-DCB	14.03	12.4	147.0
1,2,3-TCB	5.15	34.4	181.5
1,2,4-TCB	31.40	5.6	181.5
1,2,4,5-TeCB	7.91	10.4	216.0
1,2,3,4-TeCB	14.25	18.6	216.0

were carried out in triplicate, and the standard deviation was lower than 5%.

Once the equilibrium was reached, the aqueous phase in those vials without a surfactant addition was extracted with hexane, at a volume ratio of 4 (water):1 (hexane). In those vials with an added surfactant, the aqueous phase was diluted with MeOH (1:10 in volume). GC-FID/ECD was used to analyse these samples.

2.3. Oxidation runs

2.3.1. Unproductive consumption of PS by the surfactant

The unproductive consumption of PS by E3 was studied in wide oxidant and surfactant concentration ranges. The experiments were carried out in 20-mL glass vials with PTFE screw caps simulating as a stirred batch reactor. Vials were shaken intermittently, 2–5 min per day, with a magnetic stirrer to simulate the behaviour of the groundwater in the subsoil with low spatial velocity. An 18-mL volume of an alkaline aqueous solution containing the surfactant was added to the vials. Then, the PS was added as a pure solid (zero time). The concentrations of E3, NaOH and PS tested are summarized in Table S1. At each reaction time, a vial was sacrificed, the pH measured, and the oxidant concentration remaining determined.

2.3.2. Experiments regarding the oxidation of aqueous emulsions (COCs-E3)

Two sets of experiments were carried out to study the influence of surfactant, oxidant, and solubilized COCs in the S-ISCO treatment.

In the first set, 250 mL of alkaline aqueous solutions of E3 surfactant (5 or 10 g·L⁻¹) were saturated with DNAPL. The mass of DNAPL added was slightly higher than that required for total saturation to minimize the amount of non-dissolved organic phase. The mixtures were gently shaken with a magnetic stirrer for 24 h. Oxidation runs were carried out in vials with PTFE screw caps containing 18 mL of these saturated solutions. The reaction started after adding PS as a pure solid to the vials. Different concentrations of PS were tested using a NaOH:PS molar ratio of 2. Experimental conditions are summarized in Table 2. Vials were intermittently shaken with a magnetic stirrer (2–5 min per day). At different reaction times, solubilized and total COCs in vials were analysed by GC-FID/ECD. The solubilized COCs in the aqueous phase were measured by taking an aliquot of 0.1 mL of the supernatant (after 5 h of settling). The total concentration of COCs (dissolved and precipitated) was measured by taking a sample of the well-homogenized emulsion after vigorous stirring and diluting this volume in MeOH (volume ratio 1:10). The oxidant concentration and pH were also determined at each reaction time. Two replicates were carried out for each reaction time, and differences were lower than 10%.

The second set of experiments was carried with non-saturated emulsions in COCs. An 18-mL volume of the corresponding aqueous solution with the appropriate concentrations of E3 and NaOH was added to 20-mL glass vials with PTFE screw caps. Then, to obtain the desired concentration of COCs, the corresponding mass of DNAPL was added to each vial. Vials were strongly agitated with a magnetic stirrer. Once the COCs were entirely solubilized in the aqueous phase, PS was added as a pure solid (zero time). Several reaction times were used for each run, a vial being sacrificed at each reaction time. Vials were intermittently stirred (2–5 min per day) with a magnetic stirrer. Experimental conditions are summarized in Table 2. The solubilized and total COCs and PS concentrations were determined at different reaction times, and the pH of the emulsion was measured. Two replicates at each reaction time were performed, and differences were lower than 10%. Besides, two experiments were carried out without surfactant (ISCO treatment) using 168 mM of PS and 2.4 and 3.6 mM of initial COCs. The later concentrations were not completely solubilized in water, forming an organic phase. The reactions were carried out in 20 mL sealed-glass vials, and the reaction mixture in the vial was dissolved in MeOH (1:10) at each reaction time.

Table 2

Experimental conditions of the oxidation runs with COCs concentrations using a NaOH:PS of 2 mol·mol⁻¹.

Emulsion.	Cso (g·L ⁻¹)	CCOCs (mM)	CPSo (mM)	reaction time (h)
S-ISCO: Saturated	5	24.9	84	0–450
			168	
			336	
	10	59.5	84	0–450
			168	
			336	
S-ISCO: Non Saturated	1	1.2	84	0–144
			168	
			252	
		2.4	84	
			168	
			252	
	2.5	1.2	84	0–144
			168	
			252	
		2.4	84	
			168	
			252	
5	1.2	84	0–144	
		168		
		252		
	2.4	84		
		168		
		252		
10	1.2	84	0–144	
		168		
		252		
	2.4	84		
		168		
		252		
ISCO	0	2.4	0–256	
		3.6		

2.4. Analysis

The aqueous phase, with or without surfactant, was diluted at 1:10 in MeOH or extracted with 1:4 n-hexane (volume ratios), respectively. COCs in MeOH or hexane were quantified by Gas chromatography coupled with a Flame Ionization Detector and an Electron Capture Detector (GC-FID/ECD). The chromatographic method is described elsewhere (García-Cervilla et al., 2020b; Santos et al., 2018a).

Moreover, gas chromatography coupled with a mass spectrometer detector (GC-MSD) was used to identify some intermediates in the oxidation of the surfactant. The GC/MS data were processed using Software MassHunter B08 (Agilent Technologies), and the identification of the compound was carried out by comparing the mass spectra with the NIST library records (Babushok et al., 2007) (NIST011 version).

PS in aqueous phases was measured by Iodometric titration with sodium thiosulfate. A potentiometric titration analyser (Metrohm, Tiamo 2.3) was used. A basic 20-CRISON pH electrode measured the pH. Micrographs of the emulsions were taken with an electron microscope equipped with a Gatan liquid nitrogen specimen holder for cryo-EM (see Supplementary Material). The hydrodynamic diameter was measured with a Nano Zetasizer (Malvern).

3. Results and discussions

3.1. Solubility of COCs

The solubilisation of COCs in pure alkaline water or alkaline surfactant solutions was investigated. The concentration of solubilized COCs (sum of chlorobenzenes) in the aqueous phase (C_{COCs}) vs the initial surfactant concentration used is plotted in Figure S1. The amount of DNAPL added was the minimum to ensure the saturation of the aqueous solution. Therefore, the surfactant absorbed in the non-solubilized organic phase at equilibrium conditions can be neglected, considering the equilibrium surfactant concentration as the initial surfactant concentration. The solubility of the sum of COCs in pure water without surfactant addition was 0.52 mM. In the presence of surfactant, the higher C_{So} , the higher the COCs concentration (C_{COCs}) dissolved in the aqueous phase, as can be seen in Figure S1. A linear relationship was found between C_{COCs} and C_{So} , under the experimental conditions tested. Solubilisation capacity of the surfactant (SCS), defined as the ratio between the solubilized COCs in the aqueous surfactant emulsion and the amount of E3, can be calculated as the slope of the trend in Figure S1, yielding a value of $5.7 \text{ mmol}_{COCs} \cdot \text{g}_{So}^{-1}$. This value was similar to that obtained with a real DNAPL of chlorinated compounds, including chlorobenzenes and hexachlorocyclohexanes (García-Cervilla et al., 2020a) at neutral and alkaline pHs ($4.33 \text{ mmol}_{COCs} \cdot \text{g}_{So}^{-1}$ in both cases).

The molar distribution of solubilized COCs in the presence or absence of surfactant is compared in Figure S2 with the molar distribution of the COC mixture in DNAPL. As can be seen, in the absence of surfactant, CB was selectively solubilized in the aqueous phase. This finding can be explained by the higher solubility of this CB in water (Lorenzo et al., 2020). The solubility of each chlorobenzene, j , in the alkaline aqueous phase without surfactant can be calculated with Eq. (3).

$$S_j \gamma_j = \frac{C_{j, aq}}{x_j} \quad (3)$$

$S_j \gamma_j$, x_j , $C_{j, aq}$ being the solubility, activity coefficient, molar fraction of j in DNAPL and concentration in the aqueous phase, respectively, of a

compound j . Values of $S_j \gamma_j$ at alkaline conditions are summarized in Table S2. By comparison of the results at alkaline pH (>12) with those obtained elsewhere at neutral pH (Lorenzo et al., 2020), it can be seen that $S_j \gamma_j$ is lower at alkaline conditions. The solubility of COC_j at pH 12 is about half of that obtained at pH = 7.

Using E3 a similar molar distribution of solubilized chlorobenzenes and chlorobenzenes in DNAPL was obtained regardless of surfactant concentration. This effect can be explained by assuming that the surfactant solubilizes DNAPL as a single pseudo-compound (García-Cervilla et al., 2020a; García-Cervilla et al., 2021). As the oxidation occurs in the aqueous phase, the heavier and less soluble chlorobenzenes could be removed in much shorter times if surfactant is added.

3.2. COCs oxidation with PSA in the presence of surfactant

Surfactants and pollutants compete for the oxidant (Bouزيد et al., 2017; Cheng et al., 2017; García-Cervilla et al., 2021; Mendez-Diaz et al., 2010; Olmez-Hanci et al., 2014). Therefore, an appropriate dosage of surfactant and oxidant is required to minimize the unproductive consumption of the oxidant and surfactant but reducing the time needed to remove a certain mass of DNAPL.

3.2.1. Unproductive consumption of the oxidant

This section analyses the results obtained under the experimental conditions of runs summarized in Table 2. The consumption of PS (as mM) and the ratio $R_{\Delta PS/S_o}$ at different times, initial surfactant and oxidant concentrations are plotted in Fig. 1. The $R_{\Delta PS/S_o}$ value is calculated as shown in Eq (4).

$$R_{\Delta PS/S_o} = \frac{C_{PS_o} - C_{PS}}{C_{S_o}} \quad (4)$$

As shown in Fig. 1, the PS consumption is almost negligible at times of up to 450 h (conversion of less than 7%) in the absence of surfactant. As can be seen in Eqs. (1) and (2), the alkaline activation of PS promotes the formation of SO_4^- , O_2^- and OH^- , these radicals react with the surfactant and COCs. In experiments carried out without surfactant and

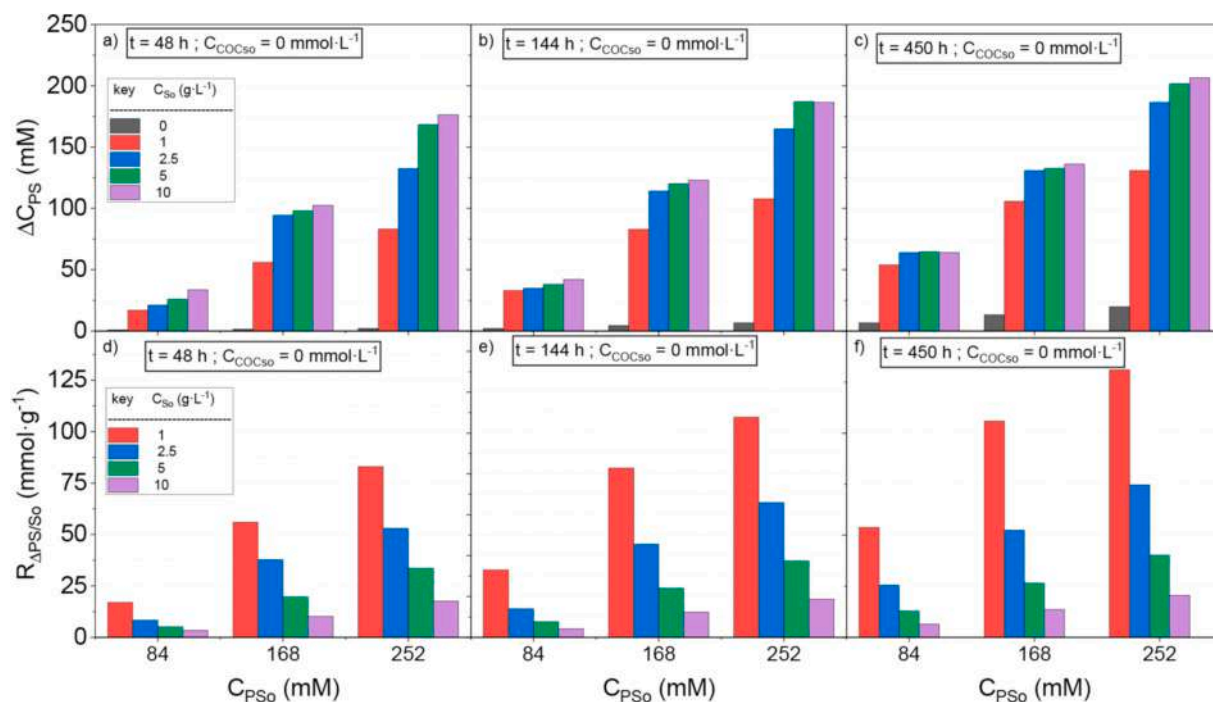


Fig. 1. PS consumption (a) 48 h and b) 144 h c) 450 h) and $R_{\Delta PS/S_o}$ (d) 48 h and e) 144 h f) 450 h) values at different oxidation times. Experimental conditions are shown in Table S1. The molar ratio NaOH:PS was 2 in all experiments.

COCs, these radicals were slowly consumed in unproductive reactions with PS and persulfate concentration remains almost constant with time. The consumption on version of PS in the absence of COCs and surfactant using 252 mM of PS and a molar ratio NaOH:PS 2:1 was lower than 15% after 21 days, as shown in Fig. 1. On the other hand, PS consumption remarkably increases when the surfactant is added.

At C_{S_0} constant, the higher the oxidant concentration, the higher the oxidant consumed, as shown in Fig. 1. However, for a given value of C_{PS_0} , the consumption of oxidant slightly increases while the initial surfactant concentration increases and the $R_{\Delta PS/S_0}$ value decreases.

The critical micellar concentration of surfactant E3 is about 80 mg L^{-1} (García-Cervilla et al., 2020a). The micelles are formed when the surfactant concentration is higher than this CMC value.

However, the shape and size of micelles change when surfactant concentration increases. It can be assumed that more complex micelle structures are formed at higher surfactant concentrations, lowering the external surface of micelles per mass of surfactant (Kosswig, 2000). The size of micelles was investigated by dynamic light scattering (DLS), using a Malvern Nano Zetasizer. With this technique, the hydrodynamic diameter (DH) of the micelles was measured for different surfactant concentrations within the range 1–100 $g \cdot L^{-1}$. It was observed that the higher the surfactant concentration, the lower the DH micelles (within the range of 13–9 nm for the surfactant concentration tested). Besides, using Cryo-EM was observed (see Figure S3 of the Supplementary Material) the amount of micelles was not appreciable increased between 5 and 10 $g \cdot L^{-1}$, this inferred the number of monomers per micell increased hindering the surfactant against oxidation.

The oxidation mechanism for the non-ionic surfactant was proposed by Brand et al. (1998) and Olmez-Hanci et al. (2014). The polyethoxylated chains in E3 are susceptible to radical oxidation (Brand et al., 1998; Olmez-Hanci et al., 2014; Wang et al., 2020). The main oxidation by-products are shortened ethoxylate chains, polyethylene glycols, aldehyde ethoxylates, carboxylated polyethylene glycols and carboxylated acids (Brand et al., 1998; Castillo et al., 2001; Olmez-Hanci et al., 2014). Some of the E3 oxidation by-products were identified by GC-MS analysis of the aqueous phases, as shown in Figures S4 and S5 of the Supporting Information. These by-products are more refractory to oxidation than the parent surfactant molecule, and the PS consumption rate slows down with time, as noticed in Fig. 1. The mineralization achieved for the surfactant was lower than 20%, in agreement with results elsewhere (Lominchar et al., 2018). Besides, E3 is formulated with limonene as a co-solvent. Limonene oxidation explains the by-products summarized in Figs. S6 and S7 of the Supporting Information.

3.2.2. Oxidation of COCs in saturated aqueous emulsions at a moderate-high surfactant concentration

Firstly, the selective oxidation of COCs in the aqueous emulsion with

a relatively high surfactant concentration and emulsified COCs were studied (runs in Table 2). The concentrations of solubilized COCs were 24.9 and 59.5 mM when the surfactant concentration was 5 and 10 $g \cdot L^{-1}$, respectively (saturation conditions). As can be seen in Table 2, three concentrations of NaOH were tested. No effect of the alkali concentration on initial solubilized COCs was found at the alkali concentration range studied.

The fraction of solubilized and total COCs remaining in the vial with reaction time was measured. Differences between solubilized and total COCs correspond to the precipitated COCs in the vial. Results using 5 and 10 $g \cdot L^{-1}$ of surfactant concentration at different PS concentrations are shown in Fig. 2.

As can be seen in Fig. 2a, COCs oxidation did not occur at 84 mM and no differences between total and solubilized COCs were noticed at this C_{PS_0} value during the time interval studied. However, a significant consumption of PS was noticed under the same conditions as shown in (Fig. 3a). This fact can be explained by taking into account the reaction between PS and the surfactant. The first surfactant oxidation by-products kept the initial surfactant capacity since the precipitation of COCs in the saturated solution did not occur.

On the contrary, at higher PS concentrations (Fig. 2b and c), the total and solubilized COCs concentrations in the vial become more different with time. After an initial period, precipitation of COCs takes place due to the progressive surfactant capacity lost. This initial period depends on the surfactant and PS concentrations. Using 168 mM of C_{PS_0} (Figs. 2b) and 5 $g \cdot L^{-1}$ of surfactant, the concentration of solubilized COCs dropped from 24.9 to 0.27 mM after 300 h in contact with PSA. However, at the same conditions of PS but using $C_{S_0} = 10 g \cdot L^{-1}$ precipitation of COCs did not occur, keeping the concentration of solubilized COCs at 59.5 mM. At 336 mM C_{PS_0} (Fig. 2c), the almost complete precipitation of COCs was noticed at 24 h and 400 h using 5 and 10 $g \cdot L^{-1}$ of C_{S_0} , respectively. This loss of surfactant capacity is due to surfactant oxidation by PSA and the corresponding PS consumed is shown in Fig. 3.

Therefore, the surfactant oxidation can be explained by two consecutive reactions. In the first reaction, the initial surfactant oxidation by-products (lumped as SOX_1 in Eq. (5)) maintain the surfactant capacity while initial solubilized COCs in the vial does not precipitated despite PS being consumed (Figs. 2a and 3a). The oxidation of first surfactant by-products (SOX_1) occurs as shorter times as PS concentration increases. The formed SOX_2 (Eq. (6)) must have a lower surfactant capacity explaining the precipitation of COCs noticed in Fig. 2b and c. The production of by-products with different surfactant capacity have been reported in the literature (Castillo et al., 2001; Olmez-Hanci et al., 2014; Wang et al., 2020). Moreover, no mineralization of the surfactant was noticed using PSA at the conditions tested.

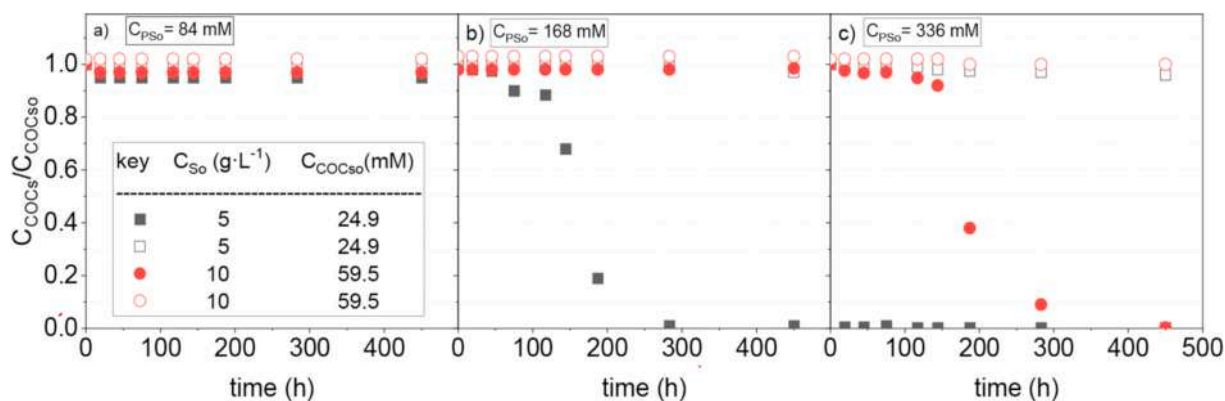


Fig. 2. Fraction of solubilized (solid symbols) and total (open symbols) COCs with time at two initial concentrations of surfactant (5 and 10 $g \cdot L^{-1}$) and solubilized COCs (24.9 and 59.5 mM). PS concentrations: a) $C_{PS_0} = 84$ mM; b) $C_{PS_0} = 168$ mM; c) $C_{PS_0} = 336$ mM. Molar ratio NaOH:PS was 2 in all experiments. Experimental Conditions in Table 2.

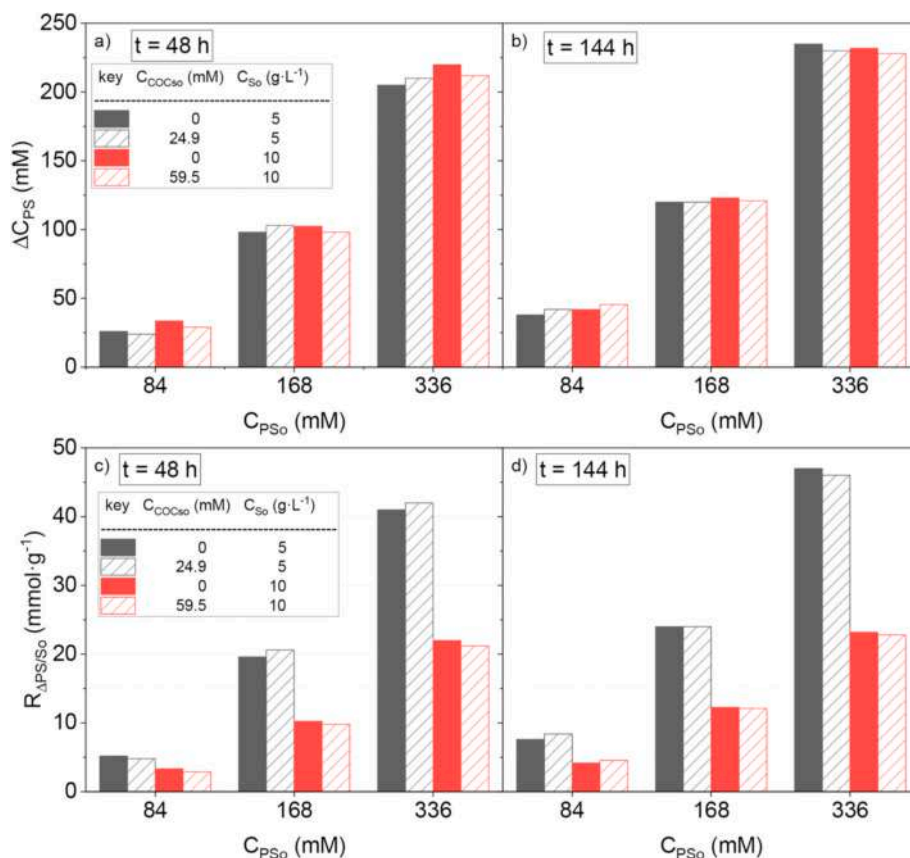


Fig. 3. PS consumption (a) 48 h and b) 144 h and $R_{\Delta PS/S_0}$ (c) 48 h and d) 144 h values at different oxidation times in runs in Table 2 at two initial concentrations of surfactant ($C_{S_0} = 5$ and 10 g·L⁻¹) and solubilized COCs ($C_{COCS_0} = 24.9$ and 59.5 mM). The molar ratio NaOH:PS was 2 in all runs.



It is worth highlighting that COCs are not oxidized under any conditions or during any runs in Table 2. Therefore, in these runs, the PS was mainly consumed by the surfactant. A similar consumption of PS in the absence (Table S1) and presence (Table 2) of COCs is noticeable by comparing results in Figs. 1 and 3.

At high enough surfactant and COCs concentration, macro-emulsions can be formed (Gupta and Mohanty, 2001; Kang et al., 2019; Okuda et al., 1996; Pennell et al., 1997; Zhou and Rhue, 2000). Macro-emulsions can contain a large amount of DNAPL as an organic phase in the micelle core (Pennell et al., 1997; Rosen and Kunjappu, 2012). (Okuda et al., 1996; Shiau et al., 1994). In Figure S8 of supplementary material, the visual aspect of the emulsion saturated with DNAPLs presented a milky phase characteristic of macro-emulsions (Kang et al., 2019; Pennell et al., 1997; Rosen and Kunjappu, 2012). The aspect of the corresponding surfactant solution in the absence of emulsified COCs is shown in Figure S9 of Supplementary Material.

On the other hand, the increase of initial surfactant concentration in Fig. 3 results only in a slight PS consumption increase. As cited in section 3.2.1, this finding can be explained by the formation of larger micelle structures as the surfactant concentration increases. These structures hinder the oxidation of surfactant and COCs molecules at the inside of the micelles. The higher the surfactant concentration, the higher the blocking of surfactant for both COCs and surfactant oxidation by PSA.

The initial concentration of surfactant in the runs in Table 2 using saturated emulsions seems to avoid the oxidation of COCs in the core of the micelle structure, hindering the contact between the oxidant, and the organic phase. Thus, the conditions tested in Table 2 are not

appropriate to apply an S-ISCO treatment with this reaction media (PSA, E3 non-ionic surfactant).

3.2.3. Oxidation of COCs in aqueous non-saturated emulsions

As deduced from previous sections, surfactant, COCs, and PS concentrations are critical parameters in the efficient application of S-ISCO. The experimental conditions for studying the oxidation of chlorobenzenes with a concentration lower than the saturation condition were summarized in Table 2.

Total COCs and solubilized COCs remaining in the vial are measured with time. Profiles are shown in Figure S10 of the supplementary information. The fraction of initial COCs that remain solubilized or precipitated with time is shown in Fig. 4. No aromatic or chlorinated by-products were detected in the oxidation of the chlorobenzenes mixture in the aqueous phase. The aspect of the solution at 3.6 mM is shown in Figure S11 of Supplementary Material.

As shown in Fig. 4 a, b, c, the higher the surfactant concentration, the lower the COCs removed (at constant initial COCs and PS concentration). This finding confirms the hindering of surfactant to COCs oxidation when the surfactant concentration increases. This fact agrees with that reported by Bouzid et al. (2017). The authors observed that the kinetic constant of phenanthrene oxidation using PS activated by temperature using Lauryl Betaine (LB) as surfactant decreased sharply with the increase of surfactant concentration.

At surfactant concentration of 1 g·L⁻¹ a remarkable decrease of total remaining COCs as the reaction time increased was noticed, achieving values of a remaining fraction of initial COCs between 0.19 and 0.3 at $C_{PS_0} = 252$ mM and 144 h of reaction time.

The ratio of the total oxidized COCs ($C_{COCS_0} - C_{COCS}$), which are shown in Figure S12a-c, and the corresponding PS consumed ($C_{PS_0} - C_{PS}$), which are shown in Figure S12d-f, defined as $R_{\Delta PS/S_0}$ in Eq. (7), is

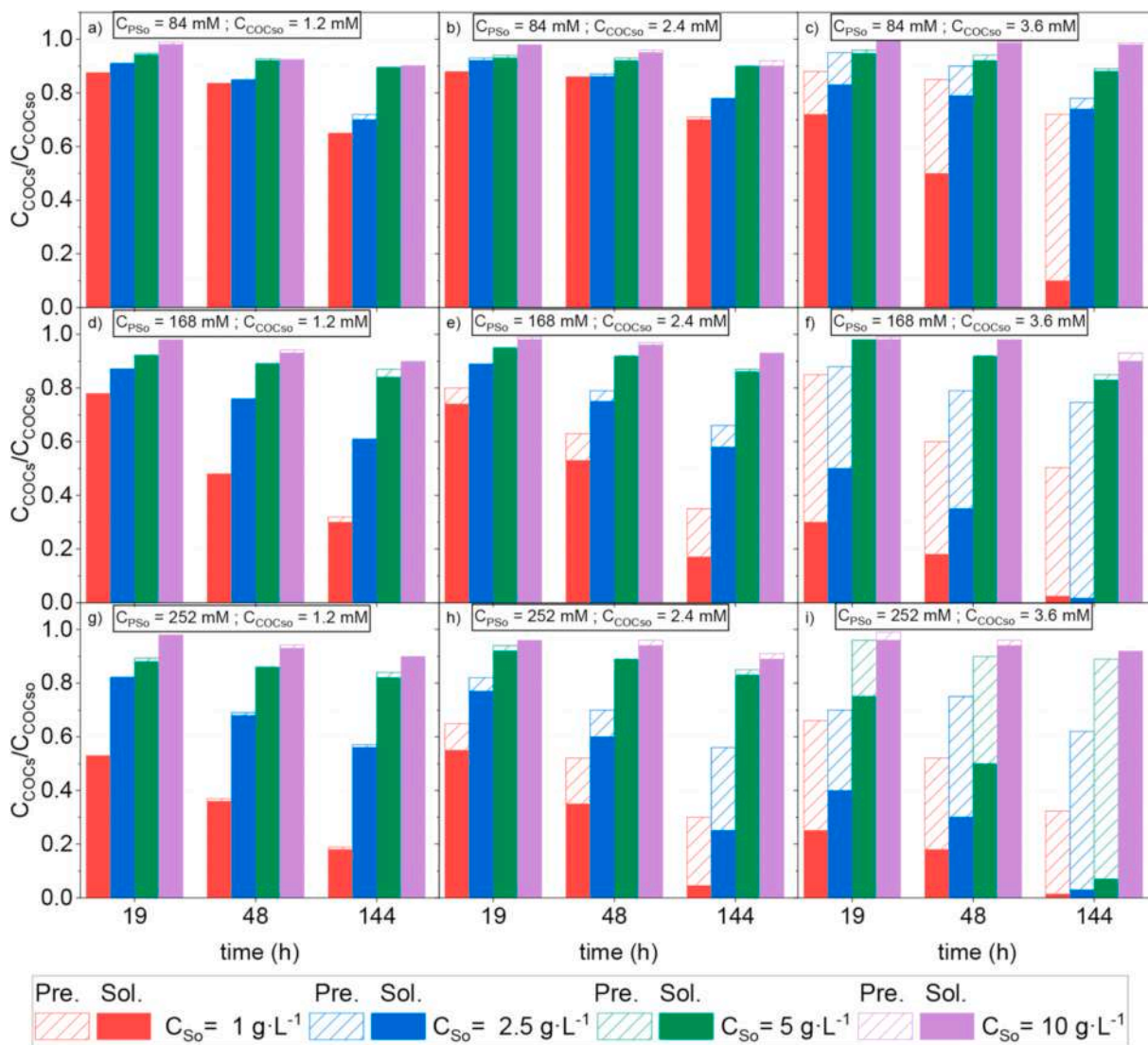


Fig. 4. Fractional remaining COCs in runs in Table 2, as the sum of solubilized COCs (Sol., filled bars) and precipitated COCs (Pre., patterned bars). Initial COCs solubilized: 1.2, 2.4 and 3.6 mM, PS concentration: 84, 168 and 252 mM and surfactant concentrations: 1, 2.5, 5 and 10 g/L. The molar ratio NaOH:PS was 2 in all runs.

shown in Fig. 5 for 144 h of reaction time. The PS consumption at different oxidation times (48 and 144 h) is shown in Figure S13 of the Supplementary Material.

$$R_{\frac{\Delta PS}{\Delta COCs}} = \frac{C_{PS_0} - C_{PS}}{\Delta COCs} = \frac{C_{COCs_0} - C_{COCs}}{\Delta COCs} \quad (7)$$

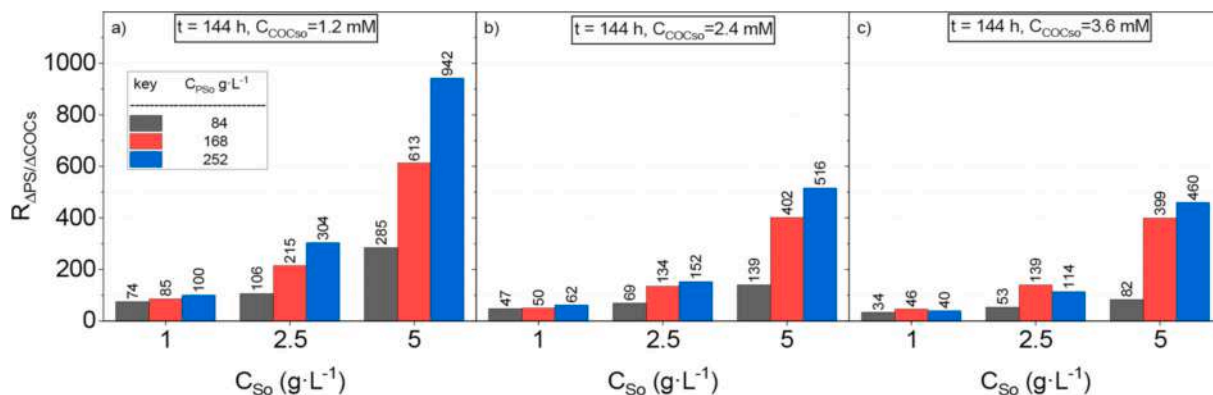


Fig. 5. Ratio $R_{\frac{\Delta PS}{\Delta COCs}}$ as a function of initial surfactant, PS and sum of chlorobenzene (COCs) concentrations calculated from results shown in Figure S12 (runs in Table 2). Initial COCs solubilized: a) 1.2, b) 2.4 and c) 3.6 mM and 144 h. The molar ratio NaOH:PS was 2 in all runs.

Higher efficiency of the oxidant in COCs abatement requires lower values of the ratio $R_{\Delta_{PS}/\Delta_{COCs}}$. In this way, better efficiencies were achieved at lower surfactant concentrations, as shown in Fig. 5. Moreover, for a given value of C_{S_0} , the higher the initial COCs solubilized, the lower the $R_{\Delta_{PS}/\Delta_{COCs}}$ value. However, if C_{S_0} decreases, the maximum amount of COCs that can be solubilized also decreases. Therefore, the surfactant dosage must be high enough to solubilize COCs at a concentration remarkably higher than the solubility achieved in the absence of surfactants but low enough to avoid the hindering of COCs to oxidation and promote a prohibited PS consumption.

A surfactant concentration of about 1 g L^{-1} has been chosen as the best value with PSA for the DNAPL mixture and surfactant used and tested reaction condition. With $C_{S_0} = 1 \text{ g L}^{-1}$, the maximum concentration of COCs that could be solubilized, according to Figure S1, is 5.2 mM. This value is about 10 times the solubilized COCs in the absence of surfactant if an equilibrium between the organic and aqueous phase is achieved.

On the other hand, the increase of initial PS concentration improves the oxidation of COCs, thus reducing the time required. However, the PS consumed per mol of removed chlorobenzenes, $R_{\Delta_{PS}/\Delta_{COCs}}$, also increases as PS concentration increases (Fig. 5). Consequently, the best value for PS initial concentration should consider both factors: the time required for COCs abatement and the unproductive PS consumption (associated with the loss of surfactant capacity and COCs precipitation). At the condition tested, a value of 168 mM can be chosen for S-ISCO runs. In addition, at a concentration of PS of 252 mM, fast precipitation of COCs occurs, as noticed in Fig. 4. However, the precipitation of COCs does not modify the COCs distribution in the aqueous phase, as shown in Figure S14 in the supplementary information.

3.2.4. ISCO vs S-ISCO

The time required in the presence (S-ISCO) or absence (ISCO) of surfactant to remove a mass of DNAPL contained in a liquid phase volume is compared in this section. Values selected for total DNAPL concentration in the vials (mass of DNAPL in a liquid volume) were 3.6 and 2.4 mM.

Selected conditions for S-ISCO in the previous section were $C_{PS_0} = 168 \text{ mM}$ and $C_{S_0} = 1 \text{ g L}^{-1}$. Moreover, with $C_{S_0} = 1 \text{ g L}^{-1}$ the maximum concentration of COCs that can be solubilized is 5.2 mM. Therefore, concentrations of 3.6 mM and 2.4 mM will be completely solubilized at zero time.

In the absence of surfactant, ISCO, the maximum concentration of solubilized COCs is 0.52 mM. The difference from this value to 2.4 or 3.6 mM will remain as an organic phase at zero time, and a partition of the DNAPL mass between aqueous and organic phases must be considered.

The time required to oxidize by PSA the COCs in a mass of DNAPL contained in a liquid volume, in the absence of surfactant, can be calculated, assuming that.

- The mass of DNAPL in the volume of the liquid phase is named as C_{DNAPL}
- C_{DNAPL} is the sum of solubilized DNAPL $C_{DNAPL_{aq}}$ and DNAPL remaining as an organic phase ($C_{DNAPL_{or}}$) (all concentrations in mM).

$$C_{DNAPL} = C_{DNAPL_{or}} + C_{DNAPL_{aq}} \quad (8)$$

- An equilibrium between organic and aqueous phases is assumed. Therefore, the aqueous concentration of compound j , j being each chlorinated compound in DNAPL, is calculated by Eq (3)
- The sum of solubilized Chlorobenzenes can be calculated as Eq (9)

$$C_{DNAPL_{aq}} = \sum S_j \gamma_j x_j \quad (9)$$

And the sum of Chlorobenzenes remaining as an organic phase can be

calculated as the difference between C_{DNAPL} and $C_{DNAPL_{aq}}$

- The oxidation of each chlorinated compound j occurs in the aqueous phase. Therefore, the removal of each j compound is calculated by Eq (10).

$$-\frac{dC_j}{dt} = k_{PS} C_{PS} C_{j_{aq}} = k_{PS} C_{PS} S_j \gamma_j x_j \quad (10)$$

C_{PS} being the concentration of PS (mM), k_{PS} the kinetic constant of reaction between PS and each chlorobenzene in the aqueous phase reported elsewhere (Santos et al., 2018b) ($k_{PS} = 1.31 \cdot 10^{-4} \frac{\text{L}}{\text{mmol h}}$) and C_j the concentration of j , sum of remaining j in the organic ($C_{j_{or}}$) and aqueous phases ($C_{j_{aq}}$)

$$C_j = C_{j_{aq}} + C_{j_{or}} \quad (11)$$

The sum of C_j being the remaining DNAPL in the media, C_{DNAPL} and the sum of $C_{j_{or}}$ the remaining DNAPL as an organic phase, $C_{DNAPL_{or}}$, both calculated by Eqs (12) and (13), respectively.

$$C_{DNAPL} = \sum C_j \quad (12)$$

$$C_{DNAPL_{or}} = \sum C_{j_{or}} \quad (13)$$

The removal of chlorobenzenes by PSA under the conditions of initial $C_{DNAPL} = 2, 4$ and 3.6 mM and $C_{PS} = 168 \text{ mM}$ has been predicted using Eqs (8)–(13). C_{PS} was considered constant with reaction time. $S_j \gamma_j$ values at $\text{pH} > 12$ and initial values of x_j for each j compound are shown in Table S2 of the supplementary information. The predicted values are compared with those obtained in the experiments carried out in absence of surfactant (ISCO experiment in Table 2). As can be seen in Fig. 6, a good agreement between the predicted and experimental values was found.

The partition of a mass of DNAPL between aqueous and organic phases when equilibrium is reached is named $R_{Aq/or}$, according to Eq. (14).

$$R_{Aq/or} = \frac{C_{DNAPL_{aq}}}{C_{DNAPL_{or}}} \quad (14)$$

The values of remaining fractional COCs with time in ISCO and S-ISCO and the profile of $R_{Aq/or}$ in ISCO are shown in Fig. 6.

As shown in Fig. 6, the time required to eliminate the COCs in the DNAPL mass in the liquid phase was remarkably reduced in S-ISCO compared with the value needed in ISCO. This fact is explained by the higher concentration of COCs in solution in S-ISCO. The ratio of DNAPL solubilized in the aqueous phase to that remaining as an organic phase, $R_{Aq/or}$, is of about 0.2 in ISCO (dotted lines in Fig. 6). If the oxidation occurs in the aqueous phase, the time required to remove a mass of DNAPL would be lower in S-ISCO.

In the absence of unproductive consumption of PS, the stoichiometric ratio for COCs mineralization is about 28 mM of PS per mM of chlorobenzenes (Dominguez et al., 2021). The consumption of PS is higher (about 40) under S-ISCO conditions (Fig. 4), but the time required for COCs abatement is remarkably lower.

On the other hand, the ISCO profiles in Fig. 6 have been calculated assuming a constant PS concentration value with time. Therefore, the DNAPL abatement simulated in ISCO has been slightly overestimated under this hypothesis. Moreover, an equilibrium between the organic and aqueous phases has been assumed. However, mass transfer between phases is usually limited under natural subsurface conditions, where DNAPL is trapped in soil fractures or low permeability zones. Therefore, the concentration of j in the aqueous phase will be lower than that considered in the ISCO simulation, and the DNAPL abatement achieved at a time by ISCO has been overestimated. Consequently, the improvement of S-ISCO has been underestimated.

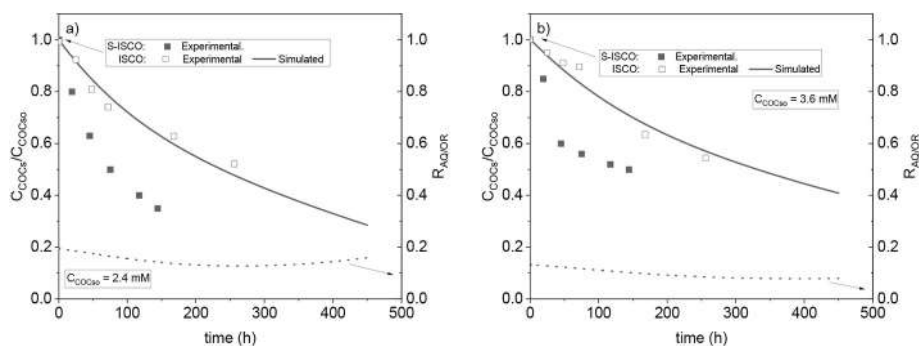


Fig. 6. Comparison of remaining fractional chlorobenzenes by S-ISCO (symbols, $C_{SO} = 1 \text{ g L}^{-1}$) and ISCO (solid lines). $C_{PSO} = 168 \text{ mM}$. Total COCs a) 2.4 mM and b) 3.6 mM. The dotted lines correspond to the fraction $C_{DNAPL\ aq} / C_{DNAPL\ OR}$ with time.

4. Conclusions

The simultaneous addition of PSA and surfactant decreases the time required to eliminate a mass of DNAPL in certain conditions. The optimal PS and surfactant concentration should consider the unproductive PS consumption, the solubilized COCs and the relative reactivity of surfactant and COCs with the oxidant.

The surfactant concentration increase slightly increases the PS consumption but produces a remarkable hindering of the COCs abatement. The formation of more complex micelle structures at higher surfactant concentrations could explain this phenomenon. The abatement of COCs was negligible due to a hindering effect of the surfactant. Using Emulse 3® as surfactant and a mixture of CB, DCB, TCB and TetraCBs as DNAPL, it was noticed that a surfactant concentration higher than 2.5 g/L caused only unproductive reactions without COCs removal.

The use of surfactant improved the solubility of COCs in water, solubilizing the DNAPL as a single pseudo-compound. The increase of surfactant concentration will increase the COCs solubilisation but hinder the COCs oxidation. Therefore, the surfactant concentration selected to eliminate this COCS with PSA was 1 g L^{-1} , considering affordable cost and time application. Besides, the increase of initial PS concentration improves the oxidation of COCs reducing the time required. However, the PS consumed per mol of removed chlorobenzenes increases with the initial PS concentration used. The PS concentration selected here was 168 mM. In general, the optimal value of these variables will depend on the nature of the COCs and surfactant and their relative reactivity against the oxidant. Each case requires laboratory studies before application to pilot or full scale to improve the efficiency of the treatment at a lower cost. Understanding the behaviour of oxidants, organic pollutants, and surfactants in the aqueous phase is critical to optimizing the operating conditions. However, the reactions taking place in the aqueous phase should be combined with the interaction between the specific soil and the aqueous phase for the design of each real case. The presence of soil can introduce adsorption phenomena that can be studied in each particular case.

Two reactions in series can explain the surfactant oxidation. The generation of the first surfactant by-products consumes PS, but the surfactant capacity is maintained. These by-products are further oxidized with an associate loss of the initial surfactant capacity promoting the COCs precipitation. Surfactant mineralization can be considered negligible.

Credit author statement

Raúl García-Cervilla: Methodology, Investigation, Writing – original draft. Aurora Santos: Funding acquisition, Resources, Conceptualization, Supervision. Arturo Romero: Funding acquisition, Resources. David Lorenzo: Conceptualization, Methodology, Supervision, Writing – original draft.

Declaration of competing interest

The authors declare that they have no known competing financial interests or personal relationships that could have appeared to influence the work reported in this paper.

Acknowledgements

This work was supported by the Regional Government of Madrid, through the CARESOIL project (S2018/EMT-4317), and the Spanish Ministry of Economy, Industry, and Competitiveness, through the project PID2019-105934RB-I00 and for the EU Life Program (LIFE17 ENV/ES/000260). Raúl García-Cervilla acknowledges the Spanish FPI grant (ref. BES-2017-081782).

Appendix A Supplementary data

Supplementary data to this article can be found online at <https://doi.org/10.1016/j.jenvman.2022.114475>.

References

- Acharya, K.R., Bhattacharya, S.C., Moulik, S.P., 1997. The surfactant concentration-dependent behaviour of safranine T in Tween (20, 40, 60, 80) and Triton X-100 micellar media. *J. Photochem. Photobiol. Chem.* 109, 29–34.
- Albergaria, J.T., Nouws, H.P., 2016. *Soil Remediation: Applications and New Technologies*. CRC Press, London.
- Babushok, V.I., Linstrom, P.J., Reed, J.J., Zenkevich, I.G., Brown, R.L., Mallard, W.G., Stein, S.E., 2007. Development of a database of gas chromatographic retention properties of organic compounds. *J. Chromatogr. A* 1157, 414–421.
- Bacocchi, R., D'Aprile, L., Innocenti, I., Massetti, F., Verginelli, J., 2014. Development of technical guidelines for the application of in-situ chemical oxidation to groundwater remediation. *J. Clean. Prod.* 77, 47–55.
- Bai, X., Wang, Y., Zheng, X., Zhu, K., Long, A., Wu, X., Zhang, H., 2019. Remediation of phenanthrene contaminated soil by coupling soil washing with Tween 80, oxidation using the UV/S2O8²⁻ process and recycling of the surfactant. *Chem. Eng. J.* 369, 1014–1023.
- Besha, A.T., Bekele, D.N., Naidu, R., Chadalavada, S., 2018. Recent advances in surfactant-enhanced In-Situ Chemical Oxidation for the remediation of non-aqueous phase liquid contaminated soils and aquifers. *Environ. Technol. Innovat.* 9, 303–322.
- Boutonnet, J.C., Thompson, R.S., De Rooij, C., Garny, V., Lecloux, A., Van Wijk, D., 2004. 1,4-Dichlorobenzene marine risk assessment with special reference to the OSPARCOM region: North Sea. *Environ. Monit. Assess.* 97, 103–117.
- Bouzdid, I., Maire, J., Brunol, E., Caradec, S., Fatin-Rouge, N., 2017. Compatibility of surfactants with activated-persulfate for the selective oxidation of PAH in groundwater remediation. *J. Environ. Chem. Eng.* 5, 6098–6106.
- Brand, N., Mailhot, G., Bolte, M., 1998. Degradation photoinduced by Fe(III): method of alkylphenol ethoxylates removal in water. *Environ. Sci. Technol.* 32, 2715–2720.
- Brusseau, M.L., 2013. The Impact of DNAPL Source-Zone Architecture on Contaminant Mass Flux and Plume Evolution in Heterogeneous Porous Media. ARIZONA UNIV TUCSON.
- Castillo, M., Penuela, G., Barcelo, D., 2001. Identification of photocatalytic degradation products of non-ionic polyethoxylated surfactants in wastewaters by solid-phase extraction followed by liquid chromatography-mass spectrometric detection. *Fresen. J. Anal. Chem.* 369, 620–628.
- Checa-Fernandez, A., Santos, A., Romero, A., Dominguez, C.M., 2021. Remediation of real soil polluted with hexachlorocyclohexanes (alpha-HCH and beta-HCH) using

- combined thermal and alkaline activation of persulfate: optimization of the operating conditions. *Separ. Purif. Technol.* 270.
- Cheng, M., Zeng, G., Huang, D., Yang, C., Lai, C., Zhang, C., Liu, Y., 2017. Advantages and challenges of Tween 80 surfactant-enhanced technologies for the remediation of soils contaminated with hydrophobic organic compounds. *Chem. Eng. J.* 314, 98–113.
- CLU-IN, 1991. Dense Nonaqueous Phase Liquids (DNAPLs). Clu-In.
- Dahal, G., Holcomb, J., Succi, D., 2016. Surfactant-oxidant Co-application for soil and groundwater remediation. *Remediation* 26, 101–108.
- Djohan, D., Yu, Q., Connell, D.W., 2005. Partition isotherms of chlorobenzenes in a sediment-water system. *Water Air Soil Pollut* 161, 157–173.
- Dominguez, C.M., Rodriguez, V., Montero, E., Romero, A., Santos, A., 2019. Methanol-enhanced degradation of carbon tetrachloride by alkaline activation of persulfate: kinetic model. *Sci. Total Environ.* 666, 631–640.
- Dominguez, C.M., Romero, A., Checa-Fernandez, A., Santos, A., 2021. Remediation of HCHs-contaminated sediments by chemical oxidation treatments. *Sci. Total Environ.* 751, 141754.
- EthicalChem, 2016. SEPR Pilot Test for Remediation of Creosote at Superfund Site Louisiana, US.
- Furman, O.S., Teel, A.L., Watts, R.J., 2010. Mechanism of base activation of persulfate. *Environ. Sci. Technol.* 44, 6423–6428.
- García-Cervilla, R., Romero, A., Santos, A., Lorenzo, D., 2020a. Surfactant-enhanced solubilization of chlorinated organic compounds contained in dnapl from lindane waste: effect of surfactant type and ph. *Int. J. Environ. Res. Publ. Health* 17, 1–14.
- García-Cervilla, R., Santos, A., Romero, A., Lorenzo, D., 2021. Partition of a mixture of chlorinated organic compounds in real contaminated soils between soil and aqueous phase using surfactants: influence of pH and surfactant type. *J. Environ. Chem. Eng.* 9, 105908.
- García-Cervilla, R., Santos, A., Romero, A., Lorenzo, D., 2020b. Remediation of soil contaminated by lindane wastes using alkaline activated persulfate: kinetic model. *Chem. Eng. J.* 393, 124646.
- García-Cervilla, R., Santos, A., Romero, A., Lorenzo, D., 2021. Compatibility of nonionic and anionic surfactants with persulfate activated by alkali in the abatement of chlorinated organic compounds in aqueous phase. *Sci. Total Environ.* 751, 141782.
- Gligorovski, S., Strekowski, R., Barbati, S., Vione, D., 2015. Environmental implications of hydroxyl radicals ($^{\bullet}\text{OH}$). *Chem. Rev.* 115, 13051–13092.
- Gupta, D.K., Mohanty, K.K., 2001. A laboratory study of surfactant flushing of DNAPL in the presence of macroemulsion. *Environ. Sci. Technol.* 35, 2836–2843.
- Interstate Technology Regulatory Council, 2000. Dense Non-Aqueous Phase Liquids (DNAPLs): Review of Emerging Characterization and Remediation Technologies.
- Kang, S., Lim, H.S., Gao, Y., Kang, J., Jeong, H.Y., 2019. Evaluation of ethoxylated nonionic surfactants for solubilization of chlorinated organic phases: effects of partitioning loss and macroemulsion formation. *J. Contam. Hydrol.* 223.
- Kosswig, K., 2000. Surfactants. Ullmann's Encyclopedia of Industrial Chemistry.
- Lanoue, M., Kessell, L., Athayde, G., 2011. Surfactant-enhanced in situ chemical oxidation (S-ISCO®). *Águas Subterráneas*. In: International Congress on Subsurface Environment, pp. 1–4.
- Lecloux, A.J., 2003. Scientific activities of Euro Chlor in monitoring and assessing naturally and man-made organohalogenes. *Chemosphere* 52, 521–529.
- Li, Y., Liao, X., Huling, S.G., Xue, T., Liu, Q., Cao, H., Lin, Q., 2019. The combined effects of surfactant solubilization and chemical oxidation on the removal of polycyclic aromatic hydrocarbon from soil. *Sci. Total Environ.* 647, 1106–1112.
- Li, Z.H., 2004. Surfactant-enhanced oxidation of trichloroethylene by permanganate - proof concept. *Chemosphere* 54, 419–423.
- Lin, C.M., Chang, G.P., Tsao, H.K., Sheng, Y.J., 2011. Solubilization mechanism of vesicles by surfactants: effect of hydrophobicity. *J. Chem. Phys.* 135.
- Lominchar, M.A., Lorenzo, D., Romero, A., Santos, A., 2018. Remediation of soil contaminated by PAHs and TPH using alkaline activated persulfate enhanced by surfactant addition at flow conditions. *J. Chem. Technol. Biotechnol.* 93, 1270–1278.
- Long, A., Lei, Y., Zhang, H., 2014. Degradation of toluene by a selective ferrous ion activated persulfate oxidation process. *Ind. Eng. Chem. Res.* 53, 1033–1039.
- Lorenzo, D., García-Cervilla, R., Romero, A., Santos, A., 2020. Partitioning of chlorinated organic compounds from dense non-aqueous phase liquids and contaminated soils from lindane production wastes to the aqueous phase. *Chemosphere* 239, 124798.
- Mendez-Diaz, J., Sanchez-Polo, M., Rivera-Utrilla, J., Canonica, S., von Gunten, U., 2010. Advanced oxidation of the surfactant SDBS by means of hydroxyl and sulphate radicals. *Chem. Eng. J.* 163, 300–306.
- Mobile, M., Widdowson, M., Stewart, L., Nyman, J., Deeb, R., Kavanaugh, M., Mercer, J., Gallagher, D., 2016. In-situ determination of field-scale NAPL mass transfer coefficients: performance, simulation and analysis. *J. Contam. Hydrol.* 187, 31–46.
- Okuda, I., McBride, J.F., Gleyzer, S.N., Miller, C.T., 1996. Physicochemical transport processes affecting the removal of residual DNAPL by nonionic surfactant solutions. *Environ. Sci. Technol.* 30, 1852–1860.
- Olmez-Hanci, T., Arslan-Alaton, I., Genc, B., 2014. Degradation of the nonionic surfactant Triton (TM) X-45 with HO center dot and SO4 center dot - based advanced oxidation processes. *Chem. Eng. J.* 239, 332–340.
- Pardo, F., Rosas, J.M., Santos, A., Romero, A., 2015a. Remediation of a biodiesel blend-contaminated soil with activated persulfate by different sources of iron. *Water Air Soil Pollut* 226.
- Pardo, F., Rosas, J.M., Santos, A., Romero, A., 2015b. Remediation of soil contaminated by NAPLs using modified Fenton reagent: application to gasoline type compounds. *J. Chem. Technol. Biotechnol.* 90, 754–764.
- Pennell, K.D., Adinolfi, A.M., Abriola, L.M., Diallo, M.S., 1997. Solubilization of dodecane, tetrachloroethylene, and 1,2-dichlorobenzene in micellar solutions of ethoxylated nonionic surfactants. *Environ. Sci. Technol.* 31, 1382–1389.
- Petitgirard, A., Djehiche, M., Persello, J., Fievet, P., Fatin-Rouge, N., 2009. PAH contaminated soil remediation by reusing an aqueous solution of cyclodextrins. *Chemosphere* 75, 714–718.
- Qiu, Y., Xu, M., Sun, Z., Li, H., 2019. Remediation of PAH-contaminated soil by combining surfactant enhanced soil washing and iron-activated persulfate oxidation process. *Int. J. Environ. Res. Publ. Health* 16.
- Rodrigo, M., Dos Santos, E., 2021. Electrochemically Assisted Remediation of Contaminated Soils.
- Rosen, M.J., Kunjappu, J.T., 2012. Surfactants and Interfacial Phenomena. John Wiley & Sons.
- Santos, A., Fernandez, J., Guadano, J., Lorenzo, D., Romero, A., 2018a. Chlorinated organic compounds in liquid wastes (DNAPL) from lindane production dumped in landfills in Sabinanigo (Spain). *Environ. Pollut.* 242, 1616–1624.
- Santos, A., Fernandez, J., Rodriguez, S., Dominguez, C.M., Lominchar, M.A., Lorenzo, D., Romero, A., 2018b. Abatement of chlorinated compounds in groundwater contaminated by HCH wastes using ISCO with alkali activated persulfate. *Sci. Total Environ.* 615, 1070–1077.
- Schaefer, C.E., Callaghan, A.V., King, J.D., McCray, J.E., 2009. Dense nonaqueous phase liquid architecture and dissolution in discretely fractured sandstone blocks. *Environ. Sci. Technol.* 43, 1877–1883.
- Schaefer, C.E., White, E.B., Lavorgna, G.M., Annable, M.D., 2016. Dense nonaqueous-phase liquid architecture in fractured bedrock: implications for treatment and plume longevity. *Environ. Sci. Technol.* 50, 207–213.
- Shiau, B.J., Sabatini, D.A., Harwell, J.H., 1994. Solubilization and microemulsification of chlorinated solvents using direct food additive (edible) surfactants. *Ground Water* 32, 561–569.
- Siegrist, R.L., Crimi, M., Simpkin, T.J., 2011. In: *Situ Chemical Oxidation for Groundwater Remediation*. Springer-Verlag New York, New York.
- Soga, K., Page, J.W., Illangasekare, T.H., 2004. A review of NAPL source zone remediation efficiency and the mass flux approach. *J. Hazard Mater.* 110, 13–27.
- Stroo, H.F., Leeson, A., Marqusee, J.A., Johnson, P.C., Ward, C.H., Kavanaugh, M.C., Sale, T.C., Newell, C.J., Pennell, K.D., Lebron, C.A., Unger, M., 2012. Chlorinated ethene source remediation: lessons learned. *Environ. Sci. Technol.* 46, 6438–6447.
- Tomlinson, D.W., Rivett, M.O., Wealthall, G.P., Sweeney, R.E.H., 2017. Understanding complex LNAPL sites: illustrated handbook of LNAPL transport and fate in the subsurface. *J. Environ. Manag.* 204, 748–756.
- Tsai, T.T., Kao, C.M., Yeh, T.Y., Liang, S.H., Chien, H.Y., 2009. Application of surfactant enhanced permanganate oxidation and biodegradation of trichloroethylene in groundwater. *J. Hazard Mater.* 161, 111–119.
- van Liedekerke, M., Prokop, G., Rabl-Berger, S., Kibblewhite, M., Louwagie, G., 2014. Progress in the Management of Contaminated Sites in Europe.
- van Wijk, D., Cohet, E., Gard, A., Caspers, N., van Ginke, C., Thompson, R., de Rooij, C., Garry, V., Lecloux, A., 2006. 1,2,4-Trichlorobenzene marine risk assessment with special emphasis on the OSPARCOM region North Sea. *Chemosphere* 62, 1294–1310.
- Van Wijk, D., Thompson, R.S., De Rooij, C., Garry, V., Lecloux, A., Kanne, R., 2004. 1,2-Dichlorobenzene marine risk assessment with special reference to the OSPARCOM region: North Sea. *Environ. Monit. Assess.* 97, 87–102.
- Wang, L., Peng, L., Xie, L., Deng, P., Deng, D., 2017. Compatibility of surfactants. And thermally activated persulfate for enhanced subsurface remediation. *Environ. Sci. Technol.* 51, 7055–7064.
- Wang, L., Wu, H., Deng, D., 2020. Role of surfactants in accelerating or retarding persulfate decomposition. *Chem. Eng. J.* 384.
- Wang, M.J., Jones, K.C., 1994. Behavior and fate of chlorobenzenes (CBS) introduced into soil-plant systems by sewage-sludge application - a review. *Chemosphere* 28, 1325–1360.
- Wang, W.H., Hoag, G.E., Collins, J.B., Naidu, R., 2013. Evaluation of surfactant-enhanced in situ chemical oxidation (S-ISCO) in contaminated soil. *Water, Air, Soil Pollut.* 224, 1–9.
- Zheng, F., Gao, B., Sun, Y., Shi, X., Xu, H., Wu, J., Gao, Y., 2016. Removal of tetrachloroethylene from homogeneous and heterogeneous porous media: combined effects of surfactant solubilization and oxidant degradation. *Chem. Eng. J.* 283, 595–603.
- Zhou, M.F., Rhue, R.D., 2000. Screening commercial surfactants suitable for remediating DNAPL source zones by solubilization. *Environ. Sci. Technol.* 34, 1985–1990.



Simultaneous addition of surfactant and oxidant to remediate a polluted soil with chlorinated organic compounds: Slurry and column experiments

Raul Garcia-Cervilla, Aurora Santos, Arturo Romero, David Lorenzo*

Chemical and Materials Engineering Department, Complutense University of Madrid, Spain

ARTICLE INFO

Keywords:

S-ISCO
Column
Persulfate
Nonionic surfactant
Chlorinated organic compounds

ABSTRACT

The inadequate management of wastes associated with chlorinated organic compounds (COCs) has become a huge environmental problem. Surfactant Enhanced In-Situ Chemical Oxidation (S-ISCO) was studied as a successful technique to remediate polluted sites. This work investigated the reaction between an aqueous solution of nonionic surfactant (Emulse-3®) and an oxidant (sodium persulfate activated with NaOH) with a real polluted soil with a complex mixture of COCs from lindane liquid wastes. Two experimental setups were used. In the first one, the reactions were carried out in batch mode under slurry conditions using different surfactant concentrations (0–10 $g \cdot L^{-1}$), 210 mM of persulfate and 420 mM of NaOH with an aqueous to soil ratio $V_L/W = 10 L \cdot kg^{-1}$. The runs were carried using a column loaded with the soil in the second experimental setup. The solution of surfactant, oxidant and activator was put in contact with soil in four pore volumes with a ratio aqueous to soil ratio $V_L/W = 0.2 L \cdot kg^{-1}$. Under these experimental conditions, the surfactant addition improved the reduction of COCs compared with the application carried out without surfactant, from 40.1% to values of conversion of 64.8–90.4%. However, an excess of surfactant hindered the COCs oxidation and increased the unproductive consumption of the oxidant, resulting in an optimal value of surfactant in the aqueous phase (1–2 $g \cdot L^{-1}$). A remarkable drop in the surfactant concentration in the aqueous phase and COCs solubilized was noticed in column runs due to the surfactant adsorption.

1. Introduction

Hydrophobic organic compounds (HOCs) such as chlorinated pesticides or solvents has been widely produced worldwide. The inadequate management of the production wastes has become a huge environmental problem [20,27,36,39].

The remediation of polluted sites with mixtures of HOCs is a challenge attracting the researchers interest [38]. In situ chemical oxidation (ISCO) has been successfully applied [1,33–35]. However, ISCO only takes place in the aqueous phase. The low solubility in water of HOCs [39] limits the ISCO application [38], increasing the time needed to remove the contamination on soil heavily contaminated [4,6,37]. To overcome this disadvantage, the simultaneous application of surfactants and oxidants (S-ISCO) has recently gained attention [4,5,23,25]. The surfactant enhances the HOCs solubilization in the aqueous phase [29,31] and improves the abatement reaction rate [4,8].

The selection of surfactant and the dose used in the S-ISCO application is not a trivial task. The surfactant must be biodegradable and

have low toxicity and adequate capacity for solubilization [40]. Among the different types of surfactants, the nonionic ones have been tested successfully in the S-ISCO applications ([6,10,44], Wang et al., 2019a, 2019b).

Despite, the higher the surfactant concentration, the higher amount of pollutants solubilized in the aqueous phase [21], the dose of surfactant must be optimized because of the following aspects: i) the surfactant reacts with the oxidant [18,28,43]; ii) the increase of surfactant concentration promotes a hindering effect in the contaminants avoiding the direct attack of the oxidant [5,19]; iii) the use of a high concentration of surfactant can produce the dispersion of contaminants in the polluted sites.

The application of surfactant and oxidant in polluted soil has been studied at a laboratory scale using well-agitated reactors where the polluted soil and the aqueous solution were put in contact in slurry experiments, using high ratios of aqueous volume to the soil. Li et al. used a 5 $L \cdot kg^{-1}$ of aqueous to soil ratio to study the simultaneous solubilization and oxidation of chlorinated organic compounds [22]; On the

* Corresponding author.

E-mail address: dlorenzo@quim.ucm.es (D. Lorenzo).

<https://doi.org/10.1016/j.jece.2022.107625>

Received 21 January 2022; Received in revised form 2 March 2022; Accepted 27 March 2022

Available online 30 March 2022

2213-3437/© 2022 The Author(s). Published by Elsevier Ltd. This is an open access article under the CC BY-NC-ND license (<http://creativecommons.org/licenses/by-nc-nd/4.0/>).

other hand, Wang et al. used a ratio of 200 $L \cdot kg^{-1}$ in the remediation of polyaromatic hydrocarbons from coal tar [43] with heat-activated persulfate and several anionic and nonionic surfactants. However, the S-ISCO technology at the field scale (in soils with effective porosity between 0.15 and 0.3) requires lower ratios between the injected aqueous phase and soil mass than those used in the literature.

Under these last conditions, where the ratio of aqueous phase to mass soil is low, the adsorption of surfactant injected on the polluted soil could significantly modify the partitioning of pollutants adsorbed and surfactant between soil and the aqueous phases [30,45]. The latter aspects even reduce the surfactant concentration in the aqueous phase, which means the surfactant capacity losses [16]. In addition, the oxidation reaction can contribute to the overall oxidation rate in soils with a high surface [17]. These aspects can be studied in a realistic way using column experiments. From our knowledge, the S-ISCO works in column experiments are very scarce [25,42]. These works were focused on determining the efficiency of pollutants removal without studying the surfactant adsorption, the HOCs oxidation in the soil surface and the consumption of oxidants by the adsorbed surfactants.

To fill this gap, this work studies the simultaneous addition of oxidant and surfactant in slurry and column ways to remediate heavily polluted soil. The selected soil was obtained from a polluted landfill where the liquid residue from lindane production was uncontrolled dumped [12,33,34]. This residue is composed of a mixture of chlorobenzenes (CB), hexachlorocyclohexanes (HCH) and hexachlorocyclohexanes (HeptaCH). These compounds have low solubilities in water and high adsorption in soil, forming a complex mixture adsorbed. The oxidant selected was sodium persulfate (PS) activated by alkali (PSA). PSA was successfully applied in a similar soil without surfactant [17]. In addition, NaOH promotes a quick dehydrochlorination of HCHs and HeptaCH to Trichlorobenzenes (TCB) and Tetrachlorobenzenes (TetraCBs), respectively, at $pH > 12$ [26].

From our knowledge, the S-ISCO applied to remediate real soil polluted by wastes of lindane production has not been carried out. The partition equilibrium and the oxidation of COCs and surfactants in both phases will be considered. Moreover, results obtained in slurry and column setups will be compared.

2. Material and methods

2.1. Materials

The soil used in this work was obtained from the Sardas landfill in Sabiñánigo (Spain), from a permeable layer heavily contaminated with the residues of the lindane production located at 13.5–14.0 m b.g.l. The subsoil of Sardas landfill is segmented into horizontal permeable and impermeable layers, being the soil used in the permeable layer (alluvium) where the groundwater flows. The alluvium contain gravel-sand with some clay interbedded [32]. Soil from the same well and depth was characterized elsewhere [15]. The characterization revealed a high carbonates content (higher than 43%w, expressed as $CaCO_3$). The total organic carbon in this soil was also determined, and the measured value was adequately explained by the COCs concentration in the soil. Therefore, the amount of other natural organic matter was considered negligible. Furthermore, different contamination levels were noticed in previous works depending on the soil size [15]. Therefore, the soil from the alluvium was sieved in two soil fractions: F (< 0.25 mm) and G (0.25–2 mm).

The surfactant used was E-Mulse® 3 (E3), a commercialized by EthicalChem. This surfactant was successfully applied in field remediation processes [11] applying S-ISCO in polluted sites with light and dense Non Aqueous Phase Liquids [4]. E3 is a non-toxic and biodegradable polyethoxylated nonionic surfactant. In addition, E3 was selected considering the results obtained from previous studies where different surfactants were tested [14,16,18]. The experimental results

showed that E3 presented a better solubilization ratio of COCs and compatibility with the PS activated with NaOH system than SDS, Tween 80 or Span 20.

Sodium persulfate (PS, Fisher Scientific) activated with alkali (NaOH, Fisher Scientific) was used as the oxidant agent. This oxidant system effectively eliminated COCs from the soil in the aqueous phase without surfactants [9,17]. The high amount of carbonates in the soil [16] make unbearable the use of the Fenton reagent with this soil due to the decomposition of H_2O_2 and Fe precipitation [9]. Regarding the activation methods of the PS, temperature, Fe or UV-light cannot be used since the contamination was found at depths higher than 15.

Commercial standards from Sigma-Aldrich were used for the identification of COCs from soil samples: chlorobenzene (CB), dichlorobenzene isomers (1,2-DCB; 1,3-DCB; 1,4-DCB), trichlorobenzene isomers (1,2,3-TCB; 1,2,4-TCB; 1,3,5-TCB), tetrachlorobenzene isomers (1,2,3,4-TeCB; 1,2,4,5-TeCB; 1,2,3,5-TeCB), pentachlorobenzene (PCB) and hexachlorocyclohexane isomers (α -HCH; β -HCH; γ -HCH; δ -HCH; ε -HCH). Standards of different solutions of DNAPLs in methanol (MeOH, Fisher Scientific) were used for the non-commercial isomers (pentachlorocyclohexenes, hexachlorocyclohexenes and heptachlorocyclohexanes), which were quantified elsewhere [33,34]. The COCs compositions in the soil fractions F and G, before any treatment, are summarized in the Table SM-1. As can be seen, a complex mixture of chlorinated compounds was identified. Most of the lighter chlorinated benzenes (chlorobenzene and dichlorobenzenes) were lost during soil transportation, storage, drying and milling.

Sodium sulfate (Fisher Scientific) was used to dry the soil samples. Hexane (Honeywell) and MeOH were used as extractants. Potassium iodide (Fisher Scientific), sodium hydrogen carbonate (Panreac), sodium thiosulfate pentahydrate (Sigma-Aldrich), and acetic acid (Sigma-Aldrich) were used in the analysis of oxidant concentration in the aqueous phases. Milli-Q water was used in all aqueous solutions.

2.2. Slurry experiments

Fraction F, with the highest COCs content (35.04 $mol \cdot kg^{-1}$, 10063 $mg \cdot kg^{-1}$) has a low hydraulic permeability due to the small particle sizes and cannot be used in column experiments. Experiments using F fraction were carried out in slurry mode using well-mixed vials of PTFE. An amount of 2 g of soil (W) was put in contact with 0.02 L of a NaOH (V_L) solution (100 $mmol \cdot L^{-1}$), to achieve the total dehydrochlorination of all non-aromatic COCs (HexaChlorocycloHexanes, HCH, and HeptaChlorocycloHexanes, HeptaCHs) in the soil to TriChloroBenzenes and TetraChloroBenzenes, respectively [17].

After 24 h the samples were centrifugated and the supernatant was replaced by 0.019 L of a solution with the corresponding concentration of surfactant (E3). Once the equilibrium between the aqueous and the solid phases was reached (< 24 h) [16], 0.001 L from an PS and NaOH concentrated solution with a molar ratio NaOH:SP = 2 was added. The experimental conditions of the runs carried out are summarized in Table 1. As can be seen, initial NaOH and PS concentrations in the vials in all the runs were 420 $mmol \cdot L^{-1}$ and 210 $mmol \cdot L^{-1}$. The surfactant concentration was 0 $g \cdot L^{-1}$ (run B0), 2.5 $g \cdot L^{-1}$ (run B2), 5 $g \cdot L^{-1}$ (run B5) and 10 $g \cdot L^{-1}$ (run B10). The water to soil (V_L/W) ratio was 10 $\cdot kg^{-1}$.

Zero time was considered after the oxidant and alkali addition. Vials were agitated (20–30 rpm) in a Labolan rotatory agitator. 5 vials were used for each experiment, and each vial was sacrificed at a reaction time.

Table 1
Experimental conditions of slurry runs. Aqueous to soil ratio $V_L/W = 10 L \cdot kg^{-1}$.

Name	E3 ($g \cdot L^{-1}$)	PS ($mmol \cdot L^{-1}$)	NaOH ($mmol \cdot L^{-1}$)
B1	0	210	420
B2	2.5	210	420
B3	5	210	420
B4	10	210	420

All experiments were conducted in duplicate, finding discrepancies between the experimental results lower than 6%. Aqueous and soil phases were separated by centrifugation, being remaining COCs analyzed in each phase.

A schematic of slurry runs and procedure can be seen in Figure SM-1 a) of the [supplementary material](#).

2.3. Column experiments

The soil with a higher size (G) was placed in glass columns. Each column has a diameter of 0.03 m with a side-feed (0.03 m from the bottom end) and a side-outlet (0.03 m from the top end). The effective length of the column is 0.0475 m. The bottom end of the column was closed with a cap of flexible silicone with a folding skirt. The bottom was filled with glass spheres (0.25 mm of diameter), on which fibreglass was placed (completely covering the feed). After this, the polluted soil (fraction G, 10.83 mmol·kg⁻¹ of COCs) was added (0.05 kg). The column interior was completed by placing the fibreglass (covering the side-outlet), the glass spheres, and the cap (for the top end of the column). Finally, the side-feed was connected to a peristaltic pump (Spetec Perimax 12) to add the feed solutions from a glass bottle, and a tube was connected to the side outlet to collect the output solutions. A metallic mesh was always placed between the soil bed and the fibreglass. Figure SM-1 b) of the [supplementary material](#) shows a schematic of the column assembly.

Milli-Q water was injected in the glass column to reach pore water saturation as a previous treatment. Following, 100 mL of an aqueous solution 100 mmol·L⁻¹ in NaOH was injected at 0.3 mL·min⁻¹, being reposed in the columns during 24 h. These conditions were enough to convert non-aromatic COCs of soil into TCBs and TetraCBs [17]. It was confirmed that nor HCHs nor HeptaCHs were detected in the aqueous phase after this period. In this process, the total COCs removed from the soil to the aqueous phase were quantified being less than 1% of the initial COCs in soil.

After the alkaline treatment, an aqueous solution containing oxidant/activator and surfactant was injected into each column at 0.3 mL/min. The oxidant concentration at the column exit was monitored by finding a S profile, with an average retention time of 35 min. A 95% of the inlet oxidant concentration was measured in the outlet stream after 40 min of injection time (12 mL injected). In plug flow, the breakthrough curve for the oxidant concentration would correspond to a step profile after injecting the PV (10 mL) for 34 min at the flow rate employed (0.3 mL/min). Therefore, the small axial dispersion of the injected fluid can be inferred.

After 40 min, the flow stopped, and the aqueous solution injected remained the chosen reaction time in the column. Moreover, it should be noticed that the reaction time between injections was 70–170 times higher than the time required for injection of each PV.

After each reaction time selected, the aqueous phase in the columns was flushed by injecting another pore volume of an aqueous solution containing the same concentrations of reagents used in the previous pore volume injected. The aqueous phase flushed with each pore volume injection was collected and analyzed, and this procedure was repeated four times. Finally, a pore volume of Milli-Q water was injected to flush the last pore volume injected with the reagents, and the column was disassembled. Then, the remaining COCs in the soil were analyzed by triplicate. The soil was divided into three fractions: column bottom, center and top.

The conditions of column experiments are summarized in.

Table 2. As can be seen, in column C1 no surfactant was injected (ISCO run), while in columns C2 and C3 (S-ISCO), a concentration of 5 and 10 g·L⁻¹ of surfactant was injected, respectively, with each pore volume. Oxidant (PS) and activator (NaOH) at each pore volume injected were 210 and 420 mmol·L⁻¹, respectively. Injection flow rate was of each pore volume was 0.3 mL·min⁻¹.

Table 2

Experimental Conditions in column runs. COCs in soil G 10.94 mmol·kg⁻¹ PS= 210 mM,.

Parameters	C1	C2	C3
Soil height (m)	4.75·10 ⁻²	4.75·10 ⁻²	4.75·10 ⁻²
Soil mass (kg)	0.053	0.052	0.051
Pv (L)	1.12·10 ⁻²	1.09·10 ⁻²	1.08·10 ⁻²
C _{E3} injected (g·L ⁻¹)	0	5	10
C _{PS} injected (mM)	210	210	210
C _{NaOH} injected (mM)	420	420	420
reaction times (h): Pv1/Pv2/ Pv3 /Pv4	113/48/ 48/113 (all columns)		

2.4. Analytical methods

The soil was analysed at each reaction time in the slurry experiment or at the final time in column runs. The soil moisture was removed by adding anhydrous sodium sulfate, and 30 mL of MeOH was added to 2 g of soil and COCs were extracted by ETHOS ONE microwave (Milestone). This procedure was carried out following EPA 3546. The liquid phase obtained was filtered (0.45 μm, nylon), and the COCs were analyzed in Gas Chromatograph equipped with a flame ionization detector and electron capture detector (GC-FID/ECD). The chromatographic method was described elsewhere [15]. The soil before the treatments described above was dried at room temperature (23 ± 2 °C), however the extraction of COCs was carried out following the same methodology.

In the aqueous phases collected, pH COCs and PS concentrations were analyzed. In the absence of surfactant, the COCs were extracted from the aqueous phase using hexane in a volume ratio of 1:1, and GC-FID/ECD analyzed the organic phase. In the presence of E3, the COCs were analyzed directly from the aqueous phase after dilution of the sample with MeOH (volume ratio 1:10). The oxidant in the aqueous phase was analyzed by potentiometric titration (Metrohm, Tiamo 2.3) using a titrant solution of sodium thiosulfate. A Basic 20-CRISON pH electrode determined the pH.

3. Results and discussion

3.1. Alkaline pretreatment

The COCs composition in F and G soil fractions after the alkaline treatment is summarized in Table SM-1 in the [supplementary material](#). In slurry and column experiments, the alkaline treatment converted the non-aromatic cyclic chlorinated HCHs-PentaCXs and HexaCXs-HeptaCHs, respectively, in TCBs and TetraCBs. as described elsewhere [15,26]. These compounds were produced by the dehydrochlorination of the non-aromatic COCs in the alkaline pretreatment. As shown in Table SM-1, the COCs molar content in soils is similar before and after the alkaline treatment, but the average molecular weight of COCs in soils has been reduced due to reactions schematized in Figure SM-2.

Although the soil fractions F and G have different COCs content, the COCs distributions are similar, as shown in Figure SM-3. After alkaline treatment, COCs removed from the soil phase (in slurry and column experiments) were a small fraction (less than 2%) of the initial COCs in soil.

3.2. Slurry experiments

The amount of COCs (in mmol) in the aqueous and soil phases in the presence and absence of surfactant (runs B1, B2, B3 and B4) before the oxidant addition (zero time) are plotted in Fig. 1. As can be seen, the concentration of COCs in the aqueous phase remarkably increased by adding surfactant. The surfactant promotes the desorption of COCs from the soil ([16], Wang et al., 2019a,2019b, [16,21]). The solubilization of hydrophobic organic compounds is carried out by micelles formed by the surfactant molecules in the aqueous phase [21,31]. COCs solubilization in micelles is expected as the surfactant concentrations used here

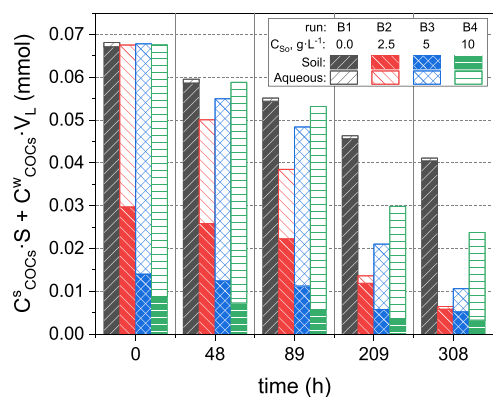


Fig. 1. Total amount of COCs (mmol) in soil (solid bars) and aqueous phases (lined bars) at different reactions times and initial surfactant concentration. $C_{PSO} = 210 \text{ mmol} \cdot \text{L}^{-1}$, $C_{NaOH} = 420 \text{ mmol} \cdot \text{L}^{-1}$ and $V_L/W = 10 \text{ L} \cdot \text{kg}^{-1} = 10$, with $V_L = 20 \text{ mL}$ $W = 2 \text{ g}$ and $(C_{COCs,soil})_o = 33.8 \text{ mmol kg}^{-1}$.

were higher than CMC of E3 ($\text{CMC} = 80 \text{ mg} \cdot \text{L}^{-1}$) [13,45,46]. The higher the initial surfactant concentration, the higher the solubilization of COCs in the aqueous phase. However, the solubilization increases more slowly when the surfactant concentration increases, confirming the Langmuir type isotherm noticed elsewhere [16]. In the absence of surfactant (B1) solubilized COCs are less than 2% of the initial COCs in soil. Adding 2.5, 5, and 10 g L^{-1} of surfactant, the solubilized COCs are 56%, 80% and 88% of the initial COCs in soil, respectively.

Moreover, surfactant adsorption should be considered. As was previously reported, the surfactant added in the aqueous phase is adsorbed in polluted soil, reducing the amount of active surfactant in the aqueous phase. After the surfactant addition, a new equilibrium of surfactant and COCs are reached between the aqueous and soil phases. Considering the results in previous works [16], surfactant concentrations in soil when equilibrium is reached (at zero time) are calculated, being approximately 11000, 20100, 23900, $\text{mg} \cdot \text{kg}^{-1}$ in runs B2, B3 and B4, respectively (zero time). Taking into account that $V_L/W = 10$, the surfactant adsorption only changes the active surfactant concentration significantly in the aqueous phase when the initial surfactant added was 2.5 $\text{g} \cdot \text{L}^{-1}$ (B2 run). In run B2 the surfactant concentration in the aqueous phase at equilibrium conditions was calculated as 1.4 $\text{g} \cdot \text{L}^{-1}$. In runs B3 and B4, negligible differences between the initial surfactant added and the active surfactant concentration in the aqueous phase were obtained when the equilibrium was reached (zero time). The active surfactant concentration was defined as the concentration of virgin surfactant with the same COCs solubilization capacity as that observed in the surfactant aqueous solutions after oxidation.

The partition equilibrium of COCs between the aqueous and soil phases is defined in Eq. (1) as:

$$K_D = \frac{C_{COCs,soil}}{C_{COCs,aq}} \quad (1)$$

Being $C_{COCs,soil}$, in (mmol kg^{-1}), and $C_{COCs,aq}$, in ($\text{mmol} \cdot \text{L}^{-1}$), the COCs concentration in the soil and aqueous phases at the corresponding reaction times. In a previous work [16] the partition equilibrium of surfactant and COCs between the soil and the aqueous phase was studied in slurry experiments. It was found that the partitioning equilibrium between phases was achieved in less than 2–3 h [16], and this time is much shorter than reaction times required for COCs abatement. In that way, it can be considered that the equilibrium of COCs and surfactants between soil and aqueous phases is reached with the reaction progress. Corresponding K_D values are calculated and shown in Fig. 2. The partition coefficient remarkably decreases after the surfactant addition. This parameter is influenced by the active surfactant concentration in the aqueous phase, in agreement with previously reported results [16]. The active surfactant in the aqueous phase with at zero and 308 h were

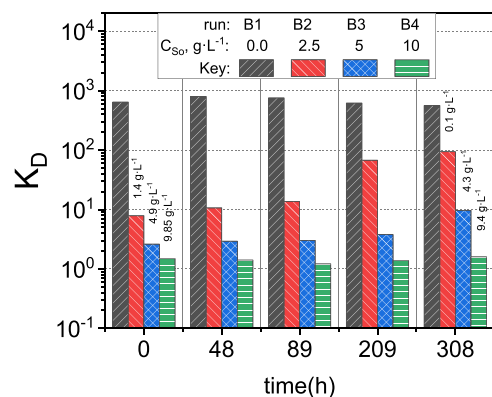


Fig. 2. Partitioning coefficient of surfactant between soil and aqueous phases in $\text{L} \cdot \text{kg}^{-1}$ calculated with Eq. (1) for runs in Table 1. Active surfactant concentration at zero time and after 308 h were measured and given as numbers above the bars.

measured following the procedure given elsewhere [18] by knowing the amount of COCs dissolved in the aqueous solution. These values are shown in Fig. 2 above the bars. As shown in Fig. 2, the active surfactant concentration in the aqueous phase decreases with time due to the unproductive consumption of the oxidant at 2.5 $\text{g} \cdot \text{L}^{-1}$, whilst this reduction was lower.

The molar distributions of COCs in both soil and aqueous phases at equilibrium conditions before the oxidant addition (zero time) are shown in Figures SM-4–6. Similar COCs distributions were obtained in the soil and the aqueous phases of runs B2, B3 and B4. On the contrary, in the absence of surfactant, the percentage of TCBS (in the total COCs) in the aqueous phase is higher than the TCBS percentage in the soil phase. Therefore, the surfactant solubilizes the COCs mixture initially adsorbed on the soil as a single phase. On the contrary, in the absence of surfactant, the preferential solubilization of the lighter compounds (TCBs) was noticed, in agreement with previously reported [7,26].

Once the equilibrium between soil and aqueous phases was reached, PS and NaOH were added to the reaction medium. The concentration of COCs in the aqueous and soil phases was analyzed at different reaction times for runs B1 to B4 in Table 1. The total amount of COCs (in mmol) remaining in each phase at different reaction times are also plotted in Fig. 1. The conversion of COCs has been calculated from the sum of remaining COCs in both phases, according to Eq. (2).

$$X_{COCs,batch} = \frac{C_{COCs,soil} W + C_{COCs,aq} V_L}{(C_{COCs,soil})_o W} \quad (2)$$

being $(C_{COCs,soil})_o$ the concentration of COCs in the soil before it was in

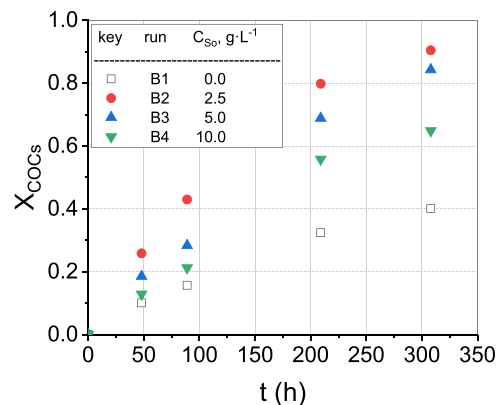


Fig. 3. COCs conversion in slurry runs with reaction time in runs summarized in Table 1.

contact with the aqueous phase. Values of $X_{COCs_{batch}}$ with time are shown in Fig. 3.

As shown in Fig. 1, the sum of COCs in both phases decreased as the reaction time increased. Accordingly, the COCs conversion increases with reaction progress (Fig. 3). When a surfactant is added, a significant decrease in the total COCs in the reaction media is noticed at the final time studied (308 h) compared to the decrease obtained in the absence of surfactant (run B1). The higher conversion observed using surfactant can be explained by the increase of COCs concentration in the aqueous phase. The solubilization capacity of the surfactant improved the availability of COCs to the oxidant in this phase [4,22,24]. Li, Liao et al. Li et al., [22] studied the oxidation of different hydrophobic organic compounds, initially adsorbed in soil samples, using several oxidants in the presence and absence of surfactant. They found that the combination of surfactant and oxidant enhanced the elimination of the contaminants compared with using only the oxidant.

However, an increase in the initial surfactant concentration above 2.5 g L^{-1} did not result in a higher conversion of COCs, as shown in Fig. 1 and Fig. 3. On the contrary, COCs conversion decreases when the initial surfactant concentration rises from 2.5 to 5 g L^{-1} . The X_{COCs} values at 380 min were 0.4, 0.9, 0.86 and 0.62 when initial surfactant concentration added was 0, 2.5, 5 and 10 g L^{-1} . This trend of COCs conversion with the surfactant concentration increase was also noticed in the aqueous phase in the absence of soil ([5], Wang et al., 2019a,2019b). It can be related to higher surfactant concentrations that prevent COCs oxidation in the micelles. Moreover, higher surfactant concentration in the aqueous phase favours the unproductive consumption of PS to the COCs oxidation. The higher the surfactant concentration, the higher the COCs in solution, the higher the surfactant hindrance to COCs oxidation, and the higher unproductive PS consumption. Therefore, the solubilized COCs is more efficient at lower surfactant concentration because higher surfactant concentration hinders the oxidation of COCs in the micelles [5,41]. Therefore, the decrease in the COCs conversion with the increase of the surfactant concentration, Fig. 3, was due to the protective effect of the micelles on the COCs solubilized inside of the micelles [41]. However, the lower the surfactant in the aqueous phase, the lower the COCs solubilized. As a result, there is an optimal value of surfactant in the aqueous phase to increase the overall oxidation rate of COCs, in agreement with previously reported [2,3,5].

The PS conversion in runs in Table 1 is shown in Figure SM-5. The higher the initial surfactant concentration, the higher the PS conversion. In the absence of surfactant (run B1), the PS conversion increases gradually with time. On the contrary, the higher the initial surfactant concentration, the higher the initial consumption of PS. The initial fast consumption of PS could be related to the unproductive consumption of PS by reaction with the surfactant micelles in the aqueous phase. However, the increase in PS conversion is not linear with the surfactant concentration added, in agreement with previously reported in the soil absence [19].

With the results in Figure SM-5 and Fig. 3, it can be deduced that higher PS consumption does not imply higher COCs conversion. In fact, despite the lower PS consumed in B2, COCs conversion obtained in runs B3 and B4 are lower than that obtained in B2, confirming the relevance of unproductive PS consumption at higher surfactant dosages. The PS consumed per mol of COCs reacted (θ_{PS}) was calculated by Eq. (3):

$$\theta_{PS_{batch}} = \frac{V_L(C_{PS0} - C_{PS})}{[(C_{COCs})_0 W - C_{COCs_{soil}} W + C_{COCs_{aq}} V_L]} \quad (3)$$

where C_{PS0} and C_{PS} are the PS concentrations (mmol L^{-1}) in the aqueous phase at zero time and at the corresponding reaction time, respectively. The time profiles of θ_{PS} in runs B1 to B4 are plotted in Fig. 4.

It was noticed that higher $\theta_{PS_{batch}}$ are obtained when surfactant concentration increases, confirming the competitive reaction between surfactant and COCs for the oxidant in the aqueous phase. However, lower values of θ_{PS} are obtained in the presence of soil compared to those

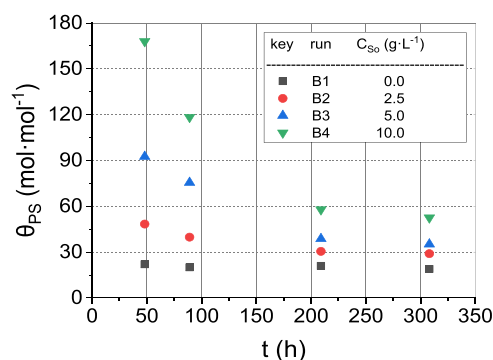


Fig. 4. Consumption of PS per sum of the total COCs consumed in slurry runs summarized in Table 1.

obtained previously in the soil absence [19]. This difference can be due to the contribution of the reaction between adsorbed COCs and PS to overall COCs conversion. The direct reaction of COCs adsorbed on the soil surface with the oxidant has been reported in the absence of surfactant [17]. Thus, it can be inferred that both dissolved COCs in the aqueous phase and adsorbed COCs react with the oxidant.

In the presence of surfactant, the partition coefficient increases with time, as shown in Fig. 2. This rise corresponds to a surfactant decrease in the aqueous phase with time. Two reasons can explain this drop. The first reason is the surfactant oxidation in the aqueous phase since PS can react with surfactant and COCs in a competitive reaction, as was reported in experiments performed in the absence of the soil [26]. The second reason is the oxidation of adsorbed COCs with time, causing a new equilibrium between soil and aqueous phases, resulting in continuous adsorption of surfactant micelles with COCs from the aqueous phase to the soil phase, and the corresponding decrease of the surfactant in the aqueous phase. Considering the initial surfactant concentration in the aqueous phase and the VL/W ratio used, the effect of surfactant adsorption on active surfactant concentration change in the aqueous phase is more relevant in B2 than in B3 and B4. This fact explains that the rise in K_D in Fig. 2 follows the trend $B2 > B3 > B4$. The higher the surfactant concentration added, the lower the K_D increase with the reaction time.

The molar distributions of COCs in both phases at 308 h of reaction time in runs B1, B2, B3, and B4 are shown in Figure SM-6 (aqueous phase) and Figure SM-7 (soil phase). These figures also provide the initial molar distribution of COCs in the initial soil (fraction F). Comparing the results in Figure SM-4 (zero time), Figure SM-6 and Figure SM-7, it is found that when a surfactant is added, similar COCs distributions were found in the initial soil, aqueous phase and soil phase with the reaction progress.

3.3. Column experiments

The column experiments were carried out with the soil fraction G (0.25–0.2 mm) with higher permeability than fraction F ($<0.25 \text{ mm}$), allowing experiments with water flow. As mentioned previously, soil fractions F and G have a similar distribution of COCs. The initial concentration of contaminants in the F fraction was higher than in the G fraction (Table SM-1).

In the column experiments, the surfactant (E3) concentrations tested were 0 (C1), 5 (C2) and 10 g L^{-1} (C3) maintaining the oxidant and activator concentration in the solution fed in 210 and 420 mmol L^{-1} , respectively. The experimental procedure has been described in the Experimental section, and the operating conditions are summarized in Table 2.

The mmol of COCs in each flushed pore volume (PV1 to 4, shown in Table 2) after remaining a specific time in the soil column is shown in Fig. 5a. The mmol of COCs flushed from the column with the injection of

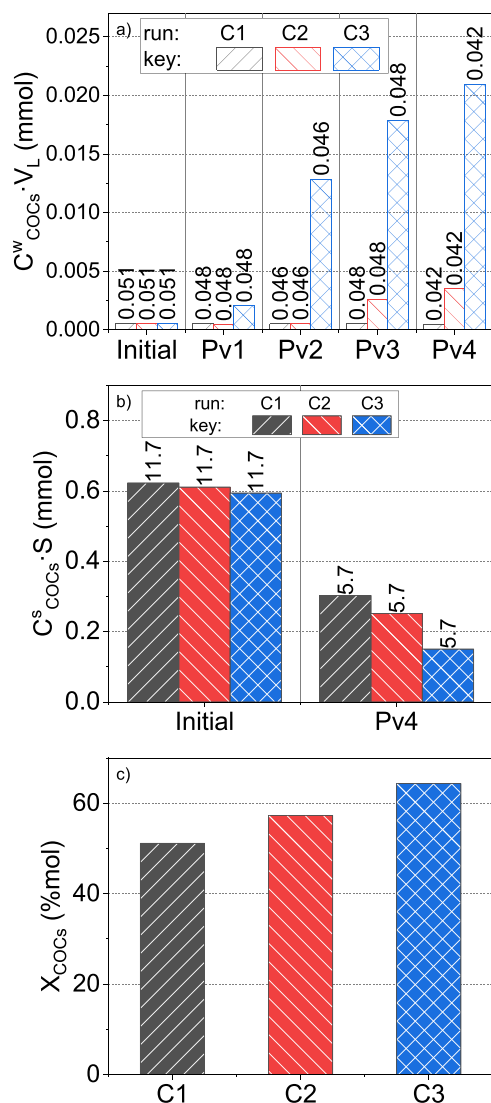


Fig. 5. (a) mmol of COCs in each Pore Volume flushed from the column (b) mmol of COCs in the initial soil in the column and in the soil after the column disassembling. (c) COCs conversion calculated by Eq. (4) after column disassembling. The concentration of COCs as $mmol \cdot L^{-1}$ (aqueous phase) or $mmol \cdot kg^{-1}$ (soil phase) are indicated at the top of the bars (experimental conditions in Table 2).

the first pore volume (named as initial) is also shown in Fig. 5a. The amount of COCs (mmol) in the initial soil placed in the column and the amount of COCs (mmol) remaining in the soil after the columns disassembling are shown in Fig. 5b. The COCs concentration ($mmol \cdot L^{-1}$) in the aqueous phase of each PV flushed and the COCs concentration in soil ($mmol \cdot kg^{-1}$) after the column disassembling are indicated at the top of the bars.

As shown in Fig. 5a, the surfactant injected into the column improved the solubilization of the COCs in the aqueous phase. The higher the surfactant concentration in the pore volume injected, the higher the solubilized COCs in the pore volume extracted. Moreover, as more pore volumes with a surfactant are injected, more COCs are solubilized in the Pore Volume extracted. This last observation can be mainly related to surfactant adsorption in soil. As more pore volumes with a surfactant are injected or higher surfactant concentrations are injected in the column, the partition equilibrium of surfactant between the soil and aqueous phases yields higher surfactant concentration and COCs dissolved in both phases. In the absence of surfactant injections (run C1) the COCs concentration in the four pore volumes flushed have

similar values.

The total conversion of COCs in each column after the column disassembling has been calculated considering the mmol remaining in the soil and the mmol of COCs eluted in the four-pore volume flushed, according to Eq. (4). The remanent amount of COCs in soil was measured at the bottom, centre and top, finding similar values between the different fractions (standard deviation lower than 5%).

$$X_{COCS} = \frac{((C_{COCS})_o - C_{COCS})W - \sum_1^{4VP} C_{COCSVP}VP}{(C_{COCS})_o W} \quad (4)$$

Overall COCs conversion after column disassembling is shown in Fig. 5c. As can be seen, the simultaneous injection of E3 and oxidant (experiments C2 and C3) promotes COCs oxidation. Accordingly, the higher the concentration of surfactant injected, the higher the total conversion obtained in the column experiments. There is a significant conversion of the COCs in C1 without surfactant. In a previous work [17], an ISCO treatment was applied to the same soil in slurry way, being noticed that reaction took place not only in the aqueous phase but also in the soil surface.

The COCs distributions in each PV flushed, and the COCs molar distribution in the soil after the column disassembling are plotted in Fig. 6. In run C1 (carried out in the absence of the surfactant, ISCO), there is lower solubilization of COCs in the aqueous phase, with similar values of solubilized COCs at all the pore volumes flushed. Moreover, in C1 the TCBS in soil are selectively dissolved to TetraCBs, as noticed in slurry runs in the absence of surfactant (Figure SM-6). This selectivity in the COCs solubilization was also observed in the first and second PV flushed from the column C2 ($5 \text{ g} \cdot L^{-1}$ of surfactant was injected into the column). The amounts and distribution of COCs solubilized in these first two pore volumes in C2 are like the corresponding values found in C1 (in the absence of surfactant). On the other contrary, the molar distribution of COCs in flushed PV3 and PV4 (C2) was similar to that found in initial soil. When the surfactant concentration in the pore volume injected was $10 \text{ g} \cdot L^{-1}$ (column C3), the molar distribution of COCs in all the PV flushed was always like the initial molar distribution of COCs in the soil placed in the column.

As shown in Fig. 5, the concentration of solubilized COCs increases with the number of PVs injected. Using $10 \text{ g} \cdot L^{-1}$ of surfactant (C3), the highest solubilization of COCs in the aqueous phase was noticed (up to $2 \text{ mol} \cdot L^{-1}$ in the four pore volume flushed). As a first approach, the surfactant remaining in the aqueous phase of each PV flushed can be calculated from the isotherms provided in previous work [16]. Taking into account the desorption isotherms in the Molar Solubilization Ratio in the aqueous phase is approximately linear in the range $0.2\text{--}2 \text{ g}_{surf} \cdot L^{-1}$. A value of 2 mM of COCs in the aqueous phase (noticed in PV4, C3) can be approximately related to $2 \text{ g} \cdot L^{-1}$ of surfactant in the aqueous phase if desorption equilibrium is faster than oxidation in the aqueous phase. From results in Fig. 5 and data previously reported [19] the surfactant in the aqueous phase in all the PV and columns have been estimated and values are shown in Figure SM-8. As can be seen, the maximum surfactant concentration in any of the PVs flushed in C2 and C3 was lower than $2 \text{ g} \cdot L^{-1}$. The low solubilization of COCs in flushed PV1 and PV2 in C2, and the selective solubilization of TCBS suggest the absence of surfactant in the aqueous phase, explained by the surfactant adsorption.

The first and fourth pore volumes injected remains similar times in the column before being flushed. As can be seen in Fig. 5 and Figure SM-8, COCs solubilized and active surfactant concentration in flushed PV4 in C3 were higher than those found in VP1. The increase in solubilized COCs and surfactant concentrations in solution with successive PVs indicates that surfactant adsorption is the cause of these trends.

The column experiment also investigated the oxidant consumption in the absence (C1) and presence (C2, C3) of surfactant. The conversion of PS in each PV injected is shown in Fig. 7a. In C1, C2 and C3, the PS conversion in the flushed PV1 and PV4 is higher than in PV2 and PV3.

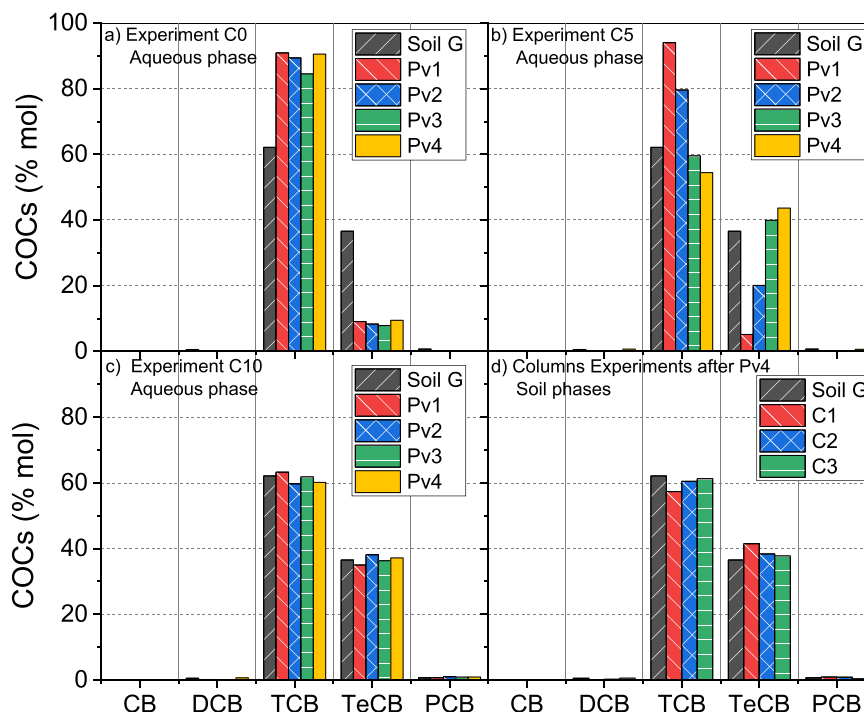


Fig. 6. Molar distribution (%) of COCs a) in the aqueous phase in column C0, b) in the aqueous phase in column C1, c) in the aqueous phase in column C2 d) in the soil after column disassembling. Black bars correspond to the soil placed in the column after alkaline treatment.

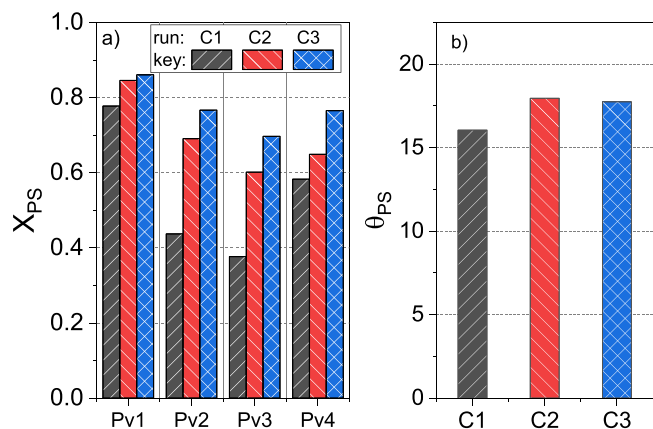


Fig. 7. (a) conversion of PS at each PV injected. (b) θ_{PS} coefficient (mmol of oxidant consumed per mmol of COCs by Eq. (5)).

This fact is explained considering that PV1 and PV4 remained in the column 113 h, more than double that of PV2 and PV3 (48 h). Moreover, the higher the surfactant concentration injected, the higher the PS conversion obtained at each PV. However, differences in PS conversion obtained in PV1 among C1, C2, and C3 are relatively low, relating to the low amount of surfactant in the column. The differences increase remarkably in PV2 and PV3.

On the other hand, PS conversion in PV1 is lower than PS conversion in PV4 in all the columns. Considering that injected PV1 and PV4 remained the same time in the column, the lower PS conversion obtained in PV4 could be due to the lower COCs concentration remaining in the soil when PV4 is injected. However, the surfactant adsorbed is higher in PV4 than in PV1, indicating that the surfactant adsorbed do not produce a substantial consumption in PS.

The ratio of PS consumed to COCs oxidized ($\theta_{PS, column}$) has been calculated according to Eq. (5), and those are shown in Fig. 7b.

$$\theta_{PS, column} = \frac{\sum_{VP} (C_{PSo} - C_{PS}) VP}{C_{COCs_0} X_{COCs} W} \quad (5)$$

being C_{COCs_0} the initial concentration of COCs adsorbed in soil, and X_{COCs} is the COCs conversion calculated with Eq. (4).

As can be seen in Fig. 7b, $\theta_{PS, column}$ in C2 and C3 are slightly higher than the observed in the run without surfactant C1. These differences can be explained by the competition between COCs and surfactants for the oxidant. However, the $\theta_{PS, column}$ values are much lower than noticed in slurry runs for the similar COCs conversion (Fig. 4). The ratio VP/W in the column is approximately 0.2 (Table 2), and VL/W in slurry runs (Table 1) was 10. Therefore, the higher values of $\theta_{PS, batch}$ can be explained by the higher contribution of the surfactant oxidation in the aqueous phase in the slurry runs. On the other hand, the slight differences noticed in $\theta_{PS, column}$ between C1, C2 and C3 suggest that the surfactant adsorbed has a small contribution on $\theta_{PS, column}$. The total amount of surfactant added in the four PVs per mass of soil was 0, 4 and 8 $g_{suf} kg_{soil}^{-1}$ in C1, C2 and C3, respectively. The active surfactant concentration in the aqueous phase was always lower than 2 $g \cdot L^{-1}$ (Fig. 5 and Figure SM-8). The differences between surfactant concentration values in injected PVs and flushed PVs are due mainly to surfactant adsorption.

4. Conclusions

This work studied the simultaneous addition of surfactant (E3) and oxidant (PS alkali activated) in the remediation of a real highly polluted soil from lindane wastes. The composition of the initial mixture of chlorinated compounds in soils changes after alkaline treatment, reducing the chlorinated non-aromatic compounds initially present in the soil to chlorobenzenes.

The simultaneous addition of surfactant and oxidant enhances the COCs reduction in both experiments (slurry and column). However, surfactant adsorption modifies the partition equilibrium of surfactant and COCs between soil and aqueous phases. It was noticed that there is an optimal value of surfactant concentration in the aqueous phase. If

surfactant concentration in the aqueous phase increases, the solubilization of COCs in the aqueous phase rises but the hindrance of the oxidation of COCs in the micelles also becomes more critical. Moreover, the reaction of PS with the COCs adsorbed in the soil have a remarkable contribution to the COCs abatement in the absence of surfactant. The high soil surface per mass of soil (due to interbedded clay) probably facilitates the reaction between COCs and PS on the soil surface. The surfactant adsorption in soil does not seem to hinder or decrease the COCs oxidation on the soil surface in the column runs.

The treatment of the Sardas landfill by S-ISCO treatment using E3 as surfactant and PS activated with NaOH seems to be an effective technology, and promising results have been obtained in this work. However, to optimize the S-ISCO process, further study is necessary. The surfactant concentration injected must be enough to increase the solubilization of the COCs but maintain the surfactant concentration under a selected value in the aqueous phase (in this work, about $1.5\text{--}2\text{ g}\cdot\text{L}^{-1}$) to avoid unproductive oxidant consumption. Therefore, the surfactant concentration and the strategy of PV injections will depend on the soil properties (surfactant adsorption isotherms, COCs desorption isotherms) and the COCs and surfactant properties. In general, a higher concentration of surfactant in the first injections can be recommended. Monitoring of surfactant and COCs concentration with time will be required for further injections.

CRedit authorship contribution statement

Raúl García-Cervilla: Methodology, Investigation, Writing – original draft. **Aurora Santos:** Funding acquisition, Resources, Conceptualization, Supervision. **Arturo Romero:** Funding acquisition, Resources. **David Lorenzo:** Conceptualization, Methodology, Supervision, Original draft.

Declaration of Competing Interest

The authors declare that they have no known competing financial interests or personal relationships that could have appeared to influence the work reported in this paper.

Acknowledgements

This work was supported by the Regional Government of Madrid, through the CARESOIL project (S2018/EMT-4317), and the Spanish Ministry of Economy, Industry, and Competitiveness, through the project PID2019–105934RB-I00 and for the EU Life Program (LIFE17 ENV/ES/000260). Raúl García-Cervilla acknowledges the Spanish FPI grant (ref. BES-2017–081782).

Appendix A. Supporting information

Supplementary data associated with this article can be found in the online version at [doi:10.1016/j.jece.2022.107625](https://doi.org/10.1016/j.jece.2022.107625).

References

- R. Baciocchi, L. D'Aprile, I. Innocenti, F. Massetti, J. Verginelli, Development of technical guidelines for the application of in-situ chemical oxidation to groundwater remediation, *J. Clean. Prod.* 77 (2014) 47–55.
- X. Bai, Y. Wang, X. Zheng, K. Zhu, A. Long, X. Wu, H. Zhang, Remediation of phenanthrene contaminated soil by coupling soil washing with Tween 80, oxidation using the UV/S2O8²⁻ process and recycling of the surfactant, *Chem. Eng. J.* 369 (2019) 1014–1023.
- X. Bai, Y. Wang, X. Zheng, K. Zhu, A. Long, X. Wu, H. Zhang, "Remediation of phenanthrene contaminated soil by coupling soil washing with Tween 80, oxidation using the UV/S2O8²⁻ process and recycling of the surfactant.", *Chem. Eng. J.* 369 (2019) 1014–1023.
- A.T. Besha, D.N. Bekele, R. Naidu, S. Chadalavada, Recent advances in surfactant-enhanced In-Situ Chemical Oxidation for the remediation of non-aqueous phase liquid contaminated soils and aquifers, *Environ. Technol. Innov.* 9 (2018) 303–322.
- I. Bouzid, J. Maire, E. Brunol, S. Caradec, N. Fatin-Rouge, Compatibility of surfactants with activated-persulfate for the selective oxidation of PAH in groundwater remediation, *J. Environ. Chem. Eng.* 5 (6) (2017) 6098–6106.
- M. Cheng, G. Zeng, D. Huang, C. Yang, C. Lai, C. Zhang, Y. Liu, Advantages and challenges of Tween 80 surfactant-enhanced technologies for the remediation of soils contaminated with hydrophobic organic compounds, *Chem. Eng. J.* 314 (2017) 98–113.
- C.T. Chiou, D.W. Schmedding, M. Manes, Improved prediction of octanol-water partition coefficients from liquid-solute water solubilities and molar volumes, *Environ. Sci. Technol.* 39 (22) (2005) 8840–8846.
- G. Dahal, J. Holcomb, D. Socci, Surfactant-oxidant co-application for soil and groundwater remediation, *Remediat. - J. Environ. Cleanup Costs Technol. Tech.* 26 (2) (2016) 101–108.
- C.M. Dominguez, A. Romero, A. Checa-Fernandez, A. Santos, Remediation of HCHs-contaminated sediments by chemical oxidation treatments, *Sci. Total Environ.* 751 (2021), 141754.
- P.J. Dugan, R.L. Siegrist, M.L. Crimi, Coupling surfactants/cosolvents with oxidants for enhanced DNAPL removal: a review, *Remediat. Journal* 20 (3) (2010) 27–49.
- EthicalChem. (2016c). "S-ISCO Remediation of Coal Tar Contamination at NYC Brownfield Site, Queens, New York." Retrieved February, 27, 2016, from http://media.wix.com/ugd/9b5eec_3b8b10eb81f84e2bbb9f88775d626d4.pdf.
- J. Fernández, M. Arjol, C. Cacho, POP-contaminated sites from HCH production in Sabiñánigo, Spain, *Environ. Sci. Pollut. Res.* 20 (4) (2013) 1937–1950.
- R. García-Cervilla, A. Romero, A. Santos, D. Lorenzo, Surfactant-enhanced solubilization of chlorinated organic compounds contained in DNAPL from lindane waste: effect of surfactant type and pH, *Int. J. Environ. Res. Public Health* 17 (2020) 12.
- R. García-Cervilla, A. Romero, A. Santos, D. Lorenzo, Surfactant-enhanced solubilization of chlorinated organic compounds contained in dnapl from lindane waste: Effect of surfactant type and ph, *Int. J. Environ. Res. Public Health* 17 (12) (2020) 1–14.
- R. García-Cervilla, A. Santos, A. Romero, D. Lorenzo, Remediation of soil contaminated by lindane wastes using alkaline activated persulfate: kinetic model, *Chem. Eng. J.* (2020) 393.
- R. García-Cervilla, A. Santos, A. Romero, D. Lorenzo, Partition of a mixture of chlorinated organic compounds in real contaminated soils between soil and aqueous phase using surfactants: Influence of pH and surfactant type, *J. Environ. Chem. Eng.* 9 (2021) 5.
- R. García-Cervilla, A. Santos, A. Romero, D. Lorenzo, Remediation of soil contaminated by lindane wastes using alkaline activated persulfate: kinetic model, *Chem. Eng. J.* 393 (2020), 124646.
- R. García-Cervilla, A. Santos, A. Romero, D. Lorenzo, Compatibility of nonionic and anionic surfactants with persulfate activated by alkali in the abatement of chlorinated organic compounds in aqueous phase, *Sci. Total Environ.* 751 (2021), 141782.
- R. García-Cervilla, A. Santos, A. Romero, D. Lorenzo, Abatement of chlorobenzenes in aqueous phase by persulfate activated by alkali enhanced by surfactant addition, *J. Environ. Manag.* 306 (2022), 114475.
- Interstate Technology Regulatory Council (2000). "Dense Non-Aqueous Phase Liquids (DNAPLs): Review of Emerging Characterization and Remediation Technologies."
- S. Kang, H.S. Lim, Y. Gao, J. Kang, H.Y. Jeong, Evaluation of ethoxylated nonionic surfactants for solubilization of chlorinated organic phases: effects of partitioning loss and macroemulsion formation, *J. Contam. Hydrol.* (2019) 223.
- Y. Li, X. Liao, S.G. Huling, T. Xue, Q. Liu, H. Cao, Q. Lin, The combined effects of surfactant solubilization and chemical oxidation on the removal of polycyclic aromatic hydrocarbon from soil, *Sci. Total Environ.* 647 (2019) 1106–1112.
- Z.H. Li, Surfactant-enhanced oxidation of trichloroethylene by permanganate - proof concept, *Chemosphere* 54 (3) (2004) 419–423.
- J.-W. Liu, K.-H. Wei, S.-W. Xu, J. Cui, J. Ma, X.-L. Xiao, B.-D. Xi, X.-S. He, Surfactant-enhanced remediation of oil-contaminated soil and groundwater: a review, *Sci. Total Environ.* (2021) 756.
- M.A. Lominchar, D. Lorenzo, A. Romero, A. Santos, Remediation of soil contaminated by PAHs and TPH using alkaline activated persulfate enhanced by surfactant addition at flow conditions, *J. Chem. Technol. Biotechnol.* 93 (5) (2018) 1270–1278.
- D. Lorenzo, R. García-Cervilla, A. Romero, A. Santos, Partitioning of chlorinated organic compounds from dense non-aqueous phase liquids and contaminated soils from lindane production wastes to the aqueous phase, *Chemosphere* 239 (2020), 124798.
- M. Mobile, M. Widdowson, L. Stewart, J. Nyman, R. Deeb, M. Kavanaugh, J. Mercer, D. Gallagher, In-situ determination of field-scale NAPL mass transfer coefficients: performance, simulation and analysis, *J. Contam. Hydrol.* 187 (2016) 31–46.
- T. Olmez-Hanci, I. Arslan-Alaton, B. Genc, Degradation of the nonionic surfactant Triton (TM) X-45 with HO center dot and SO4 center dot - based advanced oxidation processes, *Chem. Eng. J.* 239 (2014) 332–340.
- S. Paria, Surfactant-enhanced remediation of organic contaminated soil and water, *Adv. Colloid Interface Sci.* 138 (1) (2008) 24–58.
- S. Paria, K.C. Khilar, A review on experimental studies of surfactant adsorption at the hydrophilic solid-water interface, *Adv. Colloid Interface Sci.* 110 (3) (2004) 75–95.
- M.J. Rosen, J.T. Kunjappu, Surfactants and Interfacial Phenomena, John Wiley & Sons, 2012.

- [32] A. Santos, C.M. Domínguez, D. Lorenzo, R. García-Cervilla, M.A. Lominchar, J. Fernández, J. Gómez, J. Guadaño, Soil flushing pilot test in a landfill polluted with liquid organic wastes from lindane production, *Heliyon* 5 (11) (2019), e02875.
- [33] A. Santos, J. Fernandez, J. Guadano, D. Lorenzo, A. Romero, Chlorinated organic compounds in liquid wastes (DNAPL) from lindane production dumped in landfills in Sabinanigo (Spain), *Environ. Pollut.* 242 (2018) 1616–1624.
- [34] A. Santos, J. Fernandez, S. Rodriguez, C.M. Dominguez, M.A. Lominchar, D. Lorenzo, A. Romero, Abatement of chlorinated compounds in groundwater contaminated by HCH wastes using ISCO with alkali activated persulfate, *Sci. Total Environ.* 615 (2018) 1070–1077.
- [35] R.L. Siegrist, M. Crimi, T.J. Simpkin, In situ chemical oxidation for groundwater remediation, Springer Science & Business Media, 2011.
- [36] K. Soga, J.W. Page, T.H. Illangasekare, A review of NAPL source zone remediation efficiency and the mass flux approach, *J. Hazard Mater.* 110 (1–3) (2004) 13–27.
- [37] H.F. Stroo, A. Leeson, J.A. Marqusee, P.C. Johnson, C.H. Ward, M.C. Kavanaugh, T. C. Sale, C.J. Newell, K.D. Pennell, C.A. Lebron, M. Unger, Chlorinated ethene source remediation: lessons learned, *Environ. Sci. Technol.* 46 (12) (2012) 6438–6447.
- [38] H.F. Stroo, C.H. Ward, In Situ Remediation of Chlorinated Solvent Plumes, Springer Science & Business Media, 2010.
- [39] D.W. Tomlinson, M.O. Rivett, G.P. Wealthall, R.E.H. Sweeney, Understanding complex LNAPL sites: Illustrated handbook of LNAPL transport and fate in the subsurface, *J. Environ. Manag.* 204 (2017) 748–756.
- [40] C. Trellu, E. Mousset, Y. Pechaud, D. Huguenot, E.D. van Hullebusch, G. Esposito, M.A. Oturan, Removal of hydrophobic organic pollutants from soil washing/flushing solutions: a critical review, *J. Hazard. Mater.* 306 (2016) 149–174.
- [41] C. Trellu, N. Oturan, Y. Pechaud, E.D. van Hullebusch, G. Esposito, M.A. Oturan, Anodic oxidation of surfactants and organic compounds entrapped in micelles - selective degradation mechanisms and soil washing solution reuse, *Water Res.* 118 (2017) 1–11.
- [42] T.T. Tsai, C.M. Kao, T.Y. Yeh, S.H. Liang, H.Y. Chien, Application of surfactant enhanced permanganate oxidation and biodegradation of trichloroethylene in groundwater, *J. Hazard. Mater.* 161 (1) (2009) 111–119.
- [43] L. Wang, L. Peng, L. Xie, P. Deng, D. Deng, Compatibility of surfactants and thermally activated persulfate for enhanced subsurface remediation, *Environ. Sci. Technol.* 51 (12) (2017) 7055–7064.
- [44] W.H. Wang, G.E. Hoag, J.B. Collins, R. Naidu, Evaluation of surfactant-enhanced in situ chemical oxidation (S-ISCO) in contaminated soil, *Water, Air, Soil Pollut.* 224 (12) (2013) 1–9.
- [45] K. Yang, L. Zhu, B. Xing, Enhanced soil washing of phenanthrene by mixed solutions of TX100 and SDBS, *Environ. Sci. Technol.* 40 (13) (2006) 4274–4280.
- [46] G. Zheng, A. Selvam, J.W.C. Wong, Enhanced solubilization and desorption of organochlorine pesticides (OCPs) from soil by oil-swollen micelles formed with a nonionic surfactant, *Environ. Sci. Technol.* 46 (21) (2012) 12062–12068.



Article

Non-Ionic Surfactant Recovery in Surfactant Enhancement Aquifer Remediation Effluent with Chlorobenzenes by Semivolatile Chlorinated Organic Compounds Volatilization

Patricia Sáez, Aurora Santos, Raúl García-Cervilla , Arturo Romero and David Lorenzo *

Chemical Engineering and Materials Department, Complutense University of Madrid, 28040 Madrid, Spain; patrisae@ucm.es (P.S.); aursan@quim.ucm.es (A.S.); raugar05@ucm.es (R.G.-C.); aromeros@quim.ucm.es (A.R.)

* Correspondence: dlorenzo@quim.ucm.es

Abstract: Surfactant enhanced aquifer remediation is a common treatment to remediate polluted sites with the inconvenience that the effluent generated must be treated. In this work, a complex mixture of chlorobenzene and dichlorobenzenes in a non-ionic surfactant emulsion has been carried out by volatilization. Since this technique is strongly affected by the presence of the surfactant, modifying the vapour pressure, P_v^0 , and activity coefficient, γ , a correlation between $P_v^0 \gamma_j$ and surfactant concentration and temperature was proposed for each compound, employing the Surface Response Methodology (RSM). Volatilization experiments were carried out at different temperatures and gas flow rates. A good agreement between experimental and predicted remaining SVCOs during the air stripping process was obtained, validating the thermodynamic parameters obtained with RSM. Regarding the results of volatilization, at 60 °C 80% of SVCOs were removed after 6 h, and the surfactant capacity was almost completely recovered so the solution can be recycled in soil flushing.

Keywords: surfactant; chlorinated organic compounds; volatilization; emulsion treatment; SEAR emulsion treatment



Citation: Sáez, P.; Santos, A.; García-Cervilla, R.; Romero, A.; Lorenzo, D. Non-Ionic Surfactant Recovery in Surfactant Enhancement Aquifer Remediation Effluent with Chlorobenzenes by Semivolatile Chlorinated Organic Compounds Volatilization. *Int. J. Environ. Res. Public Health* **2022**, *19*, 7547. <https://doi.org/10.3390/ijerph19127547>

Academic Editors: Huiping Zeng, Yanan Cai and Yan Han

Received: 19 May 2022

Accepted: 16 June 2022

Published: 20 June 2022

Publisher's Note: MDPI stays neutral with regard to jurisdictional claims in published maps and institutional affiliations.



Copyright: © 2022 by the authors. Licensee MDPI, Basel, Switzerland. This article is an open access article distributed under the terms and conditions of the Creative Commons Attribution (CC BY) license (<https://creativecommons.org/licenses/by/4.0/>).

1. Introduction

The contamination of soil and groundwater by, among others, chlorinated organic compounds has become a severe environmental issue [1]. These pollutants present a high oil/water distribution coefficient and a low water solubility. The accidental release or intentional dumping of hydrophobic organic liquid phases into the environment has resulted in a separate liquid phase, termed non-aqueous phase liquids (or NAPLs), that persists in the subsurface [2].

One of the remediation treatments that was successfully applied to remove the NAPLs mass in the subsurface in a short time is Surfactant Enhancement Aquifer Remediation (SEAR) [3,4]. The surfactants enhance the removal of pollutants through two mechanisms: solubilization and mobilization. The amphoteric properties of the surfactants that reduce interface tension facilitate the transport of hydrophobic pollutants to the aqueous phase [5]. This technique involves injecting an aqueous solution containing a surfactant into the contaminated area with further extraction of the fluid injected containing the solubilized–mobilized pollutants [4,6,7].

The SEAR technique presents significant benefits compared to other technologies, such as pump and treat [8], since it increases the efficiency in remediating areas contaminated with NAPLs. However, the SEAR process moves the contamination from the subsurface into the aqueous phase but does not eliminate the contaminant, resulting in a secondary contamination [3]. The emulsion extracted is composed of a complex mixture of organic compounds and the surfactant used and must be treated to eliminate the organic pollutants. Moreover, the recovery of the surfactant is highly desired in a circular economy perspective.

Selective oxidation of organic contaminants in the emulsion has been proposed and tested successfully [9–12]. Still, the cost of reagents and the loss of surfactant capacity after treatment can decrease the sustainability of this treatment. Organic compounds are not mineralized, and the loss of surfactant stability is associated with the unproductive consumption of the oxidant by the surfactant [13]. The more refractory the contaminant is to oxidation, the higher the unproductive consumption of the oxidant. Selective adsorption of the organic pollutants in the emulsion on activated carbon and selective organic compound retention by membranes have also been proposed to treat contaminated emulsions [10,14–17]. However, membrane fouling and surfactant adsorption decrease the effectiveness of these methods.

The air stripping of volatile or semivolatile chlorinated organic compounds in soil (VCOs–SVCOCs) has been reported at the field scale [18–20]. Still, this topic has been scarcely studied in the scientific literature. This technique transfers the volatile compound from an aqueous solution to an air stream. The volatilized chlorinated organic compound (COC) can be more selectively adsorbed on activated carbon. This process is effective when the organic compounds are volatile or semivolatile [21]. However, the volatility of COCs in the emulsion should be affected by the surfactant presence, being that this topic is not studied in the literature. Moreover, the loss of surfactant capacity during air stripping has not been considered.

This work aims to study and model an air stripping process to eliminate a mixture of chlorobenzene and dichlorobenzene isomers in a non-ionic surfactant emulsion (Emulse-3[®] as surfactant). These chlorinated compounds are often used as solvents or reagents, and leaks from storage tanks result in soil and groundwater contamination [22–24].

The temperature applied during the volatilization process could modify the surfactant stability, and this aspect has also been studied in this work. The volatility of chlorinated organic compounds in the emulsion has also been determined. From our knowledge this topic has not been studied in the literature. The influence of the surfactant presence in the aqueous phase on SVCOCs volatility has been analyzed determining the $P_{v_j}^0 \gamma_j$ values at different surfactant and SVCOCs concentration and temperatures. The volatilization of SVCOCs in the emulsion by air streaming at different conditions has been modelled and validated.

2. Materials and Methods

2.1. Chemicals

The mixture of SVCOCs used in this work consisted of chlorobenzene (CB), 1,2-dichlorobenzene (1,2-DCB), and 1,4-dichlorobenzene (1,4-DCB) prepared from commercial compounds (Sigma Aldrich, Darmstadt, Germany, analytical grade). The distribution of each compound, expressed as molar percentage, was 53% of CB, 29% of 1,2-DCB, and 18% of 1,4-DCB.

The quantification of SVCOCs was carried out using calibration curves prepared from standard samples of known concentration in methanol from commercial compounds (Sigma Aldrich, analytical grade). Additionally, the limonene ((R)-(+)-Limonene, Sigma Aldrich) (cosolvent of surfactant) was also calibrated. Bicyclohexyl ($C_{12}H_{22}$, Sigma Aldrich) and tetrachloroethane ($C_2H_2Cl_4$, Sigma Aldrich) were used as internal standards (ISTD) for quantification by gas chromatography (GC). The chromatographic method is explained elsewhere [25].

The surfactant selected to carry out the experiments was E-Mulse 3[®] (E3) (EthicalChem), which is a non-ionic surfactant with a critical micelle concentration (CMC), measured of $80 \text{ mg} \cdot \text{L}^{-1}$. This surfactant has been successfully applied in the solubilization of 28 different chlorinated organic compounds present in a real dense non-aqueous phase liquid (DNAPL) to the aqueous phase, including CB and DCBs [26].

The air employed to perform the air stripping experiments was supplied by Carburos Metálicos, with an air purity of 99.999% (*Alphagaz*TM 1 AR, *Air Liquid*). The aqueous

solutions were prepared with high-purity water from a Millipore Direct-Q system with resistivity $>18 \text{ M}\Omega\cdot\text{cm}$ at $25 \text{ }^\circ\text{C}$.

2.2. Experimental Procedure

The experimental procedure comprised three experiment blocks. In the first one (B1), the surfactant stability was studied at different temperatures. In the second one (B2), the influence of surfactant concentration, temperature, and chlorinated compounds concentration on each COC (CB, 1,2-DCB, and 1,4-DCB) volatility was analyzed. The product of vapour pressure by the activity coefficient ($P_{v_i}^o \gamma_j$) was obtained and correlated with the variables studied. Finally, SVCOCs volatilization in the emulsion (B3) was carried out by passing an airstream through the aqueous emulsion at several temperatures and air flow rates.

2.2.1. Surfactant Stability (B1)

Surfactant stability experiments were performed in batch mode employing sealed 20 mL glass vials for gas chromatography without headspace closed with PTFE (polytetrafluoroethylene) caps in the absence and presence of SVCOCs. In the last case, the aqueous phase was saturated with the mixture of VCOCs, adding the corresponding amount of SVCOCs to obtain a saturated emulsion of organic phase in the aqueous surfactant emulsion. The amount of VCOCs added was calculated from the molar solubilization ratio MSR (amount of SVCOCs that can be solubilized in the surfactant solution when saturation is reached) obtained elsewhere for a complex mixture of chlorinated compounds in this surfactant [26] ($\text{MSR} = 4.33 \text{ mmol SVCOCs}\cdot\text{g}_{\text{surf}}^{-1}$). The emulsions were agitated during 4 h and left to settle 24 h without agitation, checking the total solubilization of VCOCs added.

The vials were prepared with 19 mL of surfactant emulsion (with or without contaminant). Vials were heated in a thermostatic bath to obtain the desired temperature ($25\text{--}60 \text{ }^\circ\text{C}$) and agitated using a magnetic stirrer for up to 48 h. Zero time was considered when the desired temperature was reached. The experimental conditions are summarized in Table 1 (runs E1 to E6).

The remaining surfactant concentration was analyzed by sacrificing a vial at the corresponding time, including zero. In the experiments carried using emulsion saturated in SVCOCs, the remaining surfactant concentration was calculated from the remaining SVCOCs in solution, considering the MSR value as shown in Equation (1).

$$C_s \left(\text{g L}^{-1} \right) = \frac{C_{\text{SVCOCs}} \left(\text{mM} \right)}{4.33 \left(\frac{\text{mmol}_{\text{SVCOCs}}}{\text{g}_{\text{surf}}} \right)} \quad (1)$$

where C_s is the surfactant concentration ($\text{g}_{\text{surf}}\cdot\text{L}^{-1}$), C_{SVCOCs} is the concentration of the sum of the three chlorinated organic compounds ($\text{mmol}_{\text{VCOCs}}\cdot\text{L}^{-1}$), and 4.33 is the solubilization mass solubilization ratio of E3 with the chlorinated compounds in $\text{mmol}_{\text{VCOCs}}\cdot\text{g}_{\text{surf}}^{-1}$.

In the absence of pollutant, the remaining surfactant concentration at each time was calculated by dissolving 1,2,4-trichlorobenzene (1,2,4-TCB), measuring the solubilized concentration of this compound in the aqueous phase and using Equation (1) taking into account that $\text{MSR}_{1,2,4\text{-TCB}} = 4.33 \text{ mmol}_{1,2,4\text{-TCB}}\cdot\text{g}_{\text{surf}}^{-1}$. All the experiments were replicated, with differences among experimental results lower than 7%. The average values were used as the experimental results.

Table 1. Experimental conditions for the experimental set. SVCOCs distribution (as molar percentage) was 53% of CB, 29% of 1,2-DCB, and 18% of 1,4-DCB.

Set B1					
Exp	T (°C)	C_{S0} (g·L ⁻¹)	C_{SVCOCs} (mmol·L ⁻¹)		
E1	20	10	0		
E2	40	10	0		
E3	60	10	0		
E4	20	10	94.11		
E5	40	10	94.11		
E6	60	10	94.11		
Set B2					
Exp	T (°C)	C_{S0} (g·L ⁻¹)	C_{VCOCs} (mmol·L ⁻¹)		
P1	30, 40, 60	1.5	3.1, 6.3		
P2	30, 40, 60	3.5	7.5, 19.6		
P3	30, 40, 60	7.0	7.8, 23.5, 39.2		
P4	30, 40, 60	15.0	15.6, 31.3, 62.8		
Set B3					
Exp	T (°C)	C_{S0} (g·L ⁻¹)	C_{SVCOCs} (mmol·L ⁻¹)	Q_{gas} (L·h ⁻¹)	$V_{emulsion}$ (L)
V1	40	3.5	23.5	1.8	0.3
V2	60	3.5	23.5	1.8	0.3
V3	40	3.5	23.5	3.6	0.3

2.2.2. B2. Estimation of P_{vj}^0, γ_j (B2)

This set of experiments was proposed to estimate the product of P_{vj}^0, γ_j , of CB, 1,2-DCB, and 1,4-DCB in the presence of surfactant at several temperatures.

Firstly, certain amounts of CB and DCB isomers were solubilized in an aqueous solution of the surfactant at the corresponding concentration. The emulsion was prepared in 100 mL flasks, without headspace, to avoid the volatile loss. Surfactant E3 concentration ranged from 1.5 g·L⁻¹ to 15 g·L⁻¹. The amount of SVCOCs was varied from 3.1 mmol·L⁻¹ to 62.8 mmol·L⁻¹ being always less than that required for saturation at the surfactant concentration used. After 2 h of agitation, the solution was settled, checking that all the SVCOCs added were dissolved by GC-FID. Following, 10 mL of the emulsion was transferred to 20 mL glass vials for gas chromatography, closed, and agitated at different temperatures (30–60 °C) for 1 h in the incubator of Headspace Gas Chromatography (HS-GC), Agilent GC Sampler 120. This time was enough to reach the equilibrium between liquid and vapour phases generated. The SVCOCs in the vapour phase were analyzed by Headspace coupled with GC/FID/ECD. Table 1 summarizes the conditions of the experiments carried out (runs P1 to P4).

2.2.3. Volatilization Tests (B3)

The volatilization of volatile chlorinated organic compounds from aqueous surfactant emulsion passing an air flow rate was performed in the experimental setup schematized in Figure 1. The air was bubbled in the aqueous emulsion from pressurized air in a cylinder, and the gas flowrate was controlled using a mass flow controller (*EL – FLOW* Select Series Mass Flow Meters/Controllers for gases, Bronkhorst). The air was introduced into the emulsion by a diffuser to favour the gas–liquid equilibrium. The system temperature was regulated with a hotplate (IKA C-MAG HS 7) and controlled with a thermometer with a PID (Proportional Integral Derivative) controller (IKA ETS-D5). The gas phase leaving

the emulsion was saturated in SVCOCs, conducted through an iron mesh (100 μm) to prevent excessive foams formation, and bubbled in MetOH, which acted like a liquid trap. The MetOH traps were introduced into an ice bath to avoid volatile loss. Samples were taken periodically from the emulsion to monitor the remaining amount of VCOCs and the surfactant concentration. The surfactant concentration in the aqueous phase with time was measured employing 1,2,4-TCB as explained in B1.

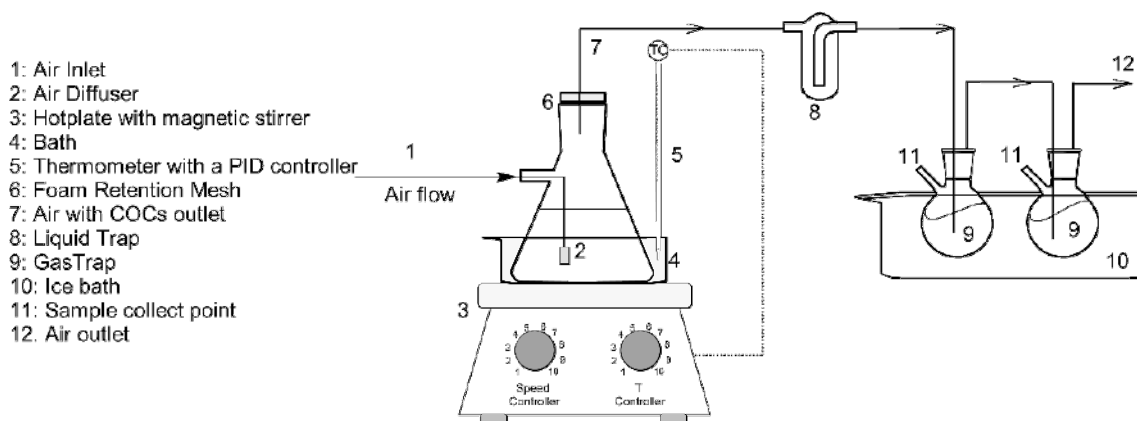


Figure 1. Scheme of the installation used for volatilization tests.

The volatilization experiments were maintained for 8 h when the airflow was stopped. The experiments were carried out at $3.5 \text{ g}\cdot\text{L}^{-1}$ of surfactant, $23.5 \text{ mmol}\cdot\text{L}^{-1}$ of initial VCOCs concentration in a volume of 0.30 L. Table 1 provides a summary of the conditions of the experiments carried out (runs V1 to V3).

2.3. SVCOCs Analysis

The concentration of SVCOCs in emulsion was analyzed by gas chromatography (Agilent 8860) with autosampler (Agilent GC Sampler 120) coupled with a flame ionization detector and an electron capture detector (GC-FID/ECD). The column was Agilent HP5-MSUI (19091S-433UI, $30 \text{ m} \times 0.25 \text{ mm ID} \times 0.25 \mu\text{m}$). Two microliters of samples were injected using helium as carrier gas (flow rate of $2.9 \text{ mL}\cdot\text{min}^{-1}$). The GC injection port temperature was set at $250 \text{ }^\circ\text{C}$, and GC oven worked at a programmed temperature gradient, starting at $80 \text{ }^\circ\text{C}$ and raising the temperature at a rate of $15 \text{ }^\circ\text{C}\cdot\text{min}^{-1}$ until $180 \text{ }^\circ\text{C}$, and then keeping it constant for 15 min. Additionally, a split ratio of 10:1 was employed in the analysis. The samples were previously diluted 1:10 with methanol.

The SVCOCs concentrations in the vapour phase in B2 experiments were measured by Headspace Gas Chromatography (HS-GC). Twenty milliliter glass vials for gas chromatography closed with PTFE caps, were filled with 10 mL of the emulsion of SVCOCs mixture. The vials were agitated and heated at constant temperature (depending on the experimental conditions tested from $30 \text{ }^\circ\text{C}$ to $60 \text{ }^\circ\text{C}$) for 1 h, ensuring the equilibrium between liquid and vapour was reached. After this time, 2.5 mL of the vapour phase was to the GC using a 10:1 split ratio. The column and the method conditions employed were the same as described for analyzing SVCOCs dissolved. More details of the method are shown in Table S1.

3. Results and Discussions

3.1. Surfactant Stability

The experiments summarized in Table 1 for the B1 experiment set were carried out to study the surfactant stability. The results obtained are expressed as the evolutions of Surfactant Capacity Loss (SCL) with the time. SCL is calculated with Equation (2) and refers to the fractional remaining surfactant capacity express in percentage.

$$SCL = \left(1 - \frac{C_S}{C_{S0}}\right) \cdot 100 \quad (2)$$

where C_S is the surfactant concentration at each time by Equation (1) ($\text{g}\cdot\text{L}^{-1}$) and C_{S0} is the initial surfactant concentration ($\text{g}\cdot\text{L}^{-1}$). Figure 2 shows the results obtained from the experiments without SVCOCs (a) and with SVCOCs (b).

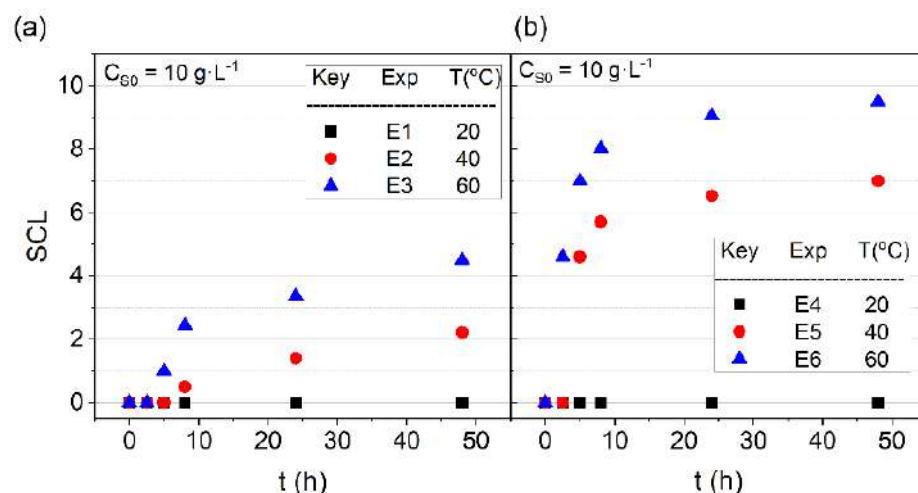


Figure 2. SCL profiles with time. $C_{S0} = 10 \text{ g}\cdot\text{L}^{-1}$, temperature = (20, 40 and 60) °C (a) absence of SVCOCs; (b) presence of SVCOCs.

As shown in Figure 2, the SCL obtained for all the experiments is lower than 10% after 40 h, even at the maximum temperature used, 60 °C, indicating the stability of the surfactant in the operation range studied. The presence of SVCOCs slightly modifies the surfactant stability. The SCL values without SVCOCs range from 2% to 4% at 40 °C and 60 °C, respectively. In the presence of SVCOCs, the SCL ranges from 7% to 9% at 40 °C and 60 °C, respectively. The differences found in the experiment carried out with and without SVCOCs can be attributed to the modification of the partial pressure of the surfactant, being higher in the presence of organic compounds.

Nevertheless, the SCL is always less than 10% in the time interval, and the temperature range studied being considered negligible. Therefore, the active surfactant concentration with time corresponds to the initial value, $C_S = C_{S0}$.

3.2. $P_{v_j}^0 \cdot \gamma_j$ Estimation and Correlation

The estimation of $P_{v_j}^0 \cdot \gamma_j$ of each SVCOC j was carried out from data obtained in the surfactant presence in set B2 summarized in Table 1. The vapour–liquid equilibrium (VLE) of the component j can be described by modified Raoult’s law Equation (3), assuming the vapour phase is an ideal gas phase and the effect of the surfactant and VCOCs in the liquid phase is taken into account with the values of the product of the vapour pressure, P_{v_j} , and the activity coefficient, γ_j .

$$P_T \cdot y_j = P_{v_j}^0 \cdot \gamma_j \cdot x_j \quad (3)$$

where P_T is the total pressure in the vial (bar) at the temperature T , y_j is the molar fraction of chlorinated organic compound j in the vapour phase; $P_{v_j}^0$ is the saturation vapour pressure (bar) of compound j ; x_j is the molar fraction of compound j in the liquid phase; γ_j is the activity coefficient of the j compound.

In Equation (3), the total pressure in the vial (bar) is calculated assuming that at the conditions tested water and air are the main compounds in the gas phase in the vial, according to Equation (4).

$$P_T \approx P_{air} + P_w = P_{o\ air} + P_w^o(T) \quad (4)$$

where P_T is the sum of the air pressure (P_{air} , bar) which can be considered the atmospheric pressure at 20 °C ($P_{o\ air}$, bar) and water pressure (P_w , bar) which is equals to water vapour pressure at T ($P_{W(T)}^o$, bar), assuming that the molar fraction of water in the liquid phase is almost the unity.

In the literature, there is scarce information regarding how the surfactants modify the ideality of the liquid phase. For that, experimental values of $P_{v_j}^o \gamma_j$ for each compound j at different temperatures, surfactant, and SVCOCs concentrations in the liquid phase were determined according to Equation (5), after measuring the gas phase composition of the vial by GC, as explained in SVCOCs analysis section.

$$P_{v_j}^o \gamma_j \approx \frac{n_j}{n_{gas}} P_T \quad (5)$$

where n_j is the moles of j compound in the vial gas phase, n_{gas} is the sum of moles of all compounds (including organic, air, and water) in the vial gas phase, respectively, P_T is the total pressure (bar) calculated with Equation (4), and x_j is the molar fraction of the compound j in the liquid phase.

The experimental results of the $\ln(P_{v_j}^o \gamma_j)$ are shown in Figure S1. The effect of temperature, SVCOCs, and surfactant concentrations on the value of $\ln(P_{v_j}^o \gamma_j)$ were studied. The red points correspond to the values of $\ln(P_{v_j}^o \gamma_j)$ under different conditions. As can be seen, SVCOCs concentration did not affect $\ln(P_{v_j}^o \gamma_j)$ values at the same surfactant concentration and temperature. For this reason this variable was not taken into account in the estimation of $\ln(P_{v_j}^o \gamma_j)$. On the other hand, the higher the temperature, the higher the $\ln(P_{v_j}^o \gamma_j)$ values under the same conditions of surfactant concentration. In this way, the compounds have a major tendency to pass to the vapour phase. Lastly, regarding surfactant concentration, when keeping a constant temperature, the values of $\ln(P_{v_j}^o \gamma_j)$ decrease with the increase in C_S . By raising the surfactant concentration, a higher concentration of micelles is generated [5], which results in the DNAPL being more protected. Therefore, the higher the surfactant concentration, the lower the volatilization of the compounds.

The interaction between surfactant concentration and temperature to $\ln(P_{v_j}^o \gamma_j)$ was modelled using the response surface methodology (RSM). In the RSM, the parameters in Equation (6) were fitted to the experimental $\ln(P_{v_j}^o \gamma_j)$ data in Figure S1.

$$P_{v_j}^o \gamma_j = \exp(a + b \cdot C_S + c \cdot T + d \cdot C_S^2 + e \cdot T^2 + f \cdot C_S \cdot T) \quad (6)$$

where T is the temperature (°C), a - f are the parameters obtained from response surface methodology (Figure S1), and C_S is the surfactant concentration ($\text{g} \cdot \text{L}^{-1}$) when VLE is reached (1 h). C_S is the initial surfactant concentration since the surfactant does not lose capacity.

The results of the parameters a - f in Equation (6) and the statistical parameters obtained from the analysis of variance (Coefficient of variation (R^2), Fischer's test value (F-value), and probability (p -value)) obtained from the fitting are summarized in Table 2. As can be seen, the value of R^2 is close to one for all the compounds present in SVCOCs, indicating the good compromise between the data obtained by experiments and those predicted by

the model. Additionally, the F-values are large ($\gg 1$), and the p-values are small enough (< 0.05) for the compounds, then, the model proposed for $P_v^0 \gamma_j$ estimation can be considered valid and the values can be estimated accurately for a given surfactant concentration and temperature regardless of initial SVCOCs concentration.

Table 2. Parameters obtained from the fitting of $P_v^0 \gamma_j$ to Equation (6). The statistical parameters were obtained from variance analysis. Coefficient of variation (R^2), Fischer's test value (F-value), and probability (p-value) are also shown.

	<i>a</i>	<i>b</i>	<i>c</i>	<i>d</i>	<i>e</i>	<i>f</i>	R^2	F-Value	<i>p</i> -Value
CB	2.86	−0.27	0.06	8.73×10^{-3}	-1.32×10^{-4}	-6.74×10^{-5}	0.99	414	1.86×10^{-22}
1,4-DCB	0.29	−0.30	0.09	1.21×10^{-2}	-2.85×10^{-4}	-8.10×10^{-4}	0.99	473	3.73×10^{-23}
1,2-DCB	0.31	−0.30	0.08	1.19×10^{-2}	-2.34×10^{-4}	-8.13×10^{-4}	0.99	666	6.52×10^{-25}

3.3. Volatilization of SVCOCs from Emulsion

Volatilization of SVCOCs in the emulsion can be modelled considering those values that influence the volatility of the chlorinated organic compounds. These variables are temperature, airflow, and surfactant concentration in the aqueous phase. The molar balance of each chlorinated organic compound *j* in the emulsion in the batch experiment schematized in Figure 1 can be calculated using Equation (7).

$$-\frac{dn_j}{dt} = -\frac{V_L C_T dx_j}{dt} \quad (7)$$

where n_j is the moles of *j* in the emulsion; V_L is the volume of the aqueous emulsion (L); C_T is the total molar concentration of the emulsion (approximately corresponding to water: $55 \text{ mol} \cdot \text{L}^{-1}$), and x_j is the molar fraction of the compound *j* in the liquid phase.

The gas flow rate which leaves the bottle (Figure 1) is assumed to be in equilibrium with the emulsion by applying Raoult's law. The molar fraction of *j* compound in the gas phase is calculated with Equation (8).

$$y_j = \frac{P_v^0 \gamma_j \cdot x_j}{P_T} \quad (8)$$

The molar flow rate of the *j* compound disappearing from the emulsion is the same as the molar flow of this *j* compound that leaves the bottle in the gas phase (both phases in equilibrium), as described in Equation (9).

$$-\frac{V_L \cdot C_T \cdot dx_j}{dt} = \frac{F_{gas} \cdot P_v^0 \gamma_j \cdot x_j}{P_T} \quad (9)$$

where F_{gas} is the gas molar flow rate ($\text{mol} \cdot \text{h}^{-1}$) fed to the system.

The molar fraction of *j* in the emulsion with time can be predicted by integrating Equation (9) as shown in Equation (10), where *K* is a constant defined in Equation (11).

$$\frac{x_j}{x_{j0}} = \exp(-K_j \cdot t) \quad (10)$$

$$K_j = \frac{F_{gas} \cdot P_v^0 \gamma_j}{V_L \cdot C_T} \quad (11)$$

The value of $P_v^0 \gamma_j$ at each time is obtained by Equation (6), considering that surfactant concentration is the initial one since it keeps constant with the time.

The ratio x_j/x_{j0} also corresponds to the concentration ratio of j compound in the emulsion (Equation (12)).

$$\frac{x_j}{x_{j0}} = \frac{C_j}{C_{j0}} \quad (12)$$

The consistency of $P_{vj}^o \gamma_j$ obtained in the surfactant presence was validated by comparing the experimental and predicted values of each compound in the emulsion obtained in runs in Table 1 (set B3). Experimental values with time of each time in emulsion (as symbols) and those predicted with Equation (10) (as lines) are shown in Figure 3.

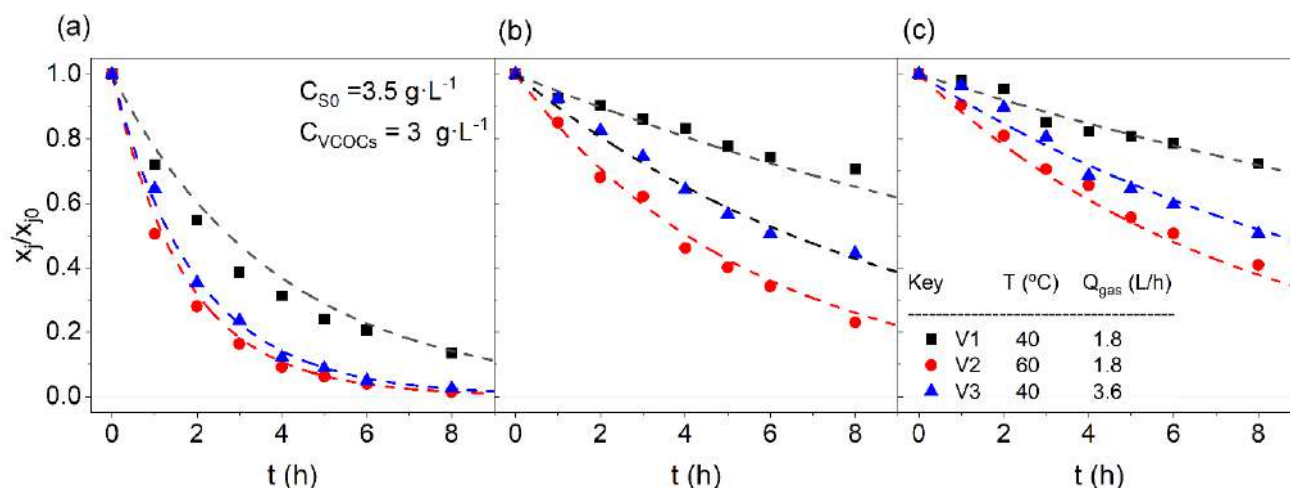


Figure 3. Volatilization of SVCOCs in the emulsion for (a) CB; (b) 1,4-DCB; (c) 1,2-DCB. Conditions $C_{SVCOCs} = 23.5 \text{ mmol}\cdot\text{L}^{-1}$; $C_{S0} = 3.5 \text{ g}\cdot\text{L}^{-1}$; $V_{aq} = 0.3 \text{ L}$. SVCOCs distribution (as molar percentage) was 53% of CB, 29% of 1,2-DCB, and 18% of 1,4-DCB. Symbols depict experimental results and line values predicted using Equation (10).

In Figure 3, either experimental values (as symbols) or simulated ones (as lines) have been plotted. As can be seen, the values of x_j/x_{j0} for each compound j ($j = \text{CB}, 1,4\text{-DCB}, 1,2\text{-DCB}$) are in good agreement with the experimental results, so the model is validated.

The effects of temperature and flow of air were studied. Experiments V1 and V2 were carried out at different temperatures. The higher the temperature (V2 experiment), the lower the fraction of SVCOC that remained in the aqueous emulsion, as was shown in Figure 3. Under the most favourable temperature conditions (60 °C), the CB removal was completed, whilst the values for 1,4-DCB and 1,2-DCB were 0.23 and 0.41, respectively. The temperature increase from 40 to 60 °C yielded an improvement of 89, 67, 44% value of the remaining ratio of SVCOCs after 8 h of volatilization treatment.

On the other hand, experiment V3 was carried out using a two-fold air flow rate, compared to the one used in V1. This variable presented a lower impact than the temperature increase in the remaining ratio of SVCOCs after 8 h. The improvement performed using a higher air flow were 81, 37, and 30% for CB, 1,4-DCB, and 1,2-DCB, respectively. As concerns each SVCOC, chlorobenzene is the compound that is more easily volatilized because it has the highest value of $P_{vj}^o \gamma_j$ (Figure S1), reaching almost complete elimination of the emulsion for experiments V2 and V3 in 8 h of treatment. For 1,2-DCB and 1,4-DCB, the results obtained are very similar between them, where the volatilization treatment was slightly more efficient for 1,4-DCB because of its slightly higher values of $P_{vj}^o \gamma_j$ (Figure S1). After 8 h of aeration, the values reached were 0.2 for 1,4-DCB and 0.3 for 1,3-DCB for the V3 experiment. Therefore, to obtain an increase in the volatilization of SVCOCs, it is necessary to use higher temperature and air flow, controlling the surfactant capacity loss and costs.

The surfactant capacity loss (SCL) during volatilization has also been measured and estimated for runs in Table 1. These aim to analyze if the surfactant can be reused in SEAR remediation treatments. The results obtained are summarized in Figure 4:

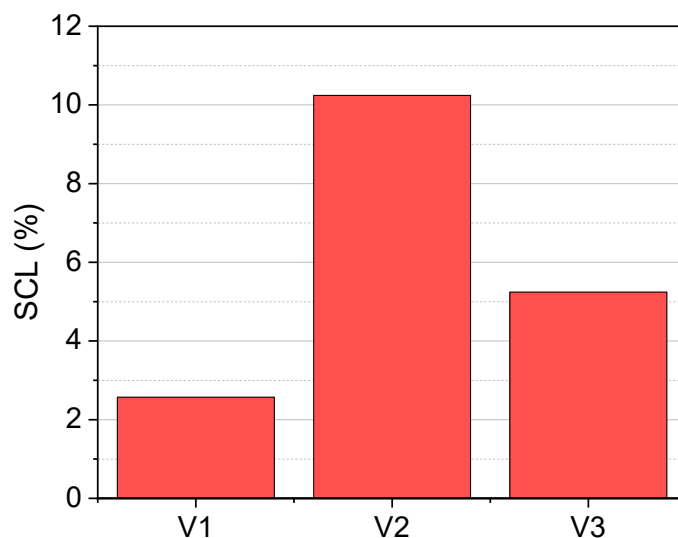


Figure 4. SCL values for each volatilization experiment.

As observed in Figure 4, the SCL caused in the SVCOCs air stripping is lower than 12% for all the experiments, indicating that the surfactant can be reused. This surfactant would be employed in a new cycle of SEAR treatment (in situ), reducing the operational costs. The use of E-Mulse® in SEAR treatment has been successfully applied in a real soil polluted with DNAPL. This DNAPL is formed by a complex mixture of chlorinated compounds among which are chlorobenzene and dichlorobenzene isomers [8].

The emulsion extracted from the new SEAR cycle will be treated by SVCOCs volatilization, which will have better results since the $P_v\gamma$ values increase with a decrease in surfactant concentration. However, it is important to point out that with each new cycle of volatilization, the surfactant capacity will decrease around 10%, so the dissolved SVCOCs in the next SEAR treatment will also decrease, taking into account that the MSR is $4.33 \frac{\text{mmol SVCOCs}}{\text{g surfactant}}$. This process can be repeated until the quantity of SVCOCs dissolved does not support the reuse of the surfactant.

It is important to point out that the volatilization process results forms the need to treat the resulting effluent after SEAR treatment, as it contains chlorinated compounds that require elimination.

4. Conclusions

In this work, the mixture of semi-volatile chlorinated organic compounds has been successfully volatilized from a non-ionic surfactants emulsion, reducing remarkably the concentration of SVCOCs in the emulsion, but keeping the surfactant capacity for recycling the emulsion in further SEAR treatments.

Regarding surfactant stability, it has been observed that surfactant capacity keeps constant at temperatures up to 60 °C during 48 h, with Surfactant Capacity Loss lower than 10%.

From the experimental results, the thermodynamic behavior of the SVCOCs in the emulsion was remarkably affected by surfactant concentration and temperature. $P_{vj}^o\gamma_j$ estimated values were correlated with surfactant concentration and temperature using surface response methodology. SVCOCs concentration does not affect the $P_v^o\gamma$ values. It has been concluded that $P_v^o\gamma$ is increased with the temperature due to the significant tendency of the organic compounds to pass to the vapour phase and reduce with the surfactant concentration.

The model proposed to simulate the evolution of SVCOCs in the emulsion during the air stripping process was successfully to predict the experimental values. Therefore, the estimated $P_{vj}^o\gamma_j$ values were validated. The SCL, after eliminating more than 80% of COCs

in the emulsion, was lower than 10%, and the resulting emulsion could be used in further soil flushing in a circular economy scenario.

Supplementary Materials: The following supporting information can be downloaded at: <https://www.mdpi.com/article/10.3390/ijerph19127547/s1>, Table S1. HS-GC conditions. Values of $P_{v_i}^0, \gamma_j$ for the experiments summarized in Table S1 (red points) and the response surfaces for the different compounds.

Author Contributions: Conceptualization: A.S. and D.L.; Methodology: P.S. and R.G.-C.; Software: D.L.; Investigation: P.S. and R.G.-C.; Data curation: P.S., R.G.-C. and D.L.; Writing-original draft preparation: P.S.; Writing-review and editing: D.L. and A.S.; resources: A.S. and A.R.; supervision: D.L. and A.S.; project administration: A.S. and A.R.; funding acquisition: A.R. and A.S. All authors have read and agreed to the published version of the manuscript.

Funding: Through the project, this work was supported by the Regional Government of Madrid through the CARESOIL project (S2018/EMT-4317), the Spanish Ministry of Economic, Industry and Competitiveness PID2019-105934RB, and for the EU Life Program (LIFE17 ENV/ES/000260). Raúl García-Cervilla acknowledges the FPI grant from the Spanish Ministry of Economy, Industry and Competitiveness (ref. BES-2017-081782).

Institutional Review Board Statement: Not applicable.

Informed Consent Statement: Not applicable.

Data Availability Statement: Not applicable.

Acknowledgments: The authors thank the Department of Agriculture, Livestock and the Environment, Government of Aragon, Spain, as well as EMGRISA, for kindly supplying the samples.

Conflicts of Interest: The authors declare no conflict of interest.

References

1. Payá Perez, A.; Rodríguez Eugenio, N. *Status of Local Soil Contamination in Europe*; European Commission: Brussels, Belgium, 2018.
2. Siegrist, R.L.; Crimi, M.; Simpkin, T.J. *In Situ Chemical Oxidation for Groundwater Remediation*; Springer Science & Business Media: Berlin/Heidelberg, Germany, 2011; Volume 3.
3. Huo, L.; Liu, G.; Yang, X.; Ahmad, Z.; Zhong, H. Surfactant-enhanced aquifer remediation: Mechanisms, influences, limitations and the countermeasures. *Chemosphere* **2020**, *252*, 126620. [[CrossRef](#)] [[PubMed](#)]
4. Ramezanzadeh, M.; Aminnaji, M.; Rezanezhad, F.; Ghazanfari, M.H.; Babaei, M. Dissolution and remobilization of NAPL in surfactant-enhanced aquifer remediation from microscopic scale simulations. *Chemosphere* **2022**, *289*, 133177. [[CrossRef](#)] [[PubMed](#)]
5. Rosen, M.J.; Kunjappu, J.T. *Surfactants and Interfacial Phenomena*; John Wiley & Sons: Hoboken, NJ, USA, 2012.
6. Babaei, M.; Copty, N.K. Numerical modelling of the impact of surfactant partitioning on surfactant-enhanced aquifer remediation. *J. Contam. Hydrol.* **2019**, *221*, 69–81. [[CrossRef](#)] [[PubMed](#)]
7. Liu, J.W.; Wei, K.H.; Xu, S.W.; Cui, J.; Ma, J.; Xiao, X.L.; Xi, B.D.; He, X.S. Surfactant-enhanced remediation of oil-contaminated soil and groundwater: A review. *Sci. Total Environ.* **2021**, *756*, 144142. [[CrossRef](#)]
8. Santos, A.; Domínguez, C.M.; Lorenzo, D.; García-Cervilla, R.; Lominchar, M.A.; Fernández, J.; Gómez, J.; Guadaño, J. Soil flushing pilot test in a landfill polluted with liquid organic wastes from lindane production. *Heliyon* **2019**, *5*, e02875. [[CrossRef](#)] [[PubMed](#)]
9. Domínguez, C.M.; Romero, A.; Santos, A. Selective removal of chlorinated organic compounds from lindane wastes by combination of nonionic surfactant soil flushing and Fenton oxidation. *Chem. Eng. J.* **2019**, *376*, 120009. [[CrossRef](#)]
10. Hanafiah, S.A.; Mohamed, M.A.; Caradec, S.; Fatin-Rouge, N. Treatment of heavy petroleum hydrocarbons polluted soil leachates by ultrafiltration and oxidation for surfactant recovery. *J. Environ. Chem. Eng.* **2018**, *6*, 2568–2576. [[CrossRef](#)]
11. Huang, K.; Liang, J.; Jafvert, C.T.; Li, Q.; Chen, S.; Tao, X.; Zou, M.; Dang, Z.; Lu, G. Effects of ferric ion on the photo-treatment of nonionic surfactant Brij35 washing waste containing 2,2',4,4'-terabromodiphenyl ether. *J. Hazard. Mater.* **2021**, *415*, 125572. [[CrossRef](#)]
12. Li, Y.; Hu, J.; Liu, H.; Zhou, C.; Tian, S. Electrochemically reversible foam enhanced flushing for PAHs-contaminated soil: Stability of surfactant foam, effects of soil factors, and surfactant reversible recovery. *Chemosphere* **2020**, *260*, 127645. [[CrossRef](#)]
13. García-Cervilla, R.; Santos, A.; Romero, A.; Lorenzo, D. Compatibility of nonionic and anionic surfactants with persulfate activated by alkali in the abatement of chlorinated organic compounds in aqueous phase. *Sci. Total Environ.* **2021**, *751*, 141782. [[CrossRef](#)]
14. Ahn, C.K.; Woo, S.H.; Park, J.M. Selective adsorption of phenanthrene in nonionic-anionic surfactant mixtures using activated carbon. *Chem. Eng. J.* **2010**, *158*, 115–119. [[CrossRef](#)]

15. Rosas, J.M.; Santos, A.; Romero, A. Soil-Washing Effluent Treatment by Selective Adsorption of Toxic Organic Contaminants on Activated Carbon. *Water Air Soil Pollut.* **2013**, *224*, 10. [[CrossRef](#)]
16. Ahn, C.K.; Lee, M.W.; Lee, D.S.; Woo, S.H.; Park, J.M. Mathematical evaluation of activated carbon adsorption for surfactant recovery in a soil washing process. *J. Hazard. Mater.* **2008**, *160*, 13–19. [[CrossRef](#)]
17. Virga, E.; Parra, M.A.; de Vos, W.M. Fouling of polyelectrolyte multilayer based nanofiltration membranes during produced water treatment: The role of surfactant size and chemistry. *J. Colloid Interface Sci.* **2021**, *594*, 9–19. [[CrossRef](#)] [[PubMed](#)]
18. Cao, W.; Zhang, L.; Miao, Y.; Qiu, L. Research progress in the enhancement technology of soil vapor extraction of volatile petroleum hydrocarbon pollutants. *Environ. Sci. Processes Impacts* **2021**, *23*, 1650–1662. [[CrossRef](#)] [[PubMed](#)]
19. Ma, J.; Yang, Y.; Dai, X.; Li, C.; Wang, Q.; Chen, C.; Yan, G.; Guo, S. Bioremediation Enhances the Pollutant Removal Efficiency of Soil Vapor Extraction (SVE) in Treating Petroleum Drilling Waste. *Water Air Soil Pollut.* **2016**, *227*, 465. [[CrossRef](#)]
20. Lee, J.H.; Woo, H.J.; Jeong, K.S. Removal of non-aqueous phase liquids (NAPLs) from TPH-saturated sandy aquifer sediments using in situ air sparging combined with soil vapor extraction. *J. Environ. Sci. Health A Toxic Hazard. Subst. Environ. Eng.* **2018**, *53*, 1253–1266. [[CrossRef](#)]
21. Huan, J.C.; Shang, C. Air Stripping. In *Advanced Physicochemical Treatment Processes. Handbook of Environmental Engineering*; Wang, L.K., Hung, Y.T., Shammas, N.K., Eds.; Humana Press: Totowa, NJ, USA, 2006; Volume 4. [[CrossRef](#)]
22. Pitt, R.; Shirley, C.; Field, R. Groundwater contamination potential from stormwater infiltration practices. *Urban Water* **1999**, *1*, 217–236. [[CrossRef](#)]
23. Braeckevelt, M.; Mirschel, G.; Wiessner, A.; Rueckert, M.; Reiche, N.; Vogt, C.; Schultz, A.; Paschke, H.; Kusch, P.; Kaestner, M. Treatment of chlorobenzene-contaminated groundwater in a pilot-scale constructed wetland. *Ecol. Eng.* **2008**, *33*, 45–53. [[CrossRef](#)]
24. Lin, X.; Xu, C.; Zhou, Y.; Liu, S.; Liu, W. A new perspective on volatile halogenated hydrocarbons in Chinese agricultural soils. *Sci. Total Environ.* **2020**, *703*, 134646. [[CrossRef](#)]
25. Santos, A.; Fernandez, J.; Guadano, J.; Lorenzo, D.; Romero, A. Chlorinated organic compounds in liquid wastes (DNAPL) from lindane production dumped in landfills in Sabinanigo (Spain). *Environ. Pollut.* **2018**, *242*, 1616–1624. [[CrossRef](#)] [[PubMed](#)]
26. García-Cervilla, R.; Romero, A.; Santos, A.; Lorenzo, D. Surfactant-enhanced solubilization of chlorinated organic compounds contained in dnapl from lindane waste: Effect of surfactant type and ph. *Int. J. Environ. Res. Public Health* **2020**, *17*, 4494. [[CrossRef](#)] [[PubMed](#)]

Regeneration of Granulated Spent Activated Carbon with 1,2,4-Trichlorobenzene Using Thermally Activated Persulfate

Andrés Sánchez-Yepes, Aurora Santos, Juana M. Rosas, José Rodríguez-Mirasol, Tomás Cordero, and David Lorenzo*



Cite This: *Ind. Eng. Chem. Res.* 2022, 61, 9611–9620



Read Online

ACCESS |



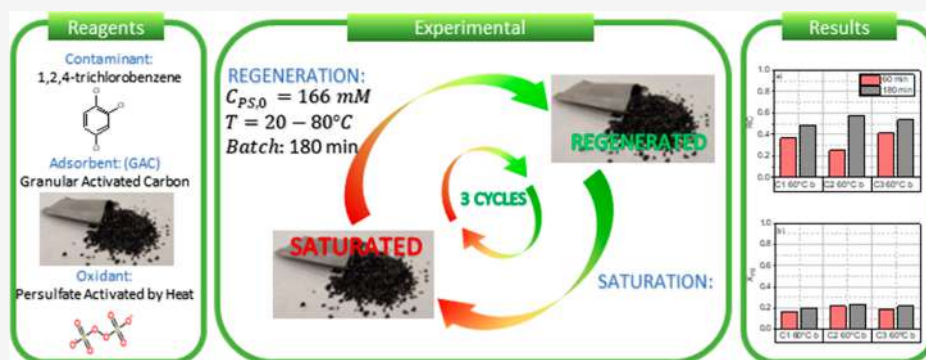
Metrics & More



Article Recommendations



Supporting Information



ABSTRACT: Chlorinated organic compounds (COCs) are persistent organic pollutants often found in groundwater near industrial sites or in industrial wastewaters. Adsorption into activated carbon is a common strategy to remediate these waters, but spent activated carbon results in a toxic residue to manage. To avoid the transport of the chlorinated compounds out of the site, the in-situ regeneration of the spent activated carbon can be considered for reuse to implement a circular economy. In this work, the regeneration of a commercial granular activated carbon (GAC) has been carried out using thermally activated sodium persulfate (TAP). GAC was previously saturated in 1,2,4-trichlorobenzene (124-TCB) as the model compound. The initial adsorption value was $350 \text{ mg}_{124\text{-TCB}} \cdot \text{g}_{\text{GAC}}^{-1}$. First, the nonproductive consumption of sodium persulfate was studied at different temperatures using nonsaturated GAC. Then, the regeneration of the saturated GAC (5 g) was studied by an aqueous solution (166 mM) of TAP (1 L) at a temperature range from 20 to 80 °C. The possible recovery of the adsorption capacity was studied after 3 h of treatment in three successive adsorption–regeneration cycles at the selected temperature (60 °C). The physicochemical changes of the GAC were also investigated before and after the regeneration treatments. The results evidence the significant deposition of sulfate on the GAC after each treatment of regeneration, which avoids the recovery of the initial adsorption capacity. Therefore, each regeneration cycle was necessarily followed by a washing step at 60 °C to remove this sulfate. After that, the regeneration treatment achieved a stable and high recovery of the initial adsorption capacity of about 48.2%.

1. INTRODUCTION

The presence of chlorinated organic compounds (COCs) in industrial wastewaters and groundwaters is a serious environmental problem. According to the EU Water Framework Directive (Directive 2000/60/EC), several COCs have been added to the list of substances to be monitored in recent decades, limiting their production and use. Examples are 1,1,1-trichloroethane, 1,1,2-trichloroethane, 1,2,4-trichlorobenzene, or 1,4-dichlorobenzene, among others. However, due to their widespread and common use as wood preservatives, pesticides, solvents, hydraulic fluids, or dielectric oil, these COCs still pose an elevated risk to the environment^{1–7} due to their persistent character, so the design of abatement techniques must be accomplished.

One of the most common strategies for treating COCs in polluted groundwater is the groundwater pump and treatment

using adsorption into granular activated carbon (GAC) as a hydraulic barrier for this contamination.^{8,9} Activated carbon is also used to treat runoff water collected from contaminated sites. Specifically, GAC is an adsorbent with highly developed porous structures. Its high initial BET surface area close to its amphoteric and hydrophobic properties renders GAC as a suitable adsorbent for retaining organic materials from an aqueous medium.¹⁰ The latter properties make activated

Received: February 9, 2022

Revised: June 16, 2022

Accepted: June 16, 2022

Published: June 28, 2022

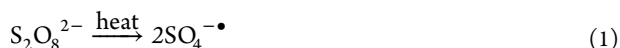


carbon a common strategy for treating wastewaters generated in many processes.^{10–16}

However, the high content of COCs in spent GAC makes this adsorbent a highly toxic waste that should be also managed appropriately. Moreover, a remarkable amount of spent GAC waste is produced when a large volume of water needs to be treated. Traditional procedures to manage spent GAC consisting^{17–21} of (i) storing the spent adsorbent in temporary chemical waste landfills or underground storage facilities by burying the waste and (ii) burning this waste in ovens, where all the organic matter will be transformed into CO₂ and water. However, this latter procedure involved a remarkable risk of production of highly toxic chlorinated species (as dioxins) during burning, due to the presence of chlorinated compounds in GAC. On the other hand, the storage of such toxic waste is also against sustainable environmental policies.

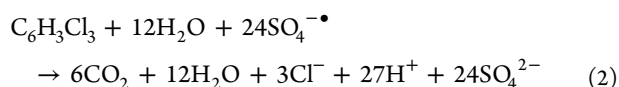
Recently, the chemical regeneration of the spent GAC by advanced oxidation processes has been gaining attention for the reuse of spent GAC, minimizing environmental impacts, increasing the circular economy of the process, and reducing the volume of spent adsorbent material waste.²² COCs are removed from the aqueous medium, and the adsorbent is regenerated and reused, preferably in the same location.^{23,24}

For this purpose, sodium persulfate (PS) activated by temperature (TAP) was studied as an oxidant in this work. Thermal activation of PS generates the sulfate radical, SO₄^{•-}, which has a redox potential of 2.6 V^{25–28} according to eq 1.



In the literature, few works deal with temperature-activated PS (TAP) for the regeneration of spent GAC, used for the removal of pollutants from aqueous streams, neither of them from chlorinated contaminants. In this sense, Jatta et al.²⁷ investigated the regeneration of a spent activated carbon saturated in toluene, with 211 mg·g_{GAC}⁻¹. In the regenerative process, they achieved 90% char recovery when applying a 100 mM PS solution at 80 °C. This degree of regeneration was stable during three consecutive regeneration cycles. Similarly, Huling et al.²⁹ studied the recovery of a GAC saturated in MTBE after removal of MTBE from an aqueous stream, achieving a saturation of 44.9 mg·kg_{GAC}⁻¹. The GAC recovery achieved was 40.9% after a single contact cycle with a 40 g·L⁻¹ PS solution at 55 °C. Despite the interest in results shown in these cited works, little attention was paid to the changes in the adsorbent through different cycles of regeneration with TAP.

This work has selected 1,2,4-trichlorobenzene (124-TCB) as a model organochlorine pollutant.^{2,30,31} This COC is a semivolatile compound with a moderate water solubility (28 ppm). Moreover, due to its toxicity and persistence, this pollutant poses a risk to human health and environmental safety.^{2,3,5,6} In previous studies, different recalcitrant compounds such as chlorobenzenes in the aqueous phase were degraded by TAP.^{25,26} Specifically, for 124-TCB, the complete mineralization reaction by application of TAP is shown in eq 2:



The main scope of this work is to analyze the regeneration of a GAC saturated with 124-TCB by TAP in successive adsorption–regeneration cycles. Moreover, attention will be paid to GAC physicochemical changes after the saturation and

regeneration cycles. To our knowledge, this is the first time that GAC properties (porosity and surface chemistry) during the intermediate stages of the regenerative process have been evaluated.

2. MATERIALS AND METHODS

2.1. Materials. Analytical-grade 1,2,4-trichlorobenzene (124-TCB) was purchased from Sigma-Aldrich. Pure 124-TCB was dissolved in *n*-hexane to plot the calibration curves. Quantification of the contaminants in the reaction samples was carried out using bicyclohexyl as a standard internal compound (ISTD), also purchased from Sigma-Aldrich.

The original (GAC-O) has a BET surface area of 905 m²·g⁻¹ and a total pore volume of 0.42 cm³·g⁻¹. Initially, GAC was previously washed with acidic water (GAC-F) as follows: 5 g of GAC was placed in a mesh and left in 1 L of Milli-Q water at pH = 3 for 24 h, with magnetic agitation. The mesh with GAC-F was recovered, rinsed twice with Milli-Q water, and dried 24 h at 50 °C in an oven. After this procedure, the GAC-F surface area and pore volume were reduced to 871 m²·g⁻¹ and 0.39 cm³·g⁻¹, respectively. The GAC-F was used as the adsorbent to conduct the adsorption–regeneration experiments.

Sodium PS, used as an oxidant, was supplied by Sigma-Aldrich. Other reagents used to quantify PS, such as potassium iodide (KI) and sodium bicarbonate (NaHCO₃), were also supplied by Sigma-Aldrich. The concentration of chloride and short-chain organic acids was determined by ion chromatography. The following compounds were used: sodium carbonate, sodium bicarbonate, sulfuric acid, and acetone (all from Sigma-Aldrich).

2.2. 124-TCB Adsorption. GAC (2 g) was placed in a stainless-steel mesh and immersed in the upper part of a 1 L closed flask containing 800 mL of water (Milli-Q purity), following which 3 g of pure 124-TCB was added as a liquid organic phase. A scheme of the experimental setup used is given in Figure S1 of the Supporting Information. The multiphase medium (organic–aqueous–GAC) was stirred to ensure that no external diffusional resistances were present. The amount of 124-TCB added was sufficient to saturate the GAC, with some of the added TCB remaining as an undissolved organic phase. In this way, the solubilized 124-TCB in water was kept at 28 mg·L⁻¹ (solubility of pure 124-TCB in water at 25 °C) during the whole adsorption time, thanks to the excess of 124-TCB organic phase present. Equilibrium between 124-TCB in the aqueous phase (28 mg·L⁻¹) and 124-TCB adsorbed on the GAC was reached before 72 h. After this time, the mesh with GAC was withdrawn and rinsed with water twice, dried at 50 °C for 24 h, and used in the regeneration experiments.

The excess of 124-TCB remaining in an organic phase and the 124-TCB solubilized in the aqueous phase was extracted by adding 200 mL of hexane to this medium containing the organic and aqueous phases. The mixture was stirred for 60 min to ensure the complete extraction of 124-TCB in hexane. GC–MS quantified the total concentration of 124-TCB extracted in hexane. The mass of 124-TCB adsorbed on GAC was calculated as the difference between the initial 124-TCB added as an organic phase and the final 124-TCB extracted in hexane. This procedure was accomplished in triplicate, and differences lower than 10% were obtained.

2.3. Experimental Procedure. Porosity and surface chemistry of original and pretreated GAC were characterized by adsorption–desorption of N₂ at –196 °C, X-ray photo-

electron spectroscopy (XPS), and temperature-programmed desorption (TPD), as described in the next sections.

Two sets of experiments were carried out: using the pretreated activated carbon without contaminant (GAC-F) and the saturated one in 124-TCB (GAC-S).

2.3.1. Reactivity of TAP with GAC-F. In the first set of experiments, the reaction between PS and GAC-F was studied batchwise at different temperatures (20–80 °C) and GAC loadings (0–10 g·L⁻¹). A 50 mL closed glass flask containing 50 mL of Milli-Q water was immersed in a thermostated glycerin bath. Constant temperature and good agitation were achieved using a mixing plate (IKA C-MAG HS 7). Once the temperature was reached, 1.97 g of PS was added to obtain a concentration of 166 mM in the aqueous phase, and a mass (0, 0.25, or 0.5 g) of pretreated GAC was confined in a stainless-steel mesh basket and introduced in the aqueous PS solution (zero reaction time). The GAC loading corresponds to 0, 5, and 10 g_{GAC}·L⁻¹ in the batch reactor, respectively. Experimental conditions are summarized in Table 1. A volume

Table 1. Experimental Conditions for Runs Carried out Using GAC-F without COCs Adsorbed^a

run	T (°C)	C _{GAC-F,0} (g·L ⁻¹)	cycle	procedure
B1	20	0	1	
B2	20	5	1	
B3	20	10	1	
B4	40	0	1	
B5	40	5	1	
B6	40	10	1	
B7	60	0	1	
B8	60	5	1, ^b 2, 3 ^b	a, ^b b ^b
B9	60	10	1, 2, 3	a, b
B10	80	0	1	
B11	80	5	1, 2, 3	a, b
B12	80	10	1, 2, 3	a, b

^aC_{PS,0} = 166 mM. ^bThe GAC after these cycles was characterized by adsorption–desorption of nitrogen at −196 °C, XPS, and TPD.

of 0.10 mL of the aqueous phase sample was taken at several reaction times to quantify the PS concentration. At the final reaction time (6 h), the mesh with the GAC was recovered and treated in two different ways

- Used directly in the following cycle (runs B8, B9, B11, and B12) and carried out under the corresponding reaction conditions.
- Washed in a 50 mL agitated flask with 50 mL of Milli-Q water at 60 °C for 2 h and used in the following cycle (runs B8 and B9), under the corresponding reaction conditions.

The number of cycles and type of procedure for each run are also summarized in Table 1. Samples of GAC obtained in the B8 run after the first and third cycles in procedure b were also characterized after washing at 60 °C with water for 2 h and then were dried at 50 °C in an oven for 24 h.

2.3.2. Regeneration of GAC-S. In the second set of experiments, the GAC-S regeneration by TAP was studied. The pretreated GAC was saturated in 124-TCB (selected as the model COC).

The runs (summarized in Table 2) were conducted batchwise in a 50 mL magnetically stirred reactor. A 50 mL closed glass flask containing 50 mL of Milli-Q water was

Table 2. Experimental Conditions of Runs Carried Out for the Regeneration of GAC-S with TAP, C_{PS,0} = 166 mM, and GAC Loading of 5 g·L^{-1a}

run	T (°C)	regeneration cycles	resaturation cycles	procedure
R1	20	1	1	a, b
R2	40	1	1	a, b
R3	60	1, ^b 2, 3 ^b	1, 2, 3	a(1, 2), b(1, 2, 3) ^b
R4	80	1	1	a, b

^aV_L = 50 mL, GAC-S = 0.25 g. ^bThe GAC was characterized after regeneration, after water rinsing, and, finally, after resaturation.

immersed in a thermostated glycerin bath controlled by a proportional–integral–derivative controller coupled with a heating and mixing plate (IKA C-MAG HS 7) to maintain a constant temperature. Once the temperature was reached, the required amount of PS was added to the aqueous phase. A mass (0.25 g) of GAC (saturated in 124-TCB or not) was confined in a stainless-steel mesh basket and introduced in the aqueous PS solution (zero reaction time). The mass of GAC added corresponds to a loading of 5 g_{GAC}·L⁻¹ in the batch reactor.

Several flasks were used in each experiment, a flask being sacrificed each time. Experiments were carried out in duplicate or triplicate. At the corresponding time, the mesh with GAC was withdrawn from the aqueous phase, and the remaining PS and pH in the aqueous phase were determined. The recovered GAC samples were analyzed to determine the recovery of GAC adsorption capacity after oxidation. The analysis of the recovered GAC adsorption capacity after regeneration was evaluated by saturating the oxidized GAC again in a 124-TCB aqueous solution (28 mg·L⁻¹) in the following way: (1) Regenerated GAC recovered in the basket mesh (0.25 mg) was placed (with or without previous washing with water at 60 °C) in a 50 mL closed glass flask containing 40 mL of Milli-Q water and 125 mg of 124-TCB (as an organic phase to ensure the saturation of 124-TCB in the aqueous phase at 28 mg·L⁻¹). The vial was agitated (300 rpm) for 72 h. After 4 h of settling, the mesh containing the GAC was withdrawn. (2) A volume of 10 mL of hexane was added to the flask, and the liquid phases were agitated for 60 min. After settling for 20 min, GC–MS was used to analyze the concentration of 124-TCB in the hexane phase. (3) The recovery of the adsorption capacity (RC) was calculated using eq 3:

$$RC = \frac{w_{124\text{-TCB},0} - C_{124\text{-TCB,extracted}} \cdot V_{\text{hexane}}}{C_{124\text{-TCB,sat}} \cdot w_{\text{GAC-F}}} \quad (3)$$

where $w_{124\text{-TCB},0}$ is the mass of 124-TCB added to saturate the oxidized GAC (in mg), $C_{124\text{-TCB,extracted}}$ is the 124-TCB concentration remaining in *n*-hexane in mg·L⁻¹, $C_{124\text{-TCB,sat}}$ is the concentration of 124-TCB in the saturated GAC-F (mg_{124-TCB} g_{GAC-F}⁻¹), $w_{\text{GAC-F}}$ is the mass of GAC-F added, and $V_{\text{n-hexane}}$ is the volume of hexane used in extraction in liters.

The mass of $w_{\text{GAC-F}}$ must be calculated from the mass of saturated GAC added, $w_{\text{GAC-S}}$, after the mass of 124-TCB adsorbed is subtracted.

$$w_{\text{GAC-F}} = \frac{w_{\text{GAC-S}}}{(1 + C_{124\text{-TCB,sat}} \times 1000)} \quad (4)$$

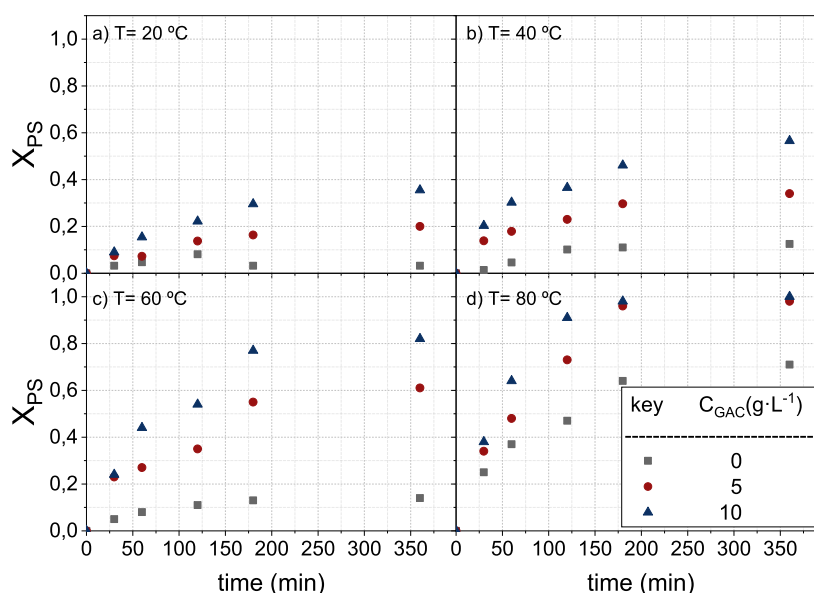


Figure 1. PS conversion profiles with reaction times in the first cycle (runs in Table 1) at different GAC-F concentrations and $C_{PS,0} = 166$ mM at (a) 20, (b) 40, (c) 60, and (d) 80 °C, respectively.

Three consecutive regeneration and adsorption cycles were performed for GAC under the reaction conditions used in run 3.

As commented previously, the recovered mesh with GAC after the oxidation treatment was handled in two ways before resaturation in 124-TCB:

- Without washing with water before resaturation in 124-TCB (run 3).
- Washing in a 50 mL agitated flask with 50 mL of Milli-Q water at 60 °C for 2 h (run 3).

The GAC was characterized by adsorption–desorption of nitrogen at -196 °C, XPS, and TPD after regeneration (GAC-R) after water rinsing (GAC-R-W) and finally after resaturation (GAC-R-W-S). Schemes of the experimental procedure are provided in the Supporting Information (Figures S1 and S2).

2.4. Analytical Methods. Quantification of 124-TCB and identification of other organic byproducts were performed by gas chromatography (Agilent 6890N, Santa Clara, CA, USA) using a mass spectrometry detector. An HP-5MS chromatographic column (30 m \times 0.25 mm ID \times 0.25 μ m) was used as the stationary phase and helium at a constant flow rate of 1.7 mL·min $^{-1}$ as the mobile phase. A 1 μ L aliquot of the liquid sample was injected (injection port temperature: 250 °C). The chromatographic oven was operated under a programmed temperature gradient (initial temperature = 80 °C, increasing the temperature at a rate of 18 °C·min $^{-1}$ up to 180 °C, and then keeping it constant for 15 min). Bicyclohexyl was used as a standard internal compound (ISTD), 8 mg·kg $^{-1}$ _{hexane}.

The concentration of PS was determined by colorimetric titration using an indicator solution of KI (100 g·L $^{-1}$) and NaHCO $_3$ (5 g·L $^{-1}$). Ionic organic byproducts, such as carboxylic acids and chlorides, were measured by ion chromatography (Metrohm 761 Compact IC), with anionic chemical suppression and a conductivity detector. The pH was measured with a basic 20-CRISON pH electrode.

The porous texture of the samples was characterized by N $_2$ adsorption–desorption at -196 °C and by CO $_2$ adsorption at 0 °C performed using an ASAP 2020 apparatus (Micro-

meritics). Samples were outgassed at 150 °C for at least 8 h. From the N $_2$ isotherm, the apparent surface area (A_{BET}) was determined by applying the BET equation. The t-method allows obtaining the values of the external surface area (A_t) and the micropore volume (V_t). The mesopore volume (V_{mes}) was determined as the difference between the adsorbed volume of N $_2$ at a relative pressure of 0.99 (V_{tot}) and the micropore volume V_t . The Dubinin–Radushkevich equation was used to calculate the apparent surface area (A_{DR}) and narrow micropore volume (V_{DR}) from CO $_2$ adsorption data.

The surface chemistry of the sample was analyzed by XPS (5700C model Physical Electronics) using Mg $k\alpha$ radiation (1253.6 eV). The maximum C 1s peak was set to 284.5 eV and used as a reference for shifting the whole spectrum.

TPD is usually used to characterize the oxygen functional groups present on the carbon surface, which are formed during carbonization/activation processes. TPD analyses were carried out using a customized quartz fixed-bed reactor placed inside an electrical furnace and coupled to both a mass spectrometer (Pfeiffer Omnistar GSD-301) and to a nondispersive infrared (NDIR) gas analyzer (Siemens ULTRAMAT 22) to quantify CO and CO $_2$ evolution (calibration error <1%). In these experiments, ca. 100 mg of GAC was heated from room temperature to 930 °C, at a heating rate of 10 °C·min $^{-1}$ under nitrogen (purity 99.999%, Air Liquide) flow (200 cm 3 ·STP·min $^{-1}$).

3. RESULTS AND DISCUSSION

3.1. GAC Characterization. The textural parameters of original carbon (GAC-O) and that washed with acid water (GAC-F) are summarized in Table S1. The N $_2$ adsorption–desorption isotherms obtained at -196 °C of both samples are given in Figure S3 of the Supporting Information. The atomic surface concentration was determined by XPS analyses, and the amount of CO and CO $_2$ evolved from TPD experiments for these samples are also collected in Table S1.

As shown in Figure S3, GAC is a microporous material presenting an isotherm of type I.³² GAC presented an initial apparent surface area of 905 m 2 ·g $^{-1}$, which was reduced by 4%

after its washing (GAC-F). An equivalent reduction of the pore volume (7%) was observed after washing it with acid water. With regard to the surface chemistry, GAC presented an atomic surface concentration of oxygen of around 10% and traces of N and S. The content of S was significantly reduced by the washing process. Meanwhile, the amount of CO and CO₂ evolved from TPD are not very significant, evidencing the low presence of carbon–oxygen surface groups. As can be seen, these amounts slightly increased after washing, mainly associated with the higher decomposition of carbonyl and quinone groups.

3.2. PS Consumption by GAC-F. The effect of the reaction between GAC without the contaminant adsorbed (GAC-F) and PS was deeply investigated at different reaction temperatures, studying the PS consumption and the changes in the carbon properties.

The consumption of PS promoted by GAC-F was tested at different reaction temperatures and using different concentrations of GAC and PS. The experimental conditions are summarized in Table 1. The PS concentration was measured, and the conversion of PS was calculated using eq 5:

$$X_{PS} = 1 - \frac{C_{PS}}{C_{PS,0}} \quad (5)$$

where $C_{PS,0}$ and C_{PS} are the initial concentration of PS and the concentration for a specific reaction time, respectively.

The profiles of PS conversion using GAC-F in the first cycle of runs carried out under the experimental conditions in Table 1 are shown in Figure 1. The higher the temperature, the higher the PS consumption, as expected in TAP. This trend was noticed with or without GAC in the medium. In GAC's absence, the PS consumption was negligible in the interval time studied in the temperature range of 20–60 °C (conversion lower than 0.15). On the contrary, consumption of PS rises at 0.71 at 360 min at 80 °C. These values are in agreement with those reported elsewhere.²⁶

The presence of GAC results in a remarkable increase in PS consumption, suggesting that PS decomposed at the GAC surface. The higher the GAC loading, the higher the PS conversion at a specific time, as shown in Figure 1. These differences were more significant at temperatures lower than 80 °C, suggesting that the activation energy of the heterogeneous reaction was lower than the activation energy of the homogeneous thermal reaction or the adsorption of PS into the carbon surface, especially at the lowest temperature.

In addition, the effect of the mesh in the reaction medium was elucidated. Experiment B8 was carried out using the GAC dispersed in the aqueous phase. The differences between the PS consumption with and without mesh were negligible (<2%).

The stability of GAC-F after oxidation with TAP was analyzed. Reactivity and structural changes of GAC caused by its reaction with PS were studied after different reaction cycles, using 5 and 10 g·L⁻¹ of GAC, at 60 and 80 °C (runs B8, B9, B11, and B12 in Table 1). At the end of each cycle (180 min), the GAC was separated, dried, and put in contact with a new solution of PS ($C_{PS,0} = 166$ mM), with or without previous washing with water, as explained in the Experimental Procedure section. The final pH reached after each cycle was 1.5 due to PS decomposition, resulting in acidic pH.

The time profiles of PS conversion obtained at each cycle, without washing the GAC recovered after TAP oxidation

(procedure a), are shown in Figure S4 of the Supporting Information. As shown in Figure S4, the PS conversion decreased with the cycle regardless of the temperature and GAC concentration used. At both concentrations tested, the PS consumption decreased dramatically between cycles 2 and 3. The drop in PS conversion in successive cycles could be due to the salt deposition on the surface of GAC.³³ The generated inorganic salts (sulfates) in the aqueous medium can be deposited on the GAC surface, hindering the PS reaction on the GAC surface. Results obtained in run 3 with and without GAC washing between cycles (at 60 °C, procedure b in the Experimental Procedure section) are compared to confirm this hypothesis. The PS conversion with time is shown in Figures S4a and S5a.

In Figure 2, PS conversion measured at each cycle in runs B8 and B9 (Table 1), with and without previous washing with

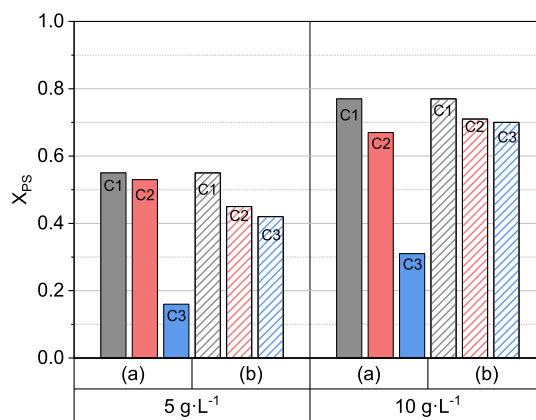


Figure 2. PS conversion at 180 min runs B8 and B9 in Table 1, with (a) and without (b) washing with water at 60 °C between oxidation cycles. PS conversions profiles with time are shown in Figures S4a,b and S5a,b.

water at 60 °C, are compared. As shown in Figure 2, if GAC is washed between oxidation cycles, the conversion of PS is stable over cycles, confirming that the deposition of inorganic salts on the GAC surface decreases the GAC reactivity with TAP.

Changes in the GAC-F porosity and BET area were measured after several cycles in run B8 (Table 1) carried out with procedure a (without washing) or b (washing with water for 2 h, at 60 °C, between the different cycles). The BET surface area and the pore volume were measured after the first cycle (GAC-B8-C1a) and after the third cycle (GAC-B8-C3b), and the results are given in Table 3. The corresponding nitrogen adsorption–desorption isotherms at −196 °C are summarized in Figure S6.

The BET surface area of the GAC-F before oxidation was 871 m²·g⁻¹ (Table S1). In GAC-B8-C1a (after the first oxidation cycle), the apparent surface area decreased by 15%. In addition, after the third oxidation cycle GAC-B8-C3b, the surface area drops to a value of 173 m²·g⁻¹, associated with 76% of porosity loss or blockage. The reaction between GAC-F and PS can explain this decrease in the specific surface area. PS oxidizes the surface, modifying the GAC textural parameters, reducing the available pores, and diminishing the accessible surface area. These data are consistent with the results obtained by XPS and TPD, where generation of many oxygen surface groups was observed.

Table 3. Physicochemical Changes in GAC-F after Reaction with TAP; Run B8 in Table 1

analytical technique	property	GAC-F	GAC-B8-C1a	GAC-B8-C3b
N ₂ adsorption	A _{BET} (m ² ·g ⁻¹)	871	737	173
	V _p (cm ³ ·g ⁻¹)	0.39	0.36	0.09
CO ₂ adsorption	A _{DR} (m ² ·g ⁻¹)	459	409	115
	V _{DR} (cm ³ ·g ⁻¹)	0.184	0.164	0.05
XPS: atomic surface concentration	C (%)	90.59	78.79	69.16
	N (%)	0.51	0.88	0.63
	O (%)	8.75	18.85	24.75
	S (%)	0.15	1.47	0.36
TPD	CO (μmol·g ⁻¹)	349	3058	3068
	CO ₂ (μmol·g ⁻¹)	41	1405	3557
	H ₂ O (μmol·g ⁻¹)	73	404	940

The reaction of TAP with GAC-F also changed the chemical composition of the GAC-F surface. As shown in Table 3, the atomic surface concentration of carbon was reduced during the cycles, favoring the formation of more oxidized surface groups, as confirmed by the high increase of the oxygen surface concentration after the different cycles determined by XPS and TPD. This oxygen increase is more significant in XPS analyses, suggesting that PS treatment strongly affects the most external surface. Specifically, the evolved CO, CO₂, and H₂O amounts from TPD analyses significantly increased with the reaction cycles. The range of evolution of these molecules is associated with the decomposition of carboxylic acids, lactones, anhydrides, and phenols/ether groups, not observed in the fresh GAC (GAC-F). In fact, after the third cycle, the amount of evolved CO₂ considerably increased, mainly due to further formation of carboxylic acids, lactone, and anhydride groups. The increase of acid groups after GAC-F's contact with PS inferred the following mechanism of carbon oxidation, proposed in eqs 6 and 7:



The sulfate radical obtained by the thermal activation of PS defined in eqs 6 and 7 attacks the GAC surface, generating the above-mentioned functional groups.

Finally, the S surface concentration determined by XPS analyses increased after reaction with TAP, as can be seen in GAC-B8-C1a, shown in Table 3, probably due to sulfate deposition. This deposition was removed after the washing steps, as evidenced in the results for GAC-B8-C3b, shown in Table 3. The initial S % content in GAC-F is 0.15, which increased to 1.47 after one cycle with TAP and decreased to 0.36 after washing with water at 60 °C, suggesting the effectiveness of hot washing in the sulfate removal. The latter was consistent with the experimental results obtained by IC where sulfates were detected.

3.3. Regeneration of GAC Saturated in 124-TCB. The saturation of GAC-F in 124-TCB (28 mg·L⁻¹ in the aqueous phase), explained in the Experimental Procedure, resulted in a GAC with 350 mg_{124-TCB}·g_{GAC-F}⁻¹ (C_{124-TCB,sat} in eq 4).

The procedure to study the recovery of GAC adsorption capacity (RC) by oxidation of GAC-S with TAP has been described in Section 2.3.2. Runs carried out are summarized in Table 2, and RC is calculated with eq 3.

3.3.1. Adsorption Capacity Recovery without Washing of Regenerated GAC. RC values obtained in the first regeneration cycle of runs R1 to R4 in Table 2, without washing with water (procedure a in Section 2.3.2) between regeneration and resaturation steps, are shown in Figure 3a, for 60 and 180 min. The corresponding consumption of PS in the regeneration step is also shown in Figure 3b.

As shown in Figure 3a, the RC was negligible at 20 °C, agreeing with the negligible PS consumption shown in Figure 3b. On the other hand, partial regeneration of the GAC-S was noticed for temperatures higher than 40 °C. As can be seen in Figure 3, the higher the temperature, the higher the PS consumption. The regeneration obtained at 80 °C (0.35) was lower than that obtained at 60 °C (0.48). Moreover, RC at 80 °C remained constant with the reaction time.

In this sense, the results shown in Figure 3a were obtained without GAC washing, between regeneration and resaturation in 124-TCB. Therefore, the RC values shown in Figure 3a can be affected by the sulfate formation on the GAC surface. This formation is higher at 80 °C due to the higher PS consumption at this temperature.³³ Moreover, the higher the PS conversion, the lower the final pH of the aqueous solution (2.07, 1.24, and 1.05 for 40, 60, and 80 °C, respectively).

The efficiency of PS consumption for 124-TCB oxidation on the GAC surface was defined as R_{OX}, this parameter being calculated from eq 8 as the ratio between the moles of PS consumed to the amount of 124-TCB oxidized (assuming that this last value is the same as the millimoles of 124-TCB adsorbed in resaturation of the regenerated GAC):

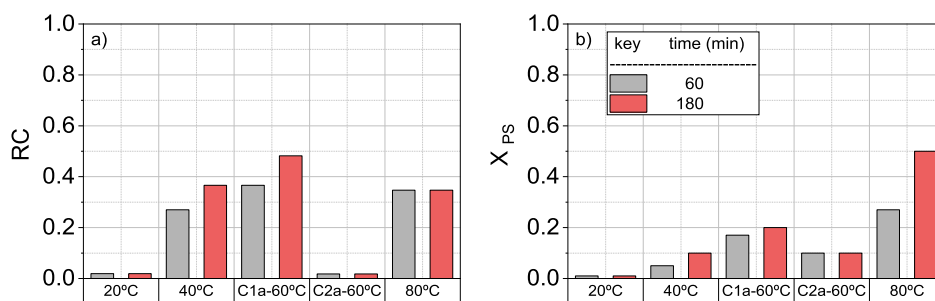


Figure 3. Experimental results of (a) regeneration capacity (RC) calculated with eq 3 of GAC-S and (b) PS conversion (eq 5) at different reaction times, using C_{PS,0} = 166 mM and C_{GAC-S} = 5g·L⁻¹. Runs in Table 2. Without GAC washing after regeneration and before resaturation for one cycle of regeneration.

$$R_{OX} = \frac{C_{PS,0} \cdot V_{AQ} \cdot X_{PS}}{C'_{124\text{-TCB},0,\text{adsorbed}} \cdot w_{GAC\text{-F}} \cdot RC} \quad (8)$$

where $C_{PS,0}$ is the initial concentration of PS used (166 mM), V_{AQ} is the aqueous volume of the aqueous phase in the reaction medium (0.05 L), $C'_{124\text{-TCB},0,\text{adsorbed}}$ is the millimoles of 124-TCB adsorbed in the initial saturated GAC-F (2.8 mmol·g⁻¹), $w_{GAC\text{-F}}$ the amount of GAC-F added, calculated from eq 4, and X_{PS} is the PS conversion.

The values of R_{OX} obtained in experiments R1–R4 (Table 2) are plotted in Figure 4. The higher the R_{OX} value, the lower

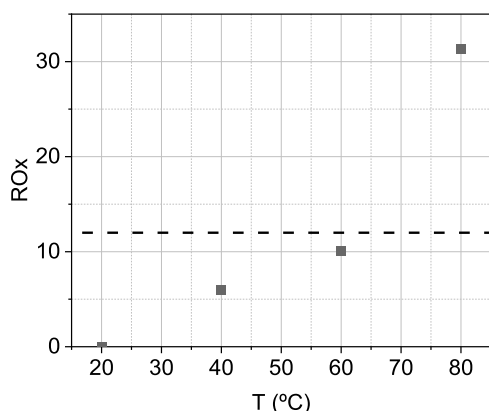


Figure 4. Oxidation yield, R_{OX} in $l_{PS,\text{reacted}} \cdot \text{mmol}^{-1}_{124\text{-TCB,regenerated}}$ for the experiments R1–R4 in Table 2, calculated using eq 8, in the first cycle of regeneration–resaturation without GAC washing between both steps.

the PS efficiency in 124-TCB oxidation and the higher the unproductive PS consumption. The theoretical value of R_{OX} for 124-TCB mineralization is close to 12 according to eq 2. A R_{OX} value lower than 12 means that the total mineralization of 124-TCB is not achieved, and a higher value of 12 implies a higher PS consumption. The closest value to 12 of R_{OX} was obtained at 60 °C (10.1 $l_{PS,\text{reacted}} \cdot \text{mmol}^{-1}_{124\text{-TCB,regenerated}}$). These conditions can be established as the best temperature to regenerate the GAC-S.

Once selected $T = 60$ °C as the best temperature tested, two cycles of regeneration–resaturation were carried out under the conditions of run R3 in Table 2. The regenerated GAC was not washed with water before resaturation in 124-TCB. The RC and PS conversion in the second regeneration–resaturation cycle are also included in Figure 3. As can be seen, a dramatic decrease in RC was noticed in the second regeneration cycle in R3 (Table 2) when the GAC was used

directly in cycles without washing, between regeneration and resaturation steps. The R_{OX} for this experiment was 121 $l_{PS,\text{reacted}} \cdot \text{mmol}^{-1}_{124\text{-TCB,regenerated}}$ due to the abatement of 124-TCB was negligible.

3.3.2. Adsorption Capacity Recovery with Washing of Regenerated GAC. The effect of GAC washing with water between regeneration and resaturation was studied at the selected temperature (60 °C). Three cycles of GAC regeneration and resaturation were carried out under the conditions of run 3 (Table 2), using procedure b (Section 2.3.2). Experimental values for RC (eq 3) and PS conversion (eq 5) at 60 and 180 min are shown in Figure 5, respectively. As shown, RC increases with time. An RC value of about 50% was held in the successive regeneration–adsorption cycles.

The R_{OX} value after each cycle was calculated with the data plotted in Figure 5, and the corresponding values obtained were 10.01, 9.09, and 8.88 $l_{PS,\text{reacted}} \cdot \text{mmol}^{-1}_{124\text{-TCB,regenerated}}$ for the first, second, and third cycles, respectively.

Values of R_{OX} lower than 12 suggest that the total mineralization of 124-TCB was not achieved. However, GC–MS or GC-FID-ECD identified neither chlorinated nor aromatic compounds in the aqueous phase. In addition, the aqueous phase after washing GAC with hot water was analyzed by two different methods. In the first one, *n*-hexane was used to extract the organic compounds; in the second, water was analyzed by HPLC. Both methods detected neither organic compound.

In addition, the chloride concentration in water after each cycle of regeneration step of the GAC was quantified. The experimental Cl^- ($(\text{Cl}^-)_{\text{exp}}$) concentration was compared to the theoretical amount of Cl^- that should be generated for the total dichlorination of 124-TCB ($(\text{Cl}^-)_{\text{stq}}$ calculated with eq 9):

$$(\text{Cl}^-)_{\text{stq}} = 350 \cdot W_{GAC} \cdot \frac{RC}{181} \cdot 3 \cdot 35.5 \quad (9)$$

where 350 mg·g⁻¹ is the total amount of 124-TCB adsorbed and 181 and 35.5 are the mass weights of 124-TCB and chloride, respectively.

The experimental chloride concentrations obtained after the three cycles were 17, 20, and 19%, respectively, of the theoretical values expected for total dechlorination of the oxidized 124-TCB. These low values can be explained by assuming the formation of more oxidized chlorinated species that were not detected³⁴ by GC/MS or HPLC and by incorporating Cl into the carbon surface (see XPS results).

On the other hand, GAC was characterized after cycles C1 and C3 to evaluate the influence of regeneration–resaturation cycles on the GAC properties. The BET surface area, pore

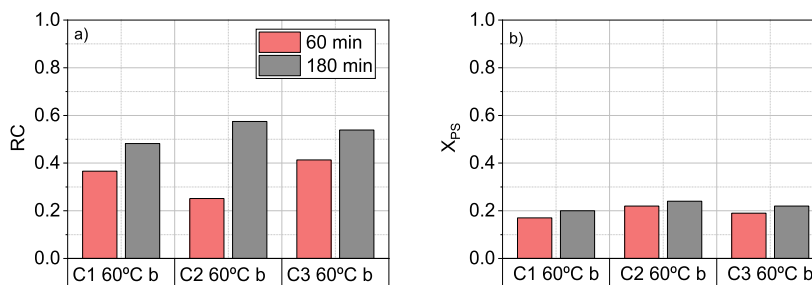


Figure 5. RC (eq 3) and PS conversion (eq 5) of GAC-S after three regeneration/adsorption cycles with washing between GAC regeneration and 124-TCB resaturation. Experimental conditions (run R3, Table 2), with $C_{PS,0} = 166$ mM, $C_{GAC\text{-S}} = 5$ g·L⁻¹, $T = 60$ °C.

Table 4. Characterization of GAC-R3 (Table 2) after First (C1) and Third (C3) Regeneration–Resaturation Cycles^a

analytical technique	property	GAC-S			C1			C3		
		initial	R	R-W	R-W-S	R	R-W	R-W-S		
N ₂ adsorption	A_{BET} (m ² ·g ⁻¹)	611	477	439	241	484	437	313		
	V_{p} (cm ³ ·g ⁻¹)	0.314	0.232	0.224	0.128	0.241	0.229	0.167		
CO ₂ adsorption	A_{DR} (m ² ·g ⁻¹)	364	328	321	333	289	306	348		
	V_{DR} (cm ³ ·g ⁻¹)	0.146	0.132	0.128	0.133	0.116	0.123	0.139		
XPS: atomic surface concentration	C (%)	89.29	81	82.77	87.13	77.25	78.94	79.01		
	N (%)	0.24	0.78	1.15	0.22	–	0.63	0.69		
	O (%)	8.33	16.48	14.6	15.00	17.56	17.11	17.94		
	S (%)	0.16	0.72	0.25	0.16	0.65	0.24	–		
	Cl (%)	1.08	1.02	1.24	0.9	4.54	2.31	1.2		
TPD	CO (μmol·g ⁻¹)	413	1403	1413	1321	1597	1784	154		
	CO ₂ (μmol·g ⁻¹)	76	446	341	337	669	714	556		
	H ₂ O (μmol·g ⁻¹)	367	506	797	609	606	628	590		

^aProperties were measured after 180 min of regeneration (R), after washing with Milli-Q water at 60 °C for 120 min (R-W), and after resaturation in 124-TCB (R-W-S).

volume, and the atomic surface concentration (by XPS) were measured for CAG after cycles C1 and C3 in R3 (Table 2) after regeneration (180 min), washing, and resaturation steps. Figure S7 collects the nitrogen adsorption–desorption isotherms obtained at –196 °C for these samples. The BET surface area and pore volume were calculated from these isotherms, and the results are summarized in Table 4.

The BET surface area and pore volume of GAC dropped from 871 m²·g⁻¹ (see Table 3) to 611 m²·g⁻¹ when the washed GAC (GAC-F) was saturated with 124-TCB. However, this value should be analyzed considering that GAC-S includes the adsorbed mass of 124-TCB (about 35% in GAC-F). After C1, the BET surface area of C1-R was 477 m²·g⁻¹ and it was kept constant after the washing step (C1-R-W). Resaturation in 124-TCB (C1-R-W-S) causes a depletion of 50% in the BET surface area. The same trend was also found in C3. However, the differences in BET surface areas from C3-R-W and C3-R-W-S were lower than the one noticed in C1. The BET surface area after C3-R was almost the same as after C1-R, suggesting that the loss of surface area caused by incorporating the contaminant was recovered with the regeneration cycles. The corresponding nitrogen adsorption–desorption isotherms are shown in Figure S7.

The comparison between the BET surface area value in samples GAC-F-B8-C3b (see Table 3) and the corresponding value of R3-C3-R-W-S (shown in Table 4) suggested that the presence of 124-TCB on GAC protected the carbon surface against the PS attack. The same conclusion can be inferred from the data of PS consumption gathered in Figures 2 and 3b. The consumption of PS was also decreased when the 124-TCB was adsorbed on the GAC surface. Both circumstances suggest that PS preferably reacts with 124-TCB, keeping the apparent surface area practically constant after three regenerative/adsorption cycles.

This conclusion is also supported by the analysis of the atomic surface concentration and the presence of carbon–oxygen surface groups (given in Table 4) after C1 and C3 in run 3 (Table 2). First, a decrease in the carbon concentration upon oxidative attack by PS can be observed. However, this decrease is less drastic in GAC saturated in 124-TCB (Table 4) than that noticed for the unsaturated GAC (Table 3). Regarding the presence of oxygen surface groups, an increase in oxygen was observed due to the increase of acidic surface groups (carboxylic groups) on the carbon surface. The

concentration of sulfur is maximum after regeneration, and this sulfur concentration is reduced after washing with water, indicating that this step is necessary to release the GAC surface.

The oxygen groups on the GAC surface increase with the regeneration (Table 4). However, the formation of carbon–oxygen surface groups, mainly as acid groups, is lower (approximately around 50%) than that noticed after the reaction of GAC-F with the oxidant (Table 3). As previously mentioned, the oxidative attack on the GAC surface in the presence of 124-TCB seems to be more selective to the pollutant, instead of leading to preferential oxidation of the carbon surface. On the other hand, some Cl incorporation into the carbon surface was also observed, even after the regeneration treatment. The analyses of the Cl 2p spectra show a unique band at 200.2 eV associated with the presence of organic Cl.

4. CONCLUSIONS

In the present work, the adsorption capacity recovery (RC) of a GAC, previously saturated with 124-TCB has been successfully carried out using PS activated with temperature. Three successive cycles of regeneration and saturation of GAC were accomplished, finding stable RC values and maintaining similar physicochemical properties of the adsorbent throughout the different reaction cycles. Between cycles, intermediate washes were implemented to remove the sulfur residues deposited during the regeneration operation. The application of these cycles ensured the promotion of the circular economy of GAC and the elimination of a highly toxic pollutant. In this sense, increasing the lifetime of the activated carbon in consecutive adsorption/oxidation cycles reduces the amount of carbon waste and the necessity of treating high amounts of activated carbons by conventional treatments.

In addition, the reaction between PS and GAC in the absence of 124-TCB adsorbed was investigated. This reaction generated mainly acidic groups on the carbon surface and reduced the apparent surface area of the carbon. The oxidation of the carbon competed with the abatement of 124-TCB. However, it was concluded that the oxidation of 124-TCB preferentially took place under the experimental conditions tested here. For saturated carbon, the sulfate radical attack was aimed at removing the 124-TCB present, avoiding the significant oxidation of the carbon surface of the adsorbent.

This work confirmed that the use of PS activated with temperature can be used to abate toxic chlorinated compounds adsorbed in GAC since the presence of the contaminant in the carbon surface favors the reaction rate and the reusability of the carbon. Further studies should be carried out to optimize the reaction conditions and to improve the efficiency of the oxidation reactions.

■ ASSOCIATED CONTENT

SI Supporting Information

The Supporting Information is available free of charge at <https://pubs.acs.org/doi/10.1021/acs.iecr.2c00440>.

Scheme of the experimental setup in the saturation and saturation/regeneration steps; characterization of the fresh and washed carbon and their adsorption isotherms; PS conversion after successive cycles without and with washing of the GAC recovered between cycles using C_{PSO} : 166 mM; adsorption isotherms for GAC obtained after C1 and C3 of experiment B1 at 60 °C with 5 g·L⁻¹ and 168 mM of initial PS; and adsorption isotherms for GAC-F, GAC-S, GAC-R3-C 1b (after regeneration, washing, and resaturation), and GAC-R3-C3b (after regeneration, washing, and resaturation) (PDF)

■ AUTHOR INFORMATION

Corresponding Author

David Lorenzo – Departamento de Ingeniería Química y de Materiales, Universidad Complutense de Madrid, Madrid 28040, Spain; orcid.org/0000-0002-4235-9308; Email: dlorenzo@quim.ucm.es

Authors

Andrés Sánchez-Yepes – Departamento de Ingeniería Química y de Materiales, Universidad Complutense de Madrid, Madrid 28040, Spain

Aurora Santos – Departamento de Ingeniería Química y de Materiales, Universidad Complutense de Madrid, Madrid 28040, Spain

Juana M. Rosas – Departamento de Ingeniería Química, Universidad de Málaga, Andalucía Tech, 29010 Málaga, Spain; orcid.org/0000-0001-9158-3413

José Rodríguez-Mirasol – Departamento de Ingeniería Química, Universidad de Málaga, Andalucía Tech, 29010 Málaga, Spain; orcid.org/0000-0003-3122-1220

Tomás Cordero – Departamento de Ingeniería Química, Universidad de Málaga, Andalucía Tech, 29010 Málaga, Spain; orcid.org/0000-0002-3557-881X

Complete contact information is available at: <https://pubs.acs.org/10.1021/acs.iecr.2c00440>

Notes

The authors declare no competing financial interest.

■ ACKNOWLEDGMENTS

This work was supported by the EU LIFE Program (LIFE17 ENV/ES/000260), the Regional Government of Madrid, through the CARESOIL project (S2018/EMT-4317), and the Spanish Ministry of Economy, Industry, and Competitiveness, through project PID2019-105934RB-I00. A.ÉS.Á-Y. would also like to thank the State Programme for the Promotion of Talent and its Employability in R&D&I of the Ministry of Science and Innovation for the support for predoctoral

contracts under FPI grant PRE2020-093195. This research was also supported by the Spanish Ministry of Science, Innovation and Universities and Junta de Andalucía through RTI2018-097555-B-I00 and UMA18-FEDERJA-110 projects, respectively.

■ REFERENCES

- (1) Li, J.-h.; Sun, X.-f.; Yao, Z.-t.; Zhao, X.-y. Remediation of 1,2,3-trichlorobenzene contaminated soil using a combined thermal desorption-molten salt oxidation reactor system. *Chemosphere* **2014**, *97*, 125–129.
- (2) Schroll, R.; Brahusi, F.; Dörfler, U.; Kühn, S.; Fekete, J.; Munch, J. C. Biomineralisation of 1,2,4-trichlorobenzene in soils by an adapted microbial population. *Environ. Pollut.* **2004**, *127*, 395–401.
- (3) Zhang, T.; Li, X.; Min, X.; Fang, T.; Zhang, Z.; Yang, L.; Liu, P. Acute toxicity of chlorobenzenes in *Tetrahymena*: Estimated by microcalorimetry and mechanism. *Environ. Toxicol. Pharmacol.* **2012**, *33*, 377–385.
- (4) Boutonnet, J.-C.; Thompson, R. S.; De Rooij, C.; Garny, V.; Lecloux, A.; van Wijk, D. 1,4-dichlorobenzene marine risk assessment with special reference to the OSPARCOM region: North Sea. *Environ. Monit. Assess.* **2004**, *97*, 103–117.
- (5) van Wijk, D.; Thompson, R. S.; De Rooij, C.; Garny, V.; Lecloux, A.; Kanne, R. 1,2-dichlorobenzene marine risk assessment with special reference to the OSPARCOM region: North Sea. *Environ. Monit. Assess.* **2004**, *97*, 87–102.
- (6) van Wijk, D.; Cohet, E.; Gard, A.; Caspers, N.; van Ginkel, C.; Thompson, R.; de Rooij, C.; Garny, V.; Lecloux, A. 1,2,4-trichlorobenzene marine risk assessment with special emphasis on the Oparcom region North Sea. *Chemosphere* **2006**, *62*, 1294–1310.
- (7) Huang, B.; Lei, C.; Wei, C.; Zeng, G. Chlorinated volatile organic compounds (Cl-VOCs) in environment — sources, potential human health impacts, and current remediation technologies. *Environ. Int.* **2014**, *71*, 118–138.
- (8) Vo, D.; Ramamurthy, A. S.; Qu, J.; Zhao, X. P. Containment wells to form hydraulic barriers along site boundaries. *J. Hazard. Mater.* **2008**, *160*, 240–243.
- (9) Marsh, H.; Rodríguez-Reinoso, F. CHAPTER 8 - Applicability of Activated Carbon. In *Activated Carbon*; Marsh, H., Rodríguez-Reinoso, F., Eds.; Elsevier Science Ltd: Oxford, U.K., 2006; pp 383–453.
- (10) Ramke, H.-G. 8.1 - Leachate Collection Systems. In *Solid Waste Landfilling*; Cossu, R., Stegmann, R., Eds.; Elsevier, 2018; pp 345–371.
- (11) Sotelo, J.; Ovejero, G.; Delgado, J. A.; Martínez, I. Adsorption of lindane from water onto GAC: effect of carbon loading on kinetic behavior. *Chem. Eng. J.* **2002**, *87*, 111–120.
- (12) Zhang, J.; Zhang, N.; Tack, F. M. G.; Sato, S.; Alessi, D. S.; Oleszczuk, P.; Wang, H.; Wang, X.; Wang, S. Modification of ordered mesoporous carbon for removal of environmental contaminants from aqueous phase: A review. *J. Hazard. Mater.* **2021**, *418*, 126266.
- (13) Obón, J. M.; Angosto, J. M.; González-Soto, F.; Asca, A.; Fernández-López, J. A. Prototyping a spinning adsorber submerged filter for continuous removal of wastewater contaminants. *J. Water Proc. Eng.* **2022**, *45*, 102515.
- (14) Abbaszadeh, S.; Wan Alwi, S. R.; Webb, C.; Ghasemi, N.; Muhamad, I. I. Treatment of lead-contaminated water using activated carbon adsorbent from locally available papaya peel biowaste. *J. Cleaner Prod.* **2016**, *118*, 210–222.
- (15) Marsh, H.; Rodríguez-Reinoso, F. CHAPTER 4 - Characterization of Activated Carbon. In *Activated Carbon*; Marsh, H., Rodríguez-Reinoso, F., Eds.; Elsevier Science Ltd: Oxford, U.K., 2006; pp 143–242.
- (16) Marsh, H.; Rodríguez-Reinoso, F. CHAPTER 2 - Activated Carbon (Origins). In *Activated Carbon*; Marsh, H., Rodríguez-Reinoso, F., Eds.; Elsevier Science Ltd: Oxford, U.K., 2006; pp 13–86.

(17) Beaumont, J. R.; Pedersen, L. M.; Whitaker, B. D. 5 - Production and operations management. In *Managing the Environment*; Beaumont, J. R., Pedersen, L. M., Whitaker, B. D., Eds.; Butterworth-Heinemann: Oxford, U.K., 1993; pp 141–178.

(18) Chen, W.-S.; Lin, C.-W.; Chang, F.-C.; Lee, W.-J.; Wu, J.-L. Utilization of spent activated carbon to enhance the combustion efficiency of organic sludge derived fuel. *Bioresour. Technol.* **2012**, *113*, 73–77.

(19) Álvarez, P. M.; Beltrán, F. J.; Gómez-Serrano, V.; Jaramillo, J.; Rodríguez, E. M. Comparison between thermal and ozone regenerations of spent activated carbon exhausted with phenol. *Water Res.* **2004**, *38*, 2155–2165.

(20) Okwadha, G. D. O.; Li, J.; Ramme, B.; Kollakowsky, D.; Michaud, D. Thermal removal of mercury in spent powdered activated carbon from Toxecon process. *J. Environ. Eng.* **2009**, *135*, 1032–1040.

(21) Huang, X.; An, D.; Song, J.; Gao, W.; Shen, Y. Persulfate/electrochemical/FeCl₂ system for the degradation of phenol adsorbed on granular activated carbon and adsorbent regeneration. *J. Cleaner Prod.* **2017**, *165*, 637–644.

(22) Parsons, S. *Advanced Oxidation Processes for Water and Wastewater Treatment*; IWA Publishing, 2005.

(23) Acevedo-García, V.; Rosales, E.; Puga, A.; Pazos, M.; Sanromán, M. A. Synthesis and use of efficient adsorbents under the principles of circular economy: Waste valorisation and electro-advanced oxidation process regeneration. *Sep. Purif. Technol.* **2020**, *242*, 116796.

(24) Singh, S.; Kumar, V.; Anil, A. G.; Kapoor, D.; Khasnabis, S.; Shekar, S.; Pavithra, N.; Samuel, J.; Subramanian, S.; Singh, J.; Ramamurthy, P. C. Adsorption and detoxification of pharmaceutical compounds from wastewater using nanomaterials: A review on mechanism, kinetics, valorization and circular economy. *J. Environ. Manage.* **2021**, *300*, 113569.

(25) Santos, A.; Fernandez, J.; Rodriguez, S.; Dominguez, C. M.; Lominchar, M. A.; Lorenzo, D.; Romero, A. Abatement of chlorinated compounds in groundwater contaminated by HCH wastes using ISCO with alkali activated persulfate. *Sci. Total Environ.* **2018**, *615*, 1070–1077.

(26) Dominguez, C. M.; Romero, A.; Lorenzo, D.; Santos, A. Thermally activated persulfate for the chemical oxidation of chlorinated organic compounds in groundwater. *J. Environ. Manage.* **2020**, *261*, 110240.

(27) Jatta, S.; Huang, S.; Liang, C. A column study of persulfate chemical oxidative regeneration of toluene gas saturated activated carbon. *Chem. Eng. J.* **2019**, *375*, 122034.

(28) Peng, J.; Wu, E.; Wang, N.; Quan, X.; Sun, M.; Hu, Q. Removal of sulfonamide antibiotics from water by adsorption and persulfate oxidation process. *J. Mol. Liq.* **2019**, *274*, 632–638.

(29) Huling, S. G.; Ko, S.; Park, S.; Kan, E. Persulfate oxidation of MTBE- and chloroform-spent granular activated carbon. *J. Hazard. Mater.* **2011**, *192*, 1484–1490.

(30) Lorenzo, D.; Santos, A.; Sánchez-Yepes, A.; Conte, L. Ó.; Domínguez, C. M. Abatement of 1,2,4-Trichlorobenzene by Wet Peroxide Oxidation Catalysed by Goethite and Enhanced by Visible LED Light at Neutral pH. *Catalysts* **2021**, *11*, 139.

(31) Lorenzo, D.; Dominguez, C. M.; Romero, A.; Santos, A. Wet Peroxide Oxidation of Chlorobenzenes Catalyzed by Goethite and Promoted by Hydroxylamine. *Catalysts* **2019**, *9*, 553.

(32) Thommes, M.; Kaneko, K.; Neimark, A. V.; Olivier, J. P.; Rodriguez-Reinoso, F.; Rouquerol, J.; Sing, K. S. W. Physisorption of gases, with special reference to the evaluation of surface area and pore size distribution (IUPAC Technical Report). *Pure Appl. Chem.* **2015**, *87*, 1051–1069.

(33) Hutson, A.; Ko, S.; Huling, S. G. Persulfate oxidation regeneration of granular activated carbon: Reversible impacts on sorption behavior. *Chemosphere* **2012**, *89*, 1218–1223.

(34) Zhang, W.; Zhou, S.; Sun, J.; Meng, X.; Luo, J.; Zhou, D.; Crittenden, J. Impact of Chloride Ions on UV/H₂O₂ and UV/

Persulfate Advanced Oxidation Processes. *Environ. Sci. Technol.* **2018**, *52*, 7380–7389.

Recommended by ACS

Comparison and Characterization of Nitrogen/Sulfur-Doped Activated Carbon for Activating Peroxydisulfate to Degrade Acid Orange 7: An Experimental and Theoretical Study

Yupan Huo, Qiang Liu, *et al.*

JULY 19, 2023

INDUSTRIAL & ENGINEERING CHEMISTRY RESEARCH

READ 

Insight into the Adsorption of Nutrients from Water by Pyrogenic Carbonaceous Adsorbents Using a Bootstrap Method and Machine Learning

Xuan Cuong Nguyen, Quang Viet Ly, *et al.*

OCTOBER 31, 2022

ACS ES&T WATER

READ 

Passive Ozone Injection through Gas-Permeable Membranes for Advanced *In Situ* Groundwater Remediation

Anwar Dawas, Ines Zucker, *et al.*

FEBRUARY 16, 2023

ACS ES&T ENGINEERING

READ 

Highly Efficient Multisubstrate Agricultural Waste-Derived Activated Carbon for Enhanced CO₂ Capture

Mardikios Maja Bade, Minaleshewa Atlabachew, *et al.*

MAY 25, 2022

ACS OMEGA

READ 

Get More Suggestions >

Treatment of a Complex Emulsion of a Surfactant with Chlorinated Organic Compounds from Lindane Wastes under Alkaline Conditions by Air Stripping

Patricia Sáez, Raúl García-Cervilla, Aurora Santos, Arturo Romero, and David Lorenzo*



Cite This: *Ind. Eng. Chem. Res.* 2023, 62, 3282–3293



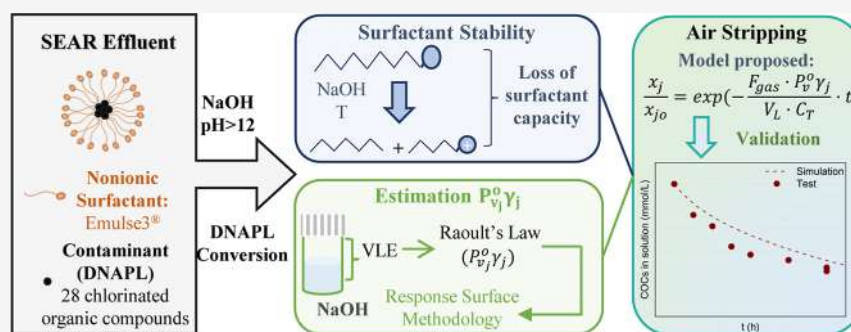
Read Online

ACCESS |

Metrics & More

Article Recommendations

Supporting Information



ABSTRACT: Surfactant-enhanced aquifer remediation is commonly applied in polluted sites with dense non-aqueous phase liquids (DNAPLs). This technique transfers the contamination from subsoil to an extracted emulsion, which requires further treatment. This work investigated the treatment of a complex emulsion composed of a nonionic surfactant and real DNAPL formed of chlorinated organic compounds (COCs) and generated as a lindane production waste by air stripping under alkaline conditions. The influence of the surfactant (1.5–15 g·L⁻¹), COC concentrations (2.3–46.9 mmol·L⁻¹), and temperature (30–60 °C) on the COC volatilization was studied and modeled in terms of an apparent constant of Henry at pH > 12. In addition, the surfactant stability was studied as a function of temperature (20–60 °C) and surfactant (2–10 g·L⁻¹), COC (0–70.3 mmol·L⁻¹), and NaOH (0–4 g·L⁻¹) concentrations. A kinetic model was successfully proposed to explain the loss of surfactant capacity (SCL). The results showed that alkali and temperature caused the SCL by hydrolysis of the surfactant molecule. The increasing surfactant concentration decreased the COC volatility, whereas the temperature improved the COC volatilization. Finally, the volatilization of COCs in alkaline emulsions by air stripping (3 L·h⁻¹) was performed to evaluate the treatment of an emulsion composed of the COCs (17.6 mmol·kg⁻¹) and surfactant (3.5 and 7 g·L⁻¹). The air stripping was successfully applied to remove COCs (>90%), reaching an SCL of 80% at 60 °C after 8 h. Volatilization can remove COCs from emulsions and break them, enhancing their further disposal.

1. INTRODUCTION

Soil and groundwater contamination by organic compounds has become a severe environmental issue.¹ The accidental release or intentional dumping of hydrophobic organic liquid phases into the environment is a widespread problem resulting in a separate liquid phase, termed non-aqueous phase liquids (or NAPLs), that persists in the subsurface.² Prolonged contact between soil and water with these NAPLs can impact the organisms of the food chain, harming human health and ecosystems.³ In the last decades, this contamination has been associated with pesticides, veterinary drugs,⁴ and heavy metals⁵ released as industrial wastes. These compounds can affect water bodies, producing significant problems like antibiotic resistance, sex organ imposition, and many others.⁶

An effective treatment to remediate polluted sites with NAPLs is the application of surfactant enhancement aquifer remediation (SEAR).⁷ This technique injects an aqueous

solution containing a surfactant into the contaminated area. Then, a polluted stream composed of a mixture of organic compounds⁸ and the surfactant injected is extracted. This stream can be a mixture of Tween-80 and total petroleum hydrocarbons (TPHs)⁹ or tetrachloroethene-nonaqueous¹⁰ and chlorinated organic compounds (COCs) with E-Mulse 3 (E3).¹¹

The surfactants enhance the removal of pollutants through solubilization and mobilization. The amphoteric properties of the surfactants that reduce interface tension facilitate the

Received: October 14, 2022

Revised: January 26, 2023

Accepted: January 27, 2023

Published: February 7, 2023



transport of hydrophobic pollutants to the aqueous phase.¹² The SEAR technique presents significant benefits compared to other technologies, such as pump and treat,¹¹ since it increases the rate of NAPL removal. However, the SEAR process moves the organic contamination into the aqueous phase but does not eliminate the contaminant, resulting in secondary contamination.⁷ A low soil permeability limits the applicability of the SEAR technology.¹¹ The adsorption of the surfactants and a possible dispersion of contaminants from the control zone affect the efficiency and safety of the process.¹³

Once these disadvantages are overcome, the SEAR process can be applied successfully.¹³ It was reported that the use of a surfactant improves the elimination of TPHs about 75 times the amount removed with water alone¹⁴ or increased by 2 orders of magnitude the elimination of tetrachloroethene (PCE) using an aqueous solution of the 6% w Tween-80 surfactant.¹⁰ In addition, using E-Mulse 3 (E3) allowed the solubilization of COCs, removing about 3.5% of COCs in the soil using only a pore volume of the aqueous surfactant solution (effective porosity of soil is less than 0.12) after 15 h of injection treatment. In these applications, the emulsion extracted from the subsoil contained a complex mixture of organic compounds, and the surfactant used and this emulsion must be managed appropriately.

Several technologies have been proposed for this scope. Some papers consider the selective oxidation of organic compounds in the mixture with the recovery of the surfactant capacity. Hanafiah et al. applied ultrafiltration and permanganate to recover the surfactant used in the remediation of a site polluted with polycyclic aromatic hydrocarbons (PAHs).¹⁵ Huang et al. used ferric ions in the photo-treatment of Brij35 washing waste containing 2,2',4,4'-tetrabromodiphenyl ether.¹⁶ Li et al. used electrochemically reversible foam-enhanced flushing for PAH-contaminated soil with FC12 as the surfactant.¹⁷ García-Cervilla et al. studied the compatibility of E3 and sodium dodecyl sulfate (SDS) with persulfate activated by alkali in the reduction of COCs.¹⁸ In these treatments, the COCs are not mineralized, and there is a loss of surfactant stability associated with the unproductive consumption of the oxidant by the surfactant.¹⁸

Selective adsorption of organic pollutants on activated carbon (AC)¹⁹ and selective retention by membranes²⁰ have also been investigated in the remediation of SEAR streams.

The air stripping of COCs in the emulsion has been reported but scarcely studied in the literature. This technique transfers the volatile compound from an aqueous solution to an air stream, and it could be effective when the organic compounds are volatile or semivolatile.²¹ When the polluted emulsion is directly sent for adsorption on AC, the efficiency of the process remarkably decreases due to the quick saturation of AC with the surfactant.¹⁹ On the contrary, the transfer of the organic pollutants from the emulsion to an air stream, free of the surfactant, remarkably improves the efficiency and economy of the further pollutant adsorption on AC.

The volatility of organic compounds from the emulsion has been studied using an apparent Henry's law constant to determine the vapor–liquid partitioning of chlorinated solvents in surfactant solutions.²² This apparent constant considers a three-phase system where the volatile organic compounds are partitioned into vapor, extramolecular (aqueous), and micellar phases.²³ Some authors have studied the partition of pure compounds between vapor and emulsion phases. Shimtory et al.²⁴ measured and estimated apparent

Henry's constants of pure compounds [TCE, PCE, *cis*-dichloroethylene (DCE), and *trans*-dichloroethylene] with different surfactants (SDS, Triton X-100, and bromuro de cetiltrimetilamónio). They found a dependence between the concentration and surfactant type.²⁴ Similar conclusions were reported by Zhang et al.²⁵ They tested three pure compounds (TCE, PCE, and DCE) separately using SDS, sodium dodecyl benzene sulfonate, Tween-80, and Triton X-100.²⁵

In the same way, Sprunger et al. studied the partition between extramolecular and micellar phases and the volatilization of several pure compounds using SDS as a surfactant.²⁶ Also, recently, Chao et al. used 1,2-dichlorobenzene (1,2-DCB), 1,3,5-trichlorobenzene (1,3,5-TCB), and 1,2,3,4-tetrachlorobenzene (1,2,3,4-TetraCB) with different Triton surfactants and reported a relationship between the volatilization and solubility of this compound and surfactant type.²⁷ In these studies, pure compounds were used as model compounds to study the COC volatilization. However, there is scarce information on using a complex mixture of COCs as wastes of pesticides such as lindane. In addition, E3 has not been previously studied as a biodegradable surfactant.

This work aims to study and model air stripping applications to volatilize COCs in an aqueous emulsion with nonionic and biodegradable surfactants. The emulsion used is a real effluent generated after a SEAR treatment of a polluted site in Sardas landfill (Sabiñánigo, Spain). In this place, the liquid wastes of lindane production, containing 28 COCs, were dumped in unlined landfills, migrating vertically through the aquifer as dense NAPLs (DNAPLs) and polluting the nearby area.²⁸ In previous studies, it was reported that alkali addition could be considered to enhance the volatility of the more chlorinated compounds since it promotes their dehydrochlorination to more volatile compounds in the aqueous and soil phases²⁹ and emulsion with E3, Tween-80, and SDS.³⁰ This effect can be managed by air stripping the contaminated emulsions obtained after SEAR treatment of sites polluted with DNAPL waste from lindane production. However, the alkali, surfactant concentrations, and temperature could affect the surfactant stability and the volatility of the COCs in the emulsion. These aspects have not been previously studied for a complex organic phase in the literature but are required for a proper air-stripping treatment design. The latter required the study of the volatility of each COC in the alkaline emulsion and the surfactant stability at different alkali concentrations and temperatures. Predicted and experimental values during air stripping runs will also be compared to validate the model proposed and the parameters obtained.

2. MATERIALS AND METHODS

2.1. Chemicals and DNAPLs. The quantification of COCs was performed using calibration curves prepared from commercial compounds (Sigma-Aldrich, analytical grade): chlorobenzene (CB), 1,2-DCB, 1,3-dichlorobenzene (1,3-DCB), 1,4-dichlorobenzene (1,4-DCB), 1,2,3-trichlorobenzene (1,2,3-TCB), 1,2,3,4-TetraCB, 1,2,3,5-tetrachlorobenzene (1,2,3,5-TetraCB), 1,2,3,4-tetrachlorobenzene (1,2,3,4-TetraCB), and hexachlorocyclohexane isomers (α , β , γ , δ , and ϵ -HCH). Additionally, limonene [(R)-(+)-limonene, Sigma-Aldrich] (cosolvent of the surfactant) was also calibrated. Bicyclohexyl (C₁₂H₂₂, Sigma-Aldrich) and tetrachloroethane (C₂H₂Cl₄, Sigma-Aldrich) were used as internal standards (ISTD) for quantification by gas chromatography (GC).

Two DNAPLs were used in this work. On the one hand, a real DNAPL (DNAPL-R) was obtained from a contaminated site in Sabiñánigo (Spain). The DNAPL-R samples were provided by the company Emgrisa and the Aragon Government. The composition of DNAPL-R used is summarized in Table S1 of the Supporting Information. DNAPL-R is composed of 28 COCs: CB, the isomers of dichlorobenzene (lumped as DCBs), trichlorobenzene (lumped as TCBs), tetrachlorobenzene (lumped as TetraCBs), pentachlorocyclohexenes (lumped as PentaCXs), hexachlorocyclohexane (lumped as HCHs), hexachlorocyclohexene (lumped as HexaCXs), and heptachlorocyclohexanes (lumped as HeptaCHs).

NaOH was used to promote the alkaline dehydrochlorination of HCHs and PentaCXs to TCBs and HeptaCHs and HexaCXs and HeptaCHs to TetraCBs, which reduced the toxicity of the effluent to be treated and increased the volatility of the COCs in the aqueous phase.³⁰ The composition of DNAPL-R after the alkalization treatment (i.e., xi pH > 12) is summarized in Table S1.

Additionally, a synthetic DNAPL (DNAPL-S) was used to simulate the COC composition of the real DNAPL-R due to the limited amount of DNAPL-R available after alkaline treatment. Commercial compounds (CB, 1,2-DCB, 1,2,4-TCB, 1,2,3-TCB, and a mixture of 1,2,4,5-tetrachlorobenzene, 1,2,3,5-TetraCB, and 1,2,3,4-TetraCB) were mixed to produce DNAPL-S. The molar fractions of these compounds in DNAPL-S are shown in Table S2.

The surfactant used to carry out the experiments was E-Mulse 3 (E3) (EthicalChem), which is a nonionic surfactant with a critical micelle concentration measure of 80 mg·L⁻¹. E3 was selected because it is a biodegradable and non-toxic surfactant¹¹ and has been successfully applied in the solubilization of COCs from DNAPL-R to the aqueous phase.³¹

The air employed to perform the experiments was supplied by Carburos Metálicos, with a quality of 99.999% (Alphagaz 1 AR, Air Liquid). The aqueous solutions were prepared with high-purity water from a Millipore Direct-Q system with resistivity >18 mΩ·cm at 25 °C.

2.2. Experimental Procedure. The experimental procedure was divided into three experiment sets. In the first one (B1), the surfactant stability was studied at different temperatures and NaOH doses, and a kinetics for surfactant capacity loss (SCL) was obtained. The second procedure studied the volatilization of each chlorinated compound in the complex mixture of the surfactant and DNAPL-R (B2). In this set of experiments, different temperatures and surfactant and COC concentrations were established to study the amount of the volatile compound transferred to the vapor phase. Finally, volatilization of COCs in the emulsion (set B3) was carried out by passing an airstream through the aqueous emulsion at several surfactant concentrations and temperatures. During these experiments, the surfactant loss by the reaction was not renewed, and the surfactant load was added at the initial time.

2.2.1. Surfactant Stability (B1). Surfactant stability experiments were conducted in the batch mode using sealed GC 20 mL glass vials without headspace closed with Teflon caps in the absence and presence of COCs. In the last case, a certain amount of DNAPL-S was added to the aqueous phase with the surfactant (2–10 g·L⁻¹) to obtain a stable emulsion. The moles of solubilized organic compounds per mole of the surfactant in micellar solution was the molar solubilization

ratio (MSR) for DNAPL-R or DNAPL-S in E3, as determined elsewhere³¹ and resulting in 4.33 mmol COCs·g_{surf}⁻¹. The emulsions were agitated for 4 h and left to settle for 24 h without agitation; after this time, the concentration of COCs in the emulsion was stable over time, and the amount of COCs was measured. The emulsions prepared following this experimental procedure, in which the ratio of the mole DNAPL and surfactant corresponds with the MSR, will be identified as saturated emulsions in COCs.

The vials were prepared with 19 mL of surfactant solution (containing or not containing DNAPL-S). Then, the vials were heated in a thermostatic bath to obtain the desired temperatures (25–60 °C). Once the temperature was reached, 1 mL of NaOH was added (zero time) into the vials from a concentrated stored aqueous solution to obtain the required NaOH concentration in the vial (2 or 4 g·L⁻¹). It is important to point out that 2 g·L⁻¹ is the minimum quantity of alkali required to get a total dehydrochlorination.²⁹ A pH of 12 was obtained with this NaOH concentration. A magnetic stirrer continuously agitated the alkalinized emulsion at the desired temperature. The experimental conditions are summarized in Table 1. The MSR and molar concentration appearing in Table

Table 1. Experimental Conditions for the Three Experiment Sets

Exp	T (°C)	C _{SO} (g·L ⁻¹)	C _{NaOH} (g·L ⁻¹)	C _{DNAPL} (mmol·L ⁻¹)
B1: Surfactant Stability				
E1	20	10	2	0
E2	20	5	2	0
E3	20	10	4	0
E4	20	5	4	0
E5	20	2	4	0
E6	40	5	4	0
E7	60	10	2	0
E8	60	10	4	0
E9	60	5	4	0
E10	20	10	2	70.3
E11	20	2	2	14.6
E12	40	5	4	35.2
E13	60	10	2	70.3
E14	60	10	4	70.3
E15	60	5	4	35.2
E16	20	10	0	0
E17	60	10	0	0
B2: Estimation of the Apparent Henry's Constant				
P1	30, 40, 60	1.5	5	2.3, 4.7
P2	30,40, 60	3.5	5	5.9, 14.6
P3	30, 40, 60	7.0	5	5.9, 17.6, 29.3
P4	30, 40, 60	15.0	5	11.7, 23.4, 46.9
B3: Volatilization Tests				
V1	40	3.5	4	17.6
V2	60	7.0	4	17.6

1 have been calculated using the averaged molecular weight obtained from the known composition of both DNAPLs used (DNAPL-S and DNAPL-R). In the case of DNAPL-R, its characterization was carried out in previous work.²⁸ The average molecular weight of DNAPL-S is 164 g·mol⁻¹ whereas for DNAPL-R is 196 g·mol⁻¹.

The remaining equivalent surfactant concentration (ESC) was analyzed by sacrificing a vial at different reaction times, including 0. In the experiments carried out with saturated

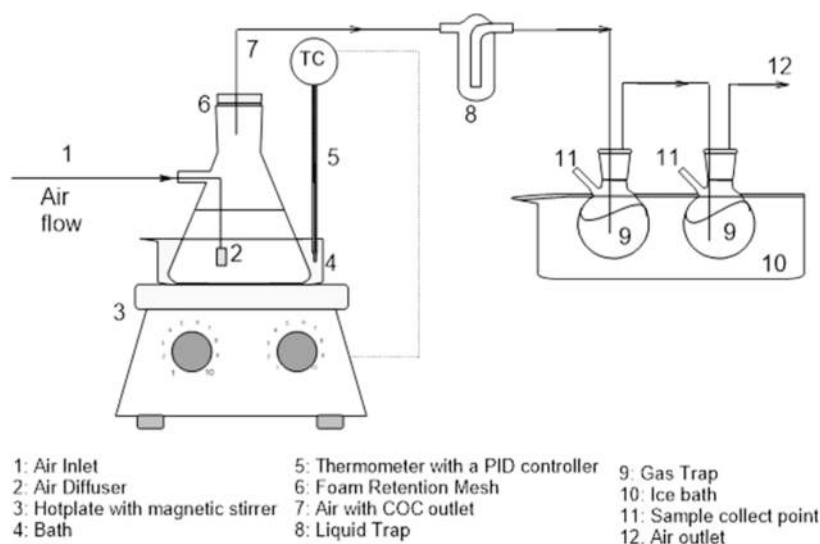


Figure 1. Scheme of the installation used for volatilization tests.

emulsion of DNAPL-S, the remaining ESC at each time was calculated from the remaining COCs in solution, taking into account the MSR value, as shown in eq 1. In the absence of DNAPL, the remaining ESC at each time was calculated by dissolving 1,3 DCB and measuring the solubilized concentration of this compound in the emulsion phase ($MSR = 4.33 \text{ mmol} \cdot \text{g}_{\text{surf}}^{-1}$). The concentration of the surfactant calculated using this method is an ESC, which considers the products and subproducts capable of dissolving COCs lumped as the surfactant. The experiments were replicated, finding a discrepancy between experimental results lower than 5%. The average values were used as the experimental results.

$$C_s = \frac{C_{\text{COCs}}}{4.33} \quad (1)$$

where C_s is the ESC ($\text{g}_{\text{surf}} \cdot \text{L}^{-1}$) and C_{COCs} is the concentration of the sum of COCs ($\text{mmol}_{\text{COCs}} \cdot \text{L}^{-1}$) and 4.33 is the MSR of E3 with the DNAPL-R and 13-DCB in $\text{mmol}_{\text{COCs}} \cdot \text{g}_{\text{surf}}^{-1}$.

2.2.2. Estimation of Apparent Henry's Constant (B2). This set of experiments was carried out to obtain the apparent value of Henry's constant of each COC (j) in the presence of the surfactant.

In 100 mL flasks, an amount of DNAPL-R (ranging from 0.04 to 0.8 g in order to get a concentration between 2.3 and 46.9 $\text{mmol} \cdot \text{L}^{-1}$) was added and filled up to 100 g with the corresponding aqueous phase containing the surfactant (E3 concentration ranging from 1.5 to 15 $\text{g} \cdot \text{L}^{-1}$). The amount of DNAPL-R added was always less than that required for saturation. After 2 h of agitation, the solution was settled, and DNAPL-R as an organic phase was not noticed. Following this, 10 mL of the emulsion was transferred to 20 mL GC glass vials, and NaOH was added to reach a concentration of 5 $\text{g} \cdot \text{L}^{-1}$ ($\text{pH} > 12$). Then, the vials were closed and agitated at different controlled temperatures (30–60 °C) for 1 h in the incubator of HeadSpace GC (HS-GC), Agilent GC Sampler 120. This time was enough to reach equilibrium between the liquid and vapor phases. The COCs in the vapor phase were analyzed by HeadSpace, following the methodology used elsewhere³² coupled with GC/ flame ionization detector (FID)/ electron capture detector (ECD). Table 1 summarizes the conditions of the experiments in set B2.

2.2.3. Volatilization Tests (B3). The volatilization of chlorinated compounds from the aqueous surfactant emulsion was carried out in the experimental setup schematized in Figure 1. An airstream was bubbled in the surfactant solution with solubilized DNAPL-S at $\text{pH} > 12$. The air was fed to the experimental system from pressurized air in a cylinder, and the flow rate was controlled using a mass flow controller (EL-FLOW Select Series Mass Flow Meters/Controllers for gases, Bronkhorst). A diffuser introduced the air into the emulsion to ensure a high interphase favoring the gas–liquid equilibrium achievement. The recipient containing the emulsion was immersed in a water bath placed on a hotplate (IKA C-MAG HS 7). The temperature was controlled using a PID controller (IKA ETS-D5) thermometer. After reaching liquid–gas equilibrium, the gas effluent saturated in COCs was passed through an iron mesh (100 μm) to prevent excessive foam formation and was bubbled in MeOH, which acted like a liquid trap. The MeOH traps were introduced into an ice bath to avoid volatile loss. Samples were taken periodically from the emulsion, the remaining COCs were analyzed, and the surfactant concentration dissolving 1,3-DCB. COC mass balance was checked for the final time by analyzing the COCs in the solvent traps.

The COC volatilization experiments were maintained for 8 h. Then, the airflow was stopped. Table 1 provides a summary of the conditions of the experiments carried out.

In Table 1, all the experiments carried out in the three experiment sets are summarized as follows: from E1 to E17 for surfactant stability (B1), from P1 to P4 for estimation of apparent Henry's constant (B2), and V1 and V2 for volatilization tests (B3).

2.3. Analytical Methods. The pH was analyzed in all experiments (B1, B2, and B3) to verify that pH was > 12 using a Metrohm 914 pH/conductometer.

The concentration of COCs in the emulsion in B1 and B3 experimental sets was analyzed by GC. Aqueous samples were diluted 1:10 in methanol and injected in a GC chromatograph (Agilent 8860) using an autosampler (Agilent GC Sampler 120) coupled with an FID and an ECD (GC-FID/ECD). The column was Agilent HPS-MSUI (19091S-433UI, 30 m \times 0.25 mm ID \times 0.25 μm). 2 μL of samples was injected using helium as carrier gas (flow rate of 2.9 $\text{mL} \cdot \text{min}^{-1}$). The GC injection

port temperature was set at 250 °C, and the GC oven worked at a programmed temperature gradient, starting at 80 °C and raising the temperature at a rate of 15 °C·min⁻¹ until 180 °C and then keeping it constant for 15 min. Additionally, a split ratio of 10:1 was employed in the analysis.²⁸

The COC concentrations in the vapor phase in B2 experiments were measured by HS-GC. GC 20 mL glass vials closed with Teflón caps were filled with 10 mL of alkaline DNAPL-R emulsions. The vials were agitated and heated at the desired temperature for 1 h. After this time, 2.5 mL of the vapor phase was injected into GC using a 10:1 split ratio. The column and the method conditions employed were the same as those described for analyzing dissolved COCs. More details of the method are shown in Table S3.

Surfactant byproducts due to alkaline hydrolysis with the temperature were studied using a Bruker AVANCE 300 MHz spectrometer. ¹H NMR spectra of the aqueous samples obtained at the final reaction times in runs E3 and E7 of experimental set B1 and 10 g·L⁻¹ of pure samples were recorded. The water content of the samples was previously removed using a rotary evaporator (Büchi Glass Oven B-585) coupled with a vacuum pump (Büchi Vacuum Pump V-300) at 20 °C and 100 mbar for 8 h. The solid residuum was diluted in dimethyl sulfoxide and used as an ISTD analyzed.

3. RESULTS AND DISCUSSION

3.1. Alkaline Hydrolysis of COCs in DNAPL-R. The addition of alkali could be considered a first step to enhancing the volatility of the more highly chlorinated compounds. It was experimentally proved that alkaline pH (>12) promotes the reaction of HCH and PentaCXs to TCBs and HeptaCHs and HexaCXs to TetraCBs in the absence and presence of the surfactant.^{29,30} TCB and TetraCB compounds presented lower risks and lower boiling points than the parent COCs. García-Cervilla et al.³¹ studied the transformation of DNAPL-R at pH 12 in the presence of the surfactant, observing distributing changes since PentaCX, HexaCX, HCH, and HeptaCH isomers were not detected in the aqueous emulsion under alkaline conditions, while the TCB and TetraCB molar percentage was increased under these conditions. Additionally, it was noted that a similar molar total concentration of COCs in solution is obtained independently of the pH employed. The molar distribution of COCs in an emulsion of DNAPL-R at pH 7 and pH 12 is also shown in Table S1.

3.2. Surfactant Stability. The influence of the initial surfactant concentration, NaOH concentration, temperature, and presence of COCs on surfactant stability was studied. The experiments are summarized in Table 1.

3.2.1. Effect of the NaOH Concentration (C_{NaOH}). The influence of the NaOH concentration was evaluated by varying the concentration between 2 and 4 g·L⁻¹ for two different initial surfactant concentrations (5 and 10) g·L⁻¹ and two temperatures (20 and 60 °C). Equation 2 calculates the fractional remaining surfactant capacity with time expressed as SCL.

$$\text{SCL} = 1 - \frac{C_{\text{ESC}}}{C_{\text{So}}} \quad (2)$$

The SCL profiles with time are shown in Figure 2. As can be seen, in the absence of NaOH in the reaction medium, negligible losses of the surfactant capacity are found under the operation conditions studied. On the contrary, a continuous

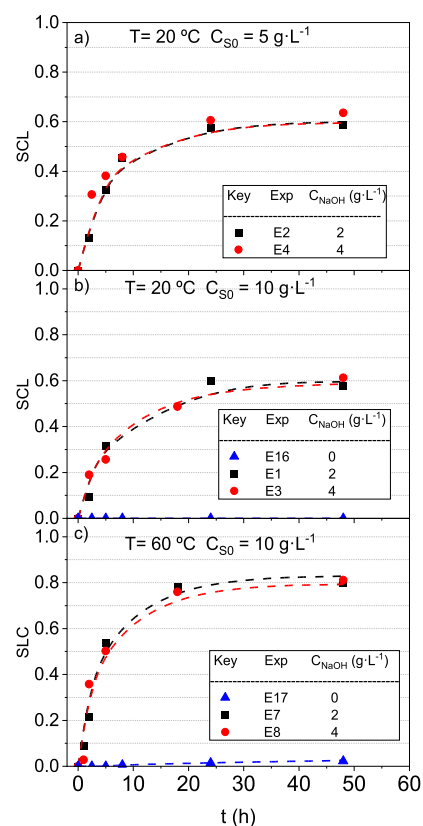


Figure 2. SCL profiles with the time for 2 and 4 g·L⁻¹ NaOH at (a) $C_{\text{So}} = 5 \text{ g}\cdot\text{L}^{-1}$ and 20 °C, (b) $C_{\text{So}} = 10 \text{ g}\cdot\text{L}^{-1}$ and 20 °C, and (c) $C_{\text{So}} = 10 \text{ g}\cdot\text{L}^{-1}$ and 60 °C. Symbols indicate experimental results, whereas line values are predicted using the surfactant stability model shown in eq 3.

loss of surfactant capacity (SCL) was observed when alkali was added, with SCL values being lower than 0.05 for both experiments (E16 and E17).

It was previously reported in the literature that OH⁻ anions attack hydrolyzable groups in the surfactant molecule. These transformations produce a consequent loss of the solubilization capacity.³³ According to the E3 maker, this surfactant is formulated with ethoxylated castor oil, ethoxylated cocamide, ethoxylated fatty acid, and limonene as cosolvents.³⁴ These compounds include ester, ether, and double-bond groups, common in polyethoxylated nonionic surfactants such as Triton X, Tween, Brij, Pluronic, and others.^{8,35} Some of these groups are susceptible to hydrolysis under strongly alkaline conditions and temperature.³³

On the other hand, as shown in Figure 2, no differences were found in the conversion of the surfactant at all the NaOH concentrations tested, regardless of the temperature and the tested initial surfactant concentrations.

3.2.2. Effect of the Initial Surfactant Concentration (C_{So}). The effect of the initial surfactant concentration on the SCL was investigated at 2, 5, and 10 g·L⁻¹ by using two temperatures 20 and 60 °C and keeping constant the NaOH concentration at 4 g·L⁻¹. The results obtained are shown in Figure 3. The higher the reaction time, the higher the SCL obtained. Moreover, the SCL was independent of its initial concentration, indicating that the reaction rate of SCL follows a first-order reaction at the surfactant concentration.

As shown in Figure 3, an asymptotic SCL surfactant value was reached in the ranges 0.60–0.64 at 20 °C and 0.79–0.83

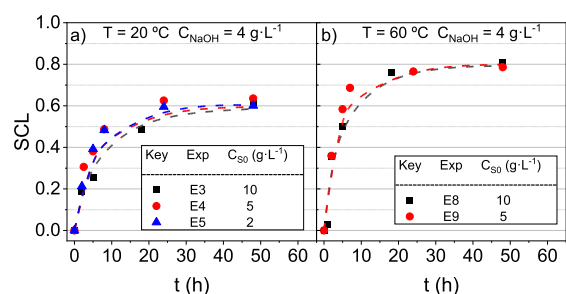


Figure 3. SCL profiles with the time. C_{NaOH} was $4 \text{ g}\cdot\text{L}^{-1}$, and temperature was (a) 20 and (b) 60 °C for an initial concentration of the surfactant of 2 , 5 , and $10 \text{ g}\cdot\text{L}^{-1}$. Symbols indicate experimental results, whereas line values are predicted using the surfactant stability model shown in eq 3.

at 60 °C. The asymptotic SCL values indicate that final byproducts of surfactant alkaline hydrolysis retain some surfactant capacity to dissolve COCs in the aqueous phase.³⁶ In addition, it can be observed that these byproducts were more reactive at higher temperatures, reducing the residual surfactant capacity. The asymptotic value of SCL depends only on temperature and not the surfactant concentration.

3.2.3. Effect of Temperature. The temperature effect on SCL was studied in the temperature range 20 – 60 °C, keeping constant the initial surfactant concentration ($5 \text{ g}\cdot\text{L}^{-1}$) and NaOH concentration ($4 \text{ g}\cdot\text{L}^{-1}$). The evolution of SCL over time is plotted in Figure 4.

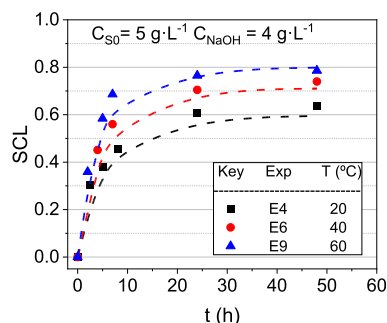


Figure 4. SCL evolution with the time. C_{S0} and C_{NaOH} were 5 and $4 \text{ g}\cdot\text{L}^{-1}$, respectively. Temperatures tested were 20 , 40 , and 60 °C. Symbols indicate experimental results, whereas line values are predicted using the surfactant stability model shown in eq 3.

As shown in Figure 4, SCL was strongly affected by temperature (20 – 60 °C). The higher the temperature, the higher the SCL with time. Moreover, as previously commented, the temperature modifies the reactivity of surfactant byproducts, resulting in different asymptotic SCLs (0.64 at 20 °C, 0.74 at 40 °C, and 0.79 at 60 °C).

The byproducts of surfactant hydrolysis were investigated using the nuclear magnetic resonance (NMR) technique. First, the NMR spectrum (shown in Figure S1) of a pure solution of E3 ($10 \text{ g}\cdot\text{L}^{-1}$) was obtained. It has been considered that E3 was composed of castor oil polyethoxylated esters (represented in Figure S2), among others. The NMR spectra of the polyethoxylated group (marked as a red square) and the hydrophobic chain (marked as a green square) were simulated using software included in the SciFinder[®] application (V11.01 Advanced Chemistry Development, Inc. ACD/LABS). The spectra obtained are summarized in Figures S3 and S4,

respectively. Upon comparing the experimental spectra of pure E-Mulse 3 (Figure S1) with the spectra predicted for the polyethoxylated groups and the hydrophobic chain (Figures S3 and S4), the different groups of the surfactant have been identified. The polyethoxylated groups were identified at chemical shifts δ 3.56 and 3.36 ppm. Meanwhile, the chemical shift associated with the unsaturated chain can be located at 5.38 ppm and between 2.10 and 1.31 ppm. The peak located at 5.38 ppm can be attributed to the double-bond on the aliphatic chain (Figure S4).

The surfactant hydrolysis byproducts were investigated using 20 °C (E3) and 60 °C (E7) samples. The NMR spectra of the aqueous solution at the final times in experiments E3 and E7 (set B1 in Table 1) are shown in Figures S5 and S6, respectively. The comparison of results in Figures S5 and S6 with those in Figure S1 reveals that the unsaturated chain disappeared by the effect of NaOH and temperature (Figure S6), confirming the attack of NaOH. On the contrary, the polyethoxylated groups were not attacked by NaOH. Under this experimental evidence, the reaction mechanism was proposed as shown in Figure S7. The surfactant alkaline hydrolysis of ester groups results in the production of an organic sodium salt (C), which maintains some surfactant capacity, and the generation of a byproduct (B) without surfactant capacity (Figure S7). These unsaturated chains were also attacked by NaOH enhanced by temperature reducing the number of intermediates capable of maintaining the surfactant capacity.³⁷

3.2.4. Effect of COCs in the Emulsion. The effect of COCs composing DNAPL-S on the SCL was evaluated by adding the amount of DNAPL-S required to reach saturated emulsions ($4.33 \text{ mmol}_{\text{COCs}}\cdot\text{g}_{\text{surf}}^{-1}$). The DNAPL-S and initial surfactant concentration ranges used were (14.6 , 35.2 and 70.3) $\text{mmol}\cdot\text{L}^{-1}$ and (2 , 5 and 10) $\text{g}\cdot\text{L}^{-1}$, respectively. Three temperatures were applied (20 , 40 and 60 °C), and the corresponding SCL values versus time obtained are shown in Figure 5.

At 20 °C (Figure 5a), it was noticed that COCs in the emulsion inhibited the SCL. At 48 h, an SCL of about 15% is obtained in experiments E10 and E11, whereas in experiments E1 and E5 (without COCs in the solution), SCL reaches 60% at the same time. However, as the temperature increases, this inhibition disappears, as shown in Figure 5b,c.

3.2.5. Modeling the SCL Rate. The effect of studied variables on the SCL of surfactant E3 has been taken into account by a kinetic model predicting the SCL rate. With the experimental results, the following assumptions have been made:

- The partial order of NaOH in the SCL reaction rate is zero.
- The SCL follows a first-order reaction on the surfactant.
- The SCL asymptotic value depends on the temperature.
- The COCs in the emulsion inhibit the SCL, but this effect changes as the temperature increases. The proposed kinetic model can be used in the presence and absence of COCs in the emulsion. The different influence of COCs at high or low temperature has been taken into account using k_1 and k_2 in eq 3.

With these assumptions, the proposed kinetic model of the SCL rate is shown in eq 3.

$$-\frac{dC_{\text{ESC}}}{dt} = k(C_{\text{ESC}} - C_{\text{S0}}x_r) \frac{(1 + k_1C_{\text{D}})}{(1 + k_2C_{\text{D}})} \quad (3)$$

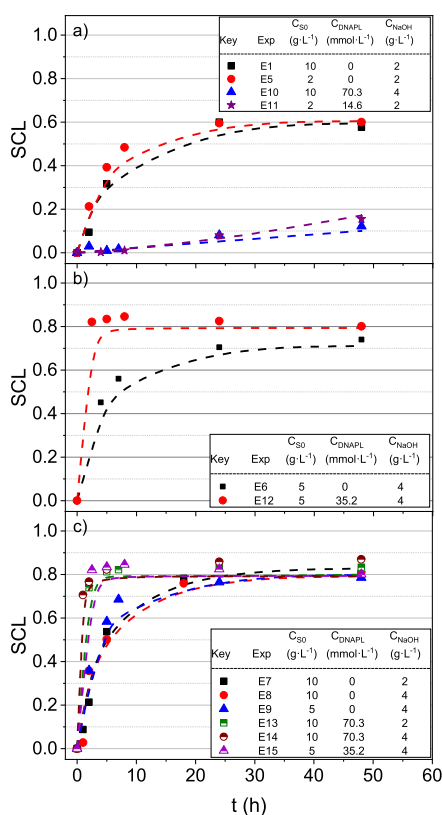


Figure 5. SCL evolution with the time at (a) 20; (b) 40; and (c) 60 °C. The COC concentration was 0 mmol·kg⁻¹ and was required for saturation of the initial surfactant solution. Symbols indicate experimental results, whereas line values are predicted using the surfactant stability model shown in eq 3.

where C_{ESC} and C_{S0} are the surfactant equivalent concentration ($g \cdot L^{-1}$) at a time t and the surfactant concentration at zero time, respectively; C_D is the COC concentration ($mmol \cdot L^{-1}$) at a time; C_{NaOH} is the NaOH concentration ($g \cdot L^{-1}$); and k is the reaction rate constant (h^{-1}). K_1 and k_2 in ($L \cdot mmol^{-1}$) are constants that take into account the effect of COCs on SCL with the temperature. k , k_1 , and k_2 follow the Arrhenius law,³⁸ expressed in eqs 4–6, respectively; x_r is the residual surfactant with temperature, being a function of the temperature as proposed in eq 7.

$$k = k_0 \cdot \exp\left(-\frac{E_a}{T(K)}\right) \quad (4)$$

$$k_1 = k_{01} \cdot \exp\left(-\frac{E_{a1}}{T(K)}\right) \quad (5)$$

$$k_2 = k_{02} \cdot \exp\left(-\frac{E_{a2}}{T(K)}\right) \quad (6)$$

$$x_r = \exp(a \cdot T(^{\circ}C)^b) \quad (7)$$

The experiments in this section using emulsions with COCs were carried out by saturating the surfactant emulsion with DNAPL. The amount of solubilized COCs in a saturated emulsion is linear with the surfactant concentration at alkaline pH.³⁰ Therefore, the decrease in the surfactant concentration with time produces a decrease in the COCs in the emulsion C_D when saturated emulsions are used at zero time. The remaining

surfactant concentration with time C_D can be calculated using eq 8.

$$C_D = C_{D_0} \cdot \frac{C_{ESC}}{C_{S0}} \quad (8)$$

Data from experiments in set B1 were fitted to the model in eqs. 3–7. The problem to be solved is composed of a mixed set of differential and algebraic equations. It was implemented in ModelBuilder 7.1.0 provided in the gPROMS suit, and the algorithm DASOLV was used to simulate the reaction system. DASOLV is based on a variable time step, variable order, and backward differentiation formulae.³⁹ The estimated parameters calculated for the SCL kinetic model by minimizing the sum of quadratic squares (eq 9) are shown in

Table 2, with the confidence interval (CI) (95%) of the parameters.

$$SQR = \sum (C_{ESC \text{ exp}} - C_{ESC \text{ pred}})^2 (g \cdot L^{-1})^2 \quad (9)$$

Table 2. Parameters Estimated for the SCL Rate^a

E_a (K)	724.1 ± 31.5
E_{a1} (K)	-2575 ± 112
E_{a2} (K)	-20835 ± 918
k_0 (h^{-1})	1.97 ± 0.06
k_{01} ($L \cdot mmol^{-1}$)	0.27 ± 0.03
k_{02} ($L \cdot mmol^{-1}$)	$1.4 \times 10^{-5} \pm 0.2 \times 10^{-5}$
A	-0.57 ± 0.02
b	$-1.68 \times 10^{-2} \pm 7.36 \times 10^{-4}$
SQR, ($g \cdot L^{-1}$) ²	3.2

^a95% CI.

3.3. Surface Responses for the Apparent Henry's Constant. The volatilization of COCs from the emulsion formed by DNAPL and E3 was studied in experiments summarized in Table 1. The vapor–liquid equilibrium (VLE) of component j can be described by Henry's law²² assuming that the vapor phase is an ideal gas phase, and the fugacity can be considered close to unity.⁴⁰ The Henry's law in eq 10 was formulated using an apparent Henry's constant in surfactant solutions.²² This constant considers the COCs to be partitioned into vapor, extracellular (aqueous), and micellar phases.²³

$$P_T \cdot y_j = H_{app,j} \cdot x_j \quad (10)$$

where P_T is the total pressure in the vial (bar) at the temperature T ; y_j is the molar fraction of COC j in the vapor phase; $H_{app,j}$ is the apparent Henry's constant of compound j ; and x_j is the molar fraction of compound j in the liquid phase. The molar fraction in the liquid phase was calculated by mass balance as the difference between the amount of compound j in the vapor phase and the initial amount prepared in the sample.

In eq 10, the total pressure in the vial (bar) is calculated assuming that under the conditions tested, water and air are the main compounds in the gas phase in the vial, according to eq 11.

$$P_T \approx P_{air} + P_w = \frac{P_{o,air} \cdot T}{273} + P_{o,w(T)} \quad (11)$$

Table 3. Parameters Obtained from the Fitting of $H_{app,j}$ to eq 13^a

	<i>a</i>	<i>b</i>	<i>c</i>	<i>d</i>	<i>E</i>	<i>f</i>	<i>R</i> ²	<i>F</i> -value	<i>p</i> -value
CB	2.54	−0.24	0.08	8.52×10^{-3}	-4.39×10^{-4}	6.90×10^{-5}	0.99	349	4.42×10^{-19}
1,4-DCB	0.26	−0.34	0.11	1.35×10^{-2}	-7.73×10^{-4}	-3.68×10^{-4}	0.97	173	6.77×10^{-17}
1,2-DCB	0.16	−0.37	0.13	1.44×10^{-2}	-9.25×10^{-4}	-4.64×10^{-5}	0.97	136	1.09×10^{-17}
1,2,4-TCB	−3.94	−0.37	0.26	1.84×10^{-2}	-2.03×10^{-3}	-2.36×10^{-3}	0.97	408	1.08×10^{-15}
1,2,3-TCB	−4.69	−0.37	0.26	1.69×10^{-2}	-1.98×10^{-3}	-2.08×10^{-3}	0.98	171	4.61×10^{-19}
a-TetraCB	−5.28	−0.60	0.27	2.63×10^{-2}	-2.19×10^{-3}	1.04×10^{-4}	0.98	320	1.82×10^{-20}
b-TetraCB	−6.05	−0.57	0.28	2.60×10^{-2}	-2.17×10^{-3}	-4.11×10^{-4}	0.98	325	1.53×10^{-20}

^aThe statistical parameters were obtained from variance analysis. The coefficient of variation (R^2), Fischer's test value (F -value), and probability (p -value) are also shown.

where $P_{0,air}$ is the initial pressure of the vial at 20 °C (water in the phase can be neglected at this temperature) and P_w is the water pressure in the vial gas phase at corresponding T (equal to water vapor pressure at T , assuming that the molar fraction of water in the liquid phase is almost the unity).

The presence of the surfactant (concentration and type) in the aqueous phase can modify Henry's constant of the chlorinated compound j .²⁴ Also, the complex mixture of DNAPL can affect this constant.

Experimental values of $H_{app,j}$ for each compound j at different temperatures and surfactant and COC concentrations in the liquid phase were determined according to eq 12, after measuring the gas phase composition of the vial by GC, as explained in the Analytical Methods section.

$$H_{app,j} \approx \frac{n_j \cdot P_T}{n_{gas} \cdot x_j} \quad (12)$$

where n_j is the moles of the j compound in the vial gas phase and n_{gas} is the sum of moles of all compounds (including organic, air, and water) in the vial gas phase.

The experimental values of $\ln(H_{app,j})$ obtained at different temperatures, surfactant concentrations, and COC concentrations in the aqueous phase are shown as red points in Figure S8. The different red points, for the same values of the temperature and surfactant concentration, refer to the different COC concentrations used at those values of T and C_{S0} (experimental conditions are detailed in Table 1). The influence of the COC concentration in emulsion on $\ln(H_{app,j})$ can be neglected if the surfactant concentration and temperature keep constant, as shown in Figure S8. On the contrary, a positive effect of temperature on $\ln(H_{app,j})$ was found. As expected, organic compounds in the emulsion have a significant tendency to pass to the vapor phase as the temperature increases. On the contrary, the higher the surfactant concentration, the lower the $\ln(H_{app,j})$ value of the j compound. The increase of the surfactant concentration results in a higher concentration of micelles,¹² inhibiting the volatilization of chlorinated compounds from the emulsion, which agrees with the conclusion reported in the literature.²⁴

The interaction between the surfactant concentration and temperature at $H_{app,j}$ values has been modeled using the response surface methodology (RSM). Experimental values of $H_{app,j}$ shown in Figure S8 have been fitted to eq 13.

$$H_{app,j} = \exp(a + b \cdot C_S + c \cdot T + d \cdot C_S^2 + e \cdot T^2 + f \cdot C_S \cdot T) \quad (13)$$

where T is the temperature (°C) and C_S is the surfactant concentration ($\text{g} \cdot \text{L}^{-1}$) when VLE is reached. Equilibrium was

achieved in 1 h, and corresponding C_S was calculated using the kinetic model proposed in Section 3.2.5. Modeling of the SCL rate has been summarized in Table S4.

The estimated values of parameters a – f in eq 13 and the statistical parameters obtained from the variance analysis [coefficient of variation (R^2), Fischer's test value (F -value), and probability (p -value)] are summarized in Table 3. As can be seen, the value of R^2 is close to 1 for all the compounds present in DNAPL-R, indicating a good agreement between experimental and predicted values. Additionally, the F -values are large ($\gg 1$), and the p -values are small enough (< 0.05) for all the chlorinated compounds studied. Therefore, the RSM model applied and the parameters obtained allow us to estimate accurately the $H_{app,j}$ values of each j compound as a function of the surfactant concentration and temperature, with the negligible effect of the COC concentration in the emulsion.

3.4. Volatilization of COCs from Alkaline Emulsions.

Emulsion of DNAPL obtained in SEAR treatment must be treated to eliminate the organic compounds. In the case of DNAPL from lindane liquid wastes, a significant fraction of COCs in emulsion correspond to low volatile HCHs and HeptaCHs. Therefore, as cited before, the previous alkalization transforms these compounds into more volatile TCBs and TetraCBs. Volatilization of COCs in the alkaline solution can be modeled by considering those values that influence the volatility of the COCs. These variables are temperature and surfactant concentrations in the aqueous phase. In addition, the surfactant concentration in the emulsion can change with time according to the SCL rate equation described in Section 3.2.5. Modeling SCL rate.

The molar balance of COC j in the emulsion in the batch experiment schematized in Figure 1 can be calculated using eq 14.

$$-\frac{dn_j}{dt} = -\frac{V_L C_T dx_j}{dt} \quad (14)$$

where n_j is the moles of j in the emulsion; V_L is the volume of the aqueous emulsion (L); C_T is the total molar concentration of the emulsion (approximately corresponding to water: $55 \text{ mol} \cdot \text{L}^{-1}$); and x_j is the molar fraction of the compound j in the liquid phase.

The gas flow rate leaving the bottle (Figure 1) is assumed to be in equilibrium with the emulsion by applying the Raoult law. The molar fraction of the j compound in the gas phase is calculated with eq 15.

$$y_j = \frac{H_{app,j} \cdot x_j}{P_T} \quad (15)$$

The molar flow rate of the j compound disappearing from the emulsion is the same as the molar flow of this j compound that leaves the bottle in the gas phase (both phases in equilibrium), as described in eq 16.

$$-\frac{V_L \cdot C_T \cdot dx_j}{dt} = \frac{F_{\text{gas}} H_{\text{app},j} \cdot x_j}{P_T} \quad (16)$$

where F_{gas} is the gas molar flow rate ($\text{mol} \cdot \text{h}^{-1}$) fed to the system.

The molar fraction of j in the emulsion with time can be predicted by integrating eq 16 as shown in eq 17.

$$\frac{x_j}{x_{j0}} = \exp\left(-\frac{F_{\text{gas}} \cdot H_{\text{app},j}}{V_L \cdot C_T} \cdot t\right) \quad (17)$$

The ratio x_j/x_{j0} also corresponds to the concentration ratio of the j compound in the emulsion (eq 18)

$$\frac{x_j}{x_{j0}} = \frac{C_j}{C_{j0}} \quad (18)$$

where C_j is the concentration of j in the aqueous emulsion a time t and C_{j0} is the concentration of j in the aqueous emulsion before the gas is fed (zero time). The concentration of the sum of COCs remaining in the emulsion can be estimated from eq 19

$$C_{\text{COCs,remaining}} = \sum C_{j0} \cdot \frac{C_j}{C_{j0}} \quad (19)$$

The value of $H_{\text{app},j}$ at each time is obtained by eq 13, with the surfactant concentration predicted by eq 3 at the time considered.

The consistency of the SCL kinetic model and $H_{\text{app},j}$ obtained in the surfactant presence were validated by comparing the experimental and predicted values of COCs in the emulsion obtained in runs shown in Table 1 (set B3). Two different temperatures were employed (40 and 60 °C) as two different initial surfactant concentrations (3.5 and 7 $\text{g} \cdot \text{L}^{-1}$) have been used. The gas flow rate employed was 3 $\text{L} \cdot \text{h}^{-1}$ (0.13 $\text{mol} \cdot \text{h}^{-1}$), the emulsion volume was 0.25 L, and the initial COC concentration in the emulsion was 17.6 $\text{mmol} \cdot \text{kg}^{-1}$. DNAPL-S was used, with a similar composition to DNAPL-R after alkalization. The air was flowing during 8 h. Experimental values with time of COCs in emulsion (as symbols) and those predicted with eq 17 (as lines) are shown in Figure 6. As can be seen, a good agreement is obtained between experimental and predicted COCs.

The SCL during volatilization has also been measured and estimated for runs shown in Table 1. Experimental and predicted values are shown in Figure 7. The excellent agreement found between the observed and predicted values of SCL inferred that the significant losses of surfactant capacity were related to the reaction between the surfactant and NaOH. The losses of the surfactant by foaming are negligible. As observed with the volatilization experiments, the SCL reached 0.8 at 60 °C and 0.62 at 40 °C during 8 h of treatment. Therefore, volatilization can be employed not only to remove COCs from emulsions but also to break them and thus facilitate their further disposal. The reduction of surfactant and pollutant contents in the processed stream permits the treatment of the water stream obtained after the air stripping

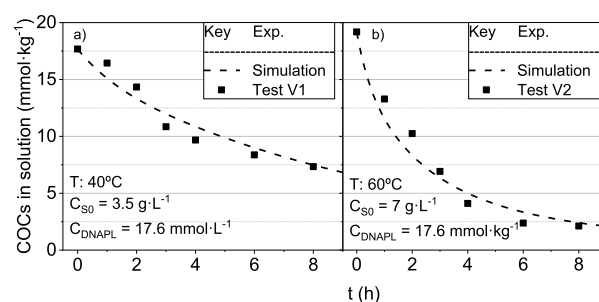


Figure 6. Volatilization of COCs in the emulsion. (a) $T = 40$ °C; $C_{S0} = 3.5$ $\text{g} \cdot \text{L}^{-1}$ and (b) $T = 60$ °C; $C_{S0} = 7$ $\text{g} \cdot \text{L}^{-1}$. Conditions $C_{\text{DNAPL-S}} = 17.6$ $\text{mmol} \cdot \text{L}^{-1}$; $V_{\text{aq}} = 0.25$ L; air flow 3 $\text{L} \cdot \text{h}^{-1}$; and $C_{\text{NaOH}} = 4$ $\text{g} \cdot \text{L}^{-1}$ NaOH. Symbols indicate experimental results, whereas line values are predicted using eq 17.

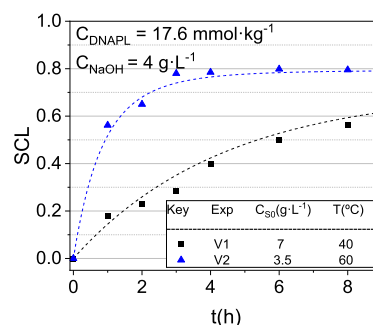


Figure 7. Evolution of SCL with the time for the volatilization experiments. Symbols indicate experimental results, whereas line values are predicted using eq 17.

step under alkali conditions, avoiding other expensive technologies such as incineration in special facilities.⁴¹

4. CONCLUSIONS

In this work, a complex mixture of chlorinated organic contaminants in a surfactant emulsion simulating a SEAR stream was successfully treated by air stripping. The emulsion was alkalized to transform the original pollutants (PentaCX, HCH, and HeptaCH) to more volatile compounds (triCB and tetraCB).

The air-stripping treatment design required studying the volatilization of COCs and the SCL. Both approaches were affected by temperature and NaOH, surfactant, and COC concentrations. It was found that temperature and alkali produced the SCL with time. Under alkaline conditions, the OH^- anions attack hydrolyzable groups in the surfactant molecule, resulting in the loss of unsaturated chains. The surfactant byproducts of alkaline hydrolysis keep some residual surfactant capacity (about 0.36 to 0.21 of the initial value). The variables' effect in the SCL was used to develop a kinetic model that can adequately explain the experimental findings.

In addition, it was observed that the surfactant presence drastically reduced the volatilization of those COCs, and their volatilization increased with temperature, while the COC concentration in the emulsion did not affect the volatilization of the COCs. The $H_{\text{app},j}$ values obtained have been adequately correlated with the variables studied using surface response methodology.

The volatilization of COCs in the alkaline emulsion by air stripping was experimentally measured and predicted. The air stripping under alkali conditions successfully reduced the initial

concentration of COCs by more than 90% after 8 h at 60 °C. In addition, SCL during air stripping was higher than 80% at 60 °C, making the emulsion disposal more straightforward. The simulated values of COCs in emulsion with time using the kinetic model of surfactant stability and the $P_v^\circ\gamma$ correlations agree well with the experimental results, validating the model.

The volatilization of COCs by air stripping was successfully applied to move and concentrate these compounds to the vapor phase. This stream can be treated by coupling different technologies, such as the adsorption in AC, whose efficiency is improved when the surfactant is removed from the feed stream.

■ ASSOCIATED CONTENT

SI Supporting Information

The Supporting Information is available free of charge at <https://pubs.acs.org/doi/10.1021/acs.iecr.2c03722>.

Additional details about the composition of DNAPL-R used and of synthetic DNAPL; additional details regarding the analysis method; NMR spectra of E3; chemical structure of a polyethoxylated ester which can be found in the surfactant employed; NMR spectrums predicted for the polyethoxylated group and aliphatic chain; NMR spectra for different experiments carried out in the article; mechanism of surfactant alkaline hydrolysis proposed; and values of $P_v^\circ\gamma_j$ for the different experiments carried out and the response surfaces for the different compounds (PDF)

■ AUTHOR INFORMATION

Corresponding Author

David Lorenzo – *Chemical Engineering and Materials Department, Complutense University of Madrid, 28040 Madrid, Spain*; orcid.org/0000-0002-4235-9308; Email: dlorenzo@quim.ucm.es

Authors

Patricia Sáez – *Chemical Engineering and Materials Department, Complutense University of Madrid, 28040 Madrid, Spain*; orcid.org/0000-0001-5041-6184

Raúl García-Cervilla – *Chemical Engineering and Materials Department, Complutense University of Madrid, 28040 Madrid, Spain*; orcid.org/0000-0002-9177-2481

Aurora Santos – *Chemical Engineering and Materials Department, Complutense University of Madrid, 28040 Madrid, Spain*

Arturo Romero – *Chemical Engineering and Materials Department, Complutense University of Madrid, 28040 Madrid, Spain*

Complete contact information is available at: <https://pubs.acs.org/doi/10.1021/acs.iecr.2c03722>

Notes

The authors declare no competing financial interest.

■ ACKNOWLEDGMENTS

This work was supported by the Regional Government of Madrid, through the CARESOIL project (S2018/EMT-4317), and the Spanish Ministry of Economy, Industry and Competitiveness, through the project PID2019-105934RB and through the EU Life Program (LIFE17 ENV/ES/000260). Raúl García-Cervilla acknowledges the FPI grant

from the Spanish Ministry of Economy, Industry and Competitiveness (ref. BES-2017-081782).

■ ABBREVIATIONS.

AC	activated carbon
BDF	backward differentiation formulae
CB	chlorobenzene
CI	95% confidence interval
CMC	critical micelle concentration
COCs	chlorinated organic compounds
DCB	dichlorobenzene
DCE	dichloroethene
DMSO	dimethyl sulfoxide
DNAPL	dense non-aqueous phase liquid
DNAPL-R	real dense non-aqueous phase liquid
DNAPL-S	synthetic dense non-aqueous phase liquid
E3	E-Mulse 3
ECD	electron capture detector
ESC	equivalent surfactant concentration
FID	flame ionization detector
GC	gas chromatography
HCHs	hexachlorocyclohexane isomers
HeptaCHs	heptachlorocyclohexane isomers
HexaCXs	hexachlorocyclohexane isomers
HS-GC	HeadSpace gas chromatography
ISTDs =	internal standards
MeOH	methanol
MSR	molar solubilization ratio
NAPLs	non-aqueous phase liquids
NMR	nuclear magnetic resonance
PAHs	polycyclic aromatic hydrocarbons
PCE	tetrachloroethene
PentaCXs	pentylcyclohexanes
RSM	response surface methodology
SCL	surfactant capacity loss
SDS	sodium dodecyl sulfate
SDBS	sodium dodecyl benzene sulfonate
SEAR	surfactant enhanced aquifer remediation
SQR	sum of quadratic squares
TCB	trichlorobenzene isomers
TCE	trichloroethene
TetraCB	tetrachlorobenzene isomers
TPH	total petroleum hydrocarbons
VLE	vapor–liquid equilibrium

■ SYMBOLS

a	fitting parameter
b	fitting parameter
c	fitting parameter
C_j	concentration of compound j in $\text{mmol}\cdot\text{L}^{-1}$ ($j = \text{COCs, DNAPL}$) or $\text{g}\cdot\text{L}^{-1}$ [$j = \text{surfactant (S), ESC, NaOH}$]
CT_{total}	total molar concentration of the emulsion (approximately corresponding to water)
c_{total}	total molar concentration of the emulsion (approximately corresponding to water) $55 \text{ mol}\cdot\text{L}^{-1}$
d	fitting parameter
e	fitting parameter

fitting parameter

E_a

activation energy in K.

f

fitting parameter

F_{gas}

gas molar flow rate in mol h⁻¹

$H_{\text{app},j}$

apparent Henry's constant of compound j in the emulsion in bar.

k

reaction rate constant in h⁻¹.

k_0

preexponential factor in L·mmol⁻¹

k_i

constants that take into account the effect of COCs on SCL in L·mmol⁻¹.

n_j

mole of compound j in mol

P

pressure in bar

$P_{v,j}$

saturation vapor pressure of compound j in bar

T

temperature in °C

t

time in h

VL

volume of the aqueous emulsion in L

x_j

molar fraction of compound j in the liquid phase

x_r

residual surfactant with temperature

y_j

molar fraction of compound j in the vapor phase

■ GREEK LETTERS

γ_j activity coefficient of the chlorinated compound j

■ SUBSCRIPTS

0 initial

air air

D COC concentration

exp experimental value

gas vapor phase

pred predicted value

s surfactant

T temperature

w water

■ REFERENCES

(1) Payá Perez, A.; Rodríguez Eugenio, N. *Status of Local Soil Contamination in Europe*; European Commission, 2018. DOI: 10.2760/093804.

(2) Siegrist, R. L.; Crimi, M.; Simpkin, T. J. *In Situ Chemical Oxidation for Groundwater Remediation*; Springer Science & Business Media, 2011.

(3) Bayabil, H. K.; Teshome, F. T.; Li, Y. C. Emerging Contaminants in Soil and Water. *Front. Environ. Sci.* **2022**, *10*. Mini Review. DOI: 10.3389/fenvs.2022.873499.

(4) Rasheed, T.; Ahmad, N.; Ali, J.; Hassan, A. A.; Sher, F.; Rizwan, K.; Iqbal, H. M. N.; Bilal, M. Nano and micro architected cues as smart materials to mitigate recalcitrant pharmaceutical pollutants from wastewater. *Chemosphere* **2021**, *274*, 129785.

(5) Rasheed, T.; Ahmad, N.; Nawaz, S.; Sher, F. Photocatalytic and adsorptive remediation of hazardous environmental pollutants by hybrid nanocomposites. *Case Stud. Chem. Environ. Eng.* **2020**, *2*, 100037.

(6) Sher, F.; Iqbal, S. Z.; Rasheed, T.; Hanif, K.; Sulejmanović, J.; Zafar, F.; Lima, E. C. Coupling of electrocoagulation and powder activated carbon for the treatment of sustainable wastewater. *Environ. Sci. Pollut. Res.* **2021**, *28*, 48505–48516.

(7) Huo, L.; Liu, G.; Yang, X.; Ahmad, Z.; Zhong, H. Surfactant-enhanced aquifer remediation: Mechanisms, influences, limitations and the countermeasures. *Chemosphere* **2020**, *252*, 126620.

(8) Liu, J. W.; Wei, K. H.; Xu, S. W.; Cui, J.; Ma, J.; Xiao, X. L.; Xi, B. D.; He, X. S. Surfactant-enhanced remediation of oil-contaminated soil and groundwater: A review. *Sci. Total Environ.* **2021**, *756*, 144142.

(9) Wang, L.; Peng, L.; Xie, L.; Deng, P.; Deng, D. Compatibility of Surfactants and Thermally Activated Persulfate for Enhanced Subsurface Remediation. *Environ. Sci. Technol.* **2017**, *51*, 7055–7064.

(10) Ramsburg, C. A.; Pennell, K. D.; Abriola, L. M.; Daniels, G.; Drummond, C. D.; Gamache, M.; Hsu, H.-I.; Petrovskis, E. A.; Rathfelder, K. M.; Ryder, J. L.; et al. Pilot-Scale Demonstration of Surfactant-Enhanced PCE Solubilization at the Bachman Road Site. 2. System Operation and Evaluation. *Environ. Sci. Technol.* **2005**, *39*, 1791–1801.

(11) Santos, A.; Domínguez, C. M.; Lorenzo, D.; García-Cervilla, R.; Lominchar, M. A.; Fernández, J.; Gómez, J.; Guadaño, J. Soil flushing pilot test in a landfill polluted with liquid organic wastes from lindane production. *Heliyon* **2019**, *5*, No. e02875.

(12) Rosen, M. J.; Kunjappu, J. T. *Surfactants and Interfacial Phenomena*; John Wiley & Sons, 2012.

(13) Paria, S. Surfactant-enhanced remediation of organic contaminated soil and water. *Adv. Colloid Interface Sci.* **2008**, *138*, 24–58.

(14) Lee, M.; Kang, H.; Do, W. Application of nonionic surfactant-enhanced in situ flushing to a diesel contaminated site. *Water Res.* **2005**, *39*, 139–146.

(15) Hanafiah, S. A.; Mohamed, M. A.; Caradec, S.; Fatin-Rouge, N. Treatment of heavy petroleum hydrocarbons polluted soil leachates by ultrafiltration and oxidation for surfactant recovery. *J. Environ. Chem. Eng.* **2018**, *6*, 2568–2576.

(16) Huang, K.; Liang, J.; Jafvert, C. T.; Li, Q.; Chen, S.; Tao, X.; Zou, M.; Dang, Z.; Lu, G. Effects of ferric ion on the photo-treatment of nonionic surfactant Brij35 washing waste containing 2,2',4,4'-tetrabromodiphenyl ether. *J. Hazard. Mater.* **2021**, *415*, 125572.

(17) Li, Y.; Hu, J.; Liu, H.; Zhou, C.; Tian, S. Electrochemically reversible foam enhanced flushing for PAHs-contaminated soil: Stability of surfactant foam, effects of soil factors, and surfactant reversible recovery. *Chemosphere* **2020**, *260*, 127645.

(18) García-Cervilla, R.; Santos, A.; Romero, A.; Lorenzo, D. Compatibility of nonionic and anionic surfactants with persulfate activated by alkali in the abatement of chlorinated organic compounds in aqueous phase. *Sci. Total Environ.* **2021**, *751*, 141782.

(19) Rosas, J. M.; Santos, A.; Romero, A. Soil-Washing Effluent Treatment by Selective Adsorption of Toxic Organic Contaminants on Activated Carbon. *Water, Air, Soil Pollut.* **2013**, *224*, 10.

(20) Trinh, T. A.; Han, Q.; Ma, Y.; Chew, J. W. Microfiltration of oil emulsions stabilized by different surfactants. *J. Membr. Sci.* **2019**, *579*, 199–209.

(21) Huan, J. C.; Shang, C. Air Stripping. In *Advanced Physicochemical Treatment Processes*; Wang, L. K., Hung, Y. T., Shammas, N. K., Eds.; *Handbook of Environmental Engineering*; Humana Press, 2006; Vol. 4.

(22) Vane, L. M.; Giroux, E. L. Henry's Law Constants and Micellar Partitioning of Volatile Organic Compounds in Surfactant Solutions. *J. Chem. Eng. Data* **2000**, *45*, 38–47.

(23) Kungsanant, S.; Kittirisawai, S.; Suriya-Amrit, P.; Kitiyanan, B.; Chavadej, S.; Osuwan, S.; Scamehorn, J. F. Study of nonionic surfactants on HVOCs removal from coacervate solutions using cocurrent vacuum stripping in a packed column. *Sep. Sci. Technol.* **2018**, *53*, 2662–2670.

- (24) Shimotori, T.; Arnold, W. A. Measurement and Estimation of Henry's Law Constants of Chlorinated Ethylenes in Aqueous Surfactant Solutions. *J. Chem. Eng. Data* **2003**, *48*, 253–261.
- (25) Zhang, C.; Zheng, G.; Nichols, C. M. Micellar Partitioning and Its Effects on Henry's Law Constants of Chlorinated Solvents in Anionic and Nonionic Surfactant Solutions. *Environ. Sci. Technol.* **2006**, *40*, 208–214.
- (26) Sprunger, L.; Acree, W. E.; Abraham, M. H. Linear Free Energy Relationship Correlation of the Distribution of Solutes between Water and Sodium Dodecyl Sulfate (SDS) Micelles and between Gas and SDS Micelles. *J. Chem. Inf. Model.* **2007**, *47*, 1808–1817.
- (27) Chao, H.-P.; Lee, J.-F.; Lee, C.-K.; Huang, F.-C.; Annadurai, G. Volatilization reduction of monoaromatic compounds in nonionic surfactant solutions. *Chem. Eng. J.* **2008**, *142*, 161–167.
- (28) Santos, A.; Fernandez, J.; Guadaño, J.; Lorenzo, D.; Romero, A. Chlorinated organic compounds in liquid wastes (DNAPL) from lindane production dumped in landfills in Sabiñanigo (Spain). *Environ. Pollut.* **2018**, *242*, 1616–1624.
- (29) Lorenzo, D.; García-Cervilla, R.; Romero, A.; Santos, A. Partitioning of chlorinated organic compounds from dense non-aqueous phase liquids and contaminated soils from lindane production wastes to the aqueous phase. *Chemosphere* **2020**, *239*, 124798.
- (30) García-Cervilla, R.; Santos, A.; Romero, A.; Lorenzo, D. Partition of a mixture of chlorinated organic compounds in real contaminated soils between soil and aqueous phase using surfactants: Influence of pH and surfactant type. *J. Environ. Chem. Eng.* **2021**, *9*, 105908.
- (31) García-Cervilla, R.; Romero, A.; Santos, A.; Lorenzo, D. Surfactant-enhanced solubilization of chlorinated organic compounds contained in dnapl from lindane waste: Effect of surfactant type and ph. *Int. J. Environ. Res. Public Health* **2020**, *17*, 1–14.
- (32) Oh, J.-H.; Park, S.-J. Isothermal Vapor–Liquid Equilibria of 2-Methoxy-2-methylbutane (TAME) + n-Alcohol (C1–C4) Mixtures at 323.15 and 333.15 K. *J. Chem. Eng. Data* **1997**, *42*, 517–522.
- (33) (a) Stjern Dahl, M.; Holmberg, K. Hydrolyzable nonionic surfactants: stability and physicochemical properties of surfactants containing carbonate, ester, and amide bonds. *J. Colloid Interface Sci.* **2005**, *291*, 570–576. (b) Lundberg, D.; Stjern Dahl, M.; Holmberg, K. *Surfactants Containing Hydrolyzable Bonds*; Springer, 2008; Vol. 218, pp 57–82.
- (34) McAvoy, B. https://www.waterboards.ca.gov/losangeles/board_decisions/tentative_orders/general/WDRs/WDR_Update/VeruSOLMSDS-Biodegradability-casestudies.pdf. Material Safety Data Sheet VeruSOL-3 Components; VeruTEK Technologies Inc, 2013. (accessed October 2022)
- (35) Prieto-Blanco, M. C.; Fernández Amado, M.; López-Mahía, P.; Muniategui Lorenzo, S.; Prada-Rodríguez, D. *Surfactants: From the Industrial Process to Environment*, 2018,
- (36) García-Cervilla, R.; Santos, A.; Romero, A.; Lorenzo, D. Abatement of chlorobenzenes in aqueous phase by persulfate activated by alkali enhanced by surfactant addition. *J. Environ. Manage.* **2022**, *306*, 114475.
- (37) (a) Castillo, M.; Peuela, G.; Barcel, D. Identification of photocatalytic degradation products of non-ionic polyethoxylated surfactants in wastewaters by solid-phase extraction followed by liquid chromatography-mass spectrometric detection. *Anal. Bioanal. Chem.* **2001**, *369*, 620–628. (b) Wang, W. H.; Hoag, G. E.; Collins, J. B.; Naidu, R. Evaluation of Surfactant-Enhanced In Situ Chemical Oxidation (S-ISCO) in Contaminated Soil. *Water, Air, Soil Pollut.* **2013**, *224*, 1713. (c) Olmez-Hanci, T.; Arslan-Alaton, I.; Genc, B. Degradation of the nonionic surfactant Triton X-45 with HO and -Based advanced oxidation processes. *Chem. Eng. J.* **2014**, *239*, 332–340.
- (38) Levenspiel, O. *Chemical Reaction Engineering*; Wiley, 1999.
- (39) Siemens Process Systems Enterprise; gPROMS, 2022. (accessed. www.psenterprise.com/gproms).
- (40) Hussam, A.; Carr, P. W. Rapid and precise method for the measurement of vapor/liquid equilibria by headspace gas chromatography. *Anal. Chem.* **1985**, *57*, 793–801.
- (41) Guadaño, J.; Gómez, J.; Fernández, J.; Lorenzo, D.; Domínguez, C. M.; Cotillas, S.; García-Cervilla, R.; Santos, A. Remediation of the Alluvial Aquifer of the Sardas Landfill (Sabiñanigo, Huesca) by Surfactant Application. *Sustainability* **2022**, *14*, 16576.

Recommended by ACS

Mechanism for Enhancing the Ozonation Process of Micro-And Nanobubbles: Bubble Behavior and Interface Reaction

Xiaolong Yang, Shu Liu, *et al.*

SEPTEMBER 20, 2023
ACS ES&T WATER

READ 

n-C₇ Asphaltenes Characterization as Surfactants and Polar Oil from the HLD_n Model Perspective

José G. Alvarado, José G. Delgado-Linares, *et al.*

JULY 21, 2023
INDUSTRIAL & ENGINEERING CHEMISTRY RESEARCH

READ 

Sulfonamide Derivatives as Novel Surfactant/Alkaline Flooding Processes for Improving Oil Recovery

Ahmed Ashraf Soliman, Attia Mahmoud Attia, *et al.*

JULY 28, 2023
ACS OMEGA

READ 

Dissipation and Efficacy of Afidopyropen for Controlling Asian Citrus Psyllids Under Field Conditions

Rachelle A. Rehberg, Thomas Borch, *et al.*

AUGUST 28, 2023
ACS AGRICULTURAL SCIENCE & TECHNOLOGY

READ 

Get More Suggestions >



European cooperation to tackle the legacies of hexachlorocyclohexane (HCH) and lindane



John Vijgen^a, Boudewijn Fokke^{a, b}, Guido van de Cotelerlet^b, Katja Amstaetter^c,
Javier Sancho^d, Carlo Bensaïah^b, Roland Weber^{a, e, *}

^a International HCH and Pesticides Association (IHPA), Elmevej 14, Holte, 2840, Denmark

^b TAUW, Handelskade 37, P.O. Box 133, 7400AC, Deventer, the Netherlands

^c CDM Smith Europe GmbH, Germany

^d SARGA, Sociedad Aragonesa de Gestión Agroambiental, Avenida Ranillas (ED A), 5 - 3 PLT, 50018, Zaragoza, Spain

^e POPs Environmental Consulting, Lindenfirststr. 23, 73527 Schwäbisch Gmünd, Germany

ARTICLE INFO

Article history:

Received 11 December 2021

Received in revised form

26 January 2022

Accepted 26 January 2022

Keywords:

HCH

Lindane

POPs

Stockholm convention

Contaminated sites

Inventory

Strategy

ABSTRACT

Hexachlorocyclohexane (HCH) waste isomers from lindane production are the largest single POPs legacy, with an estimated 4.8 to 7.4 million tonnes of disposed waste. The largest part of this waste – 1.8 to 3 million tonnes – was disposed in Europe, where most producers were located. This paper provides a short overview of projects supported by the European Union (EU) to address this waste legacy and to implement the Stockholm Convention for this group of POPs with associated protection of soil, ecosystems and human health. We report here particularly on the results of a project financed by the EU called the “HCH in EU project”, which aimed to develop a systematic inventory of sites where HCH was handled and potentially resulted in contamination. The compiled information provide guidance for competent authorities to further assess their national HCH inventory and to further develop a strategy to address this large POP legacy in future. The systematic inventory revealed that there were at least 299 sites where HCH was handled. These sites include 54 former production sites, 76 pesticide processing plants that used lindane, 59 uncontrolled HCH waste isomer deposits, 29 landfills with HCH waste, 34 former or current storage sites for stocks of obsolete pesticides including technical HCH or lindane, and 16 HCH treatment or disposal sites. Additionally, at 31 of the sites lindane/technical HCH was used in applications with significant risk of soil pollution, such as wood treatment. The number of sites in this latter category is likely higher and will need further assessment. In addition to this inventory, the “HCH in EU project” produced detailed country reports, a guidance document for how to find potentially HCH-impacted sites, and a strategy document for implementing the sustainable management of these sites EU-wide, with proposed actions at the EU, country, and site level. Furthermore, the project has facilitated information exchange and – together with other related EU projects – has led to sharing information and best practices among member states and to establishing a network of authorities and other stakeholders working on the lindane/HCH waste legacy. This collaboration will facilitate a more systematic and better coordinated process to further assess, secure, and remediate the large HCH waste legacy and reduce and control lindane/HCH releases in the EU and possibly beyond. Such a coordinated effort and exchange of information for inventorying and managing contaminated sites might also be useful for other POPs such as PFOS/PFOA or dioxins.

© 2022 The Authors. Publishing services by Elsevier B.V. on behalf of KeAi Communications Co. Ltd. This is an open access article under the CC BY-NC-ND license (<http://creativecommons.org/licenses/by-nc-nd/4.0/>).

* Corresponding author. POPs Environmental Consulting, Lindenfirststr. 23, 73527, Schwäbisch Gmünd, Germany.

E-mail address: roland.weber10@web.de (R. Weber).

Peer review under responsibility of KeAi Communications Co., Ltd.

1. Introduction

Hexachlorocyclohexane (HCH) was one of the most extensively produced pesticide, industrially manufactured mainly after the Second World War [1]. HCH was available in two formulations: technical HCH and lindane. Generally, technical HCH contains the following percentages of HCH isomers: 55–80% alpha (α), 5–14% beta (β), 8–15% gamma (γ), 2–16% delta (δ), and 3–5% epsilon (ϵ) [2]. Of these HCH isomers only the γ -isomer has specific insecticidal properties [3,4]. Lindane contains more than 90% γ -HCH produced by separation of the γ -isomer from the technical HCH mixture [1,4].

The production and application of lindane and technical HCH during the last 7 decades have resulted in environmental contamination of global proportions [1,5–7]. For each tonne of lindane, 8–12 tonnes of other HCH isomers were produced as unwanted by-products [1]. Therefore, the production of the approximately 600,000 tonnes of lindane has generated 4.8 to 7.2 million tonnes of HCH waste isomers [1]. This HCH POP-waste was mostly dumped uncontrolled at many sites in the former producing countries around the world [1,6,7] and were partly released into rivers [8]. Some of the large HCH-contaminated sites have been investigated for example in Brazil [9,10], China [11,12], France [13], Germany [14–17], India [18–20], and Spain [21–23]. Therefore in the case of HCH, the major POP contaminated site load and risk is related to the production and related disposal of HCH waste isomers at and around production sites [1]. The disposal of the major POPs share at the production sites of HCH is different from e.g. PCB where most (likely >95%) of the produced 1.5 million tonnes of PCB was sold as product and most PCB-contaminated sites were then generated along the life cycle of PCBs [24,25]. However also contamination legacies exist at the PCB production sites [26–29].

In May 2009, α -HCH, β -HCH, and lindane (industrial γ -HCH) were listed in the Stockholm Convention as persistent organic pollutants (POPs) due to their persistence, toxicity and long-range transport [30–33]. Toxic effects of HCH isomers include neurological disorders [34,35], cancer [36–38], endocrine disruption [36,39,40], and reproductive disorders [36,41,42]. Thus, as listed POPs these HCH isomers need to be addressed globally, including the obsolete stockpiles and large waste volumes remaining as a legacy from the historical production, use and disposal of HCH [1,43].

Most of the production and use of lindane took place from the 1950s to the 1990s in Europe, with minor use of technical HCH in the late 1940s and early 1950s. This resulted in HCH pollution and an estimated 1.8 to 3 million tonnes of deposited HCH waste isomers from the production of 290,000 tonnes of lindane [1,6,7,43; 44]. In a recent study it was documented for three of the European HCH-contaminated production/disposal sites that the footprint of pollution can increase over time [43]. The study also highlighted the lack of activities on the part of former HCH producing countries to manage their large HCH waste deposits and fulfil their obligations as Parties to the Stockholm Convention, and documented that HCH-contaminated sites were not appropriately addressed in the Stockholm Convention national implementation plans of several European countries [43].

Legacy POP pollution, especially in soils and sediments, is a contemporary issue and human health risk since these POPs can accumulate in free range cattle and chicken, which can lead to human exposure [24,25,45]. For example, the surroundings of an HCH production site in a rural area along the Sacco river (Sacco Valley, Central Italy) were found to be contaminated with HCH (in particular the more persistent waste isomer β -HCH), which has resulted in HCH-contamination of cows and cow's milk as well as human blood in the area [46]. Cow's milk and products from farms

located in the area had high β -HCH levels of up to 0.062 mg HCH/kg [46,47]. This was more than 20 times the regulatory limit of 0.003 mg β -HCH/kg for milk, according to European law (European Commission Regulation No 149/2008). Additionally, HCH released from such waste deposits can leach into ground water and surface water [17] and result in contamination of fish. This has been documented in the Elbe river downstream of the former production sites in Bitterfeld [17]. The release of POPs from landfills and other deposits can strongly increase due to flooding events [48–50], resulting in increased HCH (or other POPs) levels in surface water and in fish, as observed in the Elbe river after a flooding event in 2002 downstream of the former HCH production sites in Bitterfeld and Hamburg [17]. Another study reported that 120 kg HCH are released per year from one landfill in Spain into surface water [22].

The remediation or securing of two HCH deposits was recently documented. A first HCH waste deposit in France from the former lindane producer UGINE-Kuhlmann company was excavated together with the contaminated soil and sent for destruction at various waste incinerators in Europe by the current owner of the site. The remediation of that site has now been finalized [51]. An HCH dumpsite in Spain was transferred to a new established landfill [21], with some HCH releases to the environment during the transfer process [52].

The European Union and its Member States are Parties to the Stockholm Convention, which was first implemented in the EU law by Regulation (EC) No 850/2004 to assess, manage, and eliminate POPs [53]. That regulation was recently replaced by the recast Regulation (EU) 2019/1021 on POPs [54]. The EU developed a first 'Community Implementation Plan' (CIP) in 2007 (SEC (2007) 341). The CIP was first updated with a 'Union Implementation Plan' (UIP) in 2014 (COM (2014) 306 final), and further updated in early 2019 (COM(2018)848 final). In addition, the EU countries have individual national implementation plans (NIPs). Within the UIP, the European Union has financed several projects to assess and address the HCH POP legacy in Europe. An inventory of POPs waste and contaminated sites is a prerequisite for the proper management of certain POPs. Furthermore, the responsible authorities need support for managing, regulating, securing, and remediating large contaminated sites and waste deposits. Therefore, the EU financed a project aiming to develop an inventory of HCH production sites, waste deposits, landfills, and treatment centres in the EU, and to assist local, regional, or national public authorities confronted with lindane and HCH-related issues by providing them with support, expertise, advice, and consultancy. Our paper describes the major outcomes of this project and provides an overview of other EU-financed projects aiming to address the HCH/lindane legacy. This is part of the implementation of the Stockholm Convention and contributes to the protection of soils, ecosystems and human health.

2. Methods

2.1. Assessment of the HCH contamination of EU member countries and methodology development

As part of the "HCH in EU project," the European sites where HCH were handled were mapped following a stepwise approach, starting from the list of countries where lindane/HCH was produced [1]. The EU-member states on this list were Austria, Croatia, Czech Republic, France, Germany, Hungary, Italy, Netherlands, Poland, Romania, Slovakia, and Spain. In the second step draft country specific lists of known sites where lindane/HCH was handled were compiled, and these draft country specific lists of sites were shared with all known relevant stakeholders, and the lists were updated based on the feedback received.

Additionally, a literature survey of HCH-contaminated sites in

Europe was conducted and related information, including peer reviewed publications, national implementation plans, national reports, and grey literature screened and relevant information compiled. Further, information was reviewed from the thirteen Forums of the International HCH and Pesticide Association (IHPA 2013), which has been working to address this legacy for the past 30 years and has generated detailed information on HCH sites [55] and pertinent information was extracted.

Also Regional and local authorities and other stakeholders were interviewed and compiled a list of all countries with HCH production with the support of national teams. This outreach campaign ended with two open online workshops used to present the project results and request help with identifying further sites. The country specific lists of sites were again updated based on this information received during the outreach campaign.

Furthermore, different types of sites where HCH/lindane was handled were defined and compiled (see Section 3.2.1). Based on this structured assessment, a methodology was developed that can be utilized by countries to further map and assess HCH-contaminated sites in a systematic manner (Section 3.5). In addition, potential co-pollutants (POPs and other hazardous pollutants) were assessed and compiled for the different site types (see Section 3.3). Specific monitoring or analysis of soils or sediments were not conducted as part of this project since the focus of the project was the compilation of information available in institutions and literature and not to generate monitoring data.

2.2. Compilation of other EU funded projects related to HCH management

Activities of other EU funded projects dealing with the HCH legacies in the European context and supporting the implementation of the Stockholm Convention for this POP group were mapped, assessed, and summarized. For this the respective project documents were evaluated and, for some of the projects, contacts were made stakeholders involved in the current and former project activities to compile additional relevant information and for verification of findings.

3. Results and discussion

3.1. Projects conducted or currently implemented for addressing HCH and lindane contamination in the European context

In addition to our “HCH in EU project” (Section 3.1.1 and Sections 3.2–3.6), we identified five other EU-funded initiatives aiming to address the HCH/lindane legacy in Europe. Below we give an overview on the different scopes, methods, and approaches of these projects and studies and some major outcomes to date.

3.1.1. EU pilot project “HCH in EU project” reviewing the presence of lindane and HCH sites in the EU

The project consortium consisted of TAUW, CDM Smith Europe GmbH from Germany, and Sociedad Aragonesa de Gestión Agroambiental (SARGA) S.L.U from Spain. Because the project spans various international parties and locations, good cooperation and sharing of information was/is essential. To facilitate this, the project uses tailor-made digital environments including a Geographic Information Model (GIM) to collect, organize, store, interpret, assess, and report all inventory data from the different locations. The GIM Viewer is available to the project team members, the European Commission, and project stakeholders, and will be made available to the public.

The project consortium conducted the “HCH in EU project” to evaluate and address the presence of lindane and HCH in the EU. The diffuse pollution from the use of lindane/HCH in agriculture

and forestry was not in the scope of the project. This pilot project included the following objectives:

- (1) provide an overview of the legacy of the lindane and technical HCH production in Europe (for outcome see Sections 3.2 to 3.3);
- (2) to assist EU activities currently developing best practices for the sustainable management of HCH contaminate sites at six HCH contaminated pilot test sites (see Section 3.4);
- (3) a report on the use and legacy of HCH in the EU, as a guide to help identify further potentially HCH-impacted sites in addition to the ones already in the inventory (See section 3.5);
- (4) a guidance to develop an EU-wide strategy to sustainably manage HCH-impacted sites, to address the legacy of HCH and lindane in the EU (See Section 3.6).

Webinars including a final workshop were conducted within the project to inform policy makers and other stakeholders as well as the interested public (https://lnkd.in/dzjb_hD).

In total, 299 sites where HCH and lindane were produced or handled and therefore seen as potentially HCH-contaminated sites were identified. The major outcomes of this project are compiled in Sections 3.2 to 3.6 below.

3.1.2. Project LIFE DISCOVERED

The project LIFE12 ENV/ES/000761 with the acronym DISCOVERED LIFE – “Lab to field, soil, remediation demonstrative project: New ISCO application to DNAPL multicomponent environmental problem” (01/2014–06/2017). The project was led by the authorities of Aragon together with the Sociedad Aragonesa de Gestión Agroambiental (SARGA) and the International HCH & Pesticides Association.

This project addressed the contamination at the HCH/lindane megasite in Sabinanigo south of the Pyrenees, where the company Inquinosa has dumped several hundred thousand tonnes of HCH-waste over decades [22], with large associated practical challenges, health risks and remediation costs. At present, tests are being performed to destroy and eliminate the heavy layers of oily pesticide residues laying on the bottom of the aquifer.

The project dealt with a pilot scale chemical oxidation technique of dense contaminants and pesticides existing in the Bailín aquifer, Sabinanigo (Huesca). One of the main tasks is the implementation of a pilot test based on an ISCO with activated persulfate technique which addresses the oxidation of the DNAPL with the aim of assessing the risk reduction and evaluating the transferability of the technique from lab to field. The ultimate goal: to clean up the site and reduce the existing pollution load by chemical oxidation of the contaminants and pesticides and their transformation into less harmful compounds, was achieved for all the objectives set out in it: the use of the in situ chemical oxidation (ISCO) technique has demonstrated its feasibility at the site, with successful results in the degradation, greater than 90% on average, of:

- the residues of HCH (Lindane manufacture's residues)
- and of the intermediate metabolites existing in the site (polychlorinated benzenes and phenols), that on average suppose more of the 90% of the organic compounds present in the contaminated water).

The study also assessed the formation of polychlorinated dibenzo-p-dioxins and dibenzofurans (PCDD/PCDFs) as by-products (see Section 3.3.2).

The project produced a movie about this site, since pictures can

transmit another part of the story than reports and data. The film won an international award and was shown at the 13th International HCH & Pesticide Forum organized as part of the predecessor project [56]. This forum brings together all stakeholders working on HCH and other pesticide-legacy issues and technical solutions, as well as also politicians that support political solutions [55].

3.1.3. EU project LIFE SURFING

The EU LIFE SURFING 2019–2023 project is led by the authorities of Aragon together with the University of Madrid, the University of Stuttgart, and the International HCH & Pesticides Association. This project deals with the same area and contamination as in the Project LIFE DISCOVERED. The project aim to develop a practicable remediation technique for soils with non-aqueous phase liquids (DNAPL). This technique will be developed in a demonstrative project that will combine the use of chemical oxidation techniques with the action of surfactants. A project website has been established where project background and details can be found and outcomes will be reported (<http://www.lifesurfing.eu/en/life-surfing-project/>)

This project includes the organisation of the 14th International HCH & Pesticides Forum (the event was originally planned for 2021, but had to be cancelled due to COVID-19 and is currently planned for end 2022 or beginning 2023 depending on the results of the field tests).

3.1.4. EU Interreg Project LINDANET

The EU Interreg LINDANET 2019–2023 project addresses 6 EU regions that are seriously confronted with HCH problems due to the local productions of lindane: Aragon and Galicia (Spain), South Bohemia (Czech Rep), Sachsen-Anhalt (Germany), Lazio (Italy), and Silesia (Poland). These regions are represented by the Government of Aragon, the Government of Galicia (General Directorate of Environmental Quality and Climate Change), the Regional Development Agency of South Bohemia - RERA a.s., the State Office for Contaminated Soils of Sachsen-Anhalt (LAF), the Experimental Zooprofilactic Institute of Lazio and Toscana (IZSLT), and the Central Mining Institute, respectively.

The project has set the following general objectives:

- To create a network of European regions affected by contamination derived from lindane production wastes (HCH and others),
- To establish an Action Plan focused to the solutions to the problems in each region,
- To exchange experiences and knowledge that contribute to addressing the contamination derived from the HCH and lindane production wastes,
- To involve all stakeholder groups in the knowledge generation and the solution to the problem,
- To contribute to the Policy Learning Platform of the Interreg Europe programme,
- To raise public awareness about the HCH pollution and other related contamination problems derived from POPs and Obsolete Pesticides.

As of now, four Interregional Thematic Workshops have been held. The partners have also organized in their regions 18 Stakeholder workshops and meetings, and 2 exchanges with the HCH in EU project. Additionally, 1 Thematic Workshop is taking place by the end of November 2021. All workshops were in webinar format due to COVID-19. After November, the plan is for each partner to implement Action Plans during the following year, after receiving approval from the Project secretariat.

In 2021, the LINDANET project conducted a SWOT analysis that

identified the most important elements needed for remediation: long-term funding, partnerships, and political endorsement. The LINDANET project has confirmed the overall benefits of inter-regional cooperation, forward looking approach, and the need for a permanent platform for sharing knowledge and experiences derived from all aspects of lindane contamination management and remediation. The strategy going forward is also recommending to also include governance, transparency, and awareness raising as important themes in the LINDANET Action Plans now under design and implemented during 2022 and beginning of 2023. But the lack of long-term financing, partnerships, and political endorsement are seemingly insurmountable barriers that need to be tackled to achieve a final solution for the mega-sites in the LINDANET partner regions. Additionally, more R&D projects are needed, to help bring down remediation costs. Additional EU support for the Regions is also needed.

The EU Interreg Project LINDANET has developed a project website where further information can be found and followed (<https://www.interregeurope.eu/lindanet/>).

3.1.5. EU project LIFE POPWAT

The EU LIFE POPWAT 2020–2024 project is led by the University van Liberec in the Czech Republic in cooperation with the water treatment companies Photon Water (Czech Republic) and SERPOL (France) and the University of Aarhus (Denmark). With the help of so-called “Wetlands + system”, Wetland+ is a highly adaptable system that integrates a series of reactive zones along a drainage pathway avoiding the need for pumping. Reactive zones comprise zerovalent iron (reducing environment), a sorbent material zone, a biodegradation zone and a wetland zone, which is principally to polish residual biological oxygen demand from the preceding steps. HCH and lindane-contaminated waters are treated effectively in a very simple way. Two such water treatment plants are under construction at two different locations, one where lindane was produced at the former Azot factory in Jaworzno in Poland, and one in Hajek in the Czech Republic, where 3000 tonnes of HCH-containing waste were dumped. After testing the treatment plants at these two sites, the plan is to construct the same type of treatment plants at five other lindane production or HCH waste dump sites, so that these site owners can take advantage of the experiences gained at the initial two sites. Since the assessment and management of legacies from HCH production sites are complex, there is great need for such cooperation and information exchange that can eventually create synergies.

Also the EU Project LIFE POPWAT has developed a project website where further information can be found and followed (<https://cxi.tul.cz/lifepopwat/>).

3.1.6. Project Citizens' Rights and Constitutional Affairs

In 2015, a study was commissioned by the European Parliament's Policy Department for Citizens' Rights and Constitutional Affairs at the request of the Committee on Petitions (PETI). The related report, published in 2016, provided an updated mapping of the lindane production plants and HCH waste dumping sites in the EU [57]. Potential remediation techniques, including lessons learned implementing these techniques in the laboratory and field, were also provided together with a selection of best practices for contaminated site restoration and stakeholder engagement. The study also analysed information on lindane from official websites [57]. Therefore, their report served as one of the information sources for the HCH inventory of the “HCH in EU project” described in this publication.

3.1.7. EU legal framework that facilitates monitoring of HCH/POPs

The Water Framework Directive (WFD [58]; includes many POPs

and imposes monitoring obligations on Member States to progressively reduce emissions, discharges, and losses of priority substances to waters. The WFD establishes two types of environmental quality standards (EQS) for priority substances: annual average concentrations and maximum allowable concentrations. All HCH isomers are included in the list of priority substances. EQS have been established for lindane as well as for the sum of HCH isomers.

Different monitoring activities for POPs in air, including HCHs, have been conducted or are ongoing in the EU. EMEP (European Monitoring and Evaluation Programme) is the co-operative programme for monitoring and evaluation of the long-range transmission of air pollutants in Europe. It is a scientifically based and policy driven programme under the UNECE Convention on Long-range Transboundary Air Pollution. EMEP's activities are supported through the work of a number of EMEP centres and task forces (<https://www.emep.int/>). As of 2016, EMEP operates 12 active sampling sites that have long-term monitoring data for POPs in air and aerosols. Six of these sites have a co-located MONET passive sampler and were therefore selected for a recent study: Birkenes (Norway), Košetice (Czech Republic), Pallas (Finland), Råö (Sweden), Stórhöfði (Iceland) and Zeppelin (Norway/Svalbard). Each of these EMEP active samplers has been monitoring some legacy POPs since at least 2004 [59]. Such monitoring activities can

give valuable complementary information on the status of and trends in HCH emissions.

In absence of an EU soil legislation, there are currently no common provisions on the presence of lindane or HCH monitoring and assessment in soil. However, such standards and screening values exist in several national legislations. The EU Soil Strategy for 2030 recently announced that the Commission will table a new legislative proposal by 2023 to achieve good soil health across the EU by 2050. In this context, the Commission will consider proposing legally binding provisions for the identification, registration and remediation of contaminated sites.

3.2. Inventory of HCH sites in EU where HCH was handled (main task 1 of the “HCH in EU project”)

As mentioned above, a major goal of the “HCH in EU project” was the development of an inventory of sites where HCH/lindane was handled and disposed of in the past. The inventory of a POP is the basis for managing that specific POP and prioritizing action. In our earlier review of the lindane production and HCH legacy, we already compiled the major countries that had HCH/lindane production and their estimated amounts of disposed waste isomers [1].

One of the tasks of the “HCH in EU project” was to make an inventory of potentially HCH-impacted sites in Europe. By this

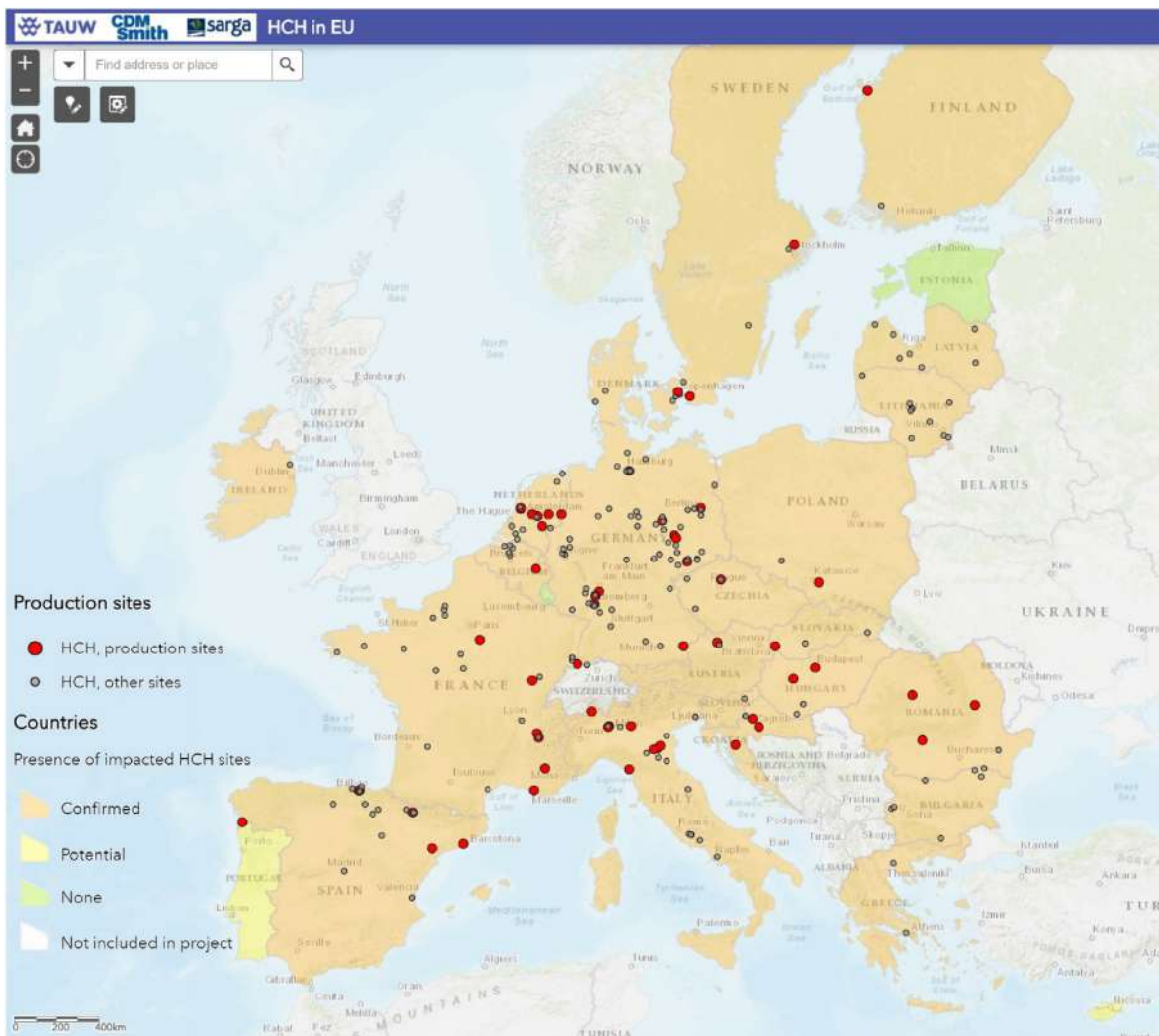


Fig. 1. EU overview map with 299 identified sites where HCHs were handled, including 54 high-risk sites.

Table 1
Summary of the EU-wide inventory of sites where lindane and HCH handling was confirmed developed and compiled within the “HCH in the EU project”.

Category	Description	Number	Remarks
Production sites	Sites where technical HCH and/or lindane were produced	54	When not remediated, these are mostly high-risk sites close to urban settlements, often with HCH-waste deposits.
Processing sites	Sites where technical HCH and/or lindane were processed or formulated into market-ready pesticides	76	This is only the tip of the iceberg, as most pesticide producers between 1950 and 1980 used lindane.
Waste deposits	Sites where lindane production wastes (HCH) were dumped without proper containment	59	Often in the direct vicinity of production sites; when not remediated, these are mostly high-risk sites.
Landfills	Sites where lindane production wastes (HCH) were disposed of with some containment measures	29	These sites are usually connected to large production facilities. The distinction between landfills and waste deposits is vague.
Storage facilities	Storage facilities for obsolete stocks of POP-pesticides, including lindane and HCH	34	Present in former socialist countries, these sites are often large collection points of obsolete pesticides where lindane is only a minor component.
Treatment centres	Incineration facilities, soil treatment centres, and recycling centres	16	These facilities are state of the art and operate in controlled environments. Environmental impacts of HCH released from these locations are unlikely.
Use sites other than agricultural use	Sites that do not fall under the above categories, but lindane/technical HCH was used there for other purposes. Examples include wood treatment/preservation facilities.	31	Alternative uses of lindane in products were found during the inventory project. These are described in a separate project report to help further expand the country specific site inventories.

Table 2
Overview of identified sites where HCH/lindane handling was confirmed developed and compiled within the “HCH in the EU project”.

Country	Total Sites	Production sites	Processing sites	Waste deposits	Landfills	Treatment centres	Storage facilities	Other
Austria (AT)	2	1	0	1	0	0	0	0
Belgium (BE)	6	1	3	1	0	1	0	0
Bulgaria (BG)	7	0	0	0	0	0	7	0
Croatia (HR)	2	1	1	0	0	0	0	0
Cyprus (CY)	0	0	0	0	0	0	0	0
Czech Republic (CZ)	4	1	1	0	1	0	0	1
Denmark (DK)	8	1	5	2	0	0	0	0
Estonia (EE)	0	0	0	0	0	0	0	0
Finland (FI)	3	1	1	1	0	0	0	0
France (FR)	38	6	7	13	2	2	0	8
Germany (DE)	98	12	32	20	13	11	6	4
Greece (EL)	2	0	2	0	0	0	0	0
Hungary (HU)	5	1	3	1	0	0	0	0
Ireland (IE)	1	0	0	0	0	0	0	1
Italy (IT)	38	8	8	6	0	0	0	16
Latvia (LV)	7	0	0	0	0	0	7	0
Lithuania (LT)	10	0	0	1	0	0	9	0
Luxembourg (LU)	0	0	0	0	0	0	0	0
Malta (MT)	0	0	0	0	0	0	0	0
Netherlands (NL)	18	7	6	0	2	2	1	0
Poland (PL)	3	1	0	0	1	0	1	0
Portugal (PT)	0	0	0	0	0	0	0	0
Romania (RO)	12	3	1	7	0	0	1	0
Slovakia (SK)	5	1	1	0	1	0	2	0
Slovenia (SL)	2	1	0	0	1	0	0	0
Spain (ES)	22	6	2	6	8	0	0	0
Sweden (SE)	6	2	3	0	0	0	0	1
Total	299	54	76	59	29	16	34	31

project now all inventory data for the discovered sites where HCH was handled or disposed in all the EU member states are stored in the Geographic Information Model (GIM). This enables now countries to localize sites where it is confirmed that HCH was handled and therefore could be potentially impacted by contamination (see Fig. 1). For each EU country a report providing a country specific list of such sites was developed (number of sites in Table 2).

The “HCH in EU project” found a total of 299 sites where HCH and lindane have been handled (Tables 1 and 2). These sites were subdivided into 7 categories (see Table 2 and description in section 3.3): Of these, 54 were former production sites which were estimated to be high-risk sites, with potentially significant impact on people and the natural environment. Many of the high-risk sites are mega-sites with large amounts of deposited HCH waste and extensive contamination of soil and groundwater, which is still spreading into the environment. Furthermore, there are 59

uncontrolled HCH waste deposits, 29 landfills with HCH, 76 pesticide formulation plants that used lindane, 34 current or former storage sites for stocks of obsolete pesticides including HCH or lindane, 16 HCH and lindane treatment or disposal sites, and 31 other sites where lindane or technical HCH was used or handled. Lindane was used in a wide variety of formulations, including: wettable powders; emulsion concentrates; suspensions; solutions; dusts and powders; granules and coarse dusts; baits; preparations for fumigations, aerosols, and special formulations such as powder, solutions, and creams for the use in the fields of human and veterinary medicine, wood treatment or use as plastic additive (see 3.2.1.7) in addition to the major use in agriculture [3]. Because of these diverse uses and formulations of lindane and considering the lindane life cycle (see Fig. 2), it is important to further investigate the category of ‘other’ sites which is certainly much larger than the 31 sites compiled in this first inventory also including the

Life cycle of HCH and Lindane

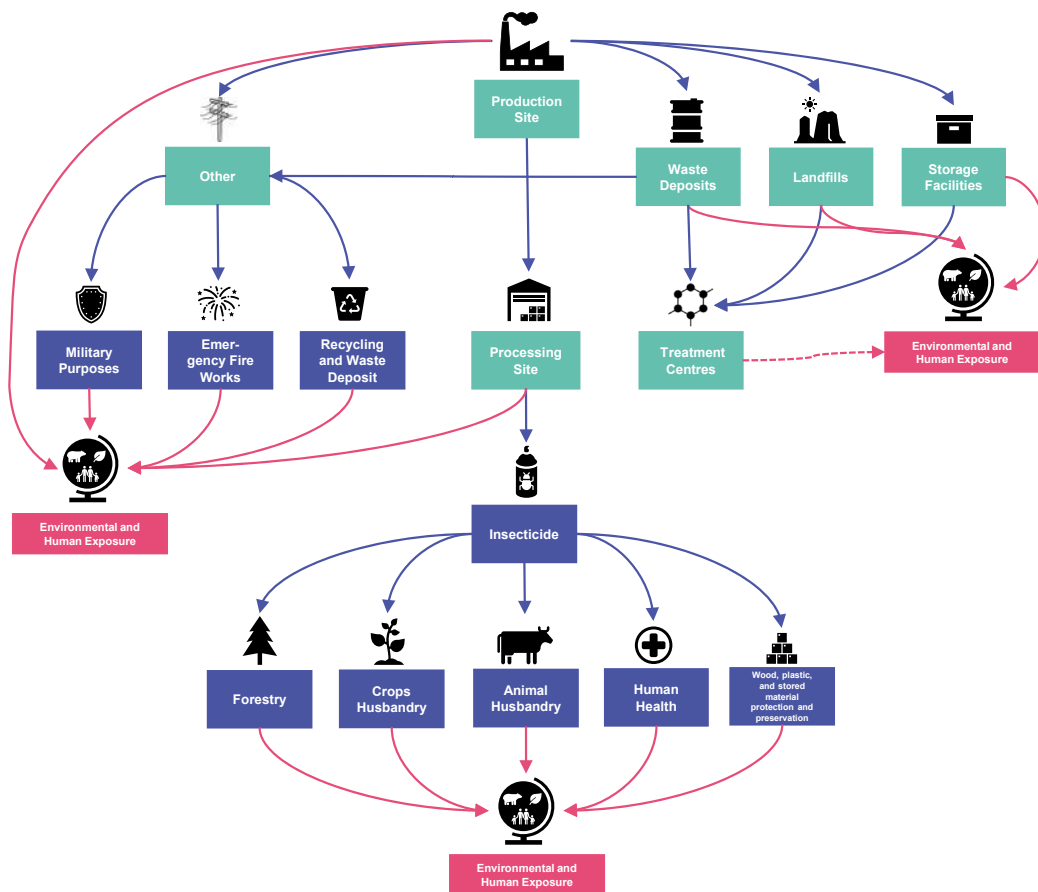


Fig. 2. Lifecycle of former HCH production and use and contemporary impact on the environment and humans.

application sites (see 3.2.1.7). This to alert authorities and owners of such sites where the onsite use of lindane might have resulted in soil contamination.

3.2.1. Categories of sites where HCH was handled

In the first phase of the project, the different categories of sites where HCH was handled were defined to develop a systematic approach for inventory development for the pilot countries. This provides a methodology for other countries to develop HCH inventories through a systematic assessment of the different site types.

Tables 1 and 2 provide an overview of the site types and the number of sites where HCH is/was handled for each of the 27 EU countries. As mentioned, a total of 299 sites have been identified in the EU where lindane or HCH were handled (Tables 1 and 2). Many other sites are suspected to have handled HCH/lindane in particular the application sites other than agricultural use (e.g. wood treatment sites, military uses or cable production), however the evidence uncovered as part of this project was insufficient to confirm more of these sites, therefore they were not added to the inventory.

3.2.1.1. Production sites. Within the entire EU, a total of **54 former production sites** were identified. The size of these production sites varies from massive production facilities such as the Inquinosa site in Spain, with up to 1000 tons/year of lindane production capacity, to small factories such as the one in Valentuna, Sweden, with 500 kg/year production capacity.

3.2.1.2. Formulation sites. A total of **76 processing sites** were identified, however this is likely only the tip of the iceberg. Lindane/HCH was a commonly available product between 1950 and 1980 and was an active ingredient in a variety of pesticides. Most pesticide production companies that operated between 1950 and 1980 have likely used lindane at some point during their existence. The exact impact of lindane/HCH use at these sites is difficult to estimate and will depend on the scale of their activities in relation to the use of lindane/HCH and the respective waste management and the sites.

3.2.1.3. Waste deposits. **59 waste deposits** were identified across the EU. Often these waste deposits received wastes from multiple sites over prolonged periods of time. HCH wastes were often mixed with other (household) wastes. This is a problem particularly common in Germany, and to a lesser extent in France.

3.2.1.4. Landfill sites. **29 landfills** were identified across the EU. Most of these landfill sites were dedicated to the receipt of HCH wastes and are connected to large production facilities. The distinction between landfill and waste dump is often vague as quite a few landfills lacked/are lacking appropriate containment measures.

3.2.1.5. Treatment centres. In total, **16 treatment centres** were identified. These include incineration facilities, soil treatment

centres, and recycling centres. Most of these facilities are state of the art, highly controlled environments, and adverse impacts of HCH released from these locations are unlikely.

3.2.1.6. (Former) storage facilities. **34 current and former storage facilities of (obsolete) pesticides** are still present, mainly in former Eastern bloc countries. Most of these storage facilities are large collection points of different obsolete pesticides, of which lindane is only a minor component. The largest storage facility identified, in Bulgaria, contains approximately 2000 kg of lindane. Most storage facilities contain less than 200 kg of lindane or have already been cleared but contamination of soils at or around these sites are likely.

3.2.1.7. Major historical uses of technical HCH/lindane and related potentially contaminated sites. As mentioned in the introduction, 290,000 t of lindane were used in Europe for different purposes with some use of technical HCH in the late 1940s and early 1950s [1], mainly for agricultural use on a large share of Europeans agricultural fields for many crops (Table 3) with major uses in Czechoslovakia, Germany, Italy, France, Hungary, Spain, Russia, Ukraine, Yugoslavia and Greece [6,7]. Some HCH contamination can be found in these areas where lindane or technical HCH was used in the past 70 years, such as in agricultural areas or where veterinary applications like sheep dips were performed [12,60–63]. Due to the moderate persistence of gamma-HCH in soil of approximately 2 years [64] and the moderate volatility, the agricultural soils treated in the 1950s–1990s with mainly lindane contain now HCH concentrations below levels considered polluted [12] and are not considered contaminated sites. However, former mixing areas and storing areas for agricultural and other uses might be contaminated at higher level (Toichuev et al., 2016). Furthermore for some uses of HCH containing pesticides, larger amounts were applied on small space which have likely resulted in elevated contamination of soils (e.g. wood treatment sites) and might possibly still be contaminated sites/hot spots. We identified five different types of such historical uses of technical HCH/lindane (see below). The inventory project identified **31 such “other” sites**, including wood treatment/preservation facilities.

3.2.1.7.1. Use site type 1: agricultural areas

3.2.1.7.1.1. Crops

HCH and lindane were used as a broad-spectrum insecticide for

a wide variety of fruit and vegetable crops (including seed treatment), tobacco, (greenhouse) vegetables, and ornamentals. HCH and lindane are applied to crops through a variety of different methods, depending on the desired pest control. Elevated concentrations of HCH are expected in areas where the insecticide was applied. Hotspots are also expected in areas where technical HCH/lindane was stored, mixed, or otherwise handled prior to application. Table 3 provides an overview of the areas of use, plant types, treatment application methods, and potential legacy.

3.2.1.7.1.2. Animal husbandry

Lindane was also used against ectoparasites in veterinary applications and in the treatment of domestic animals and fish (Table 4; [3]), leading to increased incidence of certain cancers in farmers [61,62]. The current inventory assessment in Croatia (HR-PL-01) lists a product named Gamacid® T-50, which was produced until 2005 by the pharmaceutical company Pliva Ltd., later Veterina Ltd. The preparation was registered for the treatment of sheep, by dipping them in medicinal bath containing lindane in concentration of 0.03–0.06% for pest control against ectoparasites.

For the external treatment of mange, mites, ticks, fleas etc., dips, sprays, washes, and dustings are used. To ensure optimal contact, such as for mange or lice, animals (such as sheep and other livestock; Table 4) are dipped in baths with various concentrations of pesticides. Sometimes animals are submerged two or three times, and the process can be repeated. In New Zealand assessment of the environmental contamination from sheep dips with POP pesticides have been conducted and a guideline for local authorities were developed/published for systematic assessment and risk management of such sites (Ministry for the Environment New Zealand 2006). Therefore, dipping, mixing and pesticide storage areas at farms having used cattle dipping can be considered contamination hotspots.

3.2.1.7.2. Use site type 2: health care. Lindane was also used in human health care for treatment against ectoparasites. For example, to treat lice or scabies on the head or elsewhere on the body, a lotion or shampoo with a concentration of 0.5–1% of lindane was used. The second line treatment for head lice and scabies was originally exempted under the Stockholm Convention [33], but this exemption was revoked in 2019 by Stockholm Convention decision SC-9/1 [66].

Lindane was also applied in closed rooms, by spraying,

Table 3
Principal areas of major lindane agricultural use (adapted from [3]).

Areas of use	Plant types	Application methods	Potential legacy
Field crops	Peanut, sugar beets, sugar cane, cereals (oats, wheat, barley, rye), cotton, flax, abaca, jute, kenaf, ramie, sisal, maize (American corn), sorghum, millet, oil crops (rape, mustard, castor, sunflower, safflower, sesame, oil poppy, oil palm), potatoes, rice (paddy), soya, tobacco	Bran bait, drenching, dust, fumigation, irrigation water, seed, spray, storage, soil	Hotspot areas: sites with storage, mixing, or washing of pesticides (tanks and land/spray machines) Diffuse areas: elevated concentrations in the topsoil, sediments, and drainage systems
Vegetable crops	Garlic, onions, leeks, shallots, asparagus, artichokes, chicory, okra, sweet potatoes, manioc (cassava), celery, carrots, fennel, cruciferous plants (cabbage, cauliflower, brussels sprouts, broccoli, radish), cucurbits, beans, peas, lettuce, spinach, tomatoes, aubergines, peppers, chillies, mushrooms	Casing, compost, drench, dust, foliage, root, packaging and transport materials, fumigation, spray, soil	
Fruit crops	Citrus, cacao, coffee, tea, tropical fruits (avocado, banana, date, fig, guava, lychee, mango, papaw, pomegranate, pineapple), nut fruits (walnut, hazel, Brazil nut, kola nut, pecan), olive, stone fruits (peach, plums, prunes, apricot, almond, sweet and sour cherries), small fruits (gooseberry, currants, raspberry, strawberry), pome fruits (apple, pear, quince)	Aerial treatment, drench, dust, spray, storage, soil	
Viticulture	Vine grapes	Bran bait, drench, foliage, spray	
Ornamentals	Various	Bran baits, bulb, dip, drench, soil	
Pasture and forage crops	Lucerne (alfalfa), clovers, pastures (grasses and other low plants)	Bran baits, dust, spray, soil	

Table 4

Principal areas of use for veterinary applications and treatment of domestic animals (adapted from [3,65]).

Areas of use	Animal type	Treatment type	Potential legacy
Veterinary and domestic animals	Dog	Powder	Hotspot areas: sites with pesticide storage, mixing, and dipping, and where the basin was drained
	Cattle	Spray, spot treatment, dip, powder	
	Goats, sheep	Dip, spray, spot, soil	Diffuse areas: elevated concentrations in the topsoil, sediments, and drainage systems
	Pig	Dip, spray	
	Poultry	Spot, spray houses	
	Rabbit	Not registered	
Fish (carp)	Spray or solution		

fumigating, or dusting against for example the common house fly, mosquitoes, bugs, etc. It was also used via spraying or dusting in open spaces, such as for combating mosquitos breeding sites.

An example of indoor pest control applications is for example the patented Vulcan-O fumigator bulb, which contains a heating resistor (Fig. 3). Tablets containing lindane could be inserted through holes in the outer glass, and when the lamp was switched on the tablets melted and gave off fumes. Past indoor applications of lindane have resulted in reported deaths, particularly for babies [36].

The potential legacy of these treatments is expected to be minimal due to the local application for indoor pest control, clothes, and body treatment. However, if done on larger scale and extended time, these types of applications could have led to hotspots and contamination inside houses.

3.2.1.7.3. Use site type 3: forestry. Lindane was used in forestry for pest control (Fig. 4). Different application methods were used to protect individual, rows, and groups of trees. Depending on the tree type, application methods performed included soil, spray, fogging, dust, bran baits, lure trees, and aerial foliar applications. Therefore, pesticide storing and mixing areas on forestry sites are potential contamination hotspots. In areas where aerial foliar application was used, the spraying plane, washing stations and the mixing tanks on airstrips are additional hotspots (Toichuev et al., 2016). The topsoil, sediments, and drainage systems where forestry took place are areas where diffuse contamination could have occurred.

3.2.1.7.4. Use site type 4: treatment of wood, plastic, and stored material protection and preservation. Wood treatment. Many types of industrial materials manufactured from wood and cellulose derivatives and are subject to attack by insects, especially termites, wood wasps, and beetles (woodworm). To control these pests, insecticides such as lindane were applied by dipping, immersion, painting, smoking/fumigation, spraying, and mixing paints (see Table 5). Wood protection is achieved mainly through fumigation or deep impregnation [67].

From the 1960s to the 1980s, in Germany, as well as in other countries, wood preservatives containing lindane, DDT and PCP were used on non-load-bearing components, which were often used by end consumers as well as by professional builders. Such treated wood was widely used and did not need a test mark or inspectorate approval. The EC Biocide Directive of 1998 (replaced by Regulation 528/2012) was transposed into German law by the Biocidal Act of 2002. Biocidal products are since then authorised only if it can be proven that they have no unacceptable effects on humans, animals, or the environment.

A wide range of former wood treatment sites exist in the EU [68]. These sites where lindane solutions were used as wood preservatives have normally multiple contaminants, since different cocktails of fungicides and insecticides were used for the wood treatment (see below Section 3.3.4).

The “HCH in EU project” identified a site of a company formerly known to manufacture products for interior decoration, paints, and varnishes, and which used to be the market leader in wood preservatives. It was revealed that this company was also a formulator of HCH/lindane preparations in different products.

In addition to the wood treatment sites, many older buildings containing wood structures are contaminated with lindane and other former wood treatment of lindane (and other pesticides) in Application which was for example detected in German historical buildings, such as churches [69].

Plastic additive: Lindane was used as pesticide in PVC plastic cabling in the outer sheath of the cable while it is being extruded. It was used in high tension cables, to protect against termites at levels of 0.02% [70]. The controlled release of these active ingredients from the plastic where considered to provide long-term protection.

Areas where plastic cables were produced are suspected HCH contamination sites, and areas where the wood and timber industry stored, mixed, or applied insecticides are considered contamination hotspots.



Fig. 3. Vulcan-O lamp used in combination with lindane tablets for pest control (website of lampes-et-tubes <http://lampes-et-tubes.info/sp/sp028.php?l=d>).

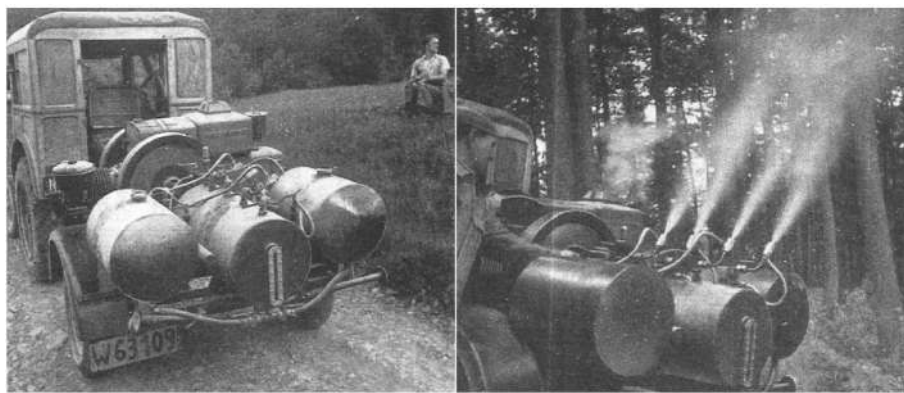


Fig. 4. Borchers' fumigation tanks used in forestry (Sinreich, A., 1952, über die Wirkung neuzeitlicher Insektizide auf die Gliedertier bei Forstschädlingsbekämpfungen 153–165, Mitteilungen der forstlichen Bundes-Versuchsanstalt Wien, Volume 48 1952).

Table 5
Principal areas of use and treatment type per parasite (adjusted from [3]).

Areas of use	Parasite type	Treatment type	Potential legacy
Timber and plywood	Ants, termites, wood wasps, beetles	Dip, painting, smoke/fumigation, spray, mixing in glue (plywood),	Hotspot areas: sites where production, storage, application, mixing and washing of pesticides occurred
Plastics	Termites	Mixing	Diffuse areas: elevated concentrations in the topsoil, sediments, and drainage systems
Storage of goods and industrial or agricultural materials	Termites, moths, silverfish, cricket, bugs, beetles	Fumigation, immersion, spray	

Storage areas. Prior to storage of goods and industrial and agricultural materials in warehouses, ships, silos, etc. prophylactic treatment could have been applied to the walls, floors, ceilings, etc. (see Table 5). The rooms were mainly disinfected using fumigation, since certain areas were difficult to reach by direct treatment. Specially constructed atomising or fumigation equipment was used, or a simple container or bucket that was gently warmed on a heater to produce smoke. Storage sites for industrial materials are also suspected contamination sites and could even be potential hotspots, since stored products needed to be protected from possible pests.

3.2.1.7.5. *Use site type 5: use of HCH isomers for military purposes.* A special application of HCH isomers is reported by Heinisch [71]. Until 1977, in the former German Democratic Republic (GDR), Falima in Magdeburg delivered annually 120 tonnes HCH isomers for “final products” to the VEB Pyrotechnik, Silberhütte in Freiberg. Here, the HCH isomers were mixed with 10% Aluminium powder to produce smoke generating devices (“Nebelkörper”), including smoke grenades for the National People's Army (Volksarmee). These products were also supplied to the Soviet Army. VEB Pyrotechnik also produced smoldering fog tools called “Hexaschwelkörpern” for mills and ship fumigation, as well as frost protection smoke creators. The related contaminated sites are mainly military training areas.

3.3. Co-pollutants at sites contaminated with HCH

Co-pollutants generated from the production or recycling process are important information for polluted site assessment and remediation. Also co-pollutants used in application sites are relevant in the same sense. This section briefly summarized information on co-pollutants considered relevant for selected HCH-contaminated sites.

3.3.1. Chlorobenzene and chlorophenol and derivatives

HCH waste isomers at some lindane production sites were recycled into chlorobenzenes (Fig. 5; [14,72,73]). These chlorobenzenes were partly sold as commercial products or used as intermediates for the production of other organochlorines, such as chlorophenols, and pesticides, such as 2,4,5-T and bromophos [14]. At one of these production sites high amounts of chlorobenzene have been discovered in soil and groundwater. It was estimated based on comprehensive monitoring that 550 tonnes of chlorobenzene are still in the soil from the recycling activities, exceeding even the amount of HCH in soil (260 tonnes) [15]. The other pesticide products, such as 2,4,5-T and bromophos and their degradation products, might also be present in soils and groundwater at these sites. There is continuous pumping at the site and the pumped residues are incinerated [15].

Additionally, high levels of chlorobenzene and chlorophenols were reported in the dense nonaqueous phase liquid (DNAPL) phase in an HCH landfill from a lindane production site in Spain [22,74].

3.3.2. Polychlorinated dibenzo-*p*-dioxin and dibenzofurans (PCDD/PCDFs)

PCDD/PCDFs were formed during HCH production, in particular in the recycling of HCH waste isomers for the production of chlorobenzenes and other pesticides, including 2,4,5-T (see Fig. 5). The α -, β - and δ -HCH waste isomers contained dioxin levels ranging from 0.8 to 300 μg toxic equivalents (TEQ)/kg [75]. Three types of waste were generated in this recycling of HCH and the related 2,4,5-T production (Fig. 5). The thermal decomposition of HCH to trichlorobenzene produced the so-called decomposer residue, with levels of PCDD/PCDFs in the percent range (1.4%–2.7%) and TEQ in the high parts per million range (90–230 mg/kg) [14,72]. The TEQ of the “Anisol” waste fractions was around and below 1 mg/kg [14]. The acidic waste fraction (so-called R-acid) formed in the production of 2,4,5-T contained 1–330 mg 2,3,7,8-TCDD (TEQ) [76]. The

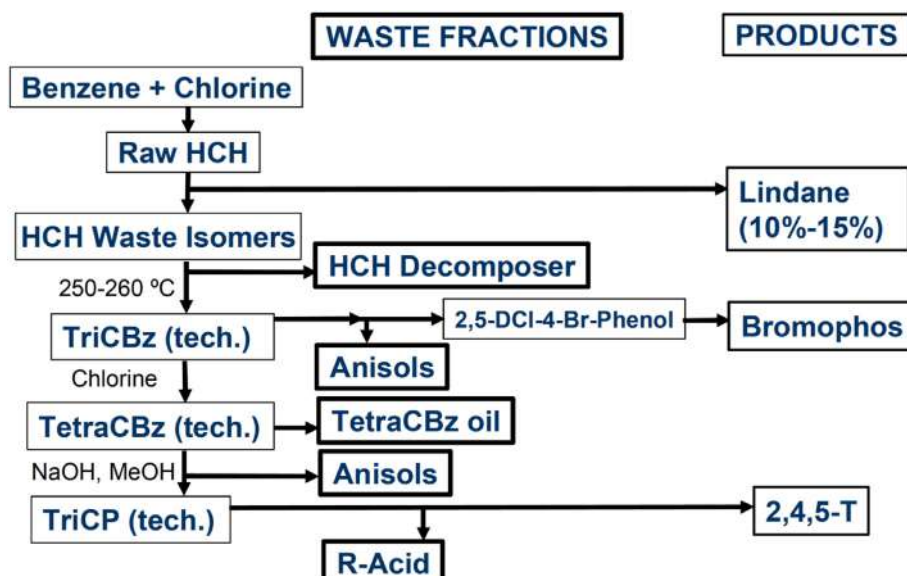


Fig. 5. Production scheme of the former pesticide factory in Hamburg, Germany, showing the major waste fractions and products [14].

final PCDD/PCDF quantity in disposed waste for two factories that were part of inventory were on the order of tonnes and the TEQ on the order of 100 kg [77]; Götz et al., 2015; [76,78]. At a German production site where a detailed inventory is available, 53–102 tonnes total sum of PCDD/PCDFs, including 333–854 kg of PCDD/PCDF TEQ, were disposed of in at least seven landfills [14]. The related production site has documented large-scale PCDD/PCDF contamination, with approximately 6 kg TEQ in the soil [15]. Such “recycling” of HCH waste isomers also occurred in the Czech Republic, France, Spain, Russia, and India [6].

At a Spanish landfill site with more than 100,000 tonnes of HCH waste disposed of, environmental monitored for PCDD/PCDFs was conducted to evaluate remediation risk [23]. Some of the disposed waste samples had up to 79 µg TEQ/kg PCDD/PCDFs, which exceeds the Basel Convention low POP content for waste (15 µg TEQ/kg). However, an initial assessment of PCDD/PCDF pollution in the vicinity of the landfills that measured soils and free range eggs as pollution indicators [79]: [24,25,45] found low PCDD/PCDF levels, suggesting no widespread PCDD/PCDF pollution at the site [23].

Furthermore, the destruction of HCH waste can lead to formation of PCDD/PCDFs, in particular when using certain non-combustion technologies (Weber 2007). A PCDD/PCDF contaminated site was generated in Brazil by the in situ “remediation” of HCH contaminated soils with calcium oxide [80]. Destruction experiments using leachates from the Spanish site mentioned above found that PCDD/PCDF contamination increased when using Fenton Oxidation but decreased with electrochemical oxidation [81]. Also bioremediation can also result in some formation of PCDD/PCDF when precursors such as chlorophenols or chlorobenzenes are present [82]; Weber 2007). Therefore, PCDD/PCDFs can be found as major contaminants at certain HCH-production sites and disposal sites and sites where certain remediation technologies were used.

3.3.3. Pollutants at lindane production and landfill sites unrelated to HCH production

Many factories that produced HCH also had other organochlorine products in their production portfolio, which caused pollution at the same production site and the related landfills. For instance, some lindane factories also produced DDT, and therefore the

related landfills contain HCH and waste DDT. This was documented for instance for one major HCH landfill in East Germany, which contains 60,000 tonnes HCH waste isomers and also 48,000 tonnes DDT waste [17].

Another prime example are chlorinated solvents (tetrachloromethane, trichloromethane, and tetrachloroethene), which were produced at several organochlorine production sites where also lindane was produced. A detailed assessment of the 60 km² of groundwater pollution at the Bitterfeld site concluded that, despite the high HCH contamination, the individual HCH isomer ranked number 8, 9, 15 and 18 on a scale indicating groundwater pollution risk, while numbers 1 through 7 were monochlorobenzene, tetrachloroethene, trichloroethene, 1,2-dichloroethene, trichloromethane, 1,1,2,2-tetrachloroethane and vinylchloride, respectively [17] generated mainly from the chlorinated solvent production. Therefore, proper risk assessment of HCH production sites and related chemical landfills must also assess the total former production portfolio of those companies and the related contamination risk.

3.3.4. Co-contaminants at technical HCH/lindane use sites

In addition to technical HCH/lindane, wood treatment used a wide range of pesticides such as pentachlorophenol (PCP), DDT, dieldrin, mirex, endosulfan, and polychlorinated naphthalenes (PCNs) [83]. Furthermore, creosote was used at many wood treatment sites, leading to contamination with polycyclic aromatic hydrocarbons (PAHs) [84]. Heavy metals, such as arsenic in the form of chromated copper arsenate, are frequently detected as major contaminants at such sites [85]. Wood treatment sites are also frequently contaminated with PCDD/PCDF, if PCP was used for some time [24,25,85].

For sheep dips, in addition to lindane/HCH, dieldrin, DDT, endrin, aldrin, and arsenic were also used as sheep dipping chemicals to treat sheep ectoparasites [86]; New Zealand Environmental Ministry 2006; Table 6). This depends however on the country. For instance, while in Iceland only lindane was used [61,62]), all these POP pesticides. The compilation of all pesticides and chemical treatments used in sheep dips in New Zealand by the government in the related guidelines can be seen as a best practice case and basis for the assessment of a contaminated site type (New

Table 6
Past and present use of pesticides and other chemicals in sheep dips [87].

Chemical ^a	Period of usage**
Arsenic	1840s - 1980
Nicotine	1840s - mid 1900s
Carbolic acid and potash	1880s
Derris	1910–1952
Lime sulphur	1849–1891
Copper	1950s - present
Zinc	1950s - present
Organochlorines/POPs^a:	
• DDT	1945–1961
• lindane	1947–1961
• dieldrin	1955–1961
• aldrin	1955–1961
Organophosphates	1960s - present
Synthetic pyrethroids	1970s - present
Insect growth regulators	Present

^a Persistent chemicals of principal concern are highlighted.

Zealand Environmental Ministry [87]: Table 6).

For cable production also PCNs, PCBs and short-chain chlorinated paraffins (SCCPs) and polybrominated diphenyl ether (PBDEs) were used as additives in cables and other plastics [88–91]. Furthermore different phthalates, lead and cadmium all restricted today have been used as additives in PVC cables [88]. Therefore at cable production sites a range of POPs and other contamination might be present from the different historic use.

At military training sites, in addition to HCH also hexachlorobenzene (HCB) and PCNs were used in fog ammunition [91]. Furthermore, PCBs and PFOS are frequent POPs contaminants at military sites [92,93,25].

These examples demonstrate that when investigating suspected lindane/HCH contamination sites, co-pollutants should also be considered depending on the site type. This requires appropriate preparation and planning for sampling and laboratory analysis.

3.4. Assisting site owners with best practice (task 2 of the “HCH in EU project”)

Task 2 of the “HCH in EU project” was to assist site-owners with best practices on sustainable contaminant site management at seven HCH-contaminated pilot sites (see Table 7). The resources provided to these pilot sites are available as reference to those involved in the remediation of similar sites. The consultancy included developing a site road map depicting how to manage the site in a sustain manner and an action plan of consultancy work that could be carried within the scope of the “HCH in EU project.” All activities were reported, and these reports are available for consultation.

Table 7
The HCH-contaminated sites provided with assistance by the “HCH in EU project”.

Site location/name	Country	Site specific issue
Wintzenheim	France	Contaminant migration from gravel pit filled with HCH from the PCUK (Ugine Kuhlmann) site of Huningue
Mulde River	Germany	Widespread sediment contamination originating from lindane and technical HCH production by VEB Chemie-Kombinat Bitterfeld (CKB)
Sardas Inquinosa	Spain	Remedial actions at the former Inquinosa lindane and technical HCH production facility and approaches for non-treated matrixes, minimizing dispersion
Valle del Sacco	Italy	Sediment contamination originating from lindane and technical HCH production and storage at the Caffaro factory
Colleferro		
Hajek	Czech Republic	Contaminant migration from a HCH landfill HCH waste from former lindane production at the Spolana Neratovice factory was disposed in a former mine
O Porriño	Spain	Contaminant migration from the lindane and technical HCH production facility of Zeltia, with widespread distribution of HCH waste
Vrakuňa	Slovak Republic	Second opinion on the selected method of containment for an HCH dump site stemming from the former lindane production at the Juraj Dimitrov Chemical Enterprises (CHZJD) in Bratislava, which caused groundwater contamination

3.5. Guidance for countries to identify sites potentially impacted by HCH

In addition to the two above-mentioned project tasks, the “HCH in EU project” team produced a report with guidance for identifying other sites potentially impacted by HCH contamination [94]. This document provides insight for authorities regarding sites where HCH might be a (co)contaminant of concern, in addition to other contaminants of concern at such sites. The document aims to direct stakeholders tasked with the management of contaminated sites to identify other sites potentially contaminated with HCH, in addition to the sites already identified in the “HCH in EU project”, which will be listed on the EU website.

The following activities were taken to provide information on the former use of lindane in this report.

1. Review the Legacy of Lindane HCH Isomer Production published on January 2006, and update the existing information.
2. Study literature on potential HCH-contaminated sites other than production sites, waste deposits, landfills, treatment centres, storage facility, processing facilities from the “HCH in EU project” inventory.
3. Select and present several examples from the current inventory
4. Compile a comprehensive report discussing the whole spectrum of lindane production and use in the EU.

3.6. Guidance to develop an EU-wide strategy to sustainably manage HCH-impacted sites

The “HCH in EU project” provided added value by delivering guidance to develop an EU-wide strategy to sustainably manage HCH-impacted sites and provide a permanent solution to the legacy of HCH and lindane in the EU. This guidance document [95] proposes an outline for a strategy to finally address the legacy of lindane production in the EU Fig. 6. This guidance is meant to inform the development of an EU-wide strategy to manage the 299 or more sites potentially impacted by HCH and lindane. The main target audience are policy makers, who can continue supporting the sustainable management of these POPs contaminated sites. Several steps are recommended to be taken at the country, regional, or site level to, once and for all, solve the problems around the legacy of past lindane production in the entire EU.

The strategy highlights that in order to solve these environmental problems, decision makers on the different levels must realize that this is an environmental legacy that needs to be solved and that the installation of one or more financial instruments (supplementing the Member States’ own investments) to pay for the long-term, expensive, and complex EU-wide clean-up

LEVEL	Identify the magnitude of the problem	Explain the need to act & Raise awareness	Develop legislation	Create HCH ownership	Build capacity	Risk-based prioritisation	Connect with funding programmes	Establish covenants between stakeholders & authorities	Construct regional development associations	Add value to the remediation site	Mitigate/control/contain environmental risks	Know why sustainable management is obstructed
EU-institutions	EU-wide inventory (Present) EU funded projects (Ongoing)	Publish paper: Need to eliminate Lindane production legacy	Develop legislation	Convince national authorities of the importance	Organize and finance R&D projects		Facilitate & stimulate	Stimulate	Stimulate			
EU Parliament	Respond & act on concerned stakeholder petitions		Establish EU legal framework for soil protection (Soil Strategy proposed) & prioritize HCH contaminated sites									
Stakeholders*	Demonstrate the problem & Submit petitions	Promote, Participate & create public pressure	Participate in public consultation	Monitor & report progress			Promote					
LINDANET	Support	Support & promote	Support based on needs of members	Extent and expand LINDANET after 2025	Establish EU community of practice, set up & extend knowledge centre	Support	Facilitate & initiate	Support & promote	Support & promote	Support & promote	Support	Support
Authorities	Detail the country specific inventory (To be completed)	Inform citizens & stakeholders	Support the Soil Strategy introduction and its implementation, develop, adapt & enforce legislation (Varies per EU member state)	Support	Facilitate pilot projects & educate	Assess preliminary sites & risks (Use standards and guidance)	Reserve national / regional funding & apply for EU funding to co-finance	Contract stakeholders to co-finance	Contract stakeholders to co-finance	Develop urban & regional development plans & make cost benefit analysis	Facilitate, co-fund & Enforce (Legislation)	Communicate with local authorities
Stakeholders*	Participate & demonstrate the problem	Participate, support create public pressure	Participate in public consultation	Set up regional/national stakeholder organisation (like in Spain)	Participate	Participate	Apply national / regional funding & EU funding to co-finance	Participate	Participate	Participate & contribute	Participate	Participate
LINDANET	Support & encourage national authorities to complete inventory	Support & promote	Support	Set up LINDANET chapter in each country with potential HCH impacted sites	Establish National communities of practice, set up & extend knowledge centres	Support	Apply for national / regional funding & EU funding to co-finance	Participate	Participate	Support	Support	Support
Site authorities	Permit, supervise evaluate (legislation)	Inform site owner & stakeholders	Apply & enforce	Development sustainable long-term town plans including HCH-sites together with site owners	Participate in R&D projects & facilitate pilot projects	Communicate, Support & advice owner	Reserve municipal budget & apply for national / regional funding & EU funding to co-finance	Participate	Participate	Develop urban development plans & make cost benefit analysis & create project teams	Permit, supervise & Evaluate (Legislation)	Communicate with owner
Site owner	Detailed site assessment (guidance)	Participate & request for assistance when needed from Site authorities		Approach authorities for participations in town plans	Participate in R&D & Pilot projects	Assess sites & risks in detail (Use standard & guidance)	Apply for municipal & national / regional funding & EU funding to co-finance	Participate	Participate	Contract stakeholders to co-finance	Survey, design, tender, contract & implement (Guidance)	Identify bottlenecks (Know current site status)
Site Stakeholders*	Participate	Participate		Set up site-specific stakeholder organisation & participate	Participate in pilot projects	Participate	Support	Participate	Participate	Participate	Participate	Participate

*Ensuring stakeholders are represented at site-, country- and EU-level

Fig. 6. Matrix of proposals for an EU-wide strategy to eliminate the legacy of Lindane production.

campaign is crucial. If this legacy receives the political priority it deserves and financial instruments are set in place, the EU soil remediation community is resourceful enough to solve the technical issues around the identification, the characterization, and finally the remediation of these sites.

An EU-wide strategy for managing HCH-contaminated site sustainably provides several advantages:

1. Leverage the successes in assessing and managing sites in Member States to prevent each country from trying to reinvent the wheel and make the same mistakes;
2. Facilitate and stimulate countries learning from each other;
3. Provide financial instruments for countries with fewer resources available to deal with this environmental legacy;
4. Guide and support parties that have taken the initiative to sustainably manage these sites.

4. Conclusion

A range of projects to address the HCH legacy have been conducted in the EU. “The HCH in EU project” developed the first comprehensive and structured inventory of sites where lindane/HCH was handled in Europe along the life cycle of production, use, and disposal. The 299 locations identified included 54 priority sites from lindane production and HCH disposal. These should be further assessed and addressed, as they may have the highest HCH release and exposure risk. Climate change and related flooding risks should be considered when assessing future risks of contaminant release. At 31 sites where certain HCH uses occurred, such as for wood treatment, the level of pollution cannot be estimated but might be significant and need further assessment.

A report detailing the assessment was developed to help local and regional authorities further refine the inventories and generate more information to best secure and remediate high-risk sites

(Fokke and Bensaiah [94]). The network of authorities responsible for large HCH sites should further be strengthened. A strategy report with needed tasks and actions Fig. 6 was also developed to support competent authorities, including the EU institutions, to further address the HCH legacy in Europe. Established networks can be used to stimulate and facilitate learning among countries. Countries and stakeholders that have taken the initiative to sustainably manage these contaminated sites should be guided and supported – best by additional EU-coordinated projects. The strategy also recommends having financial instruments so that EU countries with fewer available resources can deal with this POPs legacy. This is currently addressed in the EU Interreg Project LINDANET (See Section 3.1.3).

The first complete excavation and destruction of a large HCH deposit was completed in France in 2019 by the owner of the site and has demonstrated that this is feasible. In particular, for priority sites with high risk of contaminant release and exposure, site remediation is a sustainable solution since it does not pass on this pollution legacy to the next generation. While the cost of such excavation might be high, it is comparable to or even lower than the long-term cost of containment, which frequently involves pumping, monitoring, and other containment measures with costs that add up over decades and centuries. The indirect costs of human health impact on a global scale are impossible to assess but are significant and provide a reason to manage these sites in a sustainable manner.

Cooperative assessments of POPs contaminated sites can facilitate information exchange among affected member states. Similar HCH production, formulation, use, and disposal sites exist in Africa, Asia, and South America. Experiences gained in Europe could possibly be transferred to developing countries, taking their circumstances into account. Alternatively, developing countries with large HCH legacies from production could possibly be included in the EU network for sharing experiences and lessons learned.

Furthermore, there are other POPs with large contaminated sites (e.g., PFOS/PFOA, PCBs, HCB/HCBd) where such a coordinated assessment could be of benefit. In particular, PFOS/PFOA-contaminated sites are of increasing concern and should be systematically assessed and addressed in the EU.

Declaration of competing interest

The authors declare that they have no known competing financial interests or personal relationships that could have appeared to influence the work reported in this paper.

Acknowledgement

The financial support for this project by the European Commission (No 07.027744/2019/8120036 + 820155/ETU/ENV.D.1) is appreciated and acknowledged. We also want to thank the Commission for its support of other projects tackling the HCH/lindane legacy and promoting the implementation of the Stockholm Convention and to protect soils and ecosystems. Also the native editing by Dr. Simona Balan is appreciated.

References

- J. Vijgen, P.C. Abhilash, Y.-F. Li, R. Lal, M. Forter, J. Torres, M. Singh, M. Yunus, C. Tian, A. Schäffer, R. Weber, HCH as new Stockholm Convention POPs – a global perspective on the management of Lindane and its waste isomers, *Environ. Sci. Pollut. Res.* 18 (2011) 152–162.
- K.L. Willet, E.M. Utrich, R.A. Hites, Differential toxicity and environmental facts of hexachlorocyclohexane isomers, *Environ. Sci. Technol.* 32 (1998) 2197–2207.
- E. Ulmann, Lindane, Monograph of an Insecticide, Verlag K Schillinger, Freiburg im Breisgau, 1972.
- UNEP, Risk Profile on Lindane. Addendum Report of the Persistent Organic Pollutants Review Committee on the Work of its Second Meeting, 2006. UNEP/POPS/POPRC.2/17/Add.4.
- Y.-F. Li, Global technical hexachlorocyclohexane usage and its contamination consequences in the environment: from 1948 to 1997, *Sci. Total Environ.* 232 (3) (1999) 121–158.
- J. Vijgen, The legacy of lindane HCH isomer production. Main report. IHPA, Holte, January 2006. https://clu-in.org/download/misc/lindane_main_report_def20jan06.pdf, 2006a.
- J. Vijgen, The legacy of Lindane HCH isomer production. Annexes. IHPA, Holte, January 2006. https://clu-in.org/download/misc/lindane_annexesdef20jan06.pdf, 2006b. (Accessed 30 October 2021).
- E. Heinisch, A. Kettrup, W. Bergheim, S. Wenzel, Persistent Chlorinated Hydrocarbons (PCHC), source oriented monitoring in aquatic media 3. The isomers of Hexachlorocyclohexane, *Fresenius Environ. Bull.* 14 (6) (2005) 444–462.
- C.I.R. Fröes-Asmus, H.G.A. Alonzo, M. Palácios, A.P. Silva, M.I.F. Filhote, B. Buosi, V.M. Câmara, Assessment of human health risk from organochlorine pesticide residues in Cidade dos Meninos, Duque de Caxias, Rio de Janeiro, Brazil, *Cad. Saúde Pública Rio Janeiro* 24 (4) (2008) 755–766.
- J.P.M. Torres, C.I.R. Fröes-Asmus, R. Weber, J.M.H. Vijgen, Status of HCH contamination from former pesticide production and formulation in Brazil – a task for Stockholm Convention Implementation, *Environ. Sci. Pollut. Res.* 20 (2013) 1951–1957. <https://doi.org/10.1007/s11356-012-1089-4>.
- Y.-F. Li, D.J. Cai, Z.J. Shan, Z.L. Zhu, Gridded usage inventories of technical hexachlorocyclohexane and lindane for China with 1/6° latitude by 1/4° longitude resolution, *Arch. Environ. Contam. Toxicol.* 41 (2001) 261–266.
- Y. Ma, H. Yun, Z. Ruana, C. Lu, Y. Shi, Q. Qin, Z. Zhuming Men, D. Zou, X. Du, B. Xing, Y. Xie, Review of hexachlorocyclohexane (HCH) and dichlorodiphenyltrichloroethane (DDT) contamination in Chinese soils, *Sci. Total Environ.* 749 (2020) 141212.
- M. Forter, Umweltnutzung durch die chemische Industrie am Fall Beispiel der HCH-Fabrik Ugine-Kuhlmann, Nünigen (France), Lizentiatsarbeit, 1995, 1995 (Universität Basel, Schweiz).
- R. Götz, V. Sokollek, R. Weber, The Dioxin/POPs legacy of pesticide production in Hamburg: Part 2: waste deposits and remediation of Georgswerder landfill, *Environ. Sci. Pollut. Res.* 20 (2013) 1925–1936.
- R. Weber, G. Varbelow, The Dioxin/POPs legacy of pesticide production in Hamburg: Part 1 Securing of the production area, *Environ. Sci. Pollut. Res.* 20 (2013) 1918–1924. <https://doi.org/10.1007/s11356-012-1011-0>.
- R. Weber, C. Gaus, M. Tysklind, P. Johnston, M. Forter, H. Hollert, H. Heinisch, I. Holoubek, M. Lloyd-Smith, S. Masunaga, P. Moccarelli, D. Santillo, N. Seike, R. Symons, J.P.M. Torres, M. Verta, G. Varbelow, J. Vijgen, A. Watson, P. Costner, J. Wölz, P. Wycisk, M. Zennegg, Dioxin- and POP-contaminated sites—contemporary and future relevance and challenges, *Environ. Sci. Pollut. Res. Int.* 15 (2008) 363–393.
- P. Wycisk, R. Stollberg, C. Neumann, W. Gossel, H. Weiss, R. Weber, Integrated methodology for assessing the HCH groundwater pollution at the multi-source contaminated mega-site Bitterfeld/Wolfen, *Env. Sci. Pollut. Res.* 20 (2013) 1907–1917. <https://doi.org/10.1007/s11356-012-0963-4>.
- N. Garg, P. Lata, S. Jit, N. Sangwan, A.K. Singh, V. Dwivedi, N. Niharika, J. Kaur, A. Saxena, A. Dua, N. Nayyar, P. Kohli, B. Geueke, P. Kunz, D. Rentsch, C. Holliger, H.P. Kohler, R. Lal, Laboratory and field scale bioremediation of hexachlorocyclohexane (HCH) contaminated soils by means of bio-augmentation and biostimulation, *Biodegradation* 27 (2–3) (2016) 179–193.
- S. Jit, M. Dadhwal, H. Kumari, S. Jindal, J. Kaur, P. Lata, N. Niharika, D. Lal, N. Garg, S.K. Gupta, P. Sharma, K. Bala, A. Singh, J. Vijgen, R. Weber, R. Lal, Evaluation of hexachlorocyclohexane contamination from the last Lindane production plant operating in India, *Environ. Sci. Pollut. Res.* 18 (4) (2010) 586–597.
- J. Malhotra, S. Anand, S. Jindal, R. Rajagopal, R. Lal, *Acinetobacter indicus* sp. nov., isolated from a hexachlorocyclohexane dump site, *Int. J. Syst. Evol. Microbiol.* 62 (2012) 2883–2890.
- A. De la Torre, I. Navarro, P. Sanz, M.A. Arjol, J. Fernández, M.A. Martínez, HCH air levels derived from Bailín dumpsite dismantling (Sabiñánigo, Spain), *Sci. Total Environ.* 626 (2018) 1367–1372. <https://doi.org/10.1016/j.scitotenv.2018.01.178>.
- J. Fernández, M.A. Arjol, C. Cacho, POP-contaminated sites from HCH production in Sabiñánigo, Spain, *Environ. Sci. Pollut. Res. Int.* 20 (2013) 1937–1950. <https://doi.org/10.1007/s11356-012-1433-8>.
- J. Fernández, R. Weber, J. Guadaño, Dioxin contamination from former lindane (gamma-HCH) production in Sardas landfill and surroundings (SABIÑANIGO, Spain), *Organohalogen Compd.* 76 (2014) 696–699.
- R. Weber, C. Herold, H. Hollert, J. Kamphues, M. Blepp, K. Ballschmiter, Reviewing the relevance of dioxin and PCB sources for food from animal origin and the need for their inventory, control and management, *Environ. Sci. Eur.* 30 (2018a) 42. <https://rdcu.be/bax79>.
- R. Weber, C. Herold, H. Hollert, J. Kamphues, L. Ungemach, M. Blepp, K. Ballschmiter, Life cycle of PCBs and contamination of the environment and of food products from animal origin, *Environ. Sci. Pollut. Res. Int.* 25 (17) (2018b) 16325–16343. <https://doi.org/10.1007/s11356-018-1811-y>.
- ATSDR (Agency for Toxic Substances & Disease Registry), Anniston Community Health Survey, 2015. https://www.atsdr.cdc.gov/sites/anniston_community_health_survey/overview.html.
- A. Kocan, J. Petrik, S. Jursa, J. Chovancova, B. Drobná, Environmental contamination with polychlorinated biphenyls in the area of their former manufacture in Slovakia, *Chemosphere* 43 (2001) 595–600.
- L. Turrio-Baldassarri, S. Alivernini, S. Carasi, M. Casella, S. Fuselli, N. Iacovella, A.L. Iamicieli, C. La Rocca, C. Scarcella, C.L. Battistelli, PCB, PCDD and PCDF contamination of food of animal origin as the effect of soil pollution and the cause of human exposure in Brescia, *Chemosphere* 76 (2009) 278–285.
- S. Wimmerova, A. Watson, B. Drobná, E. Šovčíková, R. Weber, K. Lancz, H. Patayová, D. Jurečková, T.A. Jusko, L. Murínová, I. Hertz-Picciotto, T. Trnovec, The spatial distribution of human exposure to PCBs around a former production site in Slovakia, *Environ. Sci. Pollut. Res. Int.* 22 (2015) 14405–14415. <https://doi.org/10.1007/s11356-015-5047-9>.
- UNEP, Report of the Conference of the Parties of the Stockholm Convention on Persistent Organic Pollutants on the Work of its Fourth Meeting, 2009. UNEP/POPS/COP.4/38. 8 May 2009. <http://chm.pops.int/Programmes/NewPOPs/Decisions/Recommendations/tabid/671/language/en-US/Default.aspx>.
- UNEP, SC-4/10: Listing of Alpha Hexachlorocyclohexane. UNEP/POPS/COP.4/SC-4/10. May 2009, 2009.
- UNEP, SC-4/11: Listing of Beta Hexachlorocyclohexane. UNEP/POPS/COP.4/SC-4/11. 0 2009, 2009.
- UNEP, SC-4/15: Listing of Lindane. UNEP/POPS/COP.4/SC-4/15. May 2009, 2009.
- P. Grandjean, P.J. Landrigan, Developmental neurotoxicity of industrial chemicals, *Lancet* 368 (2006) 2167–2178.
- Roy A. Richardson JR, S.L. Shalat, B. Buckley, B. Winnik, M. Gearing, A.I. Levey, S.A. Factor, P. O'Suillechain, D.C. German, β-Hexachlorocyclohexane levels in serum and risk of Parkinson's disease, *Neurotoxicology* 32 (2011) 640–645.
- ATSDR (Agency for Toxic Substances & Disease Registry), Toxicological Profile for Hexachlorocyclohexanes, U.S. Department of Health & Human Services, 2005. Public Health Service. Agency for Toxic Substances and Disease Registry, 2005. <https://www.cdc.gov/TSP/ToxProfiles/ToxProfiles.aspx?id=754&tid=138,8>.
- J. Olivero-Verbel, A. Guerrero-Castilla, N.R. Ramos, Biochemical effects induced by the hexachlorocyclohexanes, *Rev. Environ. Contam. Toxicol.* 212 (2011) 1–28.
- WHO, Environmental Program on Chemical Safety. Environmental Health criteria.124. Lindane, World Health Organization, Geneva, Switzerland, 1991.
- E. Diamanti-Kandarakis, J.P. Bourguignon, L.C. Giudice, R. Hauser, G.S. Prins, A.M. Soto, R.T. Zoeller, A.C. Gore, Endocrine-disrupting chemicals: an endocrine society scientific statement, *Endocr. Rev.* 30 (2009) 293–342.
- M. Porta, E. Puigdomènech, F. Ballester, J. Selva, N. Ribas-Fitó, S. Llop, T. Lopez, Monitoring concentrations of persistent organic pollutants in the general population: the international experience, *Environ. Int.* 34 (2008) 546–561.
- F.H. Khan, P. Ganesan, S. Kumar, Chromosome microdeletion and altered sperm quality in human males with high concentration of seminal

- hexachlorocyclohexane (HCH), *Chemosphere* 80 (2010) 972–977.
- [42] M.E. Traina, M. Rescia, E. Urbani, A. Mantovani, C. Macri, C. Ricciardi, A.V. Stazi, P. Fazzi, E. Cordelli, P. Eleuteri, G. Leter, M. Spanò, Long-lasting effects of lindane on mouse spermatogenesis induced by in utero exposure, *Reprod. Toxicol.* 17 (2003) 25–35.
- [43] J. Vijgen, B. de Borst, R. Weber, T. Stobiecki, M. Forter, HCH and lindane contaminated sites: European and global need for a permanent solution for a long-time neglected issue, *Environ. Pollut.* 248 (2019) 696–705.
- [44] K. Breivik, J.M. Pacyna, J. Munch, Use of α -, β -, γ - hexachlorocyclohexane in Europe, 1970–1996, *Sci. Total Environ.* 239 (1999) 151–163.
- [45] R. Weber, L. Bell, A. Watson, J. Petrlik, M.C. Paun, J. Vijgen, Assessment of POPs contaminated sites and the need for stringent soil standards for food safety for the protection of human health, *Environ. Pollut.* 249 (2019) 703–715, <https://doi.org/10.1016/j.envpol.2019.03.066>.
- [46] D. Porta, F. Fantini, E. De Felip, F. Blasetti, A. Abballe, V. Dell'Orco, V. Fano, A.M. Ingelido, S. Narduzzi, F. Forastiere, A biomonitoring study on blood levels of beta-hexachlorocyclohexane among people living close to an industrial area, *Environ. Health* 12 (2013) 57, <https://doi.org/10.1186/1476-069X-12-57>.
- [47] F. Fantini, D. Porta, V. Fano, E. De-Felip, O. Senofonte, A. Abballe, S. D'Illo, A.M. Ingelido, F. Mataloni, S. Narduzzi, F. Blasetti, F. Forastiere, Epidemiologic studies on the health status of the population living in the Sacco River Valley, *Epidemiol. Prev.* 36 (Suppl 4) (2012) 44–52.
- [48] S.E. Crawford, M. Brinkmann, J.D. Ouellet, F. Lehmkuhl, K. Reicherter, J. Schwarzbauer, P. Bellanova, P. Letmathe, L.M. Blank, R. Weber, W. Brack, J.T. van Dongen, L. Menzel, M. Hecker, H. Schüttrumpf, H. Hollert, Remedialization of pollutants during extreme flood events poses severe risks to human and environmental health, *J. Hazard Mater.* 421 (2022) 126691, <https://doi.org/10.1016/j.jhazmat.2021.126691>.
- [49] R. Weber, A. Watson, M. Forter, F. Oliaei, Persistent organic pollutants and landfills - a review of past experiences and future challenges, *Waste Manag. Res.* 29 (1) (2011) 107–121.
- [50] J. Wölz, M. Engwall, S. Maletz, H. Olsmann, B. van Bavel, U. Kammann, M. Klempt, R. Weber, T. Braunbeck, H. Hollert, Changes in toxicity and dioxin-like activity of suspended particulate matter during flood events at the rivers Neckar and Rhine, *Environ. Sci. Pollut. Res.* 15 (2008) 536–553.
- [51] Novartis, Sanierungsprojekt ARA STEIH in Huningue Erfolgreich Abgeschlossen – Rheinuferweg Durchgängig Geöffnet, vol. 28, 2019, Oktober 2019, <https://sanierung-steih.ch/news/sanierungsprojekt-ara-steih-in-huningue-erfolgreich-abgeschlossen-rheinuferweg-durchgaengig-geoeffnet/>.
- [52] A. Pardo, C. Rodríguez-Casals, Z. Santolaria, T. Arruebo, J.S. Urieta, F.J. Lanaja, HCH isomers change in Pyrenean freshwater ecosystems triggered by the transfer operation of Bailín landfill: the case of Sabocos tarn, *Sci. Total Environ.* 787 (2021) 147655, <https://doi.org/10.1016/j.scitotenv.2021.147655>.
- [53] European Parliament and Council of the EU, Regulation (EC) No 850/2004 of 29 April 2004 on persistent organic pollutants and amending Directive 79/117/EEC, *Off. J. Eur. Union* (2004). L 158/7, 30.34.2004.
- [54] European Parliament and Council of the EU, Regulation (EU) 2019/1021 of 20 June 2019 on persistent organic pollutants (recast), *Off. J. Eur. Union* (2019). L 169/45, 25.6.2019.
- [55] J. Vijgen, G. Aliyeva, R. Weber, The forum of the international HCH and pesticides association—a platform for international cooperation, *Environ. Sci. Pollut. Res.* 20 (2013) 2081–2086, <https://doi.org/10.1007/s11356-012-1170-z>.
- [56] IHPA, Proceedings from the 13th International HCH & Pesticides Forum, the Legacy of the Lindane Production in Spain; 03–06, 2015, November 2015, Zaragoza, Spain, http://www.iHPA.info/docs/library/forumbooks/13/13thHCHForum_FORUM_BOOK_2015.pdf.
- [57] European Directorate General for International Policies, Lindane (Persistent Organic Pollutant) in the EU, Study for the Policy Department C: Citizens' Rights and Constitutional Affairs, 2016.
- [58] European Parliament and Council of the EU, DIRECTIVE 2000/60/EC establishing a framework for Community action in the field of water policy, 23 October 2000, *Off. J. Eur. Commun.* (2000). L 327/1, 22.12.2000.
- [59] J. Kalina, K.B. White, M. Scheringer, P. Příbylová, P. Kukučka, O. Audy, J. Klánová, Comparability of long-term temporal trends of POPs from co-located active and passive air monitoring networks in Europe, *Environ. Sci.: Processes Impacts* 21 (2019) 1132–1142.
- [60] E. Heinisch, K. Jonas, S. Klein, HCH isomers in soil and vegetation from the surroundings of an industrial landfill of the former GDR, 1971–1989, *Sci. Total Environ.* 134 (1993) 151–159.
- [61] V. Rafnsson, Cancer incidence among farmers exposed to lindane while sheep dipping, *Scand. J. Work. Environ. Health* 32 (3) (2006a) 185–189, <https://doi.org/10.5271/sjweh.997>.
- [62] V. Rafnsson, Risk of non-Hodgkin's lymphoma and exposure to hexachlorocyclohexane, a nested case-control study, *Eur. J. Cancer* 42 (16) (2006b) 2781–2785, <https://doi.org/10.1016/j.ejca.2006.03.035>.
- [63] R.M. Toichuev, L. Victorovna, Z.G. Bakhtiyarova, M. Timur, R. Payzildaev, W. Pronk, M. Bouwknecht, R. Weber, Assessment and review of organochlorine pesticide pollution in Kyrgyzstan, *Environ. Sci. Pollut. Res. Int.* 25 (2017) 31836–31847, <https://doi.org/10.1007/s11356-017-0001-7>.
- [64] UNEP, Proposal for Listing Lindane in Annex A of the Stockholm Convention on Persistent Organic Pollutants, 2005. UNEP/POPS/POPRC.1/8.
- [65] S. Sarig, The treatment of carp and fishponds with fish-louse, *Argulus*, in: Technical paper 15 of the General Fisheries Council for the Mediterranean, 1958.
- [66] UNEP, Stockholm Convention Decision 9/1 Exemptions. UNEP/POPS/COP.9/SC-9/1, 2019.
- [67] Deutscher Bundestag, Antwort der Bundesregierung auf die Kleine Anfrage der Abgeordneten Karin Binder, Dr. Sahra Wagenknecht, Caren Lay, weiterer Abgeordneter und der Fraktion DIE LINKE.– Drucksache 18/3691, in: Anhaltende Folgen des Holzschutzmittelskandals in den 1980er-Jahren – Verbraucherfreundliche Kennzeichnung von Giftstoffen in Holzschutzmitteln, 2015.
- [68] European Commission Joint Research Centre, Status of local soil contamination in Europe. Revision of the Indicator 'Progress in the Management Contaminated Sites in Europe', in: JRC Technical Report, 2018, <https://doi.org/10.2760/093804>. ISBN 978-92-79-80073-3 (print), 978-92-79-80072-6 (pdf).
- [69] I.C. Hennen, B. Hofestädt, U. Kalisch, H.N. Marx, H. Niewisch, U. Tostmann, Mazeration historischer Dachkonstruktionen, Erhebung und Klassifizierung des Schadensumfangs in Sachsen-Anhalt, Entwicklung und Erprobung eines Schnelltestverfahrens (MATE), Fraunhofer IRB Verlag, Fraunhofer-Informationszentrum Raum und Bau, 2010, ISBN 978-3-8167-8384-8.
- [70] F.J. Gay, A.H. Wetherly, Commonwealth Scientific and Industrial Research Organization, 1962, Australia.
- [71] E. Heinisch, Umweltbelastung in Ostdeutschland, Praxisbeiträge zur ökologischen Chemie von Chlorkohlenwasserstoffen. Wissenschaftliche, Buchgesellschaft Darmstadt, 1992.
- [72] H.-J. Jürgens, R. Roth, Case study and proposed decontamination steps of the soil and groundwater beneath a closed herbicide plant in Germany, *Chemosphere* 18 (1989) 1163–1169.
- [73] S. Sievers, P. Friesel, Soil contamination patterns of chlorinated organic compounds: looking for the source, *Chemosphere* 19 (1989) 691–698.
- [74] A. Santos, J. Fernández, J. Guadañoc, D. Lorenzola, A. Romero, Chlorinated organic compounds in liquid wastes (DNAPL) from lindane production dumped in landfills in Sabiñanigo (Spain), *Environ. Pollut.* 242 (2018) 1616–1624. Part B, November 2018.
- [75] B. Scholz, M. Engler, Determination of polychlorinated dibenzo-p-dioxins and dibenzofurans in wastes of technical hexachlorocyclohexane, *Chemosphere* 16 (1987) 1829–1834.
- [76] Universität Bayreuth, Tritschler & Partner GmbH, Dioxin-Bilanz für Hamburg, Abschlussbericht, Im Auftrag von: freie und Hansestadt Hamburg, Umweltbehörde, Kapitel 3, 1995.
- [77] Z. Bao, K. Wang, J. Kang, L. Zhao, Analysis of polychlorinated dibenzo-p-dioxins and polychlorinated dibenzofurans in pyrolysis residue of HCH, *Environ. Chem.* 13 (1994) 409–414 (in Chinese).
- [78] Universität Bayreuth, Tritschler & Partner GmbH, Dioxin-Bilanz für Hamburg, Zusammenfassender Endbericht. Hamburger Umweltberichte 51/95, Freie und Hansestadt Hamburg, Umweltbehörde, 1995.
- [79] A.D. Kudryatseva, A.A. Shelepchikov, S. Brodsky, Free-range chicken eggs as a bioindicator of dioxin contamination in Vietnam, including long-term Agent Orange impact, *Emerg. Contam.* 6 (2020) 114–123, <https://doi.org/10.1016/j.emcon.2020.02.003>.
- [80] A.M.C.B. Braga, T. Krauss, C.R.R. dos Santos, P.M. de Souza, PCDD/F-contamination in a hexachlorocyclohexane waste site in Rio de Janeiro, Brazil, *Chemosphere* 46 (2002) 1329–1333.
- [81] M. Vallejo, M.F. San Román, A. Irabien, I. Ortiz, Comparative study of the destruction of polychlorinated dibenzo-p-dioxins and dibenzofurans during Fenton and electrochemical oxidation of landfill leachates, *Chemosphere* 90 (1) (2013) 132–138, <https://doi.org/10.1016/j.chemosphere.2012.08.018>.
- [82] L. Oeberg, C. Rappe, Biochemical formation of PCDDs/Fs from chlorophenols, *Chemosphere* 25 (1992) 49–52.
- [83] UNEP, Draft Guidance on Sampling, Screening and Analysis of Persistent Organic Pollutants in Products and Recycling, Secretariat of the Basel, Rotterdam and Stockholm Conventions, United Nations Environment Programme, Geneva, 2021.
- [84] B.L. Murphy, J. Brown, Environmental forensics aspects of PAHs from wood treatment with creosote compounds, *Environ. Forensics* 6 (2) (2005) 151–159, <https://doi.org/10.1080/152759205090952829>.
- [85] A. Yanitch, H. Kadri, C. Frenette-Dussault, S. Joly, F.E. Pitre, M. Labrecque, A four-year phytoremediation trial to decontaminate soil polluted by wood preservatives: phytoextraction of arsenic, chromium, copper, dioxins and furans, *Int. J. Phytoremediation* 22 (14) (2020) 1505–1514, <https://doi.org/10.1080/15226514.2020.1785387>.
- [86] S. Gaw, G. McBride, Sheep Dip Factsheet No 2: Organochlorine Pesticides, University of Canterbury, New Zealand, 2010.
- [87] Ministry for the Environment New Zealand, Identifying, Investigating and Managing Risks Associated with Former Sheep-Dip Sites. A Guide for Local Authorities, 2006, ISBN 0-478-30106-5.
- [88] N. Aurisano, R. Weber, P. Fantke, Enabling a circular economy for chemicals in plastics, *Sustain. Chem. Pharm.* 31 (2021) 100513, <https://doi.org/10.1016/j.jcogs.2021.100513>.
- [89] Y. Guida, R. Capella, R. Weber, Chlorinated paraffins in the technosphere: a review of available information and data gaps demonstrating the need to support the Stockholm Convention implementation, *Emerg. Contam.* 6 (2020) 143–154, <https://doi.org/10.1016/j.emcon.2020.03.003>.
- [90] Y. Guida, R. Capella, N. Kajiwara, O.J. Babayemi, J.P.M. Torres, R. Weber, Inventory approach for short-chain chlorinated paraffins for the Stockholm Convention implementation in Brazil, *Chemosphere* 287 (2022) 132344, <https://doi.org/10.1016/j.chemosphere.2021.132344>.
- [91] UNEP, Draft Guidance on Preparing Inventories of Polychlorinated

- Naphthalenes (PCNs). Draft March 2017. UNEP/POPS/COP.8/INF/19, 2017.
- [92] F. Fonnum, B. Paukstys, B.A. Zeeb, K.J. Reimer, Environmental contamination and remediation practices at former and present military bases, in: Nato Science Partnership Subseries: 2, 1998, <https://doi.org/10.1007/978-94-011-5304-1>.
- [93] X.C. Hu, D.Q. Andrews, A.B. Lindstrom, et al., Detection of poly- and perfluoroalkyl substances (PFASs) in U.S. Drinking water linked to industrial sites, military fire training areas, and wastewater treatment plants, *Environ. Sci. Technol. Lett.* 3 (10) (2016) 344–350, <https://doi.org/10.1021/acs.estlett.6b00260>, 2016.
- [94] B. Fokke, C. Bensaiah, A guide to identify potentially HCH impacted sites. The use and legacy of HCH in the EU Project, in: Document for DG Environment of the European Commission, 2021, 26 October 2021.
- [95] J. Vijgen, B. Fokke, EU guidance for sustainably managing HCH impacted sites - outline of a strategy to resolve the legacy of Lindane production in the EU, in: Document for DG Environment of the European Commission 3, 2021. November 2021.



Sustainable reuse of toxic spent granular activated carbon by heterogeneous fenton reaction intensified by temperature changes

Andrés Sánchez-Yepes^a, Aurora Santos^a, Juana M. Rosas^b, José Rodríguez-Mirasol^b, Tomás Cordero^b, David Lorenzo^{a,*}

^a Chemical Engineering and Materials Department, Complutense University of Madrid, Spain

^b Universidad de Málaga, Andalucía Tech., Departamento de Ingeniería Química, Campus de Teatinos S/n, 29010, Málaga, Spain

HIGHLIGHTS

- Iron and 124-TCB adsorption on GAC decrease the unproductive H_2O_2 consumption.
- The higher the iron adsorbed, the higher the oxidant.
- The higher the iron adsorbed, the higher adsorption capacity recovery.
- A positive effect of temperature on GAC regeneration is found up to 60 °C.
- GAC surface stable during the regeneration cycles with negligible iron leaching.

GRAPHICAL ABSTRACT



ARTICLE INFO

Handling Editor: Jun Huang

Keywords:

Heterogeneous fenton
 Adsorption
 Regeneration
 Activated carbon
 Chlorinated organic compounds

ABSTRACT

A common strategy for removing highly toxic organic compounds, such as chlorinated organic compounds, is their adsorption on granular activated carbon. Spent granular activated carbon results in a toxic residue to manage; therefore, the regeneration and reuse of granular activated carbon on the site would be advisable. This work studies the regeneration of a granular activated carbon saturated in 1,2,4-trichlorobenzene, chosen as the model chlorinated organic compounds, by heterogeneous Fenton, where iron was previously immobilised on the granular activated carbon surface. This methodology avoids the addition of iron to the aqueous phase at concentrations above the allowable limits and the need for acidification. Three successive cycles of adsorption-regeneration were carried out batchwise ($5 \text{ g}_{GAC} \cdot \text{L}^{-1}$) with a granular activated carbon saturated with $300 \text{ mg}_{124-TCB} \cdot \text{g}_{GAC}^{-1}$. The recovery of the adsorption capacity after regeneration was studied with H_2O_2 (166 mM, 1.5 the stoichiometric dosage), at different concentrations adsorbed with iron adsorbed concentrations (0–12 $\text{mg}_{Fe} \cdot \text{g}_{GAC}^{-1}$) and temperatures (20–80 °C). Stable recovery of the adsorption capacity values of 65% were obtained at 180 min with $12 \text{ mg}_{Fe} \cdot \text{g}_{GAC}^{-1}$ and 60 °C. The porosity and surface chemistry of the adsorbent remained very similar after different adsorption-regeneration cycles without iron leaching into the aqueous phase. The oxidant consumption was close to the stoichiometric value for the mineralization of 1, 2, 4 – trichlorobenzene, with a low unproductive consumption of H_2O_2 with granular activated carbon. In addition, no aromatic or chlorinated by-

* Corresponding author.

E-mail address: dlorenzo@quim.ucm.es (D. Lorenzo).

<https://doi.org/10.1016/j.chemosphere.2023.140047>

Received 23 March 2023; Received in revised form 20 July 2023; Accepted 31 August 2023

Available online 1 September 2023

0045-6535/© 2023 The Authors. Published by Elsevier Ltd. This is an open access article under the CC BY-NC-ND license (<http://creativecommons.org/licenses/by-nc-nd/4.0/>).

products were detected in the aqueous solution obtained in the regeneration process. The negligible toxicity of the aqueous phase with the Microtox bioassay confirmed the absence of toxic oxidation by-products.

1. Introduction

The presence of persistent organic pollutants (POPs), particularly chlorinated organic compounds (COCs), in wastewater, surface waters, and groundwater is a significant environmental problem to solve (Rodan et al., 1999; Klecka et al., 2000; Gramatica et al., 2002; Gramatica and Papa, 2007; Loughheed, 2007). Adsorption on granular activated carbon (GAC) is a common treatment to remove these compounds from the aqueous phase (Weber and Vanvliet, 1981; Alben et al., 1983; Marsh and Rodríguez-Reinoso, 2006a, 2006b; Zhang et al., 2021). The main drawback of POPs adsorption on GAC is that large amounts of contaminated carbon are generated. Spent GAC has often been regenerated by off-site thermal treatments at 800–1000 °C (San Miguel et al., 2002; Salvador et al., 2015; Baghirzade et al., 2021), with remarkable costs and losses of GAC mass. Furthermore, if the POPs adsorbed on the spent GAC are COCs (Urano et al., 1991; Bemnowska et al., 2003; Sanchez-Yepes et al., 2022), the GAC requires particular management.

Recently, advanced oxidation processes (AOP) have been studied to regenerate spent GAC, removing the pollutant adsorbed on the carbon surface (Huling et al., 2000, 2005, 2011; Toledo et al., 2003; Horng and Tseng, 2008; Huling and Hwang, 2010; Anfruns et al., 2013; Li et al., 2013; Cabrera-Codony et al., 2015; Plakas and Karabelas, 2016; Chen et al., 2017; Jatta et al., 2019; Peng et al., 2019; Cai et al., 2020; Crincoli et al., 2020; Ma et al., 2020; Santos et al., 2020; Xiao et al., 2020; Sanchez-Yepes et al., 2022). Persulfate (PS) (Huling et al., 2011; Jatta et al., 2019; Peng et al., 2019; Xiao et al., 2020; Sanchez-Yepes et al., 2022) or hydrogen peroxide (Huling et al., 2000, 2005; Toledo et al., 2003; Horng and Tseng, 2008; Huling and Hwang, 2010; Anfruns et al., 2013; Li et al., 2013; Cabrera-Codony et al., 2015; Plakas and Karabelas, 2016; Chen et al., 2017; Cai et al., 2020; Crincoli et al., 2020; Ma et al., 2020; Santos et al., 2020) have been used as oxidants.

GAC regeneration has also been studied using hydrogen peroxide catalysed by iron cation (Fenton reagent) to produce hydroxyl radicals OH· (Huling et al., 2000, 2005; Toledo et al., 2003; Horng and Tseng, 2008; Huling and Hwang, 2010; Anfruns et al., 2013; Li et al., 2013; Cabrera-Codony et al., 2015; Plakas and Karabelas, 2016; Chen et al., 2017; Cai et al., 2020; Crincoli et al., 2020; Ma et al., 2020; Santos et al., 2020). Hydrogen peroxide and iron can be added simultaneously in the aqueous solution (Toledo et al., 2003; Huling et al., 2005; Horng and Tseng, 2008; Anfruns et al., 2013; Li et al., 2013; Chen et al., 2017; Cai et al., 2020; Crincoli et al., 2020; Ma et al., 2020; Santos et al., 2020), or iron can be previously adsorbed on the GAC (Huling et al., 2000; Huling and Hwang, 2010; Cabrera-Codony et al., 2015; Plakas and Karabelas, 2016).

Fenton Reagent (aqueous solution containing Fe cation and H₂O₂) has been used to regenerate spent GAC (Huling et al., 2000, 2005; Toledo et al., 2003; Horng and Tseng, 2008; Huling and Hwang, 2010; Anfruns et al., 2013; Li et al., 2013; Cabrera-Codony et al., 2015; Plakas and Karabelas, 2016; Chen et al., 2017; Cai et al., 2020; Crincoli et al., 2020; Ma et al., 2020; Santos et al., 2020) with adsorbed toluene (Ma et al., 2020), methyl *tert*-butyl ether (Huling et al., 2005), limonene (Anfruns et al., 2013), methylene blue (Santos et al., 2020), dyeing wastewater (Chen et al., 2017), etc. A representative work is that of Ma et al. (2020) regenerating a spent activated carbon (AC) with adsorbed toluene (512.25 mg_{tol}·g_{AC}⁻¹) using a toluene/oxidant/Fe molar ratio of 1/20/1. A recovery of adsorption capacity between 85.6 and 84.9% was obtained after 6 cycles of adsorption-regeneration (regeneration time of each cycle of 3 h). Chen et al. (2017) treated a spent AC for tertiary treatment of dyeing wastewater (240 mg g⁻¹) with a molar ratio oxidant/Fe of 20/1. They achieved less than 50% of the recovery of the adsorption capacity after 7 regeneration cycles. The main drawback is

that the use of Fenton reagent required acidic pH and a relatively high ratio of Fe to peroxide (Fe: H₂O₂ about 1:20), resulting in an iron concentration in the aqueous phase over the allowed discharged values.

The immobilisation of iron on the GAC surface has been proposed to avoid the presence of iron in the aqueous phase and the acidification of the reaction media (Huling et al., 2000; Huling and Hwang, 2010; Cabrera-Codony et al., 2015; Plakas and Karabelas, 2016). Huling et al. (2000) treated a spent GAC saturated in 2-chlorophenol (2-CP) (119 mg_{2-CP}·g_{GAC}⁻¹), using GAC with adsorbed iron (9.8 mg_{Fe}·g_{GAC}⁻¹) and an aqueous solution of H₂O₂ (2.1 M) at pH 4.6 and molar ratio pollutant: oxidant: Fe of 1:64:0.2. A recovery of the GAC adsorption capacity of 76% was obtained after three successive cycles of 24 h (Huling et al., 2000). Huling and Hwang (2010) also treated a spent AC with methyl *tert*-butyl ether (MTBE) (60 mg_{MTBE}·g_{GAC}⁻¹) using adsorbed iron on GAC (8.75 mg_{Fe}·g_{GAC}⁻¹) and an aqueous solution of H₂O₂ (0.49 mM). Recovery of adsorption capacity up to 70% was obtained at 24 h, using a pollutant: oxidant: Fe molar ratio of 1:17:0.2 (pH was kept between 2 and 4). Cabrera-Codony et al. (2015) studied the regeneration of a spent GAC with adsorbed octamethylcyclotetrasiloxane (1732 mg_{OMCTX}·g_{GAC}⁻¹) using adsorbed iron (11.5 mg_{Fe}·g_{GAC}⁻¹) and an aqueous solution of H₂O₂ (29 mM) for 24 h (without pH control). A decrease in adsorption capacity from 92.1% to 46.3% was reported after three cycles of adsorption-regeneration, using a molar ratio pollutant:oxidant:Fe of 1:20:0.04. This decrease was associated with the loss of adsorbed iron in successive cycles. Plakas and Karabelas (2016) studied the regeneration of a spent AC saturated in diclofenac (DCF) (203 mg_{DCF}·g_{GAC}⁻¹) using iron adsorbed on GAC (40.7 mg_{Fe}·g_{GAC}⁻¹) as the catalyst and an aqueous solution of H₂O₂ 3.5 mM as the oxidant, at neutral pH. A recovery of the adsorption capacity was obtained at 24 h of oxidation treatment (only one cycle was studied), using a pollutant: oxidant molar ratio: Fe of 1:73:1. These works have only studied the regeneration process at room temperature, and the effect of temperature on the process was not considered. Moreover, the oxidant consumption, changes in the physicochemical carbon properties, and presence of by-products throughout the regeneration process were scarcely considered. Furthermore, the regeneration of GAC saturated in organochlorine compounds has been barely analysed in the literature.

Among these organochlorine compounds, 124-TCB is used in many industrial processes, including the production of various pesticides (Blus, 2003; Jayaraj et al., 2016), POPs commonly found in the environment. The reduction of this compound has been studied using different oxidants. Barbash et al. (2006) indicated that persulfate could be an effective oxidiser of 1-24-TCB. In a previous work, thermally activated persulfate (TAP) was successfully applied to regenerate a spent GAC saturated in 124-TCB (Sanchez-Yepes et al., 2022). Also, the Fenton reaction has been successfully applied to treat 124-TCB. In this sense, Lorenzo et al. (2019) studied the removal of chlorobenzenes using hydroxylamine, goethite, and hydrogen peroxide to remove 124-TBC from polluted groundwater. In the same way, the abatement of 124-TCB using hydrogen peroxide and monochromatic light to activate (Lorenzo et al., 2021) or an iron complex (Conte et al., 2022) was effectively applied.

In the present work, the regeneration of GAC saturated with 124-TCB was studied by using H₂O₂ as oxidant and immobilised iron as catalyst. The influence of iron adsorbed and temperature on the regeneration of spent GAC with 124-TCB using H₂O₂ as the oxidant will be studied. The stability of GAC in the different adsorption-regeneration cycles and the unproductive consumption of the oxidant will be analysed, and the effect of the treatment on the chemical and physical properties of GAC will be fully examined. To our knowledge, this is the first study of the regeneration of GAC saturated in chlorobenzenes with adsorbed iron and hydrogen peroxide. Moreover, the effect of temperature on GAC

regeneration and the unproductive oxidant with this treatment is analysed for the first time.

2. Material and methods

2.1. Materials

The COC selected as the model pollutant, 124-TCB, is a semivolatile compound with moderate water solubility (28 mg L^{-1}) at room temperature (Schroll et al., 2004; Lorenzo et al., 2019, 2021). Analytical grade 124-TCB was purchased from Sigma-Aldrich. The calibration curves were prepared by dissolving pure 124-TCB in *n*-hexane. Bicyclohexyl was used as an internal standard (ISTD). A 35% v/v hydrogen peroxide solution was used as the oxidizing agent, iron (II) sulphate, $\text{FeSO}_4 \cdot 7\text{H}_2\text{O}$, was used as catalyst and titanium (IV) oxysulphate was used to quantify H_2O_2 concentration. Sodium carbonate, sodium bicarbonate, sulfuric acid, and acetone were used to determine the concentrations of chloride and short-chain organic acids by ion chromatography. The above compounds were analytical reagent grade and supplied by Sigma-Aldrich. Commercial GAC before pre-treatment (GAC-O) presented a surface area of $905 \text{ m}^2 \text{ g}^{-1}$ and a total pore volume of $0.42 \text{ cm}^3 \text{ g}^{-1}$ (Sanchez-Yepes et al., 2022).

2.2. Experimental procedure

2.2.1. GAC pre-treatment: acidic washing and iron adsorption

10 g of GAC-O was washed in 1 L of an acid water solution ($\text{pH} = 3$, adjusted with H_2SO_4) for 2 h (GAC-W). Subsequently, GAC-W was filtered and rinsed with H_2O milliQ and dried in an oven at 50°C for 24 h.

1 g of GAC-W was put in contact with 5 g of an aqueous solution of cation Fe (II) at different concentrations from 7.16 to 89.52 mM, adjusted at $\text{pH}_0 = 2.5$. The biphasic mixture was agitated for 72 h, and the GAC with iron (GAC-Fe) was recovered by filtration and dried at 50°C for 24 h. The remaining Fe (II) in the aqueous solution was quantified, and the iron adsorbed on the GAC was determined by the mass iron balance.

2.2.2. 124-TCB adsorption

5 g of GAC-W or GAC-Fe was placed in a stainless-steel mesh and immersed in a 1 L closed flask with 800 mL H_2O Milli-Q. A mass of 3 g of 124-TCB was added as organic liquid phase and the flask was closed and shaken at 300 rpm for 72 h at room temperature ($22 \pm 2^\circ\text{C}$). After that, the stainless steel was removed, rinsed with H_2O Milli-Q, and dried at 50°C for 24 h. The remaining 124-TCB in the flask was extracted with 200 mL of *n*-hexane and quantified by GC-MS. The mass of 124-TCB adsorbed on GAC was calculated by mass balance. This procedure provided GAC saturated in 124-TCB without iron (GAC-S) and GAC saturated in 124-TCB with immobilised iron (GAC-Fe-S).

2.2.3. Oxidation experiments

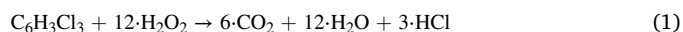
GAC (GAC-W, GAC-Fe, GAC-S, and GAC-Fe-S) reacted with hydrogen peroxide in well-mixed batch reactors. A 50 mL Milli-Q water volume was put in contact with 250 mg of GAC confined in a stainless-steel mesh basket. The reaction temperature was controlled using an agitation and heating plate coupled with a temperature-PID controller (IKA C-MAG HS 7). Once the temperature was reached, the specific amount of H_2O_2 needed was added (zero reaction time).

Two sets of experiments were carried out. In the first set, the reaction between GAC-W and GAC-Fe with H_2O_2 was studied at H_2O_2 and GAC concentrations of 166 mM and 5 g L^{-1} respectively, at two different temperatures (20 – 60°C), for 180 min. The experimental conditions are described in Table SM1. Experiments B1 and B2 were carried out using GAC-W, while runs B3–B4 were performed using GAC-Fe-12 ($12 \text{ mg}_{\text{Fe}} \cdot \text{g}_{\text{GAC}}^{-1}$). To check the catalytic role of adsorbed iron, GAC-Fe was filtered after run B4 and the solid was put in contact with a new H_2O_2

aqueous solution. This procedure was repeated three times.

The second set of experiments used GAC-S and GAC-Fe-S. The operation conditions are summarised in Table SM2. This set of experiments was designed to modify only one variable in each run to determine the effect of the studied variable avoiding the coupling effect of the variables. Runs R1 and R2 were carried out in the absence of adsorbed Fe and runs R3 to R7 were carried out at different concentrations of iron adsorbed (2 – $12 \text{ mg}_{\text{Fe}} \cdot \text{g}_{\text{GAC}}^{-1}$) and 20°C . Runs 7 to 10 were carried out at different temperatures (20 – 80°C) but using the same adsorbed iron ($12 \text{ mg}_{\text{Fe}} \cdot \text{g}_{\text{GAC}}^{-1}$). The initial pH was 7. All runs were carried out at $C_{\text{GAC}} = 5 \text{ g L}^{-1}$ and $C_{\text{H}_2\text{O}_2,0} = 166 \text{ mM}$ for 180 min (molar ratio H_2O_2 :124-TCB of 20:1). The experiments were performed in triplicate. The data are expressed as the mean \pm standard deviation.

The stoichiometry of the mineralization of 124-TCB with hydrogen peroxide is given by Eq. (1).



60% excess with respect to the stoichiometric molar ratio H_2O_2 :124-TCB required for complete 124-TCB mineralization (according to Eq (1)) was used in the experiments summarised in Table S2. The recovery of the adsorption capacity (RAC) was calculated according to Eq. (2).

$$\text{RAC} = \left(\frac{w_{124\text{-TCB,adsorbed}}/w_{\text{GAC}}}{q_{124\text{-TCB}_0}} \right) \cdot 100 \quad (2)$$

Being $w_{124\text{-TCB,adsorbed}}$ the mass of 124-TCB adsorbed after GAC regeneration, w_{GAC} the mass of GAC regenerated and $q_{124\text{-TCB}_0}$ the adsorbed 124-TCB on GAC before the first GAC regeneration treatment. Furthermore, three consecutive cycles of adsorption-regeneration were carried out under the experimental conditions of R9. The experiments were performed in triplicate. The data are expressed as the mean \pm standard deviation.

2.3. Analytical methods

124 – TBC in hexane was quantified by gas chromatography (Agilent 6890 N) with a Mass Spectrometry Detector (GC-MS). A HP-5MS chromatography column ($30 \text{ m} \times 0.25 \text{ mm ID} \times 0.25 \mu\text{m}$) was used as stationary phase and a constant flow rate of $1.7 \text{ mL} \cdot \text{min}^{-1}$ of helium as a mobile phase. $1 \mu\text{L}$ of the liquid sample was injected at a port temperature of 250°C . The chromatographic oven worked under a programmed-temperature gradient, starting at 80°C and increasing the temperature at a rate of $18^\circ\text{C} \cdot \text{min}^{-1}$ up to 180°C , then keeping it constant for 15 min. The H_2O_2 concentration was determined by colourimetry, reacting each sample with titanium (IV) oxysulphate and measuring the colour change by using a 410 nm spectrophotometer (BOECO S-20 VIS). Chloride and short-chain organic acids were determined by ion chromatography (Metrohm 761 Compact IC) with anionic chemical suppression and a conductivity detector. The pH was measured with a Basic 20-CRISON pH electrode. The iron content in the aqueous solutions was measured by spectroscopy of atomic emission (AES MP-4100 Agilent Technology) at a wavelength of 259.94 nm and a nebulizer pressure of 100 kPa. The total organic carbon (TOC) was measured using a Shimadzu TOC-V CSH analyser by oxidative combustion at 714°C accomplished with a CO_2 infrared detector.

The toxicity of aqueous phase samples after regeneration/adsorption cycles was determined using the Microtox M500 analyser (Azur Environmental) using standard bioassays following the Microtox test protocol (ISO 11348–3, 2009). The test was conducted based on the bioluminescence inhibition of *Vibrio Fischeri* bacteria when exposed to toxic substances. The method was tested at 15°C and 15 min exposure. The pH of the samples was fixed at 6–7, and the oxidant was neutralised with sodium thiosulfate to conduct the measures. The toxicity was expressed as toxicity units of the aqueous phase (TUs) calculated with Eq. (3) (Santos et al., 2004) where IC_{50} was the sample dilution ratio that

yields a 50% reduction of bacteria light emission calculated by Eq. (4).

$$TU_s = \frac{100}{IC_{50}(\%)} \quad (3)$$

$$IC_{50}(\%) = \frac{V_{\text{sample}}}{V_{\text{total}}} 100 \quad (4)$$

Where V_{sample} is the volume of the polluted sample and V_{total} the volume sum of the sample volume and the added volume of the diluent and the bacteria.

The porous texture of the GAC was characterised by N_2 adsorption-desorption at -196 °C. The samples were outgassed at 150 °C for at least 8 h. From the N_2 isotherm, the apparent surface area (A_{BET}) was determined by applying the BET equation. The t-method allows obtaining the values of the external surface area (A_t) and the micropore volume (V_t). The mesopore volume (V_{mes}) was determined as the difference between the adsorbed volume of N_2 at a relative pressure of 0.99 (V_{tot}) and the micropore volume V_t . The surface chemistry of the sample was analysed by X-ray photoelectron spectroscopy (5700C model Physical Electronics) with Mg $K\alpha$ radiation (1253.6 eV). The maximum of the C1s peak was set to 284.5 eV and was used as a reference to shift the whole spectrum. Temperature-programmed desorption (TPD) was used to characterize the oxygen functional groups on the GAC surface formed during the different treatments. TPD analyses were obtained in a customised quartz fixed-bed reactor placed inside an electrical furnace and coupled to both a mass spectrometer (Pfeiffer Omnistar GSD-301) and to a non-dispersive infrared (NDIR) gas analyser (Siemens ULTRA-MAT 22), to quantify CO and CO_2 evolution (calibration error <1%). In these experiments, c. a. 50 mg of the GAC was heated from room temperature to 930 °C at a heating rate of 10 °C·min⁻¹, in nitrogen (purity 99.999%, Air Liquide) flow (200 cm³·STP·min⁻¹).

3. Results and discussions

3.1. Iron adsorption

The adsorption of Fe (II) on the GAC-W surface was studied using different iron cation concentrations in the aqueous phase ($C_{\text{Fe(II)}} = 7.16$ to 89.52 mM) at a controlled temperature (22 ± 2 °C) for 72 h to ensure the equilibrium was reached, according to the procedure explained in the experimental section. The Fe (II) adsorbed on GAC was calculated from the iron mass balance of Fe (II) in the aqueous phase before and after Fe (II) adsorption. The obtained adsorption isotherm of Fe (II) on the GAC-W surface is shown in Figure SM1, which exhibits a typical Langmuir isotherm. The corresponding Langmuir parameters are summarised in Eq. (5), and the statistical parameters are inserted in Figure SM1. From the asymptotic value of the Langmuir isotherm, the saturation amount of Fe (II) adsorbed on the GAC surface was 12.56 mg_{Fe}·g_{GAC}⁻¹. The GAC samples with iron adsorbed have been named GAC-xFe (x the iron content in mg_{Fe}·g_{GAC}⁻¹).

$$q_{\text{Fe}} = \frac{12.56 \cdot 0.0053 \cdot C_{\text{Fe}}}{1 + 0.0053 \cdot C_{\text{Fe}}} \quad (5)$$

3.2. Effect of adsorbed Fe on 124-TCB adsorption

Incorporation of iron onto the GAC surface can affect the adsorption of pollutant (Huling and Hwang, 2010). The amount of 124-TCB adsorbed on GAC-W was 350 mg_{124-TCB}·g_{GAC}⁻¹ when the aqueous concentration of 124-TCB was 28 mg L⁻¹ (solubility of 124-TCB in the aqueous phase at 28 °C) (Sánchez-Yepes et al., 2022). The effect of adsorbed Fe on 124-TCB adsorption has been investigated, and the results are presented in Figure SM2. As shown, the highest the amount of Fe adsorbed, the lower the 124-TCB adsorption. The adsorption of 124-TCB was reduced by 14% (300 mg_{124-TCB}·g_{GAC}⁻¹) when the GAC surface was saturated with 12 mg_{Fe}·g_{GAC}⁻¹. This fact agreed to reported by

Huling and Hwang (2010). They observed that iron adsorbed on the GAC surface reduced the adsorption of methyl *tert*-butyl ether (MTBE), due to steric impediments.

3.3. Reactivity of GAC with H₂O₂

The reactivity of GAC-W with H₂O₂ with and without iron adsorbed was studied in runs B1–B4 (20 and 60 °C) (experimental conditions summarised in Table SM1). The conversion of H₂O₂ was calculated using equation (6).

$$X_{\text{H}_2\text{O}_2} = 1 - \frac{C_{\text{H}_2\text{O}_2}}{C_{\text{H}_2\text{O}_2,0}} \quad (6)$$

being $C_{\text{H}_2\text{O}_2,0}$ and $C_{\text{H}_2\text{O}_2}$ the concentration of H₂O₂ at zero time and the corresponding reaction time, respectively. Oxidant conversion values are shown in Fig. 1.

As can be seen, H₂O₂ reacted with the GAC promoting the consumption of the oxidant (H₂O₂ conversion in the absence of GAC was less than 10% in the time interval studied, 3 h, at temperatures of 20 and 6 °C, data not shown). Furthermore, both the temperature and the surface of the presence of iron on the GAC increased the conversion of H₂O₂. A H₂O₂ conversion of 0.27 and 0.38 was obtained at 180 min and 20 °C, in the absence and presence of adsorbed iron, respectively. The corresponding oxidant conversion values at 60 °C were 0.6 and 0.8. As can be seen, the reaction rate of the hydrogen peroxide consumption decreased after 150 min. For this reason, 180 min was selected as the reaction time.

These results suggested that the presence of adsorbed iron on the surface of the GAC increased the reactivity of H₂O₂, as previously reported in literature (Moreno et al., 2007; Cabrera-Codony et al., 2015).

The GAC-12Fe after 180 min of reaction under the experimental conditions of run B4 (Table SM1), named GAC-12Fe-C1, was filtered and put in contact with an H₂O₂ aqueous solution (166 mM) at 60 °C for 180 min. This procedure was repeated two times, GAC-12Fe-C2 and GAC-12Fe-C3. The consumption of the H₂O₂ at each cycle is shown in SM4.

The results in Figure SM3 showed similar H₂O₂ conversions in the three cycles carried out under the conditions of run B4 (Table SM1), suggesting a catalytic behaviour of GAC-12Fe, which allows its use in successive runs. Furthermore, iron leaching in the aqueous phase was studied during the cycles shown in Figure SM3. The iron leached at each cycle was less than 0.5% of the initial iron adsorbed on GAC-12Fe. This result indicates that the prepared material is stable during successive cycles, and a homogeneous Fenton reaction does not occur.

3.4. Regeneration of GAC saturated in 124-TCB

The oxidation of adsorbed 124-TCB and the recovery of GAC adsorption capacity (RAC) has been studied at different temperatures (20 – 60 °C) and iron contents adsorbed on GAC. (0 – 12 mg_{Fe}·g_{GAC}⁻¹). The oxidant yield (Y_{Ox}) is defined as the mol of 124-TCB removed from the GAC surface per mol of H₂O₂ consumed. The removed 124-TCB is calculated as the readsorbed amount of 124-TCB after the spent GAC regeneration, using Eq. (7).

$$Y_{\text{Ox}} = \frac{\text{mol}_{124\text{-TCB readsorbed}}}{\text{mol}_{\text{H}_2\text{O}_2 \text{ consumed}}} \quad (7)$$

The mol_{H₂O₂ consumed} corresponds to the moles of H₂O₂ consumed in the GAC regeneration run and the mol_{124-TCB readsorbed} are the moles of 124-TCB adsorbed after the regeneration with H₂O₂.

The recovery of adsorption capacity (RAC), oxidant conversion ($X_{\text{H}_2\text{O}_2}$) and oxidant yield (Y_{Ox}) after 180 min of reaction time have been calculated with Eqs. (2)–(4), respectively.

3.4.1. Effect of iron content adsorbed on the GAC

The effect of the adsorbed iron concentration on RAC, $X_{\text{H}_2\text{O}_2}$ and Y_{Ox}

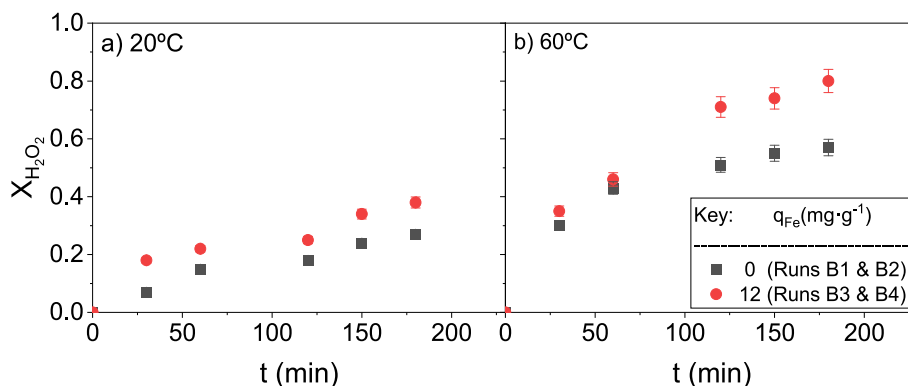


Fig. 1. H_2O_2 conversion by reaction with GAC-12Fe (runs B3 and B4) and GAC-W (runs B1 and B2) a) $20\text{ }^\circ\text{C}$ and b) $60\text{ }^\circ\text{C}$, using $C_{\text{H}_2\text{O}_2,0} = 166\text{ mM}$, $C_{\text{GAC}} = 5\text{ g L}^{-1}$ and $\text{pH}_0 = 7$. Reaction conditions for runs B1 to B4 in [Table SM1](#).

has been investigated at $20\text{ }^\circ\text{C}$ in runs R1 and R3-R7 ([Table SM2](#)). RAC, Y_{Ox} , and H_2O_2 conversion values are shown in [Fig. 2](#). The effect of the adsorbed iron concentration on RAC, $X_{\text{H}_2\text{O}_2}$ and Y_{Ox} has been investigated at $20\text{ }^\circ\text{C}$ in runs R1 and R3-R7 ([Table SM2](#)). RAC, Y_{Ox} and H_2O_2 conversion values are shown in [Fig. 2](#). The adsorbed iron concentrations (q_{Fe} values in [Fig. 2](#)) were obtained by placing contact solutions with different iron sulphate concentrations and GAC-W to reach equilibrium adsorption conditions. The amount of Fe adsorbed agreed with the Fe adsorption isotherm plotted in [Figure SM1](#).

The higher the iron adsorbed, the higher the RAC value ([Fig. 2a](#)), which means that the oxidation of 124-TCB from GAC surface was improved. Oxidant consumption also increased with increased iron concentration adsorbed. On the other hand, the highest Y_{Ox} value ($0.086\text{ mmol}_{124\text{-TCB eliminated}} \cdot \text{mmol}_{\text{H}_2\text{O}_2, \text{ reacted}}^{-1}$) is obtained at the highest amount of Fe adsorbed ($12\text{ mg}_{\text{Fe}} \cdot \text{g}_{\text{GAC}}^{-1}$). High Y_{Ox} values mean lower unproductive consumption of the oxidant and better efficiency of the oxidant in destroying the pollutant. Therefore, the best regeneration conditions correspond to $12\text{ mg}_{\text{Fe}} \cdot \text{g}_{\text{GAC}}^{-1}$. Moreover, the Y_{Ox} value of $0.083\text{ mmol}_{124\text{-TCB eliminated}} \cdot \text{mmol}_{\text{H}_2\text{O}_2, \text{ reacted}}^{-1}$ corresponds to the stoichiometric value for the total mineralization of 124-TCB (Eq. (1)).

Iron leaching was measured in the aqueous phases obtained in the regeneration runs shown in [Fig. 2](#). In all cases, the iron leached was negligible ($<1\%$ of the initial amount of iron adsorbed), ensuring that the Fenton reaction took place heterogeneously on the GAC surface. The initial pH was 7, and the final pH of the reaction medium decreased and a value between 4 and 3.5. This pH reduction was in agreement with the formation of short acids in the reaction pathway. The lower iron concentration measured in solution ($<0.2\text{ mg}_{\text{Fe}} \cdot \text{L}^{-1}$) avoids the iron sludges produced in homogeneous Fenton Reagent, carried out at higher iron concentrations in the aqueous phase (usually much higher than the values allowed for Fe discharge). The initial pH of the oxidant aqueous solution does not need acidification when the iron is previously adsorbed on GAC, and the final pH is less acidic than that obtained after applying the Fenton Reagent with both iron and hydrogen peroxide in the solution.

The molar ratio of pollutant: oxidant: iron used in this work is 1:17:0.11. This ratio is similar to that employed by [Huling and Hwang \(2010\)](#) in the elimination of MTBE in GAC by iron amendment and Fenton oxidation (ratio 1:16.5:0.23) and [Cabrera-Codony et al. \(2015\)](#) studying the regeneration of AC saturated in octamethylcyclotrisiloxane (1:20:0.023). On the contrary, [Plakas and Karabelas \(2016\)](#) applied a higher oxidant ratio to abate diclofenac adsorbed on Powered AC impregnated with iron oxide nanoparticles and H_2O_2 . Regeneration of AC saturated in 2-chlorophenol by [Huling et al. \(2000\)](#) was also achieved using higher amounts (molar ratio pollutant:oxidant: iron 1: 63.7: 0.19).

3.4.2. Effect of the reaction temperature

The effect of reaction temperature on GAC regeneration was studied with GAC-12Fe-S in the range of $20\text{--}80\text{ }^\circ\text{C}$, using an oxidant concentration of 166 mM , neutral pH, and a GAC loading of 5 g L^{-1} . The RAC, oxidant consumption and Y_{Ox} values obtained for each temperature (R7-R10 in [Table S2](#)) after 180 min of reaction are summarised in [Fig. 3](#).

As shown in [Fig. 3a](#) and b, the higher the temperature, the higher the oxidant consumption, reaching values of 0.58 at $80\text{ }^\circ\text{C}$ after 180 min of reaction time. The RAC values increased from 42% at $20\text{ }^\circ\text{C}$ to 63% at $60\text{ }^\circ\text{C}$ but did not increase further from 60 to $80\text{ }^\circ\text{C}$. The Y_{Ox} value shows a slight decrease from 20 to $60\text{ }^\circ\text{C}$ (from 0.1 to $0.086\text{ mmol}_{124\text{-TCB eliminated}} \cdot \text{mmol}_{\text{H}_2\text{O}_2, \text{ reacted}}^{-1}$), but it presents a remarkable drop from 60 to $80\text{ }^\circ\text{C}$ (from 0.086 to $0.064\text{ mmol}_{124\text{-TCB eliminated}} \cdot \text{mmol}_{\text{H}_2\text{O}_2, \text{ reacted}}^{-1}$). Therefore, increasing the temperature to $60\text{ }^\circ\text{C}$ increases the pollutant oxidation on the GAC surface, but the highest temperatures produce remarkably unproductive oxidant consumption. Similar findings were also noticed in the literature on the Fenton reaction enhanced by temperature ([Williams, 1928](#); [McLane, 1949](#)). Therefore, $60\text{ }^\circ\text{C}$ is selected as the optimum temperature for the following experiments.

The H_2O_2 conversion found at 180 min and $60\text{ }^\circ\text{C}$ in the absence of adsorbed 124-TCB (GAC-12FeC1, C2, C3 in [Figure SM3](#)) was approximately 0.80 . The H_2O_2 conversion at the same operating conditions, but with 124-TCB adsorbed on GAC (GAC-12Fe-S in [Fig. 3](#)) was about 0.47 . Therefore, it can be deduced that remarkably higher unproductive consumption of H_2O_2 takes also place in the absence of adsorbed pollutants adsorbed.

3.4.3. Stability of the regenerated GAC

Three cycles of spent GAC regeneration and 124-TCB adsorption was carried out with GAC-12Fe-S ($q_{\text{Fe}} = 12\text{ mg g}^{-1}$) at $60\text{ }^\circ\text{C}$ with $C_{\text{H}_2\text{O}_2,0} = 166\text{ mM}$, $C_{\text{GAC-12Fe-S}} = 5\text{ g L}^{-1}$ and $\text{pH} = 7$ (Run R9 in [Table S2](#)). After each regeneration cycle, the RAC, H_2O_2 consumption and Y_{Ox} were determined, and the results are summarised in [Fig. 4](#). As shown, similar values of the RAC, oxidant consumption and Y_{Ox} are obtained in the three consecutive cycles (differences lower than 5% among them). These experimental results indicate that GAC with iron adsorbed can be used in stable cyclic operation with 124-TCB adsorption and adsorbent regeneration. In addition, the Y_{Ox} was kept in a value close to the stoichiometric value required for the 124-TCB mineralization, minimizing the unproductive consumption of the oxidant. The adsorption/regeneration mechanism of the GAC previously saturated with Fe can be summarised in Eqs. (8)–(11). In step 1, 124 TC B is adsorbed, after that in [step 2](#), the H_2O_2 reacts with the adsorbed iron to produce the hydroxyl radicals, and this attacks to the 124-TCB which in several series reactions where oxidation products are generated produces the regeneration of the GAC.

Step 1. 124-TCB adsorption

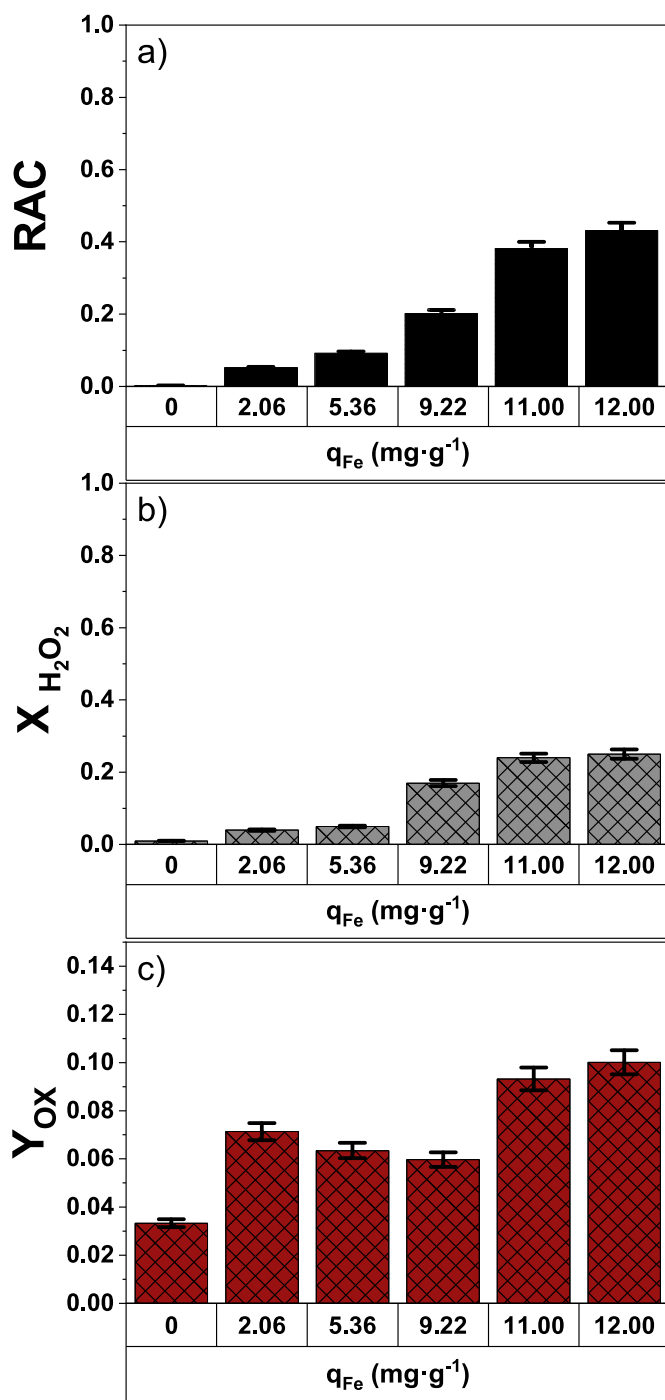
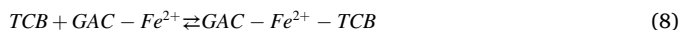


Fig. 2. Effect of adsorbed iron on a) recovered adsorption capacity (RAC), b) H_2O_2 conversion ($X_{H_2O_2}$) and c) oxidant yield (Y_{OX}) in $mmol_{124-TCB}$ eliminated $\cdot mmol_{H_2O_2}^{-1}$, reacted at 180 min of reaction time, $C_{H_2O_2,0} = 166$ mM, $C_{GAC-xFe-S} = 5$ g L⁻¹, $T = 20$ °C, and neutral initial pH. The iron leached at each cycle was less than 0.5% of the initial iron adsorbed on GAC.



Step 2. Oxidation 124-TCB and GAC regeneration

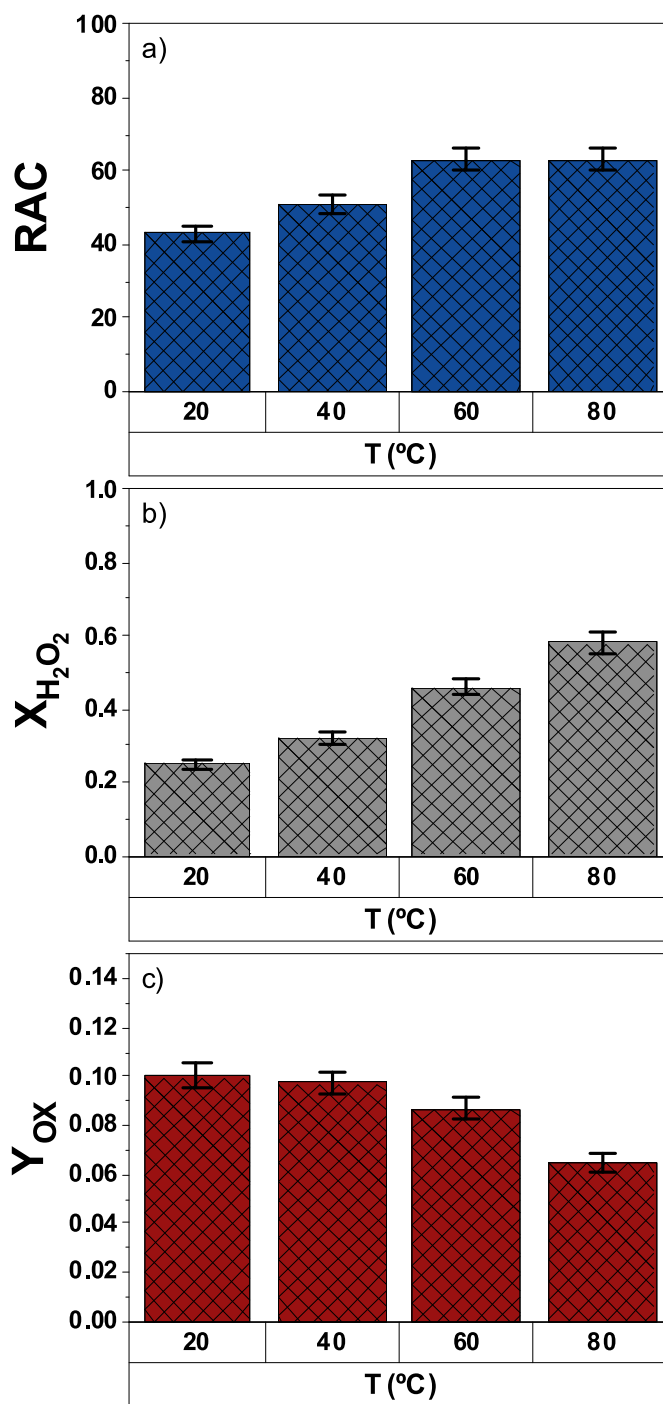
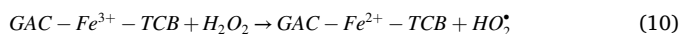
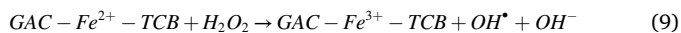


Fig. 3. Effect of temperature on a) recovery of Adsorption Capacity (RAC), b) H_2O_2 conversion ($X_{H_2O_2}$) and c) oxidant yield (Y_{OX}) in $mmol_{124-TCB}$ eliminated $\cdot mmol_{H_2O_2}^{-1}$, reacted at 180 min of reaction time, $C_{H_2O_2,0} = 166$ mM, $C_{GAC-12Fe-S} = 5$ g L⁻¹ and neutral initial pH. The iron leached at each cycle was less than 0.5% of the initial iron adsorbed on GAC.



The pH dropped from 7 to values between 4 and 3.5 at 180 min of regeneration time in the three cycles studied due to the presence of short-chain organic acids in the aqueous phase. At 180 min, only acetic acid was detected in the aqueous phase, with a concentration lower than 10 mg L⁻¹. Similar values of acetic acid concentration were found at the end of each regenerative cycle in the aqueous phase. The toxicity of the aqueous phase obtained after the regeneration cycle of the GAC was

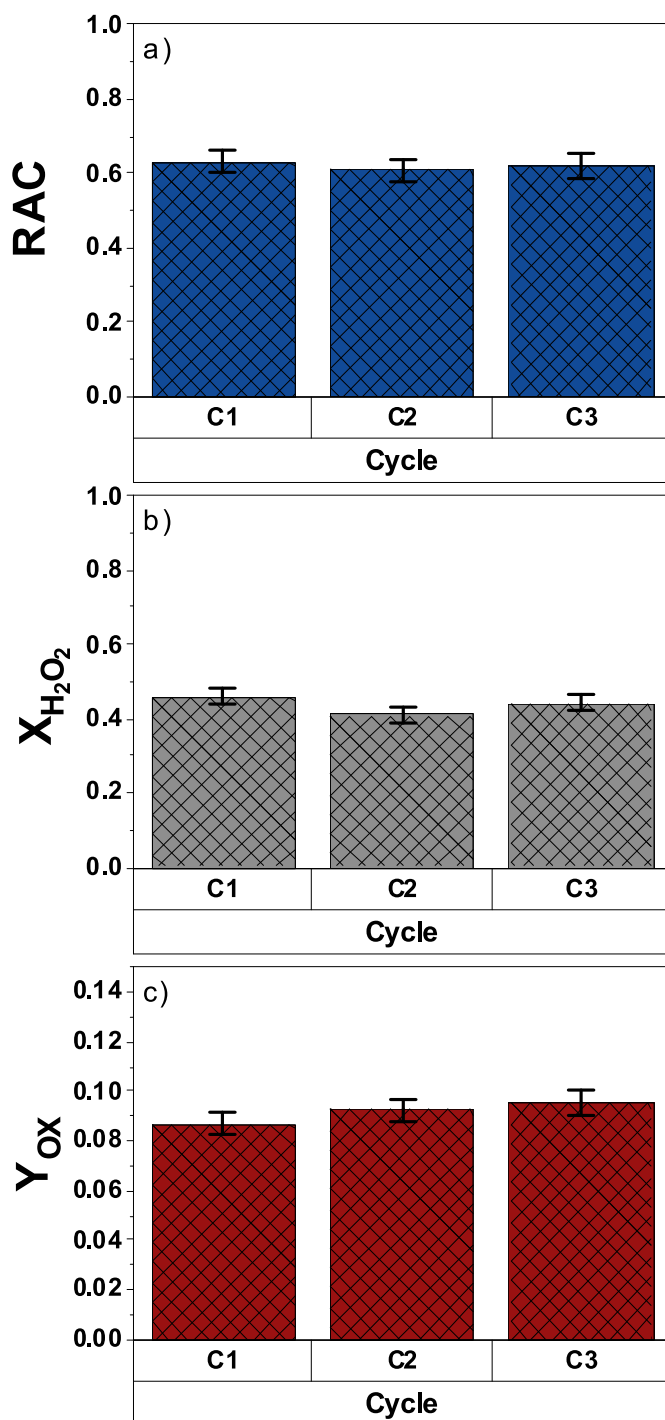


Fig. 4. Stability of GAC-12Fe in successive adsorption-regeneration cycles a) Recovery of Adsorption Capacity (RAC), b) H₂O₂ conversion (X_{H₂O₂}) and c) oxidant yield (Y_{OX}) in mmol_{124-TCB eliminated}·mmol_{H₂O₂}⁻¹, reacted at 180 min, C_{H₂O_{2,0}} = 166 mM, C_{GAC-12Fe-S} = 5 g L⁻¹, T = 60 °C and neutral initial pH. The iron leached at each cycle was less than 1% of the initial iron adsorbed on GAC-12Fe.

measured. The initial TU of the water saturated with 124-TCB (28 mg L⁻¹) was 8.92, and negligible TU values were found in the aqueous phase obtained after the regeneration step, which meant the absence of the toxic by-products generated after regeneration treatment.

TOC was also measured at 180 min in the aqueous phase with values lower than 4 mg L⁻¹. Therefore, TOC in solution corresponds to 1% of the oxidised 124-TCB. Iron concentration was also measured in the

aqueous phase at 180 min of each regeneration cycle with values lower than 0.1 mg L⁻¹. Iron leaching in the successive three regeneration cycles was less than 1% of iron adsorbed on the carbon.

3.5. Change in GAC physicochemical properties during adsorption-regeneration

The properties of the GAC surface can be modified after the adsorption-regeneration cycles. The characterisation of GAC after the different treatments is presented and discussed.

3.5.1. Effect of the acid pre-treatment, Fe and 124-TCB adsorption

The physicochemical properties of the original GAC (GAC-O) and GAC obtained after washing with acid water at pH = 3 (GAC-W) have been evaluated. The BET area, pore volume, atomic mass and acid group concentrations of GAC-O and GAC-W are summarised in Table 1. As shown, the surface area of GAC-O is 905 m² g⁻¹, being this value slightly reduced to 871 m² g⁻¹ (6%) after the acidic pre-treatment (GAC-W). An equivalent reduction in the pore volume (7%) was observed in GAC-W. Kan et al. (Kan and Huling, 2009) after pre-treatment with acid water. Still, these authors also reported that acidic pre-treatment of GAC enhanced Fe sorption, avoiding the presence of amorphous and Fe precipitates that would be obtained with untreated GAC. The N₂ adsorption isotherms obtained for GAC-O and GAC-W are summarised in Figure SM4a, showing a type I isotherm (Thommes et al., 2015) attributed to a microporous material.

The effect of Fe adsorbed on the GAC surface has been studied with samples GAC-5Fe and GAC-12Fe. The results are also shown in Table 1 and Figure SM4a. As can be seen, GAC-5Fe and GAC-W have similar surface areas. The surface area of GAC-12Fe was about 7% lower than that of GAC-W. The N₂ adsorption isotherms of GAC-xFe show the same type I isotherm found for GAC-W, as shown in Figure SM4a. (Thommes et al., 2015), keeping the microporous structure.

Regarding the surface chemistry of GAC (Table 1), it was found that the atomic mass concentration of the GAC-O was mainly composed of oxygen (around 10%) and traces of N and S. In addition, TPD profiles were represented in Fig. 5 and the amount of CO and CO₂ obtained by TPD are given in Table 1. The CO and CO₂ amounts evidenced the low presence of surface carbon-oxygen groups. As can be seen in Fig. 5, CO₂ evolution is quite lower than that of CO for all the samples, evidencing the low presence of lactone, carboxyl and anhydride groups. As shown in Table 1 and Fig. 5, the amounts of CO and CO₂ slightly increased after washing (GAC-W), as evidenced by the significant decomposition of carbonyl and quinone groups as CO at high temperatures.

However, the adsorption of Fe promoted an increase of CO and CO₂ evolution (higher formation of oxygen surface groups). The comparison between CO profile for the GAC-W and GAC-12Fe samples (Fig. 5a) showed an increase in the CO desorption rate at high temperatures (around 870 °C). This increase was associated to the oxidation of the carbon surface by the sulphur species, which were incorporated into the carbon as part of the iron salts used in the pre-treatment. As reported in the literature, an AC containing sulphur species produces a higher C consumption than other functional groups present in the AC (Lin et al., 2021), however the extent of the carbon oxidation is not very significant, as can be seen in Table 1.

The C1s, O1s and Fe2p XPS spectra were represented in Figure SM5, and the atomic mass concentration is given in Table 1. The results of XPS analysis of GAC-5Fe and GAC-12Fe confirms the highest amount of adsorbed iron in GAC-12Fe. The results of XPS analysis of GAC-5Fe and GAC-12Fe confirms the highest amount of adsorbed iron in GAC-12Fe. With regard to Fe XPS spectra in Figure SM5c, a main peak in the Fe2p_{3/2} band was observed at 711.5 eV, which was associated to Fe (III) oxides such as FeOOH or Fe₂O₃. The S and O atomic content in the GAC surface increased after Fe adsorption because sulphate iron (II) salt was used to immobilise Fe on GAC.

The effect of 124-TCB adsorption on the physicochemical properties

Table 1
Physicochemical properties in the GAC samples tested.

Analytical technique	Adsorption		N ₂ adsorption		XPS: mass surface concentration						TPD	
	q _{Fe} (mg g ⁻¹)	Saturation in 124-TCB (mg g ⁻¹)	A _{BET} (m ² g ⁻¹)	V _P (m ³ g ⁻¹)	C (%)	N (%)	O (%)	S (%)	Fe (%)	Cl (%)	CO (μmol g ⁻¹)	CO ₂ (μmol g ⁻¹)
GAC-O	0.00	0.00	908	0.420	88.82	0.25	10.60	0.33	0	0	290	18
GAC-W	0.00	0.00	851	0.380	90.59	0.51	8.75	0.15	0	0	349	41
GAC-5Fe	5.36	0.00	861	0.429	86.07	0.46	8.86	1.01	2.69	0	831	111
GAC-12Fe	12.00	0.00	806	0.408	58.59	0.65	28.05	4.32	8.40	0	1239	302
GAC-S	0.00	350	556	0.305	86.22	0.34	9.28	–	0	4.16	474	69
GAC-5Fe-S	5.36	330	662	0.338	77.67	0.31	14.85	–	4.88	2.29	564	108
GAC-12Fe-S	12.00	300	769	0.365	64.94	0.55	23.69	–	9.94	0.87	691	160
GAC-12Fe-C1	12.00	0.00	813	0.427	73.09	0.55	17.35	1.79	7.22	0	1050	263
GAC-12Fe-C3	12.00	0.00	761	0.411	66.86	0.62	20.66	1.93	9.93	0	1271	301
GAC-12Fe-S-C1-R	12.00	300	838	0.422	65.29	0.53	22.94	–	8.39	2.86	767	184
GAC-12Fe-S-C1-S	12.00	300	583	0.283	66.46	0.44	21.25	–	8.48	3.36	760	139
GAC-12Fe-S-C3-R	12.00	300	629	0.319	46.42	0.70	34.95	–	15.19	2.44	850	240
GAC-12Fe-S-C3-S	12.00	300	584	0.291	64.78	0.38	21.78	–	9.32	3.75	850	180

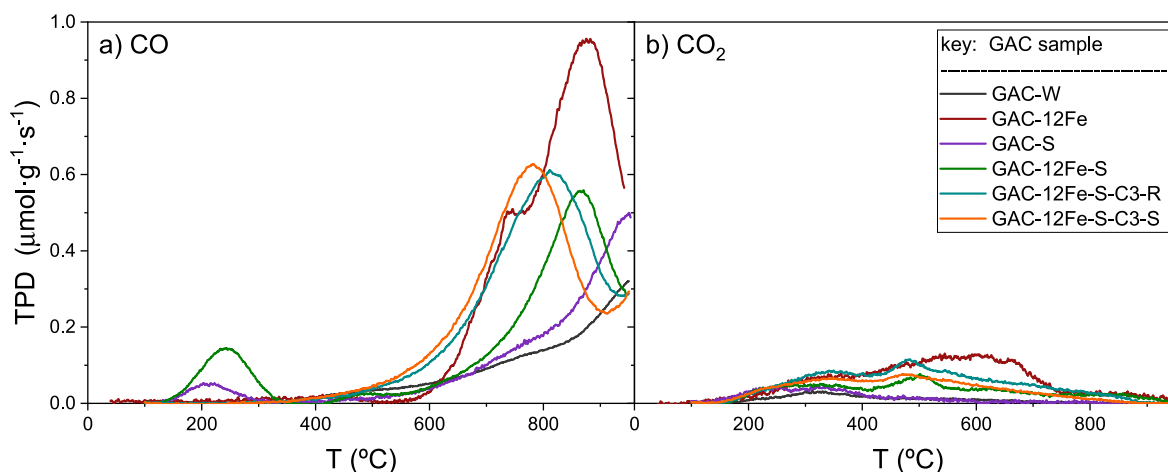


Fig. 5. TPD profile of GAC samples. a) CO desorption profile and b) CO₂ desorption profile.

has been studied in the absence and presence of adsorbed iron. As shown in Table 1, the surface area of GAC-S was 35% lower than GAC-W. On the other hand, the reduction in surface area with GAC-5Fe-S and GAC-12Fe-S was 22% and 11%, respectively (related to the area of GAC-W). Therefore, the highest the amount of Fe adsorbed, the lower the reduction of the surface area after 124-TCB adsorption. This finding can be explained by considering that the amount of 124-TCB adsorbed on GAC increases as iron adsorbed decreases. As shown in Figure SM4b, the N₂ adsorption isotherms obtained after 124-TCB adsorption show a type I isotherm [46] again, keeping the microporous structure. As shown in Table 1, the evolution of CO and CO₂ during TPD decreases after 124-TCB. As shown in Fig. 5a, the amount of CO desorbed for GAC-12Fe-S is much lower than that obtained for GAC-12Fe. These results suggest that the adsorption of 124-TCB can reduce the sulphur species present on the carbon, decreasing the formation of carbon-oxygen complexes, which decompose at high temperatures (i.e. carbonyl, quinone groups ...). On the other hand, a CO evolution was also observed at low temperature (around 200 °C), for saturated samples (GAC-S and GAC-12Fe-S), which corresponds to the desorption of the adsorbed pollutant (Berenguer et al., 2010).

As can be seen in Figure SM5a, C1s XPS spectra of the different samples were quite similar, only showing an increase of the intensity around 288.5 eV in the saturated samples, GAC-12Fe-S and GAC-

12Fe-S-C3-S, which can be associated to the formation of carbonate groups or even to the interaction of C-Cl (<https://xpsdatabase.com/>). The O1s XPS spectra (in Figure SM5b) of both GAC-12Fe and GAC-12Fe-S showed a reduction of the oxygen surface concentration, probably due to the competitive adsorption of the contaminant and the sulphate species, due to relative Fe concentrations were quite similar.

3.5.2. Effect of H₂O₂

The physicochemical properties were characterised after the reaction of GAC with H₂O₂ at 60 °C. First, these changes are studied without adsorbed 124-TCB (samples GAC-12Fe-C1 and GAC-12Fe-C3 in Figure SM3). The apparent surface area, pore volume, atomic concentration on the GAC surface, and the evolved amounts of CO and CO₂ (TPD analysis) of the GAC-12Fe-C1 and GAC-12Fe-C3 samples are summarised in Table 1 and compared to the corresponding values obtained by GAC-12Fe. The N₂ adsorption-desorption isotherms are shown in Figure SM6. The surface area, pore volume and the surface chemistry of GAC after the reaction with the oxidant in the first (GAC-12Fe-C1) and third cycles (GAC-12Fe-C3) are very similar to the values determined for GAC-12Fe (before the reaction with the oxidant). These results confirm that the reaction between H₂O₂ and the GAC surface can be considered as a catalytic process with GAC surface not significantly oxidised or modified after the reaction with H₂O₂.

The GAC physicochemical properties have been studied during the adsorption-regeneration cycles of spent GAC-12Fe-S at 60 °C. The samples obtained after the first regeneration cycle, GAC12Fe-C1-R (regeneration of GAC-12Fe-S) and GAC-12-Fe-C1-S (resaturation of GAC-12Fe-C1-R with 124 TC B) and the samples obtained at the third regeneration cycle (GAC-12Fe-C3-R and GAC-12Fe-C3-S) have been analysed. The corresponding N₂ adsorption-desorption isotherms are depicted in Figure SM7, and the surface chemistry is summarised in Table 1. As shown in Figure SM7, the type of N₂ adsorption-desorption isotherms was unchanged with the adsorption-regeneration cycles, confirming that the microporous structure of the carbon was slightly affected by the adsorption-regeneration cycles. As summarised in Table 1, the surface GAC properties measured by GAC-12Fe-C1-R and GAC-12Fe-C3-R are similar to those obtained in GAC-12Fe, confirming the surface stability of the GAC during the regeneration process. Resaturation of the regenerated GAC with 124-TCB implies a reduction in the surface area (similar to the reduction observed between GAC-12Fe and GAC-12Fe-S). Still, the recovery of the surface area and surface chemistry after regeneration indicate that the oxidant reacted selectively with the 124-TCB, also confirmed by the reduction of chloride mass concentration on the GAC surface measured by the XPS technique. In addition, the regeneration treatment produced an increase of the relative oxygen surface concentration, which was reduced after the saturation cycle, remaining very stable during the successive cycles as can be seen in the XPS spectra in Figure SM5b. The type and quantity of oxygen groups on the surface were maintained. Furthermore, the TPD results revealed that the concentration of acidic groups on the GAC did not increase after the different regeneration/adsorption cycles, in agreement with a selective attack of H₂O₂ to the 124-TCB. As can be also seen in Fig. 5a, the profile for TPD-CO for GAC-12Fe-S-C3-R and GAC-12Fe-S-C3-S were quite similar to the one obtained for GAC-12Fe-S, indicating that the activated carbon remained stable during the consecutive oxidation and adsorption cycles.

The CO and CO₂ values measured by TPD for GAC-12Fe-C1R and GAC-12Fe-C2R were slightly lower than those obtained for GAC-12Fe-C1 and GAC-12Fe-C3, due to the presence of the remaining 124-TCB adsorbed on the GAC surface.

All these results evidence the high selectivity of this process to the pollutant, which maintains the physicochemical properties of the adsorbent (GAC) almost unchanging, facilitating its reuse in consecutive cycles of adsorption-regeneration.

4. Conclusions

In this work, the abatement of 124-TCB from polluted water has been successfully achieved using a two-step method. In the first step, the 124-TCB is adsorbed onto the GAC surface with Fe previously immobilised. The spent GAC is, then, regenerated by oxidising the adsorbed pollutant using hydrogen peroxide at a temperature of 60 °C. The adsorption/regeneration was carried out during three consecutive cycles, and the GAC remained stable during these successive cycles, maintaining 65% of the original adsorption capacity of the pollutant, without significant changes in the formation of oxygen surface groups, and amount of iron adsorbed. No aromatic or chlorinated by-products were detected in the aqueous phase obtained during the regeneration step, showing low TOC values. No toxic oxidation by-products were detected using the Microtox® bioassay.

Although more research is required to implement this treatment on a full scale, this treatment is a promising technology to intensify the removal and destruction of organic pollutants. The tested method can be used to treat large volumes of polluted water, and the regeneration of GAC reduces the generation of highly contaminated solid waste. In addition, the use of immobilised iron did not require acidification of the final stream, avoiding the shortcomings of the Fenton reagent applied in a homogeneous process.

CRedit authorship contribution statement

Andrés Sánchez-Yepes: Methodology, Investigation, Writing – original draft. **Aurora Santos:** Funding acquisition, Resources, Conceptualization, Supervision. **Juana M:** Conceptualization, Investigation, Writing – original draft. **Rosas:** Conceptualization, Investigation, Writing – original draft. **José Rodríguez-Mirasol:** Funding acquisition. **Tomás Cordero:** Funding acquisition. **David Lorenzo:** Conceptualization, Methodology, Supervision, Writing – original draft.

Declaration of competing interest

The authors declare that they have no known competing financial interests or personal relationships that could have appeared to influence the work reported in this paper.

Data availability

No data was used for the research described in the article.

Acknowledgements

This work was supported by the EU LIFE Program (LIFE17 ENV/ ES /000260), the Regional Government of Madrid, through the CARESOIL project (S2018/EMT-4317), and the Spanish Ministry of Economy, Industry, and Competitiveness, through project PID 2019-105934RB-I00. A.S.-Y. would also like to thank Ministry of Science and Innovation for the support for predoctoral contracts under FPI grant PRE 2020-093195. This research was also supported by the Spanish Ministry of Science, Innovation and Universities and Junta de Andalucía through RTI 2018-097555-B-I00 and UMA18-FEDERJA-110 projects, respectively.

Appendix A. Supplementary data

Supplementary data to this article can be found online at <https://doi.org/10.1016/j.chemosphere.2023.140047>.

References

- Alben, K., Belfort, G., Benedek, A., Frick, B.R., McGinnis, F.K., Pirbazari, M., Rosene, M. R., Shpirt, E., Tien, C., Weber, W.J., 1983. Treatment of water by granular activated carbon - discussion-ii - modeling and competitive adsorption aspects. *Adv. Chem.* 269–276.
- Anfruns, A., Montes-Morán, M.A., Gonzalez-Olmos, R., Martín, M.J., 2013. H₂O₂-based oxidation processes for the regeneration of activated carbons saturated with volatile organic compounds of different polarity. *Chemosphere* 91, 48–54. <https://doi.org/10.1016/j.chemosphere.2012.11.068>.
- Baghirzade, B.S., Zhang, Y., Reuther, J.F., Saleh, N.B., Venkatesan, A.K., Apul, O.G., 2021. Thermal regeneration of spent granular activated carbon presents an opportunity to break the forever PFAS cycle. *Environ. Sci. Technol.* 55, 5608–5619. <https://doi.org/10.1021/acs.est.0c8224>.
- Barbash, A.M., Hoag, G.E., Nadim, F., 2006. Oxidation and removal of 1,2,4-trichlorobenzene using sodium persulfate in a sorption-desorption experiment. *Water Air Soil Pollut.* 172, 67–80. <https://doi.org/10.1007/s11270-005-9052-3>.
- Bembnowska, A., Pelech, R., Milchert, E., 2003. Adsorption from aqueous solutions of chlorinated organic compounds onto activated carbons. *J. Colloid Interface Sci.* 265, 276–282. [https://doi.org/10.1016/S0021-9797\(03\)00532-0](https://doi.org/10.1016/S0021-9797(03)00532-0).
- Berenguer, R., Marco-Lozar, J.P., Quijada, C., Cazorla-Amorós, D., Morallón, E., 2010. Comparison among chemical, thermal, and electrochemical regeneration of phenol-saturated activated carbon. *Energy Fuels* 24, 3366–3372. <https://doi.org/10.1021/ef901510c>.
- Blus, L.J., 2003. Organochlorine pesticides. *Handbook of ecotoxicology* 2, 313–340.
- Cabrera-Codony, A., Gonzalez-Olmos, R., Martín, M.J., 2015. Regeneration of siloxane-exhausted activated carbon by advanced oxidation processes. *J. Hazard Mater.* 285, 501–508. <https://doi.org/10.1016/j.jhazmat.2014.11.053>.
- Cai, Q.Q., Wu, M.Y., Hu, L.M., Lee, B.C.Y., Ong, S.L., Wang, P., Hu, J.Y., 2020. Organics removal and in-situ granule activated carbon regeneration in FBR-Fenton/GAC process for reverse osmosis concentrate treatment. *Water Res.* 183, 116119 <https://doi.org/10.1016/j.watres.2020.116119>.
- Chen, Q., Liu, H., Yang, Z., Tan, D., 2017. Regeneration performance of spent granular activated carbon for tertiary treatment of dyeing wastewater by Fenton reagent and hydrogen peroxide. *J. Mater. Cycles Waste Manag.* 19, 256–264. <https://doi.org/10.1007/s10163-015-0410-y>.

- Conte, L.O., Dominguez, C.M., Checa-Fernandez, A., Santos, A., 2022. Vis LED photofenton degradation of 124-trichlorobenzene at a neutral pH using ferrioxalate as catalyst. *Int. J. Environ. Res. Publ. Health* 19. <https://doi.org/10.3390/ijerph19159733>.
- Crincoli, K.R., Jones, P.K., Huling, S.G., 2020. Fenton-driven oxidation of contaminant-spent granular activated carbon (GAC): GAC selection and implications. *Sci. Total Environ.* 734, 139435 <https://doi.org/10.1016/j.scitotenv.2020.139435>.
- Gramatica, P., Papa, E., 2007. Screening and ranking of POPs for global half-life: QSAR approaches for prioritization based on molecular structure. *Environ. Sci. Technol.* 41, 2833–2839. <https://doi.org/10.1021/es061773b>.
- Gramatica, P., Pozzi, S., Consonni, V., Di Guardo, A., 2002. Classification of environmental pollutants for global mobility potential. *SAR QSAR Environ. Res.* 13, 217. <https://doi.org/10.1080/10629360290002695>.
- Hornig, R.S., Tseng, I.-C., 2008. Regeneration of granular activated carbon saturated with acetone and isopropyl alcohol via a recirculation process under H₂O₂/UV oxidation. *J. Hazard Mater.* 154, 366–372. <https://doi.org/10.1016/j.jhazmat.2007.10.033>.
- Huling, S.G., Arnold, R.G., Sierka, R.A., Jones, P.K., Fine, D.D., 2000. Contaminant adsorption and oxidation via Fenton reaction. *Environ. Eng. 126*, 595–600. [https://doi.org/10.1061/\(ASCE\)0733-9372\(2000\)126:7\(595\)](https://doi.org/10.1061/(ASCE)0733-9372(2000)126:7(595)).
- Huling, S.G., Hwang, S., 2010. Iron amendment and Fenton oxidation of MTBE-spent granular activated carbon. *Water Res.* 44, 2663–2671. <https://doi.org/10.1016/j.watres.2010.01.035>.
- Huling, S.G., Jones, P.K., Ela, W.P., Arnold, R.G., 2005. Fenton-driven chemical regeneration of MTBE-spent GAC. *Water Res.* 39, 2145–2153. <https://doi.org/10.1016/j.watres.2005.03.027>.
- Huling, S.G., Ko, S., Park, S., Kan, E., 2011. Persulfate oxidation of MTBE- and chloroform-spent granular activated carbon. *J. Hazard Mater.* 192, 1484–1490. <https://doi.org/10.1016/j.jhazmat.2011.06.070>.
- Jatta, S., Huang, S., Liang, C., 2019. A column study of persulfate chemical oxidative regeneration of toluene gas saturated activated carbon. *Chem. Eng. J.* 375, 122034 <https://doi.org/10.1016/j.cej.2019.122034>.
- Jayaraj, R., Megha, P., Sreedev, P., 2016. Organochlorine pesticides, their toxic effects on living organisms and their fate in the environment. *Interdiscipl. Toxicol.* 9, 90–100. <https://doi.org/10.1515/intox-2016-0012>.
- Kan, E., Huling, S.G., 2009. Effects of temperature and acidic pre-treatment on fenton-driven oxidation of MTBE-spent granular activated carbon. *Environ. Sci. Technol.* 43, 1493–1499. <https://doi.org/10.1021/es802360f>.
- Klecka, G., Boethling, B., Franklin, J., Grady, L., Graham, D., Howard, P.H., Kannan, K., Larson, R.L., Mackay, D., Muir, D., van de Meent, D.M., 2000. Evaluation of Persistence and Long-Range Transport of Organic Chemicals in the Environment.
- Li, X., Yang, C., Guo, J., Yang, J., Qiu, G., Yi, B., 2013. Regeneration of saturated activated carbon by Fenton reagent. *Chin. J. Environ.* 7, 3867–3873.
- Lin, Y., Li, Y., Xu, Z., Guo, J., Zhu, T., 2021. Carbon consumption and adsorption-regeneration of H₂S on activated carbon for coke oven flue gas purification. *Environ. Sci. Pollut. Res.* 28 <https://doi.org/10.1007/s11356-021-14914-2>.
- Lorenzo, D., Dominguez, C.M., Romero, A., Santos, A., 2019. Wet peroxide oxidation of chlorobenzenes catalyzed by goethite and promoted by hydroxylamine. *Catalysts* 9. <https://doi.org/10.3390/catal9060553>.
- Lorenzo, D., Santos, A., Sánchez-Yepes, A., Conte, L.O., Domínguez, C.M., 2021. Abatement of 1,2,4-trichlorobenzene by wet peroxide oxidation catalysed by goethite and enhanced by visible LED light at neutral pH. *Catalysts* 11, 139. <https://doi.org/10.3390/catal11010139>.
- Lougheed, T., 2007. Persistent organic pollutants - environmental stain fading fast. *Environ. Health Perspect.* 115, A20. <https://doi.org/10.1289/ehp.115-a20>.
- Ma, L., Wu, Z., He, M., Wang, L., Yang, X., Wang, J., 2020. Experimental study on Fenton oxidation regeneration of adsorbed toluene saturated activated carbon. *Environ. Technol.* 1–10 <https://doi.org/10.1080/09593330.2020.1797891>.
- Marsh, H., Rodríguez-Reinoso, F., 2006a. Chapter 4 - characterization of activated carbon. In: Marsh, H., Rodríguez-Reinoso, F. (Eds.), *Activated Carbon*. Elsevier Science Ltd, Oxford, pp. 143–242. <https://doi.org/10.1016/B978-008044463-5/50018-2>.
- Marsh, H., Rodríguez-Reinoso, F., 2006b. Chapter 8 - applicability of activated carbon. In: Marsh, H., Rodríguez-Reinoso, F. (Eds.), *Activated Carbon*. Elsevier Science Ltd, Oxford, pp. 383–453. <https://doi.org/10.1016/B978-008044463-5/50022-4>.
- McLane, C., 1949. Hydrogen peroxide in the thermal hydrogen oxygen reaction I. Thermal decomposition of hydrogen peroxide. *Chem. Phys.* 17, 379–385. <https://doi.org/10.1063/1.1747821>.
- Moreno, J.C., Sarria, V.M., Polo, Á.D., Giraldo, L., 2007. Evaluación del Peróxido de Hidrógeno en la Oxidación de Fenol con Hierro Soportado Sobre Tela de Carbón Activado. *IT* 18, 67–72. <https://doi.org/10.4067/s0718-07642007000200010>.
- Peng, J., Wu, E., Wang, N., Quan, X., Sun, M., Hu, Q., 2019. Removal of sulfonamide antibiotics from water by adsorption and persulfate oxidation process. *J. Mol. Liq.* 274, 632–638. <https://doi.org/10.1016/j.molliq.2018.11.034>.
- Plakas, K.V., Karabelas, A.J., 2016. A study on heterogeneous Fenton regeneration of powdered activated carbon impregnated with iron oxide nanoparticles. *Glob. Nest J.* 18, 259–268. <https://doi.org/10.30955/gnj.001894>.
- Rodan, B.D., Pennington, D.W., Eckley, N., Boethling, R.S., 1999. Screening of persistent organic pollutants: techniques to provide a scientific basis for POPs criteria in international negotiations. *Environ. Sci. Technol.* 33, 3488. <https://doi.org/10.1021/es980060t>.
- Salvador, F., Martín-Sánchez, N., Sánchez-Hernández, R., Sánchez-Montero, M.J., Izquierdo, C., 2015. Regeneration of carbonaceous adsorbents. Part I: thermal regeneration. *Microporous Mesoporous Mater.* 202, 259–276. <https://doi.org/10.1016/j.micromeso.2014.02.045>.
- San Miguel, G., Lambert, S.D., Graham, N.J.D., 2002. Thermal regeneration of granular activated carbons using inert atmospheric conditions. *Environ. Technol.* 23, 1337–1346. <https://doi.org/10.1080/09593332508618449>.
- Sánchez-Yepes, A., Santos, A., Rosas, J.M., Rodríguez-Mirasol, J., Cordero, T., Lorenzo, D., 2022. Regeneration of granulated spent activated carbon with 1,2,4-trichlorobenzene using thermally activated persulfate. *Ind. Eng. Chem. Res.* 61, 9611–9620. <https://doi.org/10.1021/acs.iecr.2c00440>.
- Sánchez-Yepes, A., Santos, A., Rosas, J.M., Rodríguez-Mirasol, J., Cordero, T., Lorenzo, D., 2022. Regeneration of granulated spent activated carbon with 1,2,4-trichlorobenzene using thermally activated persulfate. *Ind. Eng. Chem. Res.* 61, 9611–9620. <https://doi.org/10.1021/acs.iecr.2c00440>.
- Santos, A., Yustos, P., Quintanilla, A., García-Ochoa, F., Casas, J.A., Rodríguez, J.J., 2004. Evolution of toxicity upon wet catalytic oxidation of phenol. *Environ. Sci. Technol.* 38, 133–138. <https://doi.org/10.1021/es030476t>.
- Santos, D.H.S., Duarte, J.L.S., Tonholo, J., Meili, L., Zanta, C.L.P.S., 2020. Saturated activated carbon regeneration by UV-light, H₂O₂ and Fenton reaction. *Sep. Purif. Technol.* 250, 117112 <https://doi.org/10.1016/j.seppur.2020.117112>.
- Schroll, R., Brahushi, F., Dörfler, U., Kühn, S., Fekete, J., Munch, J.C., 2004. Biomineralisation of 1,2,4-trichlorobenzene in soils by an adapted microbial population. *Environ. Pollut.* 127, 395–401. <https://doi.org/10.1016/j.envpol.2003.08.012>.
- Thommes, M., Kaneko, K., Neimark, A.V., Olivier, J.P., Rodríguez-Reinoso, F., Rouquerol, J., Sing, K.S.W., 2015. Physisorption of gases, with special reference to the evaluation of surface area and pore size distribution (IUPAC Technical Report). *Pure Appl. Chem.* 87, 1051–1069. <https://doi.org/10.1515/pac-2014-1117>.
- Toledo, L.C., Silva, A.C.B., Augusti, R., Lago, R.M., 2003. Application of Fenton's reagent to regenerate activated carbon saturated with organochloro compounds. *Chemosphere* 50, 1049–1054. [https://doi.org/10.1016/S0045-6535\(02\)00633-1](https://doi.org/10.1016/S0045-6535(02)00633-1).
- Urano, K., Yamamoto, E., Tonegawa, M., Fujie, K., 1991. Adsorption of chlorinated organic compounds on activated carbon from water. *Water Res.* 25, 1459–1464. [https://doi.org/10.1016/0043-1354\(91\)90175-5](https://doi.org/10.1016/0043-1354(91)90175-5).
- Weber, W.J., Vanvliet, B.M., 1981. Synthetic adsorbents and activated carbons for water-treatment - overview and experimental comparisons. *J. Am. Water Works Assoc.* 73, 420–426.
- Williams, B., 1928. The thermal decomposition of hydrogen peroxide in aqueous solutions. *Trans. Faraday Soc.* 24, 245–255.
- Xiao, P.-f., An, L., Wu, D.-d., 2020. The use of carbon materials in persulfate-based advanced oxidation processes: a review. *N. Carbon Mater.* 35, 667–683. [https://doi.org/10.1016/S1872-5805\(20\)60521-2](https://doi.org/10.1016/S1872-5805(20)60521-2).
- Zhang, J., Zhang, N., Tack, F.M.G., Sato, S., Alessi, D.S., Oleszczuk, P., Wang, H., Wang, X., Wang, S., 2021. Modification of ordered mesoporous carbon for removal of environmental contaminants from aqueous phase: a review. *J. Hazard Mater.* 418, 126266 <https://doi.org/10.1016/j.jhazmat.2021.126266>.

ANNEX II. Abstracts

Thermal Conductive Heating (TCH): Comparison of power consumption to heat the soil between electrical resistance heating and gas fired burners

Jonathan de Grunne
Haemers Technologies

Thermal desorption is an environmental remediation technology that uses heat to increase the volatility of contaminants (organic and/or inorganic) as such that they can be removed from solid matrix (typically soil) to be recycled or destroyed. The subject will focus on two existing in situ TCH techniques: electrical and thermal heating.

The designs and calculations are made considering the injection of power per linear meter of heating element. The method of heat injection with electrical power directly injects 1 kW/m, when the method of heat injection by thermal conduction has a 50-55% efficiency, therefore needs to produce 1.8-2 kW/m to inject 1 kW/m. The question here is how is electricity produced?

Current data shows that the needed power in terms of natural gas to produce 1 kW of electricity can vary from 1.6 kW to 2.85 kW depending on the type of thermal plant (conventional or with cogeneration for example). If we take these two extremes of yields, we get to an electrical power consumption in terms of combustion of natural gas between 320 – 640 kWh/m³ of soil for the best case and 570 – 1140 kWh/m³ of soil for the worst case (when the direct natural gas consumption to heat the soil with thermal conduction can vary from 619 to 894 kWh/m³).

The difference between the two techniques in terms of power efficiency and consumption will depend on the type of thermal electricity production. Whether the electricity production is advanced or not, the advantage given to one technique can easily become the advantage of the other depending on the electricity production rates of the countries in which thermal remediation projects will take place. As of now, very few thermal plants can reach a yield of 60% with natural gas. We can globally admit that with the current sources of electricity production, the two techniques are very close to each other in terms of consumption and efficiency. Another important factor to consider is the location of remediations sites because of both the electrical power and gas supply availability.

The second part of the article will cover the energy loss related to the interdistance between heating elements. Indeed, energy efficiency in heat injection is only a part of total remediation energy efficiency. Interdistance between heating wells drives remediation time and energy losses.

Biochar - from organic waste to resource for treatment of contaminated soil

Anja Enell; Maria Larsson¹; Ludvig Landen²; Peter Flyhammar³; Yvonne Ohlsson³; Sigrun Dahlin⁴; Sara Hallin⁴; Christopher Jones⁴; Cecilia Sundberg⁵; Elias Azzi⁵; Elin Norberg⁴; Dan Berggren Kleja⁶
¹Örebro University; ²NSR-AB; ³Swedish Geotechnical Institute; ⁴Swedish University of Agricultural Sciences; ⁵KTH, Royal Institute of Technology; ⁶Swedish University of Agricultural Sciences (SLU) / Swedish Geotechnical Institute (SGI)

Biochar-RE:Source is a 2-year research project aiming to develop a remediation technique with biochar to stabilize contaminated soil and increase soil quality to reduce waste and environmental risks. In Sweden, the most common remedial action is still "dig-and-dump", leading to removal and landfilling of large volumes of soil.

Biochar could here serve as an impressive alternative leading to more sustainable soil management, great socioeconomic savings and several other environmental benefits.

Biochar is the charred solid product resulting from the pyrolysis of biomass under low oxygen environment. It is used as a soil amendment in forestry and farming due to its capacity to increase the soil quality by its ability to conserve water, sequester carbon, prevent nutrient leaching and neutralize soil acidity. Due to its porous structure, large surface area, and many functional groups it can also sorb both inorganic and organic pollutants.

We aim to find biochars produced from local organic waste streams, suitable for remediation of historically contaminated soils. The project will also investigate the conditions for biochar production from organic waste, the ability to apply the biochar technique in urban environments and quantify the environmental impact of different system alternatives in a life-cycle perspective.

During 2018, a lab study was initiated to test four biochars of different origin (produced from urban garden waste and recycled wood, processed at 500-650 °C) and two biochars modified by the addition of clay and miscanthus. Two historical contaminated soils (contaminated by metals and polycyclic aromatic hydrocarbons; PAH) were amended with 3% of each biochar. The bioavailability of PAH is being assessed using polyoxymethylene (POM) and the leachability of metals are studied at different pH using pH-static leaching tests. The soil quality of the biochar-amended soils and the untreated soils is evaluated by measuring CEC, organic carbon content, C/N-ratio, pH and available phosphate, while the characteristics of the different tested biochars are analysed by methods regulated by European Biochar Certificate (EBC).

The outcome of the lab-study will serve as the basis for choosing a suitable biochar to test in field experiment during 2019. The purpose of the field study is to determine environmental risks and biological effects under natural conditions (temperature, wind, moisture, rainfall, soil microbes, pH). We will study the impact of biochar addition to different amendment-percentage, and types of soils. The soils will be representative of masses that arise from excavation or demolition in urban environments and contain common pollutants such as PAH and metals, but differ in terms of organic content and permeability (clay content). The cultivation beds (approx. 3 x 3m) will be seeded with a crop and analysed after a growing season (summer 2019) with respect to biomass production and contamination. The bioavailability of pollutants in amended areas and controls will be assessed using leaching and ecotoxicity tests. Impact on soil respiration and effects on soil microorganisms that control the nitrogen cycle will also be studied.

Solubilization of dense non aqueous phase liquids produced as lindane wastes using non-ionic surfactants

Raul Garcia; Arturo Romero; David Lorenzo; Aurora Santos
Universidad Complutense de Madrid

The production of the obsolete pesticide Lindane (g-HCH isomer), included in the Stockholm Convention on Persistent Organic Pollutants (POPs), uses benzene as a starting material. Benzene was photochlorinated by Cl₂ and UV light with reaction in series. At each step, the number of chlorine atoms in 6-carbon ring increases. The reaction route includes Chlorobenzene (CB), Dichlorobenzenes (DCB), Trichlorobenzenes (TCB), Tetrachlorobenzenes (TetraCB), Pentachlorocyclohexenes (PentaCX), Hexachlorocyclohexanes (HCHs) and Heptachlorocyclohexanes (HeptaCH)[1]. Since the g-HCH was the only isomer with insecticidal properties, the HCH mixture was purified to produce pure lindane. Among the wastes

from lindane production, a Dense Non-Aqueous Phase Liquid (DNAPL) composed of HCH isomers, benzene and chlorobenzenes was detected in two landfills of Sabiñanigo (Spain) with an associated polluted groundwater plume[2].

Due to the low solubility of these compounds in the aqueous phase several treatment trains can be considered for the remediation of a site contaminated by NAPLs [3]. Some of them involve the use of surfactants in order to solubilize or mobilize this organic phase in the subsurface and remove it at a higher rate than achievable with pumped groundwater.

In this work, two ionic surfactants have been tested, Tween 80 from Sigma-Aldrich and E-Mulse 3[®] from EthicalChem, in order to determine the solubility of each Chlorinated Organic Compound (COCs) identified and quantified in DNAP. Two DNAPL samples were used, obtained at Bailin and Sardas landfills (Sabiñanigo, Spain), at several surfactant concentrations in the aqueous phase. Batch runs have been carried out in closed vials containing a mass of DNAPL and a volume of an aqueous solution with the surfactant tested. Analysis of the 28 identified COCs in the remaining organic phase and in the aqueous solution has been carried out. Fingerprint of COCs in the emulsion and in the organic phase were compared. Besides, partition coefficient aqueous/organic phase of each COC was obtained in absence and presence of surfactants. A high increase of the solubility was noticed with the surfactant addition, mainly for the less soluble COCs in water.

Besides, the solubility and stability of the emulsions at neutral and alkaline pH was investigated. It has been proved that at alkaline conditions (pH>12) alkaline dehydrochlorination takes place, with and without surfactants in the aqueous phase [4].

The authors acknowledge financial support from the Comunidad Autonoma of Madrid (Project S2013-MAE-2739 CARESOIL-CM) and from the Spanish MINECO (Project CTM2016-77151-C2-1-R) and the Aragon Government and EMGRISA Company for the supply of samples.

- 1.Santos, A., et al., Environmental Pollution, 2018.
- 2.Fernández, J., M. Arjol, and C. Cacho, Environmental Science and Pollution Research, 2013. 20(4): p. 1937-1950.
- 3.Tsitonaki, A., Treatment trains for the remediation of aquifers contaminated with MTBE and other xenobiotic compounds, in Department of Environmental Engineering. 2008, Technical University of Denmark: Denmark.
- 4.Santos, A., et al., Science of the Total Environment, 2018. 615: p. 1070-1077.

Between caravans and boreholes - Challenges of performing in-situ remediation on a camping site in the Black Forest, Germany

Petra Grill¹; Markus Kampschulte¹; Hans-Peter Koschitzky²; Oliver Trötschler²

¹CDM Smith Consult GmbH; ²Universität Stuttgart, Institut für Wasser- und Umweltsystemmodellierung, VEGAS

How do you quickly and inconspicuously extract volatile chlorinated hydrocarbons (CHCs) on a camping site on the outskirts of a spa town in the northern Black Forest without disturbing the relaxation of the numerous holidaymakers? CDM Smith accepted the challenge and supervised the thermal in-situ remediation at a camping site in Bad Liebenzell as consultant and project coordinator.

More than 50 years have passed since the former camera manufacturer Regula King closed its doors in Bad Liebenzell, in the Black

Forest. But the consequences of the production are still in evidence. The CHCs that Regula King used as degreasing agents until the 1960s contaminated the groundwater in the uppermost aquifer.

The Pump & Treat and Soil Vapour Extraction remediation had not achieved the desired success after ten years. The state of Baden-Württemberg / Germany decided to conduct supplementary thermal in-situ remediation of the main contaminated areas (source zone) by means of steam-air-injection.

The contaminated area of approximately 700 m² (contaminated soil volume 4,800 m³) was in the immediate vicinity of a residential area and the local open-air swimming pool and mostly located below a building on the camping site.

To develop the remediation area, 170 boreholes had to be drilled in a narrow grid under very difficult site conditions. For removal of the contaminants, a mixture of saturated steam and air was injected into the subsoil (500-700 kW steam output) and the volatilized compounds were removed by vapour extraction at a rate of approximately 1,000 m³/h.

CDM Smith supervised and coordinated the remediation with all project stakeholders. The remediation was scientifically accompanied by VEGAS - Research Facility for Subsurface Remediation, at the University of Stuttgart.

Through the supplementary operation of the steam-air-injection, the former contamination centres were successfully remediated at short notice and approximately 730 kg of CHC was removed. The CHC concentrations decreased from 7,700 to 39 µg/L. The thermal in-situ process thus removed within an effective period of just less than 2 years more contaminants than the previous Pump & Treat process over 10.5 years. For the first time, the size of the contaminated area and the small distance to the groundwater level were factors in the application of the steam-air-injection.

The remediation has been successfully completed in Spring 2017 and for now CDM Smith continues to supervise the project as part of its performance review.

Elimination of threat to one of Scandinavia's largest groundwater resources

Jesper Holm¹; Niels Ploug¹; Adis Dzafic²; Elin Remstam³; Peter Anderson³; Anders Bank⁴; Hanna Lindvall⁵

¹Kröger A/S; ²Veolia - Sweden; ³Municipality of Kristianstad; ⁴Structor Miljö Väst AB; ⁵Tyréns AB

The site Färgaren 3 in Kristianstad (Skåne, Sweden) formerly housed a dye works and dry cleaners. Releases from these activities have created one of the most contaminated sites in Skåne. The site which sits on top of one of the most valuable groundwater resources in Scandinavia. Therefore, this site was prioritized for remediation funded by the Swedish EPA and headed by the Municipality of Kristianstad.

The aim of the remediation was to make the site available for all future land use and to protect the groundwater below the site. This was to be achieved through a combination of digging away the top 2,5 meters of soil on site and implementing thermal treatment from 2,5 meters below ground until 20 meters below ground inside a 900 m² area. At the end of the digging operation, an extraction layer for the subsequent thermal remediation was installed from 2-2,5 meters below ground to be used for the thermal remediation.

The site was to be remediated down to an average concentration of chlorinated solvents of 1 mg/kg. It was estimated that the

In spring 2018 the equipment was mobilised consisting of a dredging pontoon with a hydraulic excavator fitted with a centrifugal dredging pump. Between the two largest canals a dewatering facility was set up based on two mobile soil washing plants, combined with a 250 m³/h process water treatment plant consisting of sand and activated carbon filtration. The dredging pontoon and mobile soil washing plants are optimally synchronized by means of full automation of the dewatering plants. By continuous measurement of flow rates and densities the dredge makes sure the dewatering plant can always work close to its maximum throughput of 70 tons of dry matter an hour.

The dredging and processing started in summer 2018 and will be finished in spring 2019. Around 100,000 m³ of sediments will have been removed, resulting in 30,000 tons of sand fraction and 50,000 tons of dewatered fines that will have been disposed by the client to a local landfill, and 300,000 m³ of process water that was treated.

The project is unique in its kind as dredging and full scale thorough dewatering at a high throughput were made possible by a high degree of automation of the plant.

HYdrometallurgy and phytomanagement approaches for steel slag management

*Fernando Pereira
Mines Saint-Etienne*

Metallurgical slags are major by-products generated by the steel and iron industry. Although they represent potentially important economic resources, as they still often contain significant amounts of “Strategic Metals” (SMs), slags are also considered as industrial waste that may pose public health and environmental concerns. The goal of the HYPASS project is to propose technological innovations for both a cost-effective recovery of strategic metals and an eco-friendly management of metallurgical dumps. In this respect, HYPASS will consider the process as a whole, from by-products production to slag valorization and finally rehabilitation of contaminated landfills, with the ultimate goal of developing economically feasible and environmentally acceptable “zero-waste” processes. The core of the project is the development, assessment and evaluation of two complementary valorization routes using: 1/ hydrometallurgical-based approaches (under alkaline conditions) to recover high SMs amounts, and 2/ phytostabilization approaches [and the beneficial role of “Arbuscular Mycorrhizal Fungi” (AMF)] to promote ecological restoration of slagheaps. Additionally, HYPASS proposes to list and to map existing dumpsites, to perform “Life Cycle Assessments” (LCA) for various processing methods and to develop a “Decision-Support Tool” (DST) to help identifying the best treatment options, both from an economical and from an environmental point of view. HYPASS technologies will be implemented at a large slagheap situated at Châteauneuf (Loire, France), which is registered in the SAFIR network. The project involves one industrial (Industeel France ArcelorMittal) and two academic partners (ARMINES/SPIN and BRGM) and is organized into eight complementary “Working Packages” (WPs). Strong and numerous impacts are expected from the project. Technologically, the development of new approaches to recover SMs is in itself very innovative and promising, as this could allow to process large amounts of slags that are currently weakly re-used. This is very important in relation to the ambitious targets set by the “European Union” (EU) for recycling metallurgical by-products and decreasing landfilling practices. Environmentally, using phytostabilization as a capping strategy for slagheap rehabilitation will not only improve visual aspect of degraded lands, but this will also trigger

the restoration of a local biodiversity and the construction of a technosoil. Restoring biodiversity and stimulating soil formation could give a new value to derelict slagheap, as this is directly linked to ecosystem services that a land may deliver. Additionally, HYPASS will have significant economical and societal impacts, as it could reduce the dependence of European countries to SMs importation. Finally, HYPASS could help to create new jobs in the emerging area of high added-value waste treatment and valorization.

Post-treatment of aqueous solution containing surfactant and chlorinated organic compounds from lindane wastes

Aurora Santos¹; Raul Garcia²; Carmen Maria Dominguez²; David Lorenzo²; Arturo Romero²

¹Universidad Complutense de Madrid. VAT Q-2818014-I; ²Universidad Complutense de Madrid

Injection and further extraction of a biodegradable surfactant solution to enhance the removal of DNAPLs (dense non aqueous phase liquid) in the subsurface has received increasing attention in the last years. Among the surfactant types, the non-ionic ones are preferred for soil remediation since they have lower micellar critical concentration and are more readily biodegradable than the ionic ones. Although it has been proved that the soil flushing process using surfactants as extracting agents is an efficient process to remove residual DNAPLs, the pollutants are not destroyed and further treatments are required for this scope.

Therefore, an efficient post-treatment is required for the extracted surfactant flushing solution. This post-treatment can intend the reduction of the volume to discharge/treat and/or the recovery of the surfactant with selective abatement of the pollutants. This topic has been scarcely dealt in the literature and most of these works used synthetic organic phases as a source of contamination or only a single organic compound.

In this study, a DNAPL containing 28 chlorinated organic compounds (COCs) obtained from Bailin landfill was put in contact with an aqueous solution of a commercial non-ionic surfactant-co-solvent. This DNAPL was a liquid waste produced by an old lindane factory located at Sabiñanigo (Spain). The DNAPL was dumped in unsecured landfills and it migrated by density through the subsurface, polluting the soil and groundwater.

To simulate the flushing solution extracted, 0.4 g of DNAPL from Bailin landfill was put in contact with 20 mL of an aqueous phase containing 15 g/L of the surfactant. After 24 h of stirring and 72 h of settling, the supernatant was separated and analyzed. Several vials of 15 mL of the supernatant solution, containing the COCs and the surfactant, were prepared by this procedure. The following treatments have been applied to these solutions in order to abate the pollutants and recover the surfactant:

- Addition of micro Zero-Valent Iron or nano-Zero Valent Iron
- Addition of Fenton’s Reagent (hydrogen peroxide and ferrous iron)
- Addition of Sodium Persulfate, activated by heat
- Addition of Sodium Persulfate, activated by alkali

In all cases, the COCs reduction and the remaining oxidant and surfactant concentrations were measured. The best results, in relation to the selective abatement of the pollutants, were obtained with the Fenton’s Reagent and the addition of Persulfate activated by alkali.

trains

Besides, to reduce the volume of the COCs solution, ultrafiltration (UF) with membranes of several kDa were tested (from 1 kDa to 5 kDa), finding that UF allowed to reduce the polluted fluid to less than a tenth of the initial volume. However, surfactant was remaining in the concentrate.

The authors acknowledge financial support from the Comunidad Autonoma of Madrid (Project S2013-MAE-2739 CARESOIL-CM) and from the Spanish MINECO (Project CTM2016-77151-C2-1-R) and the Aragon Government for the supply of samples.

Integrated remediation - redevelopment of contaminated sites: the ISCO-SS soil mixing technology

*Vito Schifano; Lorenz San Nicolò
Ladurner Bonifiche S.r.l.*

An in-situ remediation project was completed for a site contaminated by petroleum hydrocarbons using an innovative technology, based on in-situ chemical oxidation, for the destruction of contaminants, simultaneously with the stabilization of the soil with hydraulic binders, for the restoration of the geotechnical characteristics of the soils. Sodium Persulfate was used as a chemical oxidant together with cement to activate the oxidation reactions, promote the pozzolanic reactions that favor high-pH desorption of hydrocarbons from a solid matrix, immobilize residual contamination and any heavy metals, hydraulic isolation of the treatment area and improve the geotechnical properties of the treatment area, in particular increase the strength and bearing capacity, decrease the compressibility and permeability of the ground and thus ensure favorable conditions for the reuse of the site.

The reagent formulation was designed by means of a series of laboratory tests in which the effects of different types and combinations of reagents and binders were evaluated. The mechanical distribution of the reagent and of the binder during the execution phase was carried out with the mechanical mixing technology of Bauer "single column soil mixing".

A reagent-binder slurry was prepared in a batch mixing plant and injected at the tip of the mixing tool. Soils were mixed in-situ to a depth of 8 meters below ground surface. A design concentration of 5000mg/kg of TPH (C5-C12) and of 10.000 mg/kg of TPH (C13-C40) were targeted to be reduced below limit concentration values acceptable in soil and subsoil for commercial and industrial use.

This innovative approach to contaminated sites with a wide range of organic, inorganic and mixed contaminants is designated by the acronym ISCOSS (In-Situ Chemical Oxidation and Soil Stabilization).

Full-scale remediation of a large groundwater pollution of trichloroethene: a combination of biobarriers and hydraulic containment

*Sylvie Seurinck¹; Youri Mertens²; Beatrijs Lambie¹
¹ANTEA Belgium; ²OVAM - Flemish Waste Agency*

In this paper data from an on-going full-scale remediation of a large groundwater pollution of trichloroethene (TCE) is presented. The pollution originates from a former furniture manufacturer and is located in a partially forested and industrial area.

Two different plumes can be distinguished, each having an aerial extent of around 70 m wide and 400 m long. Plume 1 extends to a depth of 40 m-bgl and plume 2 extends to a depth of 30 m-bgl.

The groundwater pollution consists mainly of TCE but reductive dechlorination has occurred in the past given the presence of the less chlorinated daughter products, dichloroethene (DCE) en vinyl chloride (VC). Reducing conditions are established, nitrate as electron acceptor is hardly detected, sulfate is still present and methane is produced. However, TOC concentrations in the aquifer are currently too low (< 10 mg/l) to further drive significant reductive dechlorination. The contaminated formation consists of fine to medium sand containing glauconite and sand stone.

A groundwater model using Modflow coupled with MT3DMS to simulate solute transport was developed. Based on the hydrogeology of the site and the distribution of the pollution 8 model layers were defined. The groundwater model was used to assess the hydraulic performance of a proposed barrier wall to mitigate further migration of the plume.

The constructed hydraulic barrier consists of 7 pumping wells with a screen interval of 30 to 40 m-bgl. In order to prevent further spreading of the plume the hydraulic barrier has to operate at an extraction rate of 1 m³.h⁻¹ per well. The extracted groundwater is than spiked with molasses and re-infiltrated upstream of the hydraulic barrier in 16 biobarriers. No extracted groundwater is being discharged.

The 16 biobarriers are distributed over the contaminated plumes with a inter distance of 20 m. They consist of vertical infiltration filters with a 4 m screen length located at different depths. In total 362 vertical infiltration filters were installed. The shallowest infiltration depth is 9 m-bgl and the deepest infiltration depth is 40 m-bgl. In the first injection round a volume of 4 m³/m screen of 1%vol molasses solution is being infiltrated into the filters followed by flushing with groundwater at a volume of 0,5 m³/m screen. If pH in the aquifer decreases below 6, sodium bicarbonate will be dosed in line to increase the pH within the optimal interval of 6 to 7.

During the injection extraction flows, groundwater levels, injection pressures and flows and TOC concentrations are monitored. The first injection round takes up 40 days, a volume of 5755 m³ needs to be infiltrated in total. After the injection round the extracted groundwater of the hydraulic barrier will be recirculated to the biobarriers without dosing of molasses. Around 40 wells are being regularly monitored for groundwater levels, concentrations of TOC, chlorinated ethenes, nitrate, sulfate, iron(II), methane, ethane, ethane.

The presentation focuses on the conceptual site model, the final design and the installation of the full-scale remediation infrastructure. The first infiltration and monitoring results will be presented.

Biological anaerobic degradation of VOCs combined with recirculated groundwater heating

*Martin Slooijer; Rogier De Waele; Michela De Camillis; Remi Peters;
John Dijk
GreenSoil International B.V.*

The production of barium and strontium salts, followed by past production of ion exchange resins and glues, constituted harmful activities for soil and groundwater. Vertical migration of the contamination through the semi permeable unit into the underlying chalk aquifer is a potential hazard. Maximum soil contamination is found between 13,5-13,75 m-bgl with concentrations of 340 mg/kg of 1,2-DCA and 260 mg/kg of DCM. In addition, maximum groundwater contamination is detected at a depth of 8-19 m-bgl with concentrations of 435,000 µg/l of 1,2 DCA, 373,000 µg/l of DCM and 1,700 µg/l of VC. GreenSoil conducted a field test to investigate the feasibility of enhanced reductive dichlorination (ERD) to reduce the risk of spreading.

Presenters:

- Benjamin Herzog, Norbert Klaas; Research Facility for Subsurface Remediation (VEGAS), University of Stuttgart
- David Lorenzo, Aurora Santos; INPROQUIMA (Department of Chemical and Materials Engineering), University Complutense of Madrid

Groundwater and soil contamination caused by industrial activities are pervasive environmental and public health problems. DNAPLs, in particular, are usually difficult to handle due to their deeper penetration into the subsurface and pose a particular challenge for the sustainable and efficient treatment of contaminated sites.

Various in-situ remediation methods such as In-Situ Chemical Oxidation (ISCO) have been developed for the remediation of such groundwater contaminations. Remediation with ISCO involves the injection of oxidants into the affected aquifer areas with the intention to chemically transform contaminant compounds into less harmless species. However, these oxidative reactions take place in the aqueous phase and thus only the contaminants dissolved in the groundwater are being degraded. Therefore, a rebound often occurs after an ISCO remediation, i.e. the concentration of pollutants in the groundwater increases again after some time due to remaining DNAPL in the aquifer.

To avoid rebound and to increase the efficiency of ISCO applications, the use of plant-based and biodegradable surfactants in combination with oxidizing agents is being investigated as part of the EU research project "Life-SURFING". The use of surfactants is intended to increase the solubility of the contaminants in the aqueous phase, making them more accessible to the oxidant. In addition, the surfactants are able to desorb adhering organic compounds from the soil matrix, which can lead to a complete removal of contaminants from the pore spaces. In the EU project, the group INPROQUIMA (Department of Chemical and Materials Engineering at the University Complutense of Madrid) is conducting research on a field case in northern Spain, where a fractured aquifer is contaminated by a DNAPL mixture containing hexachlorocyclohexanes and other chlorinated liquid wastes from lindane production. A broader application of the Surfactant-Supported In-Situ Chemical Oxidation ("S-ISCO") is being addressed by the Research Facility for Subsurface Remediation (VEGAS) at the University of Stuttgart. Here, the transferability of the technology to other hydrogeological situations and a broader spectrum of contaminants is being investigated based on laboratory experiments of medium to large scale.

By presenting recent findings and progress regarding the S-ISCO technology, this talk will give insight into the ongoing development and research on an innovative remediation technology. The LifeSURFING project and this presentation are to motivate stakeholders to include new and innovative combinations of established and well known methods such as ISCO to increase the efficiency of treatments, shorten remediation time and save costs.

REGENERATION OF GRANULATED ACTIVATED CARBON SATURATED IN 1,2,4-TRICHLOROBENZENE BY THERMAL ACTIVATION OF PERSULFATE.

A. SANCHEZ-YEPES, D. LORENZO, A. ROMERO , A. SANTOS

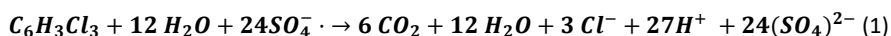
Chemical Engineering and Materials Department, Facultad de Ciencias Químicas, Universidad Complutense de Madrid, Ciudad Universitaria S/N, 28040 Madrid, Spain; andsan28@ucm.es.)

Keywords: activated carbon, 1,2,4-trichlorobenzene, persulfate, regeneration.

The growing environmental concern for chlorinated organic compounds (COCs) as pollutants in wastewater, surface water and groundwater is based on their low biodegradability and high persistence in the released medium (Lorenzo et al. 2021). The adsorption of these compounds in the activated carbon (AC) surface is frequently used to remove them. However, this process produces a large amount of spent AC, which must be treated or properly managed. Moreover, if chlorinated compounds are adsorbed, the toxicity of the spent AC residuum increases.

To reduce waste generation, authors have studied the regeneration of spent AC oxidizing the compounds adsorbed in the surface of the AC. Advanced Oxidation Processes have been recently proposed for AC regeneration. In this way, Liena et al. used persulfate and persulfate (PS) activated by iron to regenerate spent AC after trichloroethylene adsorption (Liang, Lin and Shin 2009). The activation of persulfate using temperature was successfully applied in the regeneration of methyl tert-butyl ether (MTBE) and chloroform-spent AC, (Huling et al. 2011).

In this work, the regeneration of commercial granular activated carbon (GAC), with BET surface 847m²/g, previously saturated in 1,2,4-trichlorobenzene (124-TCB), selected as a model compound, has been investigated using PS activated by temperature. The PS dosage was fixed considering the mineralization of 124-TCB with PS, as summarised in equation (1).



The GAC regeneration was carried out in a batch way with an aqueous solution of PS solution (166 mM) in contact with the GAC (5 g/L), previously saturated in 124-TCB (500 mg/g). After the regeneration reaction, the GAC used was saturated again in 1,2,4 TCB to quantify the regeneration achieved. Adsorption/regeneration cycles were carried out to study the effect of cycles on adsorption capacity. After each cycle, GAC was washed with water at the operating temperature to clean the GAC surface from salts deposited on it during regeneration and improving the subsequent adsorption of 124-TCB.

The effect of the temperature has been studied in the regeneration of GAC in the range 25 - 60°C using the stoichiometric concentration of PS to promote the total mineralization of 124-TCB. Figure (1a) and Figure (1b) show the regeneration ratio (%RE), and PS consumption obtained, respectively vs. reaction time at different activation temperatures. %RE is defined as the percentual recovery of the adsorption capacity of fresh GAC after regeneration.

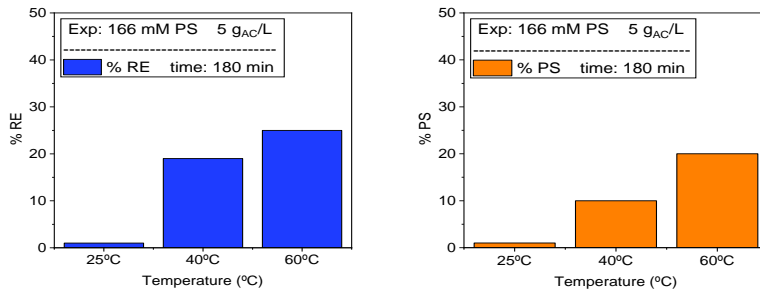


Figure 1. a) Conversion of 124-TCB by the effect of temperature. b) Conversion of PS (initial 1,4-TCB adsorbed = 500 mg/g)

As shown in **Figure 1a**, at 25°C negligible regeneration capacity of the GAC and PS conversion are noticed. However, the higher temperature used, the higher the GAC regeneration. Temperature values higher than 60°C were not tested due to the high unproductive of PS.

The loss of adsorption capacity in successive regeneration cycles was studied. The % RE obtained after 180 min of reaction time in three successive regeneration cycles are shown in **Figure 2** at 60°C and 166 mM of PS. As can be seen, at the conditions tested, the recovery of adsorption capacity after GAC regeneration at 60°C remains stable between 25-30%.

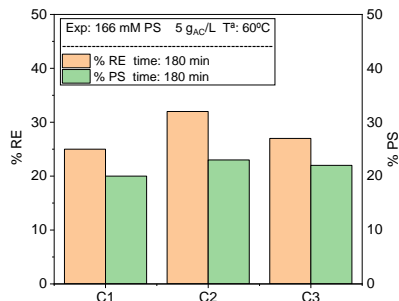


Figure 2. AC regeneration rate for each cycle at 60°C of PS 166 mM in 180 min.

The regeneration achieved in the cycles shown in Figure 2 is moderate (around 30%). This can be explained by the high initial concentration of 124-TCB adsorbed (500mg/g) and the batch procedure followed in both adsorption and regeneration. However, when experiments are carried out in a column filled with GAC the breakage curves obtained after several regeneration cycles (not shown in this summary) show lower differences, resulting in more efficient regeneration of the GAC.

Acknowledgments

This work was supported by the EU LIFE Program (LIFE17 ENV/ES/000260), the Regional Government of Madrid, through the CARESOIL project (S2018/EMT-4317), and the Spanish Ministry of Economy, Industry, and Competitiveness, through project PID2019-105934RB-I00.

References.

- Huling, S. G., S. Ko, S. Park & E. Kan (2011) Persulfate oxidation of MTBE- and chloroform-spent granular activated carbon. *Journal of Hazardous Materials*, 192, 1484-1490.
- Liang, C., Y.-T. Lin & W.-H. Shin (2009) Persulfate regeneration of trichloroethylene spent activated carbon. *Journal of Hazardous Materials*, 168, 187-192.
- Lorenzo, D., A. Santos, A. Sánchez-Yepes, L. Ó. Conte & C. M. Domínguez (2021) Abatement of 1,2,4-Trichlorobenzene by Wet Peroxide Oxidation Catalysed by Goethite and Enhanced by Visible LED Light at Neutral pH. *Catalysts*, 11, 139.

Estabilidad de surfactantes aniónicos y no-iónicos con persulfato activado por álcali y oxidación selectiva de COCs en emulsión.

D. Lorenzo^{1*}, R. García-Cervilla¹, A. Romero¹ y A. Santos¹

¹ Universidad Complutense de Madrid. Departamento de Ingeniería Química y de Materiales. Grupo INPROQUIMA.

dlorenzo@ucm.es

La contaminación del suelo por compuestos orgánicos clorados (COCs) es un problema global. Estos compuestos tienen una alta persistencia en el medio ambiente, siendo un alto riesgo para la salud humana y el medio ambiente. La baja solubilidad de la mayoría de estos compuestos en el agua hace posible la formación de fases líquidas densas no acuosas (DNAPLs) (Lorenzo, García-Cervilla et al. (2020) <http://dx.doi.org/10.1016/j.chemosphere.2019.124798>). La tecnología de oxidación química in-situ mejorada por surfactantes (S-ISCO) es un proceso prometedor que reduce los tiempos para la eliminación de DNAPLs (Besha, Bekele et al. (2018) <http://dx.doi.org/10.1016/j.eti.2017.08.004>).

La compatibilidad entre los tensioactivos y los oxidantes es un aspecto importante de la eficacia del proceso S-ISCO (García-Cervilla, Santos et al. (2021) <http://dx.doi.org/10.1016/j.scitotenv.2020.141782>). Por ello, en este trabajo se ha estudiado la estabilidad de cuatro surfactantes, tres de ellos no iónicos E-Mulse 3 (E3), Tween 80 (T80), y una mezcla de T80 y Span 80 (TS80) y el cuarto surfactante aniónico: dodecil sulfato de sodio (SDS), con el agente oxidante seleccionado (persulfato activado por álcali) para la eliminación de un DNAPL formado por 28 COCs, generado como residuo líquido en la producción de lindano. Los experimentos se llevaron a cabo en un reactor discontinuo de PTFE. Los COCs totales, la pérdida de la capacidad de solubilización y el consumo de oxidante fueron analizados. Tras 24 h de oxidación, la capacidad de solubilización de los surfactantes no iónicos se redujo considerablemente hasta alcanzar un valor constante. El E3 mostró la menor pérdida de la capacidad de solubilización (<50%). Sin embargo, T80 y TS80 perdieron más del 90%. Esta pérdida de la capacidad de solubilización se debió a la oxidación no deseada de surfactante por los radicales (OH[•]) formados por la activación alcalina del persulfato. Además, esto provocó un elevado consumo del oxidante. El SDS no se vio afectado por el oxidante y no se observó pérdida de capacidad tensioactiva ni consumo de oxidante, siendo el tensioactivo más estable. Por el contrario, el SDS tiene la menor capacidad de solubilización inicial de todos los surfactantes estudiados. El uso de surfactantes demostró una eliminación de COCs más rápida que en ausencia de estos. No obstante, aunque E3 mejoró la eliminación de COCs respecto del SDS, el consumo improductivo de oxidante y la pérdida de capacidad de solubilización de COCs fue mayor. Este estudio permitió establecer que el S-ISCO es una técnica prometedora para la eliminación de los residuos de la fabricación del lindano.

Palabras clave: Persulfato activado, DNAPL, consumo improductivo, estabilidad surfactante.

Agradecimientos: Este trabajo fue apoyado por el Programa LIFE de la UE (LIFE17 ENV/ES/000260), la Comunidad de Madrid, a través del proyecto CARESOIL (S2018/EMT-4317), el Ministerio de Economía de España proyecto (S2018/EMT-4317), y el Ministerio de Economía, Industria y Competitividad, a través del proyecto CTM2016-77151-C2-1-R. Raúl García-Cervilla agradece la subvención del FPI español (ref. BES- 2017-081782).



S7-PP23

**IN SITU CHEMICAL OXIDATION ENHANCED BY SURFACTANTS (S-ISCO):
LIFE SURFING PROJECT**

Aurora Santos¹, Jesús Fernández², Elena Cano², D. Lorenzo¹, S. Cotillas¹, Carlos Herranz³
Chemical Engineering and Materials Department, Complutense University of Madrid, Spain
e-mail: aurasan@ucm.es

¹*Chemical Engineering and Materials Department, University Complutense of Madrid, Spain.*

²*Department of Agriculture, Livestock and Environment, Government of Aragon, Spain*

³*Sociedad Aragonesa de Gestión Agroambiental SARGA, Zaragoza, Spain*

Keywords: DNAPL, Lindane, Landfill, surfactant, oxidation

During the 20th century, miles of tons of waste were generated in the lindane (γ -hexachlorocyclohexane, HCH, $C_6H_6Cl_6$) production and dumped nearby the production facilities, often in unsecured landfills. Wastes were solid (other HCHs isomers without pesticide activity) and liquid, the last being a mixture of chlorinated organic compounds from chlorobenzene to heptachlorocyclohexane. The liquid organic mixture had lower solubility in water with a density higher than water density, forming a Dense Non-Aqueous Liquid Phase (DNAPL). This DNAPL had high toxicity, containing compounds considered cancerogenic, some of them included in the list of persistent organic pollutants by the Stockholm Convention. The company INQUINOSA synthesised lindane from 1975 to May 1989 and ceased its commercialisation activity in 1992. During this period, it is estimated that INQUINOSA produced more than 150,000 tons of waste. The residues from the production of lindane, in powder and liquid form, were dumped in the Sardas landfill and later in the Bailín landfill in a practically uncontrolled manner. Bailín landfill is a fractured aquifer, and DNAPL was migrating through the fractures generating a plume of contaminated groundwater with the associated risk for the surface waters (river Gallego is 800 m from the landfill) [1]. After 16 years of pumping the dense phase (DNAPL) in the Bailín landfill aquifer (Sabiñánigo, Huesca) physical extraction is already inefficient, which makes it necessary to address the application of chemical techniques that allow cleaning the residual DNAPL and reduce the groundwater pollution.

The LIFE SURFING project has tested Surfactant Enhanced Aquifer Remediation (SEAR) and Surfactant enhanced In situ Chemical Oxidation (S-ISCO) to eliminate the residual DNAPL in the fractures. The tests were applied at a pilot scale in a cell about 60 m long, 1 m in width and 20 m in depth. The S-ISCO test was applied by injecting surfactants and oxidants (SISCO) simultaneously. The selected oxidant was persulfate (40 g/l) due to its high stability in soil. A non-ionic surfactant (E-Mulse 3 ®, 4 g/l) was chosen due to its solubilisation properties and good stability against the oxidant [2]. The persulfate was activated by an alkali (NaOH, 10 g/l). 21.6 m³ of this solution was injected into two cell wells in a 1 m³ pulse over two days. The pH of the injected fluid was strongly alkaline (pH>12). The injection procedure increases the contact time between the injected fluids and the subsoil. To maintain the aquifer strong alkaline pH and prolong the persulfate activation time, a NaOH aqueous solution has been injected into various wells downstream, compensating for the buffer effect of the carbonated medium. The oxidation of solubilised COCs by persulfate progresses in the fluid that escaped from the test cell with the distance. The fluid that reaches the river has neither remaining surfactant nor solubilised COCs. It is estimated that more than 20 kg of DNAPL has been mineralised without noticing a significant concentration rebound after two months. The S-ISCO test will be implemented in the landfill at a larger scale during the following years.

Acknowledgements: This work has been supported by EU LIFE Program (LIFE17 ENV/ES/000260) and the Aragon Government.

References

- [1] J. Fernandez, M.A. Arjol, C. Cacho, POP-contaminated sites from HCH production in Sabinanigo, Spain, *Environmental Science and Pollution Research*, 20 (2013) 1937-1950.
- [2] R. Garcia-Cervilla, A. Santos, A. Romero, D. Lorenzo, Abatement of chlorobenzenes in aqueous phase by persulfate activated by alkali enhanced by surfactant addition, *J Environ Manage*, 306 (2022) 114475.

PP-833

VOLATILIZATION OF CHLORINATED ORGANIC COMPOUNDS FROM LINDANE WASTES IN NON-IONIC SURFACTANT EMULSION AT ALKALINE CONDITIONS

P. Sáez^a, R. García-Cervilla, A. Sánchez-Yepes, D. Lorenzo, A. Romero, A. Santos

^aChemical Engineering and Materials Department, Complutense University of Madrid, Spain

e-mail: patrisae@ucm.es

Keywords: Volatilization, DNAPL, Surfactant, chlorinated organic compounds.

Surfactant enhanced aquifer remediation (SEAR) is a common treatment to eliminate dense nonaqueous phase organic liquids (DNAPL) in the subsoil in shorter times. Surfactant solution is injected and the emulsion with organic contaminants is extracted and treated on-site. One of the technologies proposed for this scope is the volatilization at moderate temperature, by passing an air stream at a certain flow rate to selectively volatilize the organic compounds in the mixture.

The DNAPL used in the current work was present in the subsoil of a highly contaminated landfill located in Sabiñánigo (Spain). This DNAPL is composed of 28 COCs including chlorobenzene, isomers of dichlorobenzene, trichlorobenze, tetrachlorobenzene, hexachlorocyclohexanes, hexachlorocyclohexenes and heptachlorocyclohexanes, whereas the surfactant employed to dissolve and mobilize this DNAPL was E-Mulse3® which is a commercial nonionic surfactant. The emulsion containing surfactant and COCs was firstly alkalized to transform the less volatile COCs (HCHs and HeptaCHs) in COCs with higher vapor pressure (Trichlorobencenes and Tetrachlorobencenes, respectively^[1, 2]). Following an air stream was bubbled in the emulsion using a gas flow rate (L/min) to liquid volume (L) of 5 min, Runs were carried out at different temperatures (40 °C and 60 °C) and surfactant concentrations (3.5 g·L⁻¹ and 7 g·L⁻¹) under alkaline conditions (pH > 12).

The reduction of COCs in the emulsion after 8 h of treatment are shown (as percentages) is shown in Figure . As can be seen, the highest the temperature or the lowest the initial surfactant concentration, the higher the COCs reduction achieved within 8h. The lower temperature the lower the vapor pressure of COCs and the highest the surfactant concentration the lower the activity coefficient of the chlorinated compound in the emulsion. The highest reduction of COCs, more than 80% of the initial value, was obtained at 60°C (Exp. 3). On the contrary, at 40 °C and 7 g·L⁻¹ of surfactant concentration (Exp. 2), the reduction of COCs was the lowest value obtained (45%).

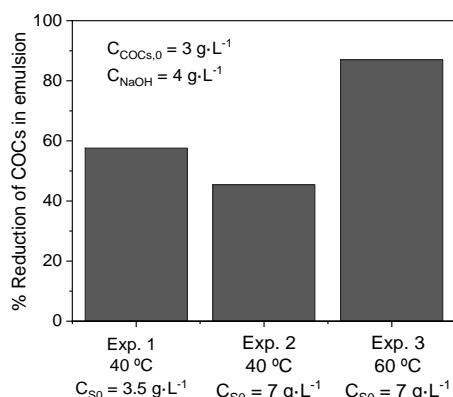


Figure 1. Reduction of COCs in emulsion after 8 h of volatilization treatment

References

- [1] D. Lorenzo, R. Garcia-Cervilla, A. Romero, A. Santos, Chemosphere, Vol. 239, 124798. 2020.
 [2] A. Santos, J. Fernandez, J. Guadano, D. Lorenzo, A. Romero, Environ. Pollut. Vol. 242(Pt B) 1616-1624, 2018.

S14-FP16

REGENERATION OF GRANULATED SPENT ACTIVATED CARBON WITH 1,2,4-TRICHLOROBENZENE BY PERSULFATE ACTIVATED BY HEAT

A. Santos^a, A. Sánchez-Yepes^a, P. Sáez^a, R. García-Cervilla, J. M^a Rosas^b, J. Rodríguez-Mirasol^b, T. Cordero^b, A. Romero, D. Lorenzo^a.

^a *Chemical Engineering and Materials Department. Complutense University of Madrid. Spain.*

^b *Universidad de Málaga, Andalucía Tech., Departamento de Ingeniería química, Campus de Teatinos s/n, 29010, Málaga, Spain*

e-mail: aursan@ucm.es

Keywords: granular activated carbon, 1,2,4-trichlorobenzene, persulfate, regeneration.

Chlorinated organic compounds (COCs) are persistent organic pollutants (POPs) present in groundwater from industrial sites or in industrial wastewater effluents [1]. A common remediation strategy for these waters is the adsorption of these COCs on activated carbon, resulting in toxic waste management. To avoid the transport of these wastes, on-site regeneration of spent activated carbon for reuse can be considered to implement a circular economy. To achieve carbon reuse, the regeneration of spent carbon by thermally activated sodium persulphate (TAP) was studied. Previously, this COCs were successfully removed from the aqueous medium using the TAP process [2], so in this work, the regeneration of a commercial granular activated carbon (GAC) saturated in 1,2,4-trichlorobenzene (124-TCB) was carried out, initially saturated with $350 \text{ mg}_{124\text{-TCB}} \cdot \text{g}_{\text{GAC}}^{-1}$.

The regeneration of saturated GAC was studied using the TAP process in a temperature range from 20 to 80°C, always maintaining an initial PS concentration of 166 mM. The adsorption recovery capacity (RC) and persulphate consumption were studied after 180 min. These experiments determined that the best regeneration ratio and PS consumption results were obtained at 60°C. Selecting the latter temperature, three successive adsorption-regeneration were accomplished with a washing step at 60 °C, to remove the sulphate deposited in the GAC surface. The results of RC and PS consumption were summarized in Figure 1. After this, the regeneration treatment achieved a stable and high recovery of the initial adsorption capacity of approximately 0.48 to 0.53. For each cycle, the oxidant consumption did not reach 0.3. In addition, the physicochemical changes of GAC before and after the regeneration treatments were also deeply investigated.

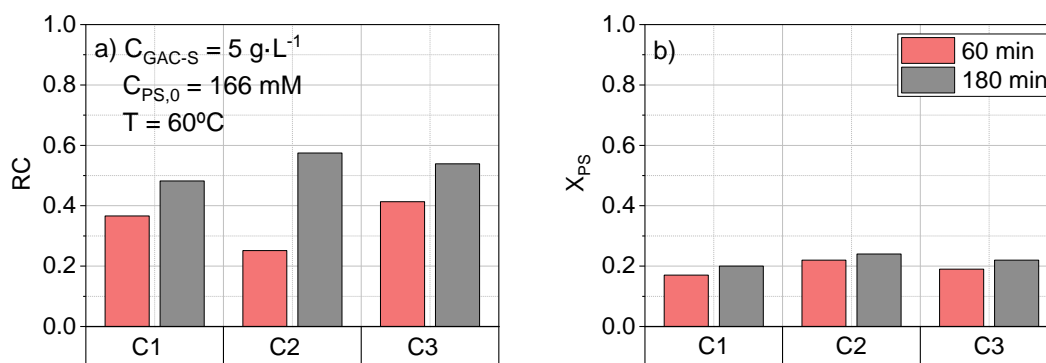


Figure 1. RC and PS conversion (X_{PS}) of GAC-S after three regeneration/adsorption cycles with washing step. Experimental conditions: $C_{\text{PS},0} = 166 \text{ mM}$, $C_{\text{GAC-S}} = 5 \text{ g} \cdot \text{L}^{-1}$, $T = 60^\circ\text{C}$.

References

- [1] D. van Wijk, E. Cohet, A. Gard, et al, 1,2,4-trichlorobenzene marine risk assessment with special emphasis on the Osparcom region North Sea. *Chemosphere*, **2006**. 62(8): p. 1294-310.
- [2] C.M. Dominguez, A. Romero, D. Lorenzo, A. Santos, Thermally activated persulfate for the chemical oxidation of chlorinated organic compounds in groundwater. *J. Environ. Manag.*, **2020**. 261.

Session 3c5 / Abstract title: DNAPL Extraction and Oxidation enhanced by Surfactant addition: LIFE SURFING PROJECT

ID: 273

Key words: Lindane, DNAPL, Fractured Aquifer, SEAR, S-ISCO

Submitter: Aurora Santos

Organization: Universidad Complutense de Madrid

Co-authors: Jesús Fernández, Department of Agriculture, Livestock and Environment, Government of Aragon, Spain; Jorge Net, Department of Agriculture, Livestock and Environment, Government of Aragon, Spain; David Lorenzo, Chemical Engineering and Materials Department, University Complutense of Madrid, Spain; Elena Cano, Department of Agriculture, Livestock and Environment, Government of Aragon, Spain; Patricia Saez, Chemical Engineering and Materials Department, University Complutense of Madrid, Spain; Carlos Herranz, Sociedad Aragonesa de Gestión Agroambiental SARGA, Zaragoza, Spain

Session: 3c5

Abstract

Surfactant Enhanced Aquifer Remediation (SEAR) and In Situ Chemical Oxidation enhanced by Surfactant addition (S-ISCO) have been successfully tested in the Bailin Landfill (Sabiñanigo, Spain) during the LIFE SURFING Project (SURFactant enhanced chemical oxidation for remediating DNAPL). DNAPL (comprising 28 Chlorinated Organic Compounds, COCs) was produced as residuum in the lindane manufacturer nearby [1] and dumped in the landfill. It was retained in the permeable sandstone layer (M) fractures, resulting in a plume of highly contaminated groundwater with the associated risk for the Gallego river and the population. After 16 years of pumping the dense phase (DNAPL) in the Bailín landfill aquifer, physical extraction is already inefficient, and advanced techniques are required to remove the residual DNAPL.

LIFE SURFING pilot test was executed from 2020 to 2022 in a test cell about 60 m in length located in the M layer of the old landfill, where most DNAPL was dumped. SEAR and S-ISCO applied ensured enough contact time between reagents and pollutants and prevented surfactant and solubilised COCs from reaching the river.

In SEAR and S-ISCO events, the groundwater composition was monitored in 29 wells in the M layer, from the cell to the river. The injection and extraction strategy in the cell and the implementation of a barrier zone between the cell and the river required a detailed previous characterisation of the groundwater flow in the fractures, carried out in 2020 and 2021. The barrier zone comprises the dosage of NaOH solution to the base of the aquifer to reach pH 12, aeration and vapour extraction and dosing Na₂S₂O₈ with alkaline activation downstream of the test cell.

Two SEAR tests were applied in the spring of 2022. E-Mulse 3® was selected as the surfactant in laboratory tests [2]. About 16 m³ of a solution of 20 g L⁻¹ of the surfactant was injected into the test cell (bromide 190 mg L⁻¹ was added as a conservative tracer). Injected fluids were recirculated during the injection. Groundwater was extracted when injection ended with a recovery of 55-60% of the tracer and 30-40% of the surfactant injected in the first and second SEAR tests, respectively, with solubilised COCs up to 3 g L⁻¹. Two weeks after the second SEAR test, 12 m³ of leachate and fines were extracted with approximately 10 kg of DNAPL in solution and 90 kg of DNAPL mixed with the fines. About 130 kg of DNAPL has been removed with the two SEAR events (ratio mass of surfactant injected/mass of DNAPL recovered about 2.5).

S-ISCO was carried out in September 2022. Oxidant (persulfate) and activator (NaOH) were selected in the previous LIFE Discovered project. The effectiveness of this oxidant and E-Mulse 3® with this DNAPL was also proved at the lab scale [3]. A volume of 21.6 m³ of a persulfate solution (40 g L⁻¹), surfactant (E-Mulse 3®, 4 g/l) and NaOH (10 g L⁻¹) was injected in pulses of 1 m³ each hour in two wells. The groundwater is pumped downstream and recirculated back to the cell during the injection. In addition, a foam barrier has been generated downstream to minimise the flow of injected fluids escaping from the cell. The injected fluid that escaped from the test cell reached the barrier zone without a dense organic phase, without surfactants and with low solubilised COCs. About 20 kg of DNAPL were oxidised in the S-ISCO event. Three months after the end of S-ISCO, the concentrations of COCs in the test cell remain very low, and no rebound has been noticed in the saturated zone. However, rebounds will be monitored during the following months.

ANNEX III. Posters

AquaConSoil Antwerp 2019

Post-Treatment of Aqueous Solution containing Surfactant and Chlorinated Organic Compounds from Lindane wastes

Aurora Santos*, Raul García, Carmen M. Domínguez, David Lorenzo and Arturo Romero.
Chemical Engineering and Materials Science Department, University Complutense of Madrid, Spain *aursan@ucm.es

ID: 21657

INPROQUIMA

Introduction

Lindane (γ -HCH): heavily used as a wide spectrum insecticide, in public health programs and as wood preservatives. **Banned by Stockholm Convenia.** Huge amounts of toxic wastes were generated and dumped in the nearby of the production sites. [1]

Liquid Wastes: DNAPL with 28 Chlorinated Compounds [2]

Objectives for Treatment of the Soil Flushing Solution [3]

- Selective Abatement of Chlorinated Organic Contaminants in the emulsion:** Oxidation/reduction of pollutants with surfactant recovery.
- Selective Retention of DNAPL from the emulsion:** Microfiltration: Surfactant preferably in the permeate and DNAPL in the retentate

Experimental

Materials

- Surfactant: **Emulse-3® (Ethical Chem)**
- Dense Non Aqueous Phase Liquid** from a Landfill in Sabiñanigo, Spain, caused by **Lindane Wastes**. 28 COCs from chlorobenzene to heptachlorocyclohexane.

Analysis of reaction effluents

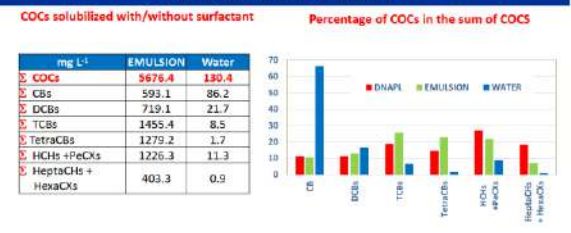
- COCs:** GC-MS, GC/ECD/FID.
- Oxidants:** Titration.
- Surfactant:** Tenslometer: Interfacial Tension. Equivalent Surfactant Concentration (ESC) by Dilution until Micellar Critical Concentration is reached (CMC=80 ppm).

Experimental Procedure:

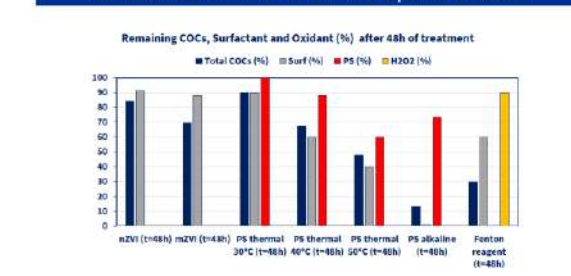
COCs Reduction	COCs Selective Oxidation	COCs selective Oxidation	COCs Selective Oxidation	Retention with Membranes
<ul style="list-style-type: none"> [mDA] = 5 g/L [mZn] = 5 g/L [COCs] = 5600 mg/L [Surf] = 15 g/L 	<ul style="list-style-type: none"> PS thermal [PS] = 250 mM T = 30-50 °C [COCs] = 5600 mg/L [Surf] = 15 g/L 	<ul style="list-style-type: none"> PS alkaline [PS] = 250 mM [NaOH] = 500 mM [COCs] = 5600 mg/L [Surf] = 15 g/L T = 20°C 	<ul style="list-style-type: none"> Fenton Reagent [F2O2] = 600 mM [Fe²⁺] = 0.012 mM [COCs] = 5600 mg/L [Surf] = 15 g/L T = 20°C 	<ul style="list-style-type: none"> Andica® Ultra-15 Centrifugal Filters Ultraflow® 3K (Merck Millipore Ltd) Permeate (BMWL A, 30, 50, 100 kDa COCs 5600, 3050 mg/L Surfactant emul-15, 7.5 g/L 10 mL + centrifugation 1h (5600 rpm)

Results

Emulsion Characterization



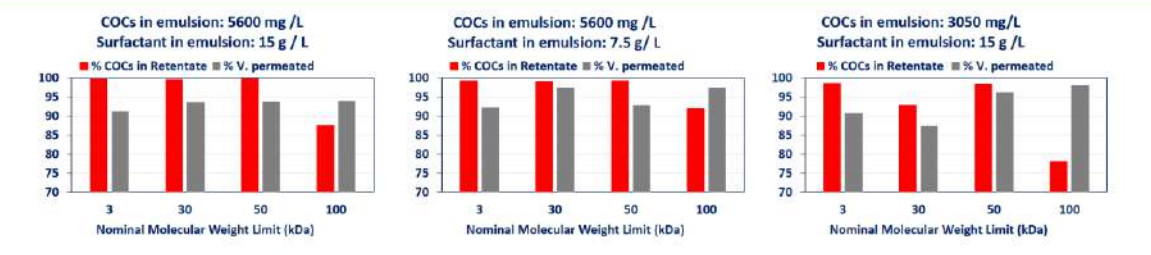
Selective Abatement of COCs in the aqueous emulsion



- As can be seen, the solubility of COCs in water is low (130 mg L⁻¹).
- To extract the trapped DNAPL into the soil the injection of the surfactant greatly enhances the COCs removal by increasing the solubility of COCs in the aqueous emulsion (5600 mg L⁻¹).
- The addition of the surfactant improved the selective extraction of the more hydrophobic COCs. The fingerprint of COCs in the emulsion is similar to the COCs distribution in the organic DNAPL phase. On the contrary, the solubility of less hydrophobic compounds (CB) is favored in water.

The best results, in relation to the abatement of the pollutants, were obtained with the Fenton's Reagent and the addition of Persulfate activated by alkali. However, the PS activated by alkali supposes a high breakage of the surfactant capacity. Then, for selective oxidation of surfactants the Fenton Reagent seems to be preferable.

Retention of COCs from the aqueous emulsion by using Membranes



- UF allowed to reduce the polluted fluid to less than a tenth of the initial volume, even at the highest NMWL tested.
- Slight differences were found with the COCs concentration in emulsion (3050-5600 mg/L) and surfactant concentration (7.5-15 g/L). However, more of 95% of the surfactant was remaining in the retentate.
- COCs in the permeate was less than 5% of the COCs in the initial emulsion. Only with NMWL 100 kDa membranes was noticed a significant increase in the concentration of COCs in the permeate.
- Therefore, the retentate could be treated by oxidation-reduction with less consume of reagents.

References:

- Fernández, J., M. Arjol, and C. Cacho, POP-contaminated sites from HCH production in Sabiñanigo, Spain. *Environmental Science and Pollution Research*, 2013, 20(4): p. 1987-1990.
- Santos, A., et al., Chlorinated organic compounds in liquid wastes (DNAPL) from lindane production dumped in landfills in Sabiñanigo (Spain). *Environmental Pollution*, 2010, 242: p. 1615-1624.
- Domínguez, C.M., Kanorio, A., Santos, A., Selective removal of chlorinated organic compounds from lindane wastes by combination of nonionic surfactant soil flushing and Fenton oxidation. *Chemical Engineering Journal*, 2013, in press, 10.1016/j.cej.2018.09.170

Acknowledgements:

This work was supported by Regional Government of Madrid de Madrid, project CORESOIL (S2018/EMT-4317), from the Spanish Ministry of Economy, Industry and Competitiveness, projects CTM2015-71151-C2-1-R and for the EU Life Program (LIFE17 ENV/ES/000260). The authors thank the Department of Agriculture, Livestock and Environment, Government of Aragón, Spain, as well as EMGRISA for their support during this work.

Solubilization of Dense Non Aqueous Phase Liquids produced as Lindane Wastes using Non-Ionic Surfactants

AquaConSoil Antwerp 2019

Raul García*, Arturo Romero, David Lorenzo and Aurora Santos
Chemical Engineering Department, University Complutense of Madrid, Spain. *raugar05@ucm.es

ID: 21662

Introduction

Lindane: γ isomer of HexachlorocycloHexane (γ -HCH) heavily used as a wide spectrum insecticide, in public health programs and as wood preservatives



ENVIRONMENTAL IMPACT [1], [2]

- Groundwater and soils are HIGHLY contaminated by lindane wastes nearby the production sites.
- Contamination was caused by solid wastes (HCH isomers) and liquid residuum (multicomponent DNAPL from chlorobenzene to heptachlorocyclohexane).
- The DNAPL had migrated by density-driven forces through the subsurface, being trapped into the soil pores or fractures at high depths below the ground level.
- The hydrophobic nature of the DNAPL trapped into the soil remains as a main source for groundwater pollution.
- In situ treatments are required for pollutant abatement: ISCO, S-ISCO.



Surfactant-Enhanced Aquifer Remediation (SEAR) can be better applied as a first step for removal of a substantial part of the DNAPL mass in the aquifer [3]

Objective

- Study the solubility of DNAPL from Sardas and Bailin Landfills in two non ionic surfactants.
- Study the stability of the emulsions.
- Study the effect of pH on the COCs solubility, chemical transformations and stability.

Experimental

DNAPL solubilization

- Dense Non Aqueous Phase Liquid from a Landfill in Sabiñánigo, Spain, caused by Lindane Wastes. 28 COCs from chlorobenzene to heptachlorocyclohexane. [4]

- Surfactant (Non ionic) Emulse-3[®] (Ethical Chem) Tween[®] 80 (Sigma-Aldrich)



Analysis of emulsions

- COCs: GC-MS, GC/ECD/FID

Surfactant:

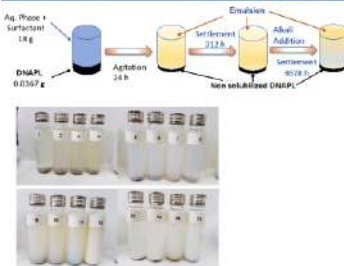
- Tensiometer: Interfacial Tension.
- GC/FID (Cosolvent Emulse 3[®]).

Variables

- DNAPL / Aqueous phase: 0.02
- Surfactant Concentration: 3 - 15 g/L
- pH: 7-13
- time of stabilization: 24 h - 3678 h

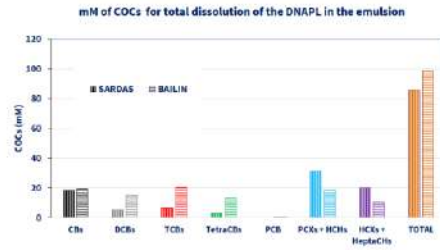
Results

PREPARATION OF EMULSIONS

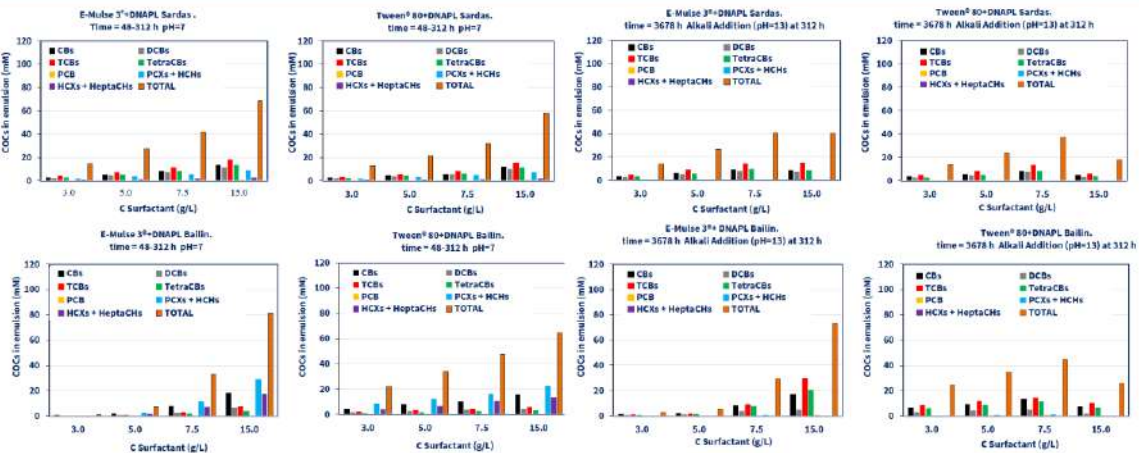


Vial	DNAPL (landfill)	Surfactant	Conc (g/L)
1	SARDAS	Tween [®] 80	3
2	SARDAS	Tween [®] 80	5
3	SARDAS	Tween [®] 80	7.5
4	SARDAS	Tween [®] 80	15
5	BAILIN	Tween [®] 80	3
6	BAILIN	Tween [®] 80	5
7	BAILIN	Tween [®] 80	7.5
8	BAILIN	Tween [®] 80	15
9	SARDAS	E-Mulse 3 [®]	3
10	SARDAS	E-Mulse 3 [®]	5
11	SARDAS	E-Mulse 3 [®]	7.5
12	SARDAS	E-Mulse 3 [®]	15
13	BAILIN	E-Mulse 3 [®]	3
14	BAILIN	E-Mulse 3 [®]	5
15	BAILIN	E-Mulse 3 [®]	7.5
16	BAILIN	E-Mulse 3 [®]	15

COCs distribution in the TOTAL DNAPL ADDED



Effect of Surfactant, pH and DNAPL origin on COCs Solubilization (Solubility in water 0.52 mM)



Addition of Surfactant (15 g/L) increases the solubility up 130 times the solubility in water. Addition of alkali decreases the stability of the emulsions. The better results are obtained with Emulse 3[®]

Addition of Alkali produces the dehydrochlorination of HCHs to TCBs and HeptaCHs to TetraCBs [4] but a remarkable solubilization of COCs is still reached at pH 13.

References:

- Fernández, J. M., Arjón, J. C., Cacho, POP-contaminated sites from HCH production in Sabiñánigo, Spain. Environmental Science and Pollution Research, 2011, 20(6): p. 1937-1950.
- Vilgen, J., et al., Hexachlorocyclohexane (HCH) as new Stockholm Convention POP—a global perspective on the management of Lindane and its waste isomers. Environmental Science and Pollution Research, 2011, 18(2): p. 152-162.
- Mao, X.H., et al., Use of surfactants for the remediation of contaminated soils: A review. Journal of Hazardous Materials, 2015, 295: p. 419-435.
- Santos, A., et al., Chlorinated organic compounds in liquid wastes (DNAPL) from lindane production dumped in landfills in Sabiñánigo (Spain). Environmental Pollution, 2018, 242: p. 1616-1624.

Acknowledgements:

[This work was supported by Regional Government of Madrid de Madrid, project CARESOIL (S2018/ENT-4317), from the Spanish Ministry of Economy, Industry and Competitiveness, projects CTM2016-77253-C2-1-R and for the EU Life Program (LIFE17 ENV/ES/000260). The authors thank the Department of Agriculture, Livestock and Environment, Government of Aragon, Spain, as well as EMGRISA for their support during this work.

27-28 septiembre 2019

LIFE SURFING

“SURfactant enhanced chemical oxidation for remediating DNAPL”

GRUPO INPROQUIMA: Aurora Santos, Carmen M^a Domínguez, Sergio Rodríguez, David Lorenzo

UNIVERSIDAD COMPLUTENSE MADRID

LIFE17 ENV/ES/000260

Departamento de Ingeniería Química y de Materiales

1

décima **noche europea** de investigadores e investigadoras



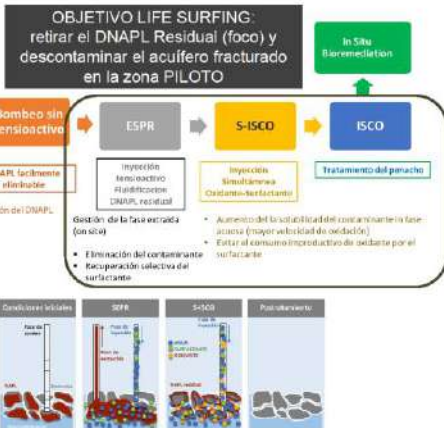
- ✓ Coordinado por el Gobierno de Aragón
- ✓ Presupuesto: 2,1 millones de euros (EU 57%)
- ✓ Duración: 2019 al 2022
- ✓ Comercializable 10% del total
- ✓ Socios :
 - Gobierno de Aragón (Departamento de Cambio Climático y Educación Ambiental)
 - Sociedad Aragonesa de Gestión Agroambiental (Sarga)
 - Internacional HCH & Pesticides Association
 - Grupo INPROQUIMA Universidad Complutense de Madrid
 - Grupo VEGAS, Universidad de Stuttgart

El problema

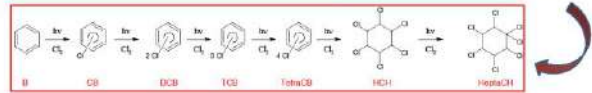
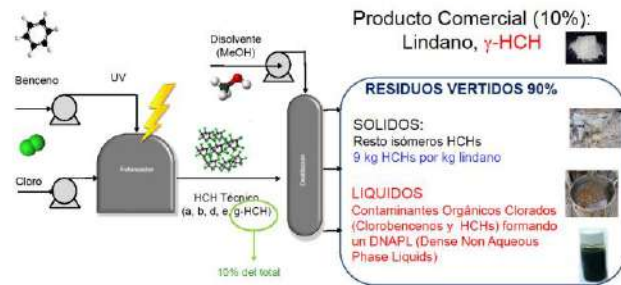
- ✓ El Lindano (isómero γ del HexacloroCicloHexano, HCH) es un plaguicida obsoleto, muy utilizado en la segunda mitad del siglo XX.
- ✓ Su uso y producción están prohibidos por el Convenio de Estocolmo.
- ✓ Su fabricación generó grandes cantidades de **residuos vertidos** cerca de los lugares de producción de forma no segura con **GRAVE CONTAMINACION DEL AGUA SUBTERRANEA Y SUELOS**



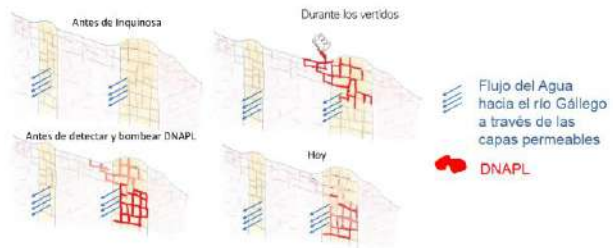
- ✓ En Sabiñanigo (Huesca) la empresa INQUINOSA fabricó lindano entre 1975 y 1988
- ✓ Generó aproximadamente 115000 toneladas de residuos de HCH, vertidos en **dos vertederos cercanos no sellados: Sardas y Bailín**, próximos al río Gallego (< 800 m) y al embalse de Sabiñanigo (< 200 m)



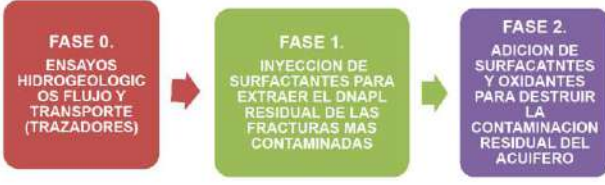
Proceso de producción de Lindano: poco selectivo (gran generación de residuos por kg de lindano)



El DNAPL vertido en el subsuelo rocoso del vertedero de Bailín ha migrado a través de las fracturas de arenisca hasta la zona saturada y es un foco continuo de contaminación del agua subterránea



Life SURFING: PROYECTO A ESCALA PILOTO EN EL VERTEDERO DE BAILIN



fundación para el conocimiento madrid

Comunidad de Madrid

OTRI OFICINA DE TRANSFERENCIA DE RESULTADOS DE INVESTIGACIÓN UNIVERSIDAD COMPLUTENSE DE MADRID



XIX SEMANA DE LA CIENCIA
4-17 NOVIEMBRE 2019

Comunidad de Madrid

**REMIEDIAR LA
CONTAMINACION
BAJO NUESTROS PIES**



Jornadas de puertas abiertas y visitas guiadas

Los **contaminantes** vertidos al suelo se dispersan en las **aguas subterráneas** y son una **amenaza** para la salud y los ecosistemas que **debe eliminarse**.

¿Quieres saber cómo?

 <p>¿Cuándo? 5 de noviembre de 2019</p>	 <p>¿Dónde? Facultad de Ciencias Químicas (UCM)</p>
---	---

<p>¿En qué consiste?</p> 	<p>Conferencia (10:30-11:15) Sala de Grados, Fac. de C.C. Químicas (UCM)</p> <p>Visita laboratorios (11:30-12:45) Laboratorios grupo INPROQUIMA (UCM)</p> 
---	--

<p>Organiza</p>  <p>Grupo INPROQUIMA, Departamento de Ingeniería Química y Materiales • Aurora Santos • Sergio Rodríguez</p>	<p>Colabora</p> <p>Programa HD CARESOL</p>  <p>Life surfing</p> <p>Proyecto SUBWATER enhanced chemical oxidation for remediation DRAC</p> 	<p>Patrocina</p>  <p>FECYT</p>
--	---	--

<p>¿Más información?</p>  <ul style="list-style-type: none"> • https://quimicas.ucm.es/actividades-semana-de-la-ciencia • http://www.madrimasd.pro/semanacienciaeinnovacion/ • http://www.madrimasd.pro/semanacienciaeinnovacion/actividad/remediar-la-contaminacion-bajo-nuestros-pies 	<p>Reserva tu plaza</p>  <p>serqioro@ucm.es</p>
---	--



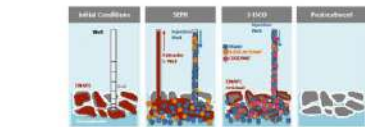
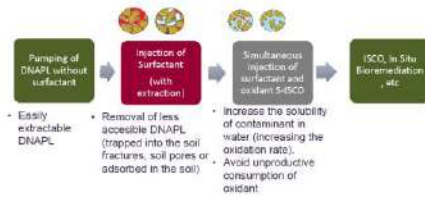
The problem

- ✓ Lindane (isomer HexachlorocycloHexane, HCH) is an obsolete pesticide, widely used in the second half of the twentieth century.
- ✓ Its use and production are banned by the Stockholm Convention. Its manufacture generated large amounts of waste discharged near production sites unsafely with HIGH CONTAMINATION OF GROUNDWATER AND SOIL.

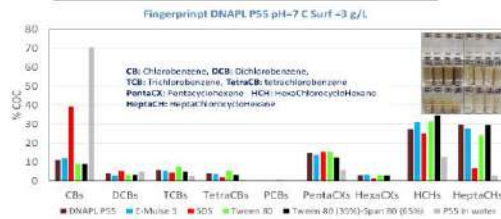
63% of total Lindane was produced in Europe (with the corresponding wastes)



Treatment train for site remediation with DNAPL



SURFACTANTS ENHANCE DNAPL SOLUBILITY in AQUEOUS PHASE



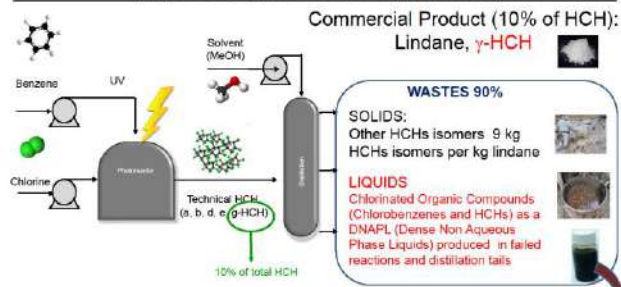
Contact: Aragon Government (Departamento de Agricultura, Ganadería y Medio Ambiente) spoolindano@aragon.es
Aurora Santos López, INPROQUIMA, Chemical Engineering and Materials Department, Universidad Complutense Madrid, [santos@quim.es](mailto:santos@quim.ucm.es)

LIFE SURFING LIFE17 ENV/ES/000260

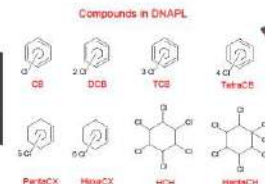
“SURFactant enhanced chemical oxidation for remediating DNAPL”

- ✓ Coordinated by Aragon Government
- ✓ Budget: 2,1 million (EU 57%)
- ✓ Duration: 2019 to 2022
- ✓ Marketable 10% of total
- ✓ Partners :
 - Aragon Government (Departamento de Agricultura, Ganadería y Medio Ambiente)
 - Sociedad Aragonesa de Gestión Agroambiental (Sarga)
 - Internacional HCH & Pesticides Association
 - Group INPROQUIMA Universidad Complutense de Madrid
 - Group VEGAS, Universidad de Stuttgart

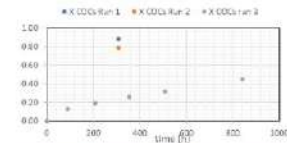
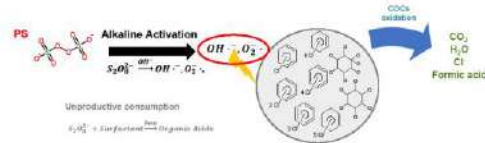
Lindane production process: unselective (large waste generation per kg of lindane)



DNAPL was dumped in the Sabinanigo Landfills, had migrated through sandstone fractures in Bailín Landfill reaching the saturated zone. Due to its hydrophobic nature is a continuous source of groundwater contamination



S-ISCO Oxidant: Persulfate activated by alkali Surfactant: Emulse 3®



Conversion of COCs in the slurry system (a) - aqueous phase in:
Run 1 (initial $C_{OCs} = 2 \text{ g L}^{-1}$, $C_{S_2O_8^{2-}} = 180 \text{ mM}$, $C_{Emulse} = 180 \text{ mM}$;
Run 2 (initial $C_{OCs} = 2 \text{ g L}^{-1}$, $C_{S_2O_8^{2-}} = 180 \text{ mM}$, $C_{Emulse} = 180 \text{ mM}$ and
Run 3 (initial $C_{OCs} = 2 \text{ g L}^{-1}$, $C_{S_2O_8^{2-}} = 180 \text{ mM}$, $C_{Emulse} = 180 \text{ mM}$). Data: UCM

Estabilidad de surfactantes aniónicos y no-iónicos con persulfato activado por álcali y oxidación selectiva de COCs en emulsión



David Lorenzo, Raúl García-Cervilla, Arturo Romero, Aurora Santos

Universidad Complutense de Madrid. Departamento de Ingeniería Química y de Materiales. Grupo INPROQUIMA. dlorenzo@ucm.es



Introducción

La contaminación del suelo por compuestos orgánicos clorados (COCs) es un problema global. La baja solubilidad de la mayoría de estos compuestos en el agua hace posible la formación de fases líquidas densas no acuosas (DNAPLs) [1].

La tecnología de oxidación química in-situ mejorada por surfactantes (S-ISCO) es un proceso prometedor que reduce los tiempos para la eliminación de DNAPLs [2].



Experimental

Reactivos:

Surfactantes:
E-Mulse 3 (E3), Tween 80 (T80), SDS

Oxidante:
Persulfato activado (PS) por álcali

Contaminante:
DNAPL formado por 28 COCs (j)

Ensayos:

Reacción improductiva

Solubilización

Oxidación selectiva

Análisis:



Resultados

Reacción improductiva oxidante surfactante

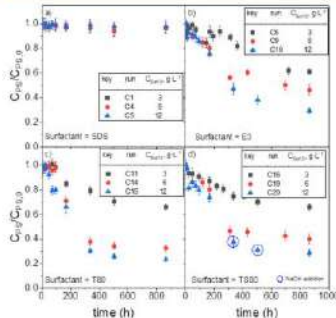


Figura 1. PS remanente vs. tiempo a diferentes concentraciones de surfactant a pH > 12.

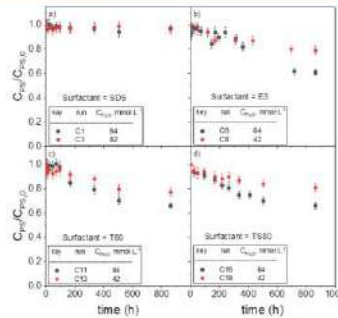


Figura 2. PS remanente vs. tiempo a diferentes concentraciones de oxidante

Los surfactantes no iónicos consumen más PS que los iónicos.



Concentración de surfactante



Consumo de PS



Concentración de oxidante



Consumo de PS

El ratio PS:NaOH no afecta al consumo de PS.

Capacidad de solubilización

Tras la oxidación de surfactante el E3 y el SDS conservan mayor capacidad surfactante (ESC).

$$MSR = \frac{(\sum C_{j,AQ})_{eq}}{(C_{surf,AQ})_{eq}} \quad ESC = \frac{\sum COC_j (mmol \cdot L^{-1})}{MSR (mmol_{COC} \cdot g_{surf}^{-1})} \quad ESC_o = \frac{C_{surf,o} \cdot V_{inj}}{V_{aq} + K_L \cdot W_{DNAPL}}$$

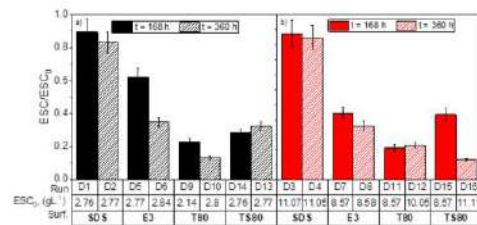
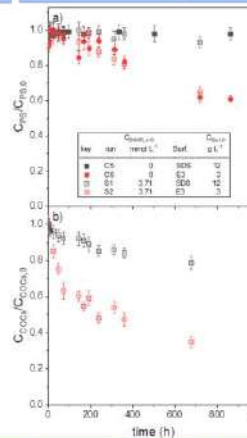


Figura 3. ESC de los surfactants parcialmente oxidados. a) $C_{surf,o} 3 g \cdot L^{-1}$ b) $C_{surf,o} 12 g \cdot L^{-1}$

Oxidación COCs.



El E3 permitió una mayor oxidación de COCs en emulsión que el SDS.

El consumo de PS en la oxidación de COCs en emulsión es despreciable.

El uso de surfactante reduce el tiempo de oxidación para las mismas condiciones sin surfactante

Figura 4. Concentración de a) PS; b) COCs empleando SDS y E3.

[1] Lorenzo, D.; García-Cervilla, R.; Romero, A.; Santos, A. *Chemosphere* 2020, 239, 124798-124808
[2] Besho, A.T.; Naidu, R.; Chadalavada, S. *Environ. Technol. Innov.* 2018, 9, 303-322

Agradecimientos: Este trabajo fue apoyado por el Programa LIFE de la UE (LIFE17 ENV/ES/000260), la Comunidad de Madrid, a través del proyecto CARESQL (S2018/EMT-4317), el Ministerio de Economía de España proyecto (S2018/EMT-4317), y el Ministerio de Economía, Industria y Competitividad, a través del proyecto CTM2016-77451-C2-1-R. Raúl García-Cervilla agradece la subvención del FPI español (ref. BE5-2017-081782). P5G



IN SITU CHEMICAL OXIDATION ENHANCED by SURFACTANTS (S-ISCO): LIFE SURFING PROJECT



Aurora Santos¹, Jesús Fernández², Elena Cano³, D. Lorenzo¹, S. Collas¹, Carlos Herranz³
¹Chemical Engineering and Materials Department, Complutense University of Madrid, Spain
 e-mail: aurasan@ucm.es
²Chemical Engineering and Materials Department, University Complutense of Madrid, Spain.
³Department of Agriculture, Livestock and Environment, Government of Aragon, Spain
⁴Sociedad Aragonesa de Gestión Agroambiental SARGA, Zaragoza, Spain



- ✓ Coordinated by Aragon Government
- ✓ Budget: 2.1 million (EU 57%)
- ✓ Duration: 2019 to 2022
- ✓ Marketable 10% of total
- ✓ Partners:
 - Aragon Government (Departamento de Agricultura, Ganadería y Medio Ambiente)
 - Sociedad Aragonesa de Gestión Agroambiental (Sarga)
 - Internacional HCH & Pesticides Association
 - Group INPROQUIMA Universidad Complutense de Madrid
 - Group VEGAS, Universidad de Stuttgart

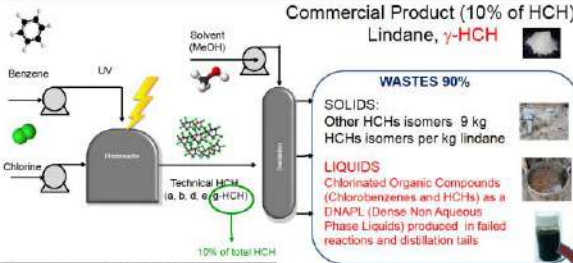
The problem

- ✓ Lindane (isomer HexachlorocycloHexane, HCH) is an obsolete pesticide, widely used in the second half of the twentieth century.
- ✓ Its use and production are banned by the Stockholm Convention. Its manufacture generated large amounts of waste discharged near production sites unsafely with HIGH CONTAMINATION OF GROUNDWATER AND SOIL

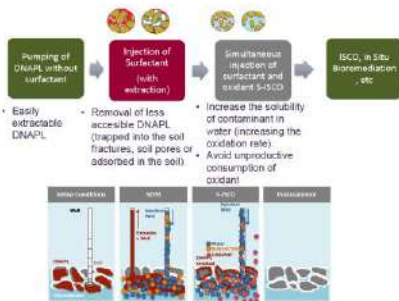
83% of total Lindane was produced in Europe (with the corresponding wastes)



Lindane production process: unselective (large waste generation per kg of lindane)



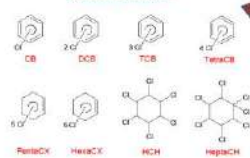
Treatment train for site remediation with DNAPL



DNAPL was dumped in the Sabiñanigo Landfills, had migrated through sandstone fractures in Bailin Landfill reaching the saturated zone. Due to its hydrophobic nature is a continuous source of groundwater contamination



Compounds in DNAPL



S-ISCO at Bailin Landfill

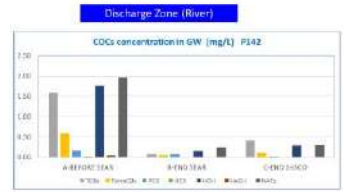


S-ISCO
Oxidant: Persulfate activated by alkali
Surfactant: Emulsi 3®

Surfactant (Biodegradable)	CMC measured (mg L ⁻¹)
E-Mulsi 3® (EthicalChem)	80
Tween 80®	20
Span 80®	10
SDS	1800

Results and Conclusions

- High decrease of HCH/TCBs ratio occurred by dehydrochlorination
- Competitive reaction of Chlorinated Organic Compounds (COCs) and surfactants by the oxidant should be taken into account
- Remarkable COCs decrease was noticed in Groundwater (GW) after S-ISCO
- Negligible COCs and surfactant concentration reached the river
- More than 10 kg of DNAPL was oxidized in S-ISCO
- Total DNAPL removed > 200 kg in SEAR+S-ISCO (1 kg DNAPL contaminates 10³ m³ water)
- No rebounds of contaminants in GW was observed after 6 months



Contact: Aragon Government (Departamento de Agricultura, Ganadería y Medio Ambiente) stopolindano@aragon.es
 Aurora Santos López, INPROQUIMA, Chemical Engineering and Materials Department, Universidad Complutense Madrid, aurasan@ucm.es

declimocuarta
noche europea
de los **investigadores**
madrid

TÍTULO: Proyecto LIFE SURFING: una lavadora para eliminar pesticidas de suelos y aguas subterráneas
AUTORES: Aurora Santos, Carmen M Domínguez, Salvador Cotillas, José Leandro Duarte, David Lorenzo
AFILIACIÓN: Departamento de Ingeniería Química y de Materiales, Facultad de Ciencias Químicas, Universidad Complutense de Madrid

PESTICIDAS CLORADOS OBSOLETOS: UNA HERENCIA ENVENENADA



¿Cómo podemos combatirlos?

Los "malos": ✓ lindano, ✓ residuos (HCHs, DNAPL)

Los "buenos": ✓ surfactantes (= jabones), ✓ oxidantes

Life surfing
LIFE17 ENV/ES/000766

Remediación de DNAPL con surfactantes y oxidación química

ZONA DE BARRERA
zona de ensayo 300m, zona de barrera 120m, Río Gállego, Barranco Ballín, FLUJO DEL AGUA

El surfactante lava el suelo arrancando los contaminantes
Tensión superficial, Solubilidad, Concentración de surfactante

Gestión de las emulsiones resultantes
1. Oxidación selectiva de contaminantes, 2. Adsorción en carbón activo y regeneración, 3. Ruptura de la emulsión

Resultados y beneficios:
Ensayar una técnica, a pequeña escala, que en una futura aplicación a gran escala, pueda eliminar el riesgo de contaminación de agua superficial en el Gállego gracias a la desaparición de la fase densa (DNAPL).

2,081M€ PRESUPUESTO TOTAL
1,182M€ FINANCIACIÓN UE
42 MESES DURACIÓN 2019-2022

Vertedero de Ballín, Sabinánigo (Huesca)

1 litro de DNAPL contamina mil millones de litros de agua equivalente a 400 piscinas olímpicas

DNAPL
10% AGUA, 30% HCl, 60% OTROS CONTAMINANTES

Proyecto financiado por la Unión Europea y coordinado por el Gobierno de Aragón

GOBIERNO DE ARAGON, IHPA, sarga, UNIVERSIDAD COMPLUTENSE MADRID, Universität Stuttgart

ORGANIZA: UCC+i UNIDAD DE CIENCIAS QUÍMICAS, fundación para el conocimiento madrid, FACULTAD DE CIENCIAS QUÍMICAS

FINANCIA: Unión Europea, LIFE17 ENV/ES/000766

decimocuarta
noche europea
de los **investigadores**



Facultad de Ciencias Químicas

Una lavadora para eliminar pesticidas de
suelos y aguas subterráneas

Proyecto LIFE SURFING

29 de septiembre
🕒 12:30 h.



ORGANIZA



UCC+i
UNIDAD DE CULTURA CIENTÍFICA



fundación para el
conocimiento
madrid

FINANCIA

